Influences on the bond behaviour of anchorages under short-term and long-term loading

Von der Fakultät Bau- und Umweltingenieurwissenschaften der Universität Stuttgart
zur Erlangung der Würde einer Doktor-Ingenieurin (Dr.-Ing.)
genehmigte Abhandlung

Vorgelegt von

Nilde Maçi

aus Tirana, Albanien

Hauptberichter:	**Prof. Dr. -Ing. Jan Hofmann**
Mitberichter:	**Prof. Dr. -Ing. Prof. h.c. Christoph Gehlen**

Tag der mündlichen Prüfung: 27.10.2023

Institut für Werkstoffe im Bauwesen der Universität Stuttgart

2023

Eigenständigkeitserklärung

Ich erkläre, dass ich die vorliegende Arbeit selbstständig verfasst und keine anderen als die angegebenen Quellen und Hilfsmittel benutzt habe. Alle Stellen der Arbeit, die wörtlich oder sinngemäß aus Veröffentlichungen oder aus anderweitigen Äußerungen entnommen wurden, sind als solche gekennzeichnet.

Stuttgart, 13.11.2023

Nilde MAÇI

Abstract

This thesis focuses on the load-bearing behaviour of adhesive anchors. The influences on the bond strength of the anchors under short-term and long-term loading are investigated.

The first part describes the current state of the art of bonded anchors under tensile loading and the influences on the load-bearing capacity under short-term loading.

In the second part, the factors influencing the long-term loading of adhesive anchors are presented. This section is a summary of various external and internal research. The influence of different parameters on the bond behaviour under long-term loading is then discussed.

The third part focuses on the influence of incremental loading on the bond behaviour of adhesive anchors. The tests were part of a research project at the Institute of Construction Materials of the University of Stuttgart. As reference tests served short-term tests where the maximum load was reached within 3 minutes. To achieve incremental loading, the anchors were loaded at five percent steps. After loading, the anchors were unloaded and then reloaded within five minutes. Different parameters are varied throughout the test program: the embedment depth, the support width, concrete condition, drilling diameter, hole cleaning and the temperature while testing.

Lastly, the short-term influence on the bond behaviour is investigated. High-strength concrete is used as anchorage base material to test epoxy adhesive anchors. This section describes this behaviour concerning the embedment depth, the bond length of the anchor, the type of steel component and the support width. A comparison between the failure load and the predicted load using the design models from the literature is carried out.

Based on the results of the previous parts, the most critical influences on the bond behaviour of adhesive anchors are presented in the last section.

Kurzfassung

Im Mittelpunkt dieser Arbeit steht das Verhalten von chemischen Befestigungssystemen. Die Einflüsse an der Trag- und Verbundfähigkeit unter Kurzzeit- und Langzeitbelastung von Verbunddübel werden untersucht.

Im ersten Teil werden der aktuelle Stand der Technik von Verbunddübel unter zentrischen Zugbeanspruchung, sowie die Einflüsse der Tragfähigkeit unter Kurzzeitbelastung erläutert.

Im zweiten Teil werden die Einflussfaktoren der Langzeitbelastung von Verbunddübel vorgestellt. Dieser Abschnitt ist eine Zusammenfassung von verschiedenen externen und internen Forschungsarbeiten. Im Anschluss wird der Einfluss verschiedener Parameter auf das Verbundverhalten unter Langzeitbelastung diskutiert.

Im Fokus des dritten Teils steht der Einfluss der stufenweisen Belastung auf das Verbundverhalten von Verbunddübel. Die Versuche waren Teil eines Forschungsprojektes am Insitut für Werkstoffe im Bauwesen der Universität Stuttgart. Kurzzeitversuche wurden durchgeführt, um die Lastschritte der Belastung zu ermitteln. Die Dübel wurden mit 5 % Lastschritten belastet und dann entlastet. Dieser Vorgang wurde innerhalb von 5 Minuten durchgeführt. In diesem Projekt werden verschiedene Parameter, wie z. B. die Verankerungstiefe, die Abstützweite, der Betonzustand, der Bohrerdurchmesser, die Bohrlochreinigung und die Temperatur während der Prüfung variiert.

Im vierten Teil dieser Arbeit wird das Verhalten von Verbunddübel unter Kurzzeitbelastung untersucht. Experimentelle Untersuchungen in ungerissenen hochfesten Beton werden durchgeführt. Der Einfluss an das Verbundverhalten wird über verschiedene Parameter beobachtet. Diese Parameter sind die Abstützweite, die Verankerungstiefe, die Verbundlänge und der axiale Druck. Ein Vergleich zwischen der Versagenslast und der berechneten Last anhand der Bemessungsmodelle aus der Literatur wird durchgeführt.

Auf Grundlage der Ergebnisse der vorherigen Teile, werden im letzten Abschnitt die wichtigsten Einflüsse an das Verbundverhalten von Verbunddübel dargelegt.

Abstrakt

Kjo tezë përqëndrohet në aftësinë lidhëse dhe mënyrën e sjelljes së fiksimeve ngjitëse me ankera në beton. Për këtë arsye u shqyrtuan ndikimet në aftësinë lidhëse të tyre nën efektin e ngarkesave të përkohshme dhe të përhershme.

Pjesa e parë përmbledh kërkimet e fundit shkencore që studiojnë sjelljen e fiksimeve ngjitëse nën ngarkesa në tërheqje qendrore dhe ndikimet në aftësinë mbajtëse gjatë ngarkimit të përkohshëm të tyre.

Në pjesën e dytë paraqiten faktorët që ndikojnë në ngarkimin e përhershëm të fiksimeve ngjitëse, si një përmbledhje e kërkimeve të ndryshme të kryera në Institutin e Materialeve të Ndërtimit të Universitetit të Shtutgardit dhe jashtë tij. Më pas, shtjellohet ndikimi i parametrave të ndryshëm në aftësinë lidhëse nën ngarkesat e përhershme.

Pjesa e tretë përqëndrohet në ndikimin e ngarkesës në rritje në aftësinë lidhëse të fiksimeve ngjitëse. Eksperimentet që përshkruhen në këtë tezë ishin pjesë e një projekti kërkimor në Institutin e Materialeve të Ndërtimit. Si teste referencë shërbyen testet ku aftësia mbajtëse maksimale e tyre u arrit brenda 3 minutave. Fiksimet u ngarkuan me hapa pesë përqind të ngarkesës maksimale. Pas njërit hap, ato u shkarkuan dhe më pas u ringarkuan përsëri brenda pesë minutave. Parametra të ndryshëm si thellësia e instalimit, gjerësia e mbështetjes së strukturës tërheqëse, gjendja e betonit (i lagur apo i thatë), diametri i shpimit, pastrimi i vrimave dhe temperatura gjatë testimit, u ndryshuan gjatë eksperimenteve.

Në vijim, u shqyrtua ndikimi i përkohshëm i faktorëve të ndryshëm në aftësinë lidhëse të fiksimeve ngjitëse. Në këto teste, u përdor beton me rezistencë të lartë si material bazë ankorimi, për të testuar fiksimet me bazë epoksidi. Kjo pjesë përshkruan aftësinë lidhëse përsa i përket thellësisë së instalimit, gjatësisë së ngjitjes së elementit metalik, llojin e elementit metalik dhe gjerësinë e mbështetjes së strukturës tërheqëse. Gjithashtu, u krye një krahasim midis ngarkesës së dështimit (failure) dhe ngarkesës së llogaritur duke përdorur modelet e projektimit nga literatura.

Në pjesën e fundit, janë paraqitur ndikimet më kritike në aftësinë lidhëse të fiksimeve ngjitëse bazuar në rezulatet e mësipërme.

Acknowledgements

This research would not have been possible without the help and support of several people. First and foremost, I wish to thank my supervisor, Prof. Dr.-Ing. Jan Hofmann for his guidance, support and encouragement. With his insights and immense knowledge, every discussion we had led to immediate and tangible improvement.

I wish to express my gratitude to Prof. Dr.-Ing. Prof. h.c. Christoph Gehlen for his careful and critical review of my work.

I am grateful for the time and the opportunity to work at the Laboratory of the Institute of Construction Materials. Being part of the team led by Dr. -Ing. Michael Potthoff was an honour and pleasure. Thank you Michael for your valuable advice and guidance. I would like to extend my deepest gratitude to Dipl.-Ing. Mehdiye Panzehir for being my go to colleague and friend at the Lab. Your countless motivating and kind words helped me accomplish my goal. I am also grateful to all my colleagues at IWB, especially Eugen Lindenmeier, Paul Geiger, Tobias Heinicke, Michael Eckstein and Jonas Weinzierle for the constructive discussions, technical support and the fond memories. To Mrs. Silvia Follmer, thank you for always encouraging me. I would like to thank Dipl.-Bibl. Monika Werner for her help with collecting the relevant literature. A special thank you to CHEMOFAST Anchoring GmbH for partially funding my research.

I am extremely grateful to my friends, especially Pamela, for their emotional support throughout the whole PhD. I cannot begin to express my thanks to my parents and my sister, who with their love, support and encouragement, were always there for me. I would not be here today without you.

Above all, the completion of my dissertation would not have been possible without the support and nurturing of my husband and best friend Mozart. Thank you for being with me every step of the way and for believing in me when I would not. Lastly, to my son, Glin, thank you for smiling and making me forget everything else.

Contents

List of Abbreviations

C	**C**oncrete cone failure
CCD	**C**oncrete **C**apacity **D**esign Method
EBM	Elastic **B**ond **M**odel
HP	**H**and **P**umping
IL	Incremental **L**oading test
IWB	Insitut für **W**erkstoffe im **B**auwesen
M1	**M**ixed pull-out and pull-out with mortar failure
M2	**M**ixed concrete cone and pull-out failure
MB	**M**achine **B**rushing
MPII	**M**anufacturers **P**rinted **I**nstallation **I**nstruction
P	**P**ull-out failure
P$_M$	**P**ull-out with **m**ortar failure
R	**R**eference test
RS2	bond line thickness equal to 2 mm
RS4	bond line thickness equal to 4 mm
S	**S**teel failure
ShT	**Sh**ort-**T**erm test
TTF	**T**ime-**T**o-**F**ailure
UBM	Uniform **B**ond **M**odel

List of Symbols

d	diameter of the anchor	mm
d_0	diameter of the hole	mm
D_c	diameter of the confined test setup	mm
d_{cut}	diameter of the drilling bit	mm
D_u	diameter of the unconfined test setup	mm
E	elastic Modulus	MPa
f_c	concrete compressive strength	MPa
$f_{c,low}$	low concrete compressive strength	MPa
$f_{c,t}$	actual concrete compressive strength	MPa
f_c'	concrete compressive cylinder strength	MPa
f_{cc}	concrete compressive strength on $150mm$ concrete cubes	MPa
$f_{cc,200}$	concrete compressive strength on $200mm$ concrete cubes	MPa
$F_{u,c}$	calculated failure load for concrete failure	kN
$F_{u,p}$	calculated failure load for bond failure	kN
$F_{u,s}$	calculated failure load for steel failure	kN
$F_{u,t}$	failure load from the tests	kN
G	shear Modulus of the mortar	MPa
h_{cone}	oncrete cone depth at minimum (controlling) failure load	mm
h_{ef}	embedment depth of the anchor	mm
k	calibration factor	$-$
$k_{1,2,3}$	calibration factors	$-$
k_{nc}	coefficient	$-$
l	embedment depth of the anchor	mm
m	coefficient	$-$
N_c	ultimate capacity calculated using the concrete cone model	kN
N_b	ultimate capacity calculated using the bond models	kN
N_u	ultimate capacity	kN
$N_{u,m}$	mean failure load	kN
$R_{p0.2}$	steel yield strength	MPa

R_m	steel tensile strength	MPa
t	thickness of the mortar layer	mm
α	angle	$^\circ$
λ	factor accounting for the stiffness of the mortar and rod	mm^{-1}
λ'	stiffness parameter of the adhesive	$\text{mm}^{-0.5}$
π	pi	3.141 59
σ	standard deviation	mm, kN
τ	uniform bond strength	N/mm^2
τ_0	bond strength at low compressive strength	N/mm^2
τ_{max}	maximum bond strength	N/mm^2
τ_u	ultimate bond strength	N/mm^2
$\tau_{u,m}$	mean ultimate bond strength	N/mm^2

1 Introduction

1.1 Problem Statement

Fastening systems are important in construction because of their adaptability. The connection of two or more parts (steel with concrete, concrete with concrete, wood with concrete, etc.) can be achieved through fasteners. Depending on the fastener type, the load is transferred from one element to the other using different transfer mechanisms.

One of the most common fastening systems in large scale constructions, such as railways, bridges, buildings, façades, etc., are adhesive anchors. These post-installed anchors have large carrying capacity and are easy to install. The focus of this research is the behaviour of adhesive anchors. The influences on the load-bearing capacity and bond strength under short-term and long-term loading are investigated.

This work is outlined as follows:

- In the first part of the research, the current state of the art of adhesive anchors under centric tensile loading, as well as the influences on the load-bearing capacity under short-term loading are explained.

- In the second part, the factors that influence long-term loading of bonded anchors are presented. This section is a summary of various external and internal researches.

- The third section focuses on the influence of incremental loading on the bond behaviour of bonded anchors. The tests were part of a research project at the Institute of Construction Materials of the University of Stuttgart. Short-term tests were carried out to determine the load steps of the loading. In this part, different parameters such as the anchorage depth, support width, concrete condition, drill diameter, borehole cleaning and temperature are varied during testing.

- In the fourth part of this paper, the behaviour of bonded anchors under short-term loading is investigated. Experimental investigations in uncracked high-strength concrete are carried out. The influence on the bond behaviour is observed via different parameters. These parameters are the support width, the anchorage depth, the bond length and the axial pressure.

- Based on the results of the previous parts, the most important parameters influencing the bond behaviour of anchorages are presented in the last section.

- A conclusion and a short outlook conclude the research.

2 Literature review

2.1 Adhesive anchor systems

Adhesive anchors or bonded anchors are fastening systems with two components: a steel component which is either a threaded rod or reinforced bar, and a chemical component. The chemical component is a cementitious material, polymer resin or a combination of the previous two. The full capacity of the anchor is influenced by different factors, which will be described in Chapter 3. Depending on the adhesive, the setting time or curing time of the anchor can be short or long.

Comité Euro-International du Béton (1994) subdivides bonded anchors according to the method of installation, in capsule systems and injection systems as illustrated in Figure 2.1.
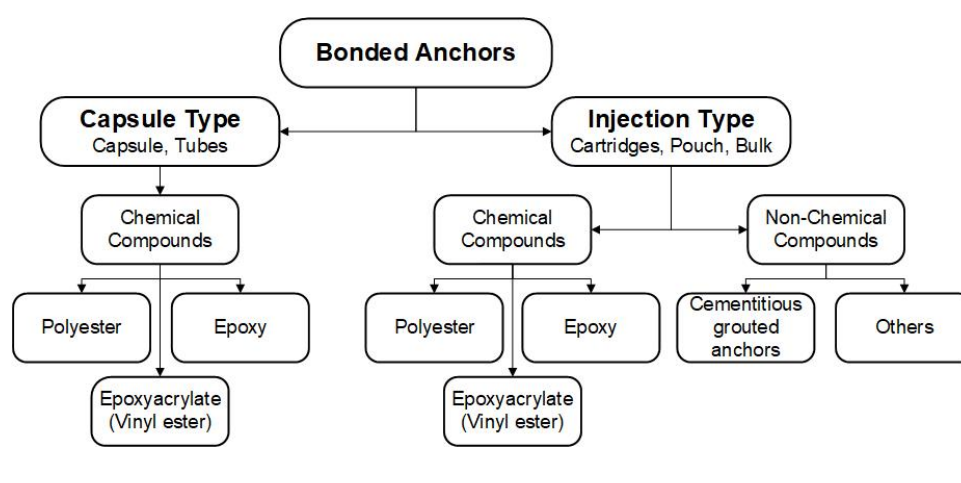
FIGURE 2.1: Adhesive anchors classification (Comité Euro-International du Béton, 1994)

2.1.1 Capsule systems

The chemical component is kept in a capsule system, which can either be a glass ampule / capsule or a foil pouch (Figure 2.2).

The capsule is inserted in a pre-drilled and cleaned hole. Depending on the depth of the hole, more capsules can be inserted.

The capsule is filled with an uncured compound, and a catalyst or an accelerator. The steel component with a sharp chiselled end is fixed to a drill and inserted in the hole with hammering and drilling motions to break the capsule or punch the foil. An alternative is inserting the rod with a hammer. When the capsule system breaks, the chemical components mix and form one polymer matrix. The resins can be classified as unsaturated polyester, vinyl ester and epoxy.
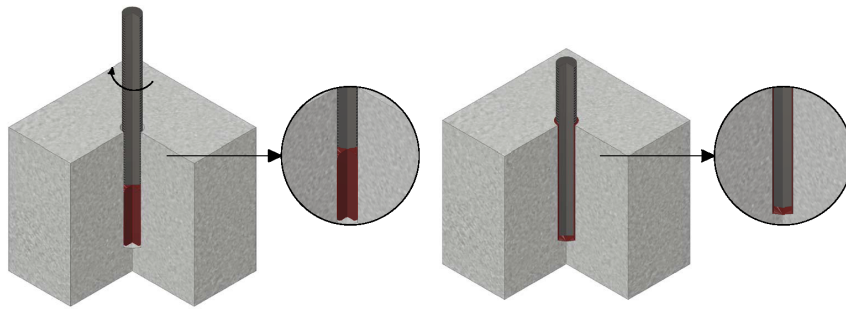
FIGURE 2.2: Capsule system (Comité Euro-International du Béton, 1994)

The installation of a capsule system with a hammer-drill motion or hammer motion is illustrated in Figure 2.3 and Figure 2.4.
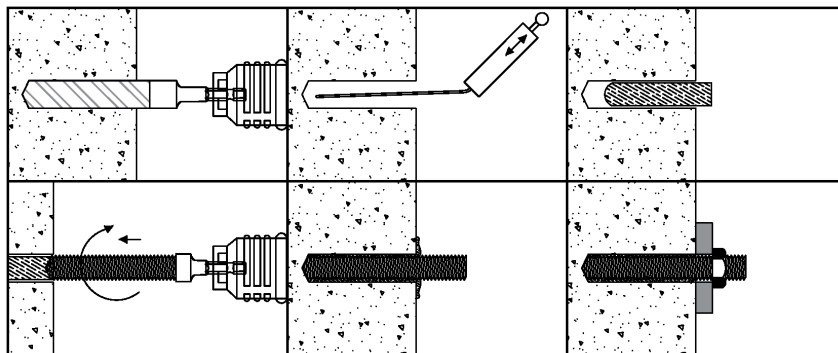
FIGURE 2.3: Capsule system installation with hammer and drilling motion (Eligehausen, Mallée, and Silva, 2006)
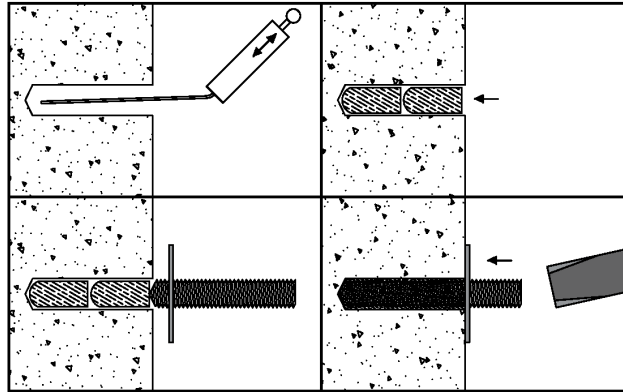
FIGURE 2.4: Capsule system installation: hammered-in capsules (Eligehausen, Mallée, and Silva, 2006)

2.1.2 Injection systems

The injection system, on the other hand, is directly injected into the hole in free form. A distinction can be made between the classic injection anchors and grouted anchors. For injection anchors, the pre-drilled hole is filled with mortar and afterwards, the rod is inserted as illustrated in Figure 2.5. Contrarily, for grouted anchors, the steel component (bolt, headed fastener, rod or reinforced bar) is placed in the hole and then the chemical component is poured in (Figure 2.6). Grouted anchors are considered a subcategory of injection anchors.
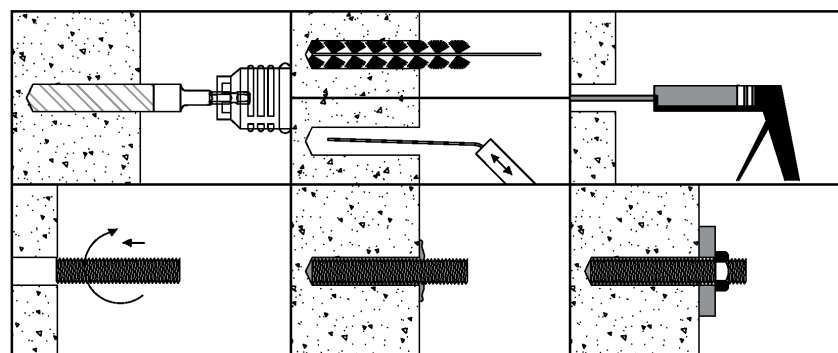
FIGURE 2.5: Injection system installation (Eligehausen, Mallée, and Silva, 2006)
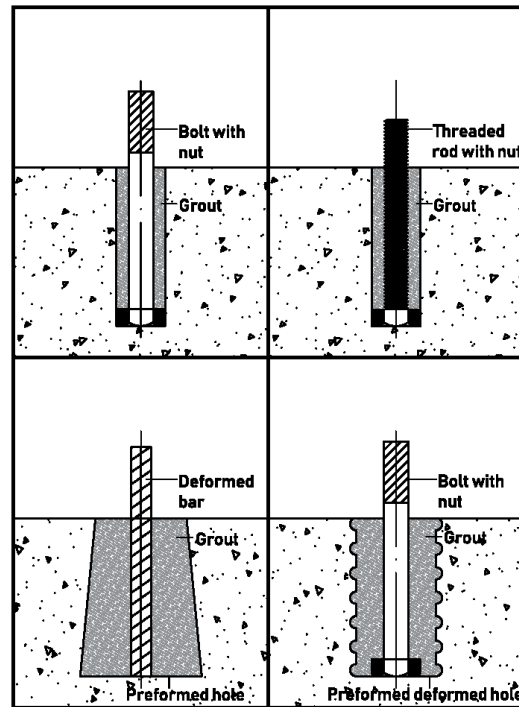
FIGURE 2.6: Injection system installation - grouted adhesives (Comité Euro-International du Béton, 1994)

The chemical components of injection anchors are packed in hard plastic cartridges or plastic foils/bulks. In the plastic cartridges, the resin and the hardener are kept in separate chambers and mixed with the help of a mixing nozzle during installation. On the other hand, in bulk injection systems, the resin and the hardener are already premixed in specific measurements before injection.

2.2   Behaviour of adhesive anchors

When a tensile load is applied to an adhesive anchor, the load is transferred from the steel component through the adhesive to concrete. Two transfer mechanisms occur in these case (Eligehausen, Mallée, and Silva, 2006; Appl, 2009): Mechanical interlock where the load is transferred from the rod or reinforcing bar to the adhesive and secondly, chemical interlock (which is a combination of micro-keying and adhesion) where the load is further transferred to the concrete member (Figure 2.7).
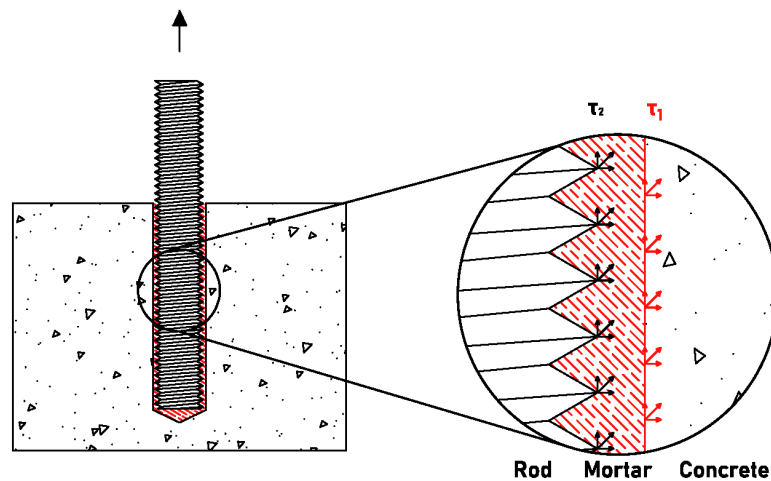
FIGURE 2.7: Load transfer mechanism for adhesive anchors loaded in tension (Appl, 2009)

2.2.1 Failure mechanism

Cook, Kunz, et al. (1998) compared the results from the world-wide database with 38 reports and over 2900 tests. The database contained a variety of tests including tests in cracked and un-cracked concrete, confined and unconfined setups, tensile and shear tests, tests near and far from the edge, tests with different anchor spacing. These tests were carried out with epoxies, unsaturated polyesters, vinyl esters, inorganic and hybrid adhesives. The steel component was either a threaded rod, inserted sleeves or reinforcing bars.

To determine the failure mechanisms Cook, Kunz, et al. (1998) limited the database to unconfined tests with threaded rods and reinforcing bars away from the edge installed in dry, clean and brushed hole.

According to the mentioned results, five typical failure modes were observed as illustrated in Figure 2.8. These failure modes were grouped into three main categories: concrete cone failure, bond failure and steel failure.

Concrete cone failure was characterized by a small embedment depth of the anchor, between $3\,d$ and $5\,d$ (Sell, 1973; Kunz
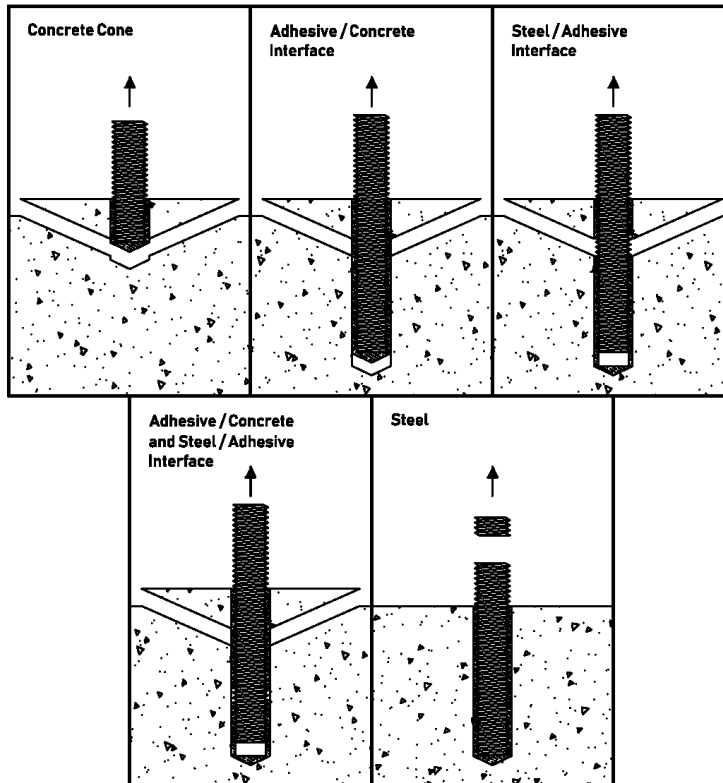
FIGURE 2.8: Failure mechanisms in adhesive anchors
(Cook, Kunz, et al., 1998)

et al., 1998). The angle of the formed concrete cone was approximately $\alpha = \angle 35$.

The bond failure happened with an increase in the anchoring depth. Three different possibilities were considered: failure of the bond between the adhesive and the concrete, the steel and adhesive or both adhesive-concrete bond and steel-adhesive bond. In each case, there was also a small concrete cone formed on the upper part of the anchor near the surface.

The increase in the embedment depths resulted in a better bond between the anchor and the concrete, therefore steel failure of the threaded rod or the reinforcing bar happened.

2.3   Bond strength calculation

This section focuses on an overview of the design models found in literature for calculating the bond strength of adhesive anchors

when concrete cone or bond failure occurs. The failure load when concrete cone failure happens can be predicted using the concrete cone model or the concrete capacity design method (CCD). Bond or pull-out failure load can be predicted using the elastic (EBM) or uniform bond model (UBM), the combined cone / bond model (using EBM or UBM), the bond model neglecting shallow concrete cone, the cone models with bond models and the two interface models. Figure 2.9 depicts a summary of these models.

FIGURE 2.9: Design models

2.3.1 Concrete cone model

Eligehausen, Mallée, and Rehm (1984) presented Equation (2.1) for predicting the capacity of adhesive anchors which show concrete cone failure. The concrete cone model illustrated the dependency of the failure load from the embedment depth of the anchor and concrete compressive strength.

$$N_c = 0.85 \cdot h_{ef}^2 \cdot \sqrt{f_{cc,200}} \qquad (2.1)$$

where: h_{ef} = embedment depth of the anchor [mm]

   $f_{cc,200}$ = concrete compressive strength on 200 mm concrete cubes [MPa]

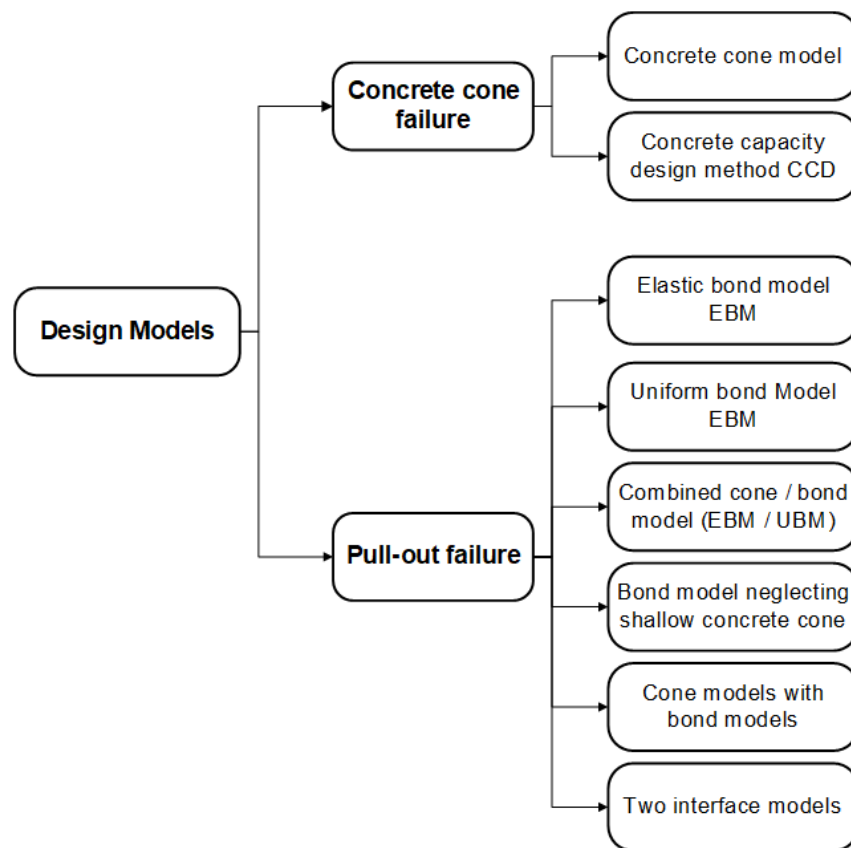Tests with anchors sizes $M\,8$ to $M\,24$ were used to calibrate this model. The effective bond length was taken as $9\,d$. The specimens had a concrete compressive strength of 15 MPa to 40 MPa. To compare the predicted loads with the experimental results, the failure loads of the tests were normalized to a compressive strength of 25 MPa. The ratio of the predicted failure load to the mean experimental results was in the range 0.94 to 1.20. The coefficient of variation of all the predicted loads was around 16 %.

2.3.2   Concrete capacity design method (CCD)

Besides the concrete cone model (Eq. 2.1), concrete failure could be predicted using the concrete capacity design method (CCD) as described in Fuchs, Eligehausen, and Breen (1995). This method was developed for different types of fasteners such as post-installed anchors and cast-in anchors. Tests were carried out with embedment depths from 20 mm to 525 mm in various concrete compressive strengths. The resulting failure loads were normalized to a compressive strength of 25 MPa.

$$N_u = k_1 \cdot \sqrt{f_{cc,200}} \cdot k_2 \cdot h_{ef}^2 \cdot k_3 \cdot h_{ef}^{-0.5} \qquad (2.2)$$

where: $k_{1,2,3}$ = calibration factors [$-$]

Equation (2.2) gives the predicted failure load according to CCD. The factor $k_1 \cdot \sqrt{f_{cc,200}}$ describes the nominal concrete tensile stress over the failure area $k_2 \cdot h_{ef}^2$, and $k_3 \cdot h_{ef}^{-0.5}$ represents the size effect. Substituting the multiplication of the calibration factors with k_{nc}, Eq. (2.2) is given as:

$$N_u = k_{nc} \cdot \sqrt{f_{cc,200}} \cdot h_{ef}^{1.5} \qquad (2.3)$$

The coefficient k_{nc} for post-installed anchors is equal to 13.5 and 9.5 for uncracked and cracked concrete, respectively.

The predicted loads were in the same range as the measured loads. An exception were some anchors with large embedment depths, where the prediction was conservative. The coefficient of variation was between 15 % and 20 % which was comparable with the tension tests.

The concrete capacity design method is easy to apply and takes into consideration the size effect of the anchor, thus it is used in current standards such as ACI 318 (2019) and DIN EN 1992-4 (2019).

2.3.3 Elastic bond model (EBM)

The elastic bond model (EBM) was developed for adhesive anchors with a diameter of 5/8" or 16 mm (Doerr and Klinger, 1989). This model considered an elastic distribution of the bond stress along the length of the anchor as seen in Figure 2.10. The development of this model took into account the total energy in the anchor system. A detailed derivation is given in Doerr and Klinger (1989).
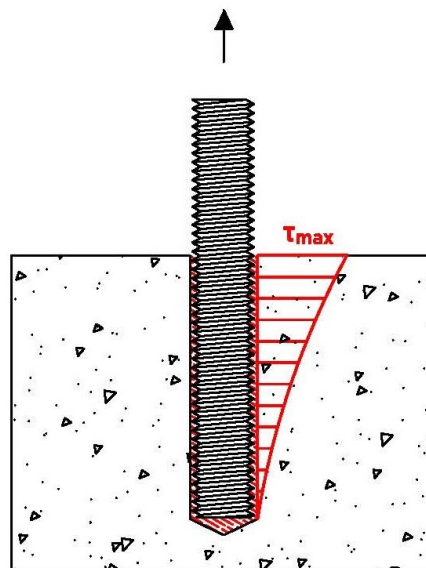

FIGURE 2.10: Elastic bond model - bond stress distribution (Doerr and Klinger, 1989)

The capacity of the anchor was given as:

$$N_u = \frac{\pi \cdot \tau_{max} \cdot d_0^{1.5}}{\lambda'} \cdot \tanh \frac{\lambda' \cdot l}{\sqrt{d_0}} \qquad (2.4)$$

where: τ_{max} = maximum bond strength [MPa]

$\quad d_0$ = the hole diameter [mm]

$\quad \lambda'$ = stiffness parameter of the adhesive [$mm^{-0.5}$]

$\quad l$ = embedment depth [mm]

From the experiments, τ_{max} ranged between 15.6 and 27.0 MPa, whereas λ' between 0.019 and 0.059 $mm^{-0.5}$ (Cook, Doerr, and Klingner, 1993).

$$\lambda' = \lambda \cdot \sqrt{d_0} = \sqrt{\frac{4 \cdot G}{t \cdot E}} \qquad (2.5)$$

where: λ = factor accounting for the stiffness of the mortar and rod [mm^{-1}]

$\quad G$ = shear modulus of the mortar [MPa]

$\quad t$ = thickness of the mortar layer [mm]

$\quad E$ = elastic modulus of the rod [MPa]

Equation (2.4) was calibrated with experiments using partially bonded anchors, where the first 50 mm of the embedment depth were unbonded to simulate the depth of the shallow cone. This model predicted the failure load of partially bonded anchors accurately. For fully bonded anchors, this model can be applied after neglecting the first 50 mm of the embedment. In this case, the model produces conservative results. Cook (1993) recommended using EBM for embedment depths higher than $40\sqrt{d_0}$.

2.3.4   Uniform bond model (UBM)

The uniform bond model (UBM) assumed a uniform distribution of the bond strength along the length of the anchor as shown in Figure 2.11 (Cook, 1993). However, the compatibility between the concrete, the adhesive and the threaded rod was not taken into account. This model showed a direct dependency of the load-bearing capacity of the anchor not only from the diameter and the embedment depth but also from the product dependent bond strength. Thus, the failure load is given as:
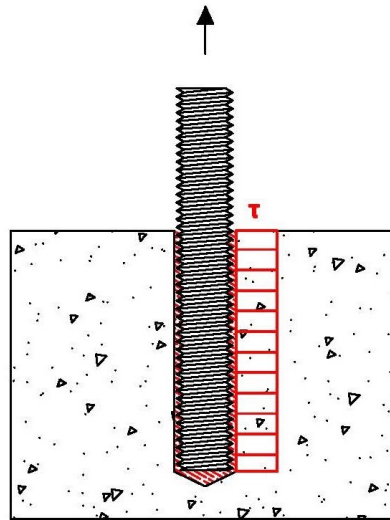
FIGURE 2.11: Uniform bond model - bond stress distribution (Cook, 1993)

$$N_u = \tau \cdot \pi \cdot d \cdot h_{ef} \qquad (2.6)$$

where: τ = uniform bond strength [MPa]
                d = anchor diameter [mm]

This model is accurate for shallow and deep embedments, which fail in the combined cone / bond mode (Cook, Kunz, et al., 1998). In Equation (2.6), it should be evaluated if the use of the anchor diameter or the hole diameter is appropriate. According to Cook (1993) using the diameter of the steel component is favourable because it does not require prior knowledge of the drill bit used.

2.3.5   Combined cone / bond model (EBM / UBM)

According to Cook (1993), a combined cone / bond model can be used to determine the bond failure of adhesive anchors. Equation (2.7) was a combination of the concrete cone failure model (Eq. 2.1) and bond failure of the anchor which was determined

using the elastic bond model or uniform bond model. In each case, the bond length was minimized by the concrete cone depth.

$$N_u = N_c + N_b \tag{2.7}$$

Using the EBM (Section 2.3.3), the failure load and the concrete cone depth were calculated as follows:

$$N_b = \tau_{max} \cdot \pi \cdot d_0 \cdot \frac{d_0}{\lambda'} \cdot \tanh \frac{\lambda' \cdot (h_{ef} - h_{cone})}{\sqrt{d_0}} \tag{2.8}$$

where: h_{cone} = concrete cone depth at minimum (controlling) failure load [mm]

$$h_{cone} = \frac{\tau_{max} \cdot \pi \cdot d_0}{1.84 \cdot \sqrt{f'_c}} \cdot \mathrm{sech}^2 \frac{\lambda' \cdot (h_{ef} - h_{cone})}{\sqrt{d_0}} \tag{2.9}$$

Alternatively, the failure load and the height of the concrete cone were determined using the UBM (Section 2.3.4):

$$N_b = \tau_0 \cdot \pi \cdot d_0 \cdot (h_{ef} - h_{cone}) \tag{2.10}$$

$$h_{cone} = \frac{\tau_0 \cdot \pi \cdot d_0}{1.84 \cdot \sqrt{f'_c}} \tag{2.11}$$

where: f'_c = concrete compressive cylinder strength [MPa]

2.3.6   Bond model neglecting shallow concrete cone

Cook, Kunz, et al. (1998) introduced another model to predict the failure load of adhesive anchors neglecting the shallow concrete cone created at approximately 50 mm or $3d$.

$$N_u = \tau \cdot \pi \cdot d \cdot (h_{ef} - 3d) \tag{2.12}$$

2.3.7   Cone models with bond models

The cone models with bond models refer to the models given in a Japanese progress report from the Japanese Concrete Institute

(JCI). These design models are described in detail in Kunz et al. (1998).

For small embedment depths, a concrete cone failure with 45 ° angle was assumed. For higher embedment depths the load was calculated as a function of the hole diameter, bond strength and embedment depth.

$$N_u = k \cdot \tau \cdot (h_{ef} + d_0 \cdot \pi) \tag{2.13}$$

$$N_u = k_3 \cdot \tau \cdot d_0 \cdot \pi \cdot h_{ef} \tag{2.14}$$

where: k, k_3 = calibration factors $[-]$

The difference between Equation (2.6) and (2.14) is that the diameter of the drill hole is considered.

2.3.8 Two interface models

The two interface bond model was developed by Marti (1993). This model was used when bond failure occurs (in the interface between the adhesive and concrete or steel and adhesive). When the interface between adhesive and concrete fails, the ultimate load was predicted as follows:

$$N_u = \tau_0 \cdot \pi \cdot d_0 \cdot h_{ef} \cdot \sqrt{\frac{f_c}{f_{c,low}}} \tag{2.15}$$

where: τ_0 = bond stress at low compressive strength [MPa]
f_c = considered concrete compressive strength [MPa]
$f_{c,low}$ = low concrete compressive strength at which τ_0 was evaluated [MPa]

When the interface between steel and adhesive fails, the load can be predicted using the uniform bond model (Eq. 2.6).

The two interface model was developed using only one type of adhesive anchor and reinforcing bars.

3 Short-term behaviour of adhesive anchors

3.1 Overview

Previous research revealed two main factors which influence the bond strength of adhesive anchors: internal and external factors (Cook and Konz, 2001). The recorded factors were:

- Internal factors:

  - Chemical formulation (type of adhesive)
  - Mixing uniformity
  - Curing time when loaded
  - Annular gap
  - Fiber content of adhesive
  - Chemical resistance

- External factors:

  - Installation factors:
    * Age of concrete
    * Anchor diameter
    * Concrete aggregates (coarse or fine)
    * Concrete strength
    * Cracked / uncracked concrete
    * Hole cleaning
    * Hole depth
    * Hole drilling
    * Hole moisture
    * Hole orientation
    * Installation temperature
    * Test Setup
    * Type of concrete

  – In-service factors:
    * Short-term cure
    * Elevated temperature
    * Long-term load (creep)

According to ACI 318 (2019) and AC 308 (2017) as in-service factors count also:

- Moisture in service

- Freeze-thaw

3.2   Internal factors

3.2.1   Chemical formulation (type of adhesive)

Previous studies have emphasized the effect of the formulation of the adhesive on the load bearing capacity of the anchor. Cook (1993) and Cook, Bishop, et al. (1994) performed confined tests on different types of bonded anchors. Cook (1993) tested 16 different formulations which are categorized in 10 epoxies with 3 using mercaptan hardeners and 7 using amine-based hardeners; 3 vinyl esters one of which was a capsule system and 3 polyesters with one capsule system, one pouch system and one pump system. Three anchor sizes with three embedment depths were tested in low-strength concrete. Cook, Bishop, et al. (1994) performed additional tension tests on 20 adhesives consisting in 10 epoxy amines, 3 epoxy mercaptans, 3 polyesters, 2 vinyl esters, 1 vinyl ester cementitious and 1 polyamide. Only one product was a self-mixing system. Three anchor sizes were tested in low-strength concrete. Figure 3.1 illustrates the influence of the product formulation in the average bond strength. The resulting strengths from the tests varied not only between the different adhesive groups but also within the same type.

Figure 3.2 illustrates the effect of the type of adhesive on the bond strength (Lehr and Eligehausen, 1998; Mészároš, 2002; Spieth, 2002). Mészároš (2002) tested the same product with three different viscosities: low, normal and high viscosity. The tests revealed a reduction of the bond strength of 2.3 % for high viscosity and 3.9 % for low viscosity.
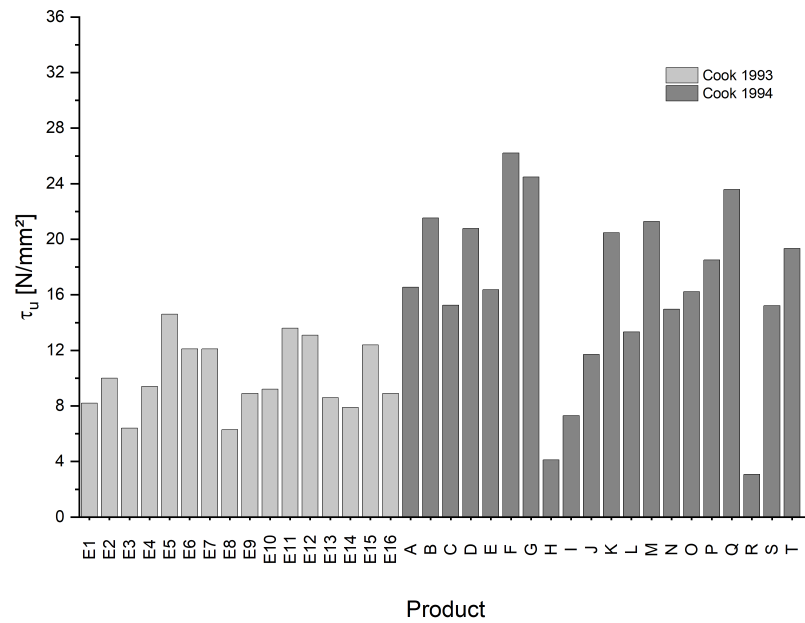
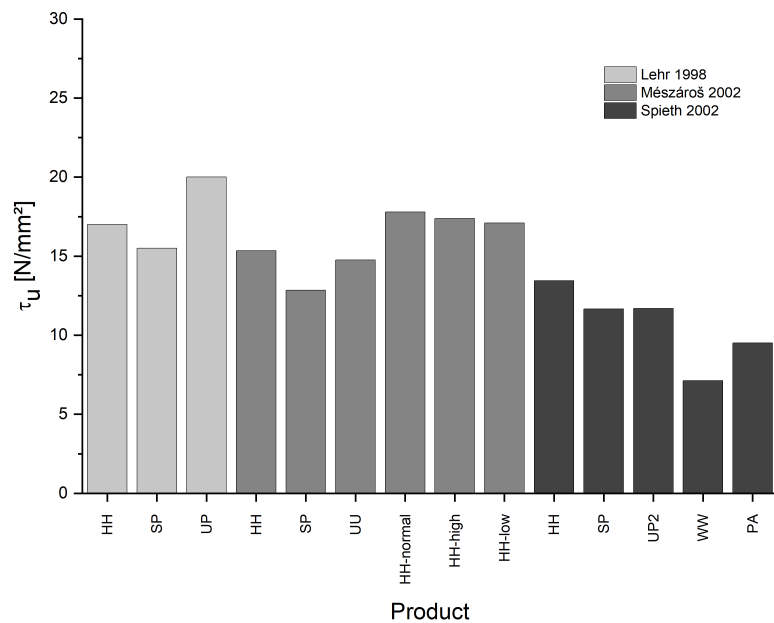FIGURE 3.1: Influence of the chemical formulation according to Cook (Cook, 1993; Cook, Bishop, et al., 1994)

FIGURE 3.2: Influence of the chemical formulation according to Lehr and Eligehausen (1998), Mészároš (2002), and Spieth (2002)

Simons (2007) performed tests on reinforcing bars. She compared the results of 5 adhesive anchors with cast-in reinforcing bars. The hybrid adhesive with a two-component system (one organic and one inorganic bonding agent) demonstrated a comparable bond strength and stiffness with the cast-in bars. On the contrary, the two epoxy-based adhesives and the cement-system showed a stiffer system. The bond strength of the epoxy adhesives was 60 % higher than the cast-in bars, as opposed to the cement-system bond which was 25 % lower. The polyester adhesive reached the peak load after 15 mm displacement due to the friction forces created in the hole. The bonded strength, in this case, was 67 % lower than the cast-in reinforcing bars.

3.2.2   Mixing uniformity

As reported above, the type of adhesive is an important factor for the load-bearing capacity of the anchor. Simultaneously, the components of the adhesive have to be mixed properly to achieve this maximum capacity. Some adhesive systems (capsule systems, injection systems) are already pre-filled with the intended ratio of each component. However, there are systems, like pouches, where the components need to be mixed manually.

Cattaneo, Locatelli, and Rago (2019) compared in their research, two different adhesives: an epoxy adhesive B, with two-paste components given in two cans and a polyester adhesive C, with one paste component given in a can and the powder component in a bag. The compared mixing methods were manual and mechanical (with a low-speed rotary hammer and a paddle). The epoxy adhesive B was mixed in each case for 3 minutes until a uniform colour was achieved. Whereas, the polyester adhesive C was mixed for 1.5 minutes until a smooth consistency was seen. Figure 3.3 illustrates the results of these tests. The bond strength of the manually mixed epoxy adhesive was 21.4 % and 37.7 % lower compared to the mechanical mixing (respectively for diameter 12 mm and 16 mm). On the other hand, for the polyester adhesive the bond strength seemed to increase for diameter 12 mm and decrease for 16 mm.
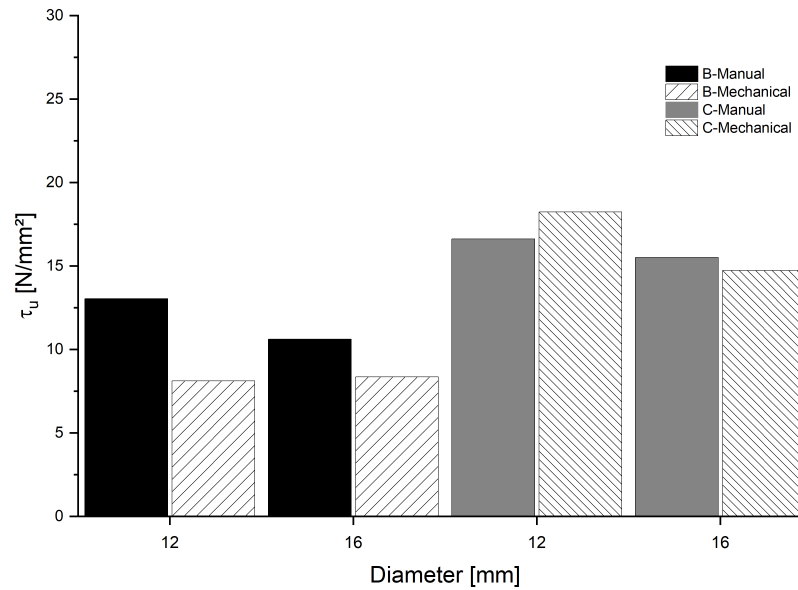
FIGURE 3.3: Influence of the mixing uniformity (Cattaneo, Locatelli, and Rago, 2019)

3.2.3 Curing time when loaded

Preliminary work on the influence of curing time in the carrying capacity of the anchor was carried out from Cook, Bishop, et al. (1994). They tested 20 products with two curing times. They loaded the anchor after 24 hours and after 7 days. More than half of the short time curing anchors reached at least 90 % of the strength compared to the reference tests (Figure 3.4).

Spieth (2002) performed tests on two-hybrid systems with a combination of vinyl ester, water and cement. He tested the anchors starting from 45 minutes to approximately 100 days as illustrated in Figure 3.5. Both systems revealed an influence of the curing time in the bond strength with an increase of around 50 % from the minimum curing time to 1000 hours.

In his PhD, Hülder (2008) studied the curing time influence in two adhesive formulations by testing their tensile strength according to the standards at two temperatures and minimal curing times as given in the Manufacturer's Printed Installations Instructions. The epoxy adhesive cured at standard temperature (23 °C) showed an increase of the strength from 32 N/mm^2 after 48 hours of curing to 36 N/mm^2 after one week. At the lower
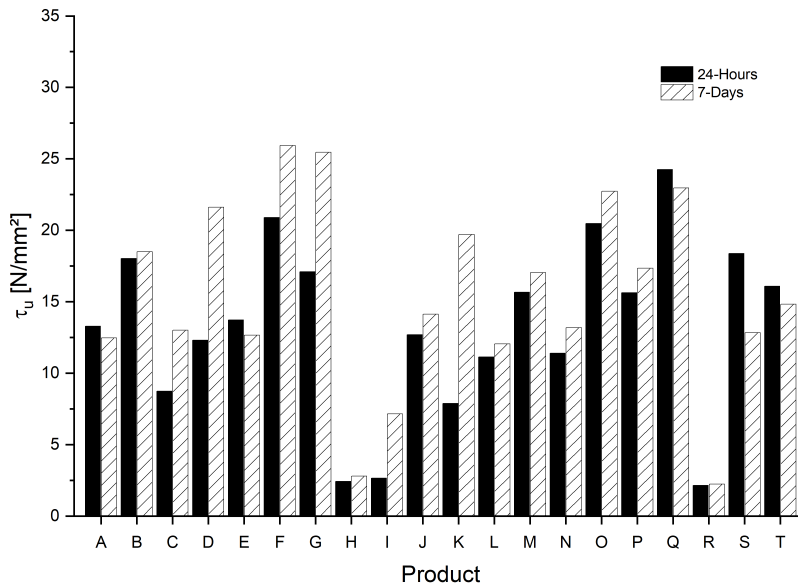
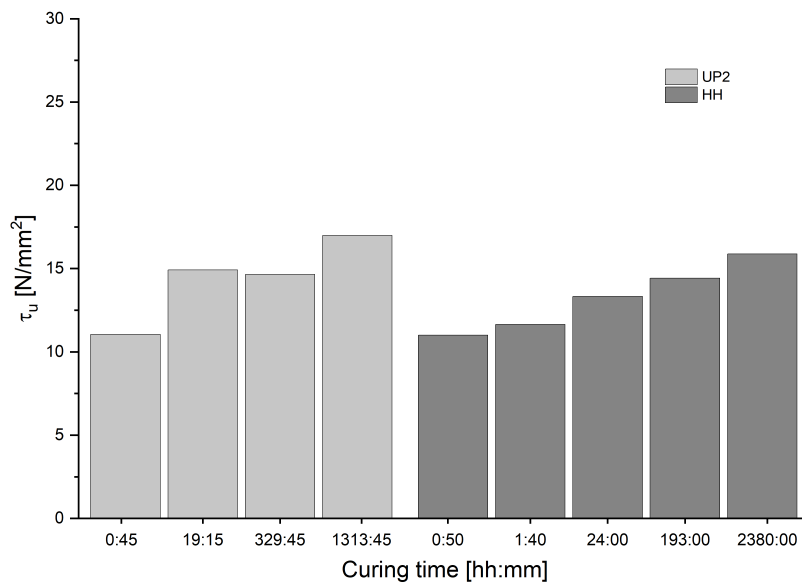FIGURE 3.4: Influence of the curing time according to Cook, Bishop, et al. (1994)

FIGURE 3.5: Influence of the curing time according to Spieth (2002)

temperature 8 °C and one-week curing time, the adhesive did not reach the value of the epoxy at 23 °C and 48 hours of curing. The other adhesive was a vinyl ester, which was tested at 0 °C

with 3 hours curing time and standard temperature 23 °C with 45 minutes of curing. Even in this case, the adhesive at the lower temperature and after one week of curing time, did not reach the tensile strength of the adhesive after only 45 minutes of curing at standard temperature.

3.2.4 Annular gap

The load-bearing capacity of a bonded anchor depends on the annular gap. The annular gap is the difference between the drill bit diameter and the steel component diameter. The relation of the drill diameter and the rod or bar is specified by the manufacturer of the adhesive and is product specific. Usually, for the same diameter of the threaded rod and reinforcing bar, the drilling diameter is larger in the second case because the nominal diameter of reinforcing bars is higher than the threaded rods.

Lehr and Eligehausen (1998) noticed, that the bond strength of the adhesive decreased with a decrease of the ratio between the annular gap and the anchor diameter. In his paper, Çolak (2001) tested 4 annular gaps: 1 mm, 2 mm, 3 mm and 4 mm. One of the tested epoxies showed an increase in bond strength with an increase of the thickness from 1 mm to 2 mm. However, afterwards, the strength decreases with the increase of the annular gap. The second epoxy formulation seemed to have almost no influence on the bond strength.

Spieth (2002) and Mészároš (2002) have demonstrated that this influence on the load-carrying capacity is product specific (Figure 3.6). Spieth compared the behaviour of a vinyl ester - cement adhesive with the given annular gap 2.5 mm to the thickness 4 mm. He observed a distinct influence on the bond strength of the anchor as well as on the displacement behaviour during testing. The system reduced the bond strength and the bond stiffness with an increase in the thickness. The load-displacement behaviour of the anchor changed drastically, the displacement at peak load quintupled. Mészároš on the other hand, tested a vinyl ester capsule system with three annular gaps: 1 mm (as given in the instructions), 1.5 mm and 2 mm. For the first two, he used only one capsule to install the anchor, whereas for the 2 mm annular gap, he used two capsules. The increase of the thickness changed the load-displacement behaviour of the anchor, where

two peak loads were observed. The increase of the annular gap with 0.5 mm reduced the load by approximately 56 % (at the first peak) and for 1 mm at 18 %, which indicated in the first case, not the influence of the thickness as much as the lack of adhesive around the rod.

Simons (2007) performed tests in cracked concrete with an increase of the annular gap from 2.5 mm to 6 mm. She observed that with increasing the thickness, higher bond strengths could be achieved but there was no influence on the bond stiffness (Figure 3.6). González et al. (2018) and Cattaneo, Locatelli, and Rago (2019) have also found, that the annular gap does not influence the bond strength of the anchor.
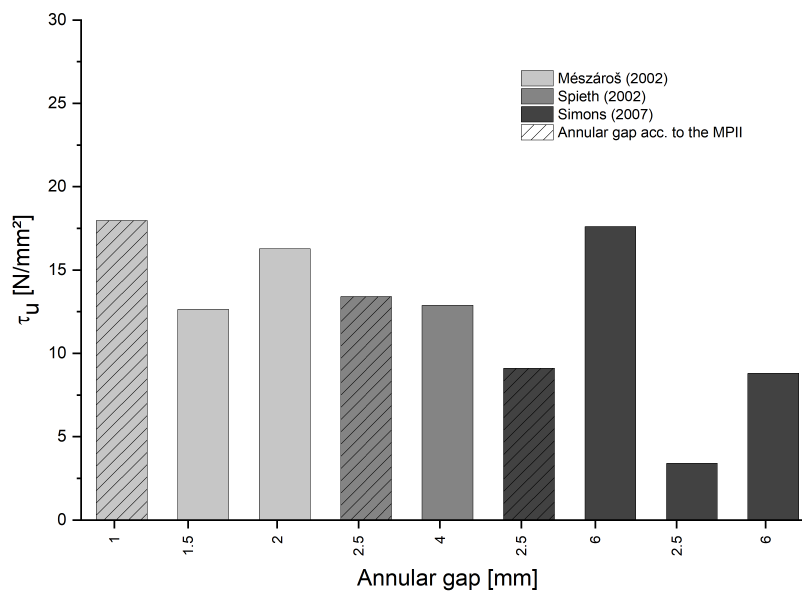
FIGURE 3.6: Influence of the annular gap according to Mészároš (2002), Spieth (2002), and Simons (2007)

3.2.5   Fiber content of adhesive

Not only the type of adhesive is important for the load-carrying capacity, but also the ratio of the fillers. Çolak (2001) carried out tests with two different epoxies with the filler concentration raging from 0 % to 72 %. He determined the adhesive shear strength in each case. The shear strength in both epoxies remained the same until the filler concentration reached 46 %. With a further

increase in the concentration, the shear strength reduced. Further research from Çolak (2007), supports the influence of the fillers in the load-bearing capacity of bonded anchors.

3.2.6 Chemical resistance

The presence of chemical compounds, such as alkalis, solvents and acids, influences the bond properties of adhesive anchors. These products as well as oils, plasticizers and greases, could penetrate in adhesive and cause it to soften which directly influences the carrying capacity of the anchors (Cognard, 2005).

3.3 Installation factors

3.3.1 Age of concrete

EAD 330499 (2018) and AC 308 (2017) define the minimum age of testing and installing on concrete slabs as 21 days.

Mészároš (2002) investigated two aspects of concrete age. He observed the influence of installation in early age concrete. He installed anchors in 7-day old and 53-day old concrete and tested them after 47 to 49 days and 1.5 to 2 hours, respectively. He experimented on 3 different adhesive systems with different hole cleaning methods (see Section 3.3.6). One adhesive system showed that the anchors which had hardened for approximately 1000 hours showed a higher failure load compared to the anchors which had 2 hours hardening time (the cleaning method was defined as good). The other two systems did not exhibit any change in the failure load. Secondly, he evaluated all his results in reference to the concrete age. Mészároš converted all his results to a standard concrete strength and compared them. The results for the confined test setup presented a relatively small increase in the bond strength of the adhesive with an increase in the concrete age.

3.3.2 Anchor diameter

A number of authors have studied the influence of the anchor diameter on the load-carrying capacity of bonded anchors. Lehr

and Eligehausen (1998) performed tests on three adhesive systems, in low and high-strength concrete with confined and unconfined setup. Each adhesive system behaved differently with an increase in diameter. Their results revealed that each adhesive system tested in low and high-strength concrete with an unconfined setup decreased the bond strength by increasing the anchor diameter. In comparison, the tests with confined setup behaved differently in each case as illustrated in Figure 3.7. For example, the system HH increased the bond strength with approximately 10 % with an increase of the diameter from 8 mm to 12 mm but decreased with a further increase of the diameter to 16 mm. On the contrary, the system SP demonstrated only a decrease in the bond strength with increasing the anchor diameter.
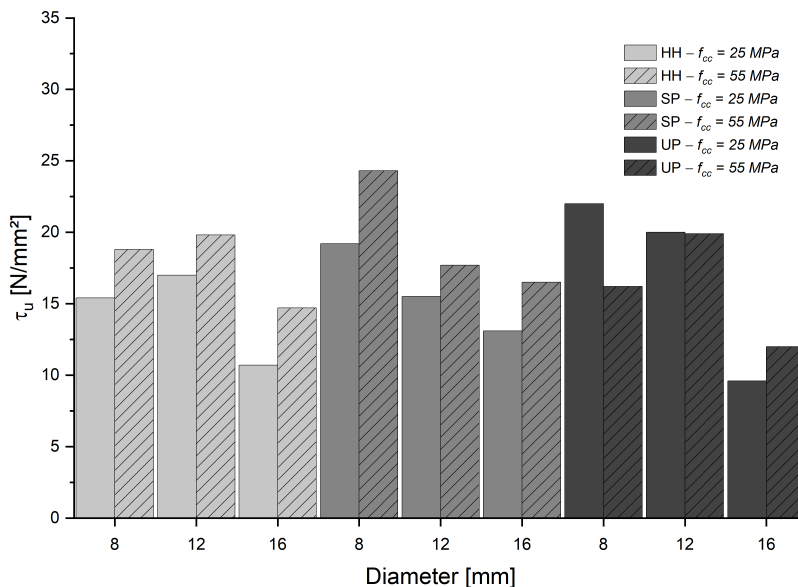

FIGURE 3.7: Influence of the anchor diameter according to Lehr and Eligehausen (1998)

Mészároš (2002) performed confined and unconfined tests in low-strength concrete with four bar diameters: 8 mm, 12 mm, 16 mm and 24 mm. The bond strength in the unconfined test decreased with an increase in the diameter of the bars. The confined test results revealed a proportional increase in the failure load with an increase in diameter. The experiments of Spieth (2002) on two diameters in low-strength concrete with confined setup concurred with the findings of Mészároš (2002).

In her research, Simons (2007) tested bars with three diameters. She demonstrated that increasing the diameter of the bar resulted partly in a decrease in the bond strength of the adhesive. Recent research from Cattaneo, Locatelli, and Rago (2019), revealed less than 6 % change in the bond strength with increasing the diameter (Figure 3.8).
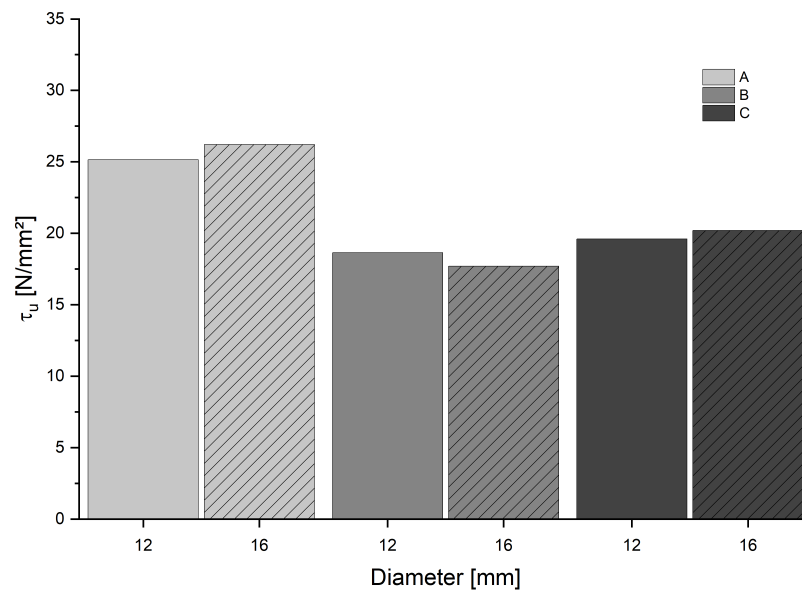

FIGURE 3.8: Influence of the anchor diameter according to Cattaneo, Locatelli, and Rago (2019)

3.3.3 Concrete aggregates (coarse or fine)

Previous research from Cook, Bishop, et al. (1994) studied the influence of the type of concrete aggregate in the behaviour of adhesive anchors. Limestone and river gravel aggregates were used (Figure 3.9). The results reported that from 15 tested products, ten adhesive systems had between 10 % to 90 % higher failure loads in the river gravel concrete, four systems had a minimal change in the load and three systems showed lower failure loads compared to the limestone concrete. Furthermore, the change in the aggregate influenced the failure mechanisms of the anchors. Six systems exhibited an adhesive - concrete interface failure with the limestone concrete, whereas in the river gravel concrete the steel - adhesive interface failed.
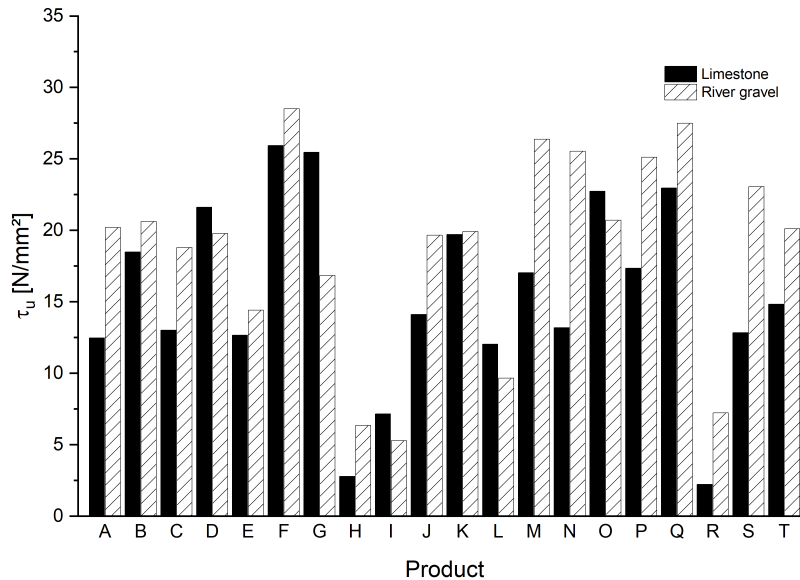
FIGURE 3.9: Influence of the type of aggregate according to Cook (1993)

Similarly, Mészároš (2002) studied the influence of the size of the aggregates in the load-carrying capacity of adhesive anchors. He tested one adhesive system in three concrete batches with aggregate sizes $0 - 8$ mm, $0 - 16$ mm, $0 - 32$ mm. The failure loads were converted to the same concrete compressive strength. The anchor installed in the concrete batch with $0 - 32$ mm aggregates revealed $10\,\%$ lower failure load compared to the other two batches. In addition, the failure mechanisms in the $0 - 8$ mm concrete was a combined adhesive - concrete and steel - adhesive failure, whereas in the other two cases was the steel - adhesive interface.

3.3.4   Concrete strength

Another factor influencing the bearing capacity of adhesive anchors is the concrete compressive strength. Lehr and Eligehausen (1998) tried to find a connection between the bond strength of the anchor and the compressive strength of concrete, however, there was no consistent relationship between the two. Cook, Bishop, et al. (1994) while testing different types of adhesive anchors, found an increase of the capacity of capsule-type adhesive anchors with

the increase of the concrete strength. In his work, Spieth (2002), pointed out that with higher concrete cover (150 mm) and higher compressive strength, the bond strength remained unaffected. On the other hand, with smaller cover (40 mm) an increase in the bond strength was shown. However, because only two compressive strengths were tested, no conclusion could be drawn. Simons (2007) tested two systems, epoxy mortar and cement type mortar, in cracked concrete with two compressive strengths. In each case, an increase in the bond strength was observed.

3.3.5 Cracked / uncracked concrete

The presence of cracks in concrete and its effect on the capacity of adhesive anchors were investigated in Mészároš (2002). Figure 3.10 illustrates the results of his research. The anchors installed in cracked concrete showed a larger scatter than the anchors installed in uncracked concrete. The failure loads for crack widths between 0.3 mm and 0.4 mm range from 25 % to 80 % of the results in uncracked concrete, with a mean value of 50 %, confirming the influence of cracks in concrete.
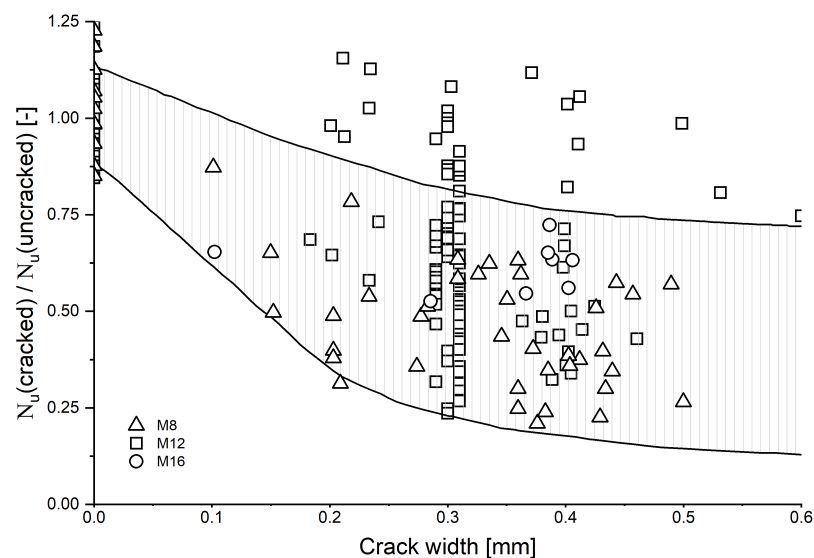

FIGURE 3.10: Influence of the cracks in concrete according to Mészároš (2002)

Similarly, Simons (2007), who tested the behaviour of reinforcing bars in cracked concrete, observed a decrease in the bond strength with an increase in the crack width.

3.3.6　Hole cleaning

Various studies have assessed the influence of hole cleaning on the carrying capacity of bonded anchors. Cook, Bishop, et al. (1994) stated that hole cleaning had different influence depending on the product type. This view is supported by the findings of different researchers (Kunz et al., 1998; Mészároš, 2002; Spieth, 2002).

Mészároš (2002) investigated the influence of hole cleaning in his thesis. Firstly, he summarized his previous research which included three categories of cleaning types: good, standard and no cleaning (Table 3.1). The results of the tests are shown in Figure 3.11.

TABLE 3.1: Cleaning methods (Mészároš, 2002)

Type [−]	No. [−]	Description of the cleaning [−]
good	1	Vacuum + 3xBrushing + Vacuum
	2	2xHand-pump + 3xBrushing + 2xHand-pump
standard	3	Vacuum
	4	2xHand-pump
no cleaning	5	Vacuum of the drilling dust
	6	Drilling dust pressed on the bottom of the hole
	7	The hole was drilled deeper
	8	Vertical drilling of a lying slab
	9	Horizontal drilling of a standing slab
	10	Hole drilled horizontally, no cleaning
	11	Hole drilled vertically upwards, no cleaning

Secondly, Mészároš (2002) tested three adhesive systems installed with four cleaning methods in 7-day old concrete. The cleaning methods observed were: A. 2$x$hand-pump, 2$x$hand-brush, 2$x$hand-pump; B. 2$x$hand-pump; C. no cleaning, the dust was pressed in the hole; D. no cleaning, the hole was drilled deeper. The type of cleaning influenced not only the load-carrying capacity of the anchors but also reduced drastically the adhesion load hence the bond strength.
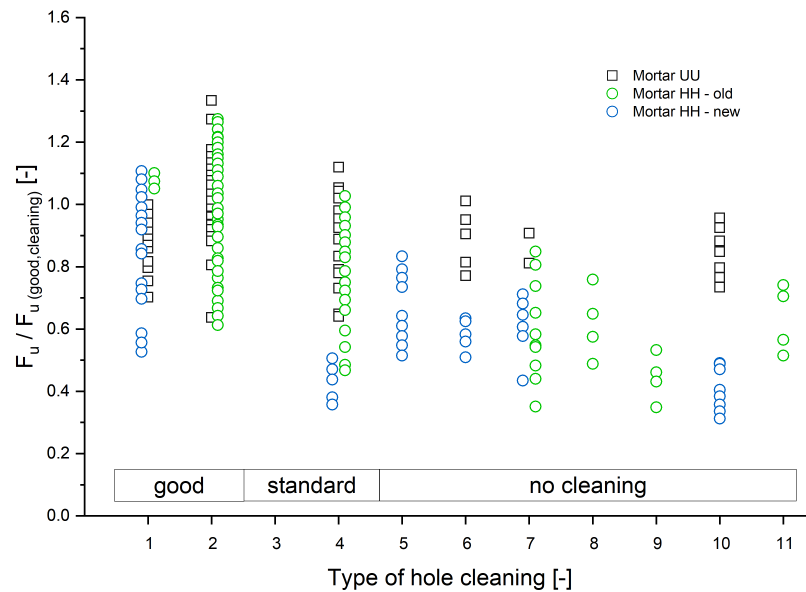
FIGURE 3.11: Influence of the hole cleaning according
to Mészároš (2002)

Spieth (2002) concluded that for each adhesive system, an op-
timal cleaning method must be developed. Simons (2007) stud-
ied this factor in cracked and uncracked concrete (Figure 3.12).
She tested one mortar with hole cleaning as described in the man-
ufacturers printed instructions (H3) and with increased cleaning
intensity (M1). The uncracked concrete tests showed no influ-
ence of the cleaning method, whereas the cracked concrete tests
exhibited higher bond strength with the higher intensity clean-
ing.

3.3.7 Hole depth

To date, several studies have investigated hole depth or embed-
ment depth of the anchor as a factor affecting the bond strength
and the carrying capacity of adhesive anchors. Mészároš (2002)
and Spieth (2002), while testing different mortars with confined
and unconfined setups, concluded that this influence was prod-
uct dependent. Such findings were also seen in the thesis of Lehr
(2003). Figure 3.13 illustrates these findings for diameters $M\,8$,
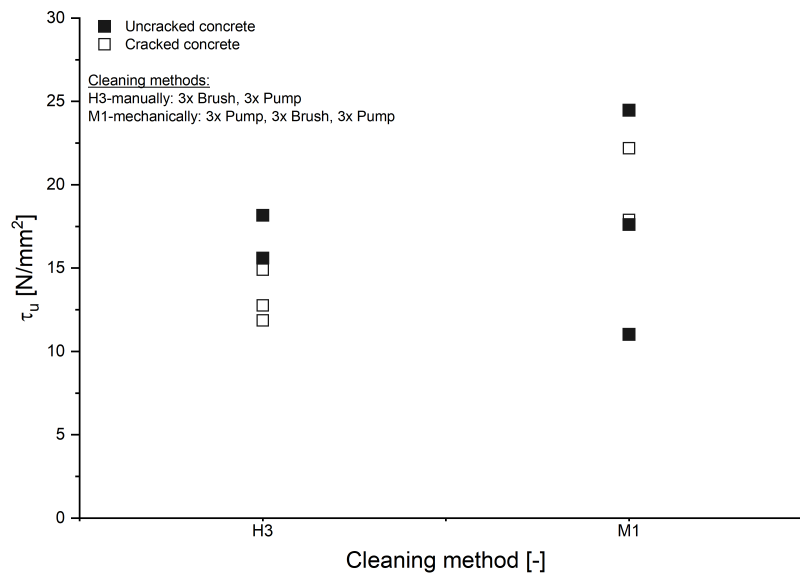$M\,12$ and $M\,16$, in low-strength concrete with unconfined setup.

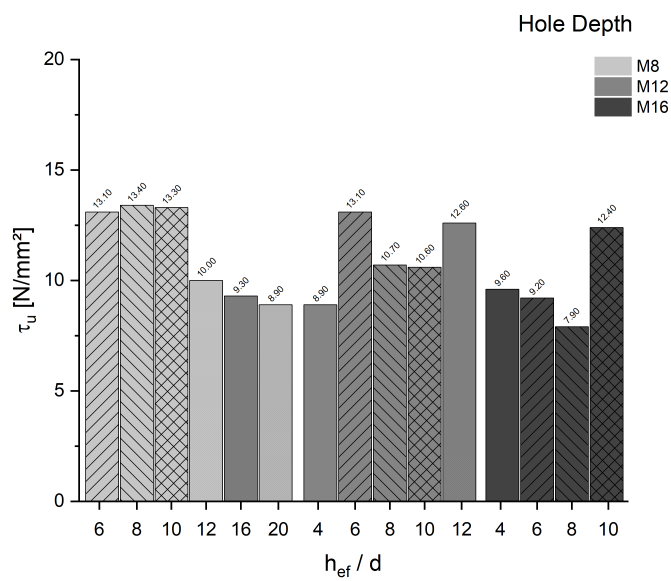FIGURE 3.12: Influence of the hole cleaning according to Simons (2007)

FIGURE 3.13: Influence of the anchor hole depth according to Lehr (2003)

3.3.8 Hole drilling

Spieth (2002) tested three drilling methods, hammer, diamond core and pneumatic hammer drilling. Firstly, he compared diamond core drilling and hammer drilling in low and high-strength concrete with small or large concrete coverage. He observed a lower bond strength for diamond core drilling compared to hammer core drilling. Furthermore, he pointed out a reduction in bond strength with increasing concrete strength only for diamond core drilling with large concrete coverage. Secondly, he tested hammer and pneumatic hammer drilling in dry and wet concrete with small and large coverage. The tests with large concrete coverage showed no influence of the drilling method or the concrete conditions, whereas for small coverage and wet concrete slightly lower failure loads were reported.

The same drilling methods were tested by González et al. (2018). In their paper, three mortar systems (epoxy resin, epoxy acrylate and cementitious grout) were installed in horizontally and vertically drilled holes in dry and wet concrete (conventionally vibrated concrete VC and self-compacting concrete SCC). Different drilling diameters and the hole cleaning methods were investigated. Figure 3.14 illustrates the results of the tests in dry concrete and Figure 3.15 in wet concrete.
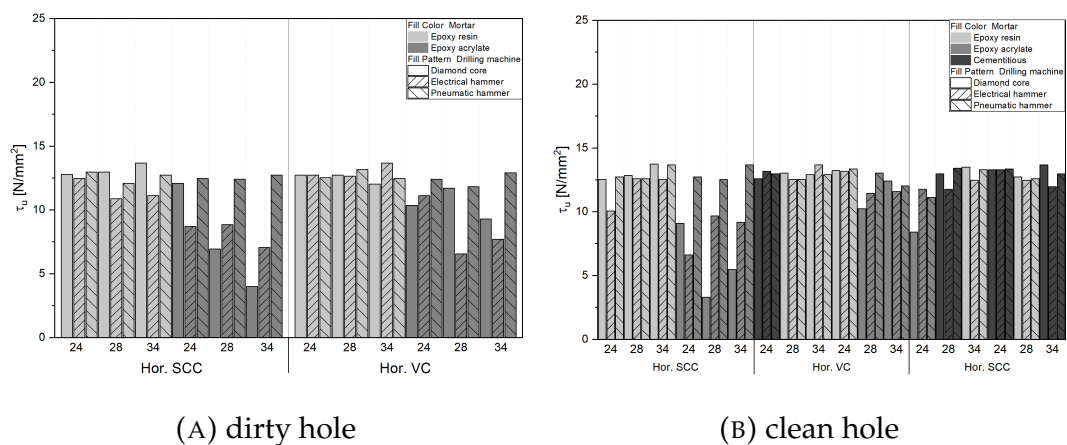

(A) dirty hole

(B) clean hole

FIGURE 3.14: Influence of the hole drilling in dry concrete according to González et al. (2018)

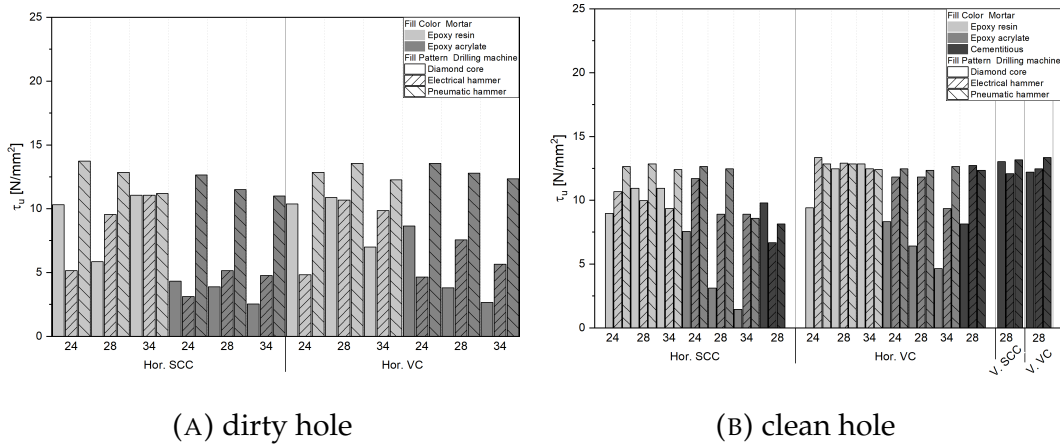(A) dirty hole   (B) clean hole

FIGURE 3.15: Influence of the hole drilling in wet concrete according to González et al. (2018)

When comparing the mean values of all the tests, the failure loads of the anchors installed in holes drilled with pneumatic hammer were higher compared to those drilled with diamond core (28 %) and electrical hammer (14 %). Depending on the type of drilling machine, the surface of the bore hole is different. Therefore, the bond between concrete and adhesive is directly affected.

3.3.9 Hole moisture

Several studies tested anchors in damp and wet concrete to observe this influence on the load-bearing behaviour of adhesive anchors (Kunz et al., 1998; Cook and Konz, 2001; Mészároš, 2002).
Cook and Konz (2001) identified a close influence on the type of adhesive used and the conditions of the hole. From all the tested products, the bond strength in moist concrete was lower than in the reference dry concrete tests and showed a higher coefficient of variation.

Mészároš (2002) investigated the sensitivity of adhesive anchors from hole moisture with two approaches as shown in Figure 3.16. Firstly, he compared anchors installed in dry slabs and in slabs which were put under 3 cm thick layer of water for one week. Secondly, he tested on slabs where the holes were drilled and cleaned, and put under water for 7 and 21 days. Afterwards, the anchors were installed without re-cleaning the holes. The

cleaning methods used are described in Section 3.3.6. In each case, Mészároš observed that every adhesive systems responded differently to the hole moisture. They were affected from the hole cleaning as well. Overall, he pointed out that the load-bearing behaviour of adhesive anchors in wet concrete was approximately 50 % less than in normal dry concrete.
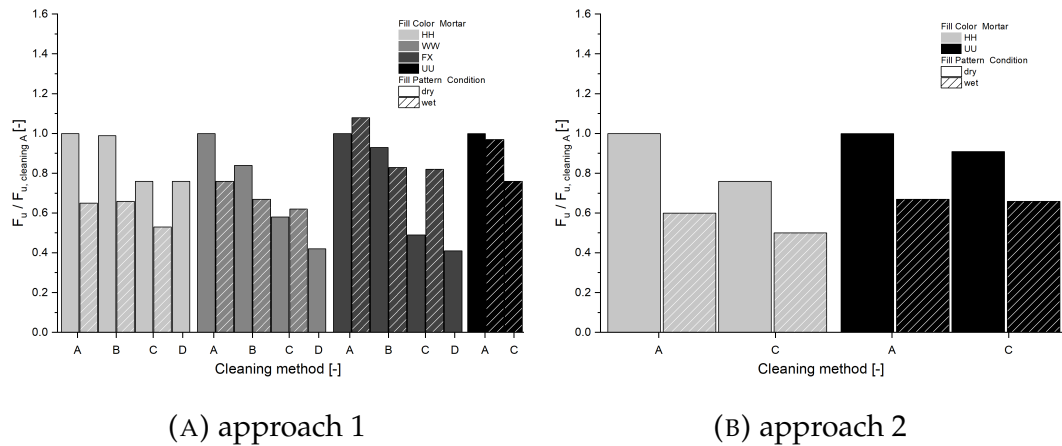

(A) approach 1   (B) approach 2

FIGURE 3.16: Influence of the hole moisture according to Mészároš (2002)

González et al. (2018) observed the influence of humidity in self-compacting concrete and conventionally vibrated concrete. They found that humidity has a higher or lesser effect on the bond strength of the anchors depending on the type of adhesive anchor and drilling method.

3.3.10 Hole orientation

There are two types of hole orientation influences, firstly hole drilling orientation and secondly hole installation orientation. Spieth (2002) tested adhesive anchors which were drilled horizontally and vertically. Because no cleaning was applied to the holes before installation, an influence on the bond strength was observed. The horizontal tests showed higher bond strength compared to vertical tests. He argued that due to the horizontal orientation, the concrete dust could fall out of the hole efficiently during drilling.

Recently, González et al. (2018) tested two adhesive anchors (epoxy and cementitious grout) in two types of concrete. The results in the conventional vibrated concrete showed higher loads

when the holes were drilled horizontally. On the other hand, for the self-compacting concrete, the vertically drilled holes showed a higher residual load.

Cattaneo, Locatelli, and Rago (2019) studied the installation direction of the anchors (Figure 3.17). They performed tests in vertically (downward), horizontally and overhead installed anchors. From the three tested adhesives, the two epoxy mortars showed very similar behaviour when installing in horizontal and overhead direction, however, one of the two showed a higher coefficient of variation. The last adhesive type (polyester mortar) exhibited a lower bond strength because of its flowability.
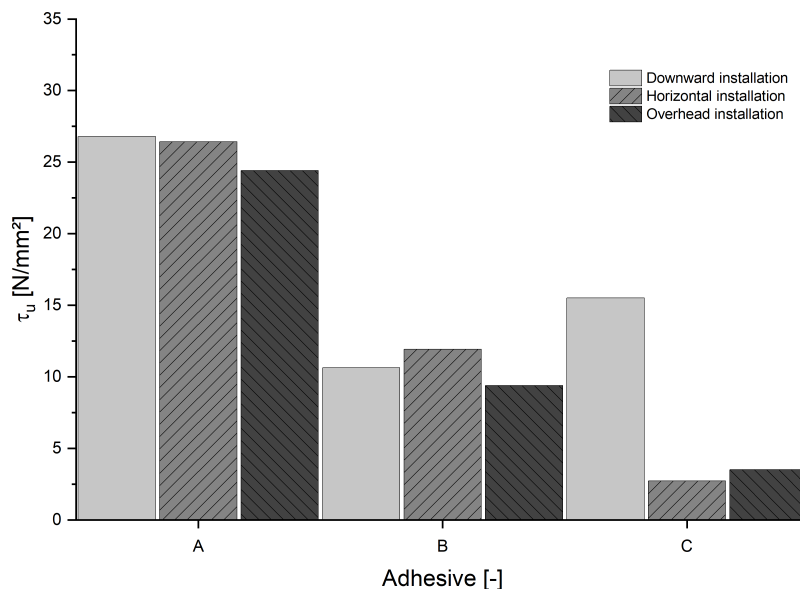

FIGURE 3.17: Influence of the hole orientation according to Cattaneo, Locatelli, and Rago (2019)

3.3.11   Installation temperature

The installation temperature is the temperature used at the time of installation of the anchor. This parameter was the object of many studies.

Spieth (2002) tested two products at $0\,°C$, $20\,°C$ and $40\,°C$. The mortar, the reinforcing bars and the concrete specimens were stored at these temperatures, except for the mortar in the case of

40 °C, which was also kept at 20 °C as per manufacturers instructions. After installation, the specimens remained at the given temperatures until the tests were carried out. The two adhesive systems showed a small influence on the installation temperature especially at 40 °C. Figure 3.18 illustrates his results. The bond strength of the anchor decreased from 5 % to 15 % with an increase in the installation temperature.
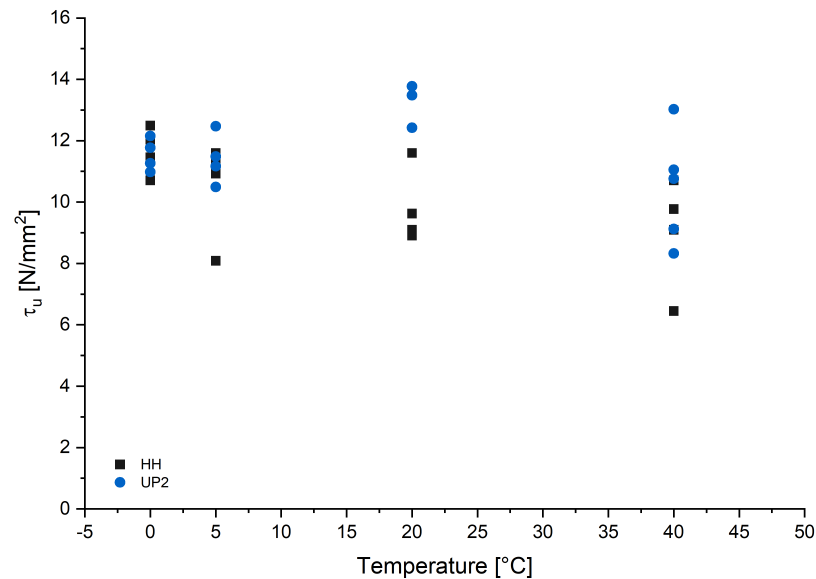

FIGURE 3.18: Influence of the installation temperature according to Spieth (2002)

Hülder (2008) tested the material properties of an epoxy and vinyl ester adhesive kept at 8 °C and 23 °C after 48 h and one week. The epoxy mortar exhibited after 48 h, a ductile behaviour at 8 °C and brittle behaviour at 23 °C. He observed that hardening at a lower temperature for both periods was not enough to reach the stiffness and strength values of the specimens stored at 23 °C for 48 h. Similarly, the vinyl ester mortar was tested at 8 °C and at room temperature after the minimum curing time, after one or seven days. The adhesive exhibited lower mechanical properties at the lower hardening temperature compared to the same time of testing at a higher temperature.

3.3.12   Test setup

Adhesive anchors are mostly tested with confined test setups to better understand the influence of the other factors (hole cleaning, moisture, drilling etc.) on the carrying capacity of the anchors. Thus, the behaviour of the anchors under unconfined setups can be derived from these results. Depending on the embedment depth, the influence of the support width changes.

Mészároš (2002) examined anchors with a ratio of h_{ef}/d equal to $4, 8, 9.17$ and 12 as seen in Figure 3.19. The ratio of the failure loads in unconfined test setups to those in confined setups were 0.7 to 0.8 for the small embedment depths ($h_{ef} = 4 \cdot d$), 0.95 to 1.0 for large embedment depths ($h_{ef} = 12 \cdot d$) and the standard depths ($h_{ef} = 8 \cdot d - 10 \cdot d$) between 0.85 and 0.95.
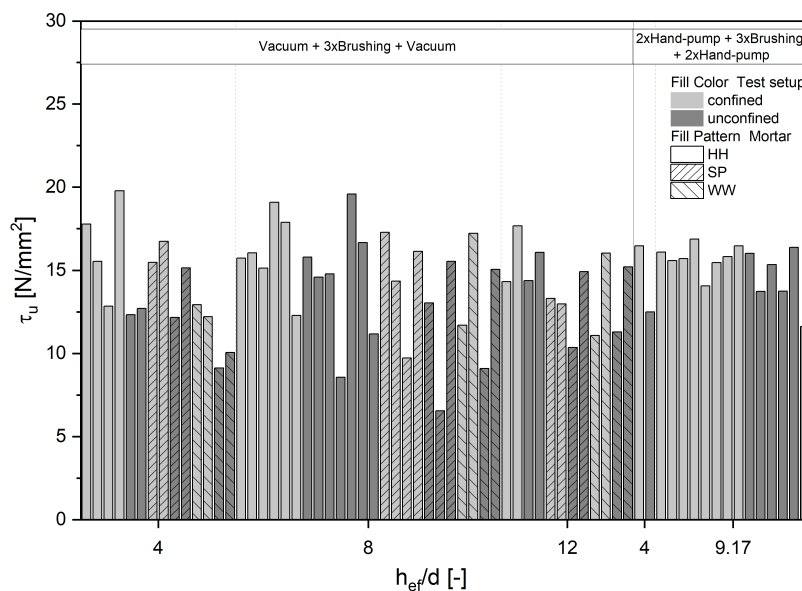

FIGURE 3.19: Influence of the test setup according to Mészároš (2002)

Further research in cracked and uncracked concrete was carried out by Appl (2009). He stated that not only the bond strength of the adhesive mortar decreases with an increase of the support width but also the stiffness of the system. He observed that the support width affected the failure loads in the cracked more than in uncracked concrete.

3.3.13   Type of concrete

Usually, concrete is created by mixing cement, aggregates, additives and water. Grzesik (2012) tested a concrete mixture where 25 % fly ash was used. The reference concrete slab had a compressive strength of 41 MPa and the fly ash concrete 38 MPa. Two adhesive anchors were used for the tests. The failure loads for both systems were comparable.

González et al. (2018) tested two concrete specimens, which were produced using conventional vibrated concrete and self-compacting concrete. The respective compressive strengths were 54 MPa and 73 MPa. The tested anchors in conventional concrete performed overall better than the anchors in the self-compacting concrete despite the compressive strength being higher.

3.4   In-service factors

3.4.1   Short-term cure

Cook and Konz (2001) tested 20 type of adhesive anchors for their short-term cure properties. The residual testing of the reference tests was performed after 7 days, whereas the short-term cure tests were tested after $24\,h$. They aimed to observe the behaviour of different anchors for the cases where they need to be loaded as soon as possible. Overall, the products tests after $24\,h$ showed approximately 88 % of the reference tests' bond strength.

As mentioned in Section 3.3.11, Hülder (2008) observed the mechanical behaviour of two types of mortars. After the minimum curing time at room temperature, the epoxy mortar revealed a tensile strength of $32\,\mathrm{N/mm^2}$. With a increase of the curing time (after a week), the tensile strength increased to $36\,\mathrm{N/mm^2}$. This also influenced the stiffness of the mortar. Similar behaviour was observed in the vinyl ester mortar.

3.4.2   Elevated temperature

During their service life, anchors are submitted to different temperature conditions. An increase in the temperature reduces the bond strength of adhesive anchors (Kunz et al., 1998). Tests carried out by Cook and Konz (2001) at room temperature and $43\,°C$

showed an influence on the bond strength. Depending on the product used, the bond strength increased or decreased with a large coefficient of variation in comparison to the reference tests.

Spieth (2002) performed tests on anchors installed at room temperature and heated from 80 °C to 180 °C. He followed two procedures to increase the temperature of the mortar. Firstly, for the tests at 80 °C, the specimens were stored in a climate chamber for 8 h directly after installation and then tested. Secondly, for the temperatures 120 °C and 180 °C, he preheated the chamber at 250 °C and inserted the specimens. Inside the mortar layer, sensors were placed at three depths to measure the temperature. Once the measured temperature reached the goal temperature, the specimens were tested to failure. Figure 3.20 illustrates the results of his research. The bond strength of the mortars was influenced by the increased temperature. Compared to the same tests, at room temperature the bond strength decreased by 35 % to 45 % at 80 °C, by 65 % to 70 % at 120 °C and by 80 % at 180 °C.
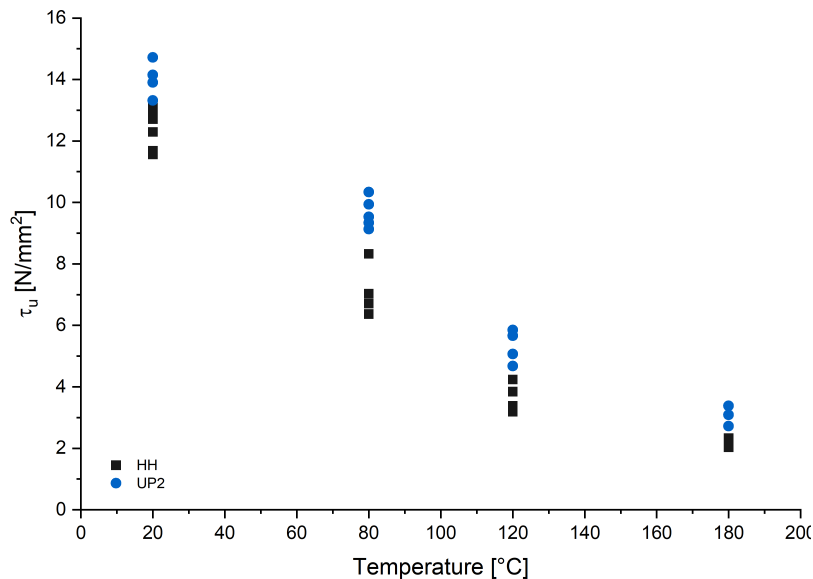

FIGURE 3.20: Influence of the elevated temperature according to Spieth (2002)

Lahouar et al. (2017) tested epoxy adhesive anchors in concrete cylinders stored at temperatures from 16 °C to 130 °C. Two thermocouples were installed at the embedment depth of the anchor and at 10 mm from the top of the cylinder to measure the

temperature in the mortar until the intended temperature was reached. The bond strength of the mortar between 20 °C and 50 °C showed almost no change. With a further increase of the temperature above 50 °C, the bond strength was reduced approximately 30 %. When the temperature of the mortar reached 130 °C, 96 % of bond strength was lost.

3.4.3 Long-term load (creep)

The long-term behaviour of adhesive anchors is influenced not only by the applied load but also by different internal and external factors. Chapter 4 will describe this behaviour in detail.

3.5 Additional factors

3.5.1 Moisture in service

Section 3.3.9 describes the influence of moisture before installation in the bond strength of the anchor. However, the presence of water even after the installation has an effect on the long term behaviour of adhesive anchors. According to Cognard (2005), for porous adhesives, the water could penetrate the adhesive and soften it slowly, it could destroy its bonding capacity or it could swell it.

3.5.2 Freeze-thaw

Freeze-thaw conditions subject the anchors not only to reduced temperatures (below 0 °C) but also to the presence of water. As mentioned in the previous sections (3.3.9, 3.3.11 and 3.4.2), the changes in temperature and the existence of water influence the bond strength of adhesive anchors.

4 Long-term behaviour of adhesive anchors

4.1 General

Adhesive anchors subjected to long-term loading start to deform slowly over time. This process is defined as creep. Figure 4.1 illustrates the three creep phases from the beginning of loading to the failure or collapse of the system.

Primary creep occurs from the moment the fastener is loaded. The behaviour of the anchor in this phase is non-linear. Usually, no lasting deformation develops if the anchor is unloaded. Secondary creep is crucial and subject to many studies. The deformation increases slightly over a long period of time. Lastly, the tertiary creep phase occurs. The deformation increases rapidly in a short time. In this case, the collapse of the system is observed.
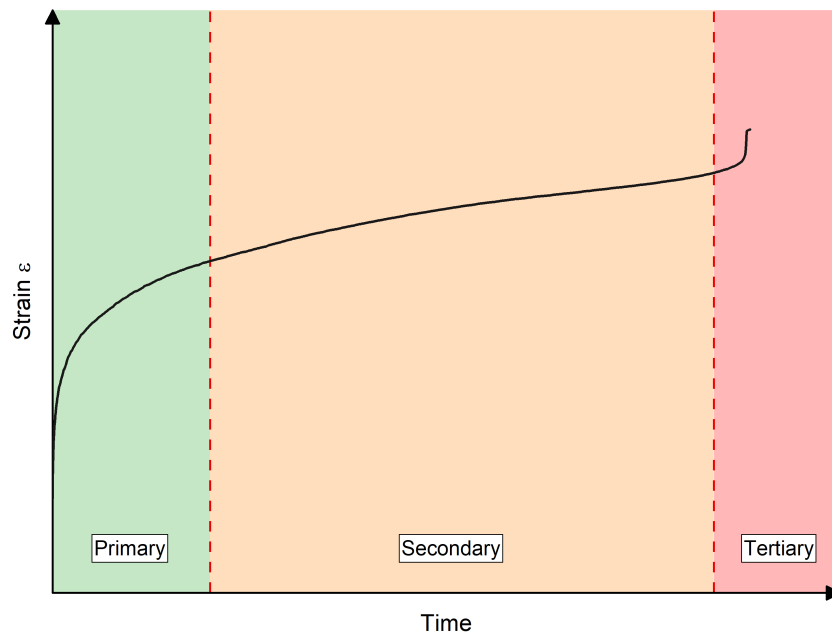

FIGURE 4.1: Creep of adhesive anchors under long-term tensile loading

Three methods for testing and evaluating the creep behaviour of adhesive anchors have been reported in the literature.

Sustained load testing. Current guidelines such as EAD 330499 (2018) and AC 308 (2017) describe sustained load testing as a method to evaluate the creep behaviour of adhesive anchors. The tests are performed as confined tests in low-strength uncracked concrete at room or elevated temperatures. After installation and curing of the fastener, a sustained load N_{sust} is applied and maintained constant. The sustained load is calculated using the results of reference confined tests in uncracked concrete.

The testing is carried out in two period of times. The sustained load is kept constant for at least three months if the long-term behaviour after 50 years should be evaluated or six months for the 100 years behaviour. Throughout the entire time, the displacement of the fasteners are recorded. At the end, the anchors are unloaded from the sustained load and tested using a confined setup until failure.

The assessment is carried out using the measured displacements. The displacements are extrapolated using Findley's approach given in Equation (4.1) (Findley, Lai, and Onaran, 1976). The extrapolation is carried out to 50 or 100 years for room temperature tests and 10 or 20 years for elevated temperature tests.

$$\delta(t) = \delta_0 + a \cdot t^b \tag{4.1}$$

where: δ_0 = initial displacement under sustained load at $t = 0$ [*mm*]

   a, b = constants determined from a regression analysis using the measured displacements during the sustained load testing

The extrapolated displacement $\delta(t)$ is then compared with the mean displacement of the reference short-term tests when the loss of adhesion occurs. If this value is higher, the tests should be repeated with a lower sustained load N_{sust}.

Time-to-failure approach. The time-to failure (TTF) method is based on the standards for the evaluation of creep in plastics ASTM D2990 (2017) and DIN EN ISO 899-1 (2018). The specimen are loaded to specific load levels and monitored until the specimen fail. The load levels should be chosen such that creep failure does not occur prior to a 1000 hours of testing. The tests

are carried out in a controlled environment (temperature and humidity). The deformation of the plastic specimen is measured in pre-described time frames. The results are plotted as a stress versus TTF graph. Through these data, a safe stress value can be determined, up to which the failure of the specimen will likely not occur.

This approach was adopted for adhesive anchors in Cook, Douglas, and Davis (2009). The specimen are kept at an elevated temperature of $43°C$ ($110°F$). The anchors are loaded at two load ranges. The first load range is 80% to 70% of the mean static load (reference tests) and the second range between 70% and 60%. The displacement are measured until failure of the specimen. The results are plotted in a stress versus TTF plot. Using the least square methods, the behaviour of the anchor after 50 years can be determined.

Modified Burgers-Model. Kränkel (2017) developed a model to predict the long-term behaviour of adhesive anchors. This model was based on the Burgers-Model, which describes the creep recovery of linear viscoelastic materials. He modified the model to take into account the inelastic response of adhesive anchors. To implement this model, three different test series have to be carried out. Firstly, static tensile strength test are performed to evaluate the elasic-plastic deformation component of the model. Secondly, long-term tests with a minimum duration of 1000 hours are carried out to determine the viscous deformation component. Lastly, the material degradation throughout time is assessed using degradation tests. The degradation tests consisted on cycle tests with loading and unloading and pause-phases where the load was kept constant before continuing to the next load increment. These increments were calculated using the bond strength from the reference short-term tests. The load was applied with a rate of 2kN. Four predefined load regimes (LR) were tested until failure of the fastener occurred.

LR1 The applied load was increased with 4% load increments. The same increment was used for three cycles, before progressing to the next one.

LR2 The first two load increments 4% and 8% were applied once. When the load increment reached 12% of the bond strength, the cycles were applied three times until failure.

LR3 Single load cycles were applied up to a increment of 20%. Afterwards, three cycles per increment were applied.

LR4 Five cycles per load increment were applied from the beginning until failure of the anchor.

Combining the three parameters (the elastic-plastic deformation component, the viscous deformation component and the degradation indicator component), the overall deformation of the anchor can be determined. The model is able to predict the time to failure of the anchors with sufficient accuracy.

Since the collapse of the ceiling in the Boston Tunnel in 2006, extensive research has been carried out on the creep / long-term behaviour of adhesive anchors (National Transportation Safety Board NTSB, 2006). Their performance under sustained loading, similar to the short-term loading, is influenced by the same factors listed in Chapter 3.

This chapter summarizes various researches focused on the creep behaviour of adhesive anchors and internal tests carried out in the recent years at the Institute of Construction Materials.

4.2   Time-to-failure approach

The time-to-failure approach was the focus of the research of Davis (2012), Blochwitz (2019) and an internal research carried out at IWB (2019). This section summarizes their findings.

4.2.1   Davis (2012)

Davis (2012) investigated in his PhD the influence of different parameters on the sustained load performance of adhesive anchors. He classified the influence parameters (Section 3.1) into three categories depending on the impact they had on the sustained load performance.

- High priority parameters: elevated in-service temperature ($20\,^\circ C$, $48\,^\circ C$), moisture in service, type of adhesive (one vinyl ester, two epoxies), adhesive curing time when first loaded (manufacturers specified curing time), hole orientation (horizontal, vertical), hole drilling (diamond drill),

hole cleaning (50 % reduced cleaning effort), moisture in installation and type of concrete (DOT - corresponding to $C25/30$ in DIN EN 206-01 (2017), fly ash, blast furnace slag concrete).

- Medium priority parameters: installation temperature (manufacturers minimum recommended temperature), unconfined test setup and early-age concrete (3, 6, 13, 20, 27 days).

- Low priority parameters: reduced in-service temperature, freeze-thaw, mixing effort, annular gap, fiber content adhesive, chemical resistance, depth of hole, anchor diameter, concrete strength, type of coarse aggregate and cracked or uncracked concrete.

The focus of his PhD were the high and medium priority parameters. The standard testing temperature was $43\,°C$. The load applied to the anchors ranged from 35 % to 88 % of the mean short-term failure load depending on the test series. The tests were perfomed at two location. Two embedment depths and two anchor diameters were considered: anchor with a diameter of 15.9 mm installed at 79.4 mm depth (University of Florida) and anchor with a diameter of 12 mm installed at 80 mm depth (University of Stuttgart).
The results of the research of Davis were:

- A logarithmic model was appropriate for the stress versus TTF relationship.

- The displacements at failure load were larger for the sustained load tests than the short-term tests.

- The final stress versus TTF curves should not include the short-term test results.

- Elevated service temperature and adhesive curing time had an influence on the sustained load performance of the anchors.

- A modification factor for the calculation of the load capacity of the anchor should be introduced if the anchor is subjected to $48\,°C$ for a significant service life time.

- The anchors used for sustained load applications should cure for an additional 24 hours to the manufacturer's minimum curing time before loading.

The results of the tests with early-age concrete were not summarized because they were performed only as short-term tests.

4.2.2   Blochwitz (2019)

In his PhD research Blochwitz (2019) studied the behaviour of four adhesive anchors under sustained loading: two epoxies and two vinyl esters. Depending on the type of adhesive, the studied parameters were defined as follows:

- tests with epoxy mortar: embedment depth (80 mm and 105 mm), test setup (confined and unconfined setup), annular gap (0.5 mm, 1 mm, 3 mm and 6 mm), and testing temperature ($43\,°C$ and $50\,°C$)

- tests with vinyl ester mortar: embedment depth (80 mm), test setup (confined), annular gap (1 mm), testing temperature ($43\,°C$)

Blochwitz divided his research into baseline tests and tests with different annular gaps. The baseline tests included all the tests with the vinyl esters (vinyl 1 and vinyl 2) and the tests with two epoxies (epoxy 1 and epoxy 2) at both embedment dephts, both confinements and with the annular gaps as specified by the manufacturers printed installation instructions MPII (1 mm). The baseline tests consisted on reference short-term tests and TTF tests with different load levels (three to six load levels).

The annular gap tests investigated the variation of the annular gap for epoxy 1 under confined setup. The fasteners were all installed at 80 mm. Short-time tests as reference tests and TTF tests (one load level per annular gap) were performed.

The testing temperature for all tests was $43\,°C$ except for the tests with epoxy 2.

Baseline tests findings

- Both types of adhesive anchors showed the same service life behaviour. The only difference was the failure mode (pull-out with mortar for epoxy and pull-out failure for vinyl ester).

- The service life of all the adhesives could not be predicted using a simple function (e.g. exponential function) because the system behaviour was complex.

- The behaviour of the TTF tests was classified in three load ranges. The failure of most anchors in less than 1000 hours characterized the service life in load range 1. In load range 2 (service load level), the anchors did not fail within the test duration (up to 15000 hours) and their displacement curves showed a trend where no failure was expected in the foreseeable future. Lastly, load range 3 was characterized as a transition region where both previous behaviours could occur. The service life behaviour in load range 3 was steady and seemed to change from load range 1 and 2. This effect was defined as the "switch effect". Using TTF test with the same failure load as in load range 3, the service life behaviour at service load level could be predicted. The upper load limit should be chosen such that the adhesive system does not exhibit any state or structural changes compared to the service load level.

- The two tested systems had a "switch load" of 40 % (vinyl ester) and 60 % (epoxy) of the mean short-term loads. Both systems were considered as failed.

- Testing using a confined setup prevents the creation of a concrete cone breakout which resulted in an earlier failure.

- The anchors tested with unconfined setup failed at a load level lower than half of the mean reference short-term tests. The anchors exhibited a mixed concrete cone and pull-out failure. The failure was dependent on the elasticity of the adhesive anchors due to loading.

- The durability of adhesive anchor systems was influenced by a number of parameters, such as concrete tensile strength, the elasticity of the mortar or its adhesive strength.

Annular gap tests findings

- The tests with annular gap 6 mm served as reference tests under the assumption that no damage occurred in the mortar during loading. The other test series suffered internal damage during loading which was determined from their initial displacement and the displacement under sustained loads. No correlation was found between the displacements and the annular gap.

- The damage of the mortar layer was more apparent in the tests with small annular gap. The "switch load" was accepted as lower compared to the other annular gap', indicating a more critical durability of the anchors with small thickness. On the contrary, their behaviour post-failure was considered not so critical due to the behaviour of the adhesive anchors as undercut anchors as a result of the small annular gap.

- After the first 800 hours, no apparent change in the displacement was observed. The displacement development started to change after the final stabilisation of the anchors occurred (the final stabilisation phase was different depending on the annular gap).

4.2.3   IWB (2019)

IWB performed TTF tests with a hybrid mortar (IWB, 2019). In this research, three parameter were varied.

- The embedment depths $5\,d$ and $7\,d$ as a function of the diameter of the anchor were investigated.

- Two setups for testing were used: confined and unconfined.

- The temperature when testing the anchors was elevated to $50\,°C$.

As reference tests served the anchors installed at $5\,d$ and tested using a confined setup at room temperature. Ten different load levels were applied to these anchors as well as the anchors tested at $50\,°C$. For the $7\,d$ embedment depth, five load levels were applied, whereas for the unconfined tests, nine load levels. The load levels started from 64 % to 94 % of the reference short-term tests. The anchors failed at different load levels and not necessarily at the high loading levels.

The results revealed that the embedment depth did not influence the bond strength of the adhesive anchor. However, the displacements for $7\,d$ embedment depth anchors were more stable through time compared to the anchors installed at $5\,d$. The results of the unconfined tests do not clearly show an influence of the type of setup on the displacement development through time. Similar to the tests at larger embedment depth, the tests at $50\,°C$ revealed that the displacements were increasing more steadily through time compared to the reference tests at room temperature.

4.3 Modified Burgers-Model

As mentioned in the previous section, Kränkel (2017) adapted the Burgers-Model to predict the long-term performance of adhesive anchors. To create and furthermore to validate his model, Kränkel performed sustained load testing on two adhesive anchors (vinyl ester and epoxy). The tested anchors were loaded in two ways: using high load levels (similar to time-to-failure tests) and using low load levels (sustained loading tests). Both cases aimed to validate the performance and prediction of the modified Burgers-Model for all types of applied loads. The load levels were defined with the help of the bond strength calculated from the short-term tests as:

- High load level tests: applied bond stress between 18.4 MPa and 23.8 MPa for the vinyl ester mortar and 28.0 MPa to 31.7 MPa for the epoxy mortar.

- Low load level tests: applied bond stress between 6.8 MPa and 16.5 MPa for the vinyl ester mortar and 11.4 MPa to 24.0 MPa for the epoxy mortar.

The long-term tests were carried out up to 30000 hours at room temperature. To validate the modified Burgers-Model, the displacement of the anchors after 100 hours of loading were implemented. The findings for the vinyl ester mortar were:

- Increasing the applied bond stress resulted in a disproportional rise of the initial displacement (for the test and the prediction) and an overall increasing displacement rate.

- The modified Burgers-Model predicted accurately the displacement value as well as the displacement propagation through time for the applied bond stress 10.0 to 16.5 MPa. The prediction for the tests with lower bond stress (from 6.8 MPa) showed the usual scatter as in the individual experiments. The time of failure for each case were predicted accurately.

- The prediction for the high load level tests delivered conservative values not only for the displacement propagation, but also for the failure time.

Below, the results of the tests with epoxy mortar are summarized:

- The initial displacement prediction was similar to the tests with vinyl ester mortar.

- The displacement development through time for the tests with applied bond stress of 11.4 MPa were predicted accurately using the modified model. The initial displacement for the tests with bond stress 19.0 MPa to 24.0 MPa was also predicted accurately. However, an unexpected propagation of the displacement in these experiments was observed from 1000 hours to 4000 hours of loading. The assumption was that something happened in the climate chamber where the anchors were stored that led to an unexplained increase in displacement. After the 4000 hours of loading, the predicted displacement was comparable to those in the tests. The modified Burgers-Model predicted the time of failure of the anchors accurately.

- The high load level tests with epoxy mortar showed similar results as the vinyl ester tests, where the prediction of the failure load was conservative.

4.4 Influence factors

This section focuses on the influence of different factors on the long-term behaviour of adhesive anchors. These factors were previously described for short-term loading in Chapter 3. The following diagrams illustrate the bond strength of the anchors versus the time of loading. The displayed data are taken from the research of Davis (2012), Blochwitz (2019) and IWB (2019). Four data points can be observed in Figure 4.2 to Figure 4.20:

- Red markers: short-term testing data

- Filled markers: the failed TTF data

- Blanked markers: the stopped TTF data

- Coloured lined: linear fit for each dataset

To compare the influence of the different parameters on the bond strength, the reference tests for standard parameters are shown in each diagram (red markers).

- Davis (2012) used for the reference tests two sets of parameters: $h_{ef} = 79.4$ mm, $d = 15.9$ mm for the tests performed at the University of Florida and $h_{ef} = 80$ mm, $d = 12$ mm for those performed at the University of Stuttgart. The testing temperature was $43\,^{\circ}C$ and confined setup was used.

- The reference parameters from the research of Blochwitz (2019) consisted on $M\,12$ anchors drilled with 14 mm drill bit (corresponding to an annular gap of 1 mm) installed at 80 mm embedment depth and tested using a confined setup at $43\,^{\circ}C$.

- $M\,12$ anchors installed at an embedment depth of 60 mm or $5\,d$ were used as reference parameters at IWB (2019). The reference testing temperature was $23\,^{\circ}C$ using a confined test setup.

4.4.1   Chemical formulation (type of adhesive)

Both, Davis (2012) and Blochwitz (2019), performed tests with different types of adhesive. Davis (2012) tested one vinyl ester (A) and two epoxy resin adhesives (B and C), whereas Blochwitz (2019) tested two of each type: vinyl ester (v1 and v2) and epoxy resin (e1 and e2).

Figure 4.2 illustrates the influence of the type of adhesive with the data from Davis (2012). These tests were performed at both locations. A comparison of the bond strength of the reference tests with the failed and the stopped tests, without taking into account the different applied load levels, shows a clear influence of the type of adhesive on the bond strength. The vinyl ester adhesive A had approximately 37 % and 60 % lower bond strength for the failed and the stopped TTF tests. The first epoxy, B showed only a 28 % reduction of the bond strength in the failed tests and 46 % in the stopped tests. Similarly, epoxy C had 34 % and 28 % lower bond strength in each case.
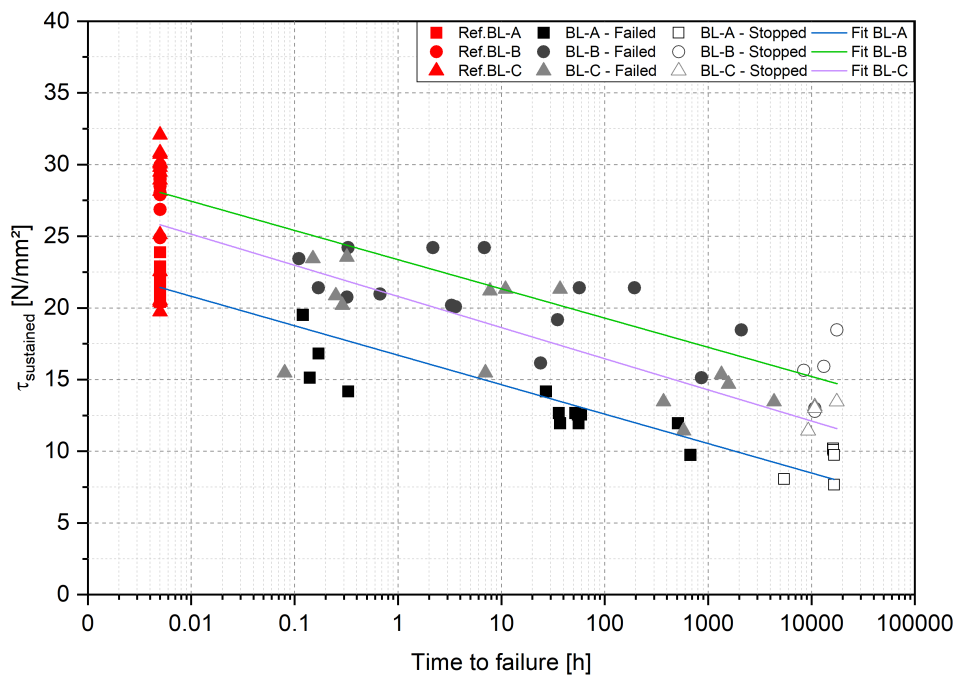
FIGURE 4.2: Influence of the type of adhesive
according to Davis (2012)

The data collected from Blochwitz (2019) is illustrated in Figure 4.3. The bond strength of failed TTF tests for both epoxy

resins dropped around $25 - 35\%$. However, for the stopped TTF tests, the epoxy e2 tests had almost 1.6 times lower bond strength as the epoxy e1 tests. The tests with vinyl ester v1 had the lower bond strength compared to the other three adhesive, approximately 53% and 67% lower (for the failed and stopped TTF tests) than the reference short-term tests. Vinyl ester v2 performed better than the first vinyl ester with 29% and 49% reduction in bond strength.
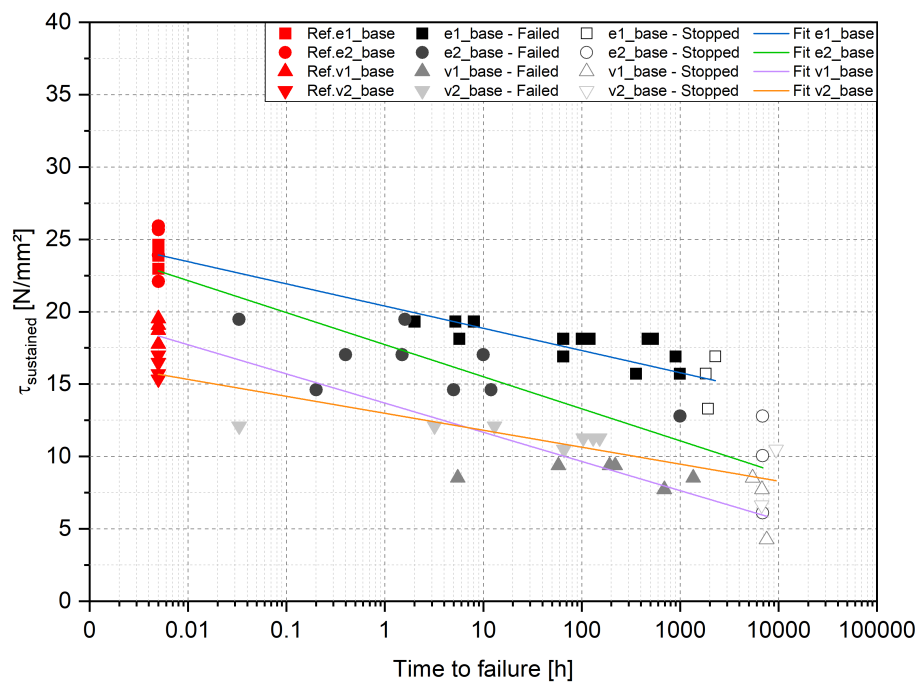
FIGURE 4.3: Influence of the type of adhesive according to Blochwitz (2019)

From these results, it is not possible to draw any strong conclusions whether epoxy resins or vinyl esters perform better under sustained loading. However, the influence of the chemical formulation of the adhesive on the long-term carrying capacity of bonded anchors is present and observed.

4.4.2   Curing time when loaded

The influence of curing time when loaded was studied by Davis (2012). Figure 4.4 illustrates not only the results of curing time when loaded corresponding to the manufacturer's curing time but also the baseline (reference) tests, tested and loaded after

seven days. No information on the manufacturer's curing time is given in the research of Davis (2012), however, it is suspected that the used adhesive anchor had a curing time of 45 minutes at room temperature. These tests were performed at the University of Florida. The baseline short-term test had twice the bond strength of the tests with shorter curing time. The bond strength under sustained loading was lower for each type of test with increasing time. The bond strength of the failed TTF tests for both cases was between $29 - 44\%$ of the reference short-term series. On the other hand, the stopped TTF tests had approximately 60% lower bond strength.
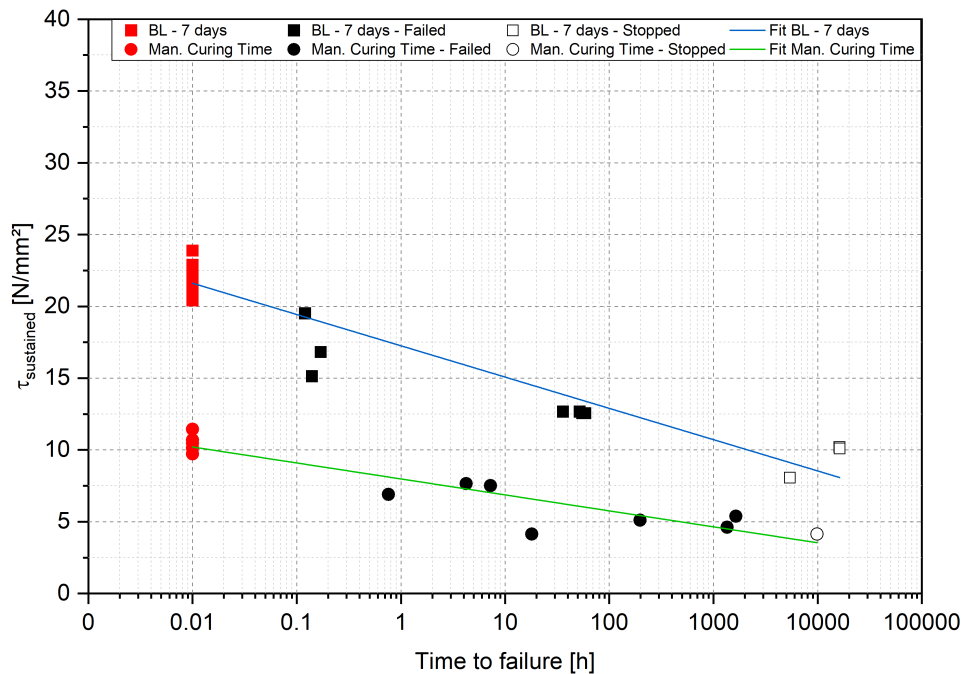
FIGURE 4.4: Influence of the curing time according to Davis (2012)

Testing using the manufacturer's curing time showed a large influence on the bond strength of anchors. At around 10000 hours, the bond strength was almost half the strength of the baseline tests.

4.4.3 Annular gap

Blochwitz (2019) performed TTF tests with an epoxy adhesive and four annular gaps: 0.5 mm - *RS*13, 1 mm - *RS*14, 3 mm - *RS*18 and 6 mm - *RS*24. The baseline tests were carried out with the annular gap specified from the manufacturer ($d_{cut} = 14$ mm or *RS*14). The results of the tests are displayed in Figure 4.5. The anchors were loaded with the same load level (59 % of the load of the baseline tests). The tests with the smaller annular gap *RS*13 had 36 % lower bond strength compared to the reference short-term tests. With increasing the annular gap, the bond strength reduced from 41 % to 70 % of the short-term tests. The lowest bond strength was observed for the *RS*18 with a larger embedment depth.
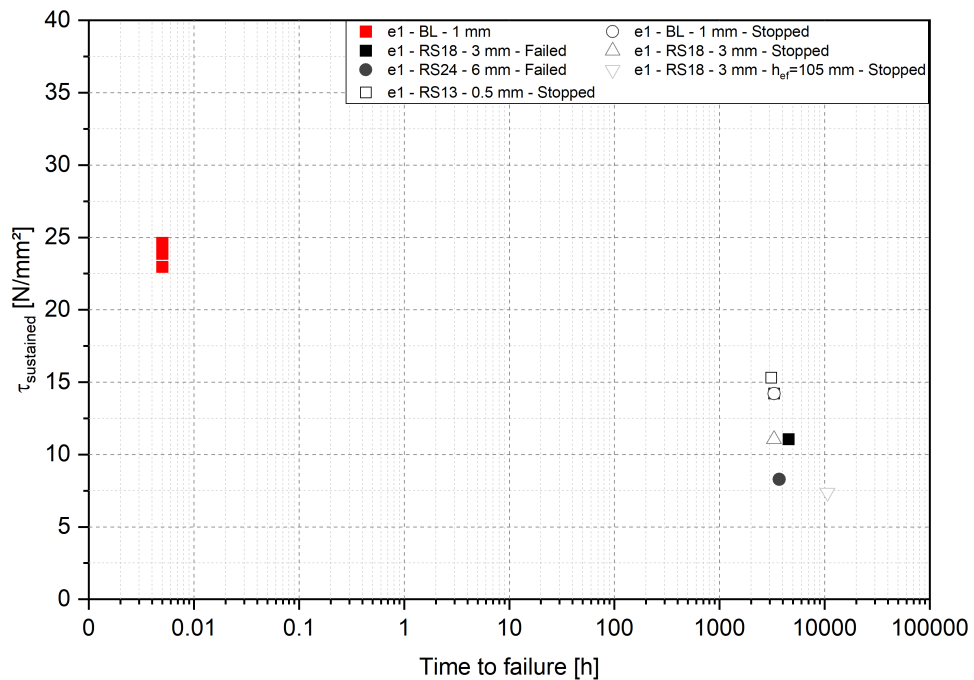
FIGURE 4.5: Influence of the annular gap according to Blochwitz (2019)

The smaller annular gap showed a higher strength compared to the larger gaps under long-term loading.

4.4.4   Hole cleaning

Another parameter studied from Davis (2012) was the reduced hole cleaning. Figure 4.6 displays the result of his tests. From the three adhesive formulations, he tested epoxy resin (C) because it was more sensitive to the cleaning effort. The full cleaning procedure was as follows:

- Blow with compressed air (4x)
- Brush with drill (1x), blow with compressed air (4x)
- these processes are repeated 4 times

The reduced cleaning effort (50 % of the full cleaning) included:

- Blow with compressed air (2x)
- Brush with drill (1x), blow with compressed air (4x)
- these processes are repeated 2 times

The tests were perfomed at the University of Florida. The reference short-term tests had approximately 6 MPa higher bond strength than the reduced cleaning tests. Comparing the failed TTF with their respective reference tests, the bond strength decreased with 32 % and 37 % for the baseline (full cleaning) and the reduced cleaning tests, respectively. Similarly, the stopped TTF revealed a similar trend with 56 % and 48 % lower bond strengths. From the plot is visible, that after 10000 hours, the change in bond strength for the baseline test and the reduced cleaning tests is less than 5 %.

4.4.5   Hole depth

Blochwitz (2019) performed TTF tests on two embedment depths: 80 mm and 105 mm. However, short-term tests only on the anchors installed at 80 mm. The bond strength of the failed TTF tests at 80 mm dropped with 25 %, whereas for the stopped TTF tests with 39 % (Figure 4.7). The TTF tests for the anchors installed at 105 mm showed a similar trend to the anchors with shorter embedment depth (37 % lower bond strength after 8000 hours).

For the tests carried out at IWB, two embedment depths were taken into account: $5\,d$ and $7\,d$ (IWB, 2019). Figure 4.8 illustrates the results of these tests. The two lines, blue and green, display
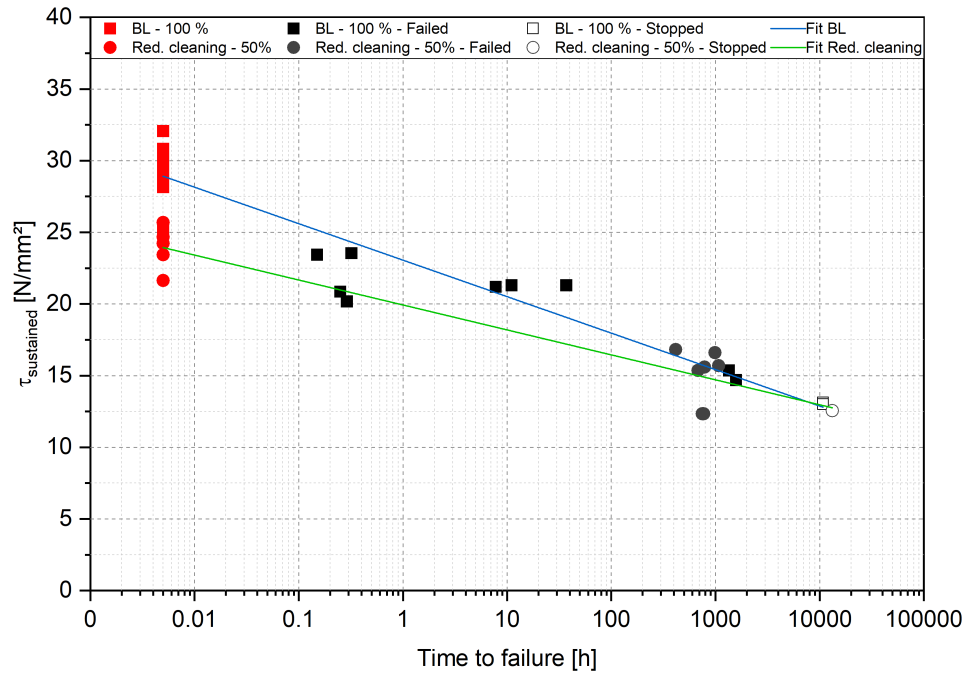
FIGURE 4.6: Influence of the hole cleaning according to Davis (2012)
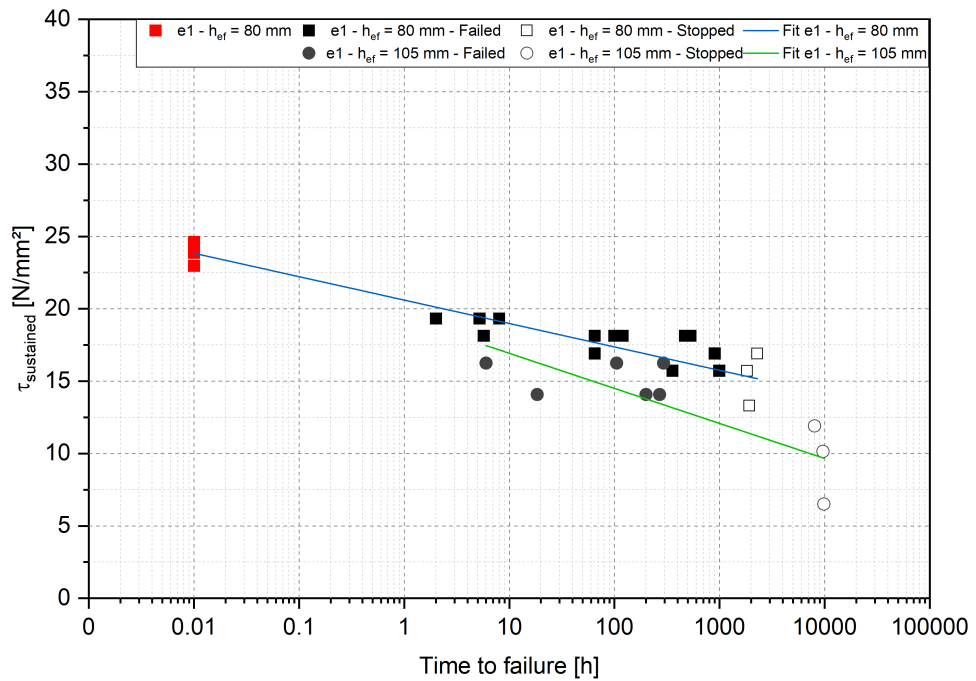
FIGURE 4.7: Influence of the hole depth according to Blochwitz (2019)

the development of the bond strength through time. The adhesive anchors revealed a similar behaviour despite the different embedment depths. The bond strength for the failed TTF was 9 % and 18 % lower compared to the reference tests for 5 d and 7 d depths, respectively. The stopped TTF tests had a further 10 % and 5 % drop compared to the stopped ones for each depth.
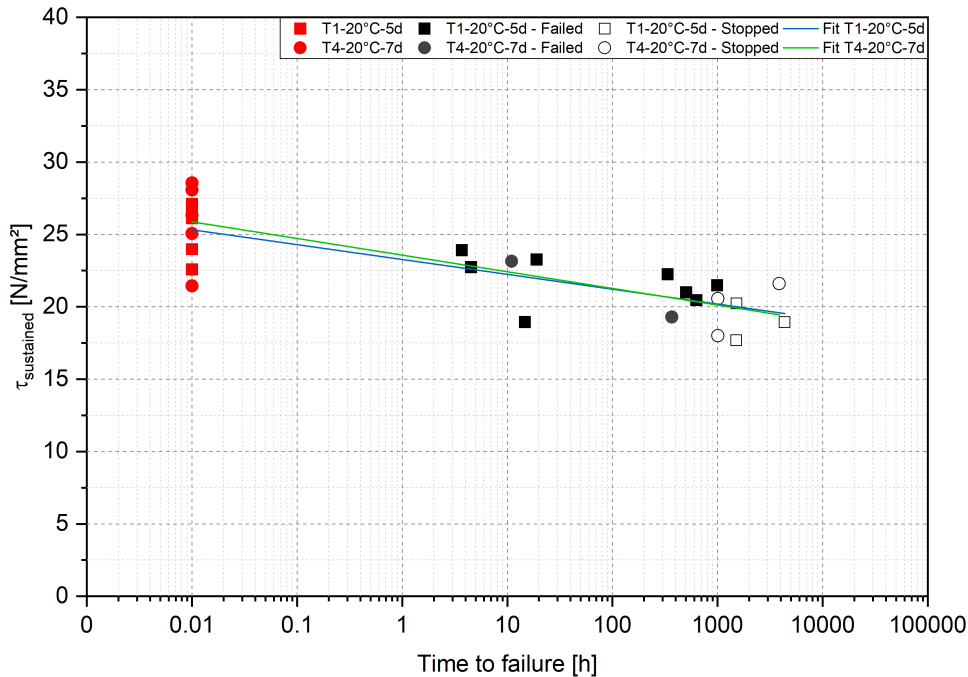
FIGURE 4.8: Influence of the hole depth according to IWB (2019)

4.4.6   Hole drilling

The influence of hole drilling on the long-term behaviour of adhesive anchors was studied from Davis (2012). Davis performed tests with hammer drilled holes (served as reference test series) and diamond core drilled holes. The tests were perfomed at the University of Florida. As seen in Figure 4.9, the hammer drilled tests showed a higher change in the bond strength throughout time: the failed TTF had 32 % lower bond strength than the short-term tests, whereas the stopped TTF had half its value. On the other hand, the core drilled anchors reduced the bond strength by approximately 32 % for both TTF series (failed and stopped).
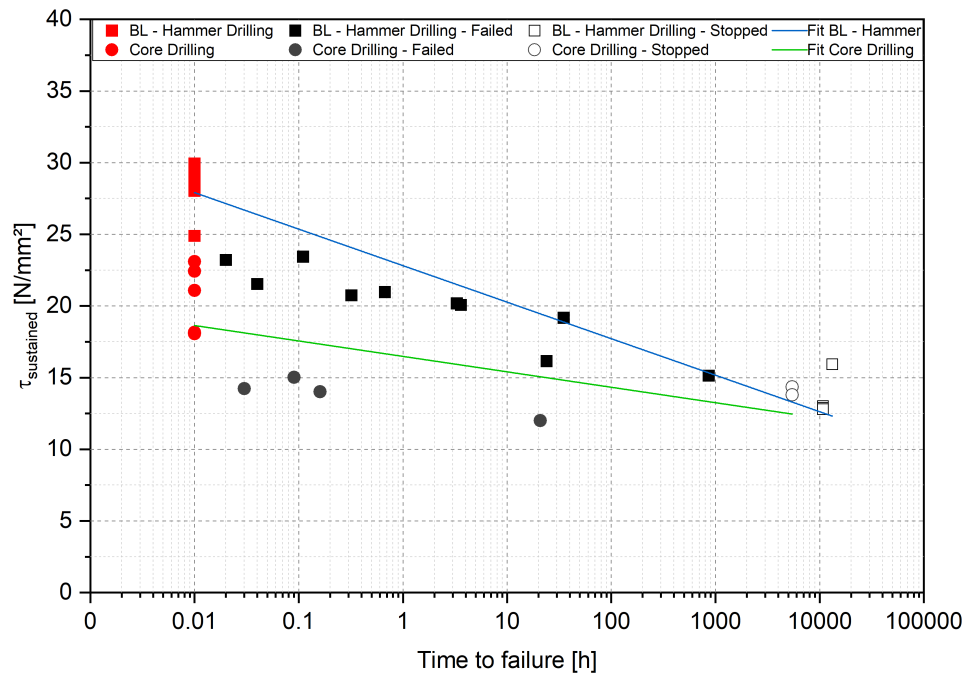
FIGURE 4.9: Influence of the hole drilling according to
Davis (2012)

4.4.7 Hole moisture

Another parameter studied by Davis (2012) was hole moisture
or moisture prior to installation. Davis conditioned the con-
crete specimen with water for eight days prior to installation.
These tests were performed at the University of Florida. Fig-
ure 4.10 displays the bond strength through time for these tests.
The failed TTF tests revealed a similar reduction in the bond
strength for both test series, 33 % of the respective short-term
tests. The stopped TTF (after at least 4700 hours) had a drop
in bond strength of 59 % for the baseline tests and 43 % for the
anchors installed in moist concrete.
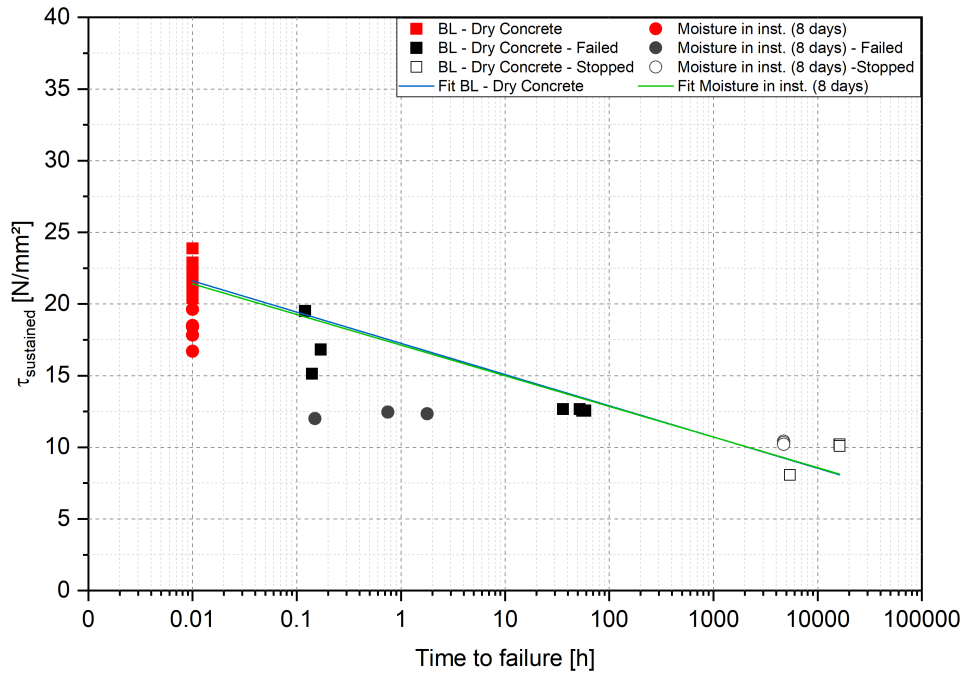
FIGURE 4.10: Influence of the hole moisture according to Davis (2012)

4.4.8 Hole orientation

The orientation of the installation of the anchors was the next parameter studied by Davis (2012). The installation direction of the baseline tests was vertical downward. Two additional installation orientations were observed: horizontal and overhead. These tests were performed at the University of Florida. The results of the short and long-term tests are illustrated in Figure 4.11. The results show, that the failed TTF tests for all three installation orientations had between 28 % and 43 % lower bond strengths compared to the short-term tests. The baseline tests, stopped after more than 10000 hours, had the highest drop in bond strength 61 %, whereas the horizontal and the vertically installed anchors only 45 %.
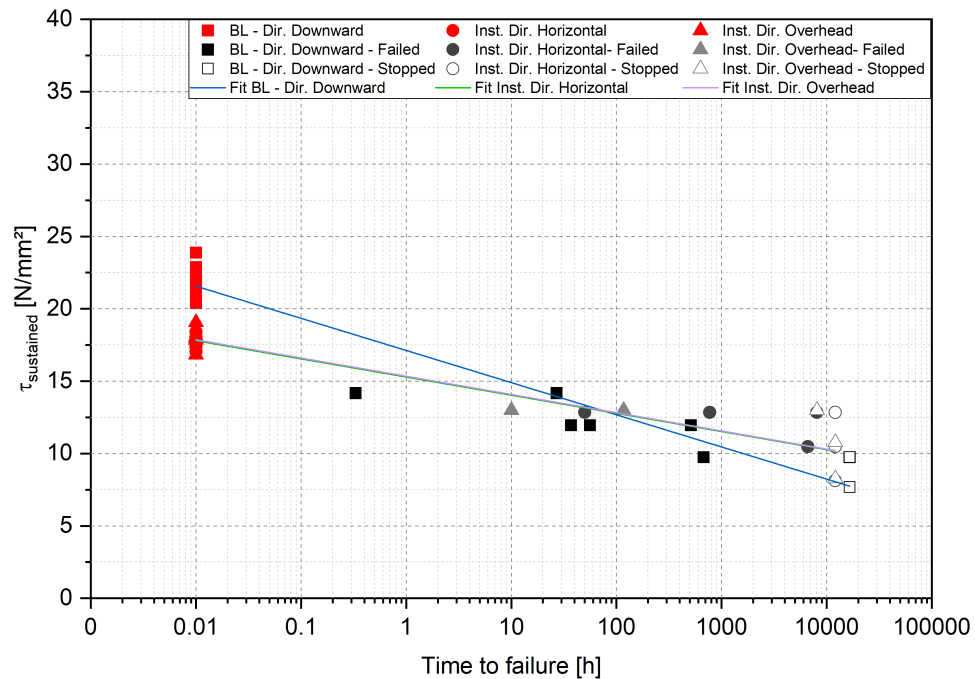
FIGURE 4.11: Influence of the hole orientation
according to Davis (2012)

4.4.9 Installation temperature

Davis (2012) observed the influence of the installation temperature on the bond strength of the adhesive anchors. The baseline tests were installed and tested at room temperature $23\,°C$. These tests were performed at the University of Stuttgart. The anchors installed at minimum temperature were tested once at the minimum service temperature $0\,°C$ and once at $43\,°C$. The bond strength of the baseline tests dropped with 42 % and 61 % for the failed and the stopped TTF, respectively. The anchors tested at minimum service temperature had 30 % lower bond strength after 1000 hours, whereas those tested at $43\,°C$ (failed TTF) had 14 % lower bond strength compared to the short-term tests.
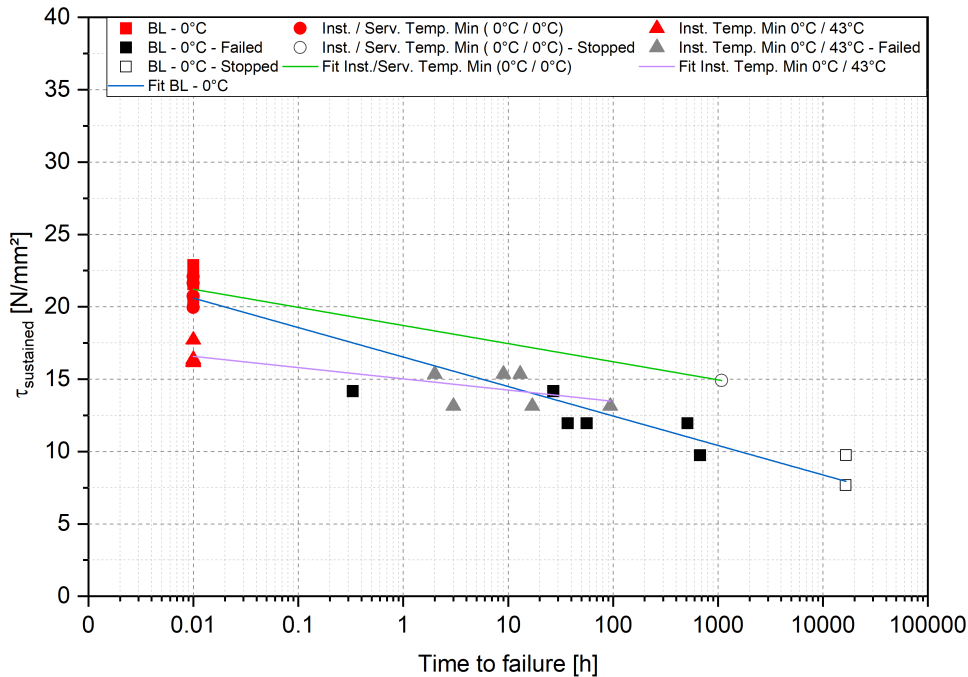
FIGURE 4.12: Influence of the installation temperature according to Davis (2012)

4.4.10　Test setup

The diameter of the confinement has a great influence on the short-term behaviour of adhesive anchors, thus its influence on the long-term performance of anchors is of importance. This influence was studied from Davis (2012), Blochwitz (2019) and IWB (2019).

Figure 4.13 shows the results of the TTF tests performed by Davis (2012). The baseline tests were performed as confined tests at the University of Florida. The results show that the long-term bond strength of the confined tests decreases significantly through time. The failed TTF had 32 % lower bond strength than the short-term tests whereas the stopped TTF more than 50 %. On the other hand, the unconfined tests had, as expected, a lower initial bond strength. However, the TTF results showed only a reduction of 23 % (failed TTF) and 16 % (stopped TTF) of the bond strength.
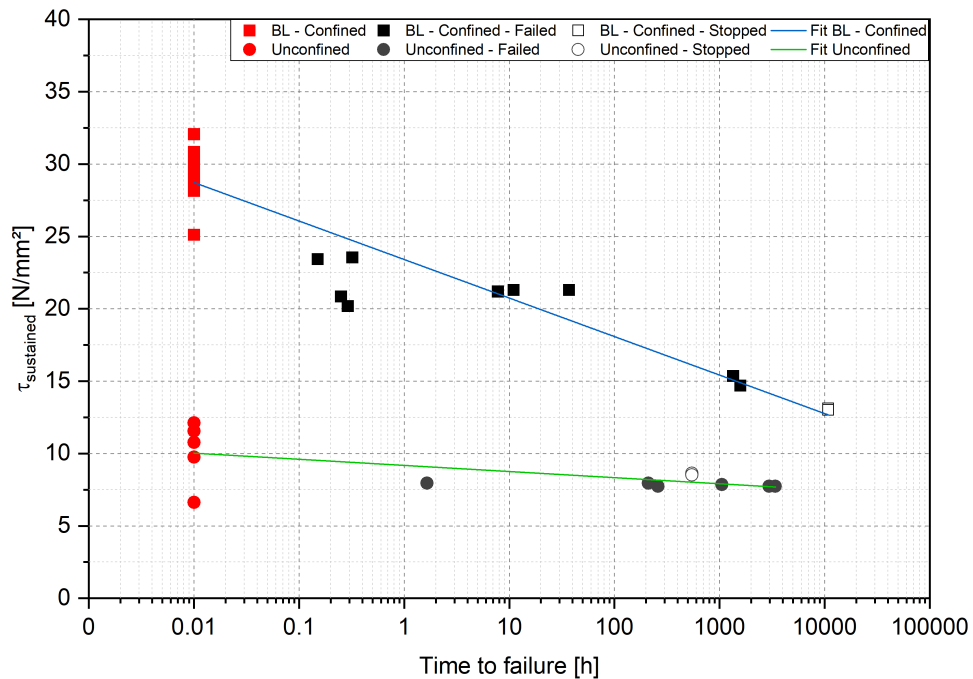
FIGURE 4.13: Influence of the test setup according to
Davis (2012)

Blochwitz (2019) tested the influence of the confinement on
anchors installed at 105 mm. No reference short-term tests were
performed with this embedment depth and confined test setup.
Figure 4.14 illustrates the results of the TTF tests. As a reference,
the short-term tests on anchors installed at 80 mm and tested
with confined setup are shown. The bond strength of the stopped
confined TTF was 37 % lower than the strength of the failed TTF.
A similar pattern showed the unconfined tests (green line), where
the bond strength decreased with 31 % for the stopped TTF.

IWB performed tests at room temperature with both confine-
ments as shown in Figure 4.15. The results show a clear trend
for the bond strength. The bond strength of the failed confined
TTF tests was 14 % lower than the short-term tests and for the un-
confined approximately 18 % lower. For both setups, the stopped
TTF tests reached 75 % of the initial bond strength.
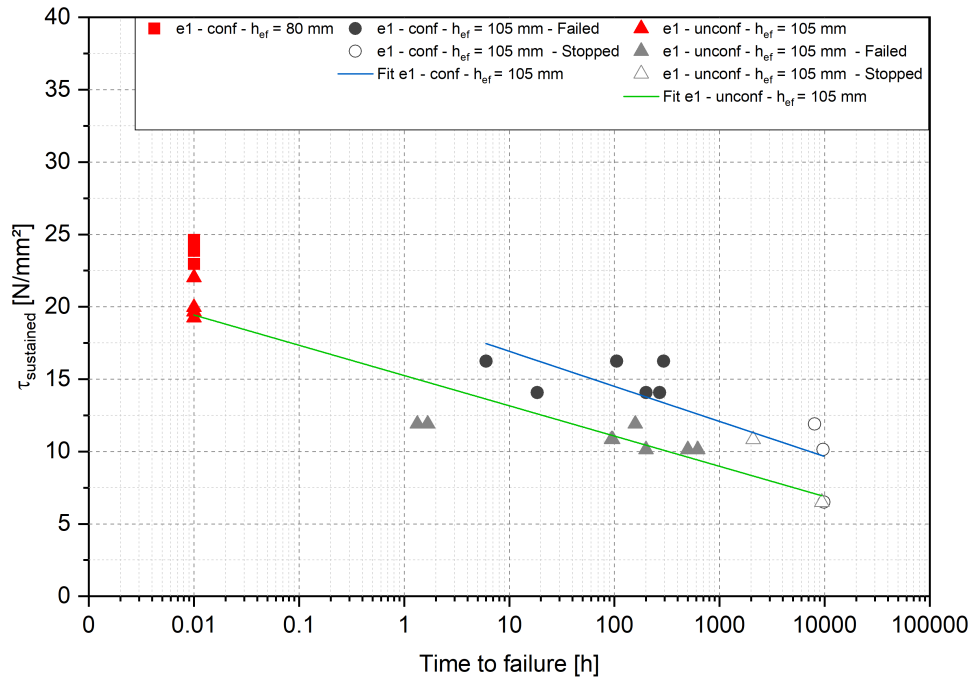
FIGURE 4.14: Influence of the test setup according to
Blochwitz (2019)
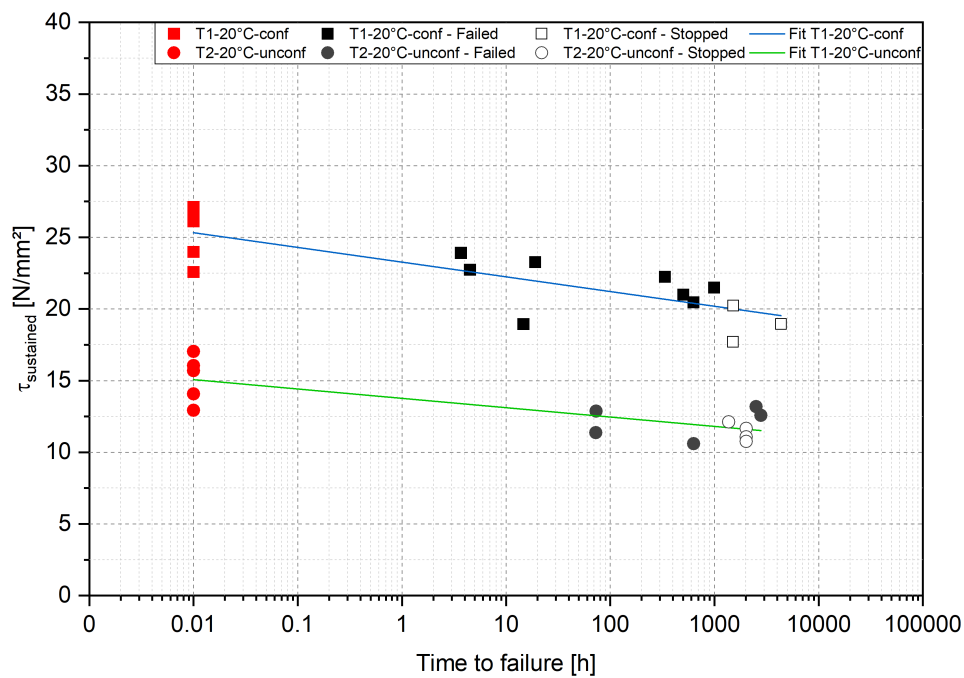
FIGURE 4.15: Influence of the test setup according to
IWB (2019)

4.4.11 Type of concrete

The influence of the type of concrete (concrete composition) was studied by Davis (2012). These tests were performed at the University of Florida. Two main concrete compositions were used A and B. Figure 4.16 illustrates the results of the short-term and long-term tests on concrete A and Figure 4.17 on concrete B. These tests were performed at the University of Florida.
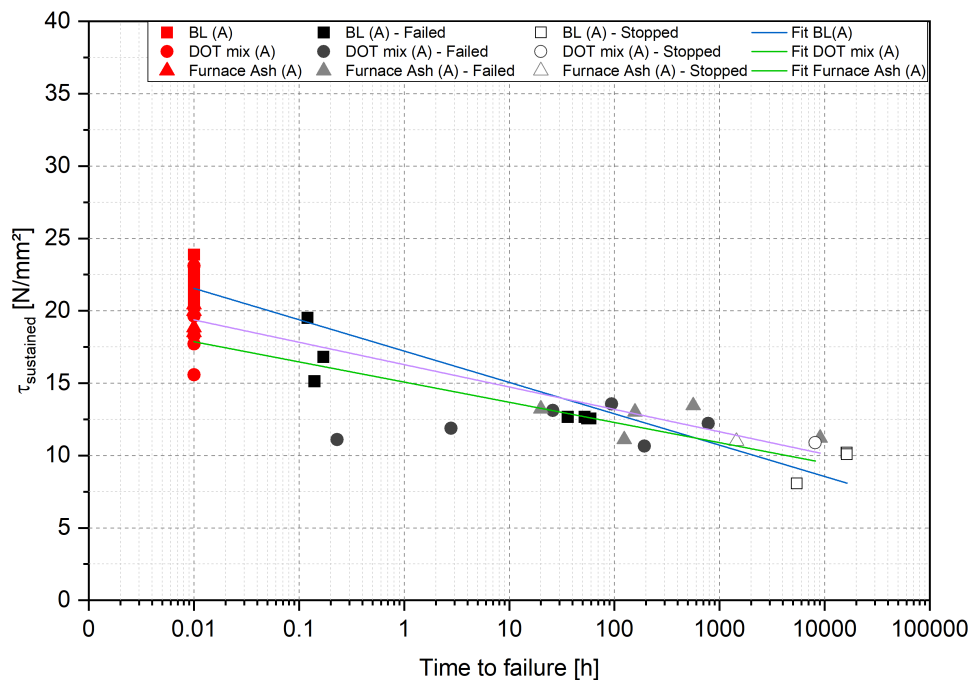
FIGURE 4.16: Influence of the type of concrete
(mixture A) according to Davis (2012)

Mixture A (BL A) was compared with a standard DOT mix (corresponding to C25/30 in DIN EN 206-01 (2017)) and with a mixture with 50 % furnace ash. The bond strength of the failed TTF baseline tests was reduced with 29 % compared to the short-term tests. Similarly, the tests with the two other concrete compositions series had 36 % lower bond strength. The strength of stopped TTF of the baseline tests was less than half (59 %) of the baseline strength. The DOT mix and the furnace ash tests, revealed a similar pattern, with 42 % and 44 % lower bond strength than the short-term tests.

Figure 4.17 displays the results for concrete composition B, where 20 % fly-ash was added to the base mixture. The baseline
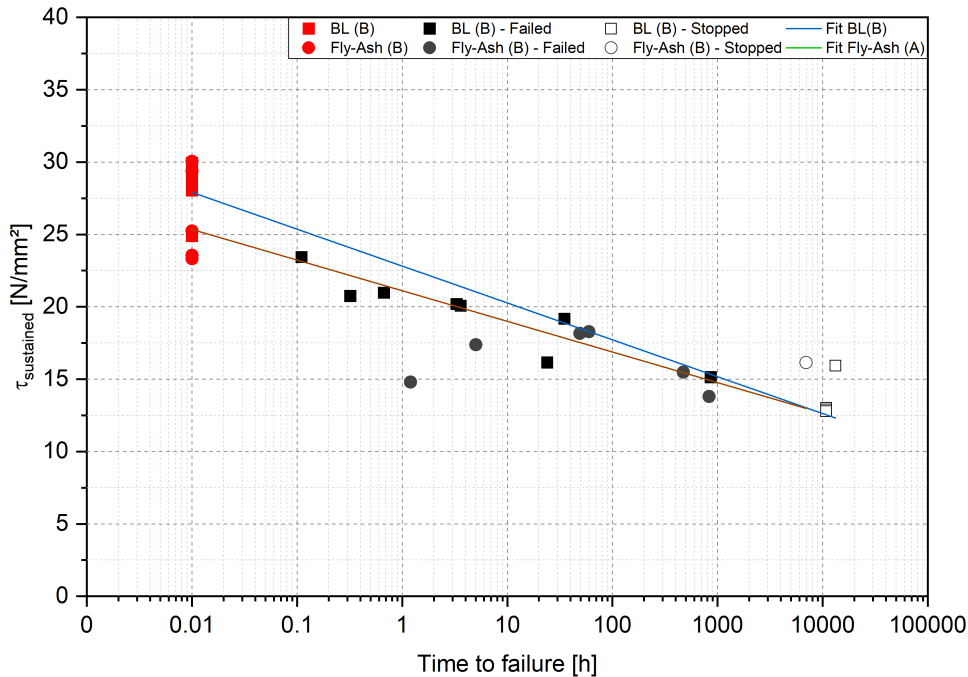
FIGURE 4.17: Influence of the type of concrete
(mixture B) according to Davis (2012)

tests showed a reduction of the bond strength with 32 % (failed TTF) and 53 % (stopped TTF). The behaviour of the concrete mixture with fly-ash was different. The bond strength for both the failed and the stopped TTF was 38 % lower than the baseline tests.

4.4.12   Elevated temperature

Davis (2012) investigated the influence of elevated temperature on the behaviour of adhesive anchors (see Figure 4.18). The anchors were installed at room temperature (24 °C) and were tested at three temperatures: 43 °C (BL), 48 °C and 20 °C. These tests were performed at the University of Stuttgart. The baseline tests and the tests at 20 °C showed a similar trend through time (blue and violet lines). The failed TTF had respectively 22 % and 25 % lower bond strength than the reference short-term tests, whereas the stopped TTF, 41 % and 31 % lower bond strength. All the anchors tested at 48 °C failed prior to reaching 300 hours with a bond strength approximately 30 % lower than the reference tests.

FIGURE 4.18: Influence of the elevated temperature according to Davis (2012)

The tests at IWB (2019) were performed at room temperature and at $50\,^\circ C$ (Figure 4.19). The room temperature TTF tests showed a reduction of $14\,\%$ (failed TTF) and $25\,\%$ (stopped TTF) in bond strength compared to the short-term tests. Surprisingly, the failed TTF at $50\,^\circ C$ had an increase of $9\,\%$ in bond strength. However, the bond strength reduced with $19\,\%$ for the stopped TTF compared to the reference tests.

FIGURE 4.19: Influence of the elevated temperature
according to IWB (2019)

4.4.13   Moisture in service

Figure 4.20 illustrated the results of the tests where the moisture
of the anchor in service was studied (Davis, 2012) at the Uni-
versity of Stuttgart. The anchors were installed in dry concrete,
however they were maintained moist through time. The short-
term tests for both cases had similar bond strength after testing.
The failed TTF tests showed 22 % and 32 % lower bond strength
than the short-term tests for the dry concrete and the wet con-
crete, respectively.
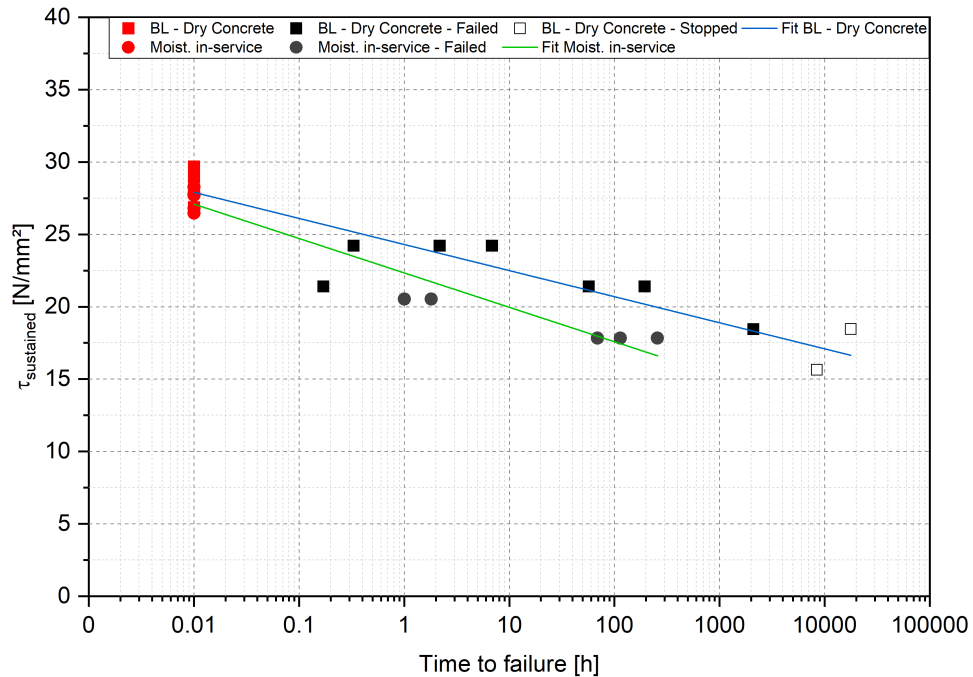
FIGURE 4.20: Influence of the moisture in service
according to Davis (2012)

4.4.14 Summary

In this chapter, thirteen influence factors considered in the research of Davis (2012), Blochwitz (2019) and IWB (2019), were described. Their influence on bond strength is given in each subsection. Using linear fit for the corresponding test results, the bond strength at 50 and 100 years was determined through extrapolation.

It is obvious, that depending on the type of adhesive, the influence factors change. Furthermore, each adhesive has a different development of the bond strength through time.

Figure 4.21 to Figure 4.25 illustrate the absolute and relative values of the estimated bond strengths grouped according to the researcher and the type of adhesive. The relative bond strength are determined as the ratio between the bond strength of TTF tests and the corresponding reference short-term tests.

Figure 4.21 to Figure 4.23 shows the bond strengths for different factors for adhesive A (vinyl ester), B (epoxy resin) and C (epoxy resin) according to Davis (2012). Adhesive A showed a higher influence of the curing time when loaded than the other

factors (hole moisture, hole orientation, installation temperature and type of concrete). In this case, the extrapolated bond strengths at 50 and 100 years were 1.71 MPa and 1.37 MPa, respectively.
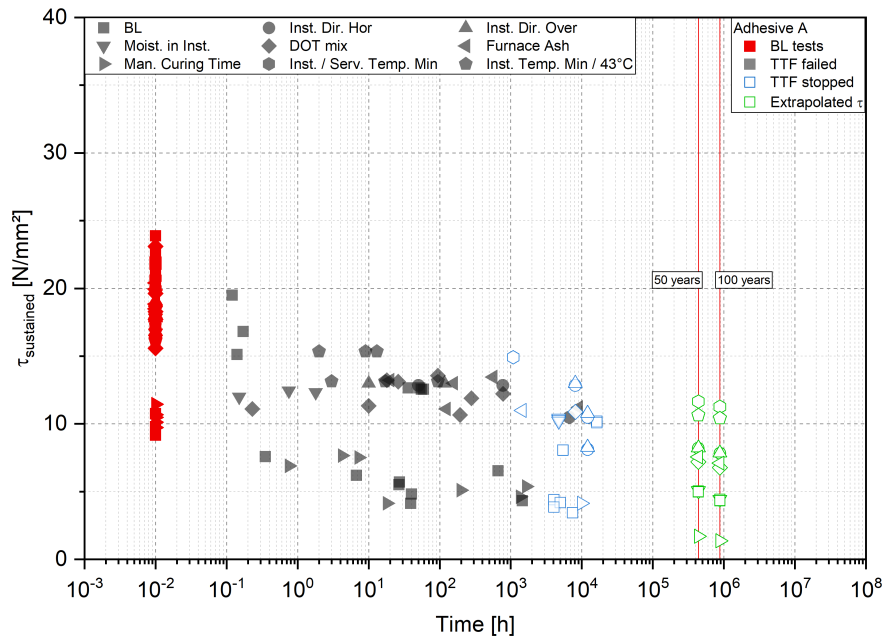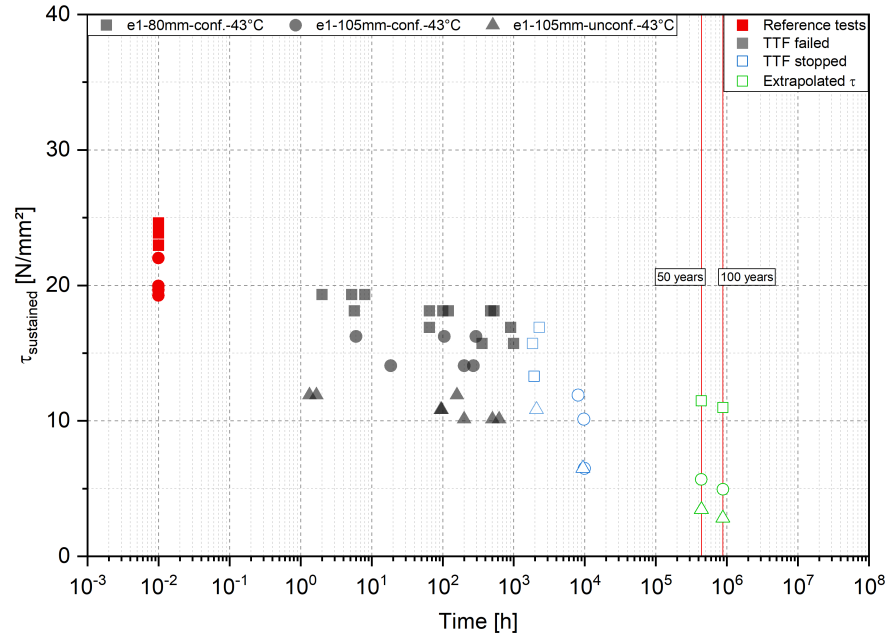

(A) Absolute values
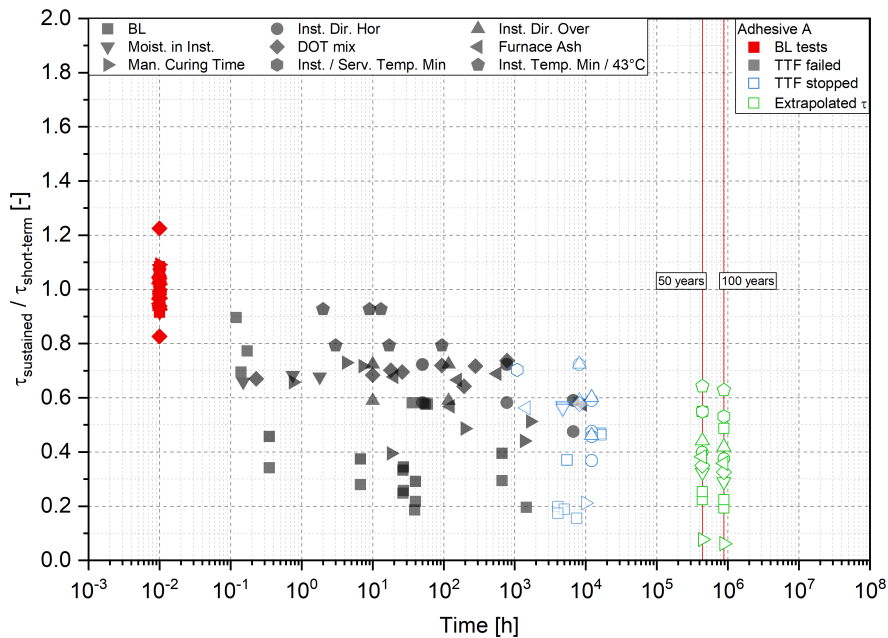
(B) Relative values

FIGURE 4.21: Influence factors on Adhesive A according to Davis (2012)

The tests with adhesive B showed more influence of the elevated temperature compared to the influence of hole drilling, hole moisture or type of concrete. The extrapolated bond strengths at 50 and 100 years were 8.57 MPa and 7.89 MPa.
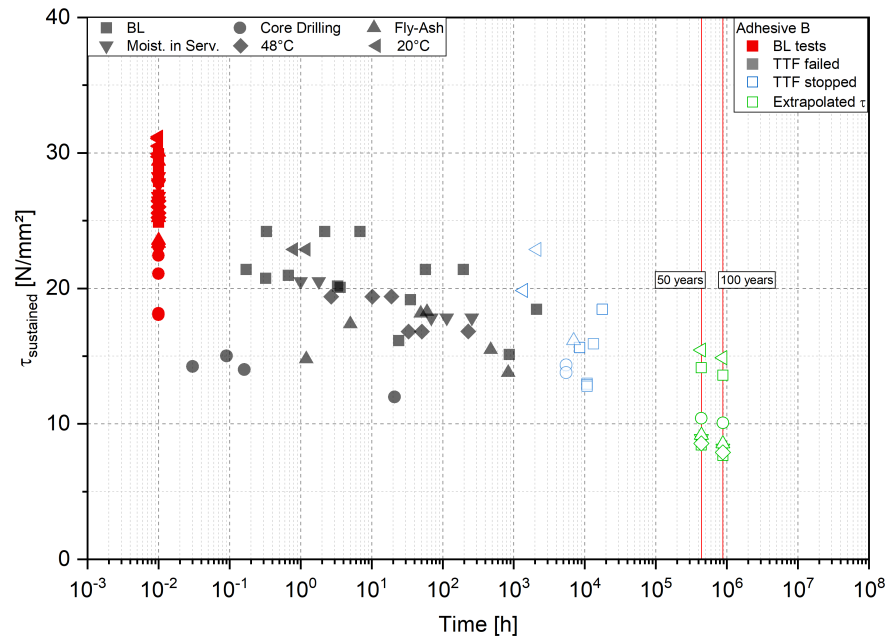
(A) Absolute values
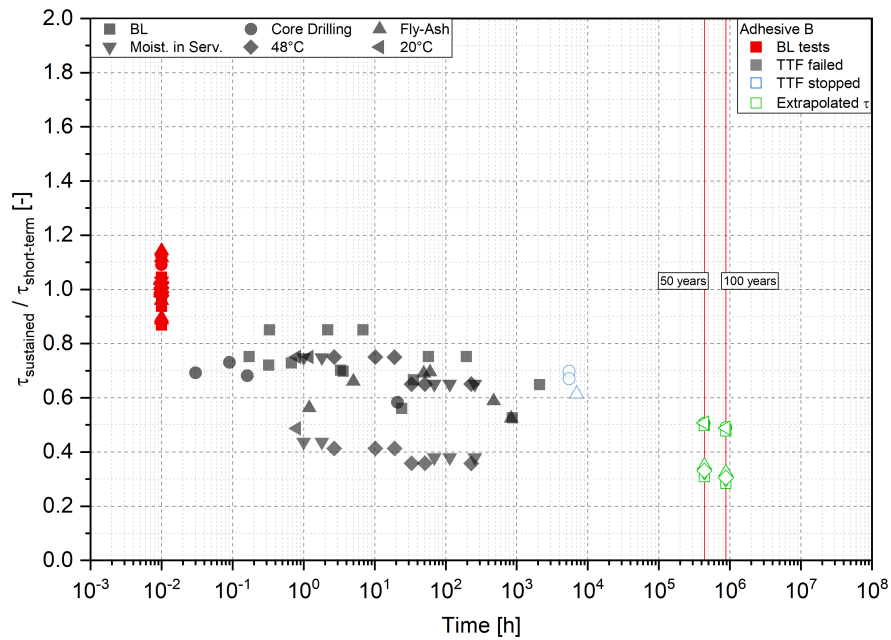
(B) Relative values

FIGURE 4.22: Influence factors on Adhesive B
according to Davis (2012)

With adhesive C only two factors were studied: the reduced cleaning effort and the testing setup. In this case, the unconfined setup affected the bond strength more compared to the reduced cleaning effort. After 50 years, the extrapolated bond strength was 6.79 MPa and after 100 years 6.67 MPa.
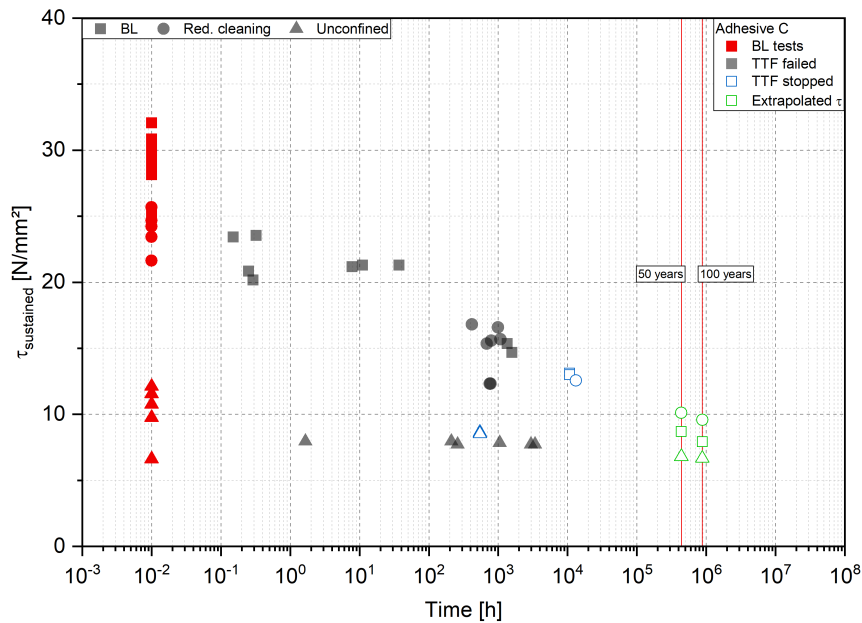
(A) Absolute values
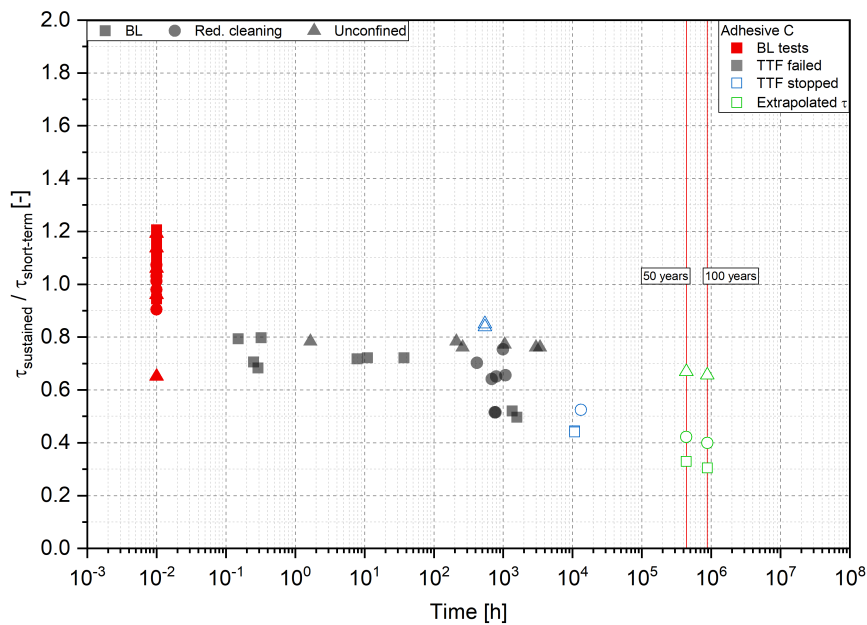
(B) Relative values

FIGURE 4.23: Influence factors on Adhesive C according to Davis (2012)

The extrapolation of the results of Blochwitz (2019) revealed a higher influence of the testing setup (unconfined setup) compared to the embedment depth (105 mm) as seen in Figure 4.24a.

(A) Absolute values
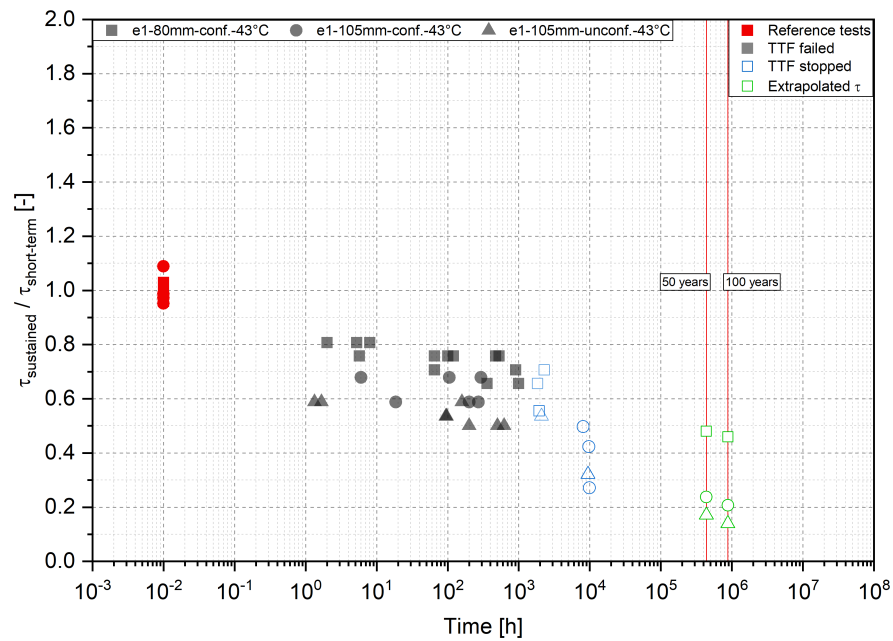
(B) Relative values

FIGURE 4.24: Influence factors according to Blochwitz (2019)

Similar to the above mentioned researches, the tests carried out at IWB (2019) demonstrated an influence of the unconfined setup on the bond strength of the adhesive followed by the elevated temperatures (Figure 4.25a).
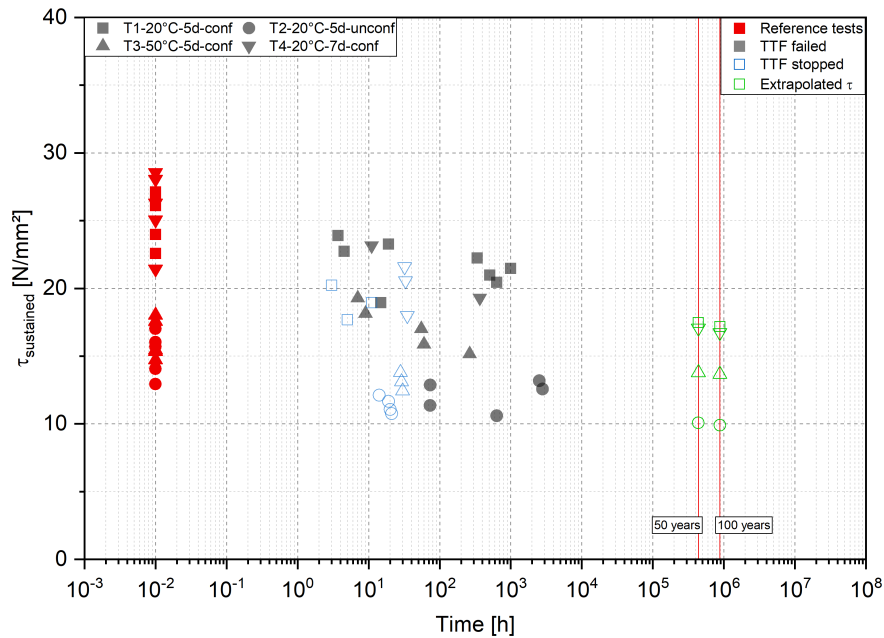
(A) Absolute values
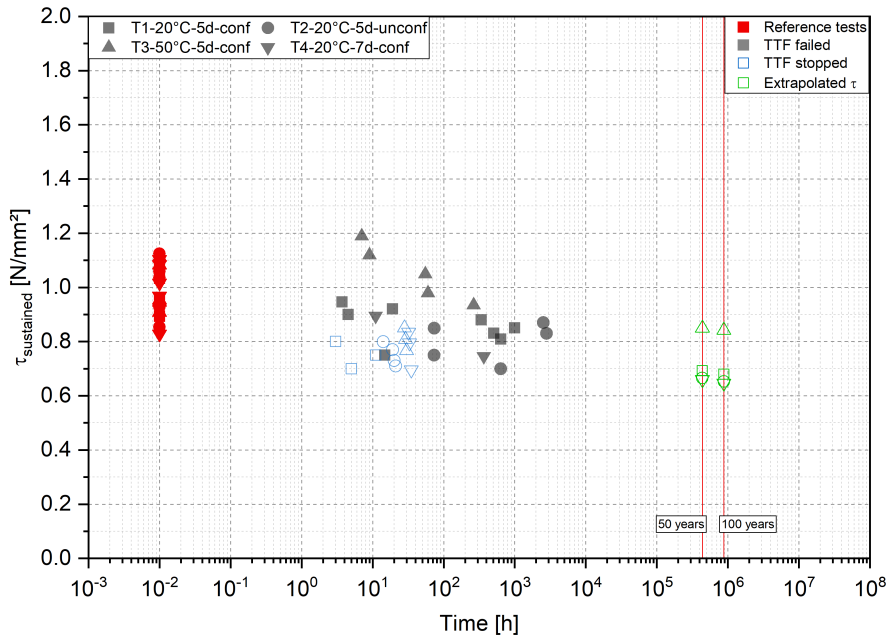
(B) Relative values

FIGURE 4.25: Influence factors according to IWB (2019)

However, observing the relative values in Figure 4.25b, the bond strengths in the TTF test at elevated temperature were approximately 15 % lower than the bond strengths at the corresponding short-time tests.

The last four figures of this chapter illustrate the relative bond strength of all the above mentioned researches grouped according to two parameters: testing setup and testing temperature. Furthermore, a linear fit of all the results (excluding the extrapolated ones) and the 95 % confidence and prediction bands are plotted in each diagram. The confidence band shows the limits of all the possible fitted lines for the selected dataset with a confidence level of 95 %. The prediction band shows that if a new datapoint is added to our existing dataset, the results will fall within this prediction band with a confidence level of 95 %.

Figure 4.26 and Figure 4.27 show the relative values of the bond strengths grouped according to the testing setup: confined and unconfined. The plotted results include tests at 23 °C and 43 °C.

The tests at room temperature (23 °C) and at elevated temperature (43 °C) are shown in Figure 4.28 and Figure 4.29, respectively. Only the confined test setup results are illustrated.
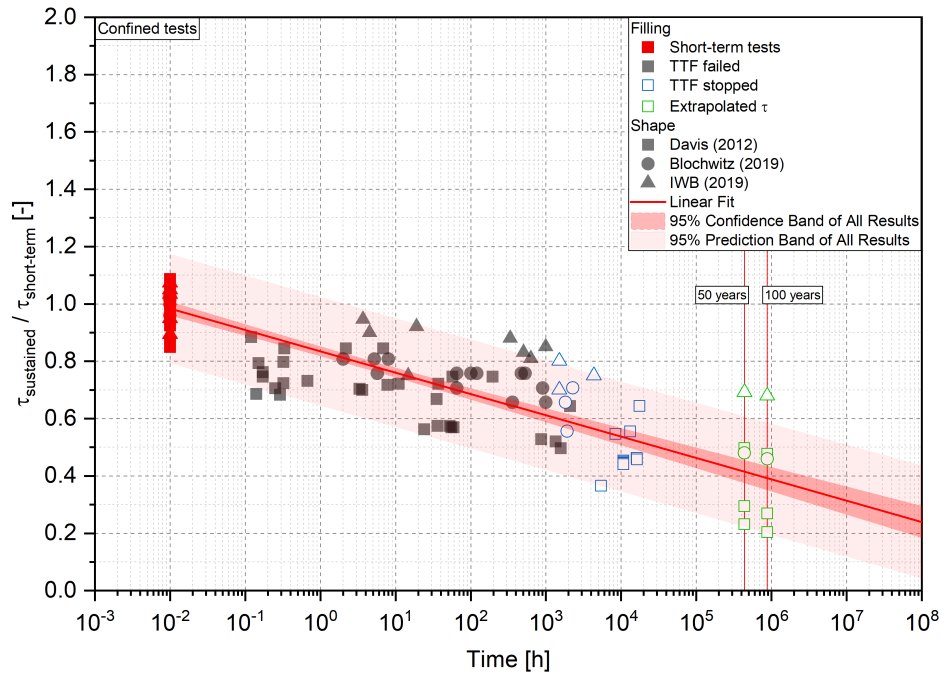
FIGURE 4.26: Summary of the relative bond strengths for confined setup tests according to Davis (2012), Blochwitz (2019), and IWB (2019)
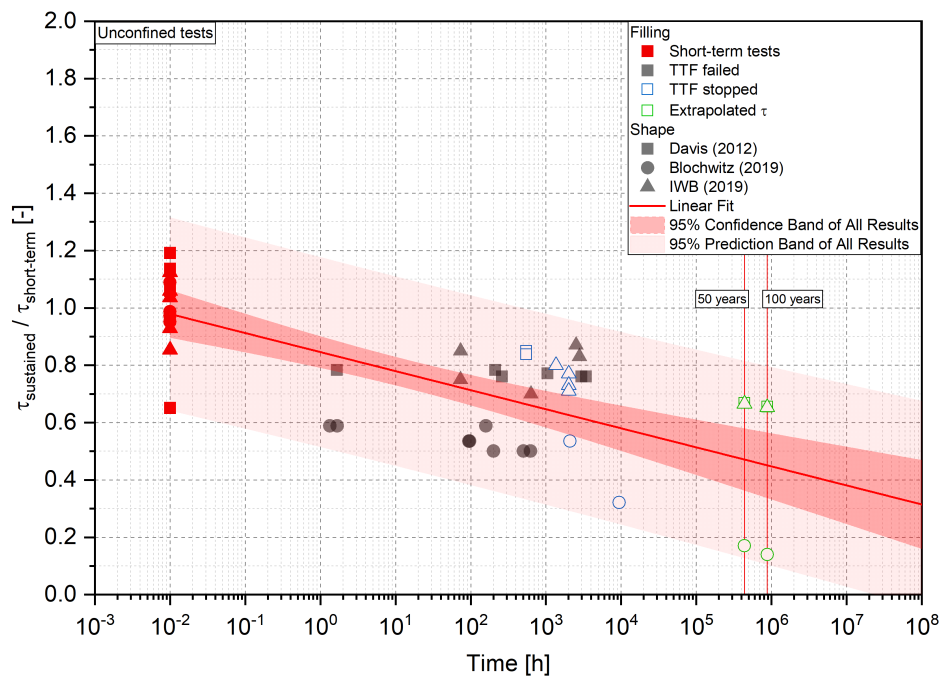

FIGURE 4.27: Summary of the relative bond strengths for unconfined setup tests according to Davis (2012), Blochwitz (2019), and IWB (2019)
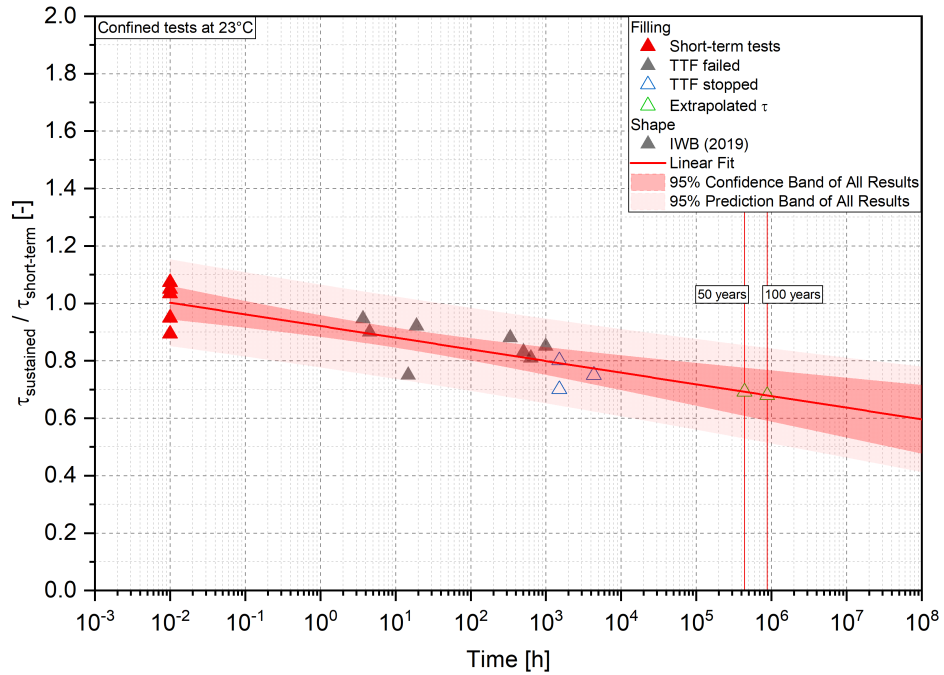
FIGURE 4.28: Summary of the relative bond strengths
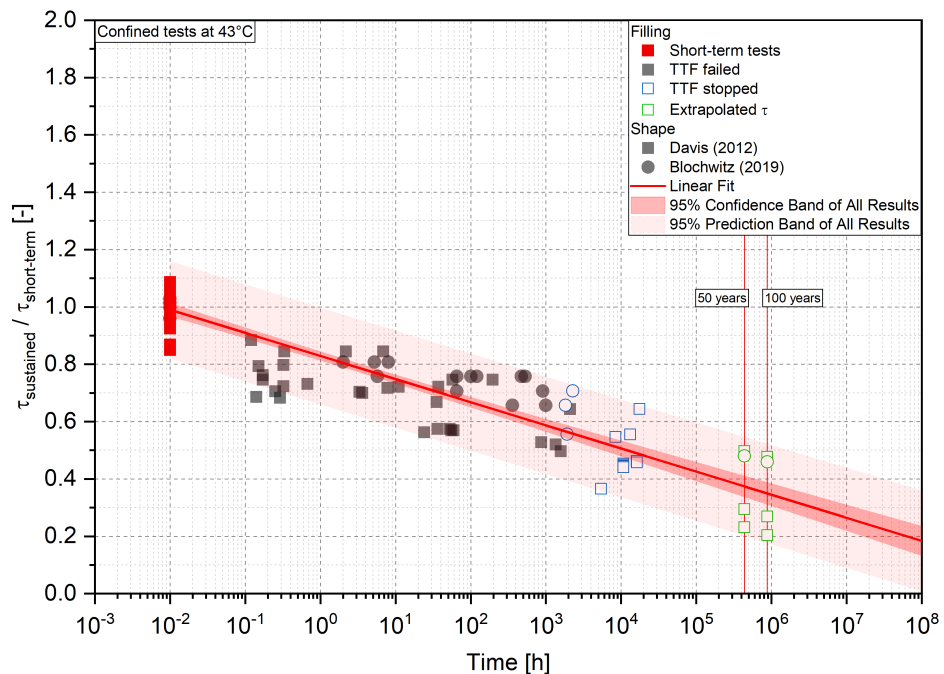at of the tests at $23\,^{\circ}C$ according to IWB (2019)

FIGURE 4.29: Summary of the relative bond strengths
of the tests at $43\,^{\circ}C$ according to Davis (2012) and
Blochwitz (2019)

5 Materials and methods

5.1 General

This chapter contains a summary of the materials and methods used in the experimental part of this thesis. The anchors were tested using four test setups: confined, unconfined, sustained loading and axial compression setup. All the tests were carried out according to the standards AC 308 (2017) and EAD 330499 (2018). A detailed overview of the materials and methods is presented in Appendix A.

5.2 Materials

5.2.1 Concrete

Concrete specimens of different compositions and dimension were used as anchorage ground for the experimental tests. Table 5.1 gives an overview of the specimens used.

TABLE 5.1: Concrete specimen

Concrete mixture	Strength	Geometry	Length	Width	Height
[−]	[−]	[−]	[cm]	[cm]	[cm]
Batch A.1	C20/25	Slab	128.5	128.5	20
Batch A.1	C20/25	Cylinder	31/20	31/20	16/15
Batch A.2	C20/25	Cylinder	31	31	16
Batch B.1	C20/25	Cylinder	20	20	15/17
Batch B.2	C50/60	Cube	20	20	20
Batch B.3	C90/105	Slab	190	190	20
Batch B.4	C90/105	Slab	190	190	30
Batch B.5	C100/115	Slab	160	160	20/25

The concrete specimens were produced by the pre-cast concrete factories Friedrich RAU GmbH & Co KG and Kaltenbach Gebr. GmbH & Co. KG according to the state of the art per DIN EN 206-01 (2017). Concrete batches A.1 and A.2 were used for

the tests described in Chapter 6, whereas batches B.1 to B.5 for those given in Chapter 7.

The compressive strength of each concrete batch was tested on concrete cubes with dimensions 15 x 15 x 15 cm according to DIN EN 12390-3 (2019).

The concrete mixtures, compressive strengths and specimen drawings are described in detail in Appendix A.

To take into account the influence of the different concrete compressive strengths, the failure loads were converted to a nominal strength. The conversion was carried out as described in EAD 330499 (2018). Equations (5.1) to (5.5) illustrate the calculation of the loads for concrete, bond and steel failure.

Concrete failure

$$F_{u,c} = F_{u,t} \cdot \left(\frac{f_c}{f_{c,t}}\right)^{0.5} \tag{5.1}$$

Bond failure

$$F_{u,p} = F_{u,t} \cdot \left(\frac{f_c}{f_{c,t}}\right)^{m} \tag{5.2}$$

The coefficient m in Equation (5.2) is determined with the results of the tests $A1, A2, R1, R2$ (see EAD 330499 (2018)) as follows:

for confined uncracked concrete

$$m = \frac{\log\left(\frac{N_{u,m,R2}}{N_{u,m,R1}}\right)}{\log\left(\frac{f_{c,R2}}{f_{c,R1}}\right)} \leq 0.5 \tag{5.3}$$

for unconfined uncracked concrete

$$m = \frac{\log\left(\frac{N_{u,m,A2}}{N_{u,m,A1}}\right)}{\log\left(\frac{f_{c,A2}}{f_{c,A1}}\right)} \leq 0.5 \tag{5.4}$$

The ratio $\frac{f_c}{f_{c,t}}$ should be smaller or equal to 1.0 to convert the loads for concrete and bond failure.

Steel failure

$$F_{u,s} = F_{u,t} \cdot \frac{f_c}{f_{c,t}} \qquad (5.5)$$

5.2.2 Adhesive anchors

Two different epoxy resin adhesive anchors were used for the tests. The two-component adhesives were filled in plastic cartridges. Epoxy 1 was used for the incremental loading tests carried out at IWB (Chapter 6). The tests described in Chapter 7 were installed using Epoxy 2.

At the time of writing, there was no information about the material properties of Epoxy 1. The material properties of Epoxy 2 are summarized in Table 5.2. These properties were used for numerical simulations.

TABLE 5.2: Material properties of Epoxy 2

Properties	Value	Units
Compressive strength	122	MPa
Flexural strength	66	MPa
Tensile strength	44.2	MPa
Young's modulus	6300	MPa
Elongation at break	1.0	%
Density	1.50	g/cm^3

5.2.3 Steel

Threaded rods ($M\,12$) and reinforcing bars ($d\,12$) were used for the tests. The threaded rods had a steel grade of 12.9, whereas the reinforcing bars, $B500B$. The reinforcing bars and the threaded rods installed at high embedment depths in high-strength concrete were hardened before use. The hardening process consisted of heating the fasteners to $950°C$ and cooling them down afterwards. The tensile strength of both steel components could not

be tested due to the short length of the specimen. Before installation, the rods and bars were cleaned with water and soap to remove any oil residue. Their length was chosen depending on the test.

5.3 Installation

5.3.1 Specimen preparation

Three methods were used to prepare the concrete specimens for installation.

Method 1: The concrete slabs and cylinders for the incremental loading tests in Chapter 6 were drilled using hammer drill bits. The diameter of the drill was taken as specified in the MPII. The drilling machine was mounted on a rig to ensure perpendicularity during drilling. An exception was the tests with increased bond line thickness, where the drill bits were chosen such that the desired bond line thickness was achieved. After drilling, the holes were cleaned as described in the MPII: hand blowing, hand brushing and hand blowing again. In the tests with reduced cleaning effort, the holes were cleaned only using hand pumping.

Method 2: A different procedure was used for the tests in wet concrete (Chapter 6). Pilot holes were drilled to the required embedment depth with a drill diameter 50 % smaller than the diameter specified in the MPII. Plastic cups with holes were glued to the concrete surface and filled with water. The holes remained with water for a minimum of 8 days. Afterwards, the water and the cups were removed, and the specimen was drilled with the drill bit specified in the MPII. Hole cleaning was carried out as mentioned in the previous method.

Method 3: The anchors in Chapter 7 were drilled using a diamond core drilling system mounted on a drill stand with a vacuum base plate to ensure perpendicularity. Two core bits diameters were used as given in the MPII. The wet method was used to drill the holes. After drilling, the boreholes were rinsed with water until clear water came out. Afterwards, the holes were brushed two times and rinsed with water again. In the end, the water was removed from the holes. To ensure that the concrete

was dry, the slabs were stored at room temperature in the laboratory for a minimum of one week. Once the concrete was dry, the boreholes were cleaned using compressed air, hand brushing and compressed air according to the MPII.

5.3.2 Installation of the anchors

After drilling and cleaning the holes, the anchors were installed at room temperature. The mortar was pressed into the holes using a mechanical dispenser (Epoxy 1) and a pneumatic dispenser (Epoxy 2). The first 10 cm of the mortar were thrown away to guarantee proper mixing of the components. The threaded rods and the reinforcing bars were inserted in the holes using rotary movements. The anchors were cured at room temperature for 24 to 48 hours. After hardening, the anchors were loaded until failure.

5.4 Testing Procedure

5.4.1 Measurement equipment

The load was measured continuously using load cells from the company GTM-GmbH. The load cells were calibrated externally from IWB. Load cells with a range up to 200 kN were used to measure the failure load of the adhesive anchors. For the axial compression tests, an additional load cell with 500 kN was utilized to record the compression load.

Displacement transducers from Novotechnik Messwertaufnehmer OHG measured the displacement. Their range was up to 75 mm. Figure 5.1 illustrates the indirect measurement method. For the sustained loading tests, the displacement was measured directly on the top of the anchor using dial gauges.

Two software programs recorded and saved the data from the tests: DIAdem, a Nation Instrument Corporation software and catman from Hottinger Brüel & Kjaer GmbH. The data was saved with a frequency of 5 Hz.
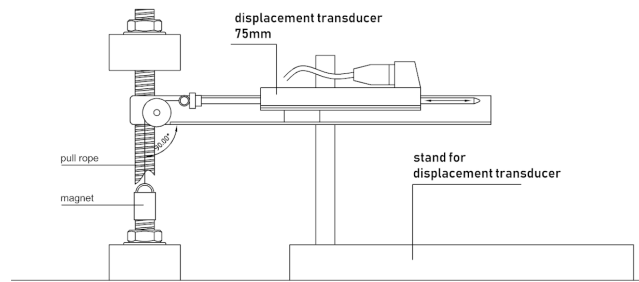
FIGURE 5.1: Indirect measurement of the displacement in the short-term tests

5.4.2   Short-term tests

Figure 5.2 illustrates the standard setup for confined tests. After installation (see Section 5.3), the anchors were axially loaded to failure within 3 minutes with the use of a hydraulic cylinder. A confinement plate was used to equally distribute the load on the concrete surface. The plate had a clearance hole with a diameter between $1.5d_{cut}$ and $2.0d_{cut}$. An exception was the test performed in Table 7.3, where the diameter of the confinement plate was varied between $0.24h_{ef}$ and $2.0h_{ef}$. The applied load was transferred with the use of a tension rod from the cylinder to the loading fixture and finally to the anchor, which was fastened with a nut. The load and displacement were measured throughout the test.

The setup used for unconfined tests is shown in Figure 5.3. The load transfer mechanism was the same as in the confined tests, however, no confinement plate was used. The rig for unconfined tests had a diameter larger than $4.0 \cdot h_{ef}$ which allowed the development of a conical concrete breakout.

Lastly, the axial compression test setup is displayed in Figure 5.4. These tests consisted of two parts, the application of the axial compression in one direction and the confined testing. The hydraulic cylinder mounted at the side of the rig helped to apply the compression to the concrete cubes. The compression was not applied to an entire concrete surface, but a surface defined by a steel plate with dimensions 80 x 200 mm. After the desired compression was achieved, the anchor was loaded to failure with a confined setup.
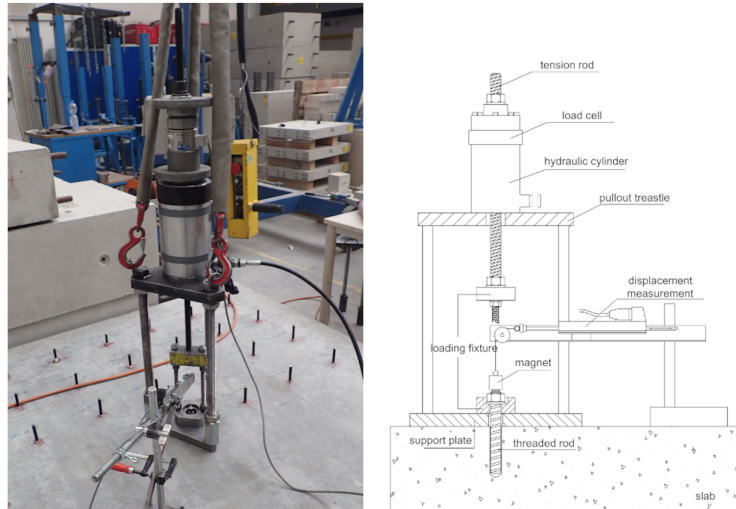
FIGURE 5.2: Confined test setup
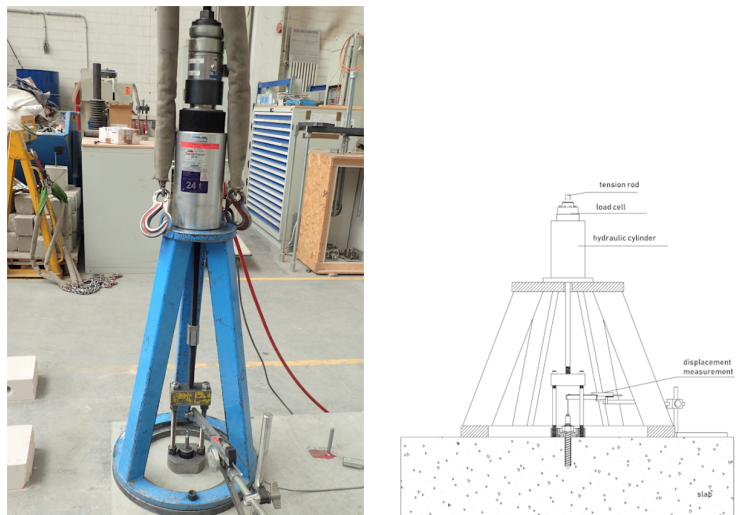
FIGURE 5.3: Unconfined test setup

Figure 5.5 illustrates the loading procedure for the anchors. At the beginning, the compression load was applied and kept constant at the specified value. Afterwards, the tension load was applied to the fastener.
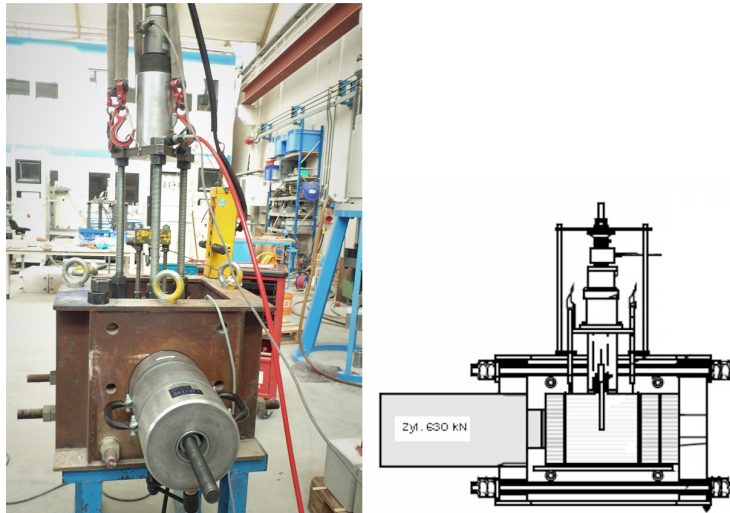
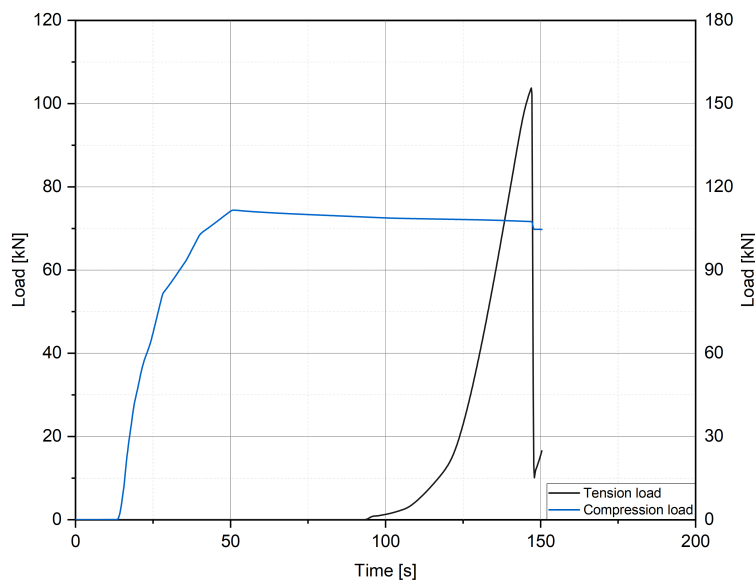FIGURE 5.4: Axial compression test setup

FIGURE 5.5: Loading procedure for axial compression
tests

5.4.3   Long-term tests

Two types of long-term tests were carried out: incremental load
and sustained load testing. For the incremental loading (Chap-
ter 6), the confined or the unconfined setups previously de-
scribed were utilized. The load was applied using 5 % increments
calculated from the short-term reference tests. After loading, the

anchor was unloaded and reload within 5 minutes. This process was repeated until the anchor failed. Figure 5.6a and 5.6b illustrate a typical loading curve for short-term tests and for incremental loading tests. The loading process and the development of the displacement are displayed in Figure 5.6c and 5.6d as a function of time. Incremental load tests were also carried out at elevated temperatures 43°C, thus, the anchors were installed in concrete cylinders. After hardening of the mortar, the cylinders were put in a climate chamber. The temperature was increased gradually from 20°C to 43°C within 24 hours and it was kept constant for 48 hours. Afterwards, the anchors were tested as previously described.
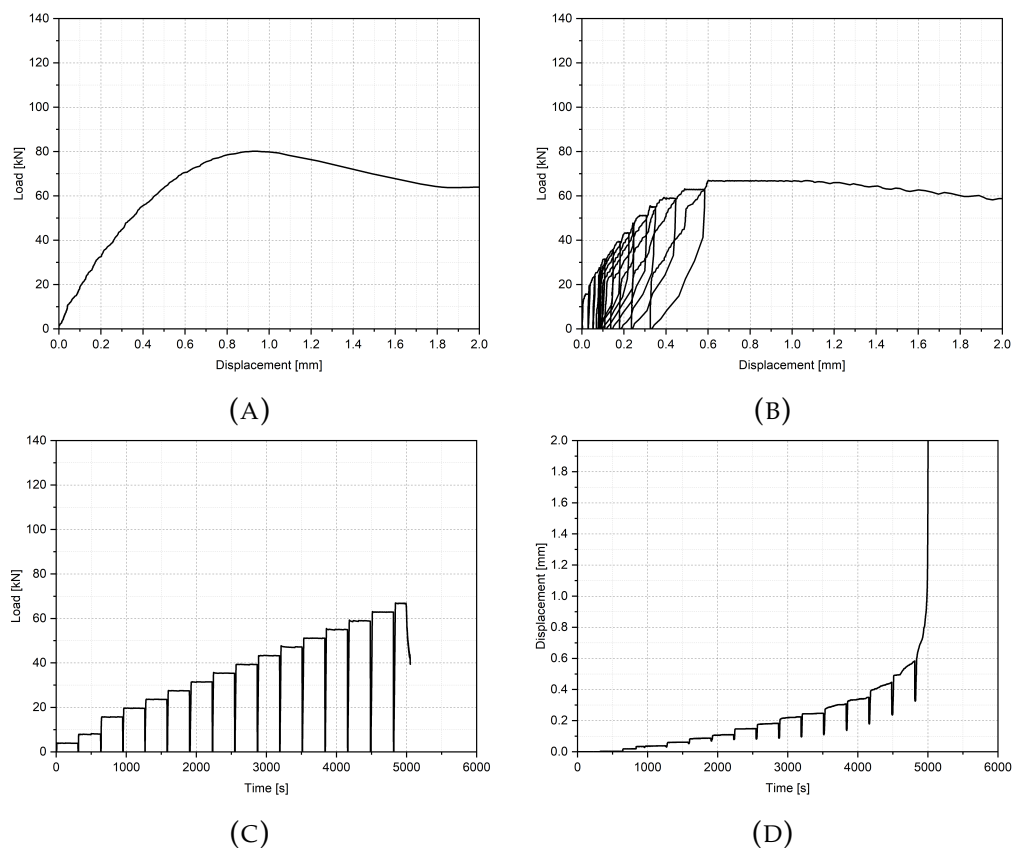
FIGURE 5.6: Illustration of: load vs displacement curves for (a) short-term and (b) incremental loading tests; (c) load vs time and (d) displacement vs time for incremental loading tests

The sustained loading (Chapter 7) was achieved using soft disc springs as seen in Figure 5.7. After preparing the anchor in

the concrete cylinder and fastening it to the loading fixture, the springs were pre-stressed using a hydraulic cylinder and a loading cell. After the sustained load value was reached, the round steel plate at the top of the setup was fastened with a nut to maintain this load. The anchors remained for 5500 hours under sustained loading (or until they failed). In the end, the anchors were unloaded and tested using a confined setup.
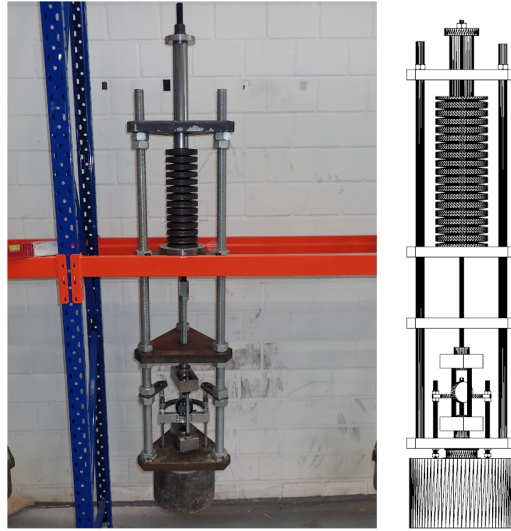
FIGURE 5.7: Long-term (sustained) loading test setup apparatus

6 Adhesive anchors under incremental loading

6.1 General

This chapter outlines the behaviour of adhesive anchors in uncracked concrete under incremental loading. The anchors were tested using confined and unconfined setups. In the following sections, the influence of incremental loading through a direct comparison between short-term tests and incremental tests is investigated. Furthermore, different parameters are varied such as hole cleaning, annular gap, hole saturation, and temperature. Their influence is observed with respect to the reference incremental loading tests or to the reference short-term tests.

6.2 Test Program

The test program for incremental loading consisted on 36 series (D028-D051 and D065-D076). The anchor tested was an epoxy resin adhesive with a $M\,12$ threaded rod. Short-term tests (as reference tests) and incremental loading tests were conducted. A summary of the test program is given in Table 6.1. The first column depicts the test series name. The second column shows the type of test carried out with the following abbreviations:

R - reference test
ShT - short-term test
IL - incremental loading test

The third column illustrates the embedment depth of the anchor, followed by the drilling diameter and the hole condition. The last two columns display the temperature when testing and the test support used to test the anchors. Three hole conditions were studied:

1 Hole cleaning: multiple times using a hand pump, one time machine brushing and finally multiple times with a hand pump (HPxMBxHP). Concrete condition: dry concrete.

2 Hole cleaning: one time using a hand pump (1xHP). Concrete condition: dry concrete.

3 Hole cleaning: multiple times using a hand pump, one time machine brushing and finally multiple times with a hand pump (HPxMBxHP). Concrete condition: wet concrete.

The results of each test series including the corresponding diagrams are described in Appendix B. The loading procedure is described in Chapter 5.

Six parameters were varied throughout the program: the embedment depth, the annular gap, hole cleaning, hole saturation, temperatures when tested and the test support width. The reference tests were drilled with a drill bit diameter 14 mm corresponding to an annular gap of 1 mm and the cleaning procedure: hand pumping to remove dust, machine brushing and hand pumping according to the manufacturers printed instructions. The anchors were installed at room temperature at three embedment depths, namely 60 mm, 80 mm and 105 mm. The annular gaps investigated were 1 mm (d_{cut} = 14 mm), 2 mm (d_{cut} = 16 mm) and 4 mm (d_{cut} = 20 mm). Two cleaning methods were tested, the standard cleaning according to the manufacturers printed instructions (HPxMBxHP) and the reduced cleaning defined as only one time hand pumping. The anchors were tested at $20°C$ and $43°C$ using confined and unconfined test setup.

TABLE 6.1: Test program

Test series [−]	Type of test [−]	Diam. anchor [mm]	Embed. depth [mm]	Drill diam. [mm]	Hole cond. [−]	Temp. [°C]	Support [−]
D028	R-ShT	12	60	14	1	20	confined
D029	R-IL	12	60	14	1	20	confined
D030	R-ShT	12	60	14	1	20	unconfined
D031& D032	R-IL	12	60	14	1	20	unconfined
D033	IL	12	60	14	2	20	confined
D034	ShT	12	60	14	2	20	confined
D035	IL	12	60	14	2	20	unconfined
D036	ShT	12	60	14	2	20	unconfined
D037	IL	12	60	16	1	20	confined
D038	IL	12	60	16	1	20	unconfined
D039	IL	12	60	20	1	20	confined
D040	IL	12	60	20	1	20	unconfined
D041& D042	R-ShT	12	80	14	1	20	unconfined
D043	R-IL	12	80	14	1	20	unconfined
D044	IL	12	80	14	2	20	unconfined
D045	IL	12	80	16	1	20	unconfined
D046	IL	12	80	20	1	20	unconfined
D047	IL	12	60	14	3	20	unconfined
D048	IL	12	60	14	3	20	confined
D049	IL	12	60	14	1	43	confined
D050	IL	12	60	14	1	43	unconfined
D051	IL	12	80	14	1	43	unconfined
D065	IL	12	60	14	2	43	confined
D066	IL	12	60	20	1	43	confined
D067	IL	12	80	14	1	43	confined
D068	IL	12	60	20	1	43	unconfined
D069	IL	12	80	20	1	43	unconfined
D070	R-ShT	12	80	14	1	20	confined
D071	R-ShT	12	105	14	1	20	unconfined
D072	R-IL	12	105	14	1	20	unconfined
D073	IL	12	105	20	1	20	unconfined
D074	R-IL	12	80	14	1	20	confined
D075	IL	12	80	14	2	20	confined
D076	IL	12	80	20	1	20	confined

6.3   Results

6.3.1   Failure modes

The anchors tested in this chapter exhibited failure modes depending on the testing setup. The failure modes are listed for each case in the tables in Appendix B. The following failure modes were observed:

P_M Pull-out failure with mortar

P Pull-out failure without mortar

$M1$ A combination of pull-out failure with and without mortar

C Concrete cone failure

$M2$ A combination of concrete cone failure with pull-out failure

The assignment of the failure modes occurred through visual examination.

6.3.2   Diagrams

The comparison between the parameters is illustrated with two types of diagrams as seen in Figure 6.1:

(A) failure load versus bond length diagram

(B) displacement versus load steps diagram

The failure load versus bond length diagram shows the failure loads for both short-term and incremental loading tests.

The displacement versus load steps diagram illustrates on the top diagram the displacement at the end of each loading increment and their average and on the bottom diagram the first derivative of the average values of each series. The first derivative of the displacement shows the rate (slope) at which the displacement increases rapidly. This point depicts the beginning of the tertiary creep. The diagram is used only for incremental loading tests.
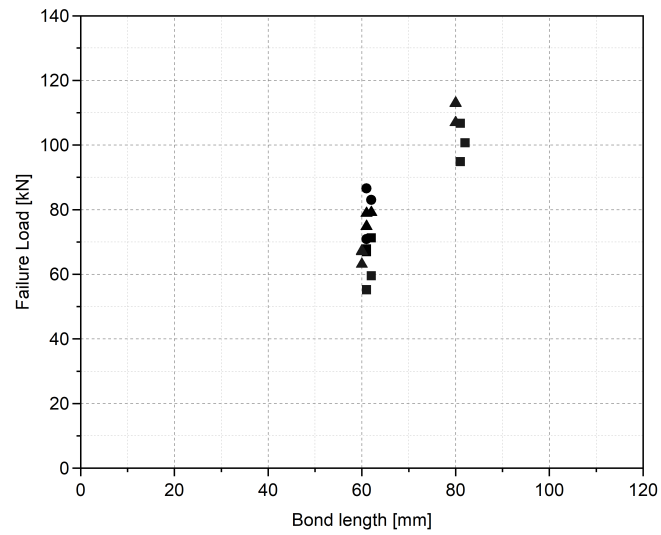
(A) failure load vs bond length
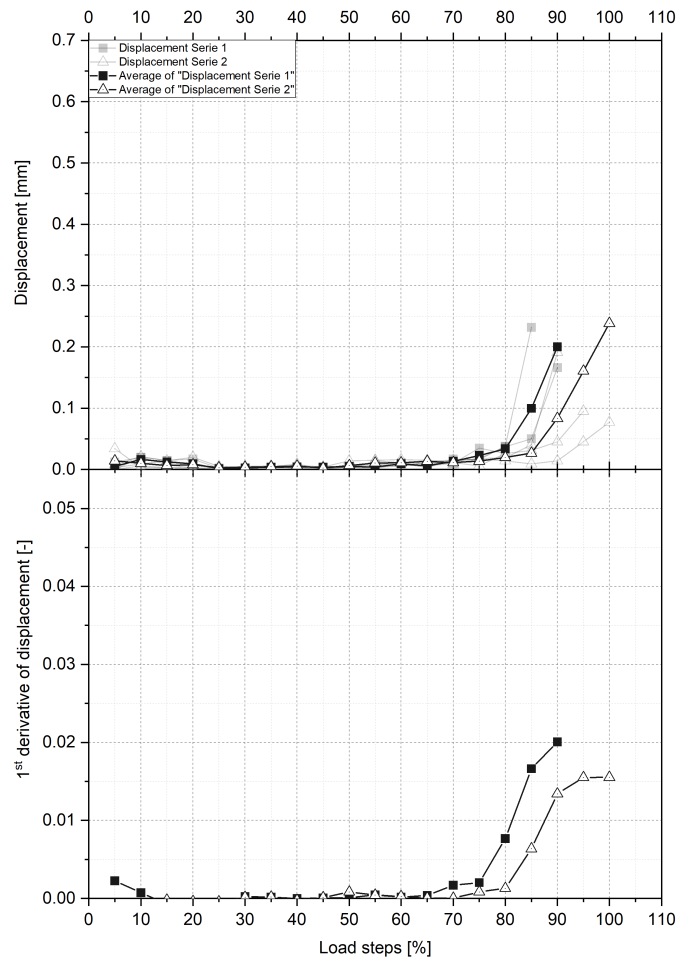
(B) displacement vs load steps

FIGURE 6.1: Example diagrams for the incremental loading tests

6.3.3   Influence of incremental loading

The direct influence of the type of loading was studied with six series for confined setup and eight series with unconfined setup. Apart from the loading methods, the embedment depth and hole cleaning procedure were varied. Table 6.2 gives an overview of the results of these tests.

TABLE 6.2: Summary of the test results for the influence of incremental loading

Test series [−]	d [mm]	h_{ef} [mm]	Support [−]	$N_{u,m}$ [kN]	σ [kN]	Failure mode [−]
D028*	12	60	confined	78.62	2.34	$1xP, 4xP_M$
D029	12	60	confined	68.71	2.27	$2xP_M, 1xM1$
D033	12	60	confined	42.13	2.36	$2xP_M, 1xM1$
D034*	12	60	confined	47.00	4.62	$3xP_M$
D070*	12	80	confined	118.23	2.35	$1xP, 1xP_M, 3xM1$
D074	12	80	confined	100.77	5.93	$1xP_M, 2xM1$
D030*	12	60	unconfined	39.22	3.33	$5xC$
D031& D032	12	60	unconfined	33.94	2.61	$5xC$
D035	12	60	unconfined	30.86	2.28	$3xM2$
D036*	12	60	unconfined	35.86	2.19	$3xM2$
D041& D042*	12	80	unconfined	57.87	3.25	$2xC, 3xM2$
D043	12	80	unconfined	46.99	3.17	$1xC, 2xM2$
D071*	12	105	unconfined	89.99	12.92	$1xC, 4xM2$
D072	12	105	unconfined	81.58	4.64	$3xM2$

*Short-term tests

The confined tests were carried out on two embedment depths: 60 mm and 80 mm, whereas for the unconfined setup, all three depths were studied. Four series: D033, D034, D035 and D036 were installed with hole condition 2 corresponding to reduced hole cleaning (1XHP) in dry concrete. Figure 6.2 illustrates the influence of incremental loading on the failure load of the adhesive anchors for both setups. It is apparent, that the short-term tests have higher failure loads compared to the incremental loading tests.

The anchors tested under confined test setup revealed a higher reduction in the residual capacity. The mean failure load
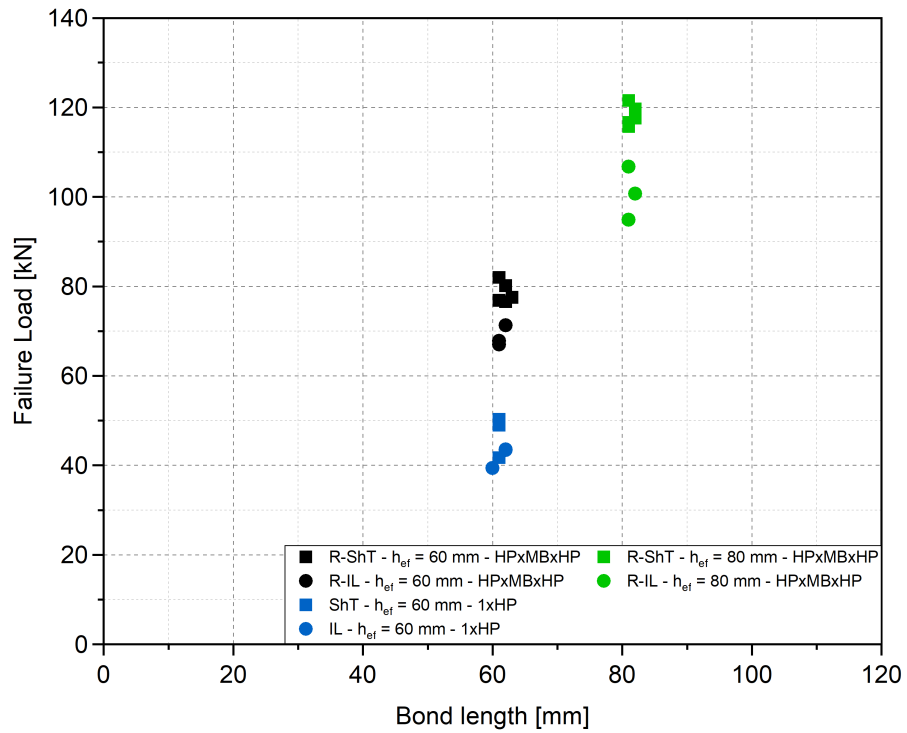
(A) confined test
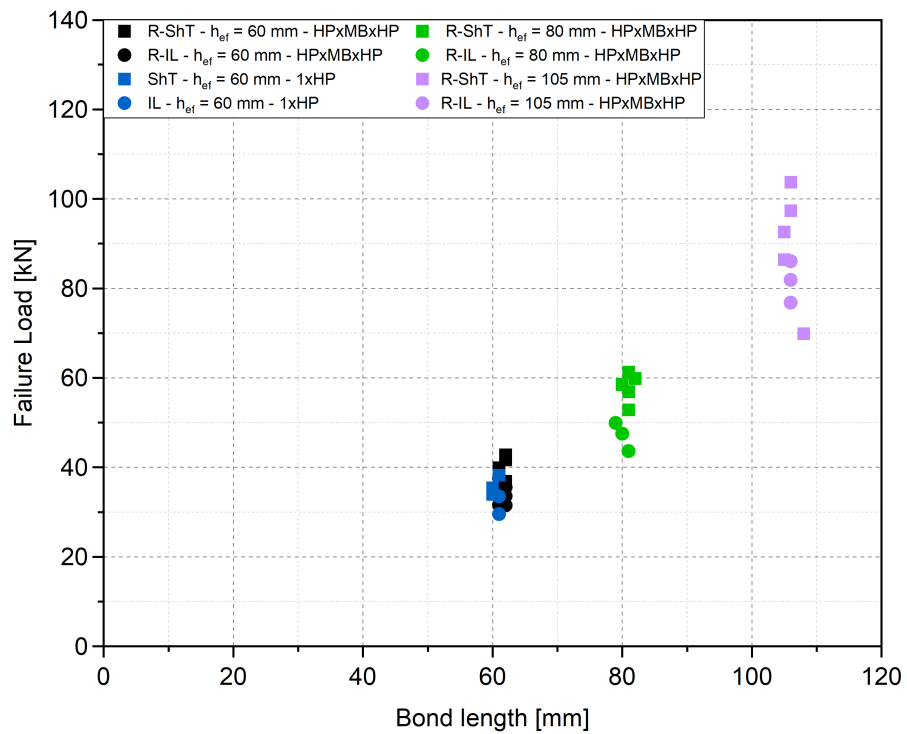
(B) unconfined test

FIGURE 6.2: Failure load vs bond length curves - influence of the type of loading

for the anchors with embedment depth 60 mm and standard hole cleaning decreased from 78.62 kN for short-term tests to 68.71 kN for incremental loading. An increase of the embedment depth to 80 mm, showed a decrease of 17 % on the failure load. Despite the reduced cleaning effort and an overall lower failure load compared to the standard hole cleaning series (see Section 5.3.1), series D033 showed 10 % lower failure load compared to its reference series D034.

Similarly behaved the tests with unconfined setup. The incremental load tests showed 13 %, 19 % and 10 % lower failure loads compared to the short-term tests for 60 mm, 80 mm and 105 mm depth, respectively. The short-term test with reduced cleaning showed 14 % increase in the failure loads compared to the incremental loading tests.

6.3.4   Influence of hole cleaning

The influence of hole cleaning was investigated on two embedment depths: 60 mm and 80 mm. Besides the tests at room temperature, test series D049 and D065, were performed at 43 °C with 60 mm depth and tested with a confined setup. Table 6.3 summarizes the test results.

Overall, the reduced cleaning effort affected the carrying capacity of the adhesive anchors. Figure 6.3 illustrates the failure loads for both testing setups.

As expected, the comparison of the short-term tests D028 with D034 and D030 with D036 revealed a decrease in the mean failure load due to the poor cleaning procedure. This decrease was equal to 40 % and 9 %, respectively. It should be highlighted, that this influence was greater in the confined setup tests.

Similar results revealed the tests with incremental loading. The confined tests at both embedment depths at room temperature showed a 39 % lower failure load due to the cleaning method whereas the anchors subjected to the increased temperature of 43 °C only 19 % drop in the load. The unconfined tests, similar to the short-term tests, failed with less than 12 % of the loads of the tests with standard cleaning procedure.

TABLE 6.3: Summary of the test results for the influence of hole cleaning

Test series	d	h_{ef}	Support	Cleaning	$N_{u,m}$	σ	Failure mode
$[-]$	$[mm]$	$[mm]$	$[-]$	$[-]$	$[kN]$	$[kN]$	$[-]$
D028	12	60	confined	HPxMBxHP	78.62	2.34	$1xP, 4xP_M$
D034	12	60	confined	1xHP	47.00	4.62	$3xP_M$
D029	12	60	confined	HPxMBxHP	68.71	2.27	$2xP_M, 1xM1$
D033	12	60	confined	1xHP	42.13	2.36	$2xP_M, 1xM1$
D049	12	60	confined	HPxMBxHP	56.68	2.48	$3xP_M$
D065	12	60	confined	1xHP	45.92	8.23	$3xP_M$
D074	12	80	confined	HPxMBxHP	100.77	5.93	$1xP_M, 2xM1$
D075	12	80	confined	1xHP	61.88	2.01	$3xM1$
D030	12	60	unconfined	HPxMBxHP	39.22	3.33	$5xC$
D036	12	60	unconfined	1xHP	35.86	2.19	$3xM2$
D031& D032	12	60	unconfined	HPxMBxHP	33.94	2.61	$5xC$
D035	12	60	unconfined	1xHP	30.86	2.28	$3xM2$
D043	12	80	unconfined	HPxMBxHP	46.99	3.17	$1xC, 2xM2$
D044	12	80	unconfined	1xHP	41.53	4.50	$3xM2$

This influence is observed in the displacements after each loading steps as well. Figure 6.4 illustrates the displacements for the confined tests. Series D028 and D070 served as reference short-term test for the tests with 60 mm and 80 mm embedment depth, respectively.

Figure 6.4 shows that the incremental tests with standard cleaning procedure failed between 65 % and 85 % of the reference short-term test, whereas the reduced cleaning tests, failed prior to the anchors reaching 50 % of the reference loads. The residual displacement for D029 and D033 (Figure 6.4a) followed the same increase pattern, which differs from the other two cases, where the mean residual displacement remained under 0.05 mm until 40 % loading.

The first derivatives show that the displacements of the tests with standard cleaning effort start increasing immediately after 60 % (Figure 6.4a), 50 % (Figure 6.4b) and 65 % (Figure 6.4c) of the reference tests' load is applied. On the other hand, the tests with reduced cleaning, show an increase after 35 % (Figure 6.4a), 30 % (Figure 6.4b) and 40 % (Figure 6.4c) of the load is applied.
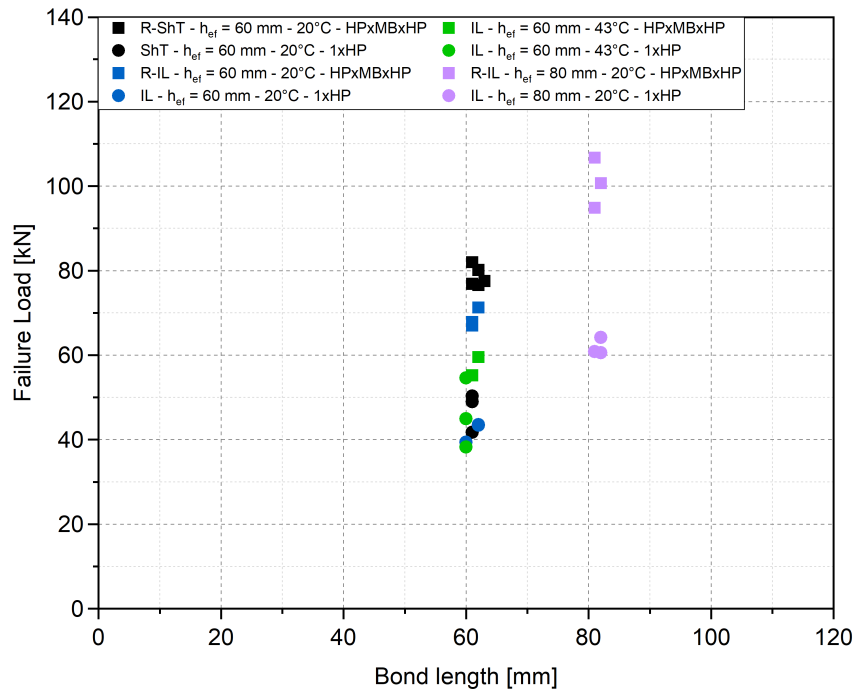
(A) confined test
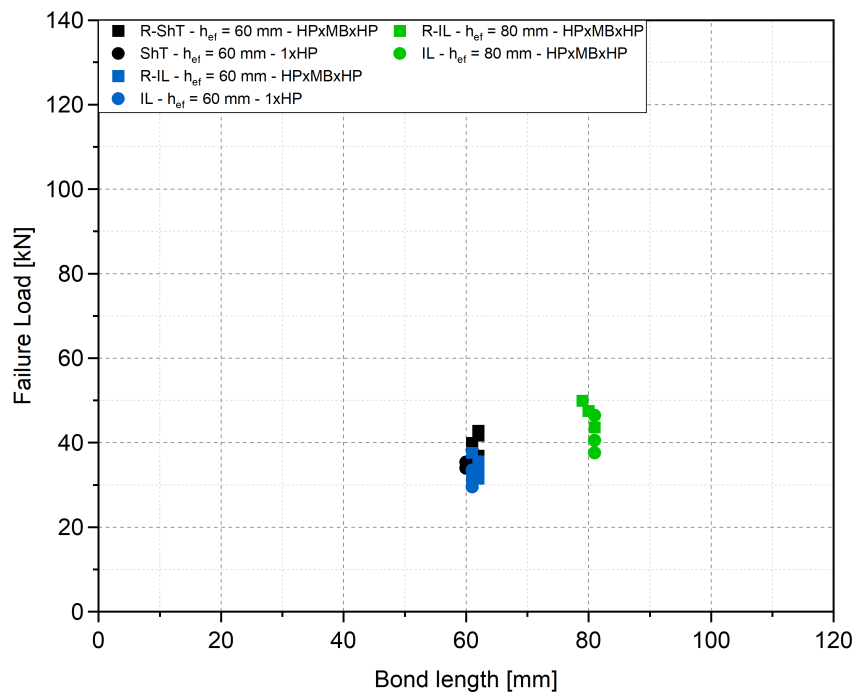
(B) unconfined test

FIGURE 6.3: Failure load vs bond length curves -
influence of the hole cleaning
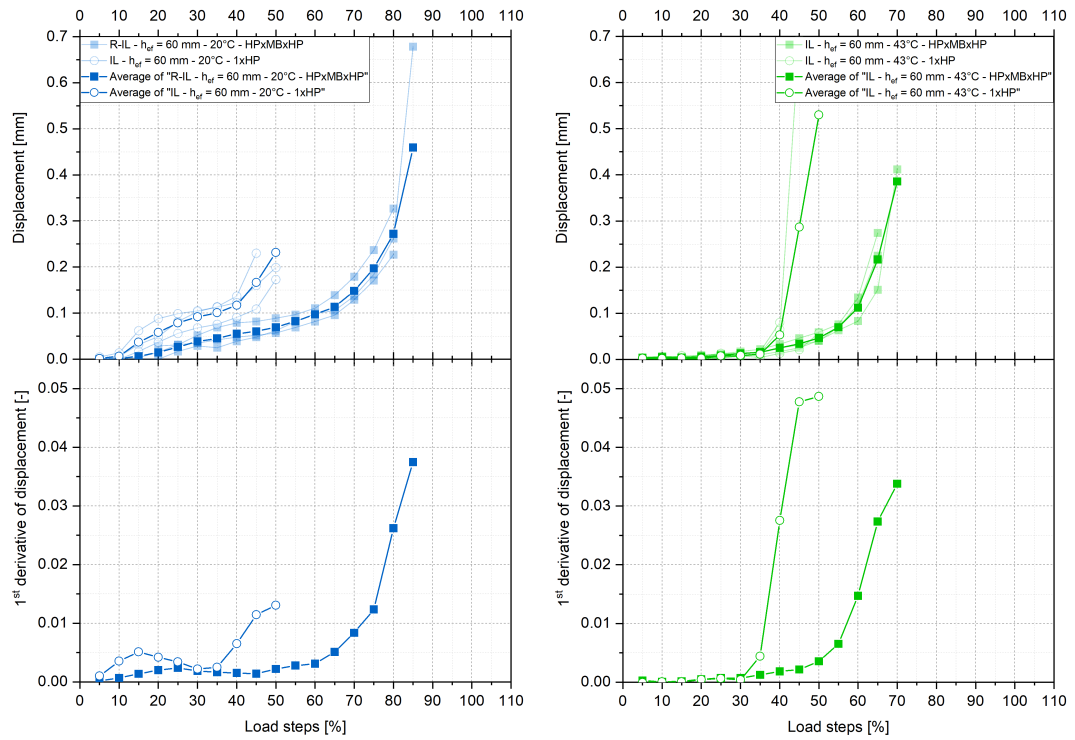
(A) $h_{ef} = 60 \text{ mm}, 20\,^{\circ}C$

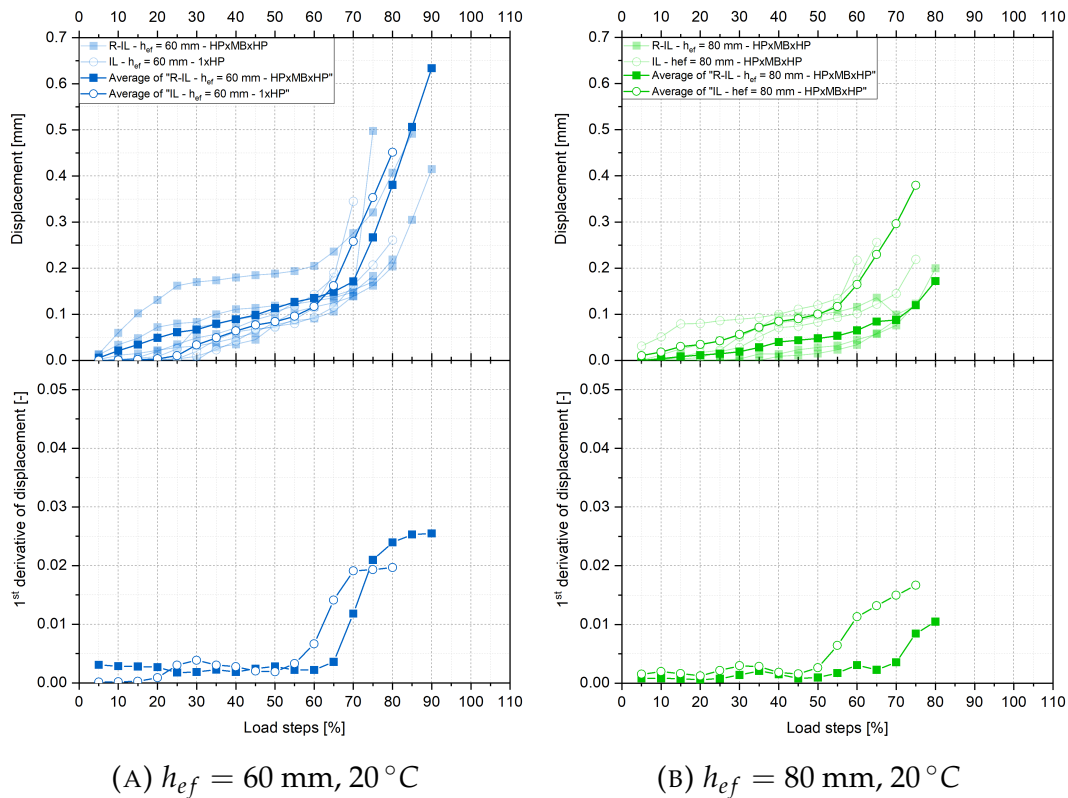(B) $h_{ef} = 60 \text{ mm}, 43\,^{\circ}C$
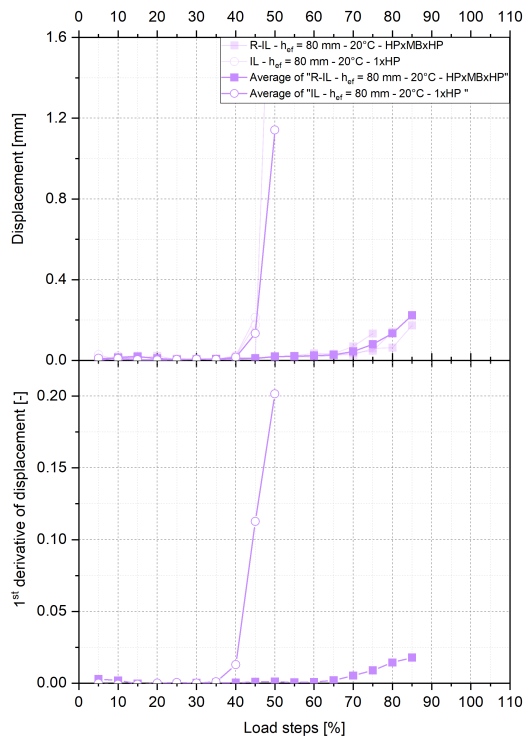
(C) $h_{ef} = 80 \text{ mm}, 20\,^{\circ}C$

FIGURE 6.4: Displacement after unloading at each load increment for confined tests - influence of the hole cleaning

Surprisingly, the unconfined tests showed a lower influence from the reduced cleaning procedure (Figure 6.5). The reference incremental loading tests failed between 70 % and 90 % of the reference short-term test load compared to the reduced cleaning effort tests which reached $60 - 80\,\%$ of these loads. The overall residual displacements for the anchors installed at 80 mm depth were lower compared to the displacement of the anchors at 60 mm depth.

The first derivatives of the displacements show that the displacements for the unconfined tests with standard cleaning effort increase rapidly at 60 % (Figure 6.5a) and 65 % (Figure 6.5b) load, whereas for the reduced cleaning tests, this change starts at 50 % of the applied load.

(A) $h_{ef} = 60$ mm, $20\,^{\circ}C$ (B) $h_{ef} = 80$ mm, $20\,^{\circ}C$

FIGURE 6.5: Displacement after unloading at each load increment for unconfined tests - influence of the hole cleaning

6.3.5 Influence of annular gap

Only incremental loading tests were carried out to investigate the influence of the annular gap on the residual capacity of the anchor as illustrated in Table 6.4. The anchors were installed using two annular gaps: RS2 - 2 mm (d_{cut} = 16 mm) and RS4 - 4 mm (d_{cut} = 20 mm). RS4 thickness was investigated for all cases, while RS2 only for the anchors tested at room temperature at 60 mm (both test setups) and at 80 mm or 105 mm under unconfined setup. The reference annular gap for M12 threaded rods was 1 mm (d_{cut} = 14 mm).

TABLE 6.4: Summary of the test results for the
influence of the annular gap

| Test series	d	h_{ef}	Support	Gap	$N_{u,m}$	σ	Failure mode
[−]	[*mm*]	[*mm*]	[−]	[*mm*]	[*kN*]	[*kN*]	[−]
D029	12	60	confined	1	68.71	2.27	$2xP_M, 1xM1$
D037	12	60	confined	2	80.16	8.24	$3xP$
D039	12	60	confined	4	77.62	2.42	$3xP$
D049	12	60	confined	1	56.68	2.48	$3xP_M$
D066	12	60	confined	4	65.80	2.32	$1xP, 2xP_M$
D074	12	80	confined	1	100.77	5.93	$1xP_M, 2xM1$
D076	12	80	confined	4	110.95	3.47	$3xP$
D031& D032	12	60	unconfined	1	33.94	2.61	$5xC$
D038	12	60	unconfined	2	39.38	0.07	$1xC, 2xM2$
D040	12	60	unconfined	4	39.02	4.45	$3xC$
D043	12	80	unconfined	1	46.99	3.17	$1xC, 2xM2$
D045	12	80	unconfined	2	58.26	0.41	$3xM2$
D046	12	80	unconfined	4	57.08	3.42	$3xC$
D050	12	60	unconfined	1	31.42	2.19	$3xC$
D068	12	60	unconfined	4	33.98	1.75	$3xC$
D051	12	80	unconfined	1	45.63	3.27	$3xM2$
D069	12	80	unconfined	4	49.44	2.97	$3xM2$
D072	12	105	unconfined	1	81.58	4.64	$3xM2$
D073	12	105	unconfined	4	90.22	4.41	$1xC, 2xM2$

Figure 6.6a presents the results of the confined tests. As it can be seen, the tests at room temperature at 60 mm embedment depth showed an increase in the failure load of 17 % for annular gap RS2, however only 13 % for RS4. At higher embedment depth (80 mm), the load for the tests with 4 mm annular gap was

10 % higher compared to its reference series. Furthermore, the anchors at elevated temperature, revealed also an increase in the failure load when drilling with a larger drill bit (16 % rise in load).

Similar behaviour exhibited the tests shown in Figure 6.6b. The results of the tests at room temperature with 2 mm annular gap at both embedment depths (60 mm and 80 mm) failed at higher loads compared to the reference tests with 1 mm annular gap (16 % and 24 %, respectively). A further increase to 4 mm, showed also an increase of the load compared to the reference tests, however a slight decrease compared to the RS2 tests. The tests at 43 °C and RS4 annular gap failed with 16 % (60 mm) and 8 % (80 mm) higher loads compared to the tests with 1 mm annular gap. Lastly, the anchors installed at 105 mm and RS4 thickness showed a rise of 11 % in the failure load.

The displacements after unloading each increment are illustrated in Figure 6.7 for the confined setup tests.

The tests with an annular gap of 2 mm failed at a minimum of 85 % of the short-term loads. Likewise, the results with 4 mm thickness failed mostly after 85 % loading at room temperature and after 75 % at 43 °C.

The residual displacements for the anchors installed at 60 mm (Figure 6.7a) were higher in comparison with the other cases, where the displacements were smaller than 0.1 mm at 50 % of the reference load (43 °C) or smaller than 0.05 mm at 60 % load (20 °C).

Comparing the first derivatives of the displacements for the confined tests, showed that the sudden increase in the displacements for the reference tests with 1 mm annular gap started prior to the increase of the displacements for the tests with 2 mm and 4 mm annular gap. Moreover, the tests at room temperature (Figures 6.7a and 6.7c) revealed a rapid rise in the displacement after 60 % (for 1 mm annular gap) and 75 % (for 2 mm or 4 mm annular gap) of the load for both embedment depths (60 mm and 80 mm). The tests at 43 °C, on the other hand, showed this increase after 45 % (for 1 mm annular gap) and 65 % (for 4 mm annular gap) of the applied load was reached (Figure 6.7b).
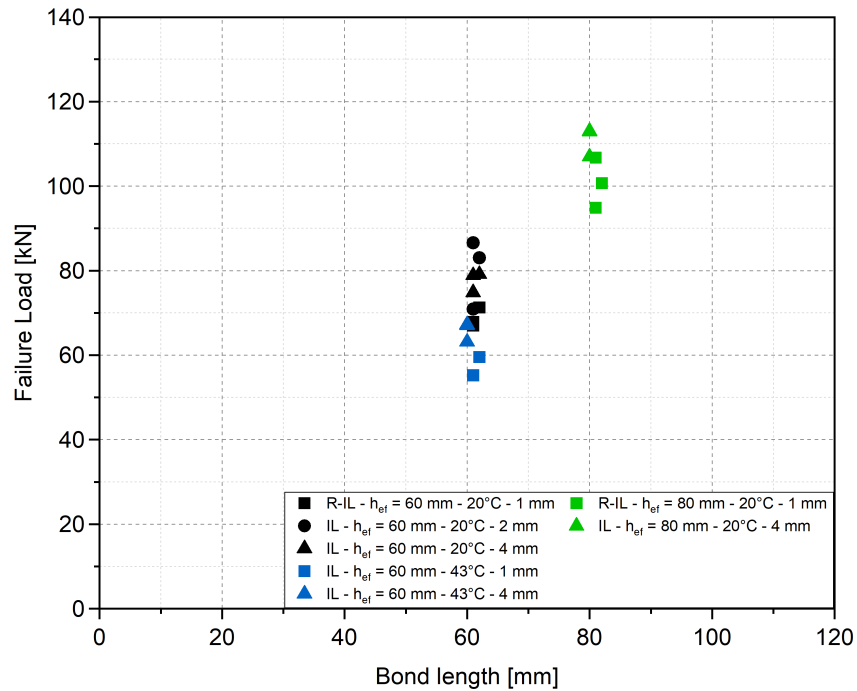
(A) confined test
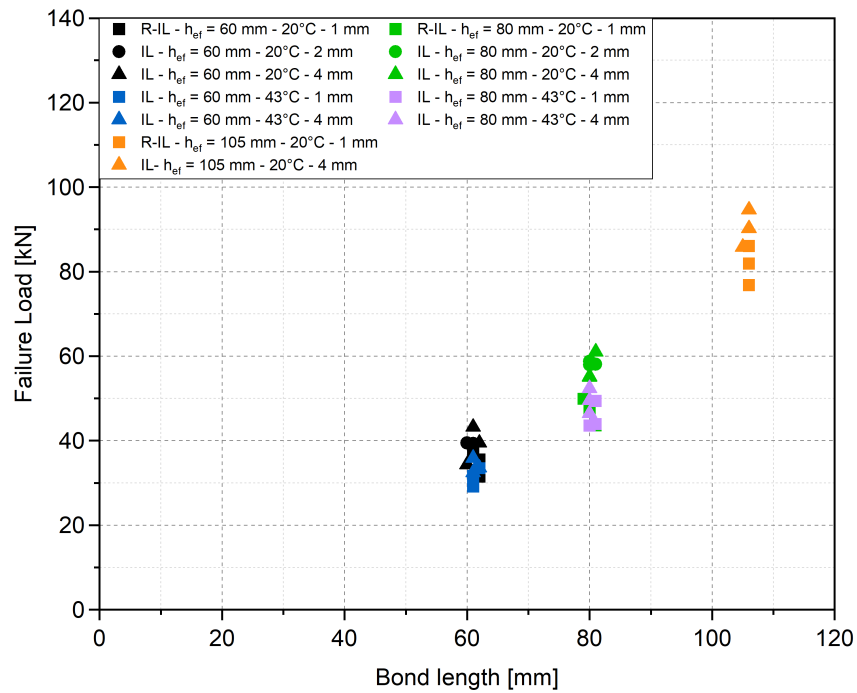
(B) unconfined test

FIGURE 6.6: Failure load vs bond length curves -
influence of the annular gap
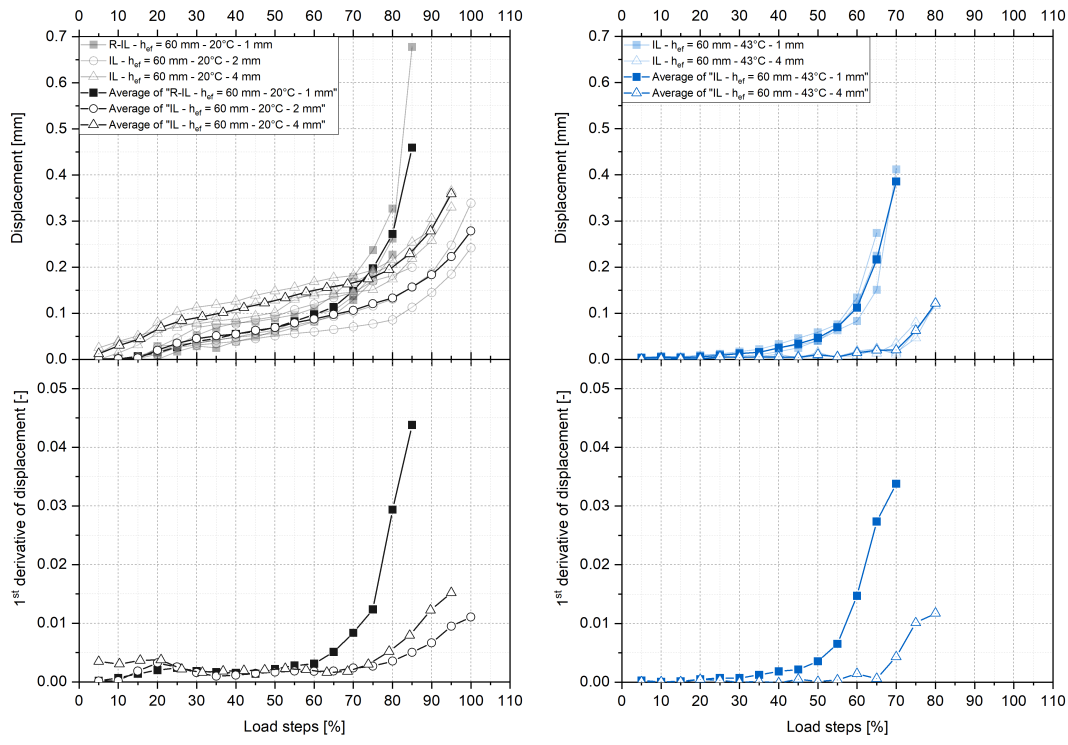
(A) $h_{ef} = 60$ mm, $20\,^{\circ}C$
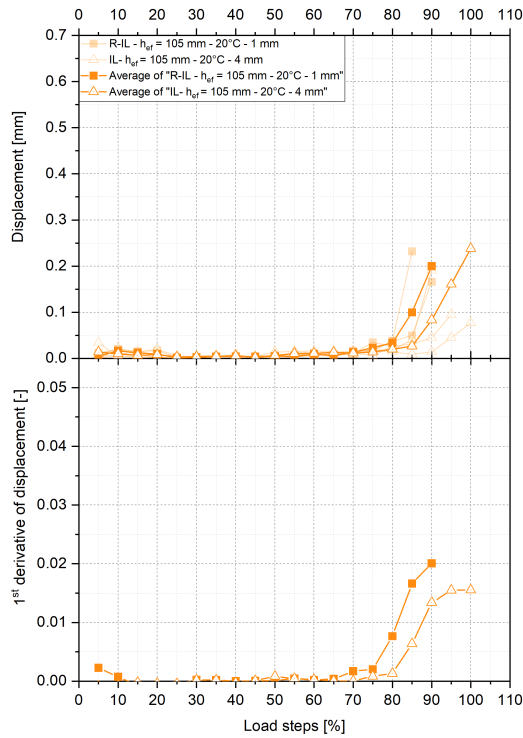
(B) $h_{ef} = 60$ mm, $43\,^{\circ}C$
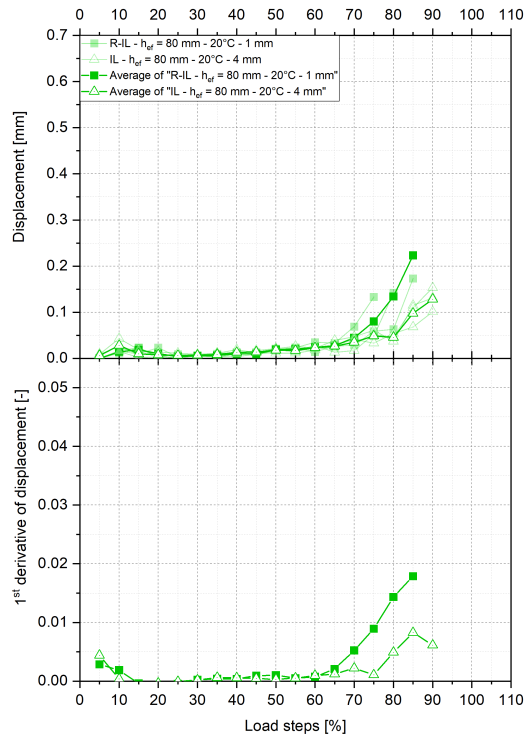
(C) $h_{ef} = 80$ mm, $20\,^{\circ}C$

FIGURE 6.7: Displacement after unloading at each load increment for confined tests - influence of the annular gap

Figure 6.8 illustrates the residual displacements and their first derivatives for the unconfined tests.

Similar to the confined tests, the tests with an annular gap of 2 mm failed at a minimum of 85 % of the short-term load in both testing setups. The anchors installed with 4 mm thickness failed mostly after 85 % loading at room temperature and after 75 % at $43\,^{\circ}C$.

The residual displacement for the anchors installed at 60 mm (Figure 6.8a) and for 80 mm (Figure 6.8c) were higher in comparison with the other cases.

The immediate increase of the displacements for the reference tests (1 mm annular gap) occurs prior to the increase of the other tests, similar to the confined tests.
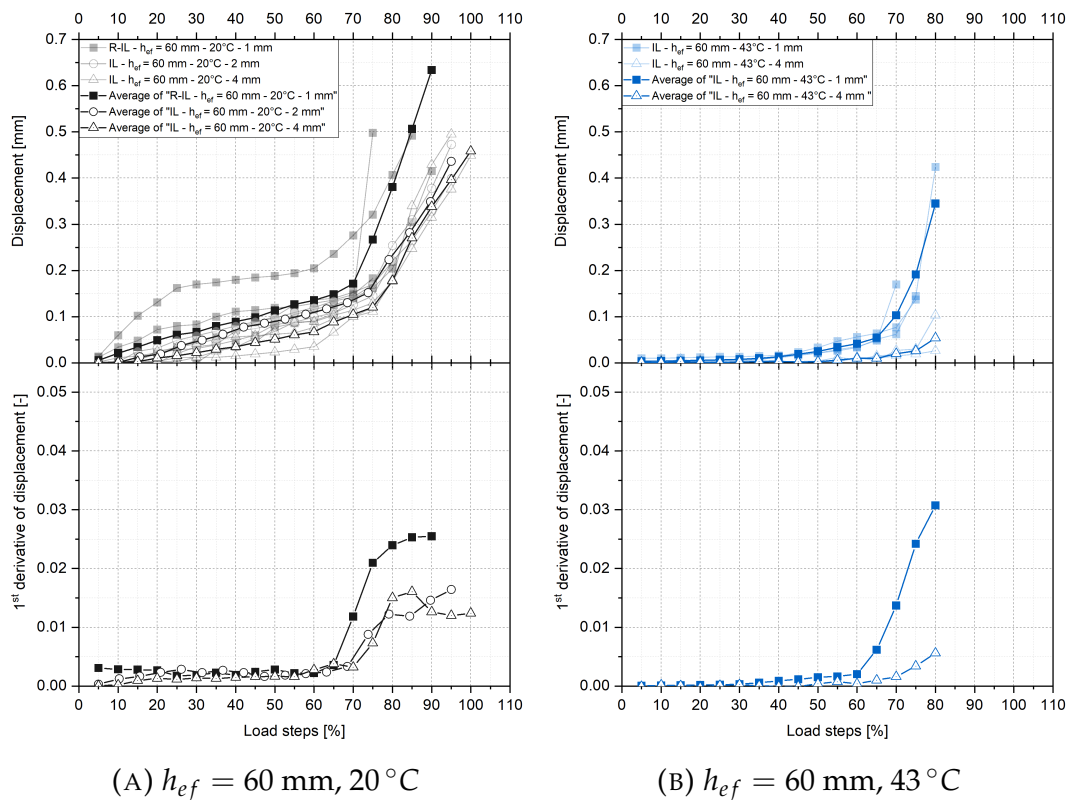
(A) $h_{ef} = 60$ mm, $20\,^{\circ}C$ \quad (B) $h_{ef} = 60$ mm, $43\,^{\circ}C$

FIGURE 6.8: Displacement after unloading at each load increment for unconfined tests - influence of the annular gap
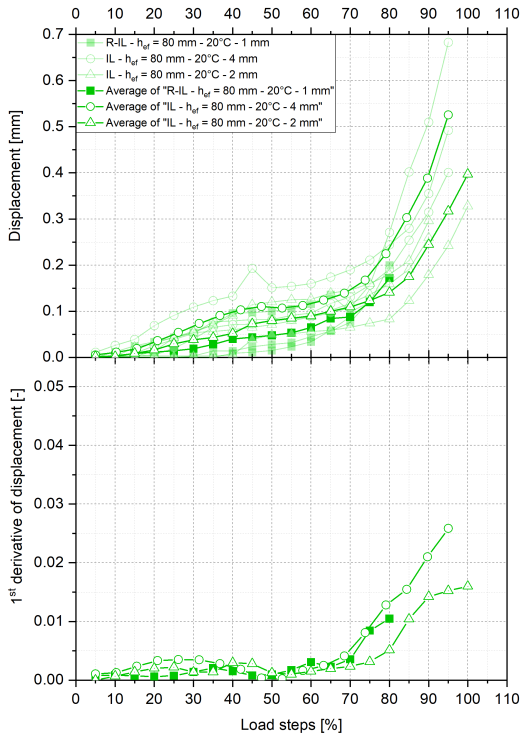
(C) $h_{ef} = 80$ mm, $20\,°C$
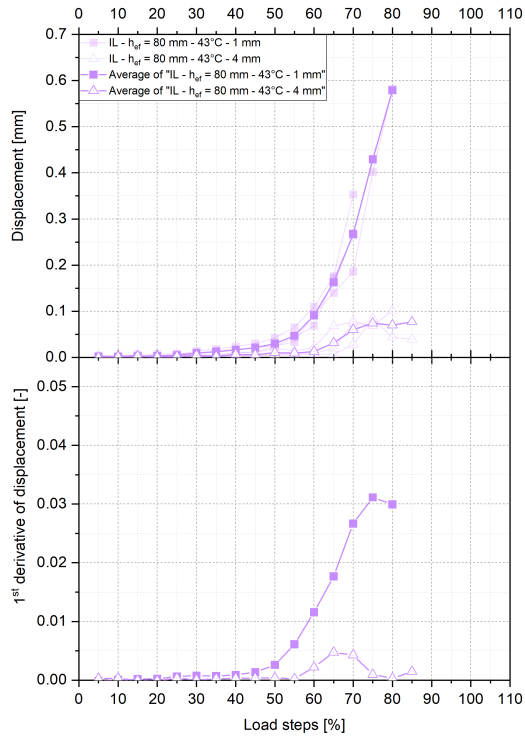
(D) $h_{ef} = 80$ mm, $43\,°C$

(E) $h_{ef} = 105$ mm, $20\,°C$

FIGURE 6.8: Displacement after unloading at each load increment for unconfined tests - influence of the annular gap

6.3.6 Influence of wet concrete

Four tests series at 60 mm embedment depth were carried out to investigate the influence of wet concrete. A summary is given in Table 6.5. As expected, the failure loads for confined tests were higher compared to the unconfined tests (see Figure 6.9). However, the installation of the anchors in wet concrete influenced the capacity of the anchor minimally. For the confined tests, the anchors installed in wet concrete showed 5 % lower failure load, whereas the unconfined tests showed only 3 % lower load.

TABLE 6.5: Summary of the test results for the
influence of concrete condition

Test series	d	h_{ef}	Support	Condition	$N_{u,m}$	σ	Failure mode
$[-]$	$[mm]$	$[mm]$	$[-]$	$[-]$	$[kN]$	$[kN]$	$[-]$
D029	12	60	confined	dry	68.71	2.27	$2xP_M, 1xM1$
D048	12	60	confined	wet	65.06	5.15	$2xP_M, 1xM1$
D031& D032	12	60	unconfined	dry	33.94	2.61	$5xC$
D047	12	60	unconfined	wet	32.83	1.20	$3xM2$
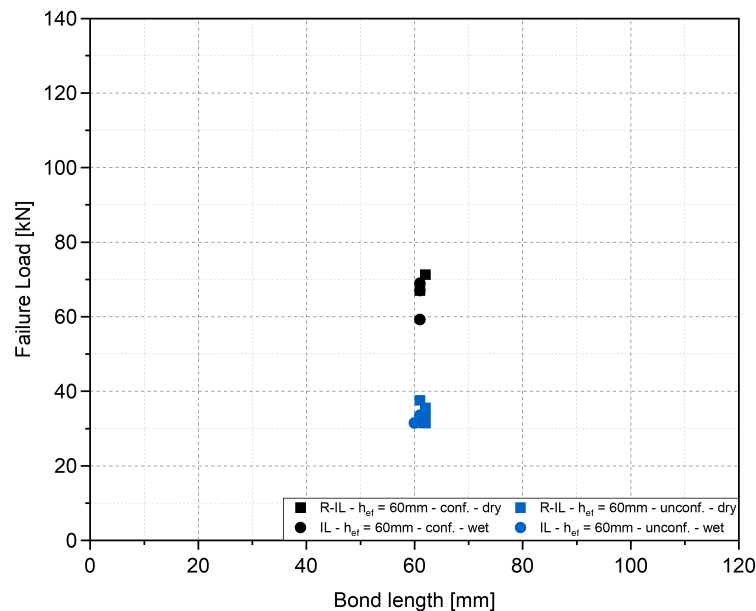
FIGURE 6.9: Failure load vs bond length curves -
influence of the concrete condition

Figure 6.10 illustrates the displacement of the anchors after unloading for confined and unconfined tests. It can be seen, that the confined tests in wet concrete failed in the range 70 % to 80 % of the reference short-term load. Similar behaviour showed the unconfined tests.

The residual displacements at the same load steps were higher for the confined tests than the unconfined tests, for example, at 50 % applied load, the average value of the displacement for confined tests was 0.11 mm whereas for unconfined 0.07 mm.

The first derivative of the displacement for the confined tests showed that the displacements in dry concrete started increasing rapidly at 60 % of the load, whereas for the anchors in wet concrete at 50 %. Different was the case for the unconfined tests, where the increase in displacement occurred for the anchors in wet concrete later than for those in dry concrete (70 % and 65 % of the applied load, respectively).
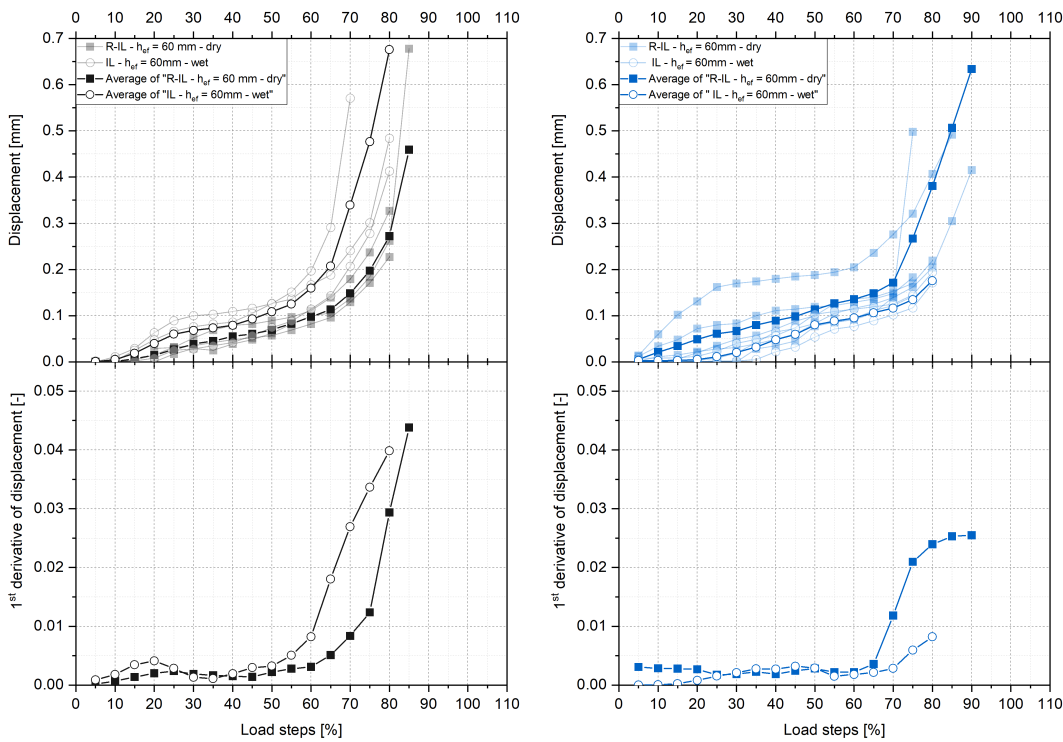
(A) $h_{ef} = 60$ mm, confined   (B) $h_{ef} = 60$ mm, unconfined

FIGURE 6.10: Displacement after unloading at each load increment - influence of the concrete condition

6.3.7 Influence temperature

Table 6.6 summarizes the results of the tests where the influence of temperature was investigated. For each support, eight test series were carried out focusing on two embedment depths (60 mm, 80 mm). Other varied parameters were cleaning effort and annular gap. The tests were carried out at room temperature and at 43 °C.

TABLE 6.6: Summary of the test results for the influence of testing temperature

Test series	d	h_{ef}	Support	Temp.	$N_{u,m}$	σ	Failure mode
[−]	[mm]	[mm]	[−]	[°]	[kN]	[kN]	[−]
D029	12	60	confined	20	68.71	2.27	$2xP_M, 1xM1$
D049	12	60	confined	43	56.68	2.48	$3xP_M$
D033	12	60	confined	20	42.13	2.36	$2xP_M, 1xM1$
D065	12	60	confined	43	45.92	8.23	$3xP_M$
D039	12	60	confined	20	77.62	2.42	$3xP$
D066	12	60	confined	43	65.80	2.32	$1xP, 2xP_M$
D067	12	80	confined	43	81.56	8.69	$3xP_M$
D074	12	80	confined	20	100.77	5.93	$1xP_M, 2xM1$
D031& D032	12	60	unconfined	20	33.94	2.61	$5xC$
D050	12	60	unconfined	43	31.42	2.19	$3xC$
D040	12	60	unconfined	20	39.02	4.45	$3xC$
D068	12	60	unconfined	43	33.98	1.75	$3xC$
D043	12	80	unconfined	20	46.99	3.17	$1xC, 2xM2$
D051	12	80	unconfined	43	45.63	3.27	$3xM2$
D046	12	80	unconfined	20	57.08	3.42	$3xP_M$
D069	12	80	unconfined	43	49.44	2.97	$3xM2$

The results showed an influence of the temperature on the carrying capacity of the anchors as seen in Figure 6.11. At 60 mm depth, the load decreased approximately 18 % for confined tests and 7 % for unconfined tests with an increased testing temperature of 43 °C. With an increase of the embedment depth to 80 mm, the same trend was observed, 19 % and 3 % lower failure loads for confined and unconfined tests.
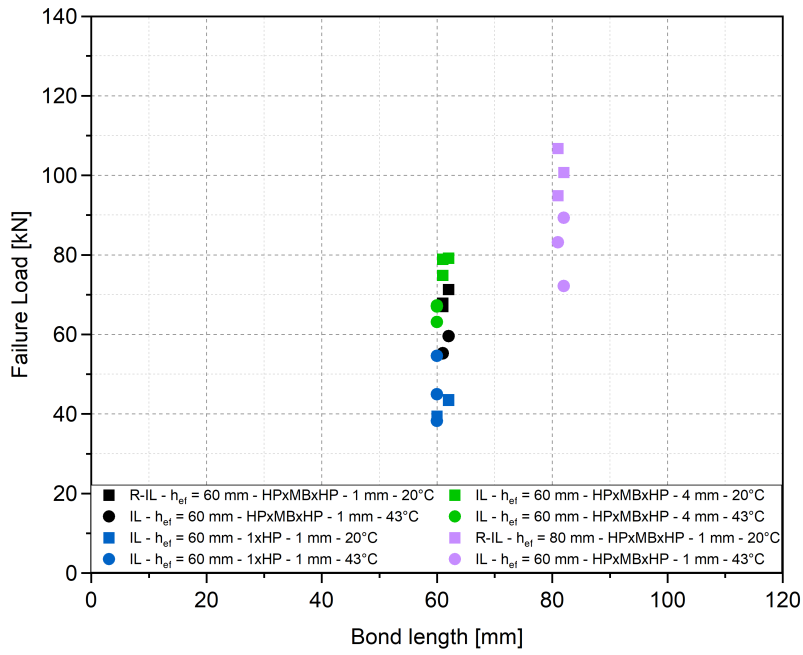
(A) confined test
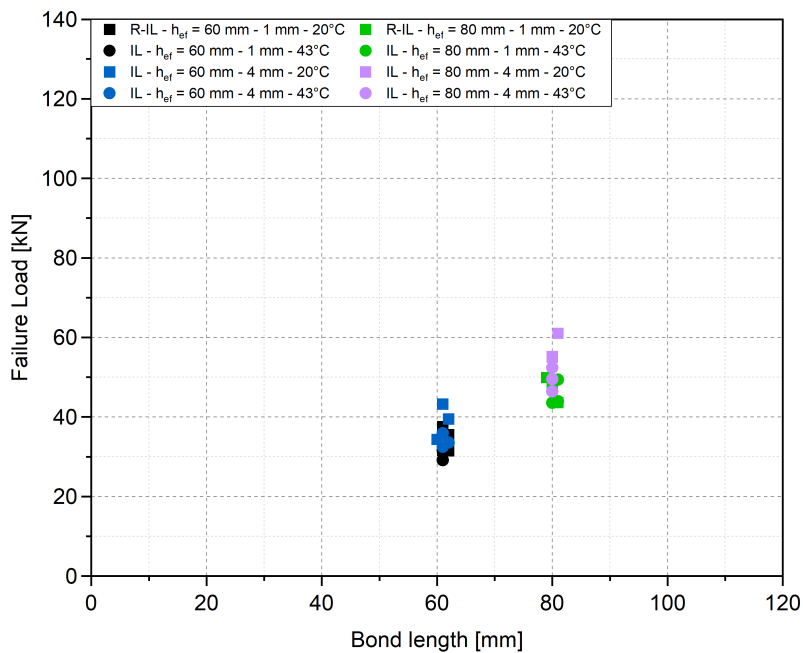
(B) unconfined test

FIGURE 6.11: Failure load vs bond length curves -
influence of the testing temperature

The next parameter taken into consideration was the annular

gap 4 mm. The confined tests at 60 mm showed 15 % lower residual capacity at increased temperature compared to the room temperature tests. Similarly, for unconfined tests, the loads dropped by 13 % for both embedment depths. The last parameter tested was the reduced cleaning effort, however only for confined setup at 60 mm embedment depth. The high testing temperature and reduced cleaning influenced positively the residual capacity of the anchors, the mean failure load increased from 42.13 kN for reference tests to 45.92 kN (9 % load increase).

By examining the displacement after unloading for the incremental loading tests, the following observations were made. The displacement of the confined tests at increased temperature 43 °C were smaller compared to the residual displacements of the anchors tested at room temperature (see Figure 6.12).
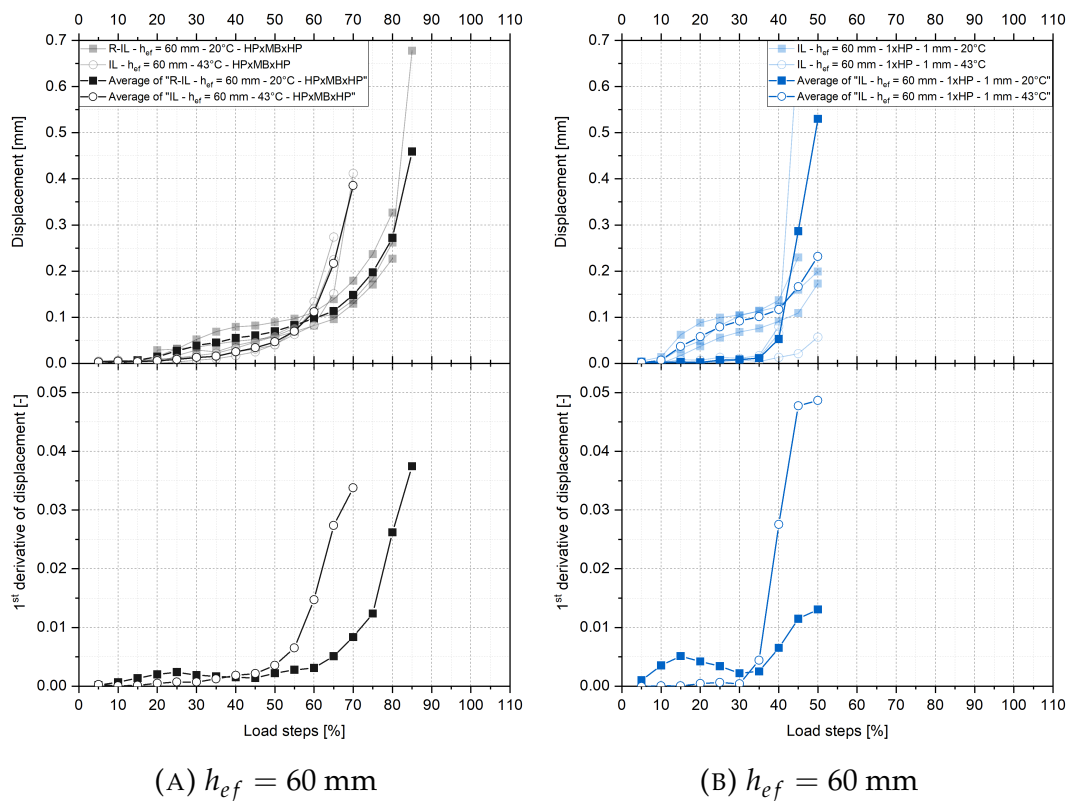
(A) $h_{ef} = 60$ mm (B) $h_{ef} = 60$ mm

FIGURE 6.12: Displacement after unloading at each load increment for confined tests - influence of the testing temperature

The anchors installed at 60 mm and 80 mm embedment depth and tested under confined setup failed between 55 % and 70 % of
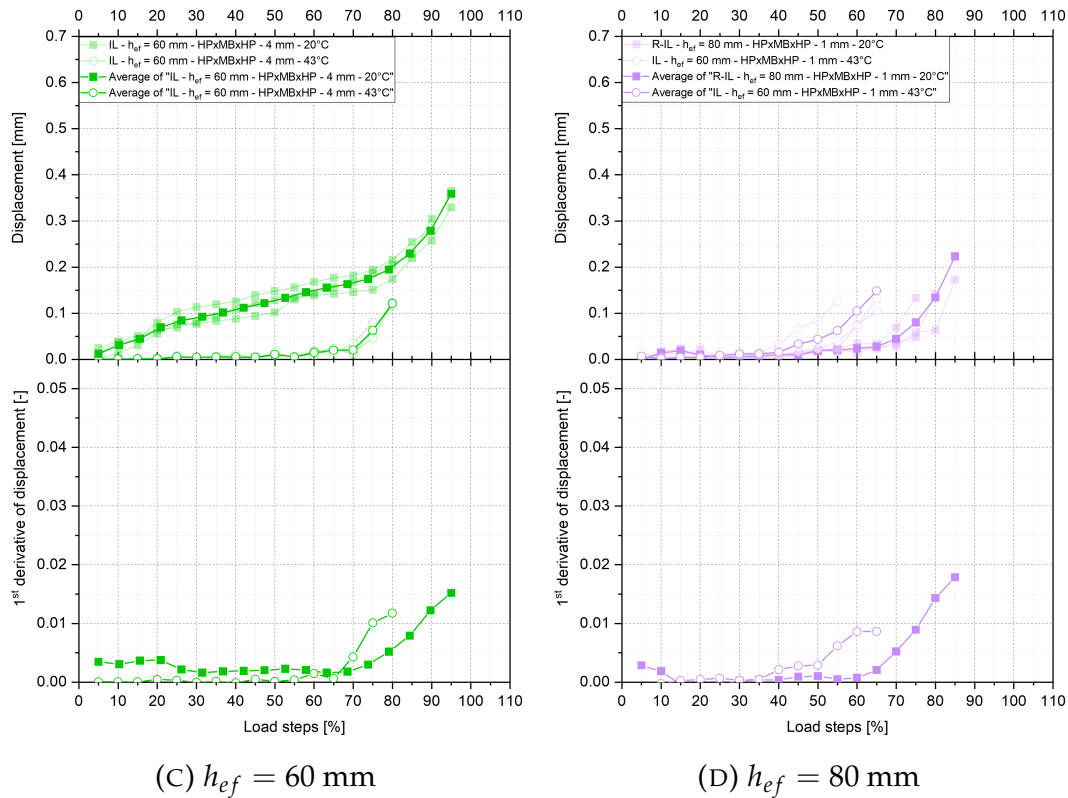
(C) $h_{ef} = 60\,\text{mm}$ (D) $h_{ef} = 80\,\text{mm}$

FIGURE 6.12: Displacement after unloading at each
load increment for confined tests - influence of the test-
ing temperature

the reference short-term load. By changing the concrete condi-
tion, the failure occurred prior to reaching 50 % of the load. On
the other hand, by increasing the drill bit diamater (annular gap),
the failure load was above 75 % of the reference short-term tests,
and the displacement up to 70 % load was below 0.05 mm.

The first derivatives of the displacements showed that rapid
increase in displacement happens for the tests at room tempera-
ture later than for the tests at 43 °C. Figure 6.12b illustrates the
influence that the cleaning effort has in the sudden increase of
the displacement for both testing temperatures.

Figure 6.13 shows the displacements for the unconfined tests.
As mentioned before, a consistent pattern appeared in this case.
The displacement of the incremental load tests was lower than
the reference incremental tests. It can also be noted, that the
displacement of the tests with 4 mm annular gap were smaller
compared to the tests with 1 mm annular gap. At 60 mm and

80 mm embedment depths, the unconfined tests failed after 75 % of the load was applied. The displacements were lower for the anchors installed at 60 mm as for those installed at higher depth. Comparing the same load level of 60 %, the mean displacements were 0.05 mm and 0.09 mm. The anchors at room temperature revealed a displacement of 0.15 mm and 0.06 mm respectively. The larger drilling diameter influenced positively the residual displacement at increase temperature. Up to 60 % of the reference short-term load, the displacements for both embedment depths were lower than 0.05 mm whereas the tests at room temperature exhibited more than 0.07 mm displacement.

Observing the first derivatives of the displacement, it can be seen that for the anchors with 1 mm annular gap at room temperature, the rapid increase of the displacement occurred at 65 % of the applied load (Figures 6.13a and 6.13c). On the other hand, for the increased temperature tests, the displacement starts to increase after 60 % and 50 % of the applied load, for embedment depths 60 mm and 80 mm, respectively. The anchors with 4 mm annular gap behaved similarly.
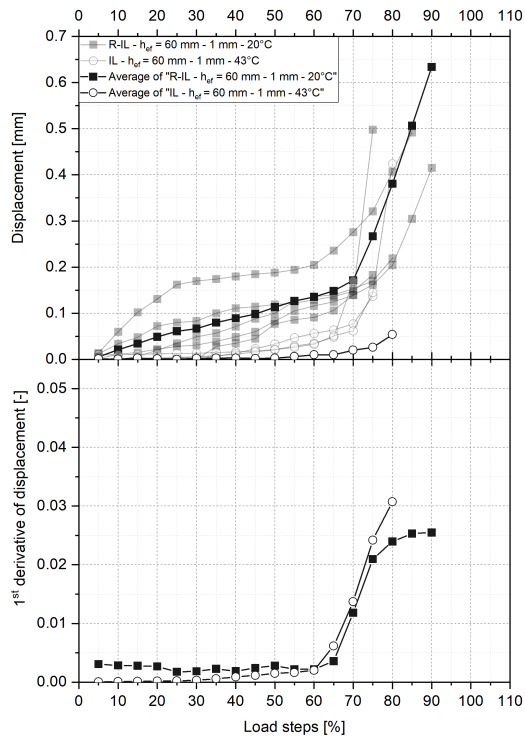
(A) $h_{ef} = 60$ mm
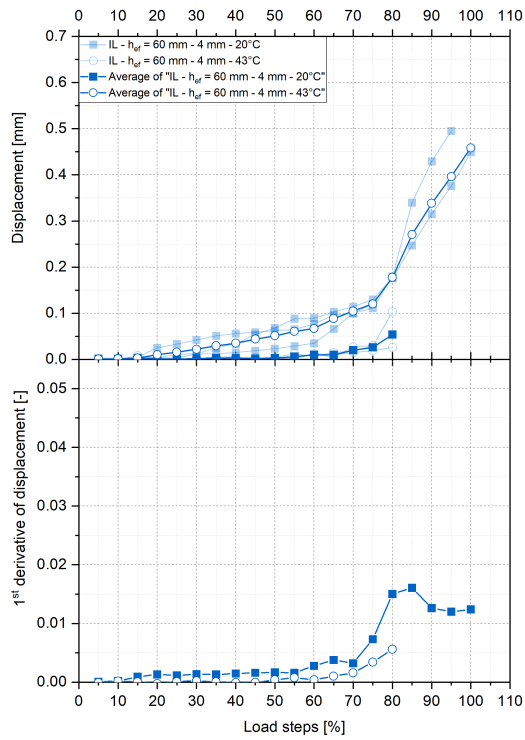
(B) $h_{ef} = 60$ mm
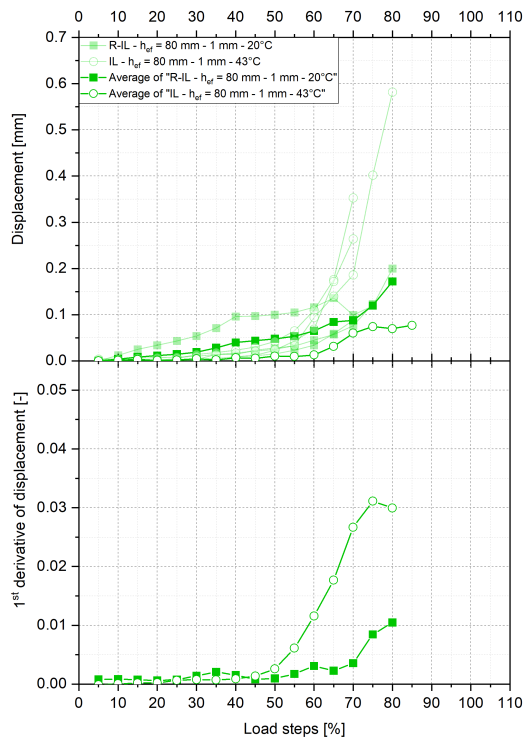
(C) $h_{ef} = 80$ mm
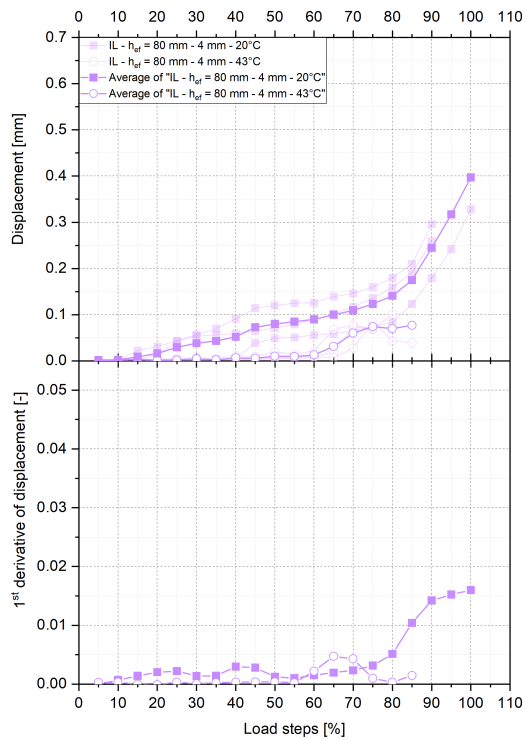
(D) $h_{ef} = 80$ mm

FIGURE 6.13: Displacement after unloading at each load increment for unconfined tests - influence of the testing temperature

6.3.8 Displacements of the incremental loading tests

Figure 6.14 to Figure 6.16 illustrate the displacements at 30 %, 50 % and 80 % of the applied reference load grouped according to the embedment depth and support width for each investigated parameter (annular gap, cleaning effort, concrete condition, increased temperature) as well as their reference tests. The mean displacements and their standard deviations are plotted.
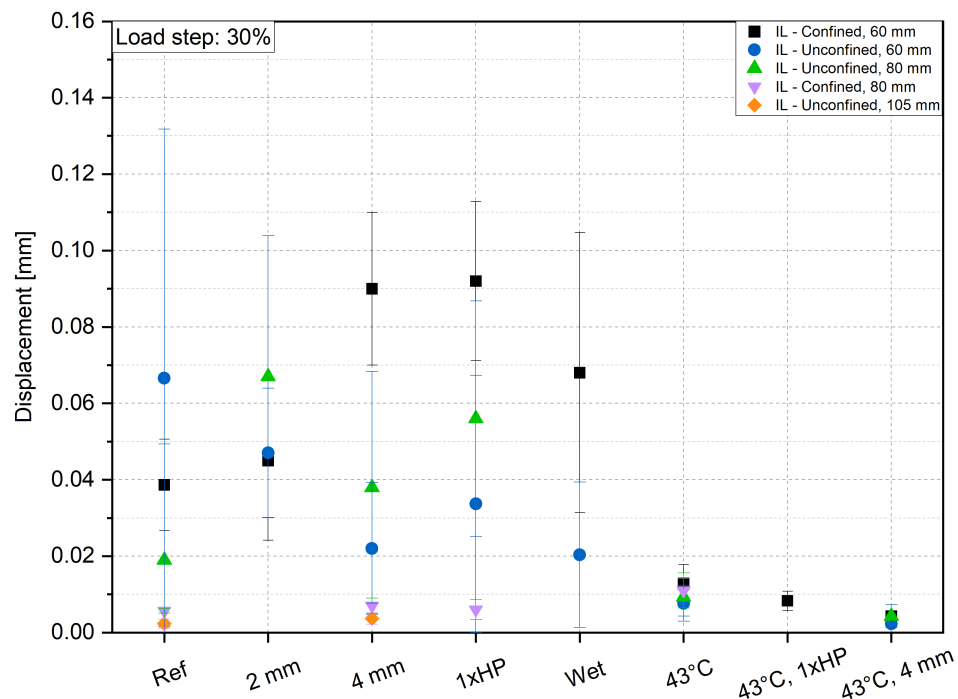
FIGURE 6.14: Summary of the displacements at load step 30 % for each embedment depth and parameter

At 30 % of the applied load, the displacements are less than 0.02 mm for the tests at elevated temperature. However, this in not the case for the other tests, where the displacements are scattered and up to 0.13 mm (e.g. reference tests with unconfined setup at 60 mm embedment depth). Surprisingly, the tests with confined setup at 60 mm depth showed larger displacements in the tests with 4 mm annular gap, in the tests with reduced cleaning effort and tests in wet concrete compared to the other embedment depths and testing setups in the same group.

Figure 6.15 illustrates the displacements at 50 % of the applied load. The overall displacements of the elevated temperature tests were still lower compared to the other tests. Similar to the displacements at 30 % load, the displacements of the anchors installed at 105 mm depth were small. The anchors with the larger displacement were those installed at 60 mm embedment depth in holes with reduced cleaning and tested at room temperature using a confined setup.
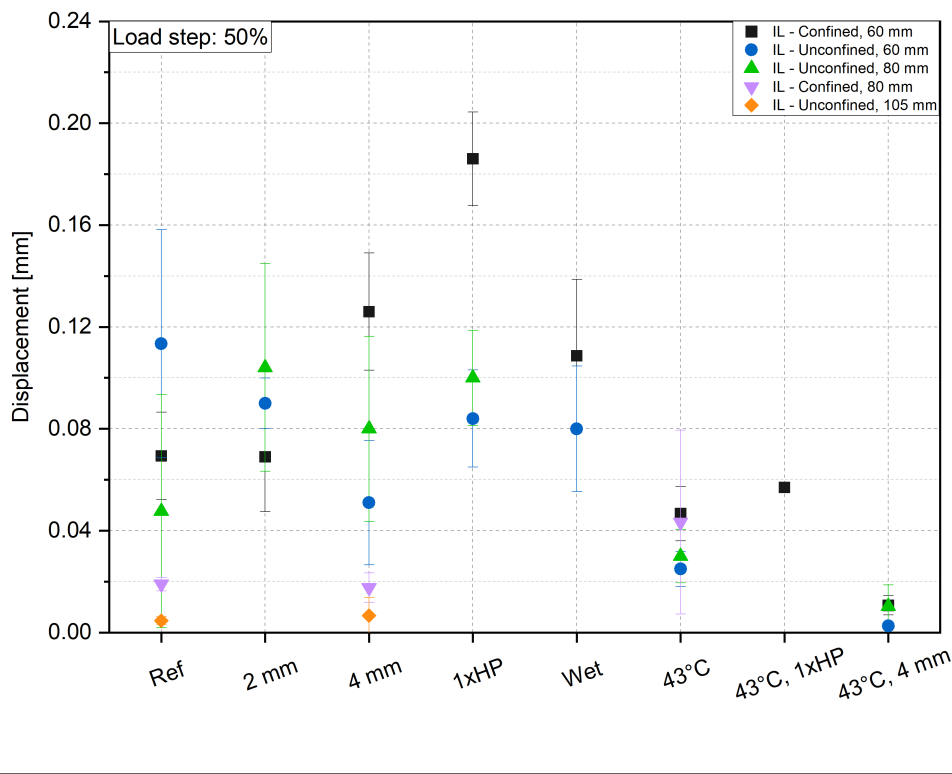
FIGURE 6.15: Summary of the displacements at load step 50 % for each embedment depth and parameter

Lastly, the displacements at 80 % of the applied load are shown in Figure 6.16. Not all the tests were loaded to 80 %. As expected, the larger displacements were reached from the elevated temperatures tests and the tests in wet concrete (anchors installed at 60 mm embedment depth and tested with a confined setup).
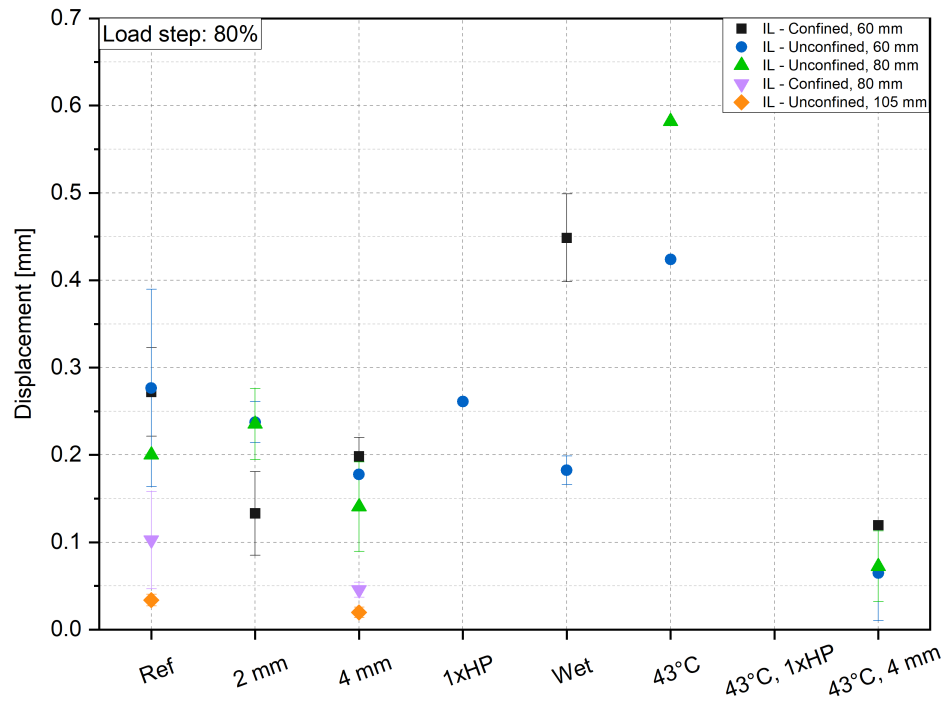
FIGURE 6.16: Summary of the displacements at load
step 80 % for each embedment depth and parameter

6.3.9 Bond strength

The calculated bond strengths for the reference incremental load
tests R-IL and incremental load tests IL are illustrated in Fig-
ure 6.17.

In this figure, the values are grouped according to the embed-
ment depth and the support width. The mean bond strengths
and their standard deviation are plotted.

The bond strength of the anchors installed at 60 mm depth
and tested with confined setup varied from 18.21 N/mm^2 (the
tests with reduced cleaning) to 34.66 N/mm^2 (the tests with an
annular gap of 2 mm). The bond strength increased by approxi-
mately 10 % with an increase of the embedment depth to 80 mm.

Similarly, the unconfined tests, exhibited lower bond strength
at 60 mm between 13.42 N/mm^2 and 17.27 N/mm^2. The anchors
installed at 80 mm embedment depth showed a bond strength
ranging from 13.60 N/mm^2 to 19.24 N/mm^2. Finally, the anchors
at 105 mm embedment depth showed a bond strength between
20.42 N/mm^2 and 22.65 N/mm^2.
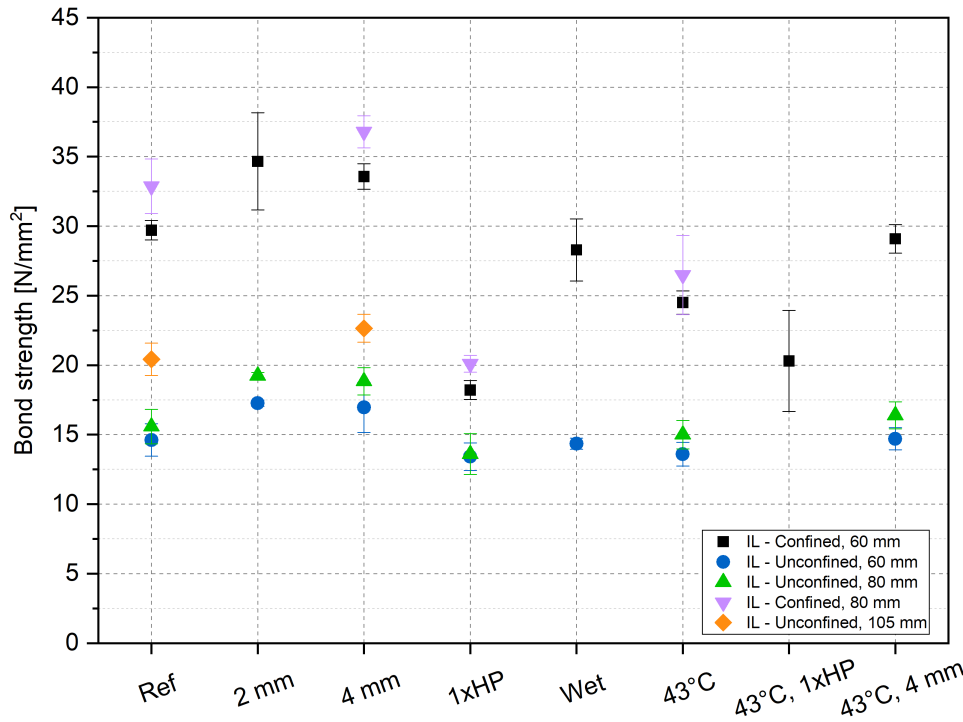
FIGURE 6.17: Summary of the mean bond strength for
each embedment depth and parameter

Considering all embedment depths and both testing setups, two factors influenced more negatively the bond strength of the incremental loading tests: cleaning effort and elevated temperature. These results agree well with existing studies on the short-term behaviour of adhesive anchors as summarized in Sections 3.3.6 and 3.4.2. Furthermore, as discussed in Sections 4.4.4 and 4.4.12, both these factors have negative influence on the long-term behaviour of adhesive anchors.

The increase of the annular gap to 2 mm showed a positive influence on the bond strength of the anchors in the incremental load tests. Çolak (2001) reported similar results in his research about short-term tests. However, more studies on the influence of annular gap on the short-term behaviour (Section 3.2.4) could not show conclusive results. The results of the incremental load tests are in contrast with the findings of Blochwitz (2019) (Section 4.4.3). He reported that the smaller annular gap resulted in higher bond strength for the anchors subjected to long-term loading.

6.4 Summary

The main focus of this chapter was the behaviour of adhesive anchors under short-term and incremental loading. Aside from the influence of the type of loading, the influence of hole cleaning, annular gap, hole saturation and increased temperature were investigated. The first derivatives of the displacements of the incremental loading tests were plotted against the applied load levels and analysed. The derivatives show when the slope of the displacement change (increase rapidly) and tertiary creep begins. The major findings of these experiments are summarized below.

Firstly, the influence of the type of loading was investigated. As expected, the anchors subjected to incremental loading failed prior to the anchors loaded within 3 minutes. The failure loads for confined and unconfined setups were in the range 10 % to 20 % lower than the reference short-term tests.

Secondly, the influence of hole cleaning was investigated. The anchors were installed in holes with the cleaning procedure as described in the manufacturers printed instructions and in holes with a reduced cleaning effort (only one hand pump to blow out the concrete dust). This influence was more obvious in the confined tests where the load was approximately 40 % lower compared to the reference tests. An exception were the anchors installed at 60 mm and tested at 43 °C with a 19 % lower failure loads. For the confined tests, the failure loads dropped by a maximum of 12 % compared to the reference tests. The residual displacement after unloading for the unconfined tests and the tests at 60 mm at room temperature (confined) with reduced cleaning were higher than the displacement of the reference incremental loading tests. The other tests showed up to the failure of the anchor, similar residual displacement as the reference tests.

Another investigated parameter, was the annular gap. The results demonstrated an increase of the failure load with the increase of the annular gap. The anchors installed in the holes drilled with $d_{cut} = 16$ mm (RS2 or 2 mm annular gap) showed higher failure loads than the reference incremental loading tests between 16 % to 24 % for both confinements. Drilling with a larger diameter ($d_{cut} = 20$ mm - 4 mm thickness), increased the failure load compared to the reference tests ($8 - 21\%$ higher

loads) despite the loads being slightly lower than those tested with 2 mm thickness.

The results showed a small influence of the hole saturation in the carrying capacity of the anchors. The failure loads were 5 % lower than the reference incremental loading tests. The residual displacements of the "poor" cleaned anchors (related to the reference tests) for the confined tests were higher than those of subjected to unconfined setup.

The last factor studied was the testing temperature. Overall, the increase of the temperature lowered the residual capacity of the anchors. The failure loads for confined tests were 15 % to 19 % lower and for unconfined tests between 3 % and 13 % lower than their reference loads. An exception was the confined tests at 60 mm with a reduced hole cleaning, where the load increased with 9 % for an increased testing temperature. The residual displacements of the anchors at the same load increment were smaller for the anchors tested at 43 °C than those tested at room temperature.

Generally, the change of the slope for the displacements happened between 35 % and 85 % of the applied short-term load. The failure of the anchor due to creep is independent from the testing setup.

The trend of the results illustrated that the bond strength of the anchors was the lowest for the anchors installed with reduced cleaning effort, followed by those tested under elevated temperatures and the highest for the increased annular gap tests (both testing setups). A reduction due to the influence parameters can be considered for the adhesive system. Nonetheless, only the reduction factor from the parameter which has the highest influence is decisive. As expected, the larger embedment depths are more favourable for long-term loading.

6.5 Comparison of the TTF and incremental loading tests

Figure 6.18 and Figure 6.19 illustrate the TTF tests summarized in Chapter 4 and the incremental loading tests.

From the TTF tests were considered only the reference TTF data tested with a confined setup at 43 °C (see Figure 4.26).

The following incremental loading tests were considered:

- D029: 60 mm embedment depth and tested at 20 °C

- D049: 60 mm embedment depth and tested at 43 °C

- D074: 80 mm embedment depth and tested at 20 °C

- D067: 80 mm embedment depth and tested at 43 °C.

The above listed series were all tested using a confined setup. The hole cleaning and the drilling diameter were specified by the manufacturer.

As load level for the incremental loading tests was taken the level at which the displacement of the anchors started increasing rapidly (tertiary creep began). The first derivative graphs given in the previous sections helped determining these levels and displacements. It was assumed that for these displacements the anchors do not fail for 50 years. The load levels ranged between 45 % and 60 % for the anchors installed at 60 mm embedment depth and between 35 % and 60 % for those installed at 80 mm depth.

Figure 6.18 shows the load levels versus time-to-failure data points as well as the linear fit of the TTF tests. The results of the incremental loading tests (black markers) fit well with the TTF results.

Figure 6.19 illustrates on the y-axis the ratio between the bond strength of the anchors after being subjected to long-term loading and the bond strength of the reference short-term tests. A ratio of $\frac{\tau_{residual}}{\tau_{reference}} \leq 1.0$ indicates that the carrying capacity of the anchor after long-term loading is less than capacity after short-term loading (which is expected). The x-axis shows the relationship between the displacement of the long-term tests and the displacement at failure load for the short-term tests.
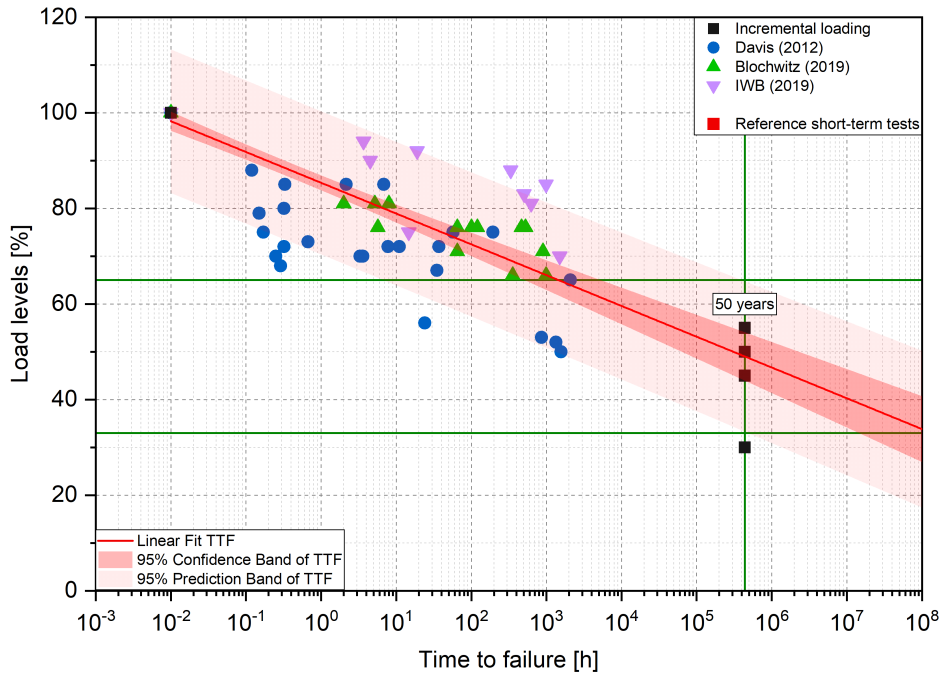
FIGURE 6.18: Comparison of the TTF and incremental
loading tests

In EAD 330499 (2018) and AC 308 (2017), the displacement
at loss of adhesion δ_{adh} determined from the short-term tests is
given as a criterion for the sustained loading tests. If the extrapolated displacements of the tests are smaller than δ_{adh}, the test
are considered successful and the adhesive anchor system is presumed as not damaged.

In Figure 6.19, a similar criterion is used to determine the state
of the adhesive after long-term loading. However, instead of the
displacement at loss of adhesion δ_{adh} [1], the displacement at failure load δ_u is used as limit. Moreover, the displacements of the
TTF tests are not the extrapolated values, but the measured displacements from the tests [2].

---

[1]It was not possible to determine δ_{adh} for the TTF tests due to lack of data.
[2]The time when these displacements were measured is shown in Figure 6.18.
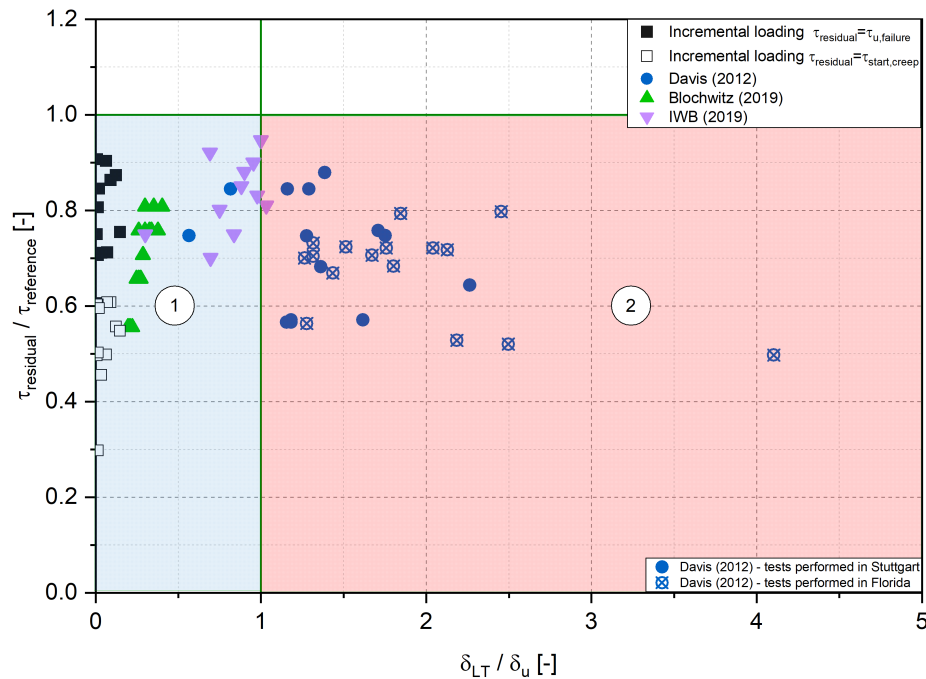
FIGURE 6.19: Relative bond strength vs. relative displacement

The following observations are made:

- Both test methods (TTF and IL) reveal that the bonding properties of the anchors decrease after long-term loading.

- The majority of the tests from Davis (2012) show that the tested adhesive systems would not remain intact for a long period of time (EAD 330499, 2018; AC 308, 2017) - Region 2 in Figure 6.18. However, the anchors did not fail even when their displacements were more than two times the displacement at short-term failure load.

- The adhesives tested by Blochwitz (2019) and IWB (2019) using TTF method and the incremental loading tests represent undamaged systems according to EAD 330499 (2018) and AC 308 (2017) - Region 1 in Figure 6.18. The displacements in this region suggest that the adhesive is close to the loss of adhesion.

- The incremental loading tests show that when creep starts, the displacement of the anchor continues to increase rapidly.

- The accuracy of the displacements' measurement is crucial to determine when the anchors fail.

The incremental tests seem to deliver comparable results with the time-to-failure tests. Using incremental loading tests to determine the long-term behaviour of adhesive anchors would be less time consuming and more cost effective compared to TTF tests. However, further investigation is necessary to evaluate the use of incremental loading tests as a method to predict the long-term behaviour of adhesive anchors.

7 Tests with alpha setup

7.1 General

The focus of this chapter is the reduction coefficient alpha setup, which is the ratio between the bond strength of the unconfined to the confined tests. Adhesive anchors in low and high-strength concrete were tested. Various parameters were changed throughout the program. The influence of the embedment depth, support diameter, bond length, axial compression, and sustained loading on the bond strength of the anchors was investigated. The bond strength for each parameter was calculated using Equation (2.6). Lastly, a comparison of the failure loads with the different design models (Section 7.5) was performed.

7.2 Test Program

The experimental investigation was divided into six main sections as listed in Tables 7.1 to 7.5. Chapter 5 describes the materials and methods used in this chapter. An overview of the results is presented in Appendix C.

7.2.1 Confined and unconfined tests with $M12$ and $d12$

The aim of these tests was the direct calculation of α_{setup} with varying embedment depth. The tests were carried out under a confined and unconfined setup. The notation of the series is in sequential order represented. The letters C and U at the end of each series depict the setup used when testing.

Table 7.1 summarizes the test program with $M12$ threaded rods. A total of ten series were carried out. The third column lists the embedment depths tested as a function of the anchor diameter d: $4d$ (48 mm), $5d$ (60 mm), $6d$ (72 mm), $7d$ (84 mm), and $8d$ (96 mm).

TABLE 7.1: Confined and unconfined test program
with $M\,12$ threaded rod

Test series [–]	Anchor diameter [–]	Embed. depth [–]	Concrete batch [–]	Support [–]
$S1.1-C$	$M\,12$	$4\,d$	Batch B.3	confined
$S1.1-U$	$M\,12$	$4\,d$	Batch B.3	unconfined
$S1.2-C$	$M\,12$	$5\,d$	Batch B.3	confined
$S1.2-U$	$M\,12$	$5\,d$	Batch B.3	unconfined
$S1.3-C$	$M\,12$	$6\,d$	Batch B.3	confined
$S1.3-U$	$M\,12$	$6\,d$	Batch B.3	unconfined
$S1.4-C$	$M\,12$	$7\,d$	Batch B.3	confined
$S1.4-U$	$M\,12$	$7\,d$	Batch B.3	unconfined
$S1.5-C$	$M\,12$	$8\,d$	Batch B.3	confined
$S1.5-U$	$M\,12$	$8\,d$	Batch B.3	unconfined

Table 7.2 lists the tests carried out with $d\,12$ reinforcing bar. Only three embedment depths ($4\,d$ (48 mm), $6\,d$ (72 mm), and $8\,d$ (96 mm)) were tested. Higher embedment depths were not tested to avoid steel failure.

TABLE 7.2: Confined and unconfined test program
with $d\,12$ reinforcing bar

Test series [–]	Anchor diameter [–]	Embed. depth [–]	Concrete batch [–]	Support [–]
$S2.1-C$	$d\,12$	$4\,d$	Batch B.4	confined
$S2.1-U$	$d\,12$	$4\,d$	Batch B.4	unconfined
$S2.2-C$	$d\,12$	$6\,d$	Batch B.4	confined
$S2.2-U$	$d\,12$	$6\,d$	Batch B.4	unconfined
$S2.3-C$	$d\,12$	$8\,d$	Batch B.5	confined
$S2.3-U$	$d\,12$	$8\,d$	Batch B.5	unconfined

7.2.2   Tests with variation of the support diameter

The tests in Table 7.3 were performed with different support diameters. The embedment depth was for all these series $5\,d$ or 60 mm. The support diameter was varied depending on the embedment depth: $0.24 \cdot h_{ef}$, $0.5 \cdot h_{ef}$, $1.0 \cdot h_{ef}$, $1.5 \cdot h_{ef}$, and $2.0 \cdot h_{ef}$.

TABLE 7.3: Test program with $d\,12$ and variation of the support diameter

Test series [−]	Anchor diameter [−]	Embed. depth [−]	Concrete batch [−]	Support diameter [−]
S3.1	$d\,12$	$5\,d$	Batch B.5	$0.24 \cdot h_{ef}$
S3.2	$d\,12$	$5\,d$	Batch B.5	$0.5 \cdot h_{ef}$
S3.3	$d\,12$	$5\,d$	Batch B.5	$1.0 \cdot h_{ef}$
S3.4	$d\,12$	$5\,d$	Batch B.5	$1.5 \cdot h_{ef}$
S3.5	$d\,12$	$5\,d$	Batch B.5	$2.0 \cdot h_{ef}$

7.2.3   Tests with variation of the bond length

The aim of these tests was the indirect determination of α_{setup} through the bond length of the fastener. Firstly, the definition of the phrases *bond length* and *embedment depth* should be clarified. *Embedment depth* refers to the length of the fastener embedded in concrete from the bottom of the hole to the concrete surface. *Bond length* indicates the length throughout the length fastener which is bonded to concrete. Generally, the *bond length* is smaller or equal to the *embedment depth*.

The tests were carried out using $M\,12$ threaded rods under a confined and unconfined setup. Five embedment depths ($4\,d, 5\,d, 6\,d, 7\,d$, and $8\,d$) and four bond configurations (a, b, c and d) were investigated. Figure 7.1 illustrates the bond configurations.
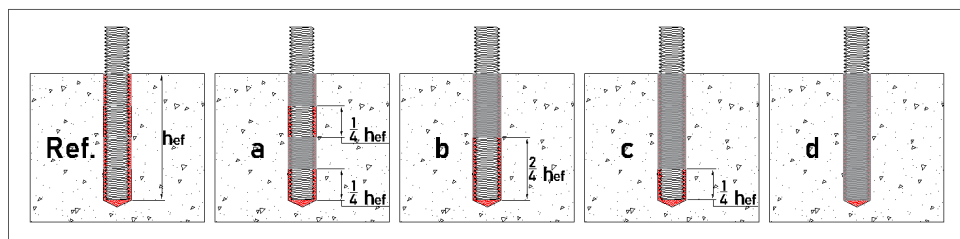
FIGURE 7.1: Configurations of the bond length

Starting from the left: the first figure shows the reference test, where the bond length is equal to the embedment depth (as reference tests, served the series described in Table 7.1). The second figure shows configuration a: the bond lengths are the first and

the third quarter of the embedment depth starting from the bottom. The following is configuration *b,*where the bond length is the bottom half of the embedment depth. The fourth figure illustrates configuration *c,* where only the bottom quarter of the embedment depth is bonded. The last configuration *d* represents the anchor fully debonded to evaluate the influence of friction on the failure load. Adhesive tape helped with the bond free surface of the threaded rods.
The tests were performed in three phases:

- Phase 1: Tests with embedment depths: $5\,d$, $6\,d$, $7\,d$, and $8\,d$. Tested configurations: *a* and *b*.

- Phase 2: Tests with embedment depth $4\,d$. Tested configurations: *a* and *b*.

- Phase 3: Tests with embedment depths: $4\,d$, $6\,d$, and $8\,d$. Tested configurations: *c* and *d*.

Table 7.4 summarizes the test series included in this section.

TABLE 7.4: Test program with $M\,12$ and variation of the bond length

Test series [−]	Anchor diameter [−]	Embed. depth [−]	Concrete batch [−]	Bond conf. [−]	Support [−]
$S4.0 - A - C$	$M\,12$	$4\,d$	Batch B.5	*a*	confined
$S4.0 - A - U$	$M\,12$	$4\,d$	Batch B.5	*a*	unconfined
$S4.0 - B - C$	$M\,12$	$4\,d$	Batch B.5	*b*	confined
$S4.0 - B - U$	$M\,12$	$4\,d$	Batch B.5	*b*	unconfined
$S4 - 4d - 3/4 - C$	$M\,12$	$4\,d$	Batch B.5	*c*	confined
$S4 - 4d - 3/4 - U$	$M\,12$	$4\,d$	Batch B.5	*c*	unconfined
$S4 - 4d - 4/4 - C$	$M\,12$	$4\,d$	Batch B.5	*d*	confined
$S4 - 4d - 4/4 - U$	$M\,12$	$4\,d$	Batch B.5	*d*	unconfined
$S4.1 - C$	$M\,12$	$5\,d$	Batch B.5	*a*	confined
$S4.1 - U$	$M\,12$	$5\,d$	Batch B.5	*a*	unconfined
$S4.2 - C$	$M\,12$	$5\,d$	Batch B.5	*b*	confined
$S4.2 - U$	$M\,12$	$5\,d$	Batch B.5	*b*	unconfined
$S4.3 - C$	$M\,12$	$6\,d$	Batch B.5	*a*	confined
$S4.3 - U$	$M\,12$	$6\,d$	Batch B.5	*a*	unconfined
$S4.4 - C$	$M\,12$	$6\,d$	Batch B.5	*b*	confined
$S4.4 - U$	$M\,12$	$6\,d$	Batch B.5	*b*	unconfined
$S4 - 6d - 3/4 - C$	$M\,12$	$6\,d$	Batch B.5	*c*	confined
$S4 - 6d - 3/4 - U$	$M\,12$	$6\,d$	Batch B.5	*c*	unconfined

TABLE 7.4: (continued)

Test series [−]	Anchor diameter [−]	Embed. depth [−]	Concrete batch [−]	Bond conf. [−]	Support [−]
$S4-6d-4/4-C$	$M\,12$	$6\,d$	Batch B.5	d	confined
$S4-6d-4/4-U$	$M\,12$	$6\,d$	Batch B.5	d	unconfined
$S4.5-C$	$M\,12$	$7\,d$	Batch B.5	a	confined
$S4.5-U$	$M\,12$	$7\,d$	Batch B.5	a	unconfined
$S4.6-C$	$M\,12$	$7\,d$	Batch B.5	b	confined
$S4.6-U$	$M\,12$	$7\,d$	Batch B.5	b	unconfined
$S4.7-C$	$M\,12$	$8\,d$	Batch B.5	a	confined
$S4.7-U$	$M\,12$	$8\,d$	Batch B.5	a	unconfined
$S4.8-C$	$M\,12$	$8\,d$	Batch B.5	b	confined
$S4.8-U$	$M\,12$	$8\,d$	Batch B.5	b	unconfined
$S4-8d-3/4-C$	$M\,12$	$8\,d$	Batch B.5	c	confined
$S4-8d-3/4-U$	$M\,12$	$8\,d$	Batch B.5	c	unconfined
$S4-8d-4/4-C$	$M\,12$	$8\,d$	Batch B.5	d	confined
$S4-8d-4/4-U$	$M\,12$	$8\,d$	Batch B.5	d	unconfined

7.2.4 Tests with axial compression

Table 7.5 lists the performed tests to observe the influence of axial compression on the bond strengths of the anchors. Five test series with the same embedment depths were tested. The anchors of $S7.R$ series served as a reference series, tested without axial compression and with a confined setup. The axial compression was increased for each series: $0.1 \cdot f_{cc}$ (112 kN), $0.2 \cdot f_{cc}$ (225 kN), $0.4 \cdot f_{cc}$ (448 kN), and $0.45 \cdot f_{cc}$ (512 kN).

TABLE 7.5: Test program for axial compression tests

Test series [−]	Anchor diameter [−]	Embed. depth [−]	Concrete batch [−]	Compressive strength [−]
$S7.R$	$M\,12$	$6\,d$	Batch B.2	$0 \cdot f_{cc}$
$S7.1$	$M\,12$	$6\,d$	Batch B.2	$0.1 \cdot f_{cc}$
$S7.2$	$M\,12$	$6\,d$	Batch B.2	$0.2 \cdot f_{cc}$
$S7.3$	$M\,12$	$6\,d$	Batch B.2	$0.4 \cdot f_{cc}$
$S7.4$	$M\,12$	$6\,d$	Batch B.2	$0.45 \cdot f_{cc}$

7.2.5   Long-term tests

Long-term tests or sustained loading tests were carried out in low-strength and high-strength concrete. The anchors were installed at 60 mm (6 d) depth.

Reference short-term series in low-strength concrete $C\,20/25$ were $S8.1-R-A$, $S8.2-R-B$ and $S1.3-C$ described in Table 7.2 for configuration a, b and full bond length, respectively.

$S4.3-C$ and $S4.4-C$ (Table 7.4) served as reference tests in $C\,100/115$ concrete for configurations a and b. The fully bonded anchor was not investigated because of the high concrete compressive strength.

TABLE 7.6: Test program for sustained load tests

Test series [−]	Anchor diameter [−]	Embed. depth [−]	Concrete batch [−]	Bond conf. [−]	Type of test [−]
$S8.1-R-A$	$M\,12$	$6\,d$	Batch B.1	a	Sh-T
$S8.2-R-B$	$M\,12$	$6\,d$	Batch B.1	b	Sh-T
$S8.3-A$	$M\,12$	$6\,d$	Batch B.1	a	Sustained
$S8.4-R$	$M\,12$	$6\,d$	Batch B.1	$-$	Sustained
$S8.5-B$	$M\,12$	$6\,d$	Batch B.1	b	Sustained
$S8.7-A$	$M\,12$	$6\,d$	Batch B.5	a	Sustained
$S8.8-B$	$M\,12$	$6\,d$	Batch B.5	b	Sustained

7.3   Results

7.3.1   Failure modes

The anchors tested in this chapter exhibited failure modes depending on the testing setup. The failure modes are listed for each case in the tables in Appendix C. The following failure modes were observed (see Figure 7.2):

P_M Pull-out failure with mortar

P Pull-out failure without mortar

$M1$ A combination of pull-out failure with and without mortar

C Concrete cone failure

M2 A combination of concrete cone failure with pull-out failure

S Steel failure

The assignment of the failure modes occurred through visual examination. Generally, pull-out failure (with mortar, without mortar or their combination) was observed in the anchors tested under a confined setup and in partially bonded anchors tested under an unconfined setup. The fasteners failed in pull-out when the interface between the fastener and adhesive or the adhesive and concrete surface broke down.

Concrete cone failure happened in fasteners installed at shallow embedment depths ($4\,d$) and tested with an unconfined setup. The cone was formed starting from the bottom of the fastener to the concrete surface. The combined failure mode: concrete cone and pull-out failure appeared with increasing embedment depth. The concrete cone did not originate from the bottom of the fastener.

The high embedment depth tests $8\,d$, in high-strength concrete, exhibited steel failure.
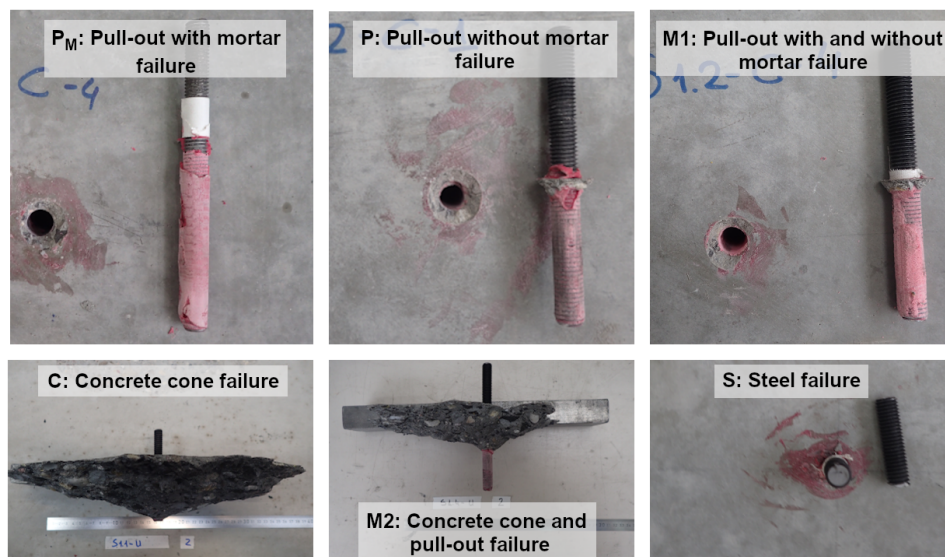
FIGURE 7.2: Examples of the observed failure modes

Table 7.7 lists the frequency of occurrence of each failure mode.

TABLE 7.7: Frequency of occurrence

Failure mode [−]	Percentage [%]
P_M	3
P	40
$M1$	26
C	3
$M2$	25
S	3

7.3.2 Load-displacement behaviour

Figures 7.3 and 7.4 [1] illustrate representative load-displacement curves observed from the experimental investigation with $M12$ and $d12$. The threaded rod and the reinforcing bar tests showed different behavioural trends. Regardless of the failure load, the main difference between the two steel element types was the displacement before reaching this load. The threaded rods achieved the maximum load at a smaller displacement than the reinforcing bars installed at the same depth.

Both figures show different steel failure curves (1, 7). The tests with reinforcing bars revealed the typical steel failure curves from literature, where the load increased slower than the displacement. The threaded rods behaviour did not conform with the findings in the literature. It is suspected that this may be due to the hardening process of the steel components. The threaded rod seemed to be more ductile than the reinforcing bars. A closer examination of the results revealed some anomalies. Test series $S1.5 - C, S1.5 - U$ and $S2.3 - C$ showed different failure modes within each series: steel, pull-out, and combined cone and pull-out failure. In these series, the smaller loads were those of the anchors which showed steel failure.

The second observed failure mode was pull-out failure (P_M,P and $M1$). The fasteners behaved nearly elastic before reaching the peak load. After reaching the ultimate failure load, the anchors behaved incoherently. This behaviour is associated with

---

[1]The x-axis depicting the displacement of the reinforcing bars is interrupted after 4 mm and restarted at 12 mm so that the whole steel failure curve could be shown.
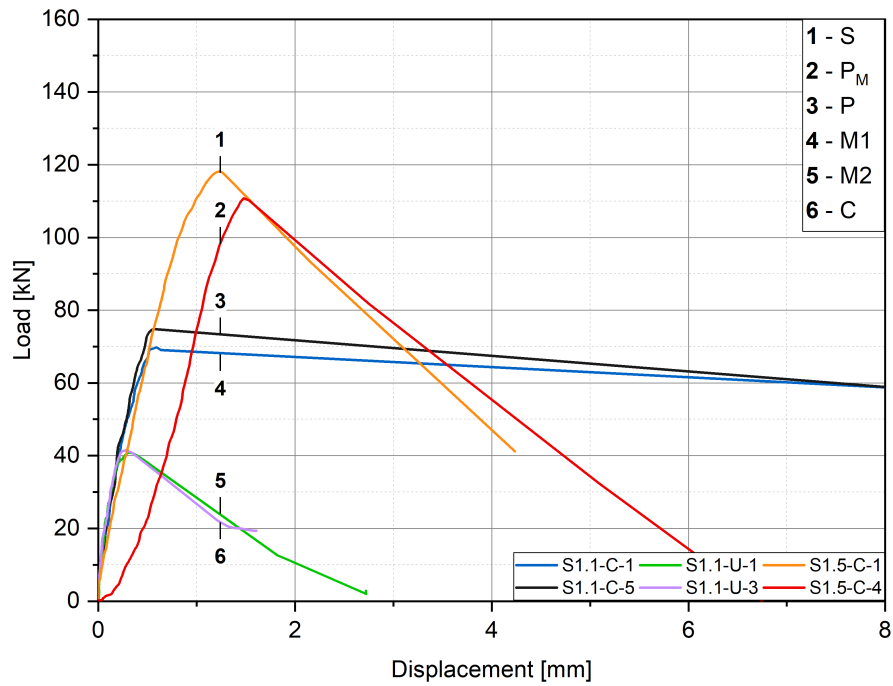
FIGURE 7.3: Representative curves of the failure modes for threaded rods
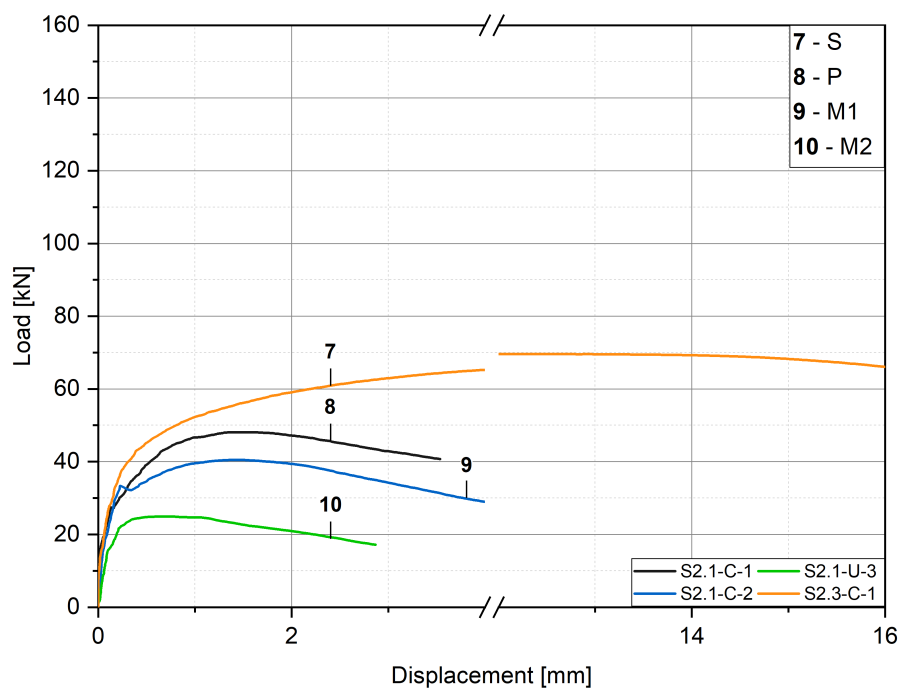
FIGURE 7.4: Representative curves of the failure modes for reinforcing bars

the adhesion strength correlated to the mechanical interlock influenced by the surface roughness where the failure happens. A part of the threaded rods exhibited a decrease in load with increasing displacement (3, 4). These results suggest that the adhesion between mortar and concrete surface was higher than the adhesion between rod and mortar. The load-displacement behaviour described by curve 2 occurred mostly in fully bonded threaded rods installed with $h_{ef} \geq 6\,d$ and showed a rapid decrease in load with increasing displacement. This indicates an excellent bond strength throughout the length of the anchor followed by a sudden drop in bond strength as a result of the initial cracking inside the mortar after peak is reached.

The partially bonded anchors with configuration *d* (the whole length of the anchor bond free) showed a continuous increase in displacement with minimal change in load. This represents the friction created inside the hole.

The reinforcing bar tests (8, 9) behaved similarly in the pre-peak region (nearly elastic), though the ultimate load was reached over a higher displacement compared to the threaded rod tests. This behaviour is attributed to the frictional resistance between the bar and the adhesive being higher than the adhesion strength. In general, there appeared to be a trend for the failure loads. The ultimate loads for failure mode *P* and *M*1 (with failure percentage $P > P_M$) were higher than the loads for P_M and *M*1 ($P < P_M$) failure.

A full concrete cone breakout developed only in the tests with threaded rods at shallow embedment depths (line 6 in Figure 7.4). Line 5 and 10 illustrate the combined concrete cone and pull-out failure *M*2. The behaviour of the anchors was linear up to a certain point (approximately 75% of the ultimate load). A slight increase in load followed the linear part of the curve up to the peak. Afterwards, the load dropped. The load decrease for the reinforcing bars was more gradual than for the rods.

The load-displacement curves for each series are illustrated in Appendix C.

7.3.3   Influence of the embedment depth

The influence of the embedment depth was studied with $M\,12$ and $d\,12$ fasteners. Figure 7.5 illustrates the failure loads as a

function of the actual embedment depths for the tests described in Table 7.1 using the threaded rods $M\,12$.
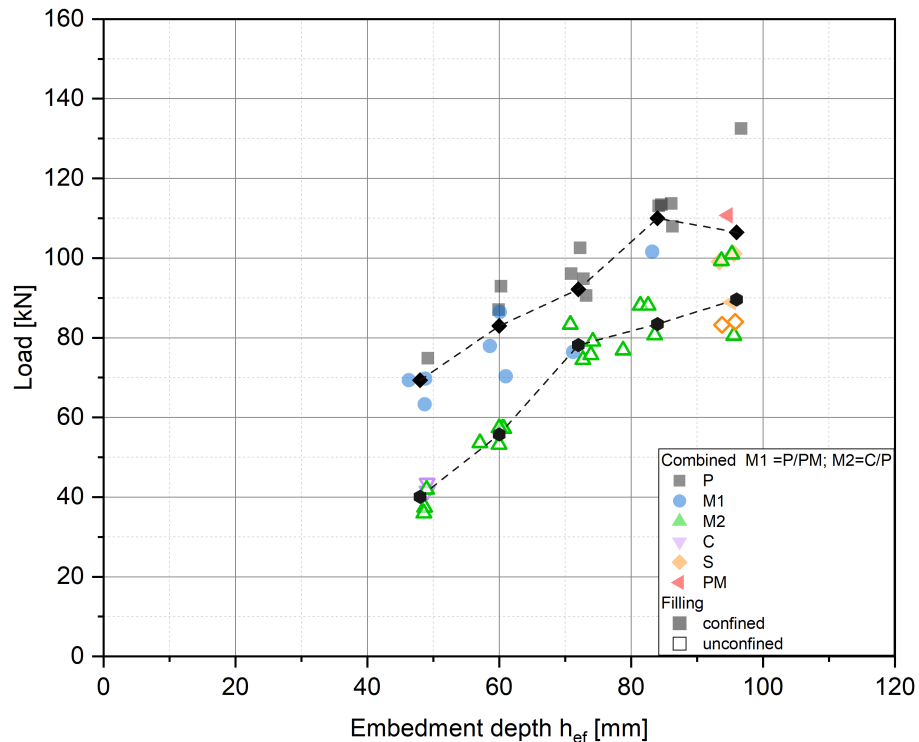
FIGURE 7.5: Influence of the embedment depth for
Table 7.1 using $M\,12$

In the figure, the results are plotted according to their failure mode and testing setup. The results showed a clear trend for both support diameters: the increase in the embedment depth yielded a higher failure load. Comparing the confined tests with each-other, the mean load changed from 69 kN (48 mm) to 110 kN (84 mm). However, with an increase to 96 mm, the load decreased to 106 kN. This drop corresponds to about 3 % lower load than the anchors tested at 84 mm but a 54 % increase concerning the anchors installed at 48 mm. The unconfined tests revealed only an increase in their ultimate load from 40 kN (48 mm) to 90 kN (96 mm). As shown in the figure, the failure load reached approximately twice the initial failure load (48 mm) at the depth of 72 mm. This value increased by a factor of 2.25 at the highest embedment depth. The relationship between the bond strength and the ratio $\frac{h_{ef}}{d}$ is presented in Figure 7.6 and 7.7 for $M\,12$.
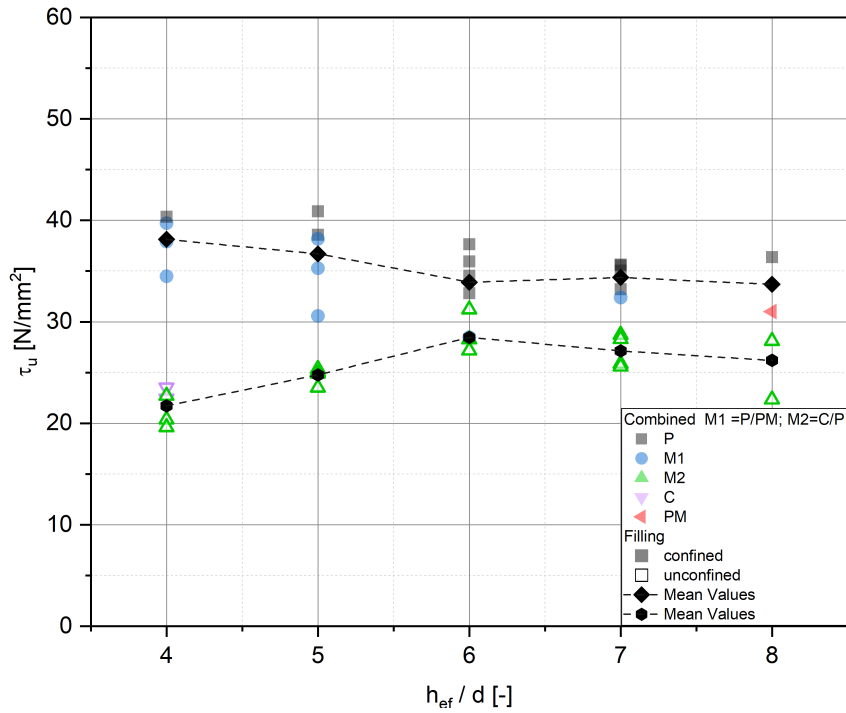
FIGURE 7.6: Influence on the bond strength of the ratio embedment depth - anchor diameter for the tests in Table 7.1 using *M* 12
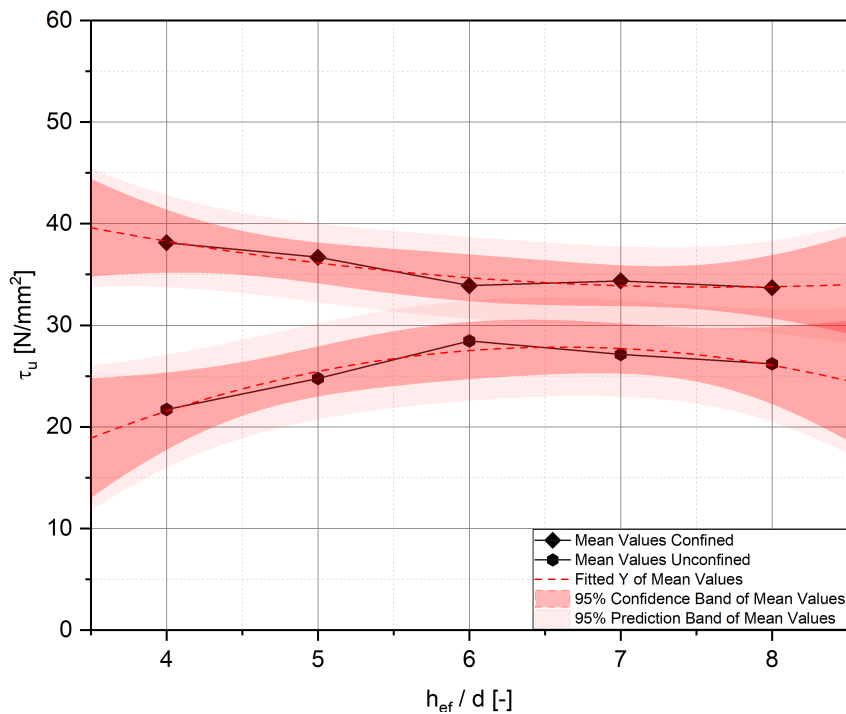
FIGURE 7.7: The development of the bond strength for the tests in Table 7.1 using *M* 12

These figures show the same results but plotted differently. The bond strength trend for both setups are illustrated with a dashed red line in Figure 7.7. The confined tests revealed a decrease of the bond strength with increasing embedment depth up to $6\,d$. Afterwards, this strength remained roughly constant ($\pm2\,\%$). The tests under an unconfined setup behaved differently. The bond strength rose almost linearly with $14-15\,\%$ up to $6\,d$. With a further increase in depth, the bond strength decreased with $5\,\%(7\,d)$ and $8\,\%(8\,d)$.

The reinforcing bars $d\,12$ behaved similarly to the threaded rods. Figure 7.8 shows the influence of the embedment depth on the failure load. The load increased for confined and unconfined test by $50\,\%$ and $70\,\%$, as the embedment depth changed from 48 mm to 72 mm. After this depth, the bars behaved differently depending on the used testing setup. The anchors tested with a confined setup revealed a slight increase of the failure load from 67.6 kN to 68.6 kN for embedment depths 72 mm and 96 mm. On the other hand, the failure load for the unconfined tests increased more rapidly by 13 %.
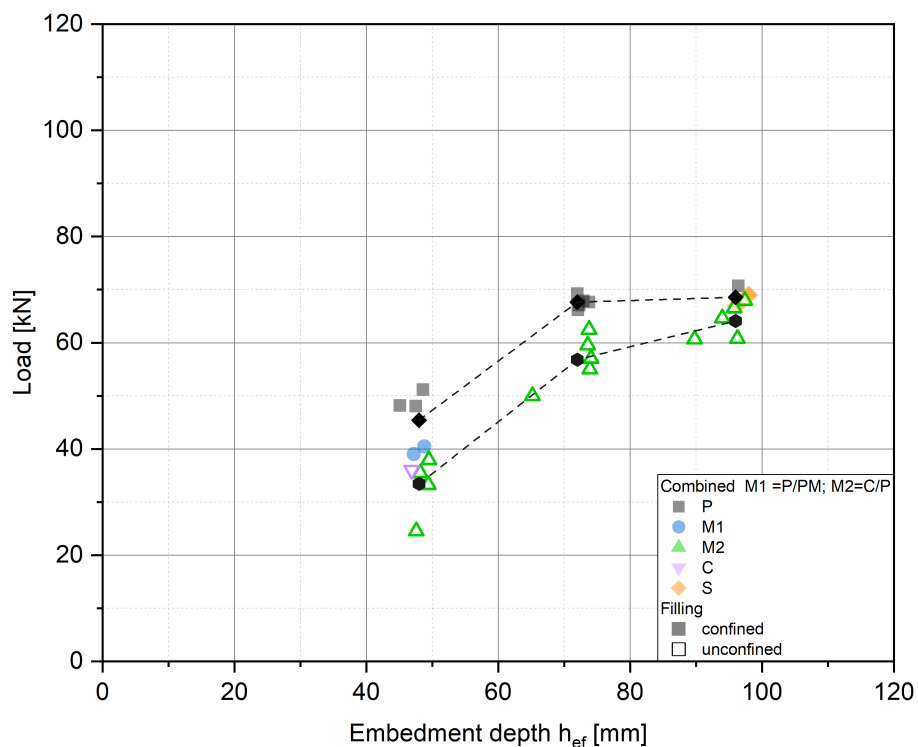
FIGURE 7.8: Influence of the embedment depth for Table 7.2 using $d\,12$

Figure 7.9 shows the dependence of the bond strength on the embedment depth - anchor diameter ratio. An interesting pattern emerged when examining the results of the unconfined tests. The bond strength increased by approximately 14 % from $4\,d$ to $6\,d$. A further increase to $8\,d$ revealed a decrease in bond strength by 13.4 % compared to this strength at $6\,d$, but only 1.4 % compared to $4\,d$. In contrast, the confined tests reduced the bond strength from $25.4\,\mathrm{N/mm^2}(4\,d)$ to $24.7\,\mathrm{N/mm^2}(6\,d)$ and finally $19.5\,\mathrm{N/mm^2}(8\,d)$.
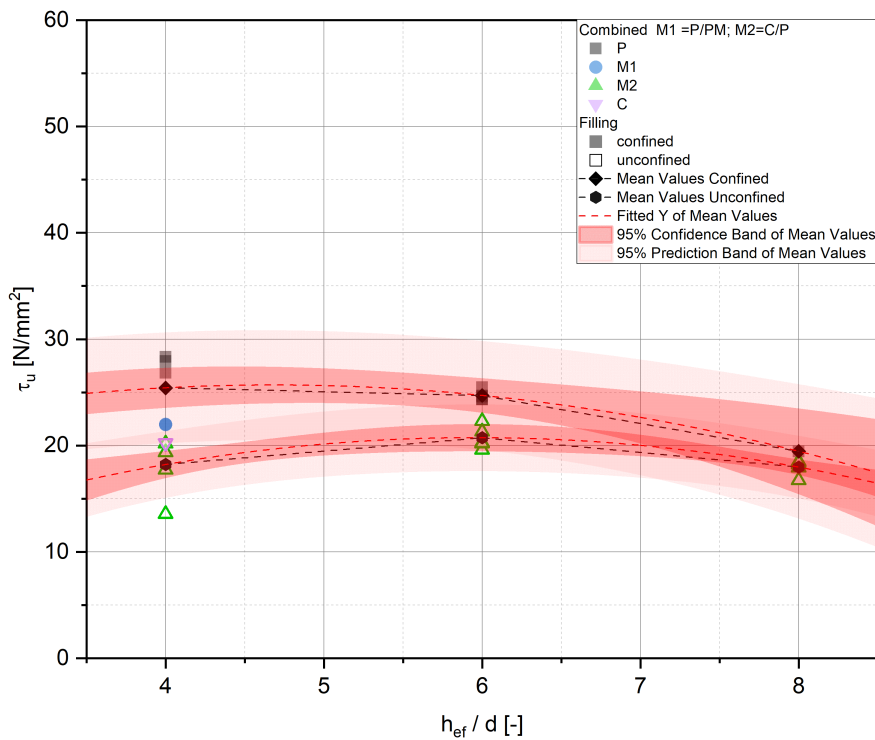
FIGURE 7.9: Influence on the bond strength of the ratio embedment depth - anchor diameter for the tests in Table 7.2 using $d\ 12$

7.3.4 Influence of the support diameter

The tests described in Table 7.3 aimed to analyse the influence of the support diameter on the carrying capacity of adhesive anchors. Figure 7.10 illustrates the failure loads as a function of the support diameter D.
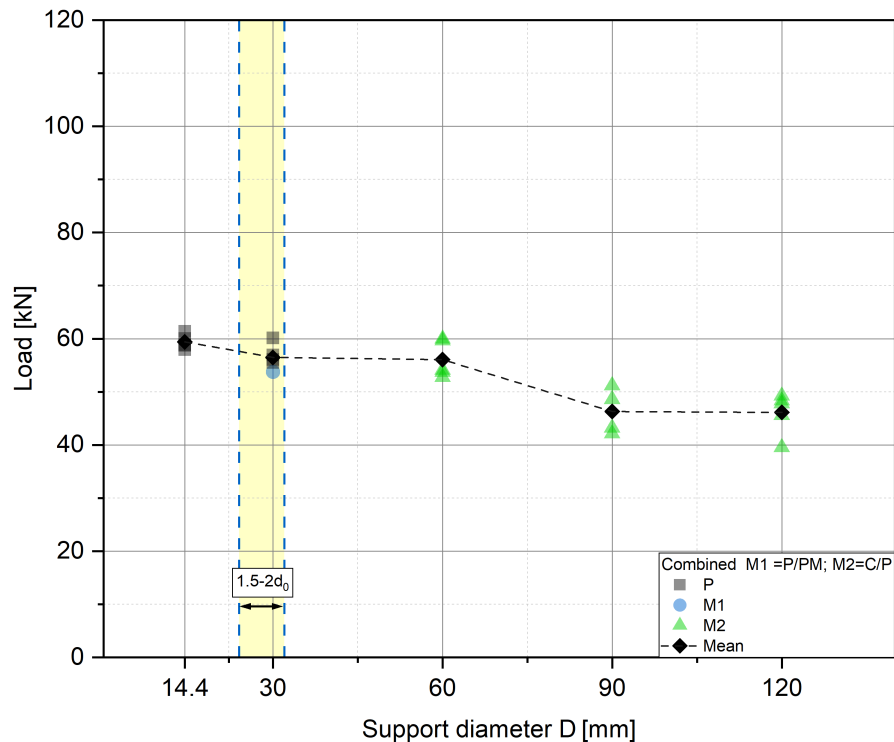
FIGURE 7.10: Influence of the support diameter for
Table 7.3

The section between the dotted blue lines illustrate the support diameter as a function of the drilling diameter d_0 as described in the current standards AC 308 (2017), ACI 318 (2019), and EAD 330499 (2018). The drilling diameter for reinforcing bars was 16 mm. Thus, the recommended support diameter was in the range of $24 - 32$ mm. The figure shows that with increasing the support diameter, the mean failure loads reduced. The load decreased by 4.9 % and 5.7 %, as the diameter increased to 30 mm and 60 mm, respectively. The mean failure loads dropped more than 22 % as the diameter D increased to 90 mm and 120 mm. From Figure 7.10, it is apparent that the scatter of the failure loads is higher the higher the support diameter is.

The effect of the ratio support diameter-embedment depth and the development trend of the bond strengths (dashed red line) are shown in Figure 7.11.

Similar to the failure loads behaviour, the bond strengths decreased with increasing the support diameter. However, the trend of reduction in bond strength changed depending on the
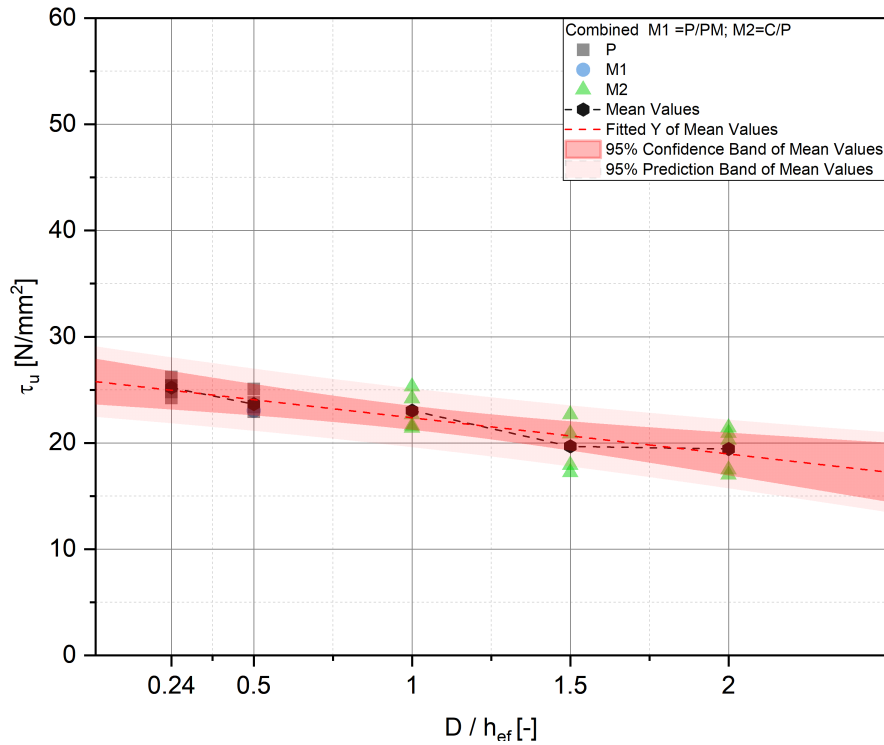
FIGURE 7.11: Influence on the bond strength of the
ratio support diameter - embedment depth for the
tests in Table 7.3 using d 12

support diameter.   Firstly, the bond strength dropped from
25.2 N/mm^2 to 23.7 N/mm^2 as the diameter D increased from
$0.24 \cdot h_{ef}$ to $0.5 \cdot h_{ef}$. A further increase in the diameter revealed
a smaller drop in the bond strength than the previous one (ap-
proximately 2.6 %). At $D = 1.5 \cdot h_{ef}$, the bond strength reached
19.7 N/mm^2.   Lastly, the pattern of the bond strength from
$1.5 \cdot h_{ef}$ to $2.0 \cdot h_{ef}$ showed a minor decrease of 1.3 %.

Except the tests described in Table 7.3, where the diameter of
the support was varied as a function of the embedment depth,
the tests in Tables 7.1 and 7.2 were also carried out with two sup-
port diameters, namely $D_c = 1.5 - 2 \cdot d_0$ (confined test setup) and
$D_u \geq 4 \cdot h_{ef}$ (unconfined test setup). Figure 7.12 and 7.13 illus-
trate these results represented for reinforcing bars and threaded
rods, respectively. The x-axis shows the support diameter given
on a logarithmic scale. The y-axis shows the ratio of the bond
strengths with the mean of the tests where pull-out failure was
observed within the same test series.

Both diagrams show visually the influence of the support diameter on the bond strength with the help of the failure modes.
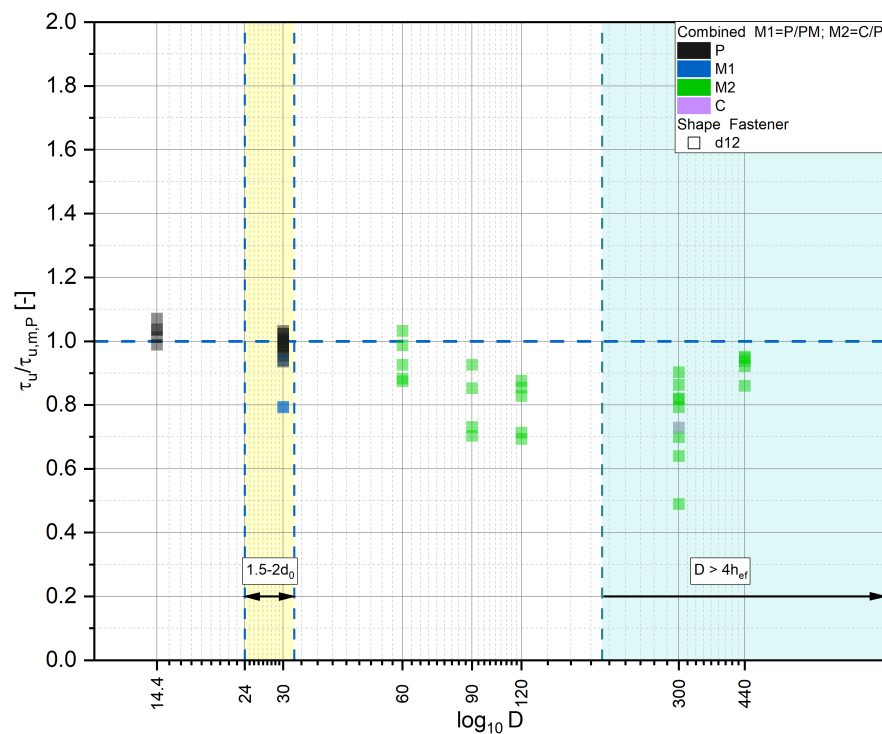
FIGURE 7.12: Relative bond strength of the reinforcing bars tests (Table 7.2 and 7.3)

The failure modes of both steel components changed as the support diameter increased. The reinforcing bars exhibited only pull-out failure (P and $M1$) for $D \leq 30$ mm. Afterwards, the fasteners showed a combined concrete cone and pull-out failure $M2$ from $D = 60$ mm. Only one fully formed concrete cone failure was observed at the support of 300 mm.

The threaded rods showed a similar behaviour. However, the difference of the failure modes at larger diameters was more obvious. The combined cone - pull out failure $M2$ was mostly observed for the ratio $\frac{\tau_u}{\tau_{u,m,P}} \leq 1$.
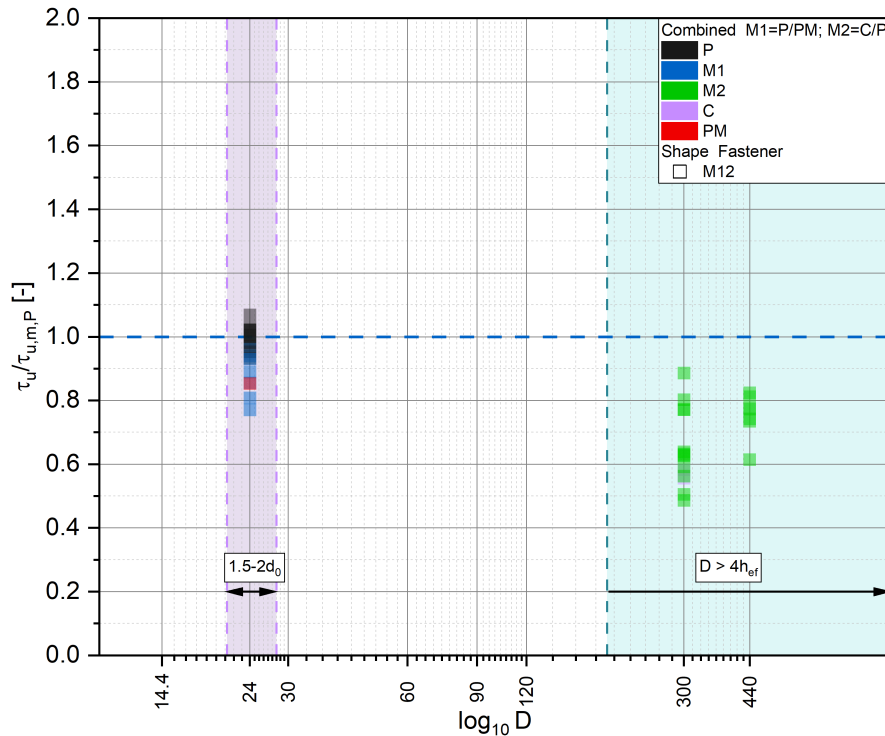
FIGURE 7.13: Relative bond strength of the threaded
rod tests (Table 7.1)

7.3.5　Influence of the bond length

Another parameter investigated was the bond length of the anchors (see Table 7.4). Figure 7.14 illustrates the failure loads of the tests for each bond length. The plotted lines (red and blue) show the trend lines for each testing setup.

Configurations *a* and *b* showed the same bond length ($50\,\% \cdot h_{ef}$), but the distribution varied as shown in Figure 7.1. Thus, a comparison between these two configurations for each type of testing setup is meaningful.

The confined tests at $4\,d$ and $8\,d$ showed the highest decrease in the failure load for configuration *b* of $13.3\,\%$ and $14.8\,\%$, respectively. The anchors with embedment depth $5\,d$ and configuration *b* showed less than $1\,\%$ lower load, whereas those installed at $7\,d$ showed approximately $4.5\,\%$. Surprisingly, the failure load for configuration *b* at $6\,d$ increased by $11.2\,\%$ compared to configuration *a*.
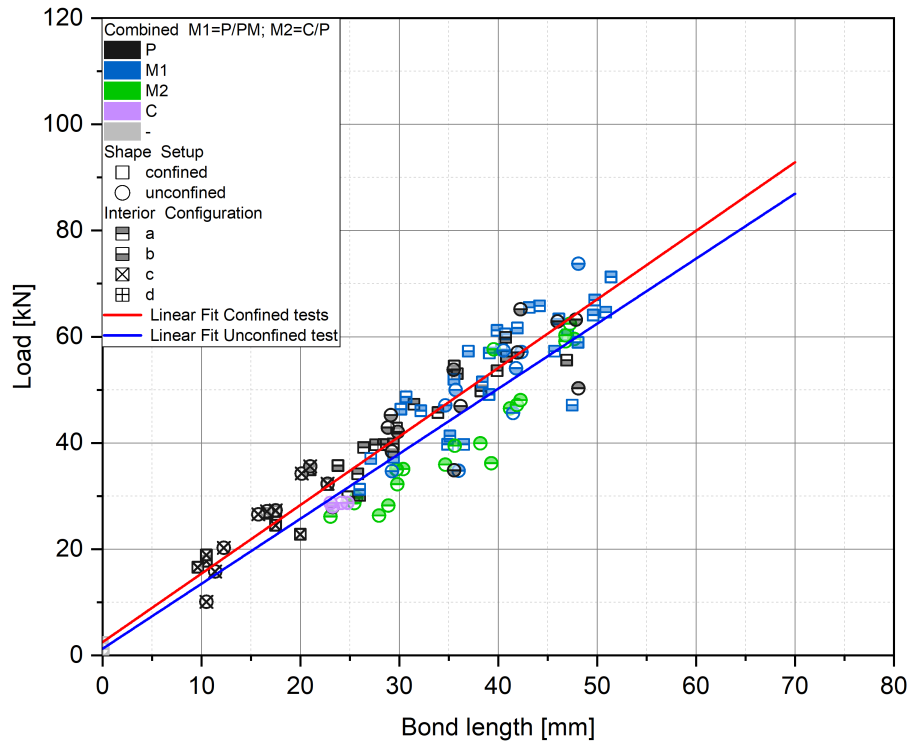
FIGURE 7.14: Influence of the bond length for Table 7.4 using *M* 12

Contrary to the confined tests, the unconfined tests resulted in increasing failure load for configuration *b*. The failure load of tests at 4 *d* increased by 1.5 %. The anchors installed at 5 *d* and 6 *d* failed with around 24 % higher loads compared to configuration *a*. Similarly, the tests carried out with embedment depths 7 *d* and 8 *d* using configuration *b* showed 19.2 % and 14.2 % larger failure loads.

Configuration *c* and *d* were investigated for three embedment depths: 4 *d*, 6 *d* and 8 *d*. The tests with configuration *c* aimed to reveal the bond strength at the bottom of the embedment depth with only 25 % bond length. As expected, the failure load increased with increasing bond length. The anchors installed at 4 *d* with 12 mm bond length showed a mean failure load of 17.8 kN and 15.4 kN for confined and unconfined setup, respectively. At 6 *d* depth with 18 mm bond length, the failure loads were 26.1 kN and 27.0 kN for each setup. Lastly, the loads for 24 mm bond length (8 *d* embedment depth) were 30.0 kN and 34.1 kN, respectively.

The failure loads of the anchors installed with configuration d (no bonding length) ranged from 0.49 kN to 2.5 kN, with a maximum mean load of 1.9 kN. The main idea behind the tests with this configuration was to find the load which represented the friction between the fastener and the hole.

Observing the trend lines in Figure 7.14, it is obvious that the confined tests exhibit higher failure loads and as a result higher bond strengths compared to the unconfined tests. The ratio between the bond strength of the unconfined and the confined tests is defined as the factor α_{setup}. For 10 mm and 50 mm bond length, $\alpha_{setup} = 0.88$ and $\alpha_{setup} = 0.93$, respectively. However, these values are calculated from the data in the linear fit. An exact calculation is given in the Section 7.3.9

The results from the partially bonded anchors were compared with those of the fully bonded anchors presented in Table 7.1. Figure 7.15 shows the failure loads for the reference bonded anchors and the partially bonded tested under confined setup.

The failure loads for all embedment depths using configuration a and b ranged between $53 - 61\,\%$ and $47 - 59\,\%$ of the results for the fully bonded anchors. For configuration c, the loads reached a maximum of $32\,\%$ of the reference tests.

Similar results showed the anchors tested under unconfined setup as shown in Figure 7.16. The tests with configuration a show a higher scatter of the results compared to the confined tests ($48 - 70\,\%$ of the fully bonded anchors). The other two configurations b and c reached $60 - 73\,\%$ and $35 - 43\,\%$ of the load, respectively.

These results agree well with existing studies on the influence of the bond length on the ultimate failure load of adhesive anchors, stating that the failure load increases with increasing bond length.
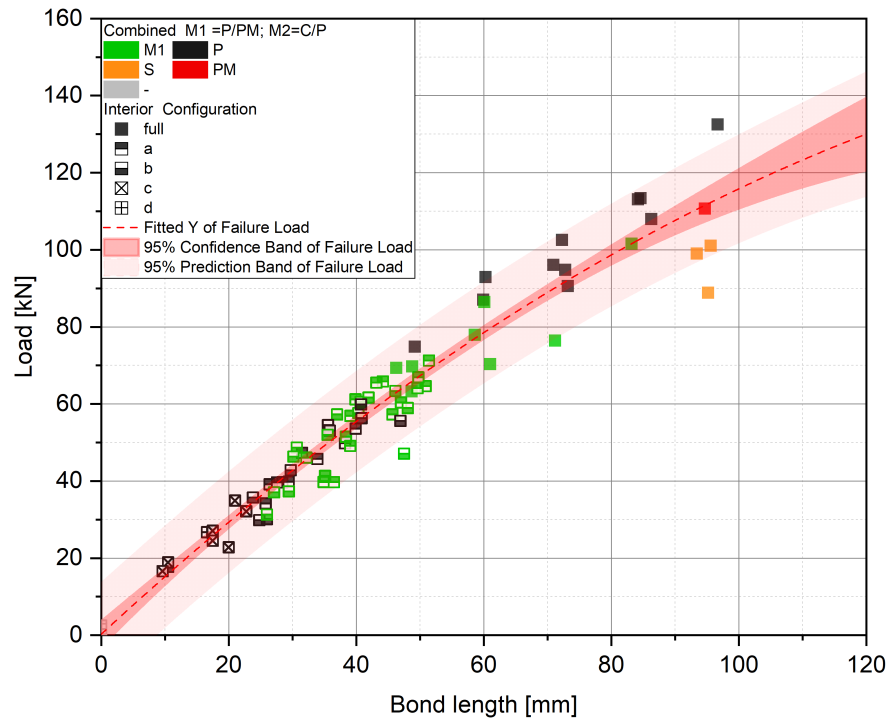
FIGURE 7.15: Influence of the bond length for the
confined tests with M 12
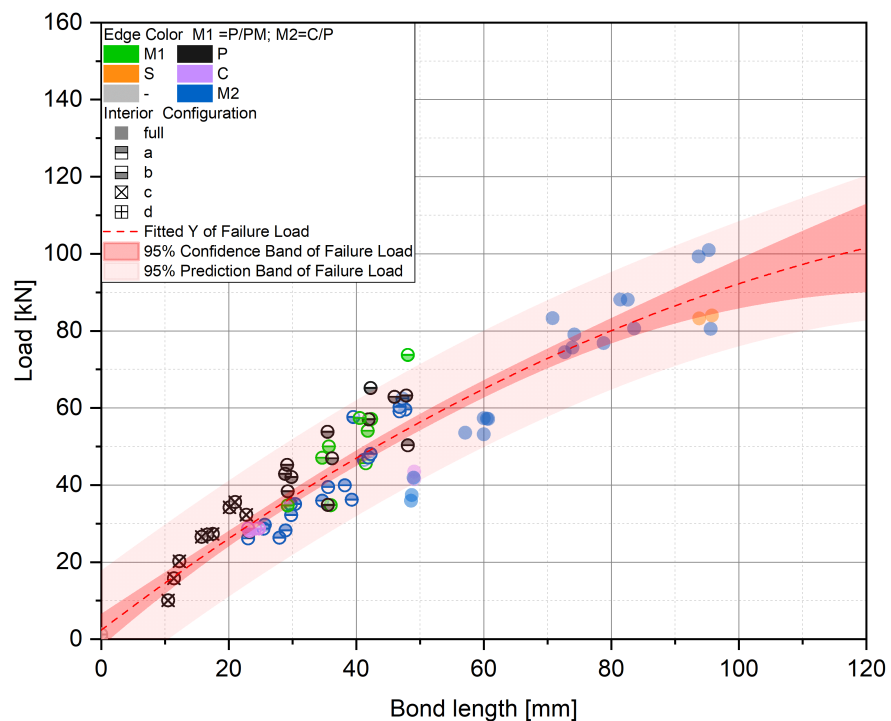
FIGURE 7.16: Influence of the bond length for the
unconfined tests with M 12

The bond strength was calculated using the uniform bond strength distribution Equation (2.6). Knowing the bond strength for the fully bonded anchors at $4\,d$, $6\,d$ and $8\,d$, and for each configuration, a, b, c and d, the bond strength for each quarter of depth was calculated.

Figure 7.17 illustrates the distribution of the bond strength for embedment depth $4\,d$ for confined and unconfined setup as well as the mean bond strength from the reference test series (Table 7.1).
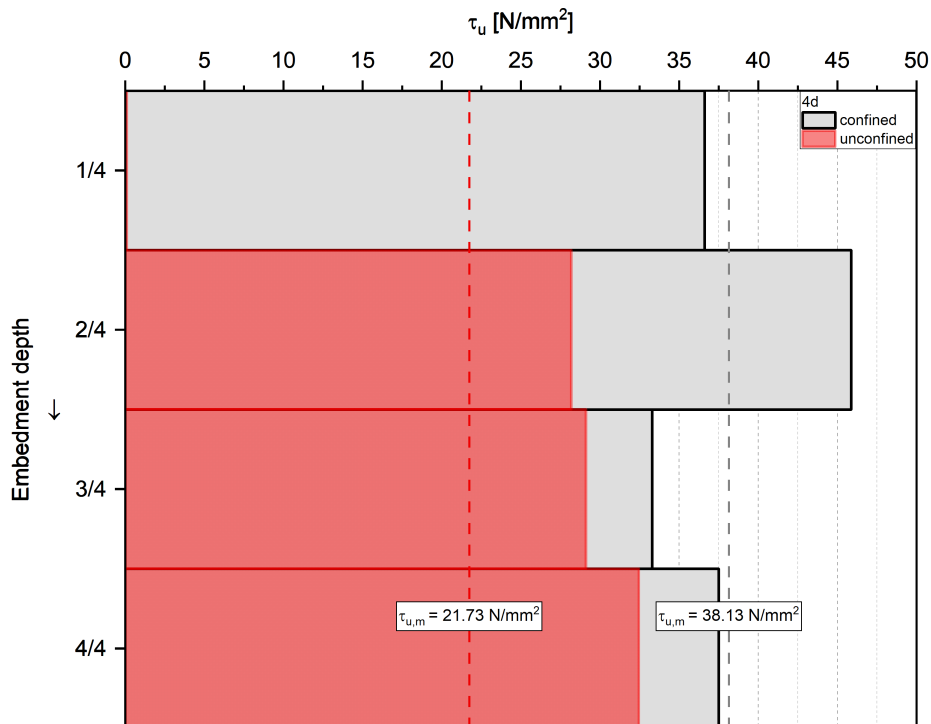
FIGURE 7.17:   Bond strength distribution along the embedment depth $4\,d$

The calculated bond strength distribution for the confined tests differed substantially from the unconfined tests. The unconfined tested anchors increased the bond strength with increasing depth. However, the confined anchors seem to behave irregularly. The bond strength at $1/4 \cdot h_{ef}$ was 36.6 N/mm^2 for the confined tests and approximately zero for the unconfined tests. At $2/4 \cdot h_{ef}$ the bond strength increased to 45.9 N/mm^2 and 28.2 N/mm^2, respectively. A further increase of the embedment depth to three-quarters, decreased the confined bond

strength to 33.3 N/mm². On the contrary, the bond strength for the unconfined increased by 3 % than the previous depth. The strength at the bottom part of the anchor rose to 37.5 N/mm² and 32.5 N/mm², for each support width.

Figure 7.18 shows the bond strength for the anchors with $6\,d$ embedment depth. Surprisingly, in contrary to the unconfined tests at $4\,d$, the anchors showed a higher bond strength at $1/4 \cdot h_{ef}$ depth (19.5 N/mm²) compared to the bond strength at $2/4 \cdot h_{ef}$ (15.1 N/mm²). Both bond strengths are illustrated in gray color in Figure 7.18. The reason for this behaviour is unclear. At $3/4 \cdot h_{ef}$ depth, the bond strength increased by approximately 48%. At the end of the embedment depth, the bond strength reached 38.5 N/mm².
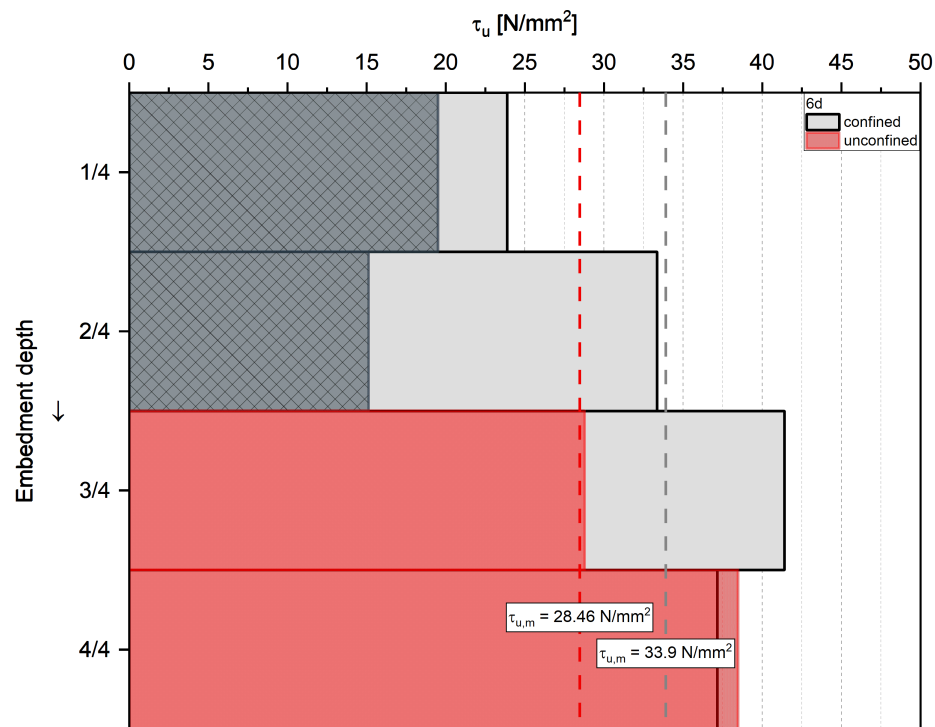
FIGURE 7.18: Bond strength distribution along the embedment depth $6\,d$

The confined tests behaved differently. The bond strength increased from 23.9 N/mm² to 41.4 N/mm² up to three-quarters of the embedment depth. At the bottom of the anchor, the strength decreased by 10% (to 37.2 N/mm²).

Lastly, the anchors installed at $8\,d$ showed the bond strength illustrated in Figure 7.19. The confined tests increased the bond strength up to $2/4 \cdot h_{ef}$ (from 29.3 N/mm^2 to 38.5 N/mm^2). Afterwards, the strength decreased to 35.6 N/mm^2 at $3/4 \cdot h_{ef}$ and 31.0 N/mm^2 at $4/4 \cdot h_{ef}$. The unconfined tests showed an increase in the bond strength throughout the length of the anchor. This strength started at 10.4 N/mm^2 up to 36.3 N/mm^2 at the bottom of the anchor.
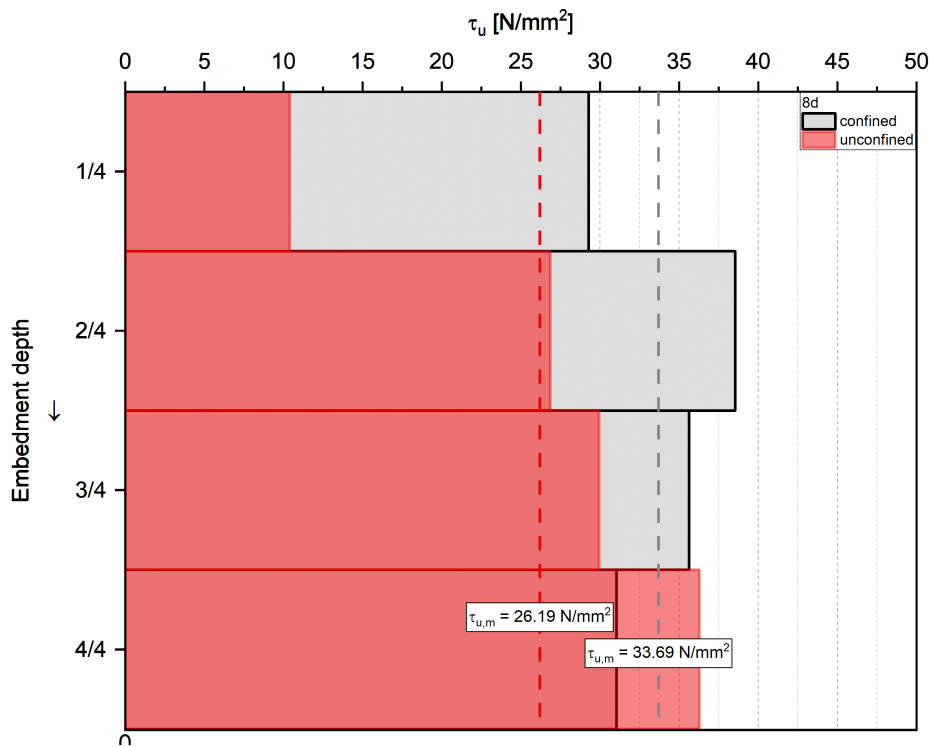
FIGURE 7.19: Bond strength distribution along the embedment depth $8\,d$

Figures 7.20 and 7.21 illustrate the bond strengths of each depth segment ($1/4 \cdot h_{ef}$ to $4/4 \cdot h_{ef}$) for the three depths ($4\,d$, $6\,d$ and $8\,d$) for confined and unconfined setup, respectively.

An interesting pattern emerged when examining the results of the confined tests. The bond strength at a depth up to $50\,\% \cdot h_{ef}$ was the lowest for the anchors installed at $6\,d$. However, for a depth between $50 - 100\% \cdot h_{ef}$, the bond strength was higher for the emebedment depth of $6\,d$. The mean value of the bond strength calculated from the tests in Table 7.1 (orange dotted line) followed the pattern of the upper part of the embedment depth,

where the bond strength at $4\,d$ is higher than at $6\,d$. Afterwards, the bond strength changes minimally with an increase of the embedment depth to $8\,d$.
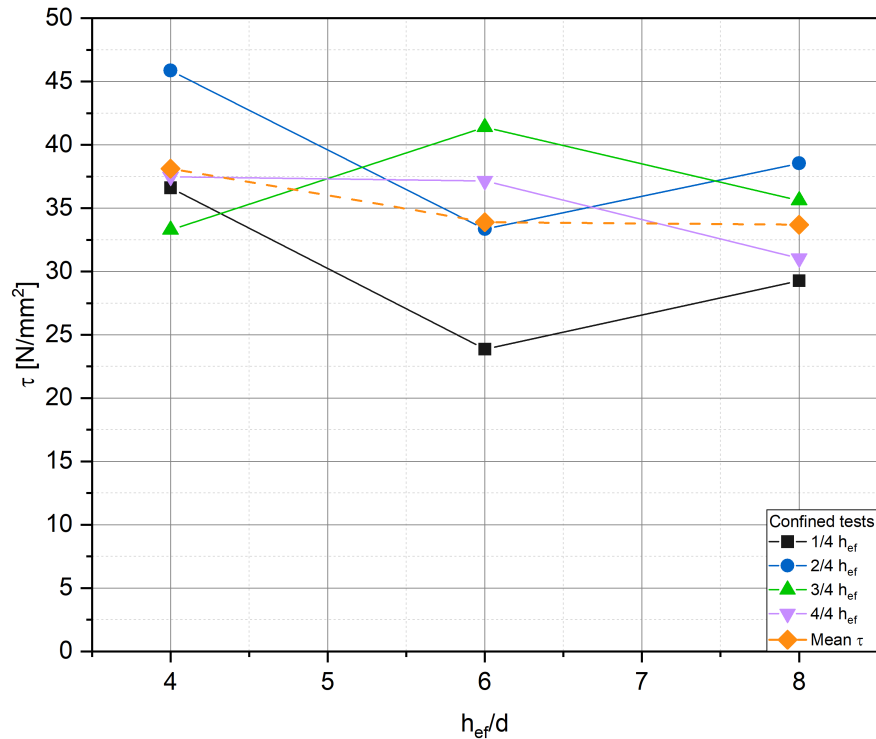
FIGURE 7.20: Comparison of the bond strengths for each depth segment

Figure 7.21 shows the results for the unconfined tests. In this case, three different behaviours can be observed. Firstly, the bond strength reaches a peak at $6\,d$ for the depths $1/4 \cdot h_{ef}$ and $4/4 \cdot h_{ef}$. Secondly, the bond strength is the lowest at $6\,d$ ($2/4 \cdot h_{ef}$). Lastly, the bond strength remains almost constant with increase of the embedment depth from $4\,d$ to $8\,d$ ($3/4 \cdot h_{ef}$). Here, the mean bond strength throughout the entire depth followed the first pattern with a higher bond strength at $6\,d$.
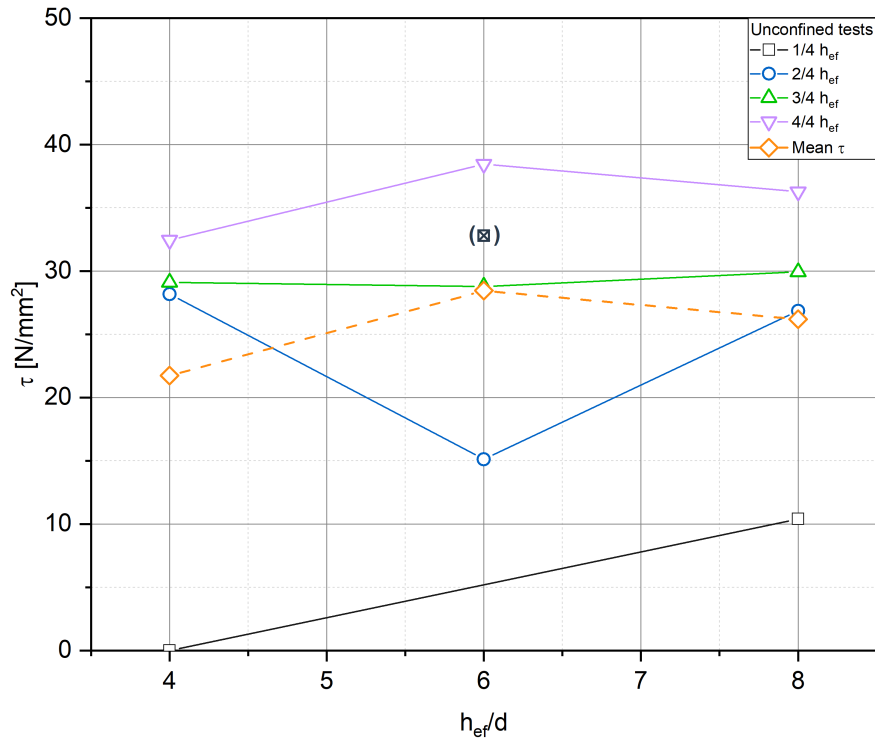
FIGURE 7.21: Comparison of the bond strengths for
each depth segment

7.3.6   Influence of the axial compression

The tests listed in Table 7.5 intended to examine the influence of
the axial compression on the bond strength and the load carrying
capacity of adhesive anchors. Figure 7.22 illustrates the results of
these tests. The x-axis shows the applied axial compression load
for each test series: 0 kN, 112 kN, 225 kN, 448 kN and 512 kN.
The reference tension tests with no axial compression revealed
a mean failure load of 78 kN. After increasing the axial com-
pression to $0.1 \cdot f_{cc}$ and $0.2 \cdot f_{cc}$, the failure load increased with
16% and 3%, respectively. Raising the compression to $0.4 \cdot f_{cc}$
and $0.45 \cdot f_{cc}$ rose the load with $9 - 11\%$ compared to the refer-
ence tests. The tests illustrate that the scatter of results within
each series reduces with increasing axial compression. The fail-
ure modes changed throughout the test series from mostly pull-
out failure for the reference tests to pull-out with mortar and
combined pull-out failure.
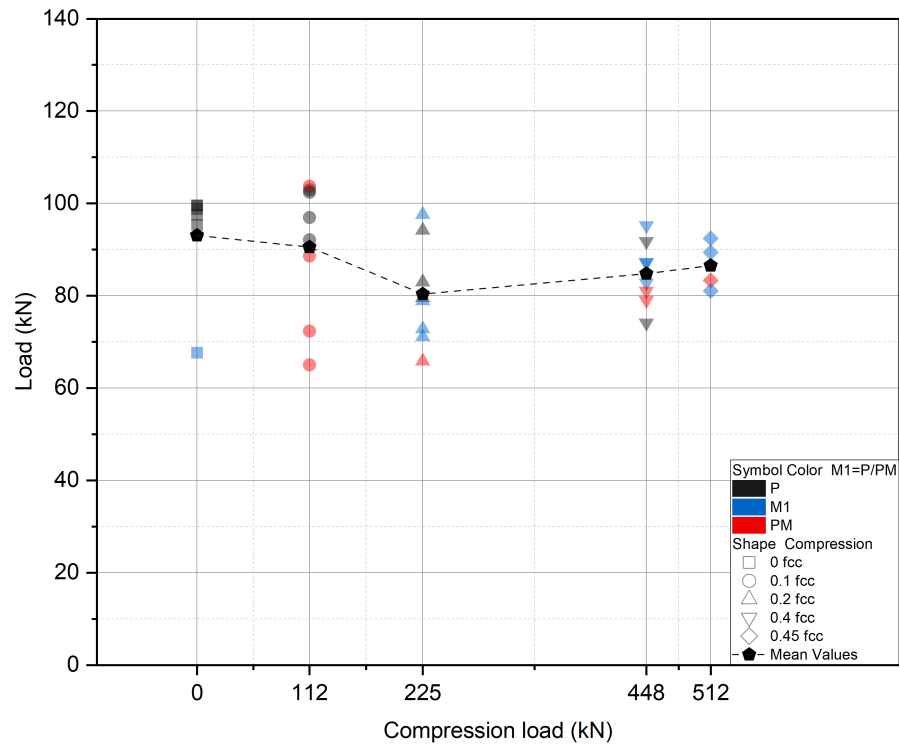
FIGURE 7.22: Influence of the axial compression for
Table 7.5 using M 12

Mészároš (2002) investigated in his dissertation the behaviour of adhesive anchors in low-strength concrete under two-axial compression. Figure 7.23 shows a comparison of the bond strengths with his results. The trend in both cases is similar. The bond strength in his tests increased up to 20% compared to the reference test and the scattering of the results reduced when the axial compression increased to $0.75 \cdot f_{cc}$.
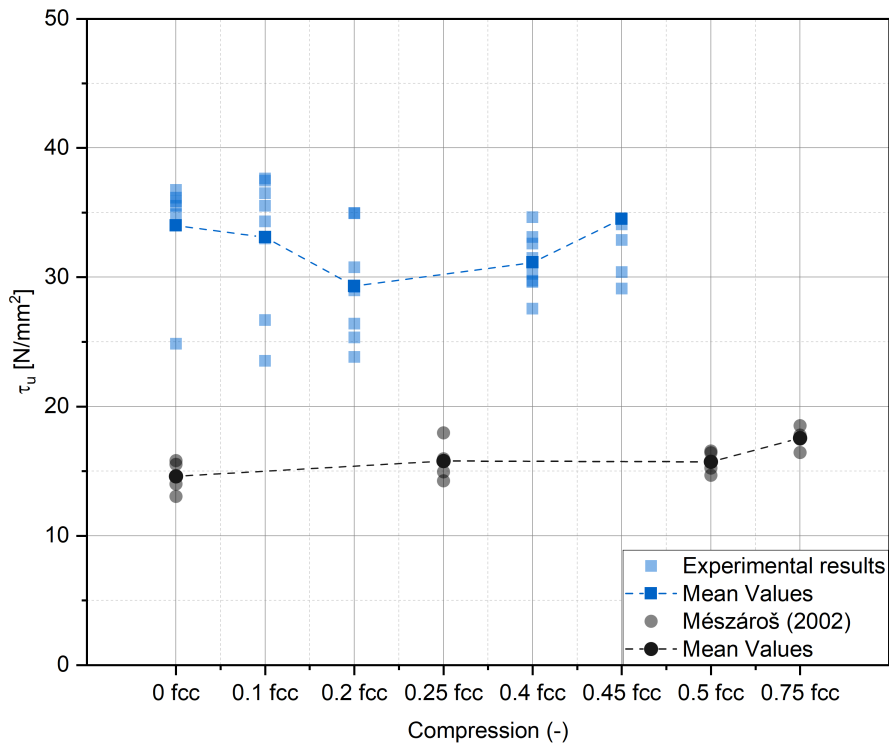
FIGURE   7.23:   Comparison of the results with
Mészároš (2002)

7.3.7   Influence of the sustained loading

Sustained load testing was carried out on low-strength and high-strength concrete (see Table 7.6). The anchors were loaded for a minimum of 5500 h. Afterwards, the anchors were unloaded and tested using a confined test setup (Chapter 5). Figure 7.24 and Figure 7.25 illustrate the displacement as a function of the loading time for $C20/25$ and $C90/105$, respectively.

Three configurations (a, b and fully bonded anchors) were installed in $C20/25$ concrete and loaded with $N_{sust} = 33$ kN (Figure 7.24). The sustained load was 32% of the short-term failure loads for the fully bonded anchors and 64% for configurations a and b. The data for the reference fully bonded anchors are denoted with black lines, for configuration a blue lines are used and for configuration b green lines. As expected, the displacement of the reference tests through time was lower compared to other two configurations. Before unloading, the mean displacement of the fully bonded anchors was 0.34 mm. Configurations

a and *b* showed more than twice the displacement of the reference anchors: 0.80 mm and 0.79 mm. After unloading, the mean residual displacement was 0.15 mm for the fully bonded anchors and 0.56 mm for configurations *a* and *b*.
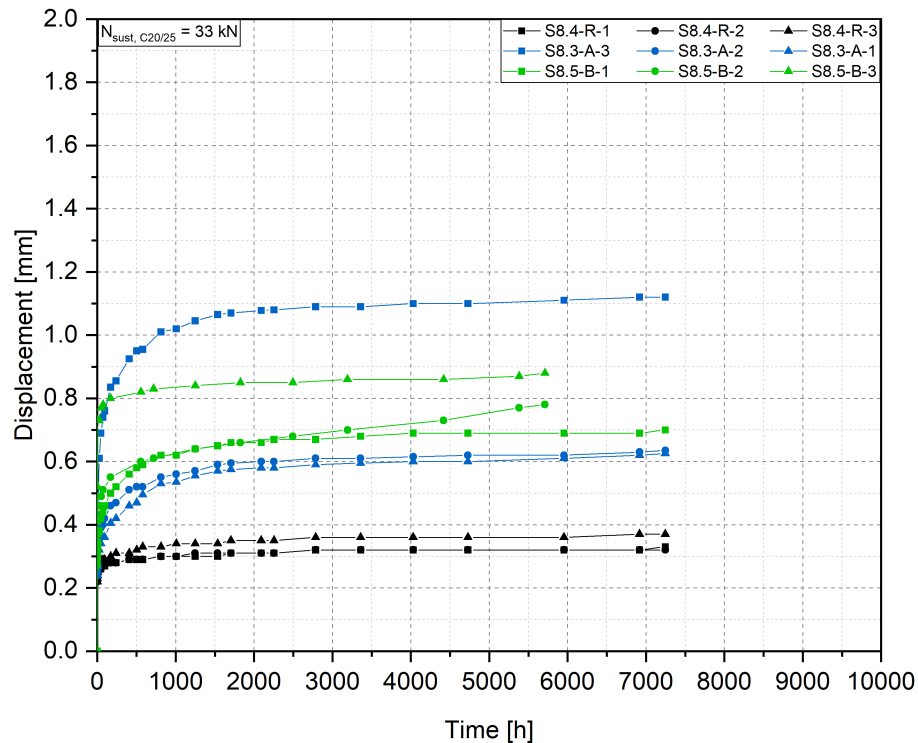
FIGURE 7.24: Influence of sustained loading in *C*20/25 concrete

Figure 7.25 presents the displacements for the anchors in *C*90/105. The anchors installed with configuration *a* were loaded with $N_{sust} = 34$ kN, whereas those installed with configuration *b* with $N_{sust} = 37$ kN. The sustained loads were 40% and 35% of the short-term failure loads. The mean displacements before unloading were 0.98 mm and 1.48 mm for each configuration. The residual displacements were 0.69 mm and 0.77 mm.

The displacement measured during the sustained load testing helped predicting the displacement after 50 years and 100 years using the Findley approach (Findley, Lai, and Onaran, 1976) described in Section 4.1. Figures 7.26 to 7.30 illustrate the Findley approximation for each test series. According to guidelines: EAD 330499 (2018) and AC 308 (2017), the approximated displacement
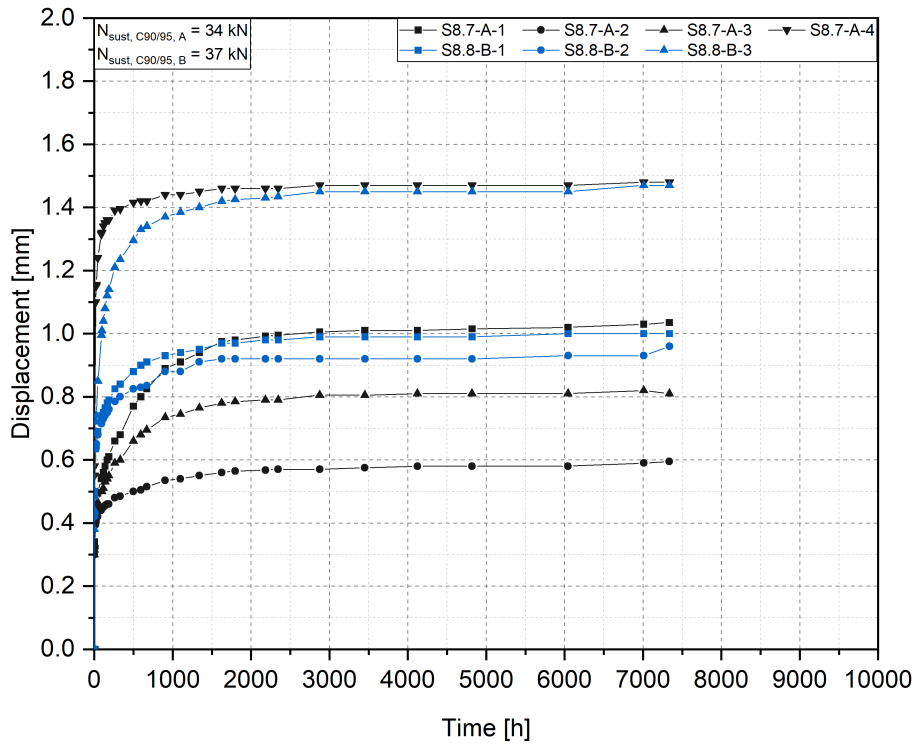
FIGURE 7.25:   Influence of sustained loading in
C90/105 concrete

shall be compared to mean displacement of the reference short-term tests where the loss of adhesion occurs δ_{adh} to establish if the tests were successful. Table 7.8 lists the displacements δ_{adh} for each loading case as well as the displacements at failure load δ_u.

TABLE 7.8: Displacements of the short-term tests

Concrete [−]	Configuration [−]	δ_{adh} [mm]	δ_u [mm]	$\delta_{50y,m}$ [mm]	$\delta_{100y,m}$ [mm]
C20/25	−	0.30	1.13	0.47	0.50
C20/25	*a*	0.36	0.46	1.31	1.43
C20/25	*b*	0.49	0.56	1.19	1.31
C90/105	*a*	0.46	0.46	1.51	1.63
C90/105	*b*	0.55	0.47	2.01	2.22

The reference sustained load tests $S8.4 − R$ results in low-strength concrete are shown in Figure 7.26. The mean extrapolated displacement after 50 years was 0.48 mm and after 100

years, 0.52 mm. Both displacements were 60% and 73% higher than the displacement at loss of adhesion.
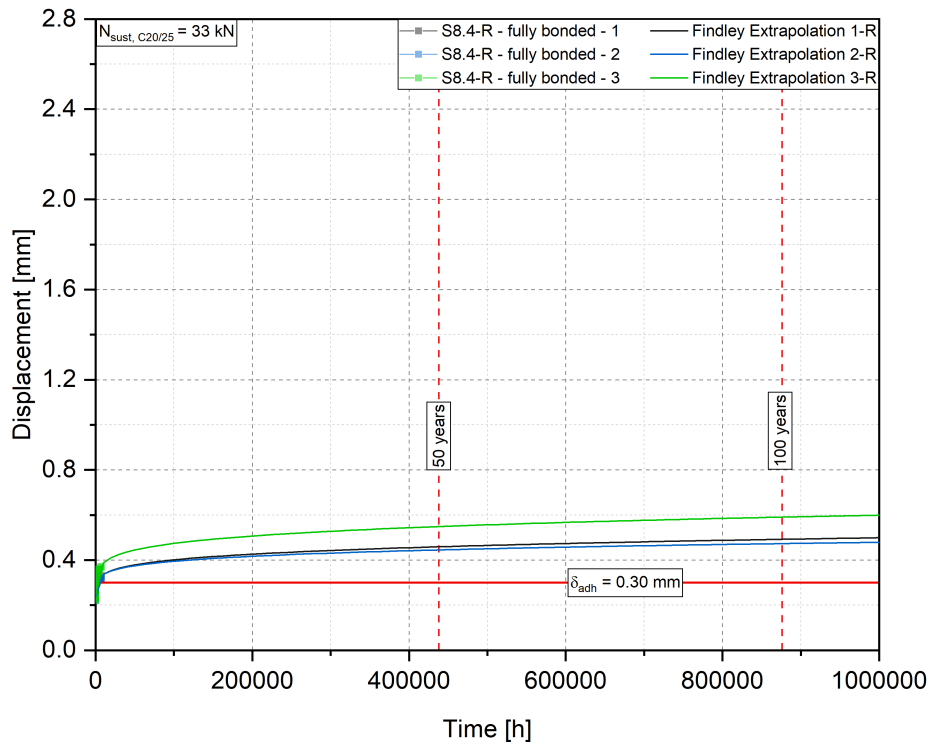
FIGURE 7.26: Findley extrapolation to 50 and 100 years for test series $S8.4 - R$

Figure 7.27 and Figure 7.28 present the extrapolated results for the series $S8.3 - A$ and $S8.5 - B$ in low-strength concrete. The displacements after 50 years were 1.49 mm and 1.24 mm for each configuration. Similarly, the extrapolation after 100 years revealed displacements of 1.64 mm and 1.33mm, respectively. The calculated values for configuration a were more than three times the displacement at loss of adhesion. Configuration b showed 1.5 and 1.7 times higher values compared to δ_{adh}.
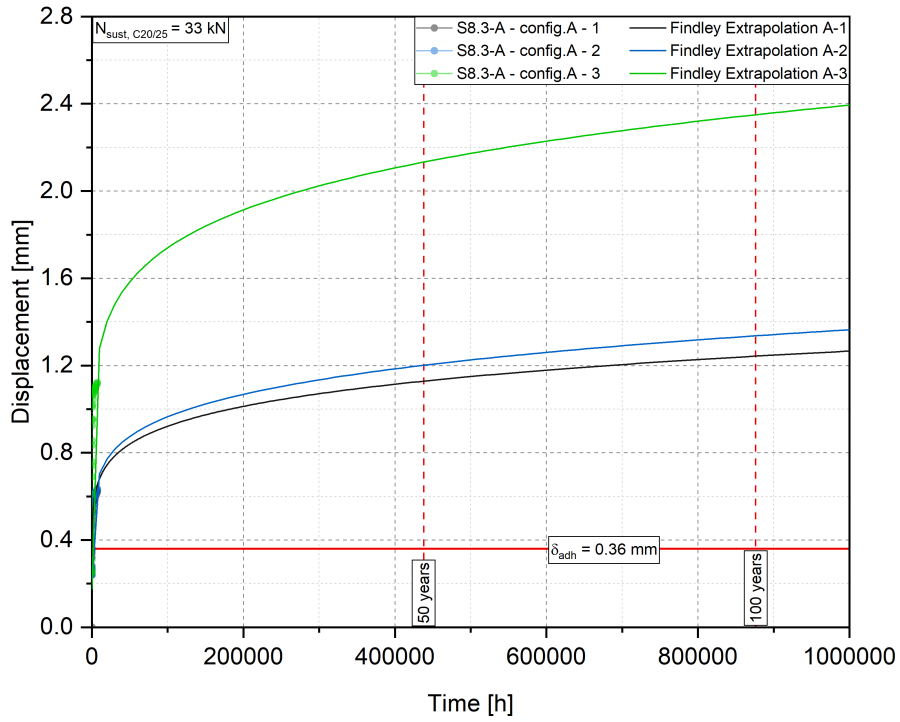
FIGURE 7.27: Findley extrapolation to 50 and 100
years for test series $S8.3 - A$
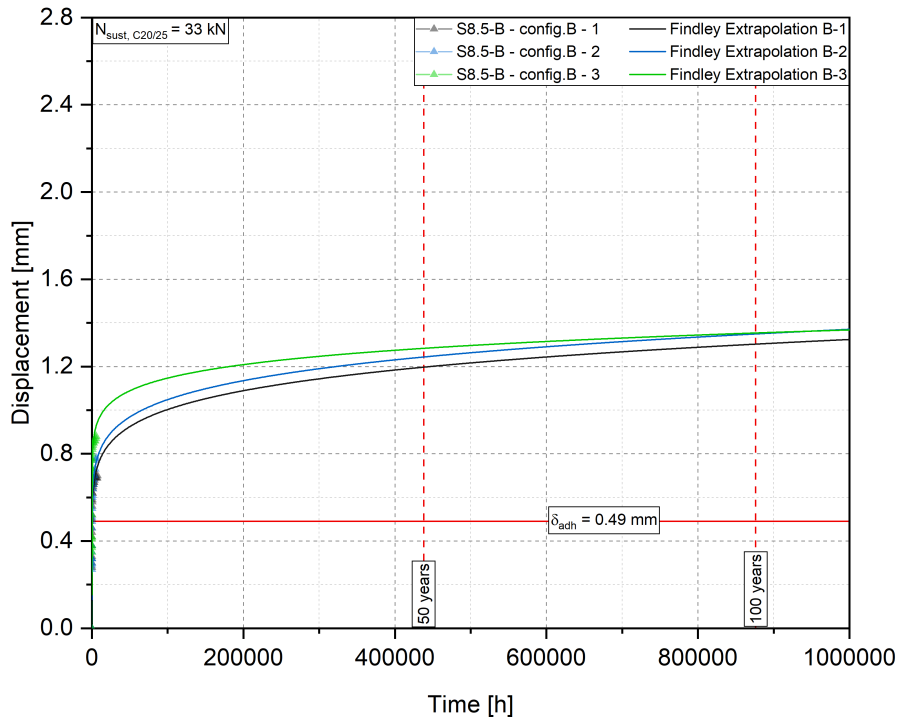
FIGURE 7.28: Findley extrapolation to 50 and 100
years for test series $S8.5 - B$

The Findley approximation for the anchors installed in high-strength concrete $C90/105$ is shown in Figure 7.29 for configuration a ($S8.7 - A$) and Figure 7.30 ($S8.8 - B$) for configuration b. The calculated displacements after 50 years were 1.69 mm and 1.89 mm and after 100 years 1.83 mm and 2.03 mm. Compared to the displacement δ_{adh}, the extrapolated displacements after 50 years were 2.7 and 2.4 times higher for each configuration. Similarly, the displacement at 100 years were at 3 and 2.7 times higher.
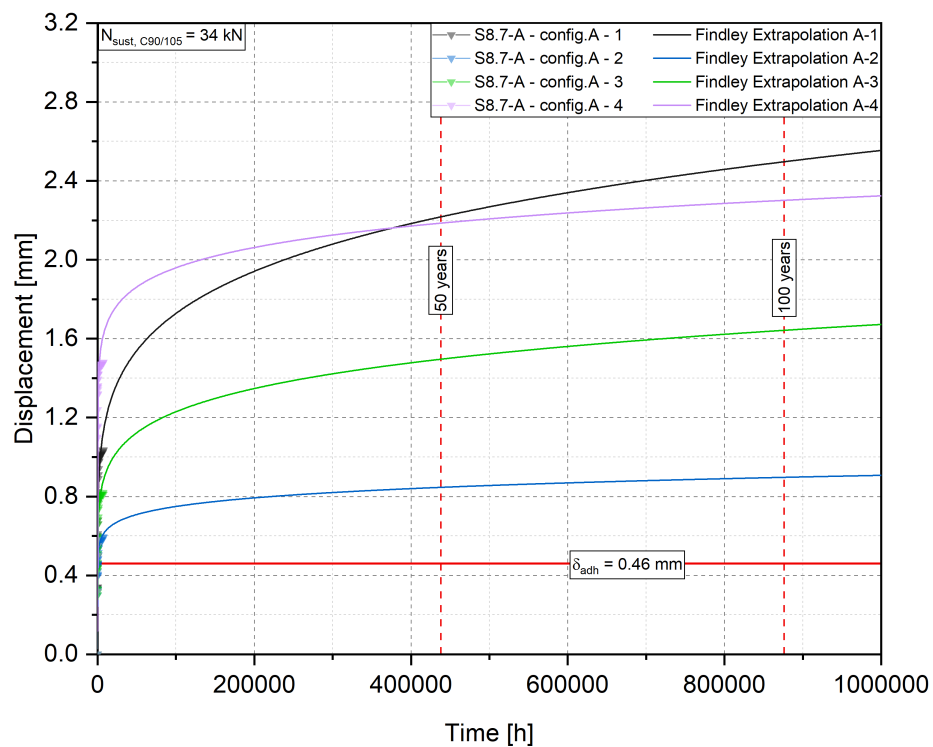
FIGURE 7.29: Findley extrapolation to 50 and 100 years for test series $S8.7 - A$

The fully bonded anchors exhibited an overall smaller displacement compared to the other configurations. According to the criteria from the current guidelines (EAD 330499, 2018; AC 308, 2017), all the performed tests failed (the extrapolated displacement was higher than the displacement at loss of adhesion), thus the tests should be repeated with a reduced sustained load. Comparing the same displacements, with the displacements of the short-term tests at ultimate failure load, only the tests with full bond length in low-strength concrete would not fail after 50
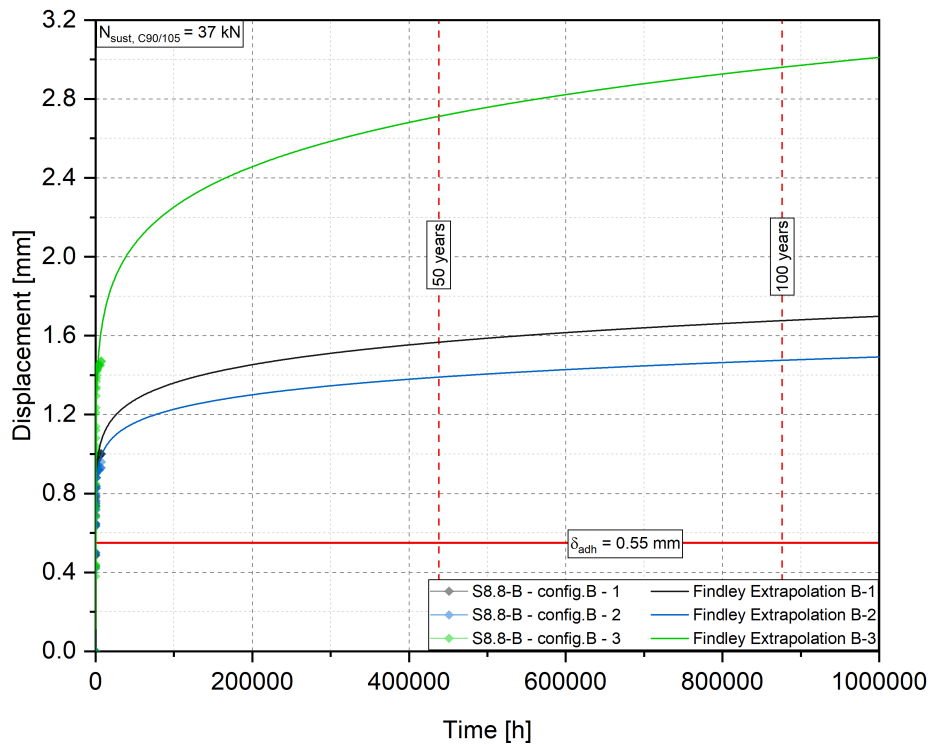
FIGURE 7.30:   Findley extrapolation to 50 and 100
years for test series $S8.8 - B$

and 100 years. The test series, exhibited distinctly higher extrapolated displacement, which pointed out to a failure of the adhesive prior to 50 years.

After unloading, the anchors were loaded to failure using a confined setup. The load displacement curves are illustrated in Appendix C. The failure loads of the long-term tests were compared to the failure loads of the correspondent short-term tests.

The anchors installed in low-strength concrete with full bonding length showed a slightly lower load compared to the short-term tests (3%). On the other hand, the anchors installed with configuration a and b showed an increase on the failure load of 18% and 20%, respectively. Similar increase showed the anchors installed in high-strength concrete $C90/105$: 24% and 11% for configurations a and b.

Figure 7.31 illustrates the bond strength of the sustained loads and the extrapolated displacement as a function of the short-term tests. Only the mean values of the tests are illustrated. The x-axis gives the ratio between the extrapolated displacements at 50

years and the displacement of the short-term tests. Two short-term displacements were considered: displacement at loss of adhesion δ_{adh} and the displacement at failure load δ_u. These two displacements were used as a criterion to evaluate if the adhesive anchors system was damaged (EAD 330499, 2018; AC 308, 2017). The y-axis shows the ratio of the residual bond strength of the sustained load tests and the short-term tests' bond strength.
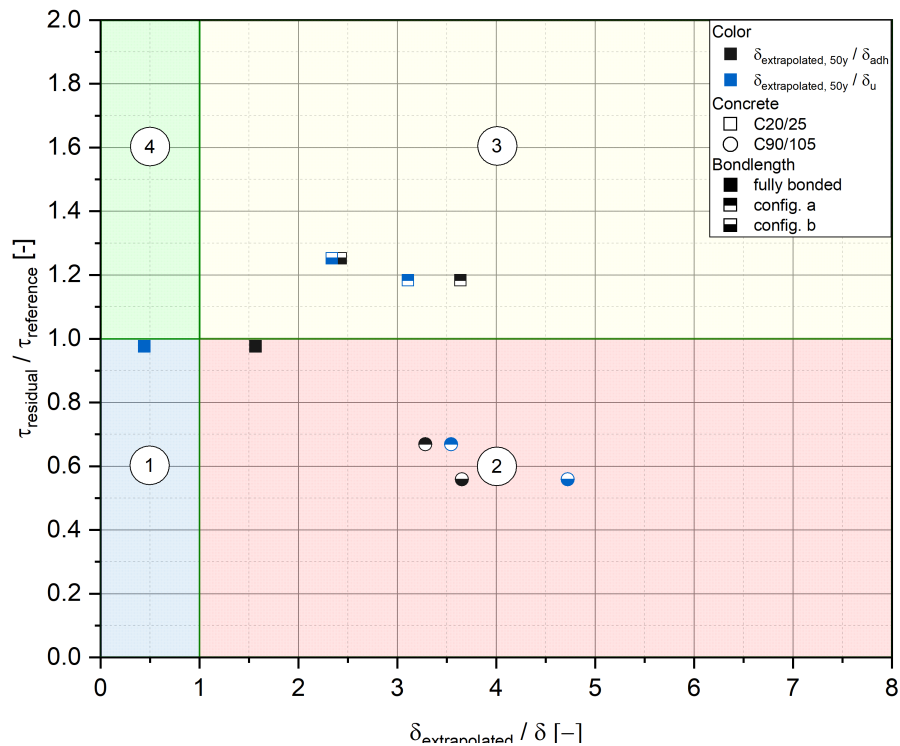
FIGURE 7.31: Relative residual bond strength for the sustained load tests

From Figure 7.31, four regions can be defined:

- Region 1: $\frac{\tau_{residual}}{\tau_{reference}} \leq 1.0$ and $\frac{\delta_{extrapolated}}{\delta} \leq 1.0$
  The adhesive anchor system is undamaged. The bond strength after sustained loaded is smaller than the bond strength of the short-term tests.

- Region 2: $\frac{\tau_{residual}}{\tau_{reference}} \leq 1.0$ and $\frac{\delta_{extrapolated}}{\delta} > 1.0$
  The adhesive anchor system is damaged. The anchors should be tested again with a lower long-term load.

- **Region 3:** $\frac{\tau_{residual}}{\tau_{reference}} > 1.0$ and $\frac{\delta_{extrapolated}}{\delta} > 1.0$

  The bond strength after sustained loading is higher than the strength of the short-term tests - Strength criterion is fulfilled. The extrapolated displacement is higher than the short-term displacements - Displacement criterion is not fulfilled. It is not possible to draw a conclusion about the long-term behaviour of the anchors in this region.

- **Region 4:** $\frac{\tau_{residual}}{\tau_{reference}} > 1.0$ and $\frac{\delta_{extrapolated}}{\delta} \leq 1.0$

  The anchor system is considered undamaged. The bond strength of the sustained loading tests is higher.

As seen in Figure 7.31, the fully bonded anchors exhibit a lower bond strength after sustained loading. However, depending on which short-term displacement is the criterion, the adhesive system is either damaged (δ_{adh}) or undamaged (δ_u). The partially bonded anchors in high-strength concrete are located in region 2, which indicates that the system is damaged. On the other hand, the partially bonded anchors in low-strength concrete are located in region 3. These anchors exhibit higher bond strengths after sustained loading. However, it is unclear if the adhesive system is damaged or if the concrete fails prior to the damage of the adhesive.

7.3.8   Comparison of the TTF and sustained loading tests

Figure 7.32 shows a comparison between the time to failure tests performed at IWB (2019) and the sustained loading tests. The TTF tests were performed at $23\,^{\circ}C$ (see Figure 4.28). In this figure, the ratio of the bond strength during sustained loading (calculated from the sustained load) with the bond strength of the short-term tests is given as a function of time. For the sustained load, the considered time depicts the time when the anchors reached the respective displacement at loss of adhesion (not the time when the tests were extrapolated or stopped). The results of the sustained load fit well with the TTF tests.
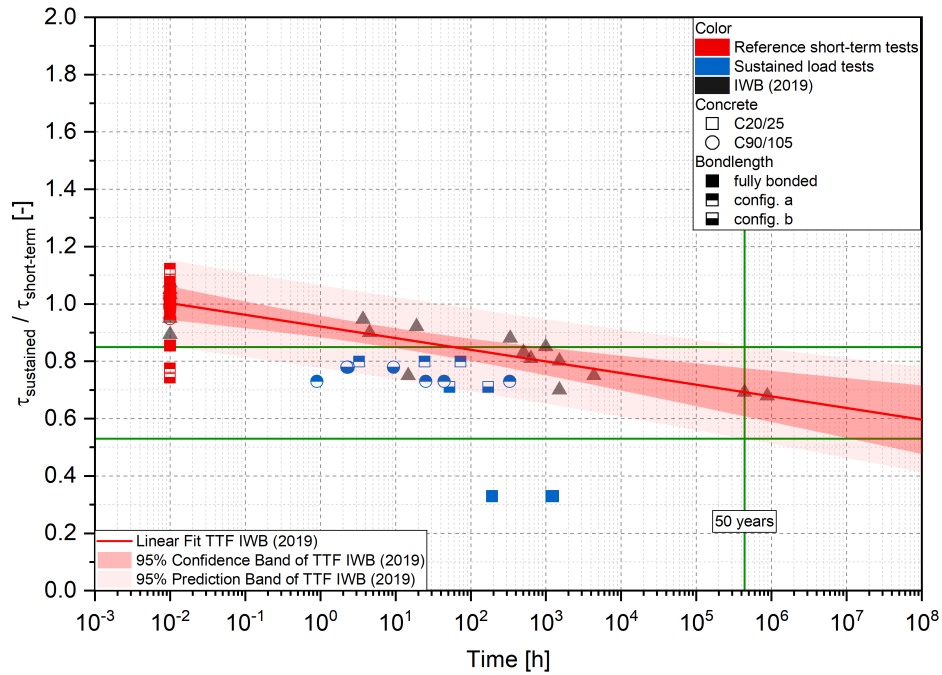
FIGURE 7.32: Comparison of the TTF tests and sustained loading tests

7.3.9 Alpha setup

The influence of the support diameter as a function of the embedment depth was discussed in Section 7.3.4. This section focuses on the relationship between the confined tests and unconfined tests which is defined as α_{setup} and given in Equation (7.1):

$$\alpha_{setup} = \frac{\tau_{unconf}}{\tau_{conf}} \tag{7.1}$$

To evaluate this relationship, the results of the tests in Tables 7.1, 7.2 and 7.4 were considered. The other results were omitted due to the lack of tests using unconfined setup.

Table 7.9 lists the bond strengths for the confined tests τ_{conf} and unconfined tests τ_{unconf}, their relationship α_{setup} and the maximum bond strength needed to activate the concrete surface τ_{max}. To calculate the maximum bond strength, the failure load needed to activate the concrete surface can be taken equal to the failure load needed to pull-out the fastener. Thus, by equating

the failure load predicted using the CCD method (Section 2.3.2) with the load predicted using the UBM (Section 2.3.4), τ_{max} is:

$$\tau_{max} = \frac{k_{nc} \cdot \sqrt{f_{cc,200}} \cdot h_{ef}^{1.5}}{\pi \cdot d \cdot h_{hef}} \tag{7.2}$$

TABLE 7.9: Calculated α_{setup} values

Series [−]	h_{ef}/d [−]	Config. [−]	τ_{conf} [N/mm²]	τ_{unconf} [N/mm²]	τ_{max} [N/mm²]	α_{setup} [−]
S1.1	4	−	38.13	21.73	23.63	0.57
S1.2	5	−	36.70	24.77	26.35	0.67
S1.3	6	−	33.90	28.46	28.88	0.84
S1.4	7	−	34.37	27.12	31.34	0.79
S1.5	8	−	33.69	26.19	33.18	0.78
S2.1	4	−	25.43	18.22	23.43	0.72
S2.2	6	−	24.71	20.74	28.99	0.84
S2.3	8	−	19.46	17.97	33.55	0.92
S4.0 − A	4	a	37.12	29.70	17.84	0.80
S4.0 − B	4	b	34.13	31.85	17.19	0.93
S4 − 4d − 3/4	4	c	46.10	35.38	10.87	0.77
S4.1	5	a	35.01	29.39	19.69	0.84
S4.2	5	b	38.66	36.86	18.66	0.95
S4.3	6	a	33.59	26.95	21.09	0.80
S4.4	6	b	39.94	34.76	20.43	0.87
S4 − 6d − 3/4	6	c	40.31	43.15	14.11	1.07
S4.5	7	a	38.64	30.99	22.21	0.80
S4.6	7	b	38.37	37.51	21.76	0.98
S4.7	8	a	34.73	32.72	23.92	0.94
S4.8	8	b	31.67	37.34	23.34	1.18
S4 − 8d − 3/4	8	c	37.29	42.58	15.68	1.14

Figure 7.33 illustrates the results of the tests. On the y-axis, the relationship between τ_{unconf} and τ_{conf} (α_{setup}) is shown. The x-axis shows the ratio between τ_{conf} and τ_{max}.

The fully bonded anchors with $M12$ threaded rods showed a ratio of the unconfined to the confined bond strengths between 0.57 and 0.84 whereas the reinforcing bars from 0.72 to 0.92. The α_{setup} for the partially bonded anchors ranged from 0.77 to 1.18. The results show that the ratios are usually above 0.75 but also below 1.0. This mean that an α_{setup} is necessary and 0.75 is generally sufficient.
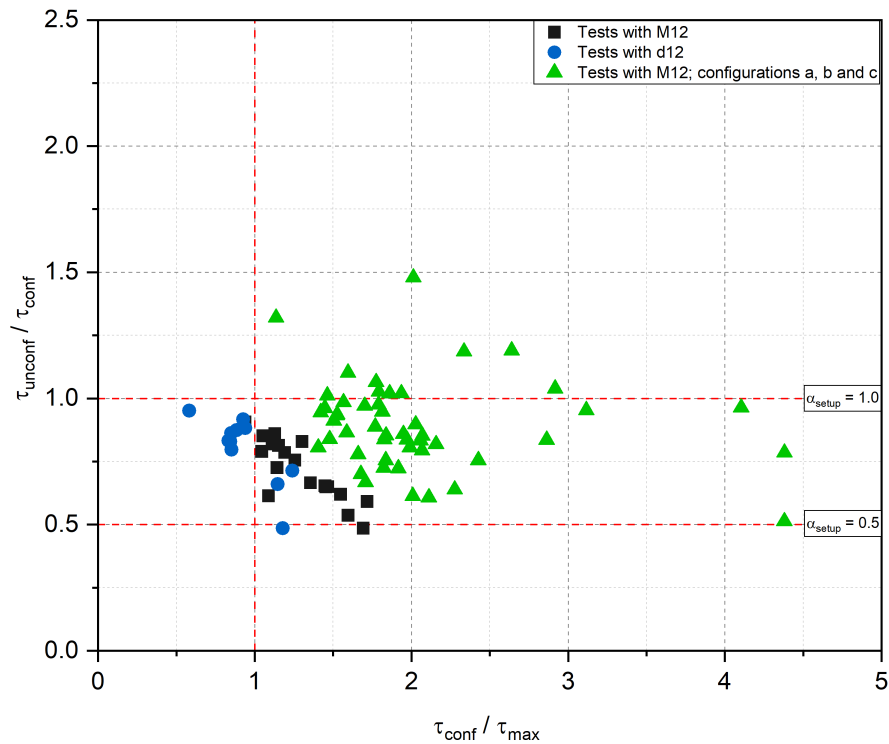
FIGURE 7.33: Influence of the setup type as a function of τ_{conf}/τ_{max} - experimental results

Figure 7.34 presents the results of this research and the data collected from the literature Mészároš (2002), Appl (2009), and Vogelgsang (2012). The plotted green line represents the reduction as a result of concrete cone failure (EAD 330499, 2018). Every point located below the theoretical Curve (green line) should be covered by α_{setup}.
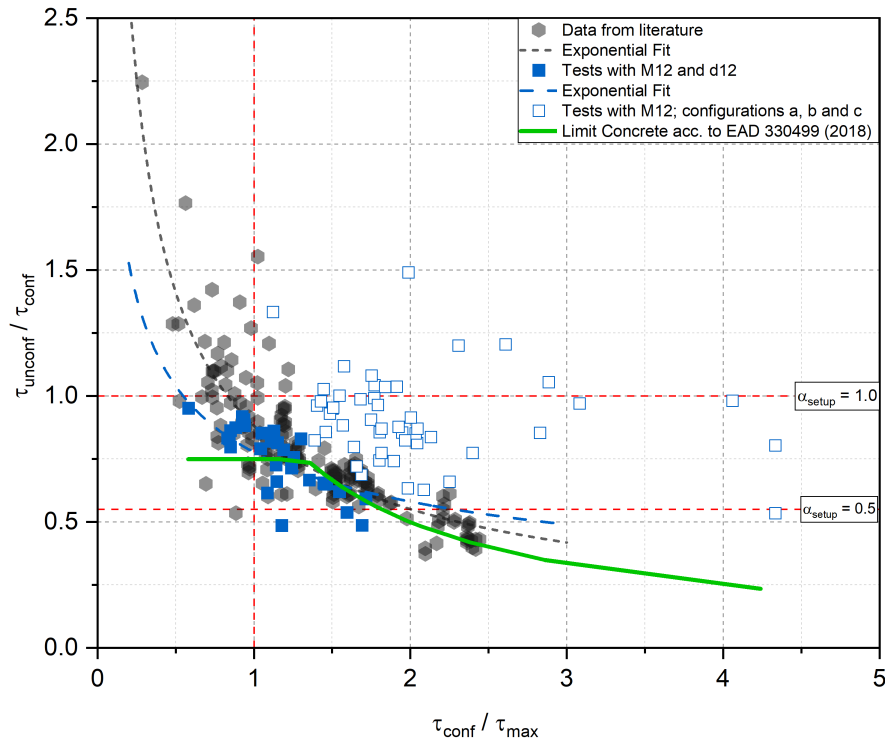
FIGURE 7.34: Influence of the setup type as a function
of τ_{conf} / τ_{max} - comparison with literature data

7.4   Summary of the results

The experimental investigations showed the influence of different factors on the carrying capacity of adhesive anchors. The studied parameters included the embedment depth, the support diameter, the bond length, axial compression and sustained loading.

Firstly, the influence of the embedment depth was studied. The finding of this research correspond with the findings in literature: The failure load of the adhesive anchors increases with an increase of the embedment depth independent of the diameter of the testing setup. The bond strength for the threaded rods $M12$ and the reinforcing bars $d12$, increased up to an embedment depth of $h_{ef} = 6 \cdot d$, afterwards it decreased.

The next investigated parameter was the support diameter on reinforcing bars $d12$. The support diameter was varied from $0.24 \cdot h_{ef}$ to $2.0 \cdot h_{ef}$. As expected, the failure load decreased when

the support diameter increased. The bond strength behaved accordingly. The results of these tests, were compared with the tests using a confined and unconfined support as given in the current standards. The observations also agree with previous findings: the larger the support diameter the lower the failure load and the bond strength.

The influence of bond length was observed on threaded rods. Four bonding configurations were tested without considering the fully bonded anchors. Two configurations consisted on 50% bond length (*a* and *b*), one configuration on 25% bond length (*c*) and the last one with 0% bond length (*d*). The tests with "no" bonding length were performed to consider for the friction between the fastener and the hole. The results from these tests were approximately 1.9 kN. Configurations *a* and *b* showed the same bond length but distributed differently (Figure 7.1). Configuration *a* revealed overall higher failure loads for the confined tests compared to configuration *b*. However, for the unconfined tests, the opposite was observed. The confined tests with configuration *c* showed almost 75% lower load compared to the fully bonded anchors, whereas the unconfined tests showed a 65% lower load.

The adhesive anchors were subjected to axial compression to investigate the shear behaviour of the mortar. Three main observations were made. Firstly, the load of the fasteners increased with increasing axial compression (compared to the reference tests with no axial compression). Secondly, the scatter of the failure loads reduced with increasing compression. Lastly, the failure modes transitioned from pull-out (reference tests) to mixed pull-out or pull-out with mortar at the highest compressive load.

Long-term tests (sustained load) were performed to determine the behaviour of the adhesive after 50 and 100 years. The displacement of the anchors was measured throughout the loading period. Using the Findley approach (1976), the displacement was calculated. Two concrete compressive strengths were studied. Three configurations were investigated in C20/25 (configuration *a*, *b* and fully bonded), whereas in C90/105 only two (*a* and *b*). According to the current standards, each of the performed tests failed to qualify because the extrapolated displacements were higher than the displacement at loss of adhesion. Similarly, comparing these displacement with the displacements

at maximum failure load, only the fully bonded anchors in low-strength concrete would not fail after 100 years. The sustained load tests were also compared with the TTF tests in Chapter 4. The results showed that the displacement criterion given in the current guidelines (EAD 330499, 2018; AC 308, 2017) is on the safe side.

Lastly, the ratio between the unconfined and confined bond strength was calculated from the tests. The minimum calculated α_{setup} for the fully bonded anchors was 0.57 and the maximum 0.92. The results show overall that an α_{setup} is necessary and 0.75 is generally sufficient.

7.5   Comparison with the design models

The design models used to predict the failure loads for bond failure and concrete failure are presented in Section 2.3. This section focuses on a comparison between the loads of the test results and the loads predicted using the design models from literature. Only the tests described in Table 7.1, Table 7.2 and Table 7.3 were considered for this comparison.

As mentioned in Section 2.3.3, the prediction of the load using the elastic bond model (EBM) can be applied if preliminary tests with partially bond anchors are carried out. In this research, only $M12$ threaded rods were tested as partially bonded anchors (Table 7.4). Their results were utilised to establish τ_{max} and λ' with the help of a least squares fit. Using these two parameters, the ultimate load was predicted.

The current standards AC 308 (2017), ACI 318 (2019), and EAD 330499 (2018) predict the characteristic resistance to pull-out failure using Equation (2.6), which assumes a uniform bond stress distribution. The characteristic resistance for concrete cone failure is calculated using Equation (2.2).

The combined cone / bond models with elastic or uniform bond model are calculated similarly. Firstly, the depth of the cone is determined using either Equation (2.9) or (2.11). The difference between these two equations is the hyperbolic secant in Equation (2.9). This model is valid when the depth of the cone is smaller or equal to the bond length $h_{cone} \leq h_{ef}$. After the cone

depth is calculated, the combined capacity of the anchor is evaluated.

The next model used to predict the bond failure load is the bond model neglecting the shallow concrete cone. Curve fitting is used on *M* 12 and *d* 12 for both confined and unconfined tests. The intersection of the confined and unconfined fit curves, represents the bond length where the shallow concrete cone can be taken into account. Thus, this model can be applied only to *d* 12.

It is important to point out, that all the above mentioned bond models, are calculated using the diameter of the anchor *d* and not the diameter of the drilled hole d_0 as given in the Equations (2.4), (2.5) and (2.8) to (2.10).

The two interface model could not be applied to predict the failure load. This model assumes pull-out or pull-out with mortar failure of the fasteners, however the anchors of this research failed mostly in a mixed failure mode (combined pull-out and pull-out with mortar).

Table 7.10 and Table 7.11 list the results from the experimental investigation and the calculations from the design models for bond and concrete failure, respectively.

TABLE 7.10: Comparison of the test results for bond failures: P, P_M and $M1$

Series	N_{test}	EBM		UBM		Combined cone / bond				Bond negl.	
						EBM		UBM		shallow cone	
		N_p	$\frac{N_t}{N_p}$	N_p	$\frac{N_t}{N_p}$	N_p	$\frac{N_t}{N_p}$	N_p	$\frac{N_t}{N_p}$	N_p	$\frac{N_t}{N_p}$
[−]	[kN]	[kN]	[−]	[kN]	[−]	[kN]	[−]	[kN]	[−]	[kN]	[−]
S1.1-C	69.33	53.3	1.31	69.8	1.00	−	−	−	−	−	−
S1.2-C	82.97	61.4	1.35	86.2	0.96	−	−	−	−	−	−
S1.3-C	92.13	68.1	1.35	103.6	0.89	−	−	−	−	−	−
S1.4-C	109.98	73.3	1.50	122.0	0.90	100.6	1.09	58.3	1.89	−	−
S1.5-C	121.65	76.5	1.59	135.6	0.88	199.8	0.61	71.9	1.69	−	−
S2.1-C	45.42	−	−	45.5	1.00	−	−	−	−	−	−
S2.2-C	67.63	−	−	69.6	0.97	−	−	42.5	1.59	67.7	1.00
S2.3-C	68.57	−	−	92.4	0.77	−	−	54.2	1.30	70.8	1.00
S3.1	59.42	−	−	58.3	1.00	−	−	31.6	1.88	59.5	1.00
S3.2	56.50	−	−	59.0	0.96	−	−	32.0	1.77	61.3	0.92

The results in Table 7.10 demonstrate that the uniform bond model predicted the failure load for all bond lengths and both types of steel components with the highest accuracy. The ratio

varied between 0.88 and 1.0. The elastic bond model produced less accurate loads with an increase in the bond length. The mean predicted failure load for all depths was between 23 % to 37 % lower than the test results. The combined cone / bond models were used to predict the failure load only for embedment depths $7\,d$ ($S1.4 - C$) and $8\,d$ ($S1.5 - C$) for $M\,12$, because only in these cases the condition of the cone depth was fulfilled. The model based on EBM showed a better approximation only for $7\,d$ with 9 % lower predicted load. For $8\,d$ the load was overestimated with 64 %. On the other hand, the model based on UBM showed an underestimation of the predicted failure load for both bond lengths of 47 % and 41 %, respectively.

It should be noted, that for the reinforcing bars $d\,12$ in Table 7.2 only one result for embedment depth $8\,d$ ($S2.3 - C$) was considered, because the other fasteners exhibited steel failure. The reinforcing bars summarized in Table 7.3 showed bond failure in test series $S3.1$ and $S3.2$. The other three series failed with mixed concrete cone and pull-out failure, thus their load was predicted with the concrete models. Similar to the tests with $M\,12$, the UBM predicted the load better than all the other models.

The elastic bond model and subsequently the combined cone /bond model based on EBM for the reinforcing bars $d\,12$ could not be determined.

The cone / bond model with UBM predicted a lower failure load compared to the test results, approximately 37 % lower for $6\,d$ ($S2.2 - C$) and 23 % lower for $8\,d$ ($S2.3 - C$). For series $S3.1$ and $S3.2$ the predicted loads were underestimation by approximately 45 %.

The bond model neglecting the shallow cone produced a good estimation of the failure loads for the reinforcing bars at both embedment depths.

Table 7.11 summarizes the predicted loads for the tests with concrete cone failure. The two prediction models were intended for full concrete failure. However, in the tests with unconfined setup, only 7.9 % of the tested anchors showed full concrete cone failure (3 anchors) and 84.2 % showed mixed concrete cone and pull-out C / P failure mode (the rest showed steel failure).

As expected, the concrete capacity design gave a better estimation of the load for all embedment depths for $M\,12$ tests. The

TABLE 7.11: Comparison of the test results for
concrete failures: $M2$ and C

Series	N_{test}	CCD		Concrete cone	
				model	
		N_p	$\frac{N_t}{N_p}$	N_p	$\frac{N_t}{N_p}$
$[-]$	$[kN]$	$[kN]$	$[-]$	$[kN]$	$[-]$
S1.1-U	40.07	43.9	0.91	19.4	2.07
S1.2-U	55.71	59.1	0.94	28.8	1.94
S1.3-U	78.15	79.9	0.87	43.0	1.83
S1.4-U	83.45	95.5	0.81	54.9	1.55
S1.5-U	93.62	118.5	0.79	72.7	1.29
S2.1-U	33.43	43.08	0.78	18.9	1.77
S2.2-U	56.81	78.6	0.72	42.1	1.35
S2.3-U	64.11	118.2	0.54	72.4	0.89
S3.3	56.05	66.4	0.84	33.7	1.67
S3.4	46.31	63.6	0.73	31.1	1.47
S3.5	46.12	64.4	0.72	32.3	1.44

predicted load ranged from 2.3 % to 27 % higher than the test results. For d 12, this load was overestimated with 30 % for $4\,d$ ($S2.1 - U$), 39 % for $6\,d$ ($S2.2 - U$) and 84 % for $8\,d$ ($S2.3 - U$). For test series $S3.3$ to $S3.5$, CCD predicted higher loads with increased support diameter, ranging from 18 % to 40 %.

The concrete cone model showed in all cases (threaded rods and reinforcing bars) better approximation with increasing bond length. This prediction for M 12 decreased from 52 % lower load for $4\,d$ ($S1.1 - U$) to 22 % lower load for $8\,d$ ($S1.5 - U$). The same behaviour was observed for d 12, where for the bond length $4\,d$ ($S2.1 - U$) the predicted load was 44 % lower and for $6\,d$ ($S2.2 - U$) was 26 % lower compared to the test results. However, for the embedment depth of $8\,d$ ($S2.3 - U$), the model overestimated the load with 13 %. The ratio of the tested loads with the predicted ones for test series $S3.3$ to $S3.5$ ranged from 1.44 to 1.67.

Figure 7.35 illustrates the ratio of the tested loads with the predicted loads as a function of the embedment depth for the threaded rods M 12 (Table 7.1) and reinforcing bards d 12 (Table 7.2). In this figure, only the uniform bond model UBM and the concrete capacity design CCD as they give the better approximations. Figure 7.36 illustrates the results of the comparison of the loads for the reinforcing bars in Table 7.3 as function of the ratio support diameter and embedment depth.
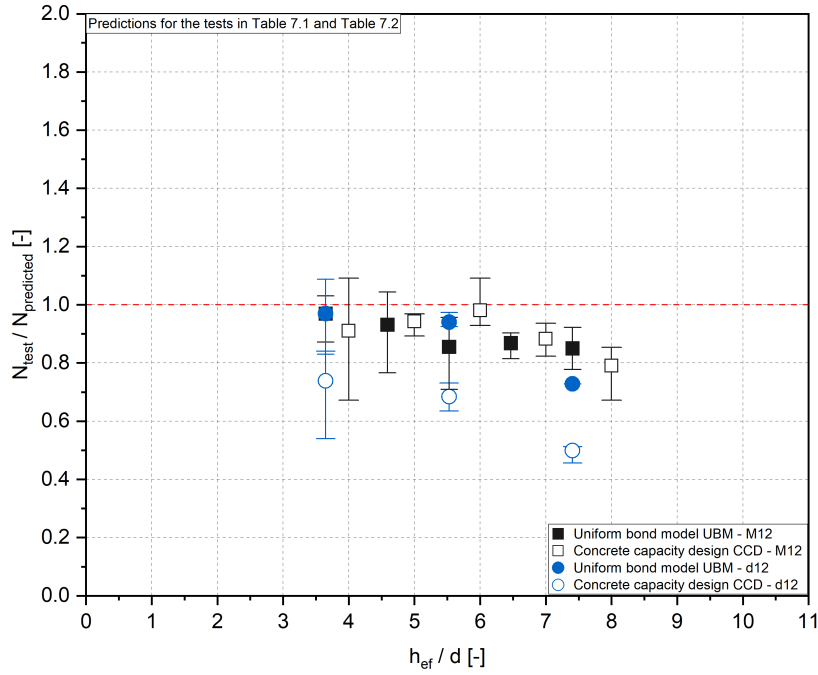
FIGURE 7.35: Ratio of the failure loads in tests and
their prediction for *d* 12 with bond and concrete
failure - Table 7.3
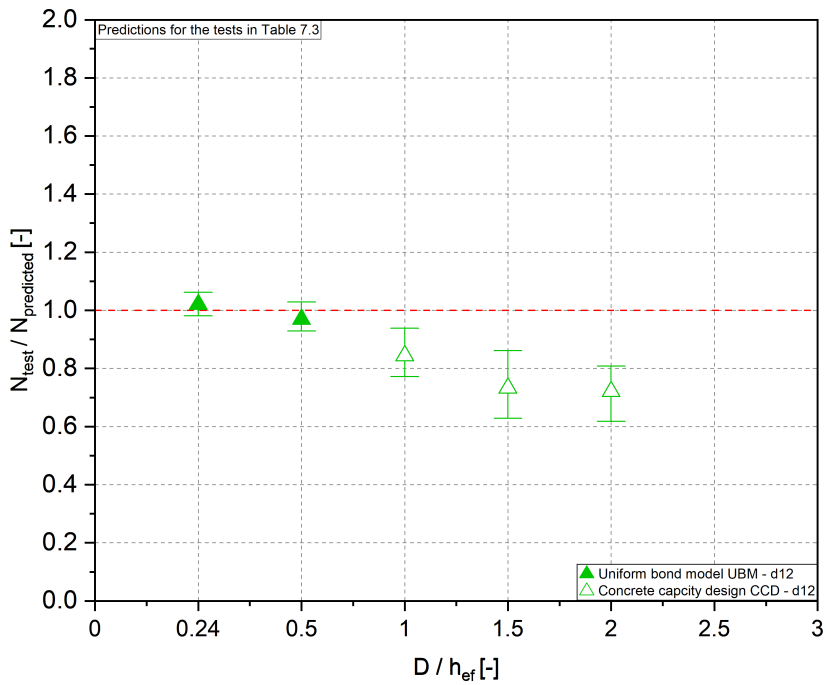
FIGURE 7.36: Ratio of the failure loads in tests and
their prediction for *d* 12 with bond and concrete
failure - Table 7.3

8 Conclusions

This research focuses on the influences on the bond behaviour of anchorages under short-term and long-term loading. The performance of single adhesive anchors subjected to centric tensile load and the factors influencing their behaviour are discussed.

Firstly, this dissertation starts with an overview on adhesive anchor systems. Their behaviour, the failure mechanisms of adhesive anchors as well as the bond strength calculation using known bond models are summarized.

Secondly, the performance of adhesive anchors under short-time loading is described. There are two main group factors which influence the bond strength of adhesive anchors under short-time loading. These are the internal factors such as chemical formulation, curing time when loaded, annular gap, etc. And the external factors such as anchor diameter, concrete strength, hole depth, sustained loading, elevated temperature, etc. In this part, the literature on each of these influencing factors is given.

These factors can be classified into four categories depending on the level they influence the bond strength of the adhesive under short-term loading:

- No influence: the annular gap.

- Little to no influence (up to 10 % change in bond strength): age of concrete, anchor diameter, concrete strength, hole cleaning, hole depth, type of concrete.

- Small influence (10 − 50 % change in bond strength): mixing uniformity, fiber content, chemical resistance, concrete aggregate, hole drilling, hole orientation (during drilling or installation), installation temperature, short-term cure, moisture in service.

- Large influence (more than 50 % change in bond strength): type of adhesive, curing time when loaded, cracked and

uncracked concrete, hole moisture, testing setup, elevated temperature, freeze-thaw.

The long-term behaviour of adhesive anchors is the next focus point of this thesis. Three approaches that help understand the long-term behaviour of adhesive anchors are described. These are: the sustained loading approach, time-to-failure approach and the modified Burgers-Model.

Moreover, similar to the short-term loading, the factors influencing the bond strength of adhesive anchors under long-term loading are presented. Understandably, these factors are dependent on the type of adhesive used. The researches from Davis (2012), Blochwitz (2019) and IWB (2019) show an influence of the increase support diameter on the bond strength of the anchors after 50 and 100 years. Another influencing factor is the curing time when loaded (Davis, 2012), embedment depth (Blochwitz, 2019) and elevated temperatures (IWB, 2019).

The next focus point of this thesis is the influence of incremental loading on the behaviour of adhesive anchors. The anchors installed in uncracked concrete are subjected to 5 % loading steps (using confined and unconfined setups) determined from the short-term tests and increased after 5 minutes until the anchor failed. Four other parameters are varied to understand this influence: hole cleaning, annular gap, hole saturation and increased temperature.

The anchors subjected to incremental loading show 10 % to 20 % lower failure loads than the reference short-term tests. The influence of the reduced hole cleaning during incremental loading is more obvious in the confined tests than in the unconfined. The experiments demonstrate an increase of the failure load with the increase of the annular gap. Increasing the testing temperature influences the carrying capacity of the anchor. The failure loads are between 3 % and 19 % lower than their reference loads. The results show a small influence of the hole saturation under incremental loading.

The results of the incremental loading tests reveal that the bond strength of the anchors is the lowest for the anchors installed with reduced cleaning effort, followed by those tested

under elevated temperatures. A reduction factors due to this parameters can be considered. However, only the factor with the highest influence is decisive. The increase of the annular gap for both testing setups increases the bond strength.

The time-to-failure tests and the incremental loading tests seem to deliver comparable results. Using incremental loading tests to determine the long-term behaviour of adhesive anchors would be less time consuming and more cost effective compared to the TTF tests.

The last point of this research investigates the influence of different factors on the carrying capacity of adhesive anchors in high-strength concrete. Two types of steel components are studied: threaded rods $M\,12$ and reinforcing bars $d\,12$. The studied parameters include the embedment depth, the support diameter, the bond length, axial compression and sustained loading.

The increase of embedment depth shows an increase in the failure load of the adhesive anchor independent of the testing setup. The support diameter of reinforcing bars is varied from $0.24 \cdot h_{ef}$ to $2.0 \cdot h_{ef}$. The increase of the support diameter decreases the failure load and as a result the bond strength. Both these findings concurs with the findings in literature.

The influence of bond length is observed using four bonding configurations excluding the fully bonded one. Two configurations consist on 50% bond length (*a* and *b*), one configuration on 25% bond length (*c*) and the last one with 0% bond length (*d*). Configuration *d* tests with "no" bonding length are performed to consider for the friction between the fastener and the hole. Even though configurations *a* and *b* have the same bond length (distributed differently), configuration *a* reveal higher failure loads for the confined tests and configuration *b* for the unconfined ones. Configuration *c* test reach up to a fourth of the fully bonded anchors failure load.

The observations made for the anchors subjected to axial compression are: 1. an increase in axial compression increases the the failure load of the fasteners; 2. the scatter of the failure loads reduces with increasing compression and 3. the failure modes transition from pull-out (reference tests) to mixed pull-out or pull-out with mortar at the highest compressive load.

The long-term performance of adhesive anchors (after 50 and 100 years) using the Findley approach (1976) is determined through the sustained load testing. The extrapolated displacements are higher than the displacement at loss of adhesion. Therefore, the performed tests would not qualify according to the current standards. The sustained load tests are then compared with the time-to-failure tests. The results show that the displacement criterion given in the current guidelines (EAD 330499, 2018; AC 308, 2017) is on the safe side.

Another important point of this thesis is the factor α_{setup}. Through the tests in high-strength concrete, the ratio between the unconfined and the confined bond strength is determined in the range 0.57 to 0.92, which concurs with the data in literature. The results show overall that an α_{setup} is necessary and 0.75 is generally sufficient.

Lastly, the failure loads from the tests are compared with the predicted load using design models for concrete and pull-out failure. As expected, the uniform bond model and the concrete capacity design predict the failure loads with the highest accuracy.

9 Schlussfolgerung

In der vorliegenden Arbeit werden die Einflüsse von chemischen Befestigungssystemen auf das Verbundverhalten unter Kurzzeit- und Langezeitbelastungen untersucht. Dazu wurde das Verhalten von Einzelverbunddübeln unter zentrischer Zugbelastung mit verschiedenen Einflussparametern ermittelt.

Die vorliegende Arbeit beginnt mit einem allgemeinen Überblick über Verbunddübelsysteme. In diesem Zusammenhang werden das Tragverhalten, die Versagensmechanismen von Verbunddübeln, sowie die Berechnung der Verbundfestigkeit anhand bekannter Verbundmodelle dargestellt.

Im zweiten Schritt wird das Tragverhalten von Verbunddübeln unter Kurzzeitbelastung beschrieben. In diesem Fall unterteilen sich die untersuchten Parameter in zwei Hauptgruppen. Diese sind zum einen interne Faktoren, wie z.B. chemische Formulierung des Mörtels, die Aushärtezeit bei der Belastung und Ringspalt. Dübeldurchmesser, Betonfestigkeit, Bohrlochtiefe, Dauerbelastung und eine erhöhte Umgebungstemperatur gehören zur zweiten Hauptgruppe. Unter Berücksichtigung des Standes der Technik werden die aufgeführten Einflussparameter näher erläutert. Des Weiteren werden die Parameter in Einflussgrade eingestuft, um deren Wirkung auf das Tragverhalten zuzuordnen. Im Folgenden sind die Einflussgrade, sowie den zugeordneten Parametern dargestellt:

- Kein Einfluss: der Ringspalt.

- Geringer bis kein Einfluss (bis zu 10 % Unterschied in der Verbundfestigkeit): Alter des Betons, Dübeldurchmesser, Betonfestigkeit, Bohrlochreinigung, Bohrlochtiefe, Betonart

- Geringer Einfluss (10 − 50 % Unterschied in der Verbundfestigkeit): Mischverhältnis vom Beton, Fasergehalt vom Beton, chemische Beständigkeit vom Beton, Zuschlagstoffe im Beton, Bohrverfahren, Richtung des Bohrvorgangs

und Setzrichtung, Montagetemperatur, Kurzzeitaushärtung, Feuchtigkeit im Betrieb

- Starker Einfluss (mehr als 50 % Unterschied in der Verbundfestigkeit): Art des Verbunddübels, Aushärtezeit bei Belastung, gerissener oder ungerissener Beton, Bohrlochfeuchtigkeit, Versuchsaufbau, erhöhte Temperatur, Frost-Tau-Wechsel

Das Langzeitverhalten von Verbunddübeln ist ein weiterer Schwerpunkt dieser Arbeit. Zur Untersuchung des Langzeitverhaltens von Verbunddübeln standen folgende Methoden zur Verfügung: Dauerstandsversuche, Zeitstandsversuche und das modifizierte Burgers-Modell. Darüber hinaus werden analog zur Kurzzeitbelastung die Faktoren vorgestellt, die die Verbundfestigkeit von Verbunddübeln unter Langzeitbelastung beeinflussen. Diese Faktoren sind naturgemäß von der Art des verwendeten Verbunddübels abhängig. Die Untersuchungen von Davis (2012), Blochwitz (2019) und IWB (2019) zeigen einen Einfluss des zunehmenden Abstützungsdurchmessers auf die Verbundfestigkeit der Dübel nach 50 und 100 Jahren. Weitere Einflussparamater sind die Aushärtezeit bei Belastung (Davis, 2012), die Verankerungstiefe (Blochwitz, 2019) und erhöhte Temperaturen (IWB, 2019).

Eine weitere Thematik dieser Arbeit ist die Untersuchung des Einflusses von stufenweisen Belastung auf das Tragverhalten von Verbunddübeln mit Gewindestangen des Durchmesser $M\,12$. Dabei werden die in ungerissenem Beton installierten Dübel 5 Minuten lang in 5 % Schritten belastet, bis der Dübel versagt. Als Referenz der Stufen dienen die Kurzzeitversuche. Neben der stufenweisen Belastung gibt es weitere Variationen der Einflussparameter, wie die Abstützweite des Versuchsaufbaus, die Bohrlochreinigung, der Ringspalt, die Bohrlochsättigung oder eine erhöhte Temperatur.

Der Einfluss der stufenweisen Belastung konnte, bezogen auf die Referenzversuche, mit 10 % bis 20 % Lastreduktion quatifiziert werden. Der Einfluss der reduzierten Bohrlochreinigung bei der stufenweisen Belastung des Verankerungssystems ist in

den Versuchen mit enger Abstützung ausgeprägter als in denen mit weiter Abstützung. Weiter zeigen die Versuche einen Zuwachs der Versagenslast mit Zunahme des Ringspalts. Bei erhöhter Temperatur ist ein negativer Einfluss auf die Tragfähigkeit des Verbunddübels ersichtlich. Dabei ergeben sich 3 % bis 19 % geringere Bruchlasten als bei den Referenzversuchen Die Ergebnisse mit Variation der Bohrlochsättigung zeigen einen geringen Einfluss auf das Tragverhalten von Verbunddübeln bei stufenweiser Belastung.

Die Versuchsergebnisse mit reduzierter Bohrlochreinigung weisen die geringste Tragfähigkeit bei stufenweiser Belastung auf, gefolgt von den Versuchen bei erhöhter Temperatur. Ein Abminderungsfaktor aufgrund dieser Parameter kann in Betracht gezogen werden. Maßgebend ist wird jedoch nur der Faktor mit dem größten Einfluss auf die Versagenslast. Die Vergrößerung des Ringspalts hat bei beiden Versuchsaufbauten eine positive Wirkung auf die Verbundfestigkeit und erhöht diese.

Die Zeitstandversuche und die stufenweisen Belastungsversuche liefern vergleichbare Ergebnisse. Es ist von Vorteil das Langzeitverhalten von Verbunddübeln mit stufenweisen Belastungsversuchen zu untersuchen, da dieses Verfahren weniger zeitaufwendig und somit auch kostengünstiger ist.

Der letzte Forschungspunkt befasst sich mit dem Einfluss verschiedener Faktoren auf die Tragfähigkeit von Verbunddübeln in hochfestem Beton. Als Ankerstangen dienten Gewindestangen der Größe $M\,12$ und Bewehrungsstäbe der Größe $d\,12$. Zu den untersuchten Parametern gehören die Verankerungstiefe, die Abstützweite, die Verbundlänge, der axiale Druck und die Dauerbelastung. Unabhängig vom Versuchsaufbau steigt mit zunehmender Verankerungstiefe die Versagenslast des Verbunddübels. Die Ab-stützweite bei Versuchen mit Bewehrungsstäben wird von $0,24 \cdot h_{ef}$ bis $2,0 \cdot h_{ef}$ variiert. Mit Vergrößerung der Abstützweite nimmt die Bruchlast ab und somit auch die Verbundfestigkeit. Dieses Verhalten stimmt mit den Erkenntnissen aus der Literatur überein.

Der Einfluss der Verbundlänge wird anhand von vier Verbundkonfigurationen untersucht. Zwei Konfigurationen haben eine Verbundlänge von 50% (*a* und *b*), eine Weitere hat eine Verbundlänge von 25% (*c*) und die letzte Konfiguration hat eine

Verbundlänge von 0% (*d*). Bei Konfiguration *d* wird die Ankerstange über die gesamte Einbindetiefe abgeklebt und installiert, um die Reibung zwischen dem Verbindungselement und dem Bohrloch zu ermitteln. Obwohl die Konfigurationen *a* und *b* die gleiche Verbundlänge aufweisen (mit unterschiedlicher Anordnung), zeigt die Konfiguration *a* höhere Bruchlasten für die Versuche mit enger Abstützung. Konfiguration *b* wurde mit weiter Abstützung geprüft. Dabei wurden geringere Versagenslasten erreicht. Die Versuche der Konfiguration *c* erreichen etwa 25 % der Bruchlast der vollständig eingemörtelten Verankerungssysteme.

Bei weiteren Untersuchungen wurden Betonkörper unter axialen Druck gesetzt, während die Verankerungs in Zugrichtung belastet wurde. Dabei konnten folgende Festellungen gemacht werden: 1. Eine Zunahme der axialen Druckkraft auf den Betonkörper erhöht die Bruchlast der Dübel; 2. Die Streuung der Bruchlasten nimmt mit zunehmender Druckkraft ab und 3. die Versagensart geht mit Zunahme der Druckkraft von Herausziehen ohne Mörtel (Referenzversuche), zu Herausziehen teilweise mit Mörtel und bei der maximalen Druckkraft zu Herausziehen mit Mörtel über.

Das Langzeitverhalten von Verbunddübeln (nach 50 und 100 Jahren) unter Verwendung des Findley-Ansatzes (1976) wird durch Dauerlastversuche bestimmt. Die extrapolierten Verschiebungen sind höher als die Verschiebung bei Verbundverlust. Daher entsprechen die durchgeführten Versuche nicht den aktuellen Richtlinien. Im Anschluss erfolgt ein Vergleich der Dauerlastversuche mit den Zeitstandversuchen. Die Ergebnisse zeigen, dass das in den aktuellen Richtlinien (EAD 330499, 2018; AC 308, 2017) angegebene Verschiebungskriterium auf der sicheren Seite liegt.

Ein weiterer zentraler Punkt dieser Arbeit ist die Untersuchung des Faktors α_{setup}. Anhand der Versuche mit weiter und enger Abstützung in hochfestem Beton wird das Verhältnis der Verbundfestigkeit bei der Versagensart Herausziehen ermittelt. Der Verhältniswert liegt im Bereich von $0,57$ bis $0,92$ welcher mit den Literaturdaten übereinstimmt. Auf Grundlage der Versuchsergebnisse ist ersichtlich, dass der Faktor α_{setup} notwendig ist und eine gute Übereinstimmung bei einem Wert von $0,75$ erreicht.

Abschließend werden die Bruchlasten aus den Versuchen mit der berechneten Last unter Verwendung von Bemessungsmodellen für Beton im Fall von Herausziehen verglichen. Wie erwartet, schätzen das Uniform Bond Modell und das CC-Verfahren die Bruchlasten mit der höchsten Genauigkeit ein.

10 Outlook

This researched focused on the influence factors on the bond behaviour of adhesive anchors under short- and long-term loading.

The parameters influencing the short-term behaviour of anchors have been the focus of many past studies, thus their influence is known. On the other hand, the long-term behaviour of adhesive anchors holds a lot of open questions. Depending on the type of adhesive anchors, some factors influence their bond strength more than others. Thus is important to see, if there is a correlation between the type of adhesive and the factors which influence their carrying capacity.

Incremental loading can be a method to investigate the long-term behaviour of adhesive anchors. In comparison with the sustained loading or the time-to-failure tests, this method is quicker, however the testing has to be supervised until completion. Further research with incremental loading is needed to better understand this method and to hopefully implement it as a predictor for long-term loading.

A Materials and Methods

A.1 Concrete

Table A.1 summarizes the concrete compressive strengths tested on concrete cubes with dimensions 15 x 15 x 15 cm.

TABLE A.1: Concrete compressive strengths

Concrete mixture [−]	Casting date [−]	Density [kg/m^3]	Compressive strength [N/mm^2]	Testing date [−]
Batch A.1	16.01.2014	2300	32.31	11.03.2014
Batch A.2	16.04.2013	2310	38.08	26.09.2013
Batch B.1	15.05.2020	2230	30.13	27.07.2020
Batch B.2	10.05.2019	2310	70.22	28.07.2020
Batch B.3	27.07.2016	2477	113.3	17.01.2020
Batch B.4	28.07.2016	2430	99.83	17.01.2020
Batch B.5	23.01.2020	2300	98.45	16.04.2020

Figure A.1 displays the general drawing of the concrete slabs used in the tests.

Table A.2 gives an overview of the concrete mixtures for all the concrete batches used in the test program.
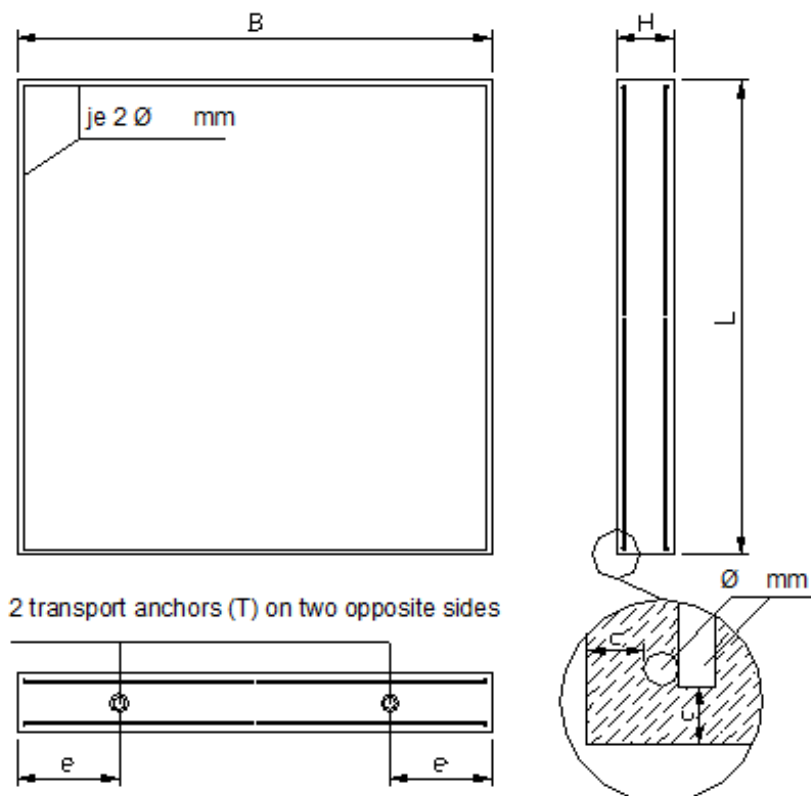
FIGURE A.1: Concrete slab drawing

TABLE A.2: Concrete mixtures

Concrete	Strength class	Cement Type	Quantity	Aggregates 0−2 mm	2−8 mm	8−16 mm	Water Quantity	W/C	Consistency Slump	Class	Additives Super plasticiser	Retarding admixtures
[−]	[−]	[−]	[kg/m³]	[kg/m³]	[kg/m³]	[kg/m³]	[kg/m³]	[−]	[−]	[−]	[%]	[%]
Batch A.1	C20/25	CEM I 32.5R	264.5	747.5	475	697.5	697	0.658	43	F3	−	−
Batch A.2	C20/25	CEM I 32.5R	240	787.4	499.4	744.5	174.5	0.727	39	F2	−	−
Batch B.1	C20/25	CEM I 32.5R	238.9	783.7	516.2	732.4	124.0	0.519	38	F2	−	−
Batch B.2	C50/60	CEM I 42.5R	374.2	708.9	482.1	683.9	150.8	0.402	43	F3	0.62	0.14
Batch B.3	C90/105	CEM I 52.5R	411.7	701.5	892.8	359.8	65.9	0.160	38	F2	2.50	1.00
Batch B.4	C90/105	CEM I 52.5R	407.5	675.8	928.3	360.8	69.1	0.169	39	F2	2.50	1.00
Batch B.5	C100/115	CEM I 42.5R	478.8	721.6	1056.6	0	76.9	0.160	43	F3	0.00	0.01

A.2 Installation

FIGURE A.2: Diamond core drilling system
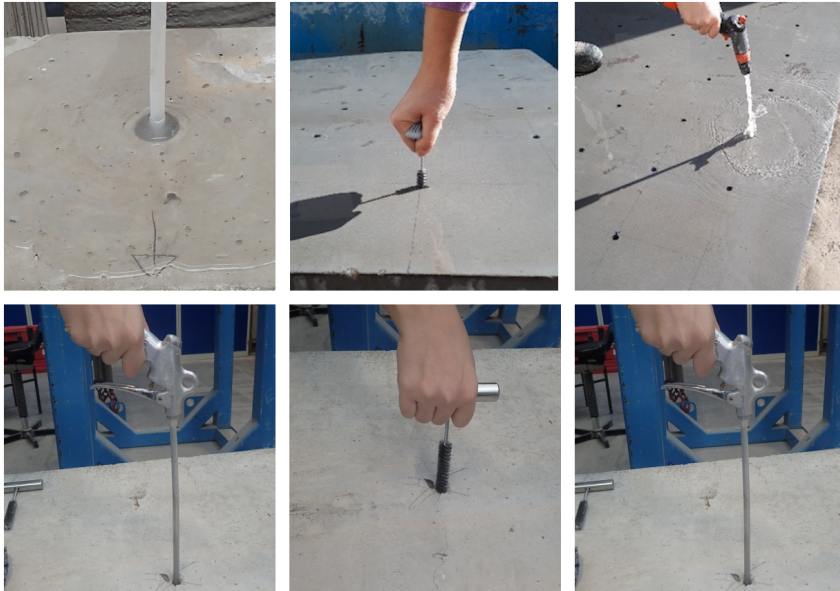
FIGURE A.3: Cleaning of the holes prior to installation

A.3 Displacement measurement
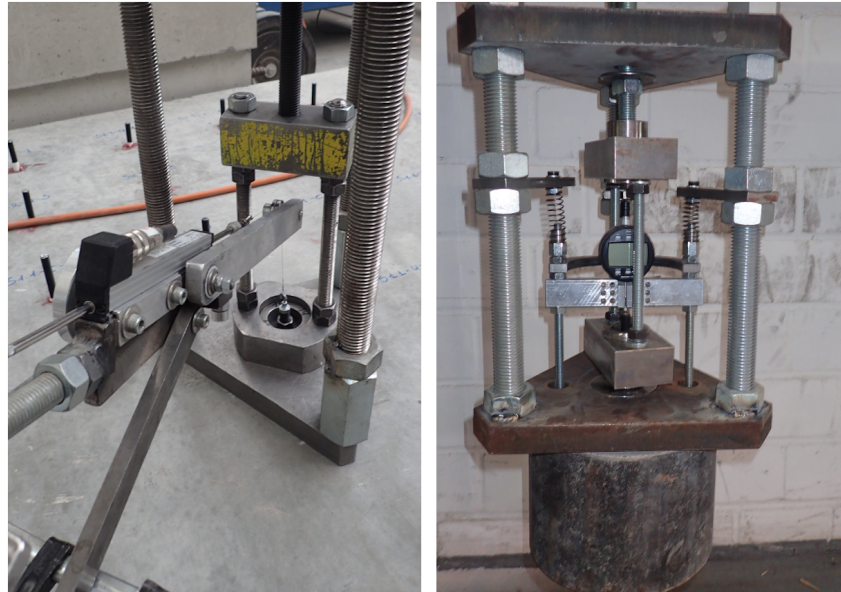
FIGURE A.4: Measurement of the displacements

A.4   Axial compression setup
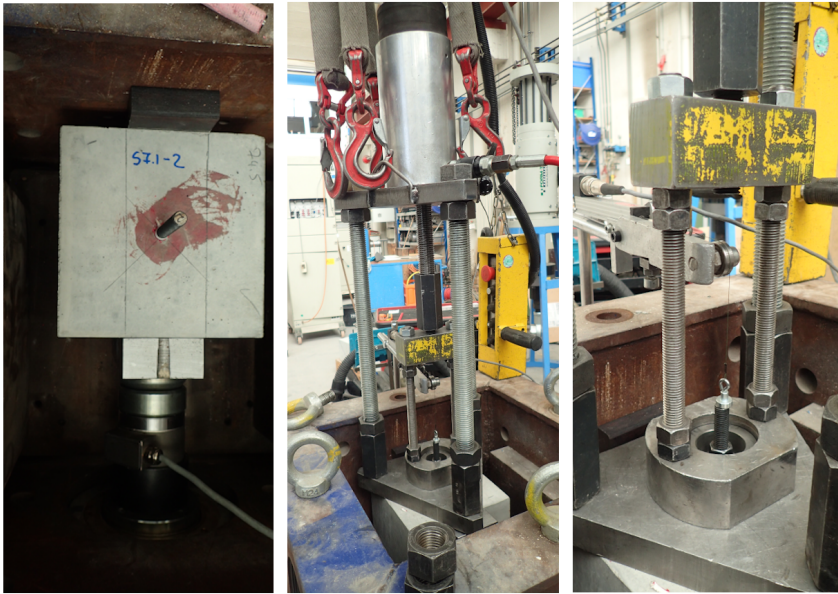
FIGURE A.5: Axial compression tests setup

B Test results for incremental loading

This appendix presents the results of the incremental loading tests carried out at the Institute of Construction Materials. Table B.1 summarizes these results. The contents of each column are described below:

- Column 1: Designation of the test series

- Column 2: Number of the tests carried out

- Column 3-13: Parameters studied

    - Column 3: Reference test
    - Column 4: Embedment depth
    - Column 5: Short-term test
    - Column 6: Incremental loading test
    - Column 7: Confined setup test
    - Column 8: Unconfined setup test
    - Column 9: Bond line thickness test 2 mm (RS2)
    - Column 10: Bond line thickness test 4 mm (RS4)
    - Column 11: Reduced cleaning effort test (1 x Hand Pumping)
    - Column 12: Hole saturation test
    - Column 13: Increased temperature test (43°C)

- Column 14: Support diameter

- Column 15: Concrete compressive strength

- Column 16: Measured embedment depth

- Column 17: Ultimate failure load

- Column 18: Mean ultimate failure load

- Column 19: Standard deviation of the ultimate load

- Column 20: Bond strength

- Column 21: Mean bond strength

- Column 22: Standard deviation of the bond strength

- Column 23: Failure mode

- Column 24: Concrete cone depth

TABLE B.1: Test results of the incremental loading testing

Series	No.	Ref.	h_{ef} [mm]	SHT	IL	conf.	unconf.	RS2	RS4	Thp	wet	43°C	Setup diam. [mm]	[MPa]	h_{ef} [mm]	N_u [kN]	$N_{u,m}$ [kN]	σ [kN]	τ_u [MPa]	$\tau_{u,m}$ [MPa]	σ [MPa]	Failure mode [–]	Cone depth [cm]
D028	1	×	60	×		×							22	32.3	61	81.98	78.62	2.34	35.65	33.76	1.24	P_M	–
D028	2	×	60	×		×							22	32.3	62	76.57			32.76			P_M	–
D028	3	×	60	×		×							22	32.3	61	76.88			33.43			P_M	–
D028	4	×	60	×		×							22	32.3	62	80.14			34.29			P	–
D028	5	×	60	×		×							22	32.3	63	77.55			32.65			P_M	–
D029	1	×	60		×	×							22	32.3	62	71.29	68.71	2.27	30.50	29.71	0.70	P_M	–
D029	2	×	60		×	×							22	32.3	61	67.81			29.49			P/P_M	–
D029	3	×	60		×	×							22	32.3	61	67.03			29.15			P_M	–
D030	1	×	60	×			×						240	32.3	62	42.78	39.22	3.30	18.30	16.88	1.35	C	6
D030	2	×	60	×			×						240	32.3	62	36.90			15.79			C	4.6
D030	3	×	60	×			×						240	32.3	61	39.87			17.34			C	5.3
D030	4	×	60	×			×						240	32.3	61	34.85			15.15			C	6
D030	5	×	60	×			×						240	32.3	62	41.69			17.84			C	4.8
D031	1	×	60		×		×						240	32.3	61	37.55	33.94	2.61	16.33	14.62	1.17	C	6
D031	2	×	60		×		×						240	32.3	62	35.51			15.19			C	5.6
D032	1	×	60		×		×						240	32.3	62	31.48			13.47			C	6
D032	2	×	60		×		×						240	32.3	62	33.58			14.37			C	6
D032	3	×	60		×		×						240	32.3	61	31.56			13.72			C	6
D033	1		60		×	×				×			22	32.3	60	39.41	42.13	2.36	17.42	18.21	0.68	P_M	–
D033	2		60		×	×				×			22	32.3	62	43.56			18.64			P_M	–
D033	3		60		×	×				×			22	32.3	62	43.42			18.58			P/P_M	–
D034	1		60	×		×				×			22	32.3	61	48.99	47.00	4.62	21.30	20.44	2.01	P_M	–
D034	2		60	×		×				×			22	32.3	61	41.72			18.14			P_M	–
D034	3		60	×		×				×			22	32.3	61	50.30			21.87			P_M	–
D035	1		60		×		×			×			240	32.3	61	29.54	30.86	2.28	12.85	13.42	0.99	P_M/C	2.6
D035	2		60		×		×			×			240	32.3	61	33.50			14.57			P_M/C	3.5
D035	3		60		×		×			×			240	32.3	61	29.55			12.85			P_M/C	2.3
D036	1		60	×			×			×			240	32.3	60	33.96	35.86	2.19	15.01	15.76	0.82	P_M/C	3.3
D036	2		60	×			×			×			240	32.3	60	35.38			15.64			P_M/C	3.1
D036	3		60	×			×			×			240	32.3	61	38.25			16.63			P_M/C	4
D037	1		60		×	×		×					22	32.3	61	70.88	80.16	8.24	30.82	34.66	3.50	P	–
D037	2		60		×	×		×					22	32.3	61	86.60			37.66			P	–
D037	3		60		×	×		×					22	32.3	62	83.00			35.51			P	–
D038	1		60		×		×	×					240	32.3	60	39.43	39.38	0.07	17.43	17.27	0.23	P/C	3.8
D038	3		60		×		×	×					240	32.3	61	39.33			17.10			P_M/C	4.3

TABLE B.1: (continued)

Series	No.	Ref.	h_{ef}	ShT	IL	conf.	unconf.	RS2	RS4	Thp	wet	43°C	Setup diam.	f_{cc}	h_{ef}	N_u	$N_{u,m}$	σ	τ_u	$\tau_{u,m}$	σ	Failure mode	Cone depth
[–]	[–]	[–]	[mm]	[–]	[–]	[–]	[–]	[–]	[–]	[–]	[–]	[–]	[mm]	[MPa]	[mm]	[kN]	[kN]	[kN]	[MPa]	[MPa]	[MPa]	[–]	[cm]
D039	1		60		×	×							22	32.3	61	74.83	77.62	2.42	32.54	33.57	0.92	P	–
D039	2		60		×	×							22	32.3	61	78.89			34.31			P	–
D039	3		60		×	×							22	32.3	62	79.15			33.86			P	–
D040	1		60		×		×		×				240	32.3	61	43.22	39.02	4.45	18.79	16.96	1.80	C	5.3
D040	2		60		×		×		×				240	32.3	62	39.49			16.90			C	5.7
D040	3		60		×		×		×				240	32.3	60	34.36			15.19			C	6
D041	1	×	80	×									350	32.3	82	59.84	57.87	3.25	19.36	18.95	1.05	P_M/C	6.1
D041	2	×	80	×									350	32.3	81	61.27			20.06			P_M/C	6.3
D041	3	×	80	×									350	32.3	81	56.91			18.64			C	7.8
D042	1	×	80	×									350	32.3	80	58.50			19.40			P_M/C	5.5
D042	2	×	80	×									350	32.3	81	52.83			17.30			C	7.2
D043	1	×	80		×		×						350	32.3	81	43.61	46.99	3.17	14.28	15.59	1.24	C	–
D043	2	×	80		×		×						350	32.3	80	47.48			15.74			P_M/C	6.6
D043	3	×	80		×		×						350	32.3	79	49.89			16.75			P_M/C	6.7
D044	1		80		×		×			×			350	32.3	81	46.44	41.53	4.50	15.21	13.60	1.47	P_M/C	4.3
D044	2		80		×		×			×			350	32.3	81	37.59			12.31			P_M/C	4.6
D044	3		80		×		×			×			350	32.3	81	40.56			13.28			P_M/C	5.3
D045	1		80		×		×	×					350	32.3	80	58.73	58.26	0.41	19.47	19.24	0.23	P_M/C	5.6
D045	2		80		×		×	×					350	32.3	81	58.08			19.02			P_M/C	5.1
D045	3		80		×		×	×					350	32.3	80	57.98			19.22			$P/P_M/C$	5.3
D046	1		80		×		×		×				350	32.3	80	55.18	57.08	3.42	18.30	18.84	0.99	C	7.2
D046	2		80		×		×		×				350	32.3	81	61.02			19.98			C	7.1
D046	3		80		×		×		×				350	32.3	80	55.03			18.25			C	7.3
D047	1		60		×		×				×		240	32.3	60	31.45	32.83	1.20	13.90	14.35	0.39	P_M/C	4.8
D047	2		60		×		×				×		240	32.3	61	33.45			14.55			P_M/C	3.9
D047	3		60		×		×				×		240	32.3	61	33.59			14.61			P_M/C	3.4
D048	1		60		×	×					×		22	32.3	61	67.02	65.06	5.15	29.14	28.29	2.24	P_M	–
D048	2		60		×	×					×		22	32.3	61	68.94			29.98			P/P_M	–
D048	3		60		×	×					×		22	32.3	61	59.21			25.75			P_M	–
D049	1		60		×	×						×	20	32.3	61	55.27	56.68	2.48	24.03	24.51	0.84	P_M	–
D049	2		60		×	×						×	20	32.3	62	59.54			25.47			P_M	–
D049	3		60		×	×						×	20	32.3	61	55.22			24.01			P_M	–
D050	1		60		×		×					×	275	32.3	61	31.66	31.42	2.19	13.77	13.59	0.85	C	5.4
D050	2		60		×		×					×	275	32.3	61	29.12			12.66			C	6
D050	3		60		×		×					×	275	32.3	62	33.49			14.33			C	5.2

TABLE B.1: (continued)

Series	No.	Ref.	h_{ef} [mm]	SHT	IL	conf.	unconf.	RS2	RS4	1hp	wet	43°C	Setup diam. [mm]	f_c [MPa]	h_{ef} [mm]	N_u [kN]	$N_{u,m}$ [kN]	σ [kN]	τ_u [MPa]	$\tau_{u,m}$ [MPa]	σ [MPa]	Failure mode	Cone depth [cm]
D051	1		80		×		×					×	275	32.3	81	43.94	45.63	3.27	14.39	15.00	1.02	P_M/C	4.8
D051	2		80		×		×					×	275	32.3	80	43.56			14.44			P_M/C	5.8
D051	3		80		×		×					×	275	32.3	81	49.40			16.18			P_M/C	4.2
D065	1		60		×	×				×		×	20	32.3	60	54.59	45.92	8.23	24.13	20.30	3.64	P_M	–
D065	2		60		×	×				×		×	20	32.3	60	44.95			19.87			P_M	–
D065	3		60		×	×				×		×	20	32.3	60	38.22			16.90			P_M	–
D066	1		60		×	×			×			×	20	32.3	60	67.26	65.80	2.32	29.74	29.09	1.03	P_M	–
D066	2		60		×	×			×			×	20	32.3	60	67.01			29.62			P	–
D066	3		60		×	×			×			×	20	32.3	60	63.12			27.91			P_M	–
D067	1		80		×	×						×	20	32.3	82	89.35	81.56	8.69	28.90	26.49	2.85	P_M	–
D067	2		80		×	×						×	20	32.3	81	83.14			27.23			P_M	–
D067	3		80		×	×						×	20	32.3	82	72.18			23.35			P_M	–
D068	1		60		×		×		×			×	275	32.3	61	35.90	33.98	1.75	15.61	14.70	0.80	C	5.1
D068	2		60		×		×		×			×	275	32.3	61	32.46			14.12			C	5.3
D068	3		60		×		×		×			×	275	32.3	62	33.58			14.37			C	6
D069	1		80		×		×		×			×	275	32.3	80	46.44	49.44	2.97	15.40	16.39	0.98	P_M/C	6.9
D069	2		80		×		×		×			×	275	32.3	80	49.51			16.42			P_M/C	4.5
D069	3		80		×		×		×			×	275	32.3	80	52.37			17.36			P_M/C	6.5
D070	1	×	80	×		×							22	32.3	81	121.55	118.23	2.35	39.81	38.53	0.77	P/P_M	–
D070	2	×	80	×		×							22	32.3	82	119.64			38.70			P/P_M	–
D070	3	×	80	×		×							22	32.3	82	117.59			38.04			P/P_M	–
D070	4	×	80	×		×							22	32.3	81	115.74			37.90			P_M	–
D070	5	×	80	×		×							22	32.3	81	116.64			38.20			P	–
D071	1	×	105	×			×						350	32.3	106	97.35	89.99	12.92	24.36	22.54	3.36	P_M/C	5.6
D071	2	×	105	×			×						350	32.3	106	103.71			25.95			P_M/C	5.2
D071	3	×	105	×			×						350	32.3	108	69.85			17.16			P_M/C	6.5
D071	4	×	105	×			×						350	32.3	105	92.59			23.39			P_M/C	6.5
D071	5	×	105	×			×						350	32.3	105	86.43			21.83			C	10.5
D072	1	×	105		×		×						350	32.3	106	81.89	81.58	4.64	20.49	20.42	1.16	P_M/C	5.4
D072	2	×	105		×		×						350	32.3	106	86.06			21.54			P_M/C	5.4
D072	3	×	105		×		×						350	32.3	106	76.80			19.22			P_M/C	7.3

TABLE B.1: (continued)

Series	No.	Ref.	h_{ef}	ShT	IL	conf.	unconf.	RS2	RS4	Thp	wet	$43°C$	Setup diam.		h_{ef}	N_u	$N_{u,m}$	σ	τ_u	$\tau_{u,m}$	σ	Failure mode	Cone depth
[–]	[–]	[–]	[mm]	[–]	[–]	[–]	[–]	[–]	[–]	[–]	[–]	[–]	[mm]	[MPa]	[mm]	[kN]	[kN]	[kN]	[MPa]	[MPa]	[MPa]	[–]	[cm]
D073	1		105		×		×		×				350	32.3	105	85.83	90.22	4.41	21.68	22.65	1.00	P_M/C	6.6
D073	2		105		×		×		×				350	32.3	106	94.64			23.68			C	10.5
D073	3		105		×		×		×				350	32.3	106	90.19			22.57			P_M/C	6.9
D074	1	×	80		×	×							22	32.3	81	94.87	100.77	5.93	31.07	32.87	1.96	P/P_M	–
D074	2	×	80		×	×							22	32.3	81	106.73			34.95			P/P_M	–
D074	3	×	80		×	×							22	32.3	82	100.71			32.58			P_M	–
D075	1		80		×	×				×			22	32.3	82	64.20	61.88	2.01	20.77	20.10	0.60	P/P_M	–
D075	2		80		×	×				×			22	32.3	82	60.60			19.60			P/P_M	–
D075	3		80		×	×				×			22	32.3	81	60.85			19.93			P/P_M	–
D076	1		80		×	×			×				22	32.3	80	112.87	110.95	3.47	37.42	36.79	1.15	P	–
D076	2		80		×	×			×				22	32.3	80	113.03			37.48			P	–
D076	3		80		×	×			×				22	32.3	80	106.95			35.46			P	–

B.1 Diagrams

B.1.1 Reference short-term test
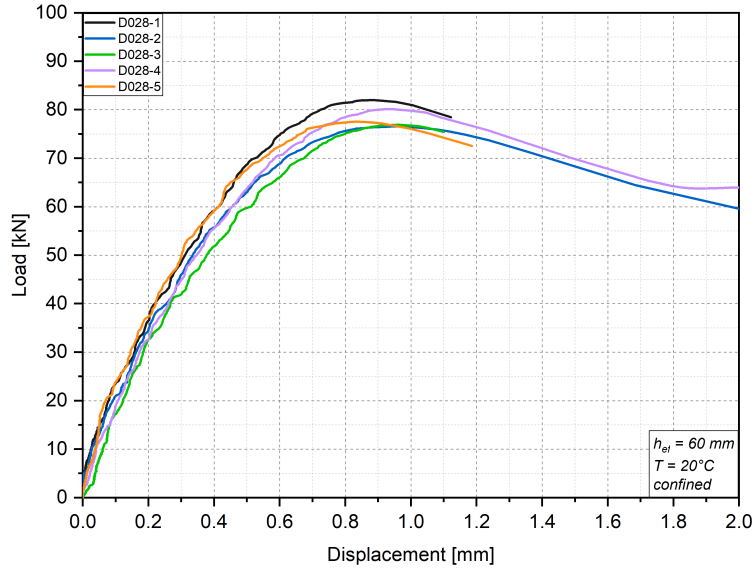
FIGURE B.1: D028 - load versus displacement curves
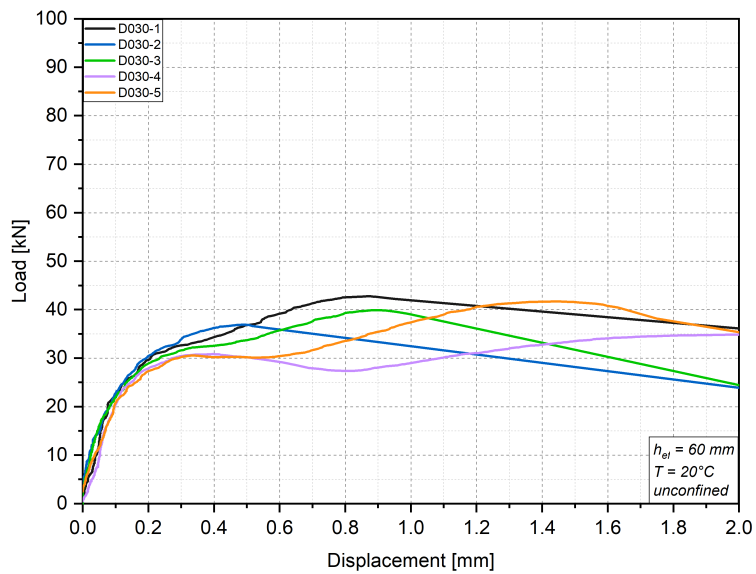
FIGURE B.2: D030 - load versus displacement curves
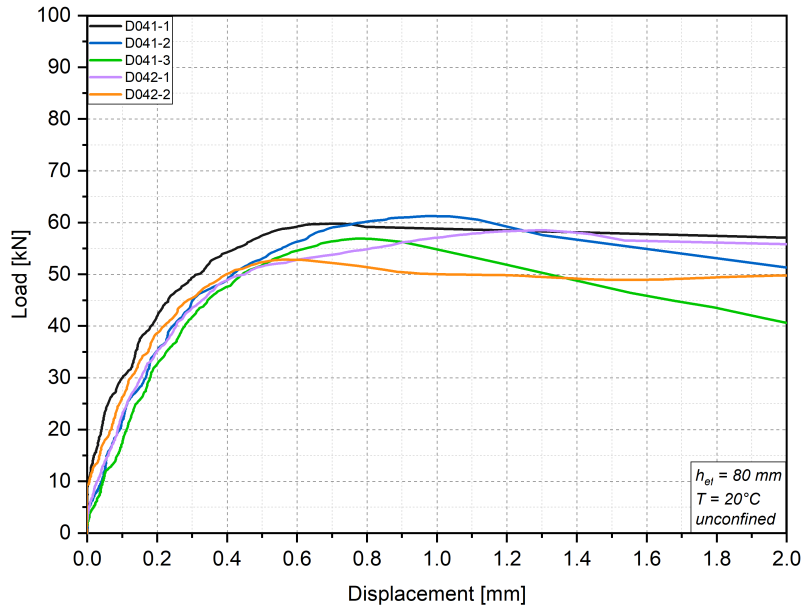
FIGURE B.3: D041&D042 - load versus displacement curves
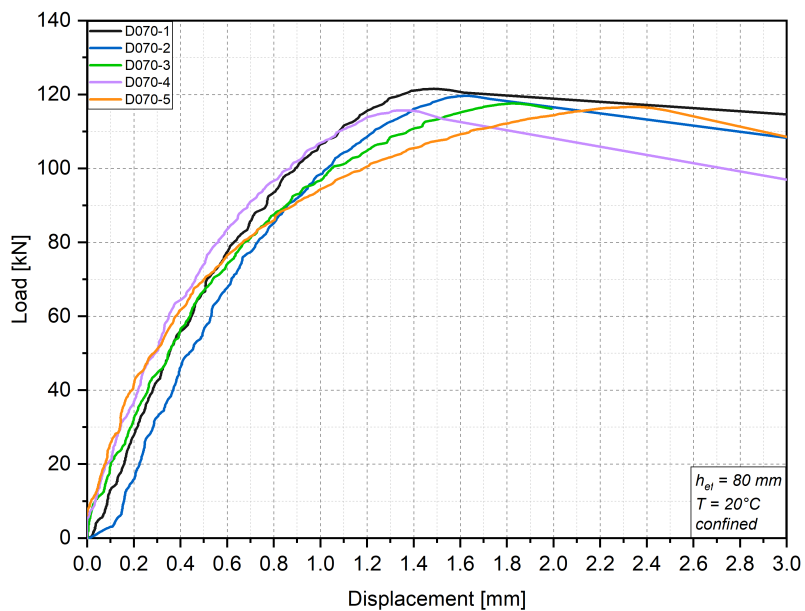
FIGURE B.4: D070 - load versus displacement curves
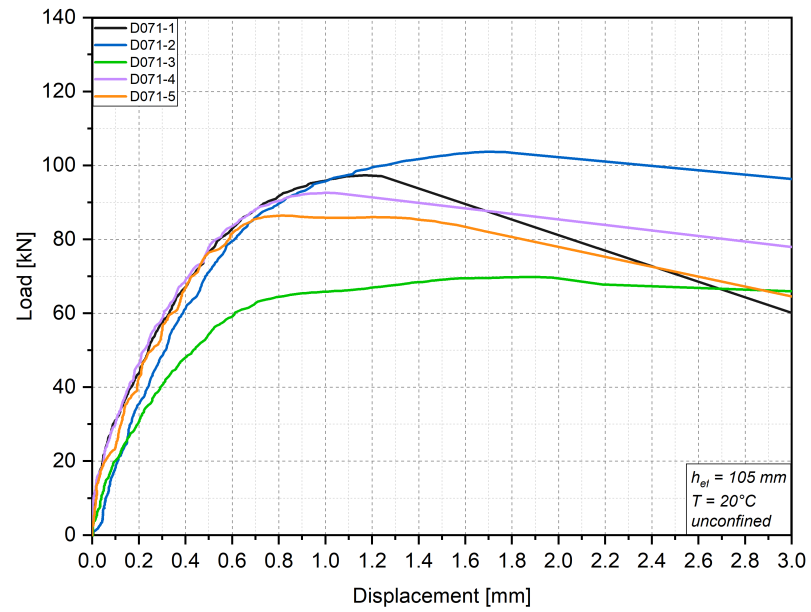
FIGURE B.5: D071 - load versus displacement curves

B.1.2   Short-term test
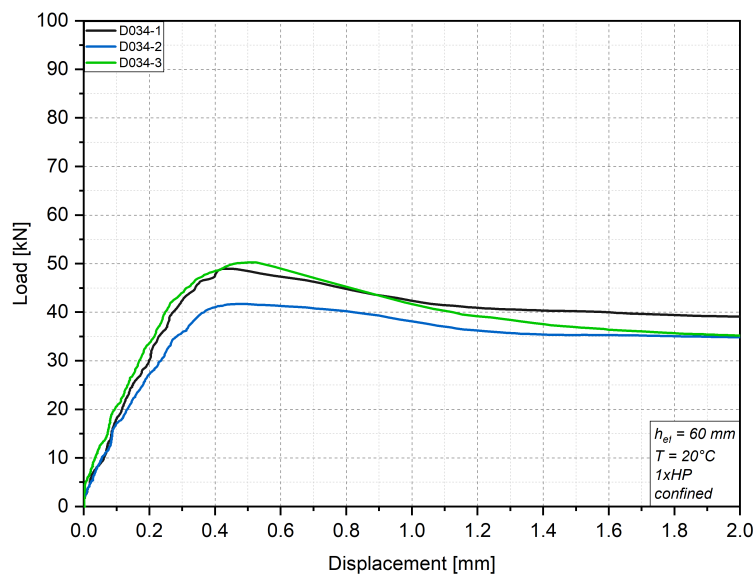
FIGURE B.6: D034 - load versus displacement curves
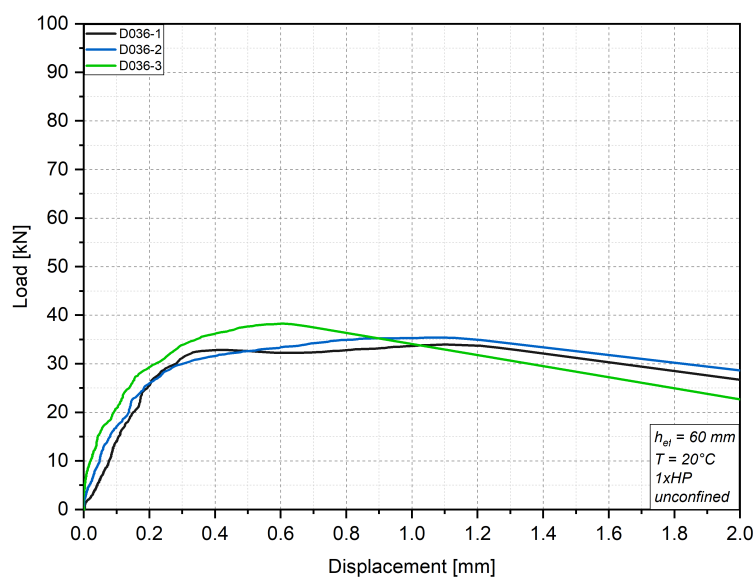
FIGURE B.7: D036 - load versus displacement curves

B.1.3   Reference incremental loading test
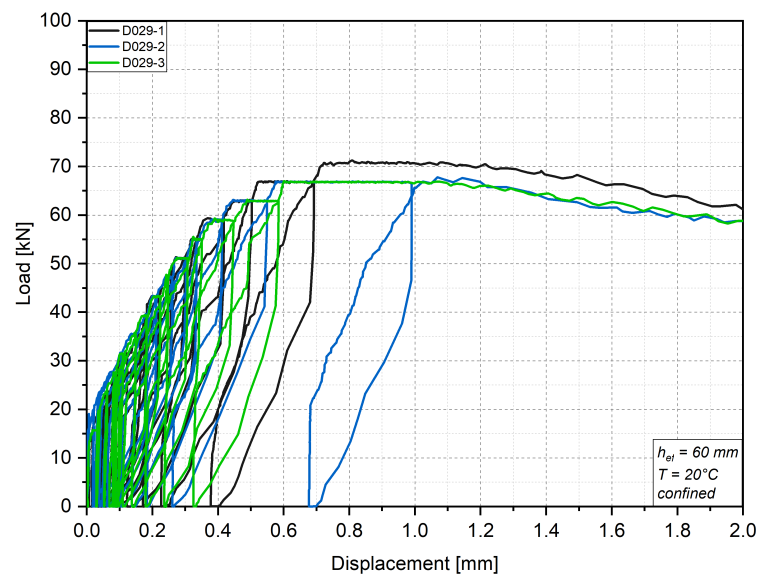
FIGURE B.8: D029 - load versus displacement curves
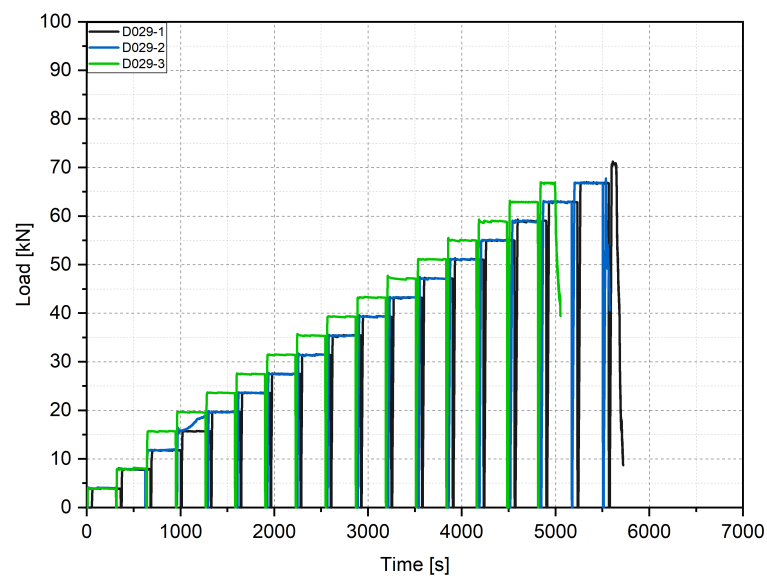
FIGURE B.9: D029 - load versus time curves
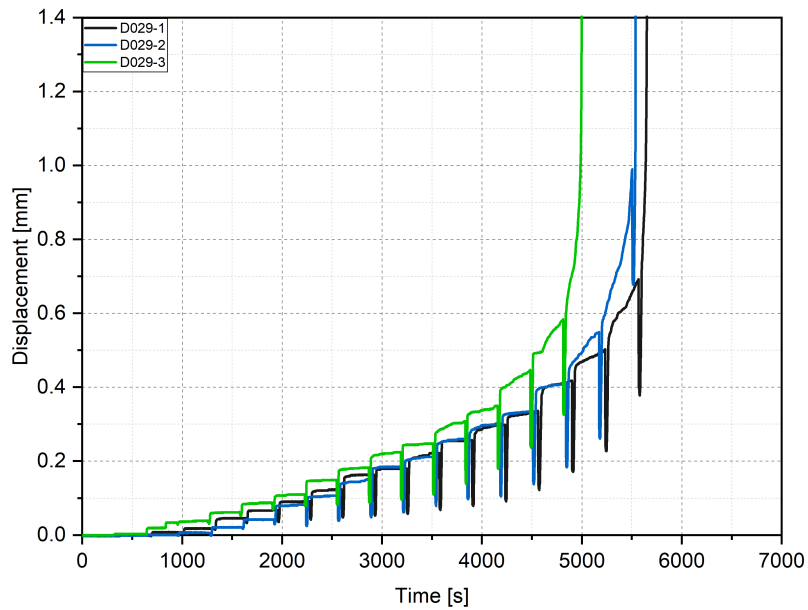
FIGURE B.10: D029 - displacement versus time curves
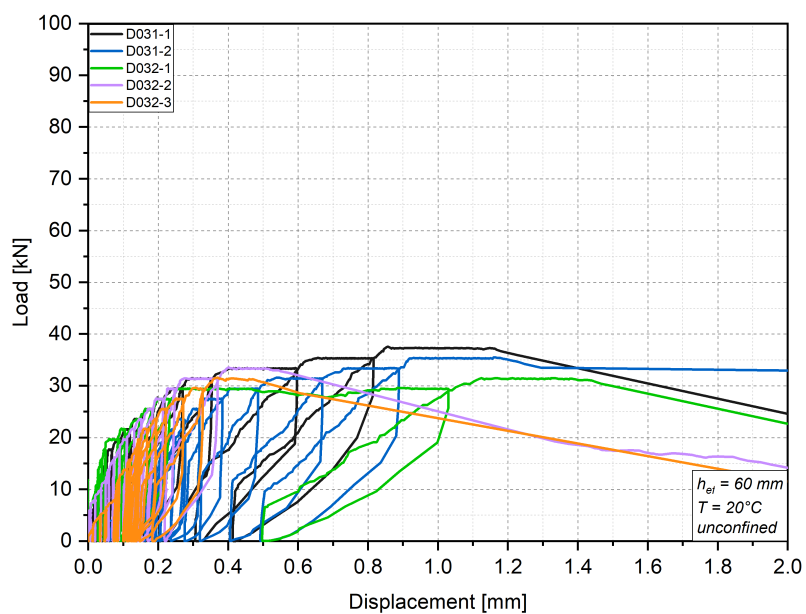
FIGURE B.11: D031&D032 - load versus displacement curves
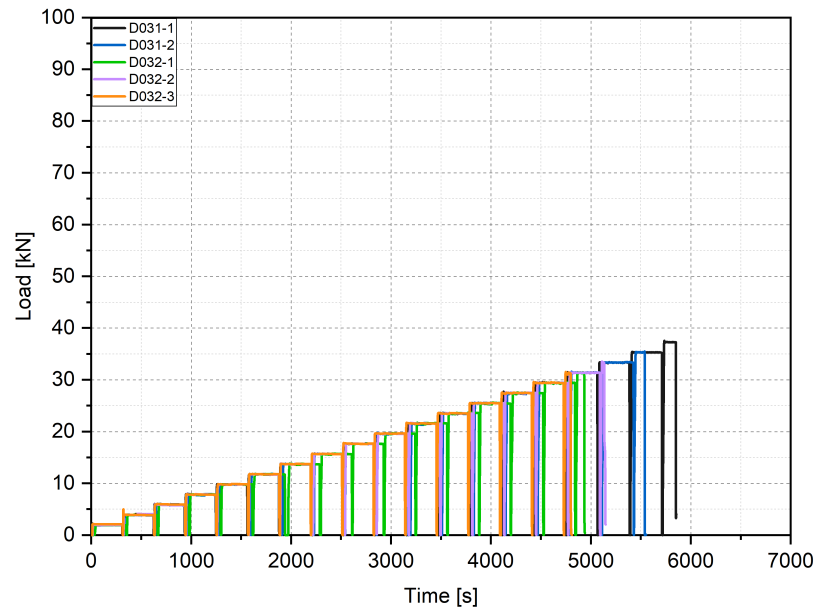
FIGURE B.12: D031&D032 - load versus time curves
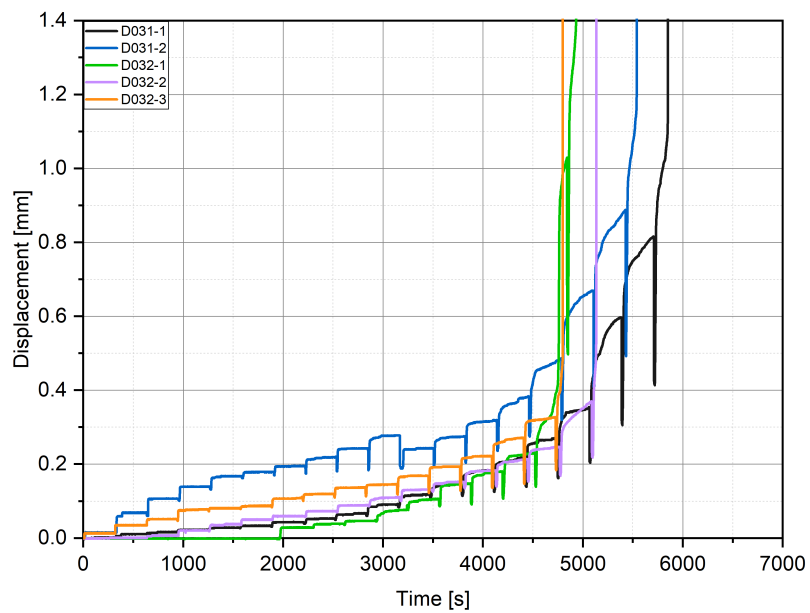
FIGURE B.13: D031&D032 - displacement versus time curves
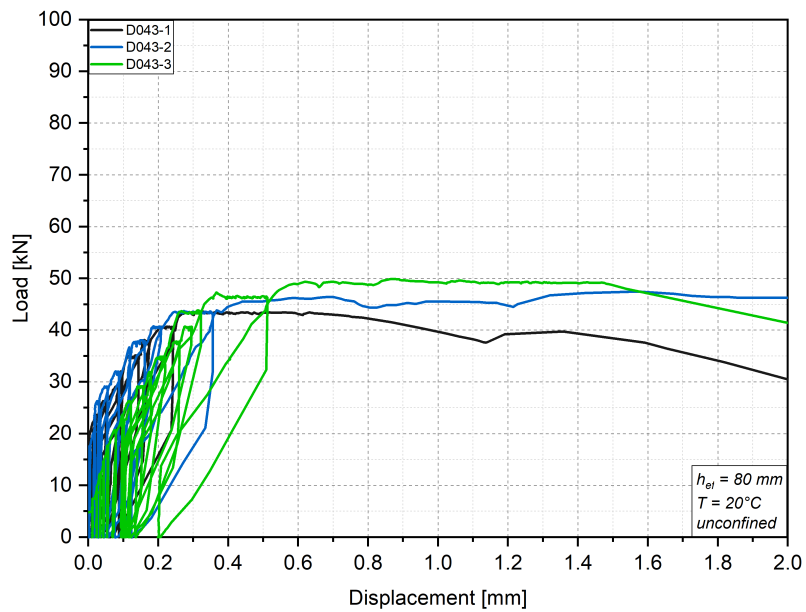
FIGURE B.14: D043 - load versus displacement curves
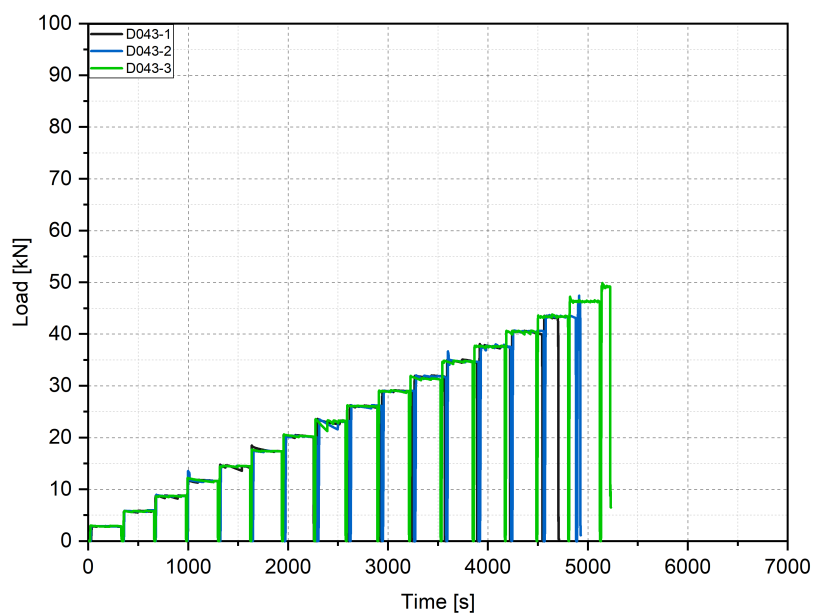
FIGURE B.15: D043 - load versus time curves
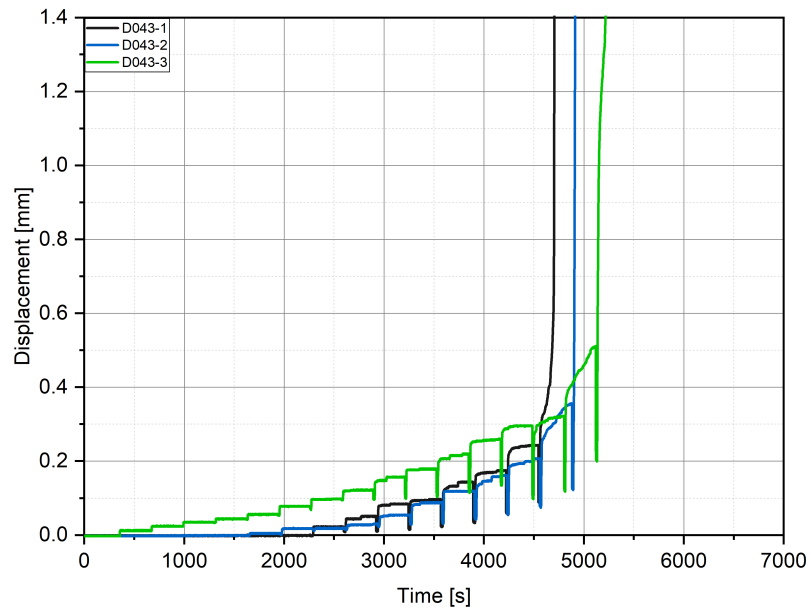
FIGURE B.16: D043 - displacement versus time curves
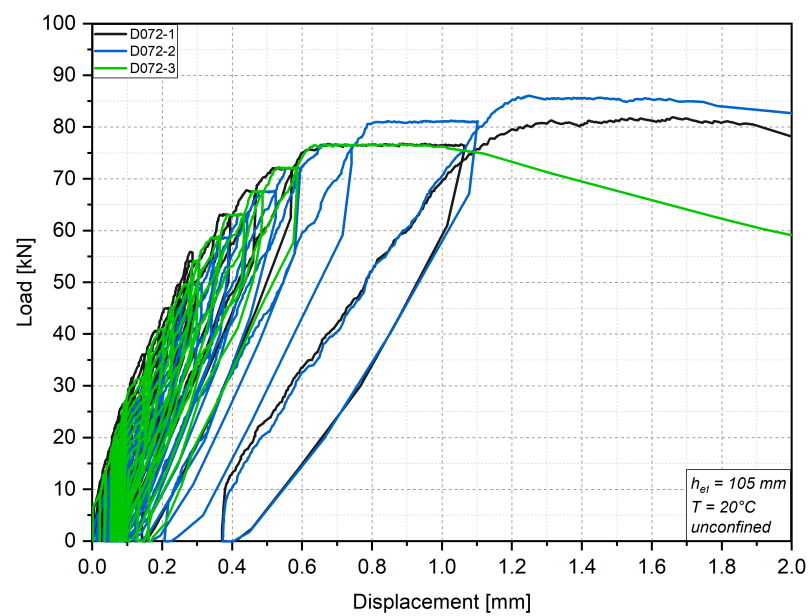
FIGURE B.17: D072 - load versus displacement curves
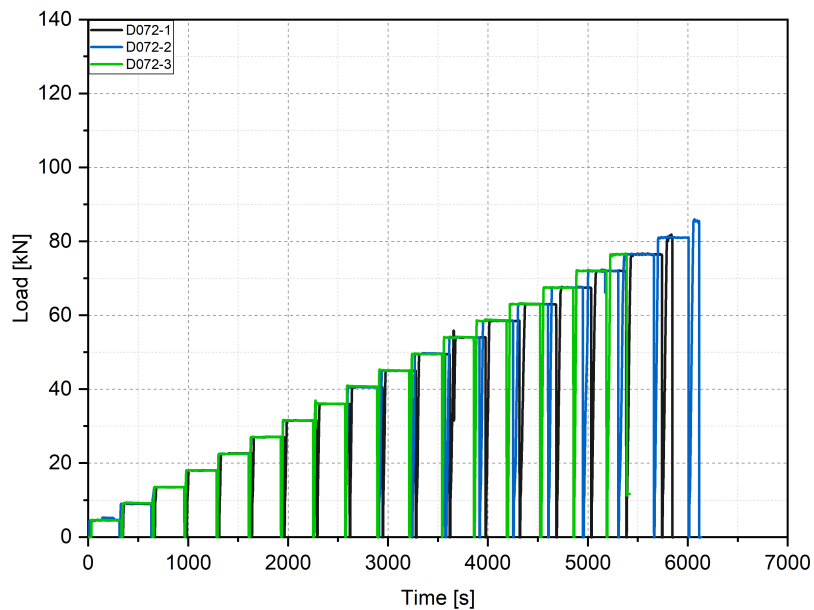
FIGURE B.18: D072 - load versus time curves
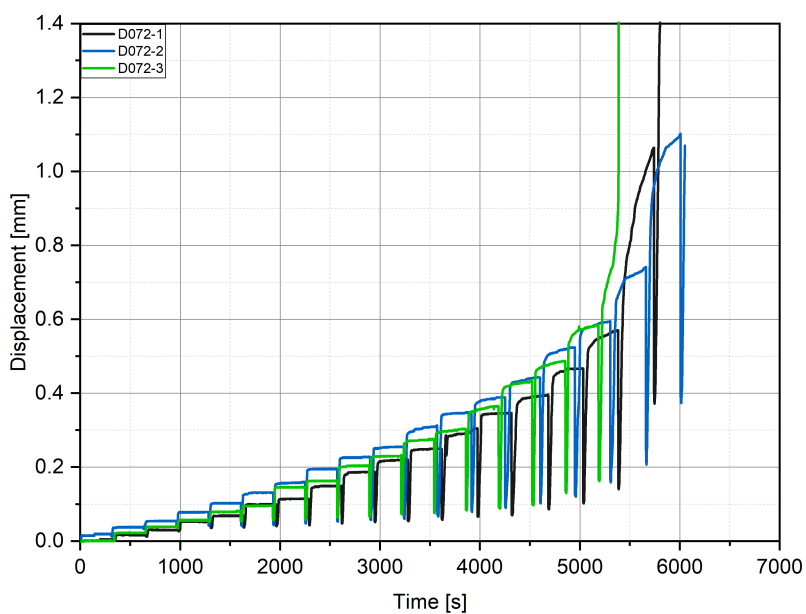
FIGURE B.19: D072 - displacement versus time curves
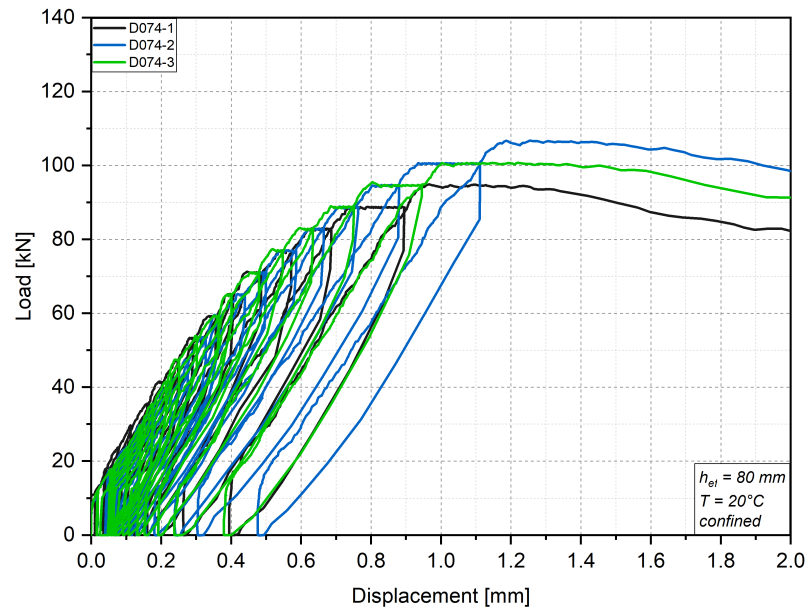
FIGURE B.20: D074 - load versus displacement curves
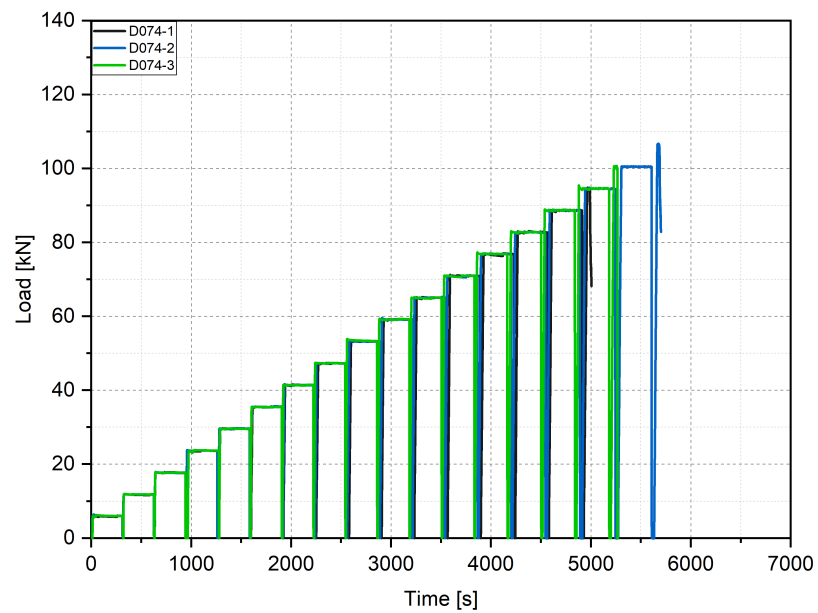
FIGURE B.21: D074 - load versus time curves
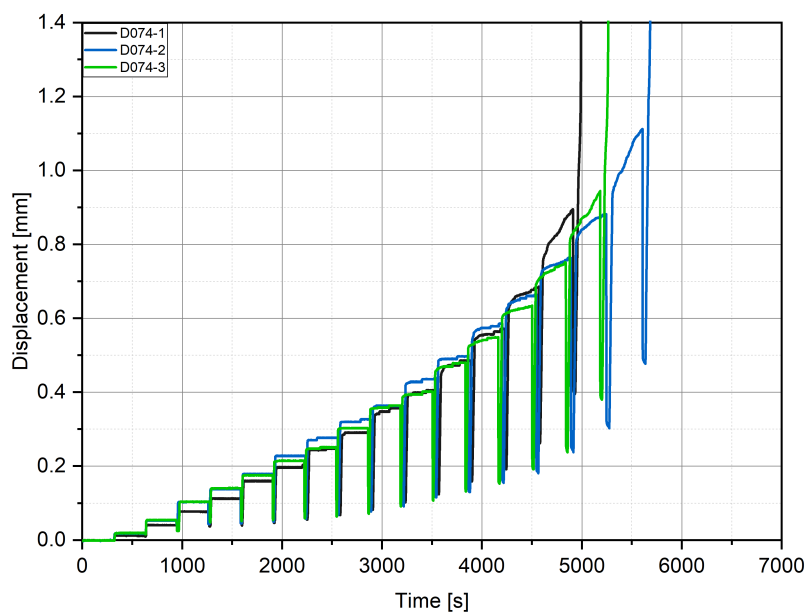
FIGURE B.22: D074 - displacement versus time curves

B.1.4   Incremental loading test
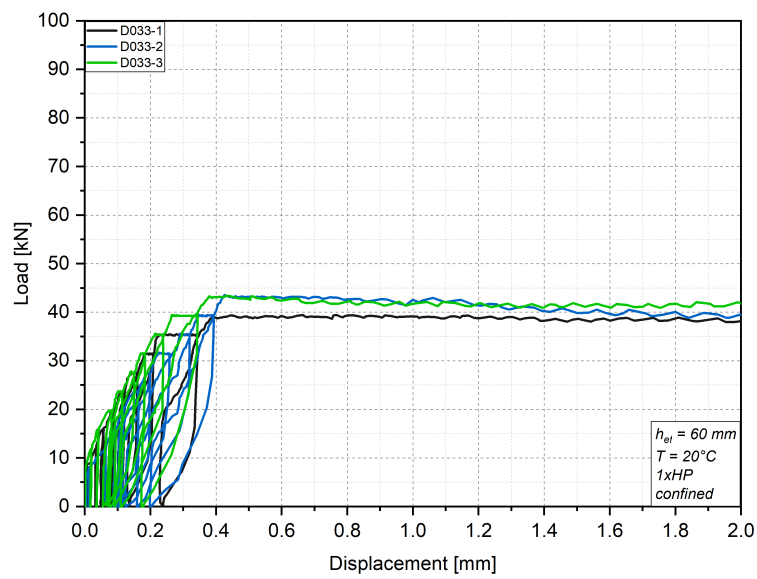
FIGURE B.23: D033 - load versus displacement curves
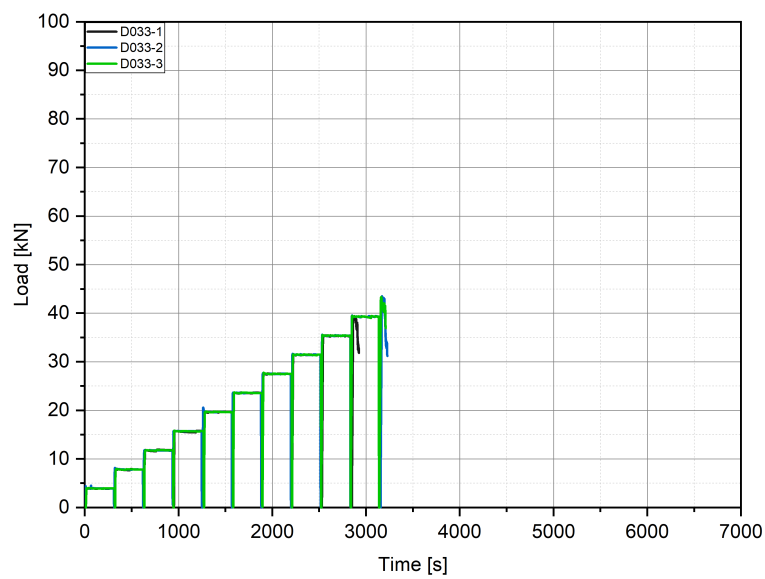
FIGURE B.24: D033 - load versus time curves
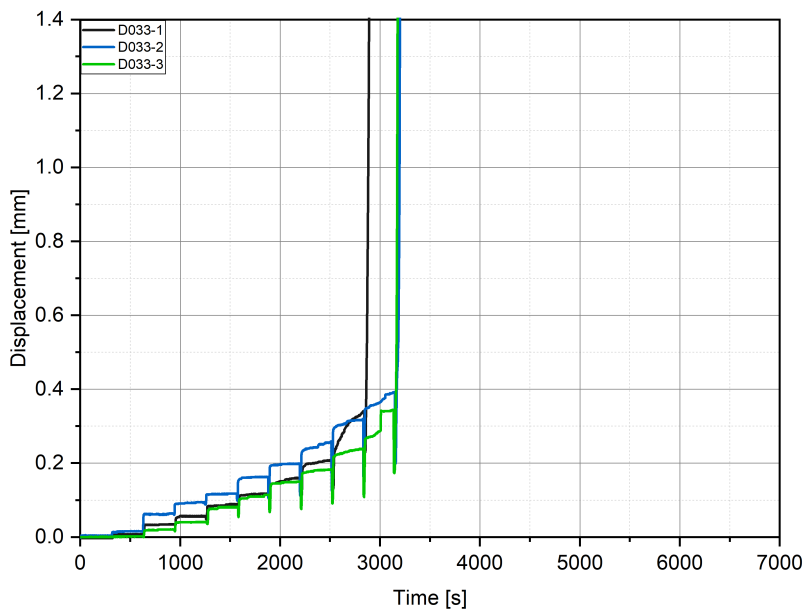
FIGURE B.25: D033 - displacement versus time curves
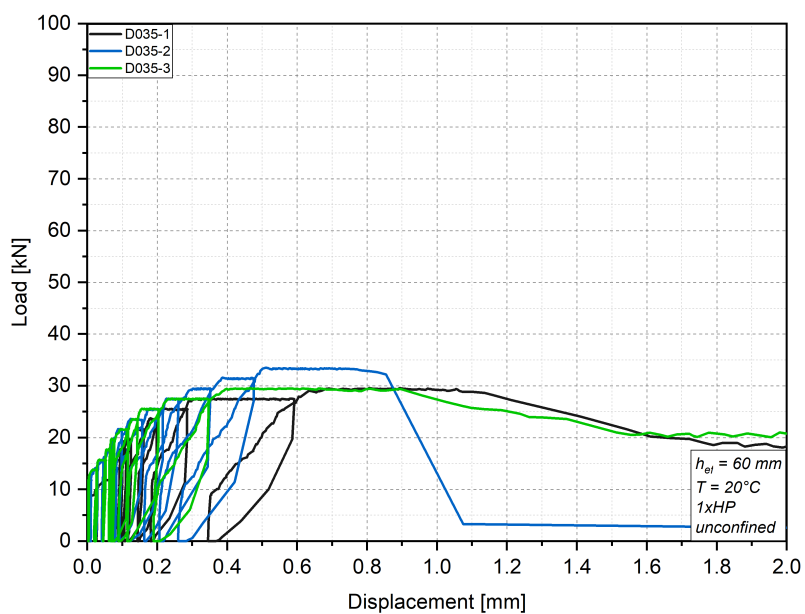
FIGURE B.26: D035 - load versus displacement curves
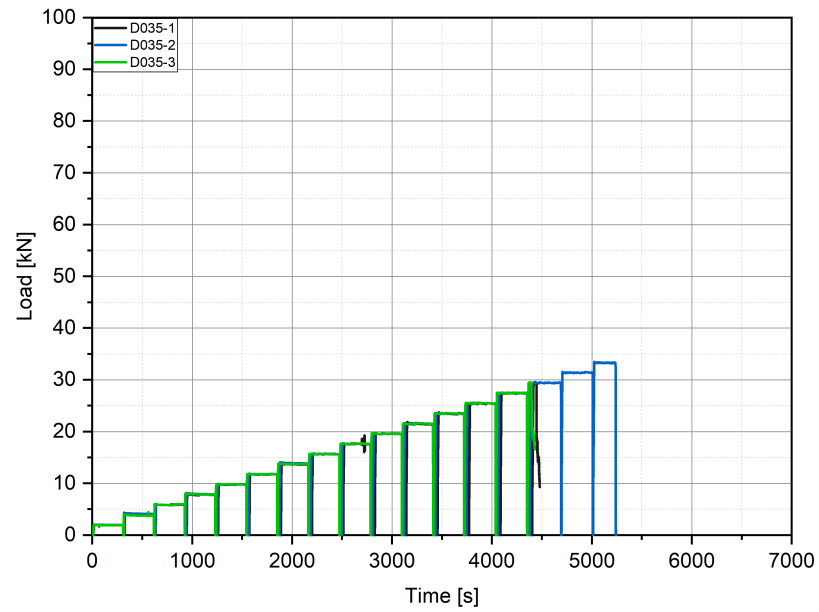
FIGURE B.27: D035 - load versus time curves
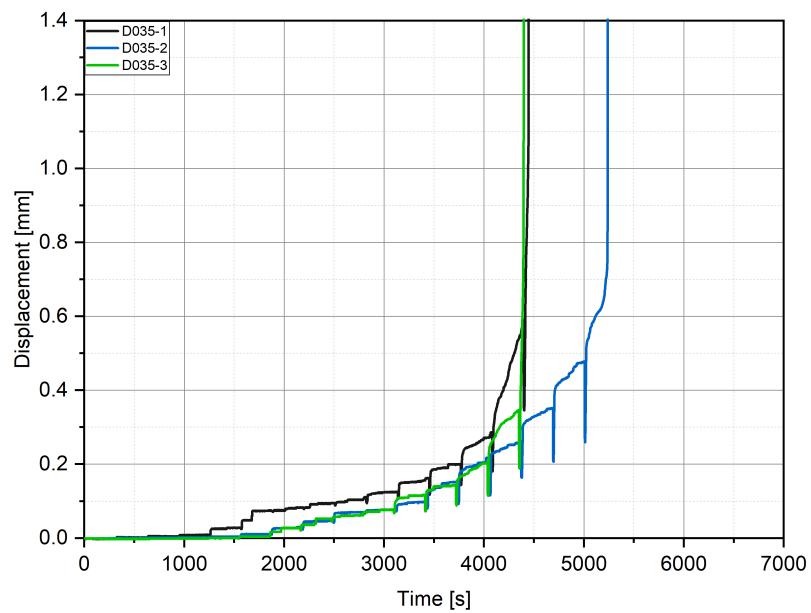
FIGURE B.28: D035 - displacement versus time curves
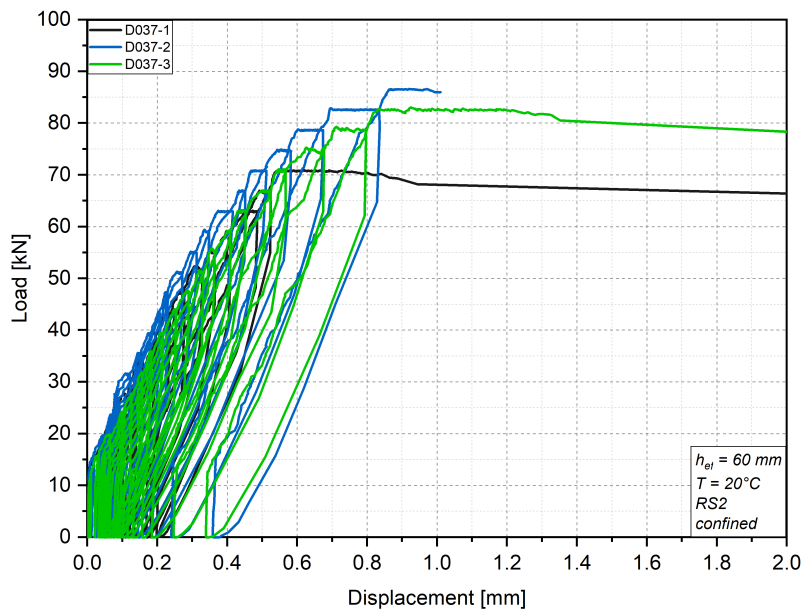
FIGURE B.29: D037 - load versus displacement curves
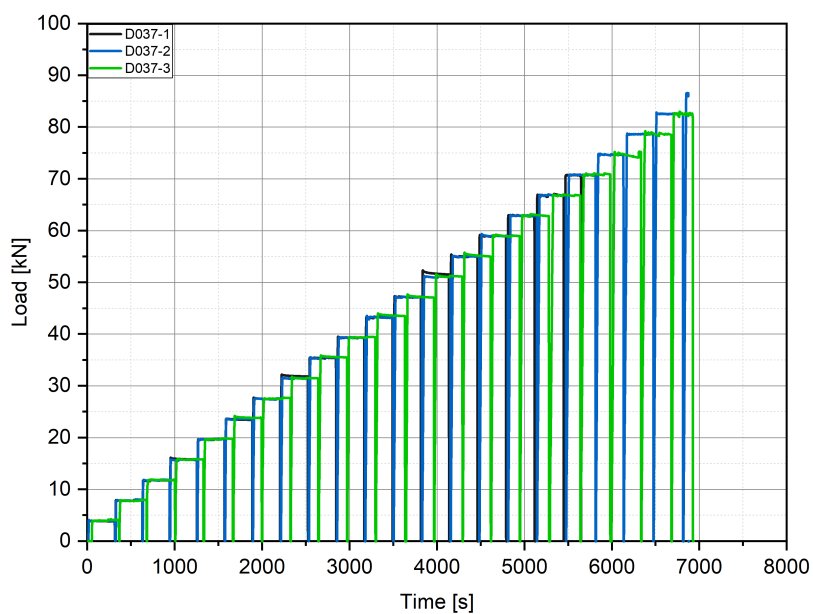
FIGURE B.30: D037 - load versus time curves
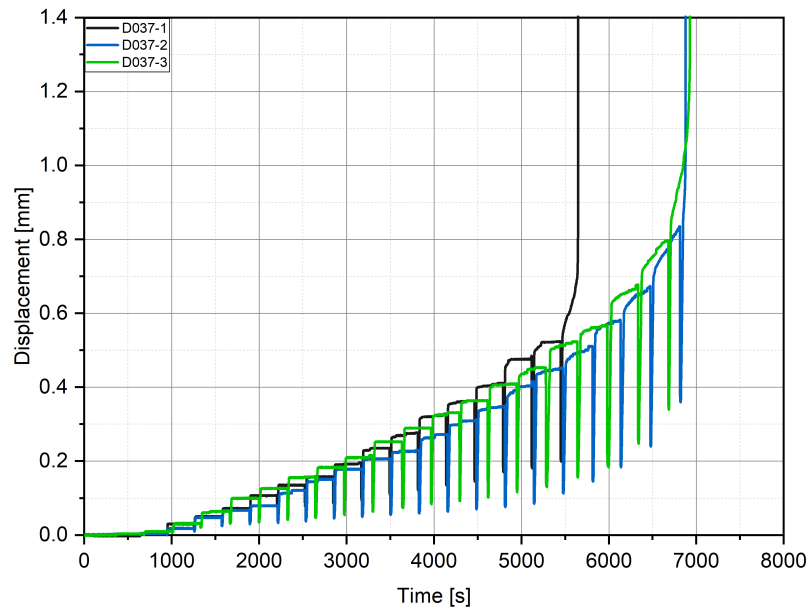
FIGURE B.31: D037 - displacement versus time curves
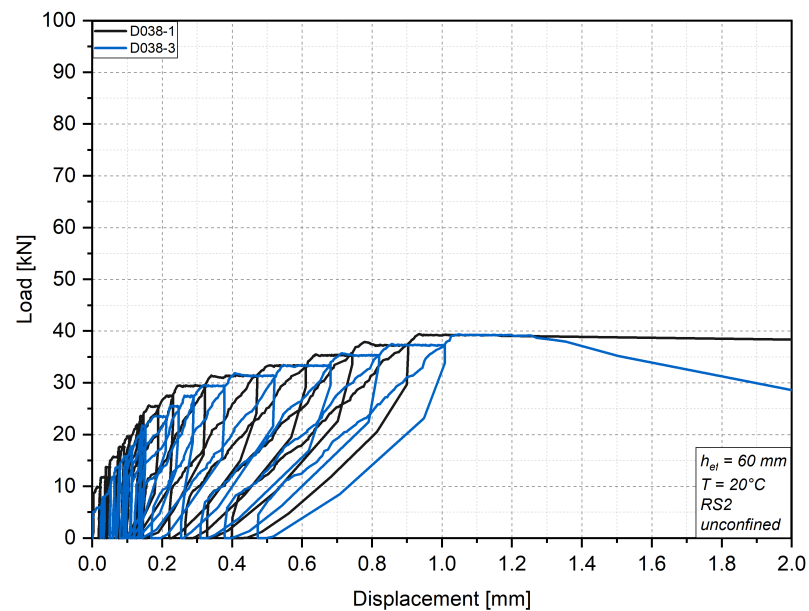
FIGURE B.32: D038 - load versus displacement curves
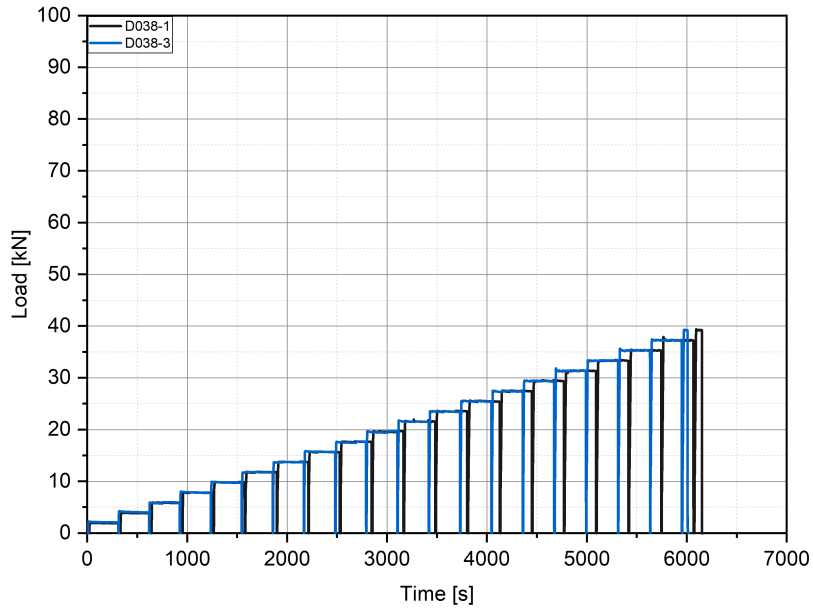
FIGURE B.33: D038 - load versus time curves
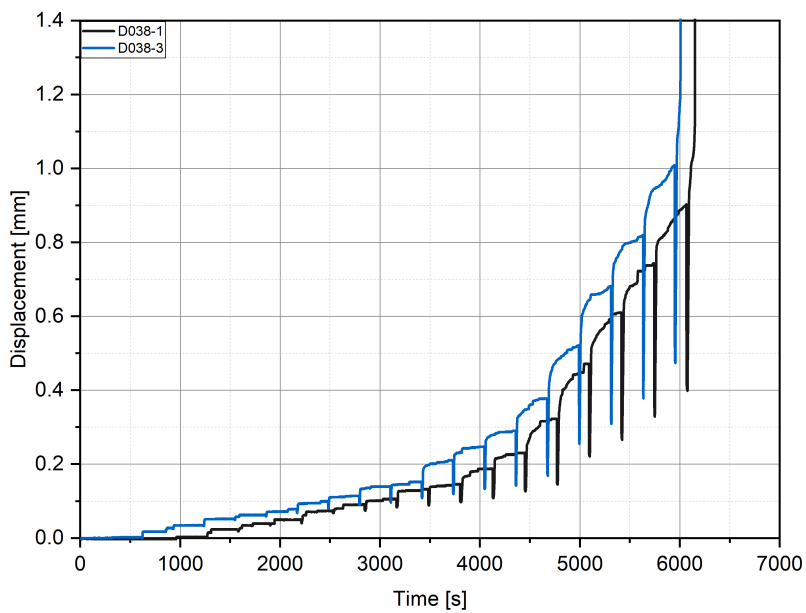
FIGURE B.34: D038 - displacement versus time curves
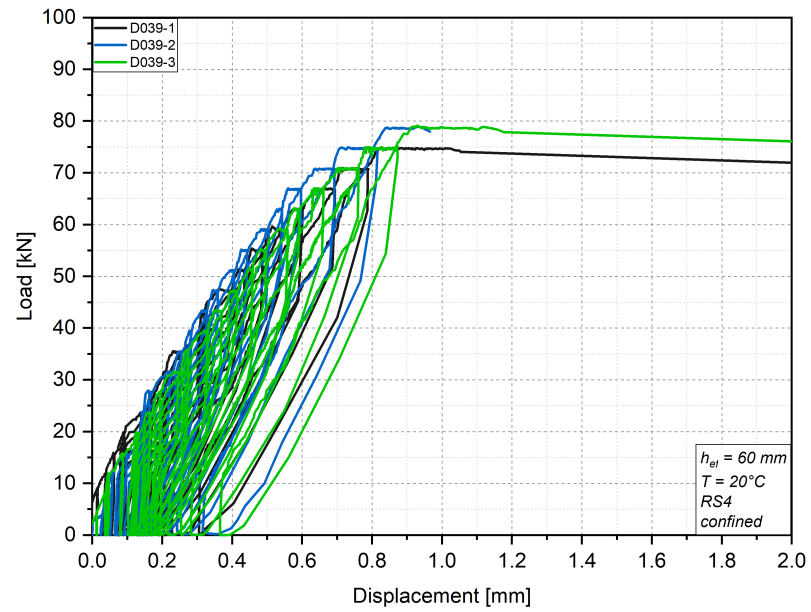
FIGURE B.35: D039 - load versus displacement curves
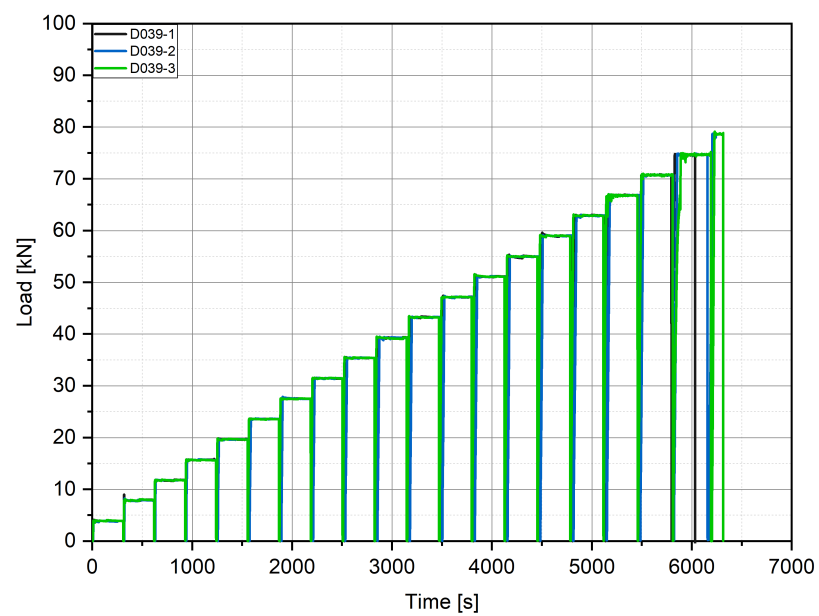
FIGURE B.36: D039 - load versus time curves
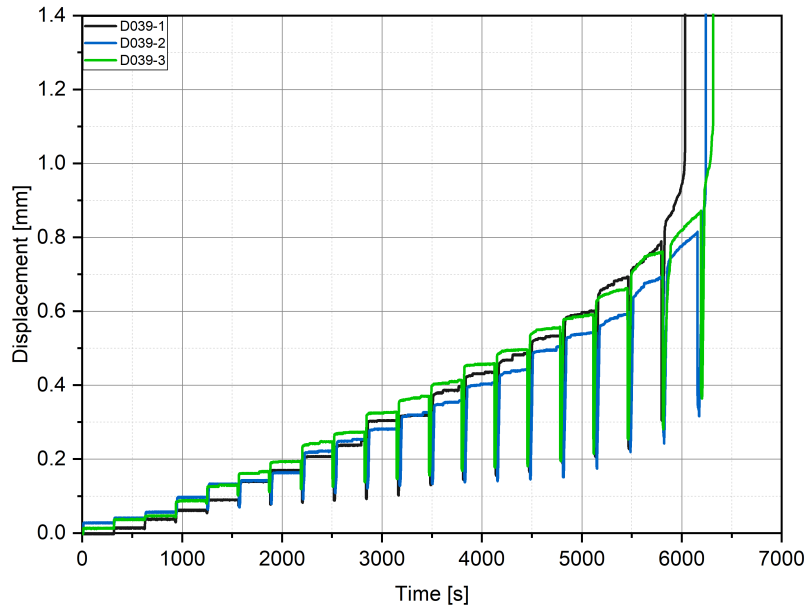
FIGURE B.37: D039 - displacement versus time curves
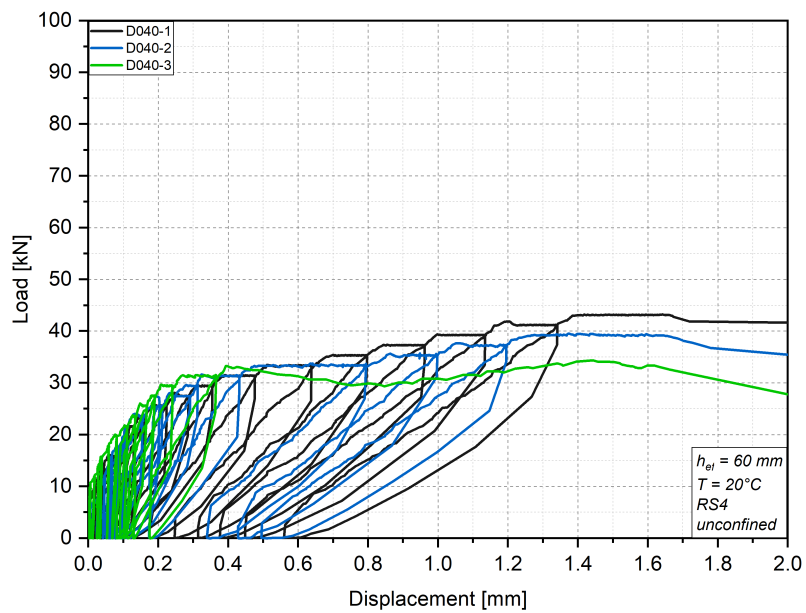
FIGURE B.38: D040 - load versus displacement curves
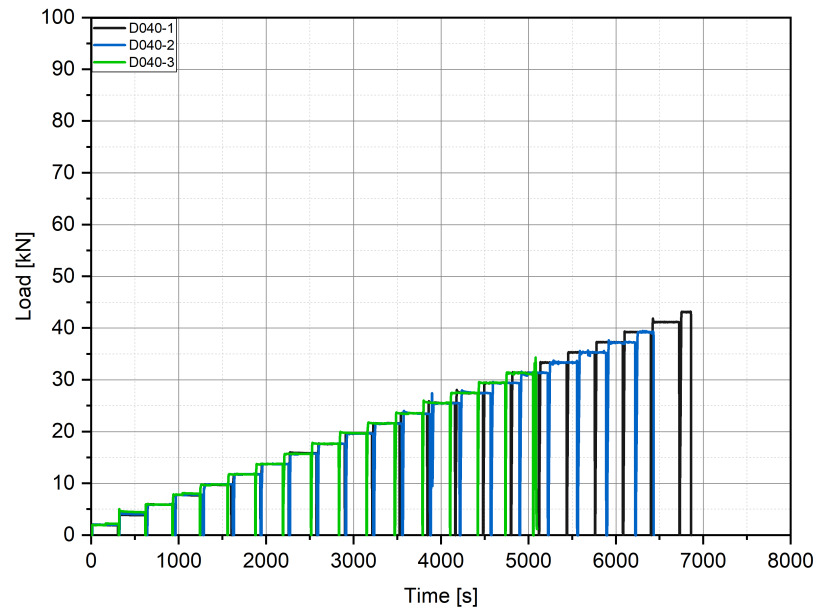
FIGURE B.39: D040 - load versus time curves
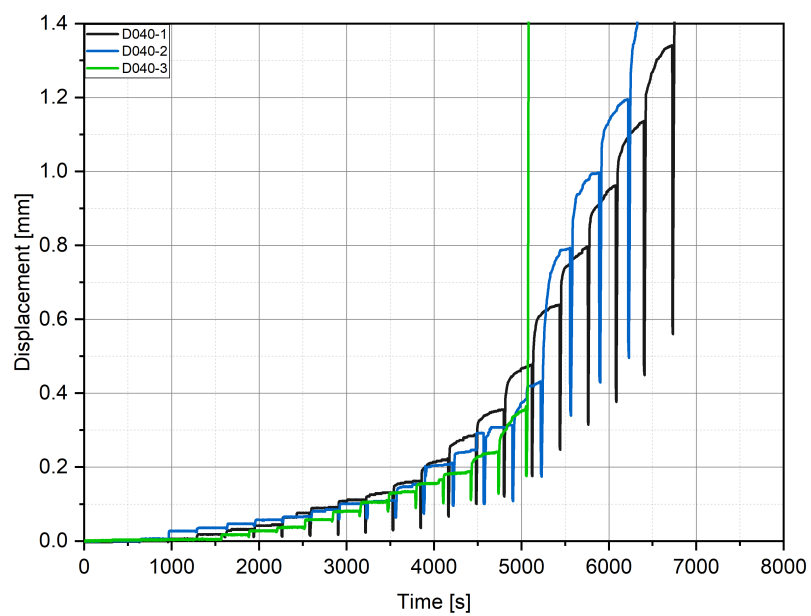
FIGURE B.40: D040 - displacement versus time curves
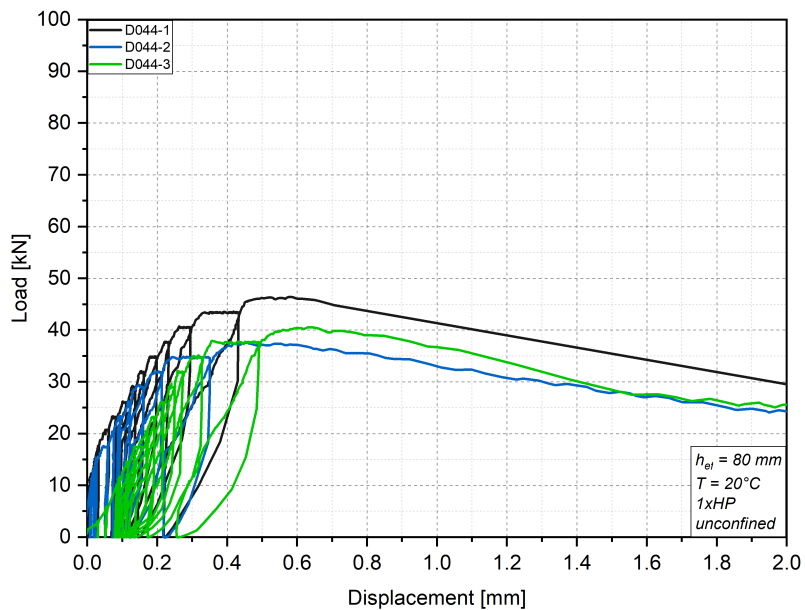
FIGURE B.41: D044 - load versus displacement curves
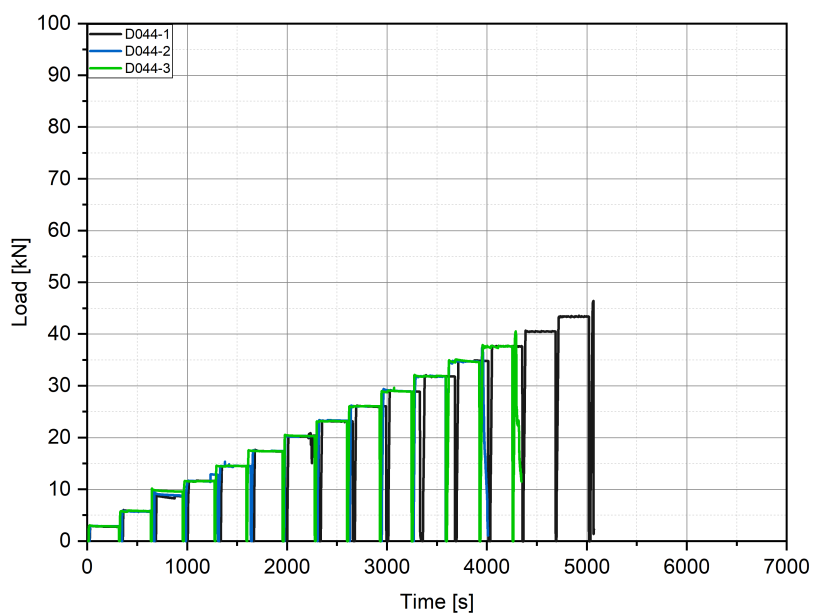
FIGURE B.42: D044 - load versus time curves
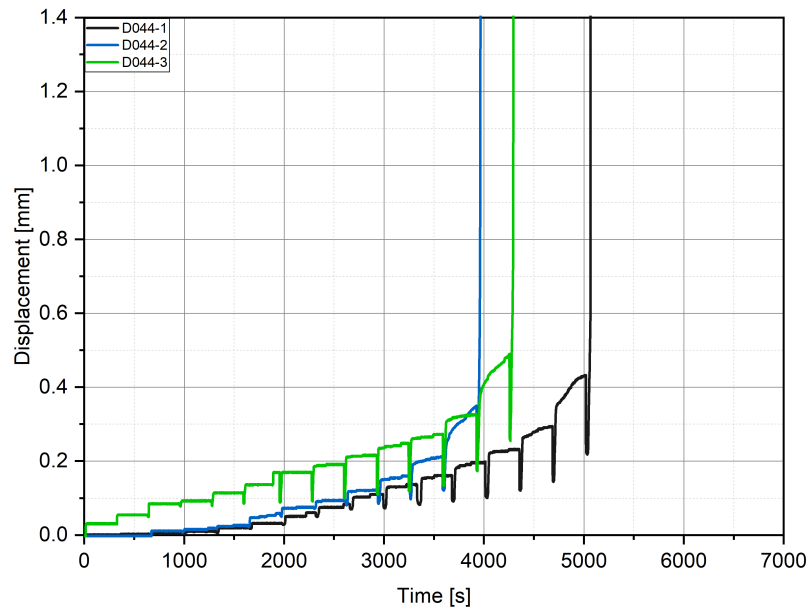
FIGURE B.43: D044 - displacement versus time curves
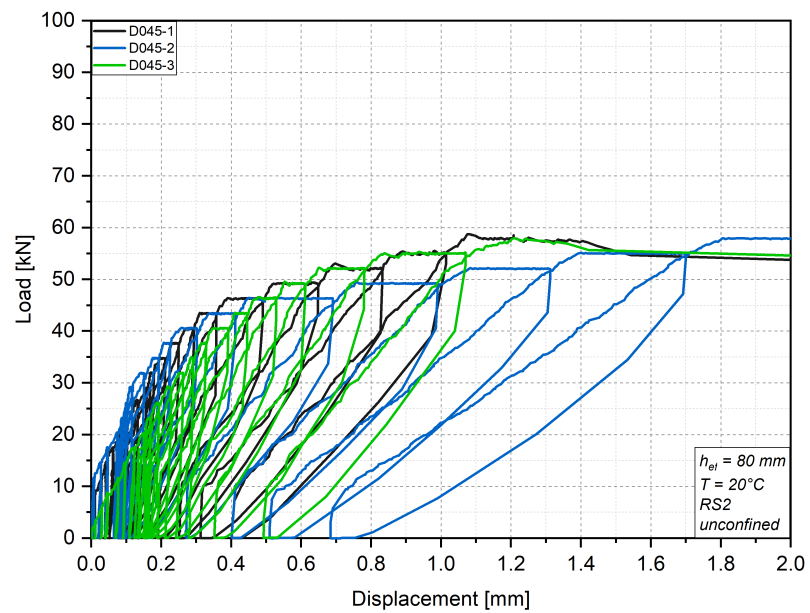
FIGURE B.44: D045 - load versus displacement curves
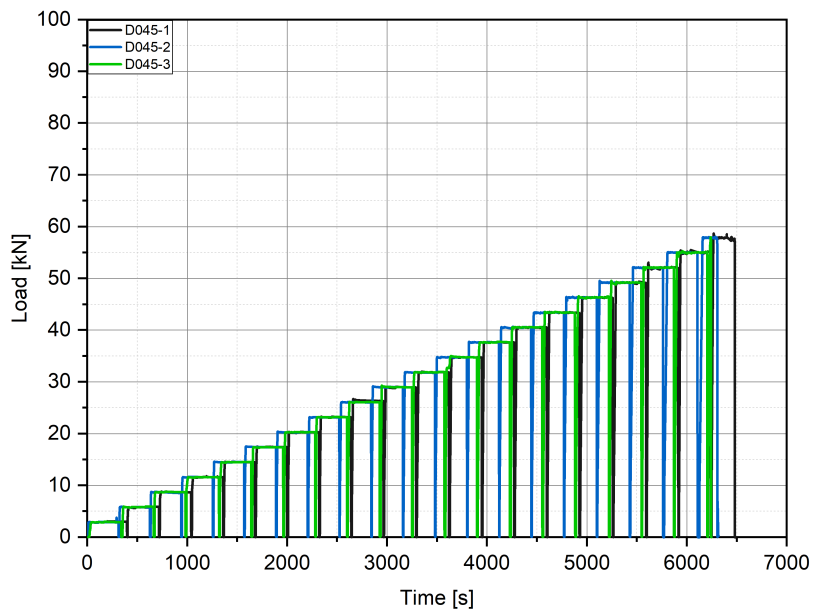
FIGURE B.45: D045 - load versus time curves
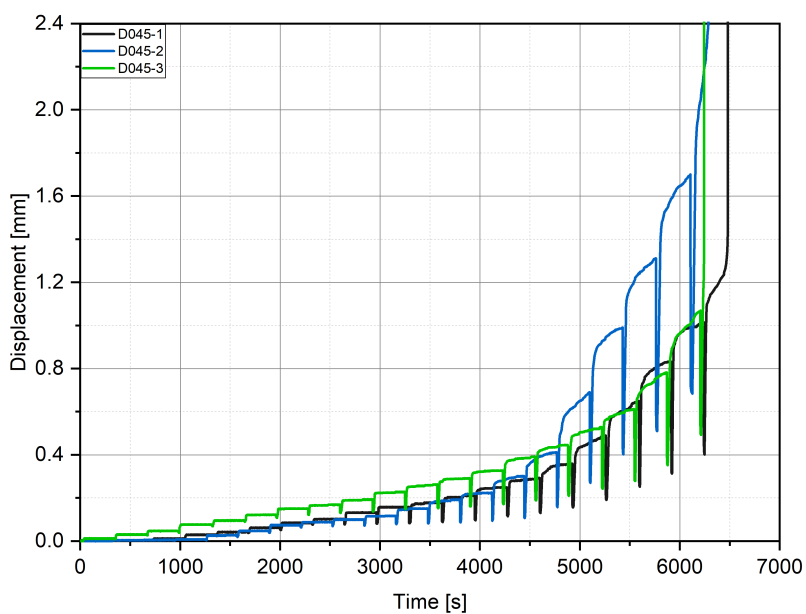
FIGURE B.46: D045 - displacement versus time curves
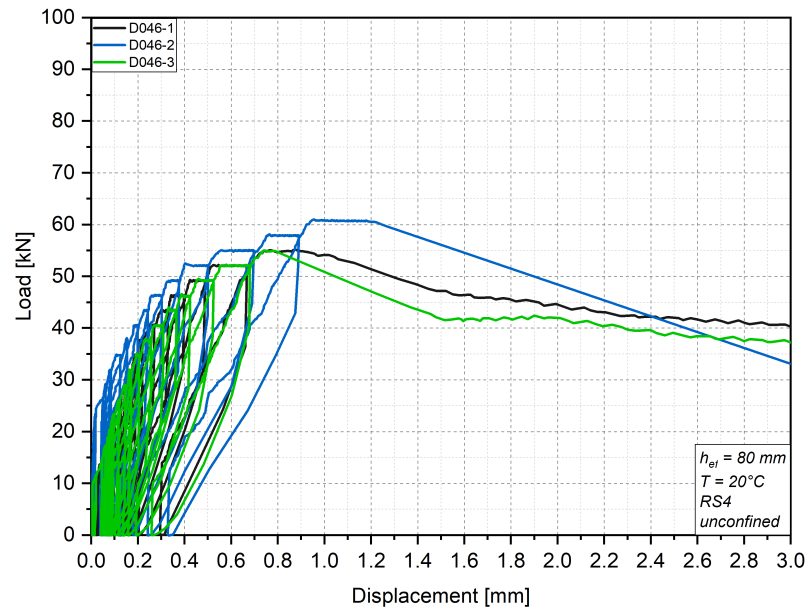
FIGURE B.47: D046 - load versus displacement curves
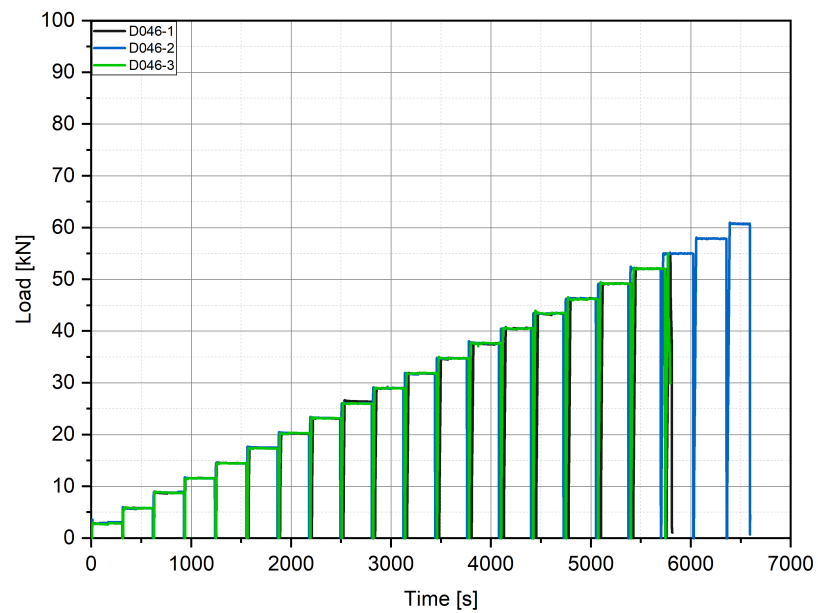
FIGURE B.48: D046 - load versus time curves
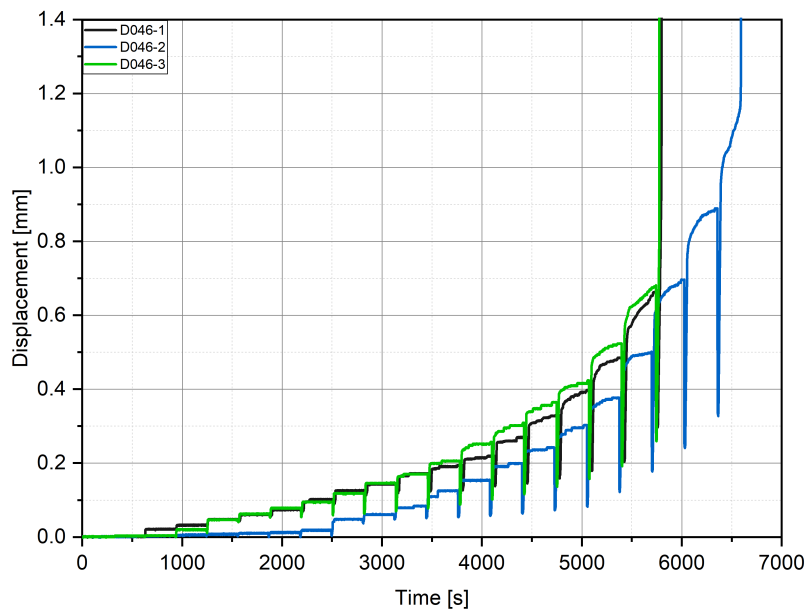
FIGURE B.49: D046 - displacement versus time curves
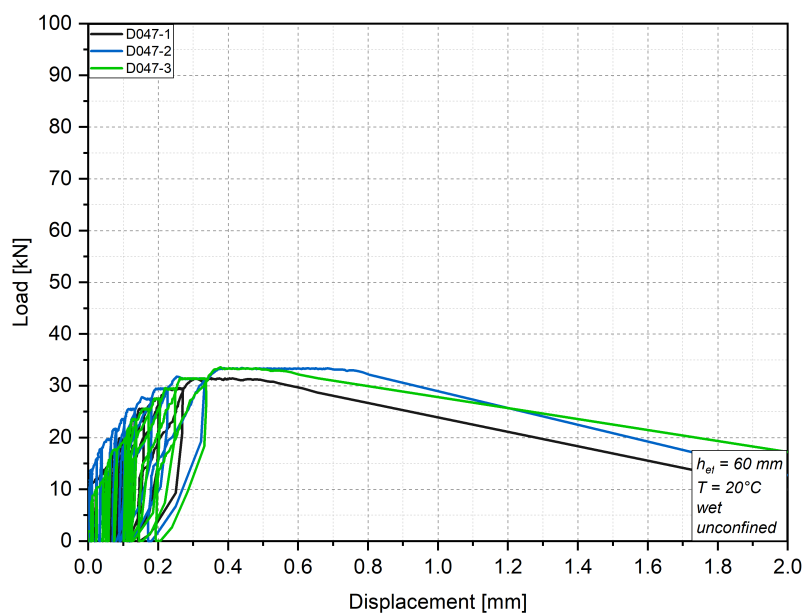
FIGURE B.50: D047 - load versus displacement curves
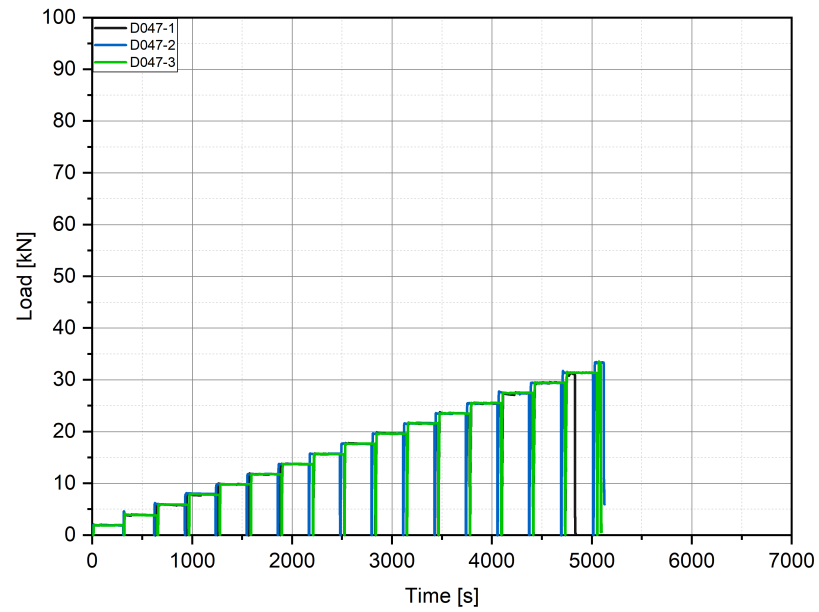
FIGURE B.51: D047 - load versus time curves
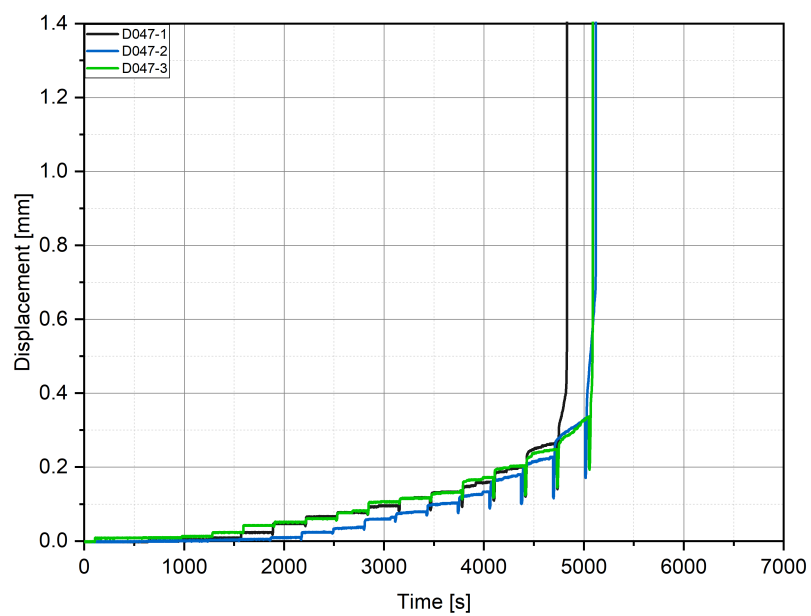
FIGURE B.52: D047 - displacement versus time curves
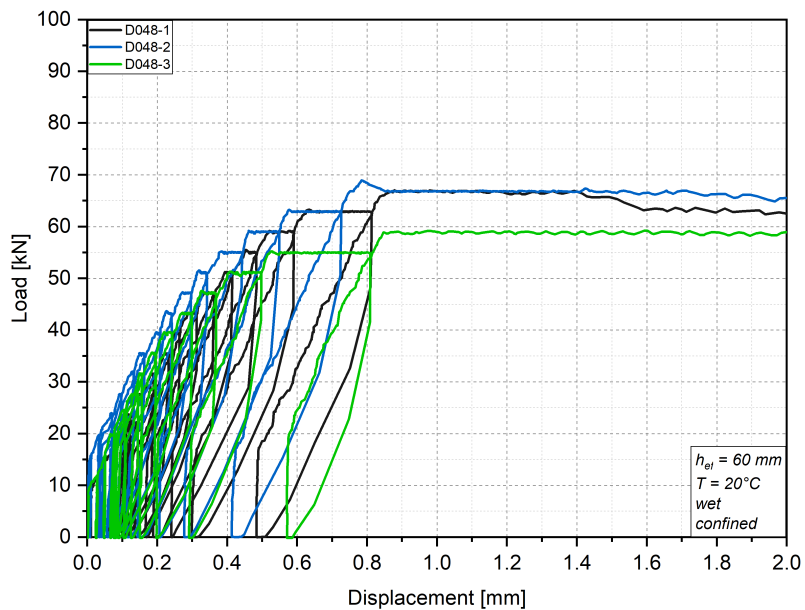
FIGURE B.53: D048 - load versus displacement curves
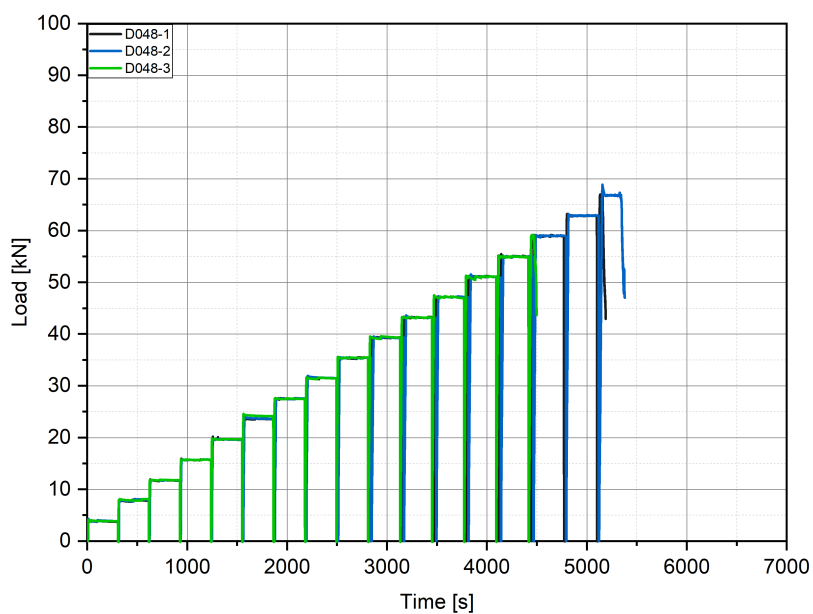
FIGURE B.54: D048 - load versus time curves
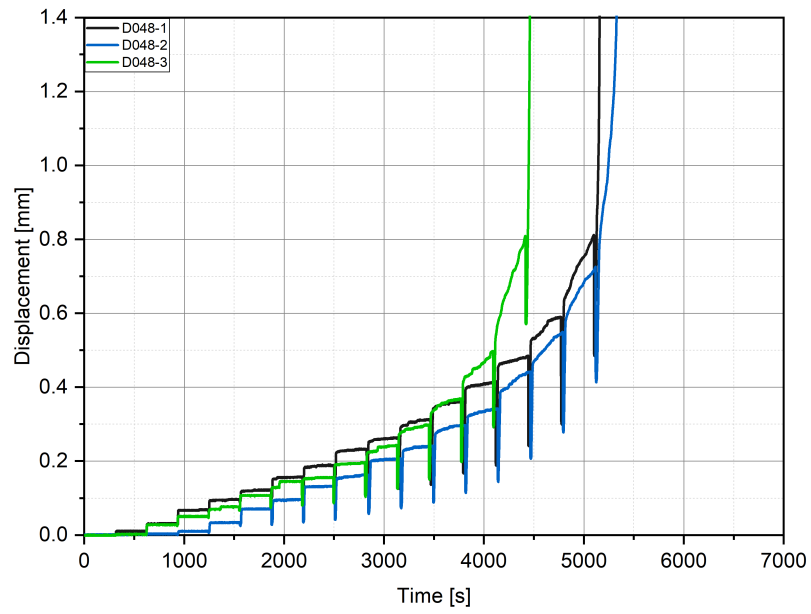
FIGURE B.55: D048 - displacement versus time curves
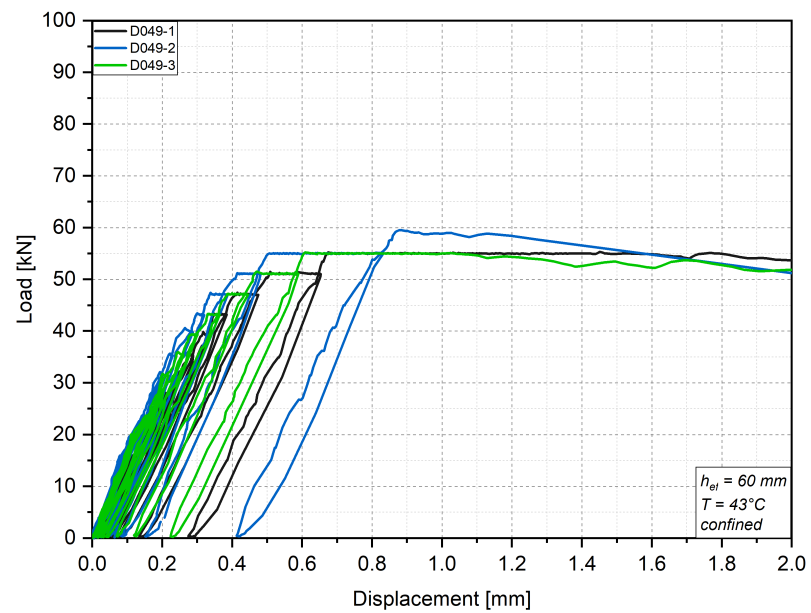
FIGURE B.56: D049 - load versus displacement curves
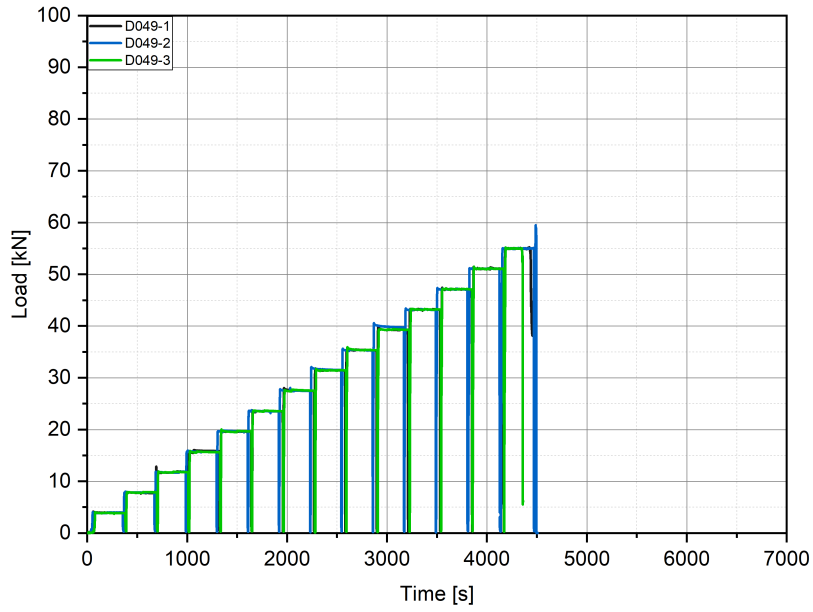
FIGURE B.57: D049 - load versus time curves
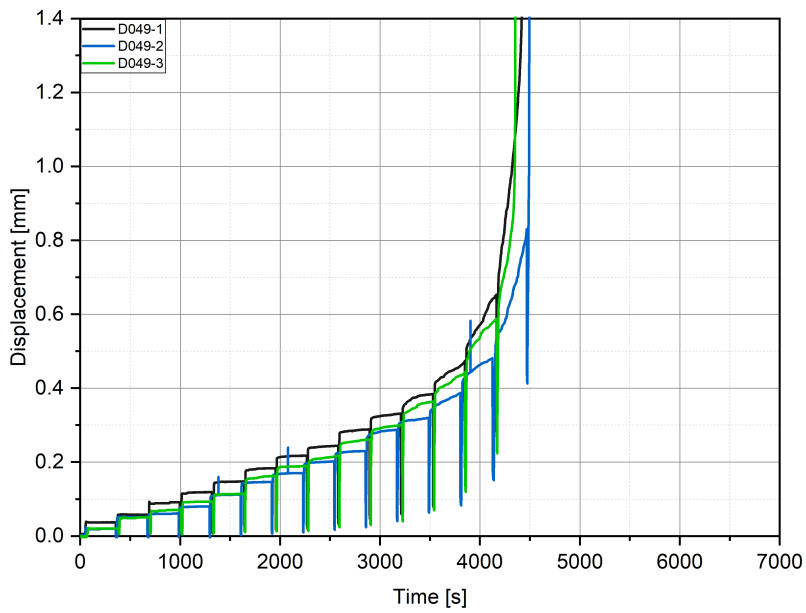
FIGURE B.58: D049 - displacement versus time curves
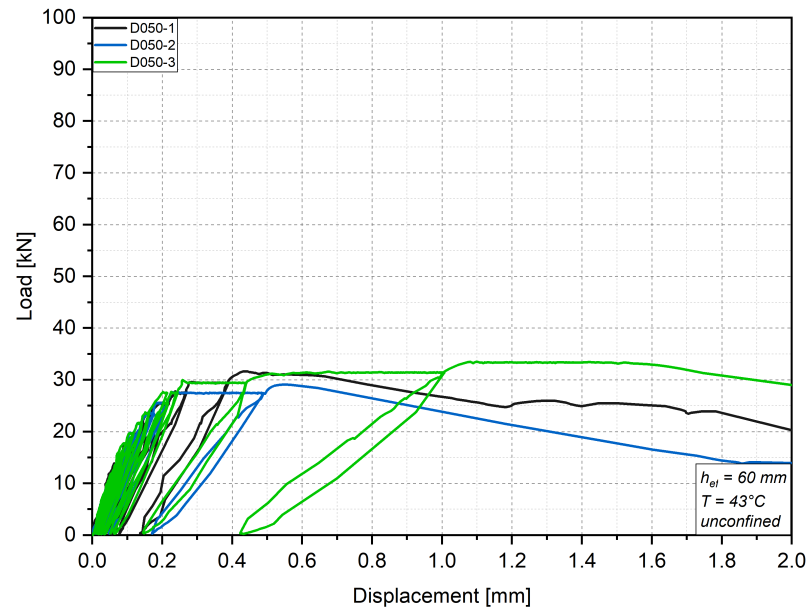
FIGURE B.59: D050 - load versus displacement curves
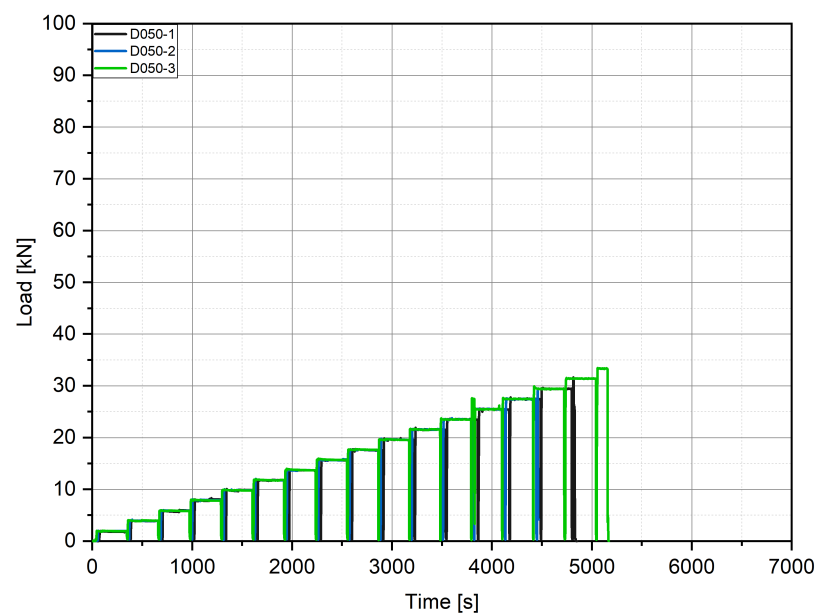
FIGURE B.60: D050 - load versus time curves
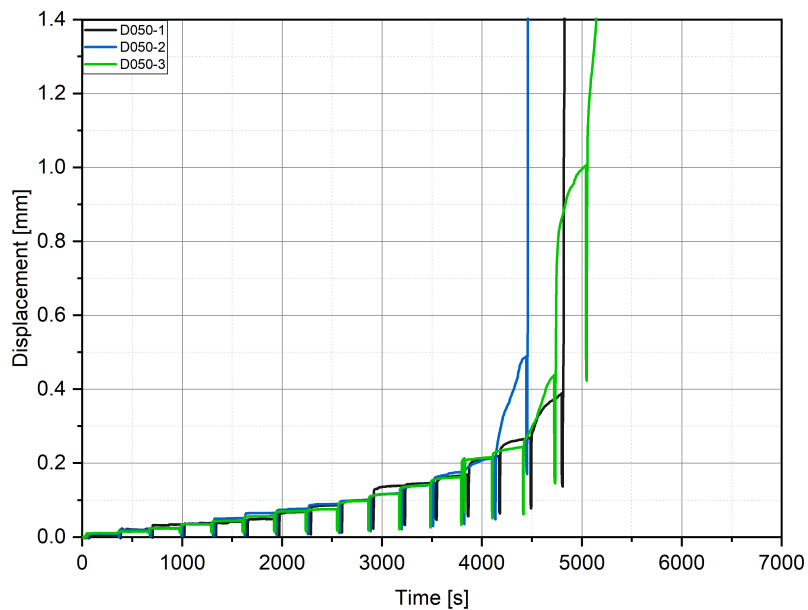
FIGURE B.61: D050 - displacement versus time curves
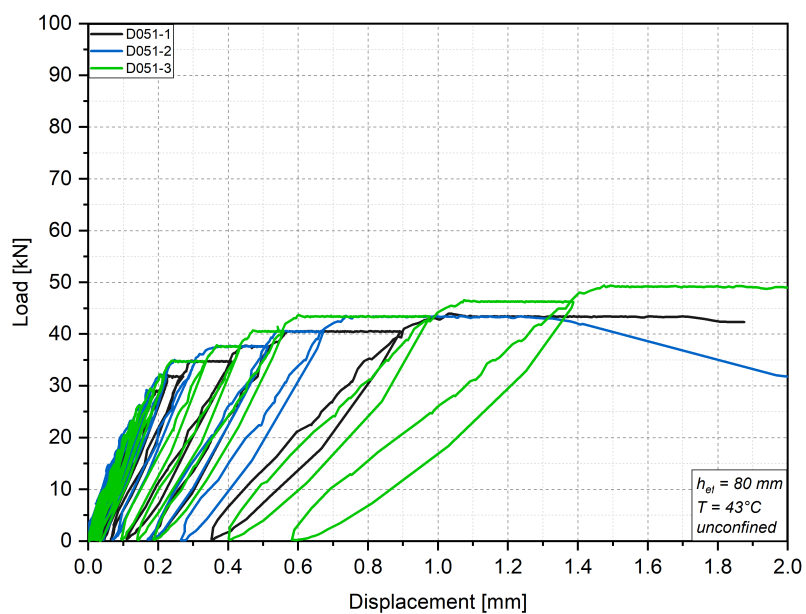
FIGURE B.62: D051 - load versus displacement curves
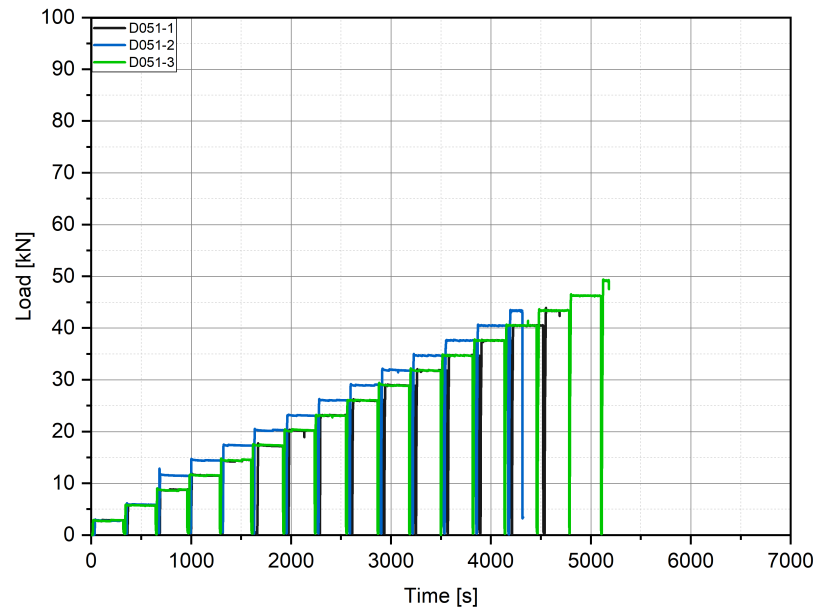
FIGURE B.63: D051 - load versus time curves
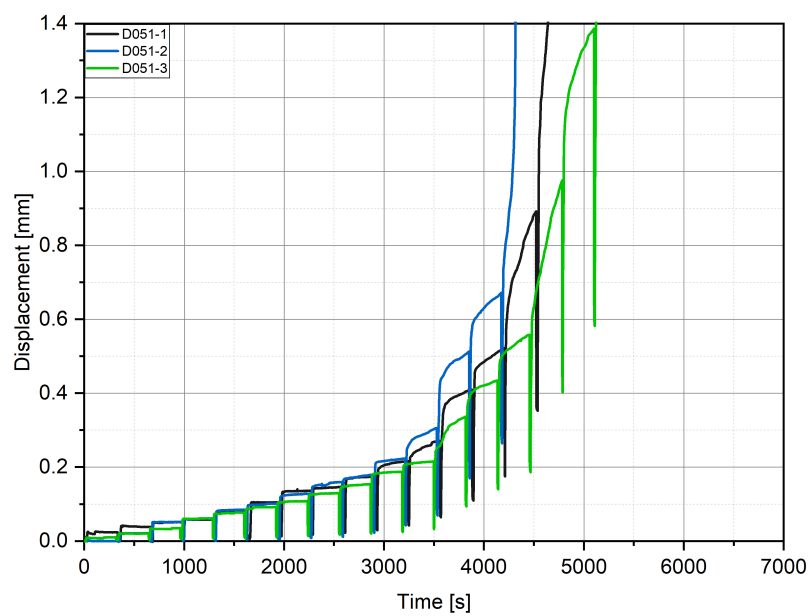
FIGURE B.64: D051 - displacement versus time curves
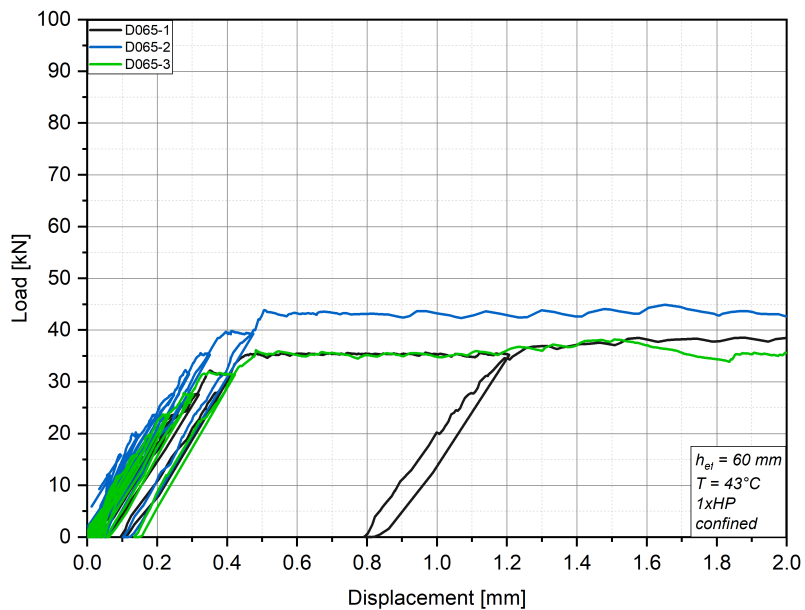
FIGURE B.65: D065 - load versus displacement curves
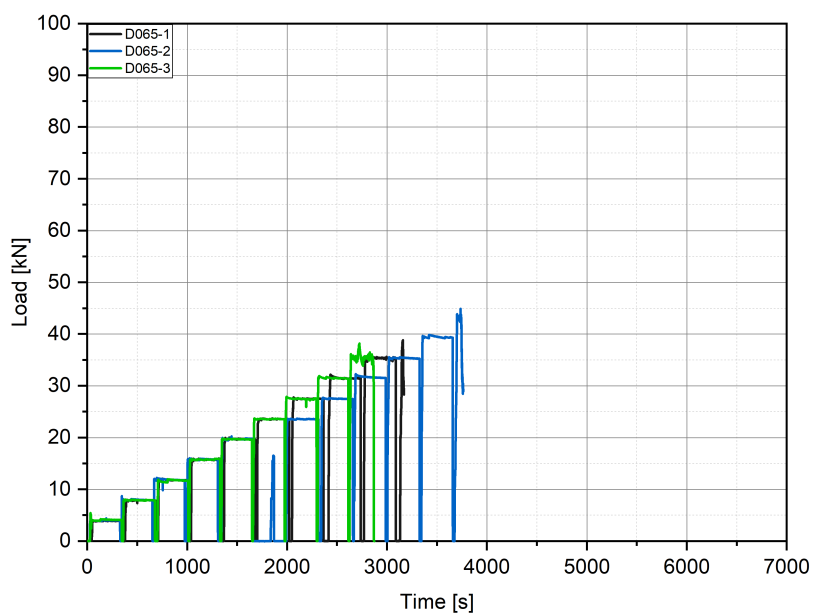
FIGURE B.66: D065 - load versus time curves
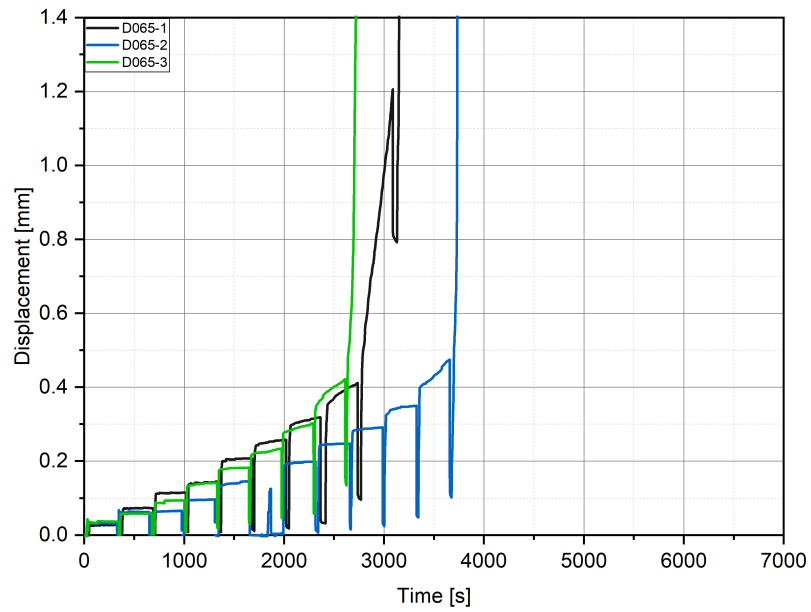
FIGURE B.67: D065 - displacement versus time curves
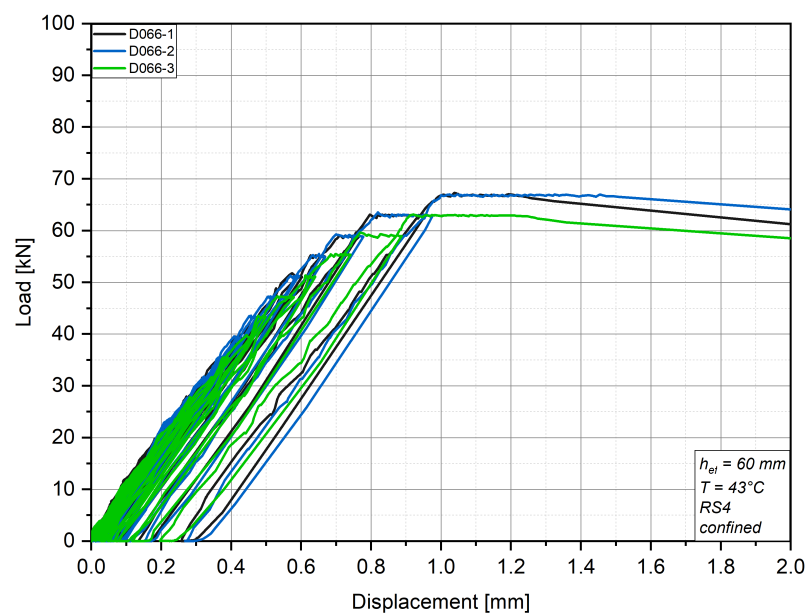
FIGURE B.68: D066 - load versus displacement curves
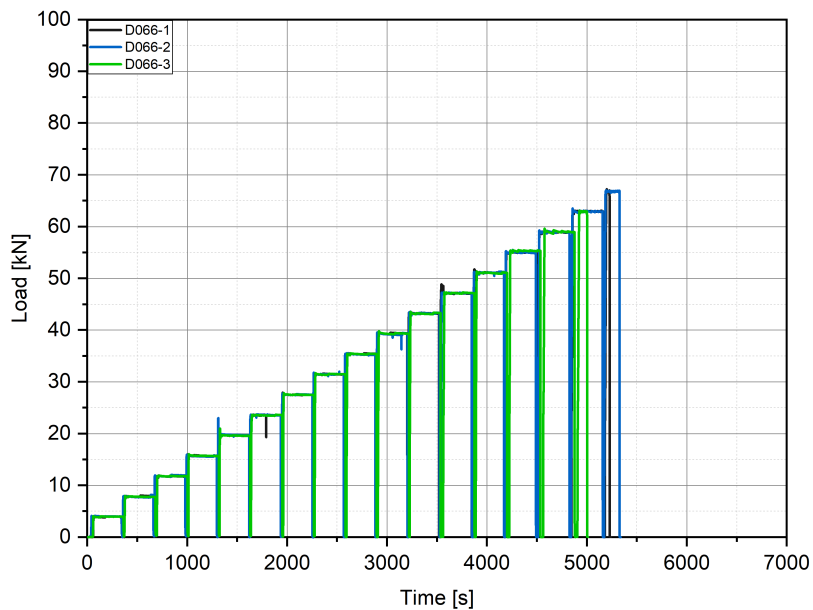
FIGURE B.69: D066 - load versus time curves
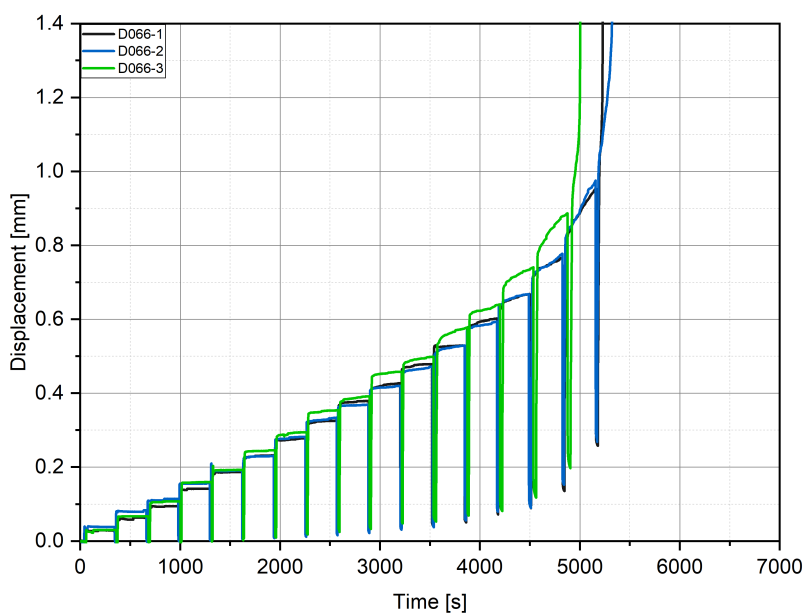
FIGURE B.70: D066 - displacement versus time curves
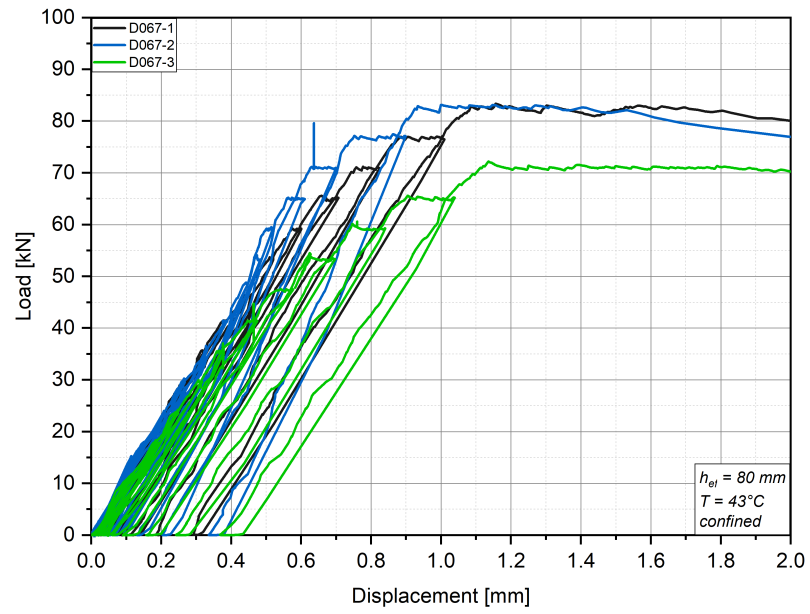
FIGURE B.71: D067 - load versus displacement curves
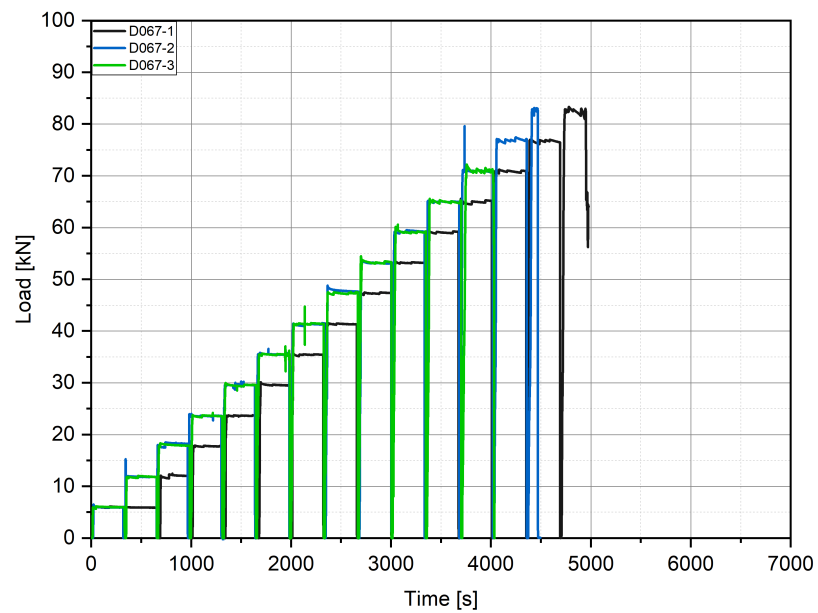
FIGURE B.72: D067 - load versus time curves
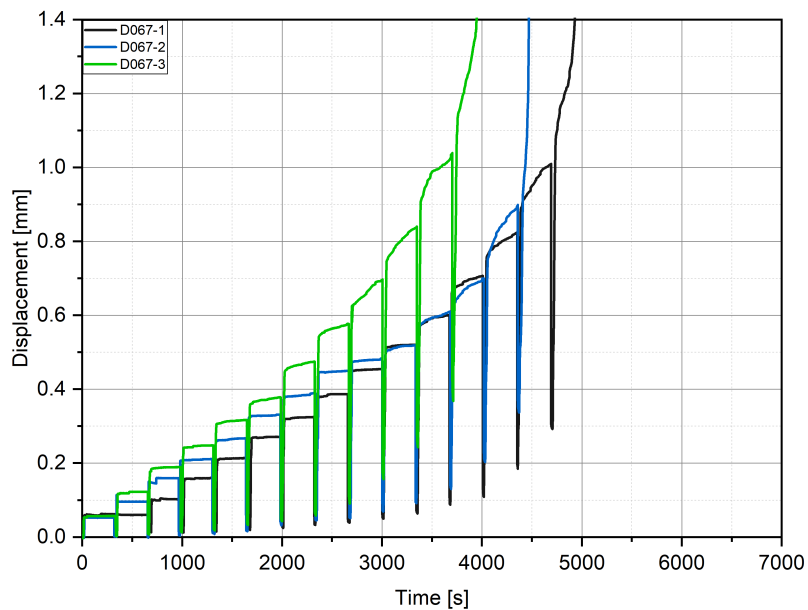
FIGURE B.73: D067 - displacement versus time curves
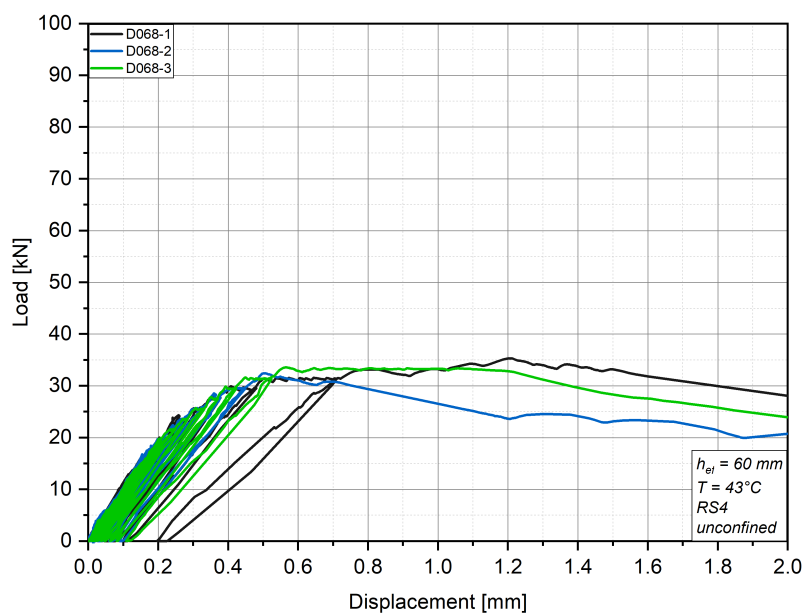
FIGURE B.74: D068 - load versus displacement curves
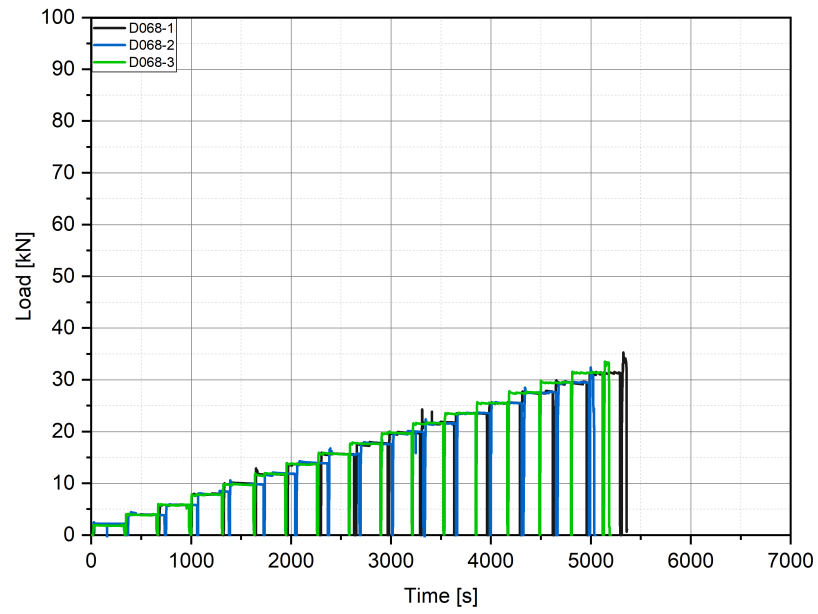
FIGURE B.75: D068 - load versus time curves
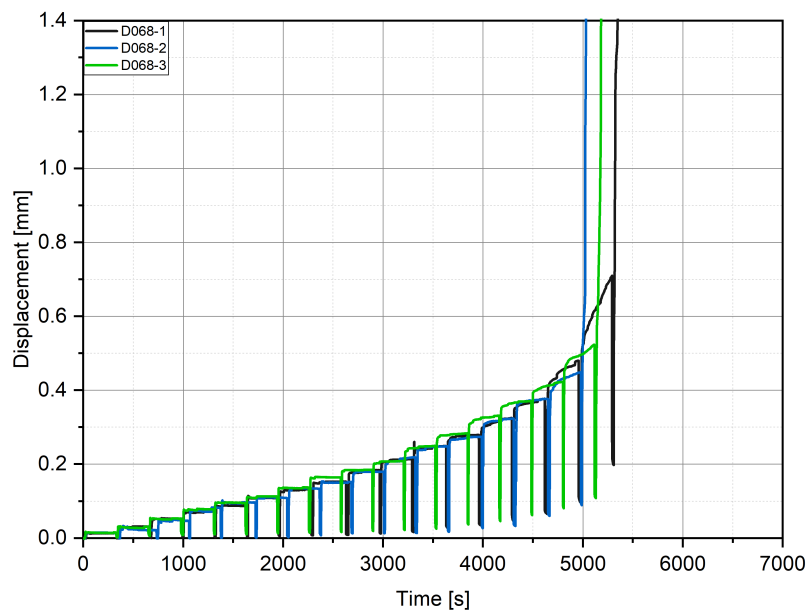
FIGURE B.76: D068 - displacement versus time curves
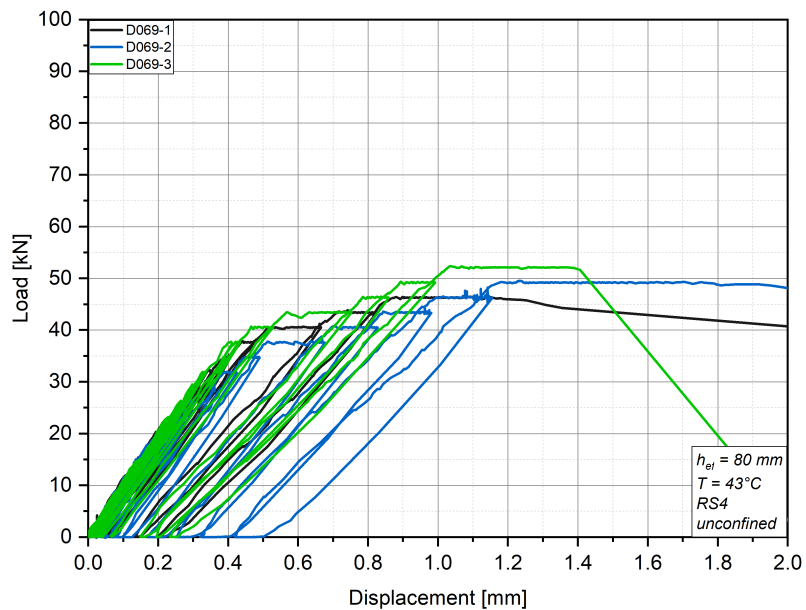
FIGURE B.77: D069 - load versus displacement curves
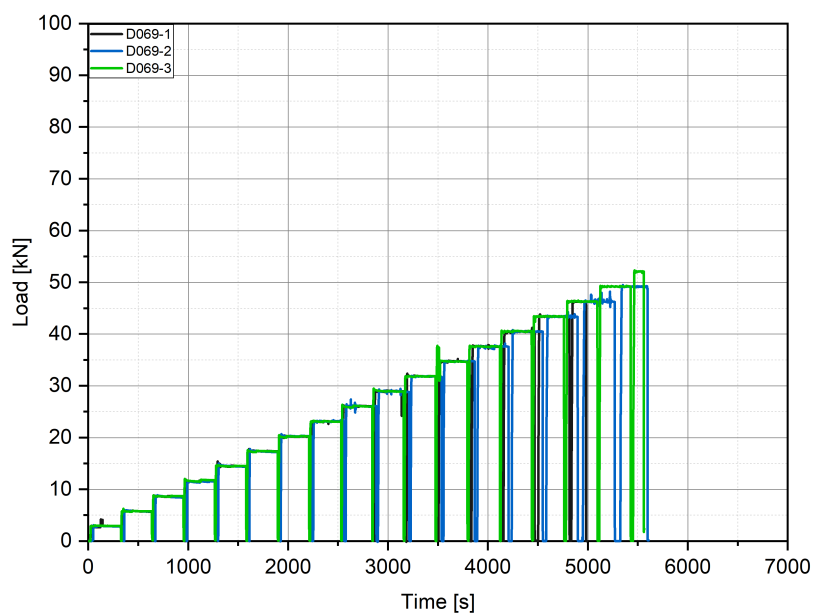
FIGURE B.78: D069 - load versus time curves
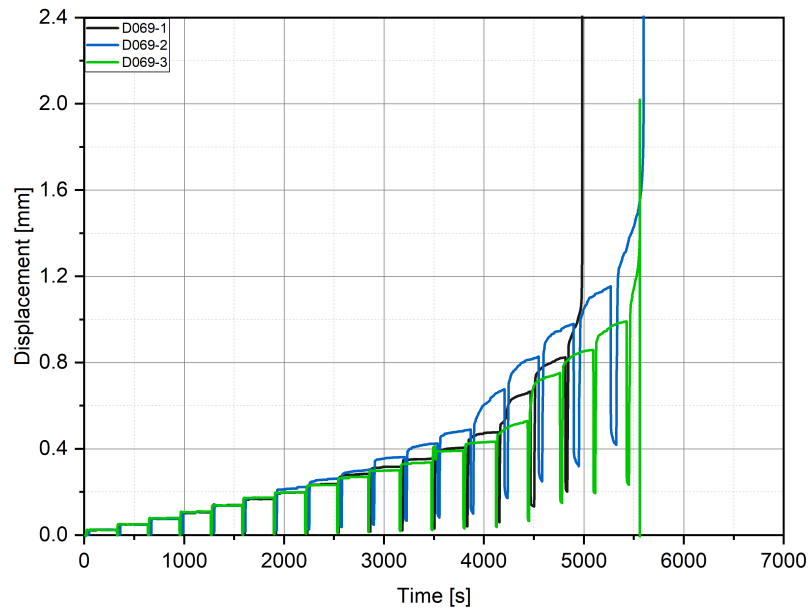
FIGURE B.79: D069 - displacement versus time curves
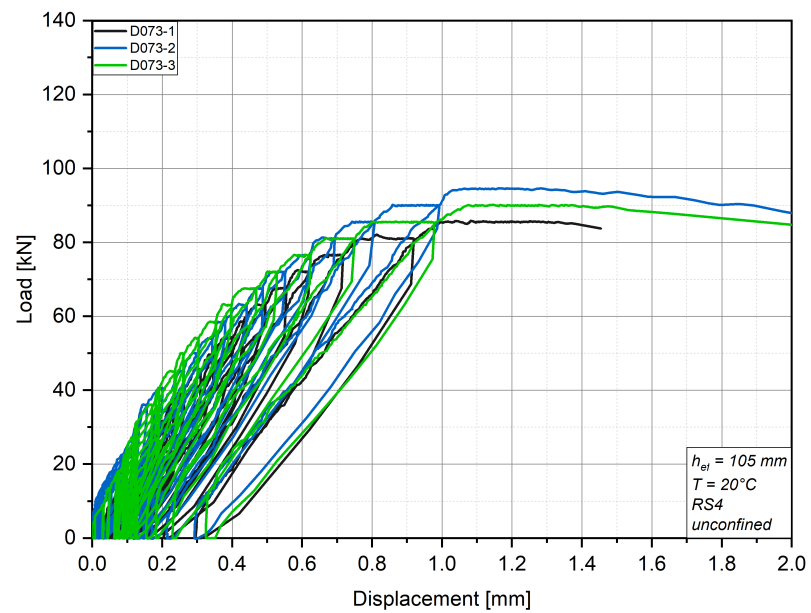
FIGURE B.80: D073 - load versus displacement curves
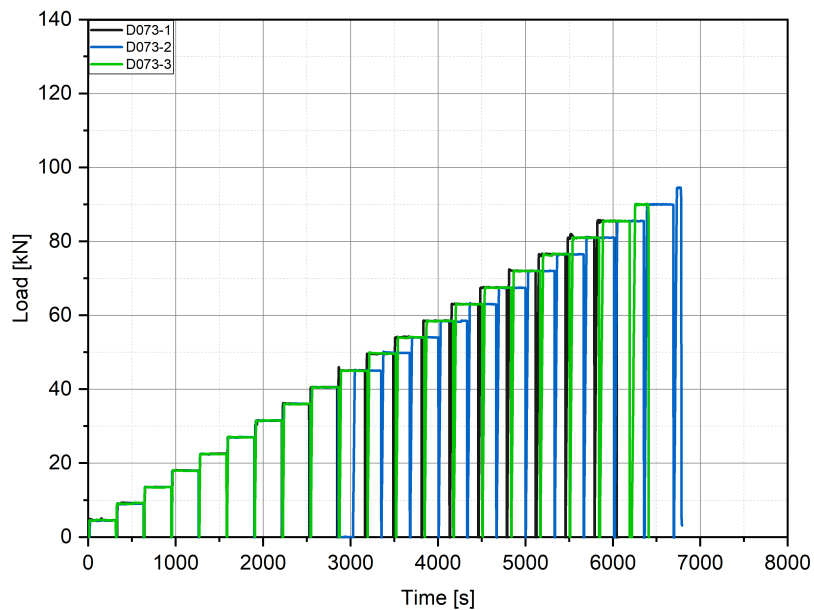
FIGURE B.81: D073 - load versus time curves
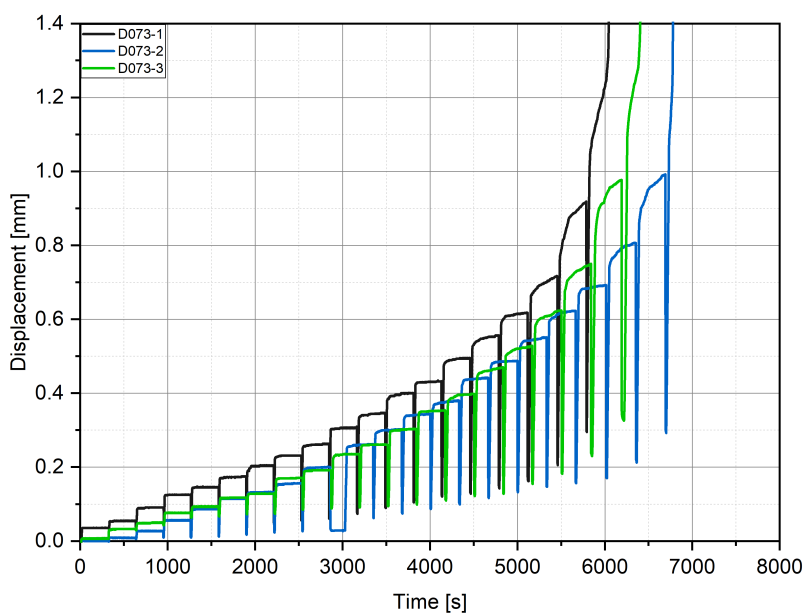
FIGURE B.82: D073 - displacement versus time curves
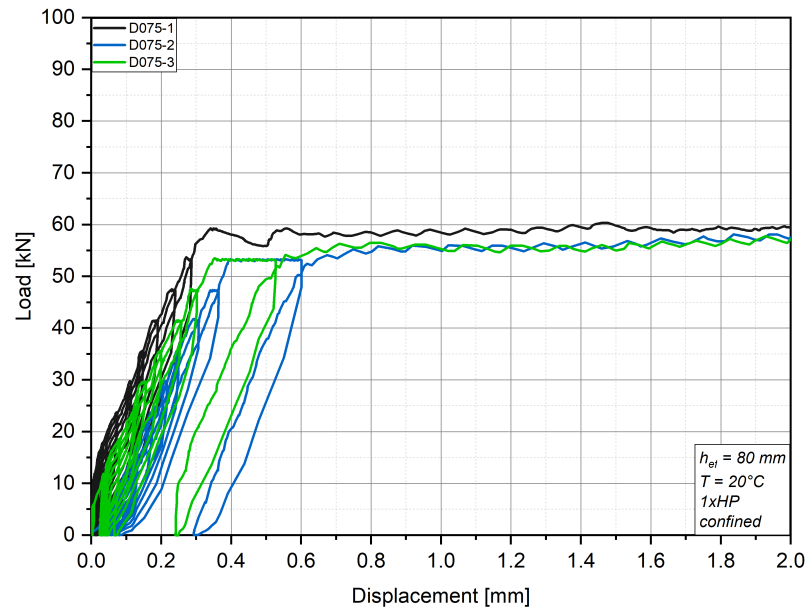
FIGURE B.83: D075 - load versus displacement curves
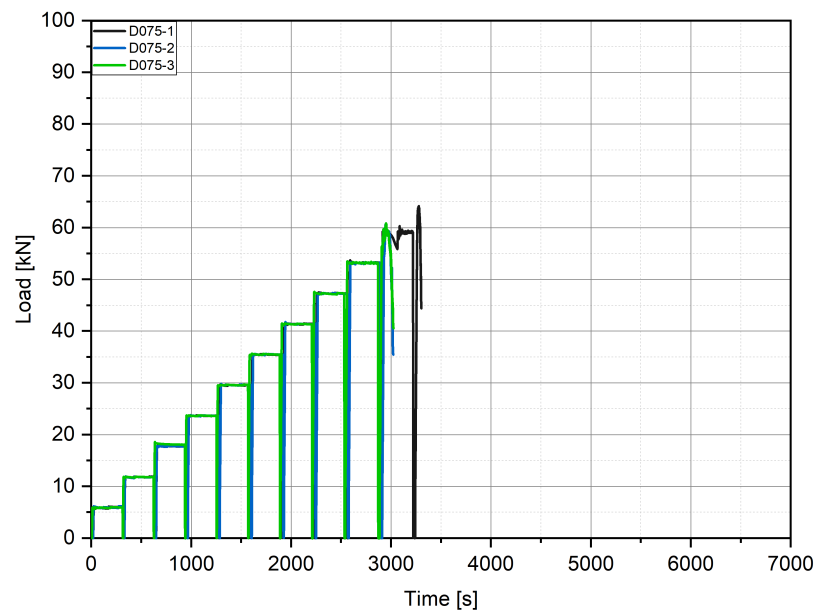
FIGURE B.84: D075 - load versus time curves
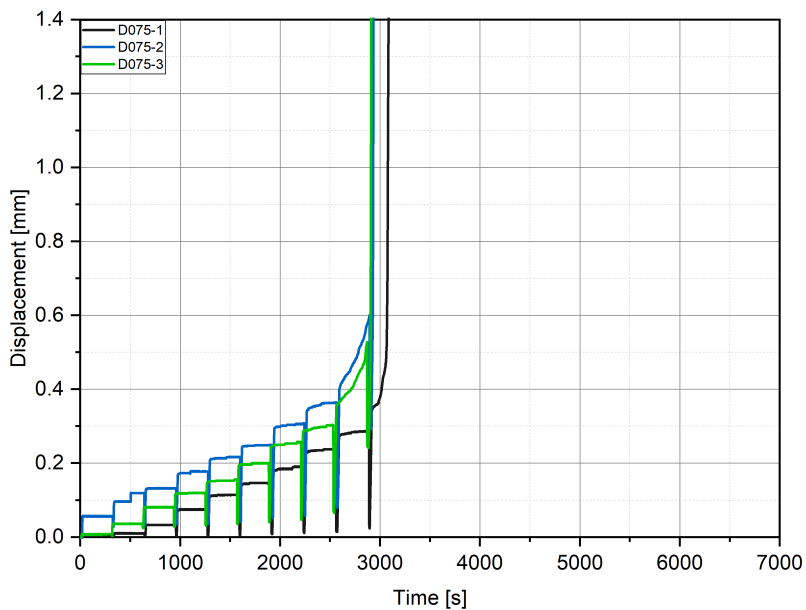
FIGURE B.85: D075 - displacement versus time curves
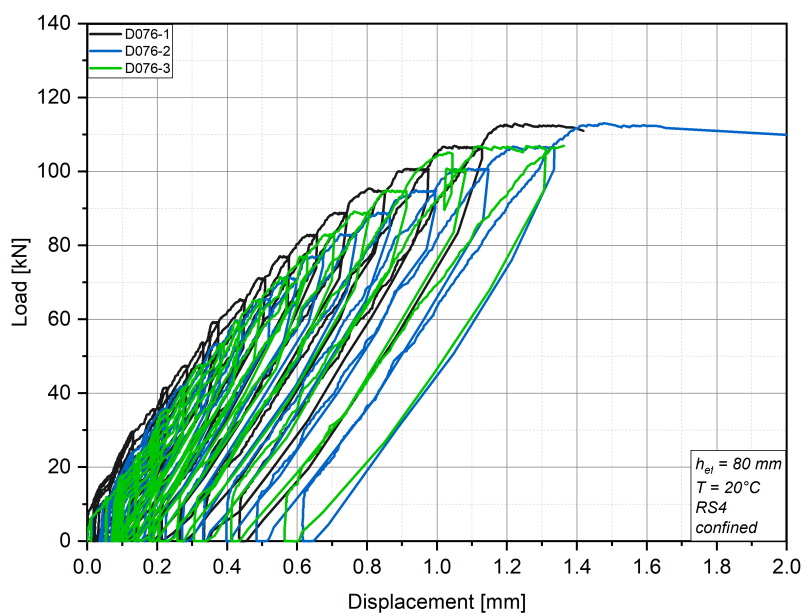
FIGURE B.86: D076 - load versus displacement curves
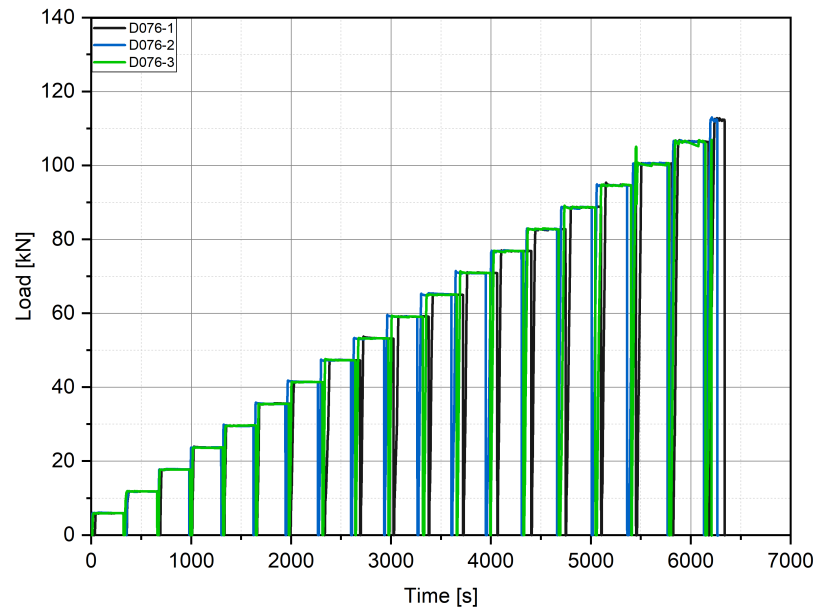
FIGURE B.87: D076 - load versus time curves
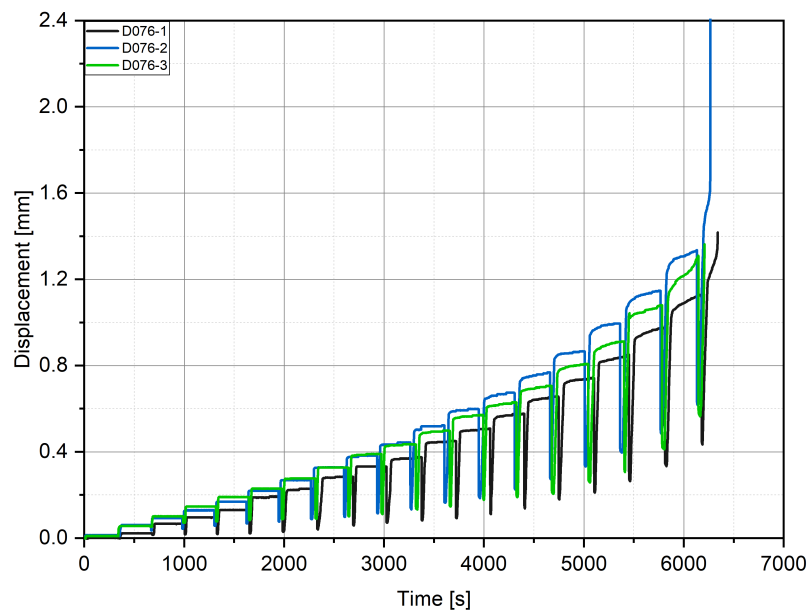
FIGURE B.88: D076 - displacement versus time curves

B.2 Failure Figures

B.2.1 Reference short-term test
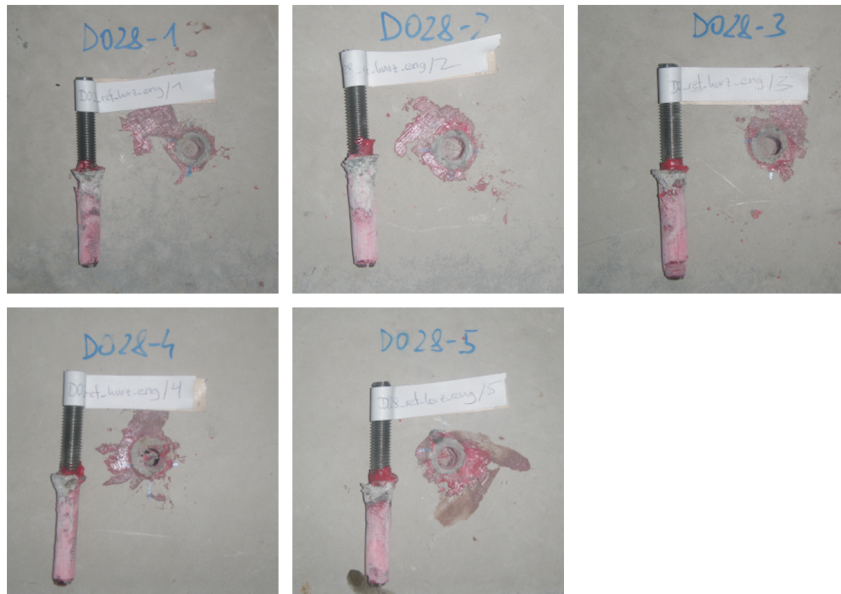
FIGURE B.89: D028 - Failure of the anchors
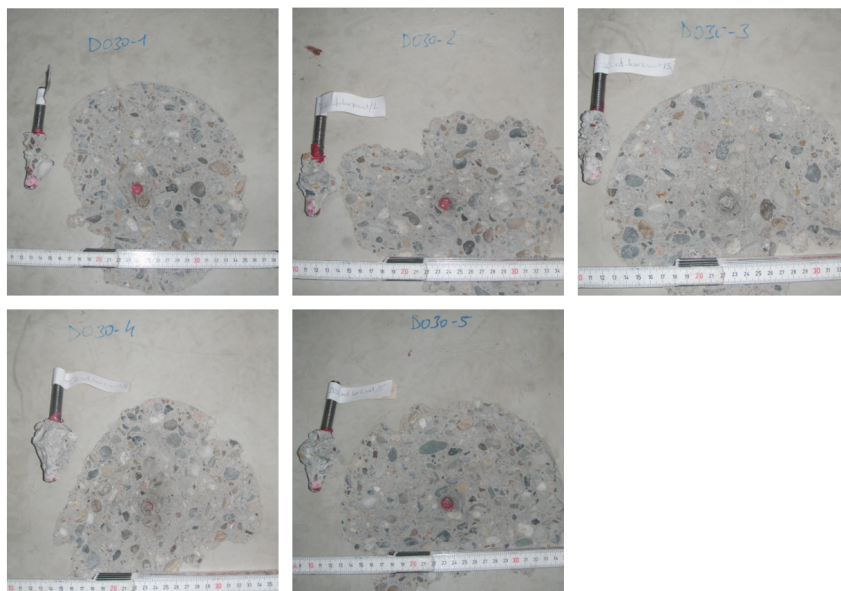
FIGURE B.90: D030 - Failure of the anchors
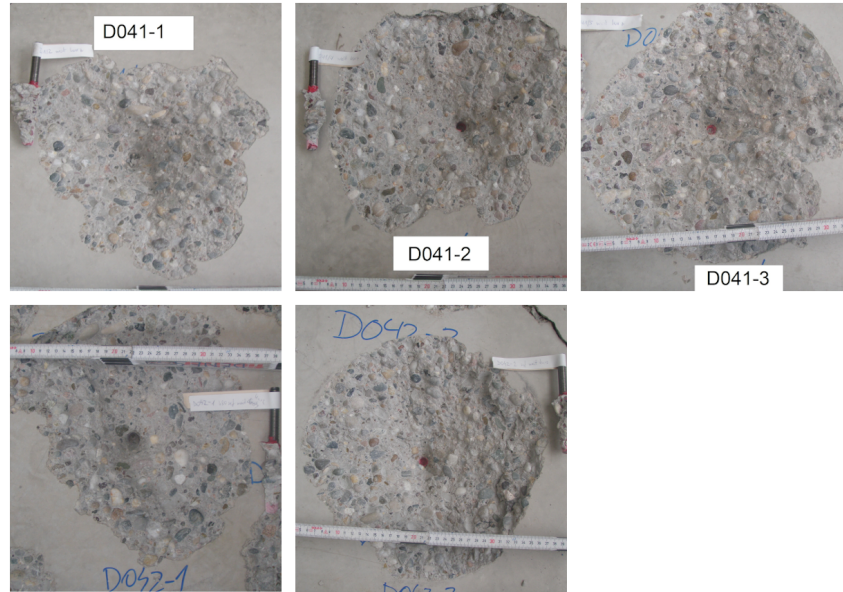
FIGURE B.91: D041&D042 - Failure of the anchors
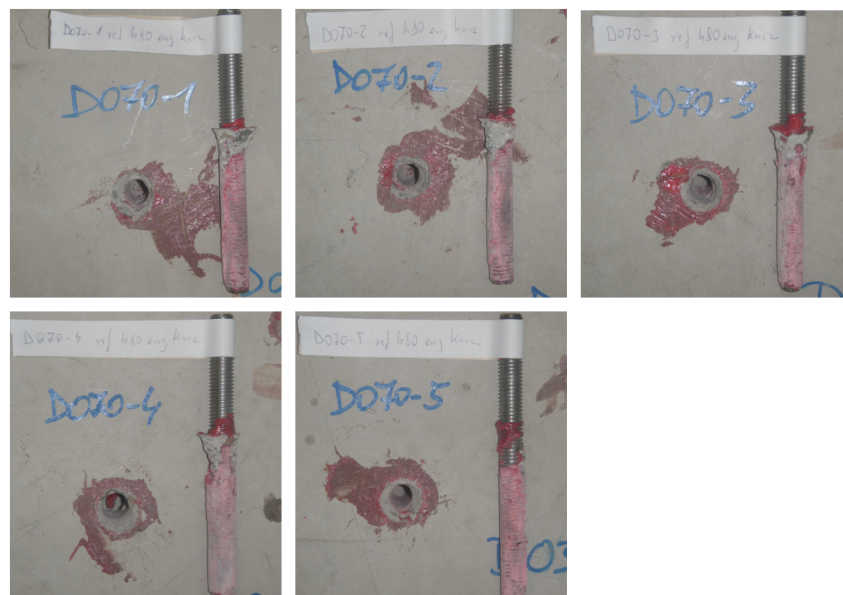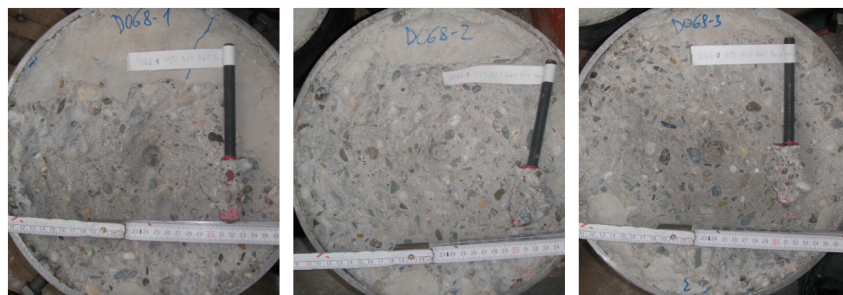

FIGURE B.92: D070 - Failure of the anchors
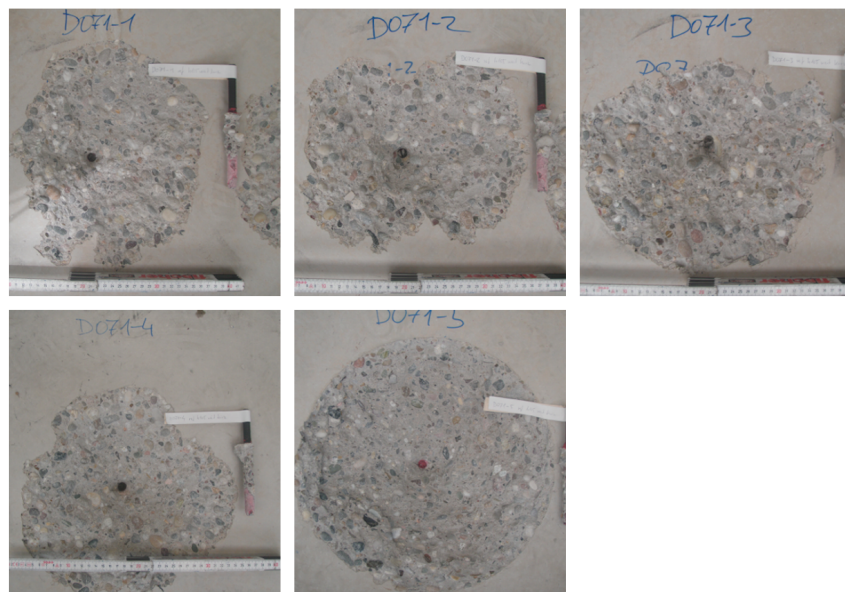
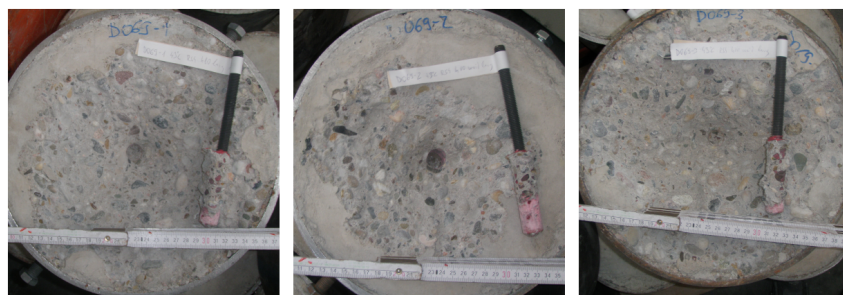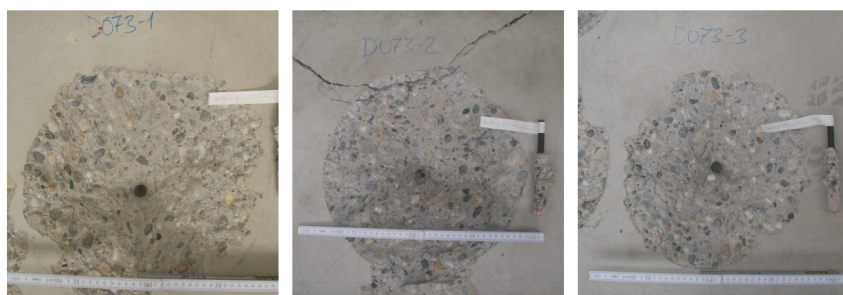FIGURE B.93: D071 - Failure of the anchors

B.2.2 Short-term test
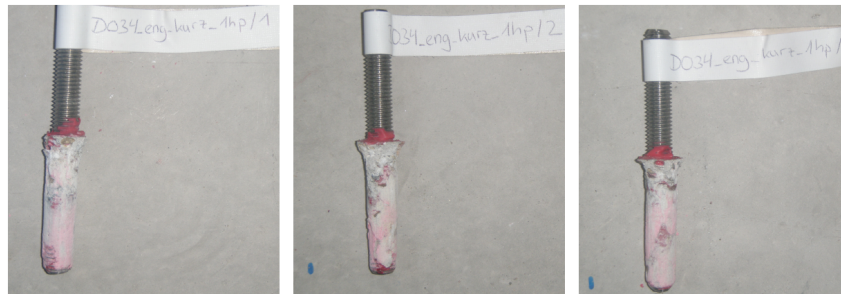
FIGURE B.94: D034 - Failure of the anchors
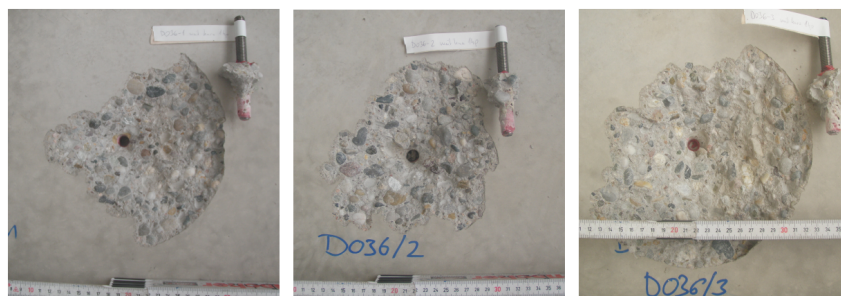
FIGURE B.95: D036 - Failure of the anchors

B.2.3 Reference incremental loading test
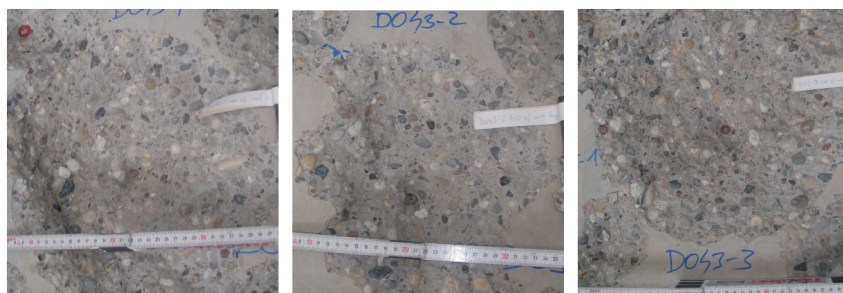
FIGURE B.96: D043 - Failure of the anchors
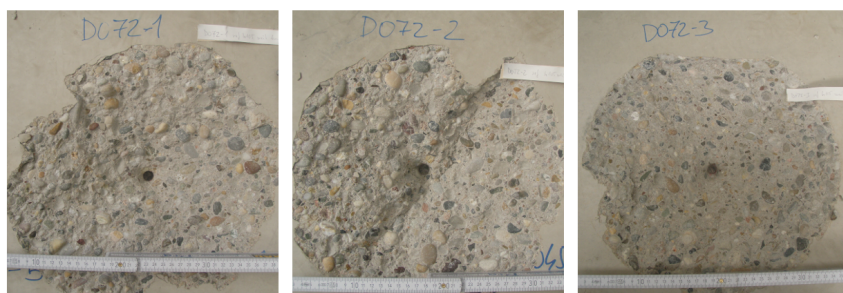
FIGURE B.97: D072 - Failure of the anchors

FIGURE B.98: D074 - Failure of the anchors

B.2.4 Incremental loading test

FIGURE B.99: D033 - Failure of the anchors
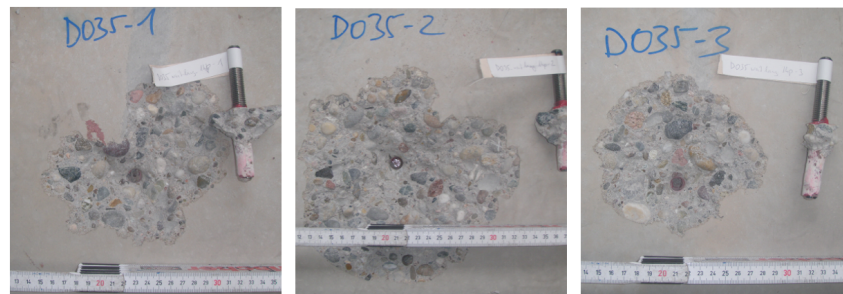
FIGURE B.100: D035 - Failure of the anchors

FIGURE B.101: D037 - Failure of the anchors
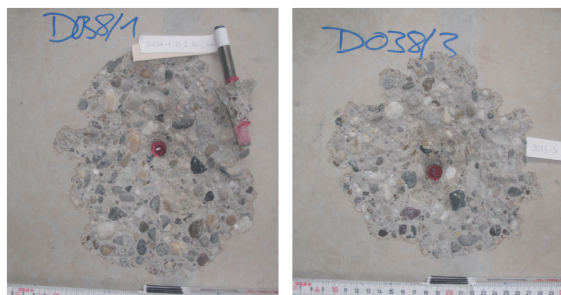
FIGURE B.102: D038 - Failure of the anchors

FIGURE B.103: D039 - Failure of the anchors
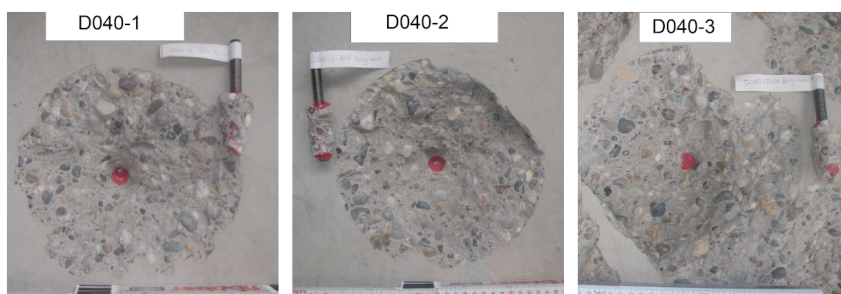
FIGURE B.104: D040 - Failure of the anchors
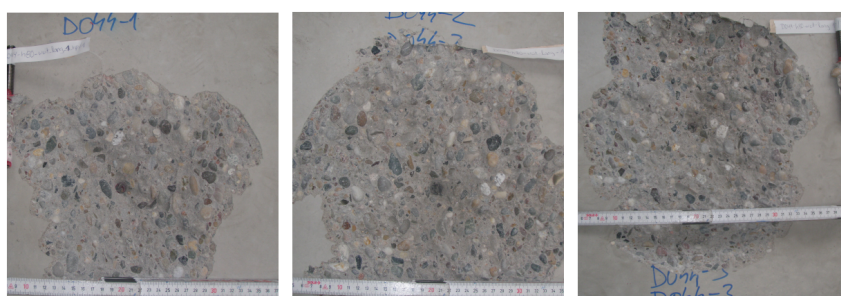
FIGURE B.105: D044 - Failure of the anchors
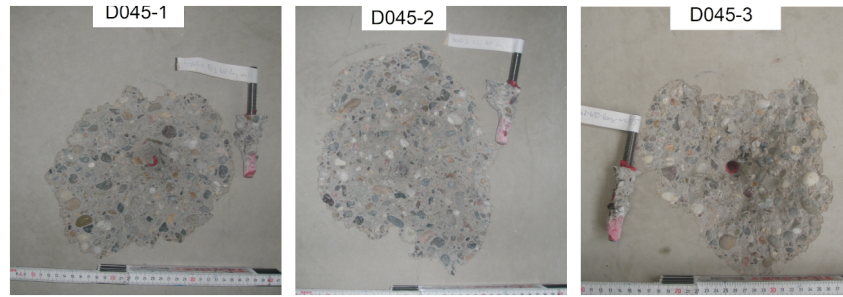
FIGURE B.106: D045 - Failure of the anchors
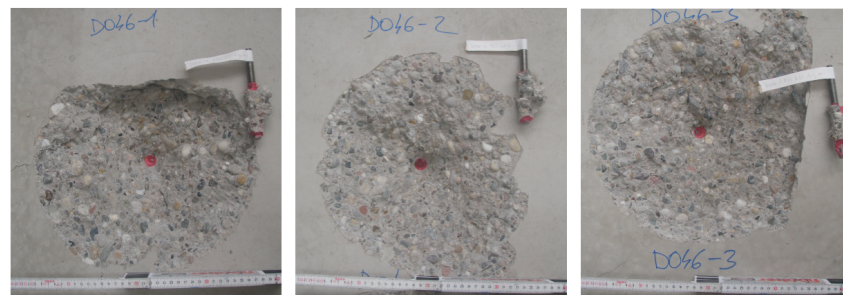
FIGURE B.107: D046 - Failure of the anchors
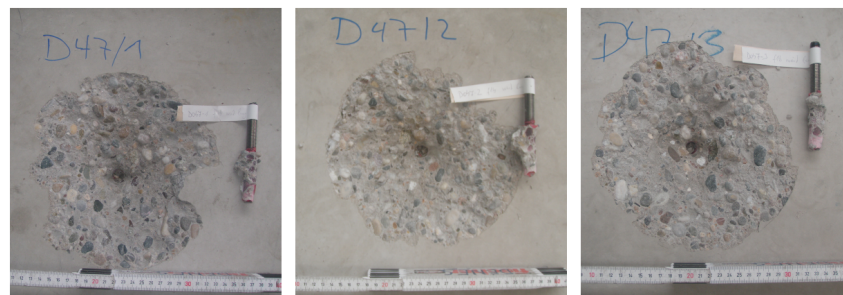
FIGURE B.108: D047 - Failure of the anchors
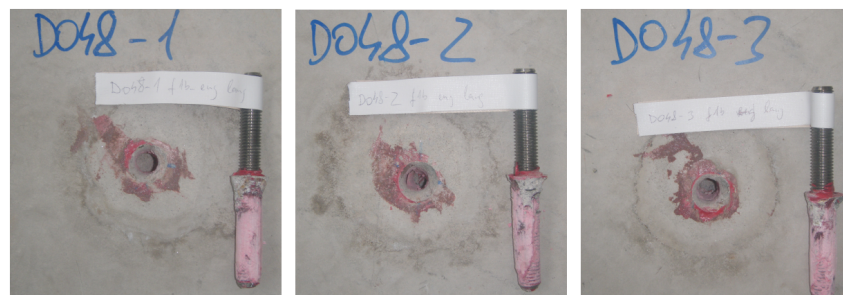
FIGURE B.109: D048 - Failure of the anchors

FIGURE B.110: D049 - Failure of the anchors
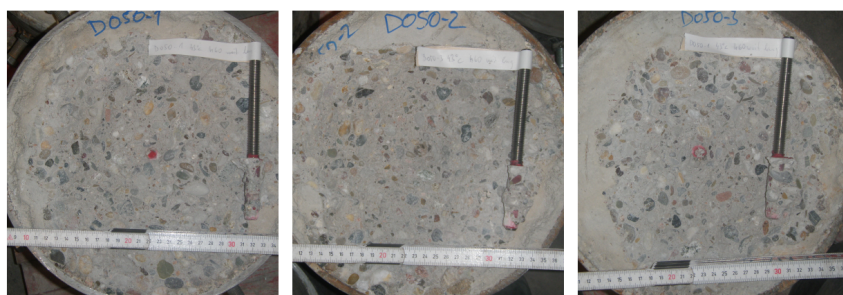
FIGURE B.111: D050 - Failure of the anchors
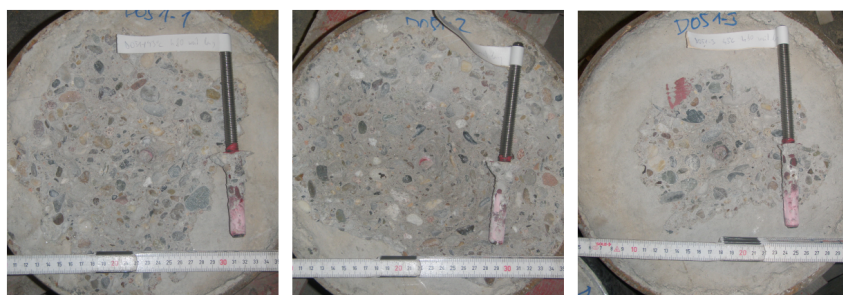
FIGURE B.112: D051 - Failure of the anchors

FIGURE B.113: D065 - Failure of the anchors

FIGURE B.114: D066 - Failure of the anchors

FIGURE B.115: D067 - Failure of the anchors

FIGURE B.116: D068 - Failure of the anchors

FIGURE B.117: D069 - Failure of the anchors

FIGURE B.118: D073 - Failure of the anchors

FIGURE B.119: D075 - Failure of the anchors

FIGURE B.120: D076 - Failure of the anchors

C Test results for alpha setup

This appendix presents the results of the tests described in Chapter 7. Table C.1 to C.6 summarizes these results. The contents of each column in Table C.1 to C.3 are described below:

- Column 1: Designation of the test series

- Column 2: Number of the tests carried out

- Column 3: Anchor diameter

- Column 4: Ratio embedment depth to anchor diameter

- Column 5: Support diameter

- Column 6: Actual concrete compressive strength

- Column 7: Normalized concrete compressive strength

- Column 8: Measured embedment depth

- Column 9: Ultimate failure load

- Column 10: Normalized ultimate failure load

- Column 11: Mean ultimate failure load

- Column 12: Standard deviation of the ultimate load

- Column 13: Normalized bond strength

- Column 14: Mean bond strength

- Column 15: Standard deviation of the bond strength

- Column 16: Failure mode

- Column 17: Percentage of the failure mode

- Column 18: Concrete cone dimensions

The contents for Table C.4 are:

- Column 1: Designation of the test series

- Column 2: Number of the tests carried out

- Column 3: Anchor diameter

- Column 4: Ratio embedment depth to anchor diameter

- Column 5: Bond length configuration

- Column 6: Support diameter

- Column 7: Actual concrete compressive strength

- Column 8: Normalized concrete compressive strength

- Column 9: Measured bond length

- Column 10: Measured embedment depth

- Column 11: Ultimate failure load

- Column 12: Normalized ultimate failure load

- Column 13: Mean ultimate failure load

- Column 14: Standard deviation of the ultimate load

- Column 15: Normalized bond strength

- Column 16: Mean bond strength

- Column 17: Standard deviation of the bond strength

- Column 18: Failure mode

- Column 19: Percentage of the failure mode

- Column 20: Concrete cone dimensions

The contents for Table C.5 are:

- Column 1: Designation of the test series

- Column 2: Number of the tests carried out

- Column 3: Anchor diameter

- Column 4: Ratio embedment depth to anchor diameter

- Column 5: Support diameter

- Column 6: Actual concrete compressive strength

- Column 7: Axial compression load

- Column 8: Normalized ultimate failure load

- Column 9: Mean ultimate failure load

- Column 10: Standard deviation of the ultimate load

- Column 11: Normalized bond strength

- Column 12: Mean bond strength

- Column 13: Standard deviation of the bond strength

- Column 14: Failure mode

- Column 15: Percentage of the failure mode

- Column 16: Concrete cone dimensions

The contents for Table C.6 are:

- Column 1: Designation of the test series

- Column 2: Number of the tests carried out

- Column 3: Anchor diameter

- Column 4: Ratio embedment depth to anchor diameter

- Column 5: Bond length configuration

- Column 6: Setup diameter

- Column 7: Actual concrete compressive strength

- Column 8: Sustained load

- Column 9: Measured bond length

- Column 10: Measured embedment depth

- Column 11: Ultimate failure load

- Column 12: Mean ultimate failure load

- Column 13: Standard deviation of the ultimate load

- Column 14: Normalized bond strength

- Column 15: Mean bond strength

- Column 16: Standard deviation of the bond strength

- Column 17: Failure mode

- Column 18: Percentage of the failure mode

TABLE C.1: Test results for confined and unconfined test program with $M12$ threaded rod (Table 7.1)

Series [-]	No. [-]	Anchor diam. [mm]	h_{ef}/d [-]	Setup diam. [mm]	f'_{cc} [MPa]	Nom. f'_{cc} [MPa]	h_{ef} [mm]	N_u [kN]	Nom. N_u [kN]	$N_{u,m}$ [kN]	σ [kN]	Nom. τ_u [MPa]	$\tau_{u,m}$ [MPa]	σ [MPa]	Failure mode [-]	Ratio [%]	Cone dim. [cm]
S1.1 – C	1	12	4	24	113.3	95	48.8	69.75	69.75	69.33	4.73	37.91	38.13	2.64	P/P_M	90/10	–
S1.1 – C	2	12	4	24	113.3	95	46.3	69.36	69.36			39.73			P/P_M	85/15	–
S1.1 – C	3	12	4	24	113.3	95	48.7	63.32	63.32			34.49			P/P_M	20/80	–
S1.1 – C	5	12	4	24	113.3	95	49.2	74.88	74.88			40.37			P	100	–
S1.1 – U	1	12	4	300	113.3	95	48.7	40.85	37.40	40.07	3.22	20.37	21.73	1.65	C/P	70/30	34x34
S1.1 – U	2	12	4	300	113.3	95	49.1	47.54	43.53			23.52			C	100	25.5x34
S1.1 – U	3	12	4	300	113.3	95	49.1	45.33	41.50			22.42			C	100	47x48
S1.1 – U	4	12	4	300	113.3	95	49.0	45.80	41.94			22.70			C/P	65/35	27.5x28
S1.1 – U	5	12	4	300	113.3	95	48.6	39.27	35.96			19.62			C/P	85/15	31x31
S1.2 – C	1	12	5	24	113.3	95	59.9	87.09	87.09	82.97	8.86	38.57	36.7	3.96	P	100	–
S1.2 – C	2	12	5	24	113.3	95	60.1	86.51	86.51			38.18			P/P_M	90/10	–
S1.2 – C	3	12	5	24	113.3	95	60.3	92.94	92.94			40.89			P	100	–
S1.2 – C	4	12	5	24	113.3	95	61.0	70.33	70.33			30.58			P/P_M	40/60	–
S1.2 – C	5	12	5	24	113.3	95	58.6	77.96	77.96			35.29			P/P_M	90/10	–
S1.2 – U	1	12	5	300	113.3	95	60.5	62.52	57.25	55.71	2.12	25.10	24.77	0.73	C/P	85/15	31x30
S1.2 – U	2	12	5	300	113.3	95	60.7	62.43	57.17			24.98			C/P	50/50	24x19
S1.2 – U	3	12	5	300	113.3	95	60.0	62.63	57.35			25.36			C/P	75/25	30.5x30
S1.2 – U	4	12	5	300	113.3	95	57.1	58.54	53.60			24.90			C/P	80/20	30x29
S1.2 – U	5	12	5	300	113.3	95	60.0	58.07	53.18			23.51			C/P	60/40	28.5x26.5
S1.3 – C	1	12	6	24	113.3	95	72.3	102.62	102.62	92.13	9.77	37.65	33.9	3.51	P	100	–
S1.3 – C	2	12	6	24	113.3	95	71.2	76.45	76.45			28.48			P/P_M	30/70	–
S1.3 – C	3	12	6	24	113.3	95	70.9	96.14	96.14			35.97			P	100	–
S1.3 – C	4	12	6	24	113.3	95	72.8	94.84	94.84			34.56			P	100	–
S1.3 – C	5	12	6	24	113.3	95	73.2	90.61	90.61			32.83			P	100	–
S1.3 – U	1	12	6	300	113.3	95	70.8	91.02	83.35	78.15	3.97	31.23	28.46	1.92	C/P	55/45	27x30.5
S1.3 – U	3	12	6	300	113.3	95	72.7	81.36	74.50			27.18			C/P	65/35	30x30
S1.3 – U	4	12	6	300	113.3	95	73.9	82.65	75.68			27.17			C/P	55/45	19x28
S1.3 – U	5	12	6	300	113.3	95	74.2	86.37	79.09			28.27			C/P	30/70	20.5x21
S1.4 – C	1	12	7	24	113.3	95	84.2	113.15	113.15	109.98	5.24	35.64	34.37	1.48	P	100	–
S1.4 – C	2	12	7	24	113.3	95	86.1	113.75	113.75			35.04			P	100	–
S1.4 – C	3	12	7	24	113.3	95	86.3	108.03	108.03			33.20			P	100	–
S1.4 – C	4	12	7	24	113.3	95	84.6	113.39	113.39			35.55			P	100	–
S1.4 – C	5	12	7	24	113.3	95	83.2	101.61	101.61			32.39			P/P_M	80/20	–
S1.4 – U	1	12	7	440	113.3	95	78.8	83.95	76.87	83.45	5.62	25.88	27.12	1.62	C/P	35/65	21.5x14.5
S1.4 – U	2	12	7	440	113.3	95	81.4	96.27	88.16			28.73			C/P	40/60	23.5x26.7
S1.4 – U	3	12	7	440	113.3	95	82.6	96.22	88.11			28.29			C/P	50/50	32x28
S1.4 – U	5	12	7	440	113.3	95	83.6	88.08	80.66			25.59			C/P	50/50	35x34

TABLE C.1: (continued)

Series	No.	Anchor diam.	h_{ef}/d	Setup diam.	f'_{cc}	Nom. f'_{cc}	h_{ef}	N_u	Nom. N_u	$N_{u,m}$	σ	Nom. τ_u	$\tau_{u,m}$	σ	Failure mode	Ratio	Cone dim.
[-]	[-]	[mm]	[-]	[mm]	[MPa]	[MPa]	[mm]	[kN]	[kN]	[kN]	[kN]	[MPa]	[MPa]	[MPa]	[-]	[%]	[cm]
S1.5 – C	1	12	8	24	113.3	95	93.4	118.16	99.08	121.65	15.45	–	33.69	3.78	S	100	–
S1.5 – C	2	12	8	24	113.3	95	96.7	132.57	132.57			36.37			P	100	–
S1.5 – C	3	12	8	24	113.3	95	95.6	120.58	101.1			–			S	100	–
S1.5 – C	4	12	8	24	113.3	95	94.7	110.72	110.72			31.01			P_M	100	–
S1.5 – C	5	12	8	24	113.3	95	95.2	106.03	88.90			–			S	100	–
S1.5 – U	1	12	8	440	113.3	95	95.6	87.95	80.53	93.62	11.36	22.35	26.19	3.33	C/P	25/75	15x17
S1.5 – U	2	12	8	440	113.3	95	95.8	100.21	84.03			–			S	100	–
S1.5 – U	3	12	8	440	113.3	95	93.7	108.46	99.31			28.11			C/P	65/5	44.5x64.5
S1.5 – U	4	12	8	440	113.3	95	95.3	110.30	101.00			28.11			C/P	40/60	30x26.2
S1.5 – U	5	12	8	440	113.3	95	93.8	90.92	83.26			–			S	100	–

TABLE C.2: Test results for confined and unconfined test program with d 12 reinforcing bar (Table 7.2)

Series	No.	Anchor diam.	h_{ef}/d	Setup diam.	f'_{cc}	Nom. f'_{cc}	h_{ef}	N_u	Nom. N_u	$N_{u,m}$	σ	Nom. τ_u	$\tau_{u,m}$	σ	Failure mode	Ratio	Cone dim.
[−]	[−]	[mm]	[−]	[mm]	[MPa]	[MPa]	[mm]	[kN]	[kN]	[kN]	[kN]	[MPa]	[MPa]	[MPa]	[−]	[%]	[cm]
S2.1 − C	1	12	4	30	99.83	95	47.5	48.10	48.10	45.42	5.31	26.86	25.43	3.19	P	100	−
S2.1 − C	2	12	4	30	99.83	95	48.8	40.49	40.49			22.01			P/P_M	95/5	−
S2.1 − C	3	12	4	30	99.83	95	48.6	51.22	51.22			27.95			P	100	−
S2.1 − C	4	12	4	30	99.83	95	47.2	39.08	39.08			21.96			P/P_M	95/5	−
S2.1 − C	5	12	4	30	99.83	95	45.1	48.19	48.19			28.34			P	100	−
S2.1 − U	1	12	4	300	99.83	95	49.4	33.85	33.25	33.43	5.25	17.73	18.22	2.79	C/P	50/50	17.5x17
S2.1 − U	2	12	4	300	99.83	95	49.5	38.62	37.94			20.19			C/P	25/75	13.5x18.5
S2.1 − U	3	12	4	300	99.83	95	47.6	24.96	24.52			13.57			C/P	30/70	14.5x8.5
S2.1 − U	4	12	4	300	99.83	95	48.2	36.08	35.44			19.37			C/P	40/60	14.5x14
S2.1 − U	5	12	4	300	99.83	95	46.9	36.65	36.00			20.22			C/P	80/20	31.5x30
S2.2 − C	1	12	6	30	99.83	95	72.0	69.24	69.24	67.63	1.11	25.51	24.71	0.48	P	100	−
S2.2 − C	2	12	6	30	99.83	95	72.3	67.09	67.09			24.62			P	100	−
S2.2 − C	3	12	6	30	99.83	95	73.8	67.70	67.70			24.33			P	100	−
S2.2 − C	4	12	6	30	99.83	95	72.9	67.90	67.90			24.71			P	100	−
S2.2 − C	5	12	6	30	99.83	95	72.1	66.24	66.24			24.37			P	100	−
S2.2 − U	1	12	6	300	99.83	95	73.8	63.60	62.48	56.81	4.73	22.30	20.74	1.07	C/P	15/85	10.5x5.5
S2.2 − U	2	12	6	300	99.83	95	73.9	56.00	55.01			19.61			C/P	40/60	16.5x21
S2.2 − U	3	12	6	300	99.83	95	74.1	58.05	57.02			20.27			C/P	25/75	14.5x12
S2.2 − U	4	12	6	300	99.83	95	73.6	60.61	59.54			21.31			C/P	25/75	14.5x9
S2.2 − U	5	12	6	300	99.83	95	65.2	50.89	49.99			20.20			C/P	80/20	31x31
S2.3 − C	1	12	8	30	98.45	95	96.5	69.61	67.17	68.57	1.55	−	19.46	−	S	100	−
S2.3 − C	2	12	8	30	98.45	95	96.4	70.71	70.71			19.46			P	100	−
S2.3 − C	3	12	8	30	98.45	95	98.1	71.47	68.96			−			S	100	−
S2.3 − C	4	12	8	30	98.45	95	96.0	69.36	66.93			−			S	100	−
S2.3 − C	5	12	8	30	98.45	95	97.9	71.60	69.09			−			S	100	−
S2.3 − U	1	12	8	440	98.45	95	96.3	61.87	60.78	64.11	3.31	16.74	17.97	0.72	C/P_M	65/35	35.5x41
S2.3 − U	2	12	8	440	98.45	95	97.4	69.16	67.94			18.50			C/P	15/85	10.5x8.5
S2.3 − U	3	12	8	440	98.45	95	89.8	61.76	60.67			17.92			C/P	5/95	3.5x8
S2.3 − U	4	12	8	440	98.45	95	94.0	65.79	64.63			18.24			C/P	20/80	7x7
S2.3 − U	5	12	8	440	98.45	95	95.8	67.74	66.55			18.43			C/P	20/80	10x11.5

TABLE C.3: Test results for test program with *d* 12 and variation of the support diameter (Table 7.3)

Series	No.	Anchor diam.	h_{ef}/d	Setup diam.	f'_{cc}	Nom. f'_{cc}	h_{ef}	N_u	Nom. N_u	$N_{u,m}$	σ	Nom. τ_u	$\tau_{u,m}$	σ	Failure mode	Ratio	Cone dim.
[−]	[−]	[mm]	[−]	[mm]	[MPa]	[MPa]	[mm]	[kN]	[kN]	[kN]	[kN]	[MPa]	[MPa]	[MPa]	[−]	[%]	[cm]
S3.1	1	12	5	14.5	98.45	95	64.3	58.75	58.75	59.42	1.34	24.24	25.21	0.75	P	100	–
S3.1	2	12	5	14.5	98.45	95	62.0	57.97	57.97			24.80			P	100	–
S3.1	3	12	5	14.5	98.45	95	62.1	61.40	61.40			26.23			P	100	–
S3.1	4	12	5	14.5	98.45	95	62.8	60.07	60.07			25.37			P	100	–
S3.1	5	12	5	14.5	98.45	95	61.5	58.93	58.93			25.42			P	100	–
S3.2	1	12	5	30	98.45	95	63.6	60.17	60.17	56.50	2.36	25.10	23.66	0.88	P	100	–
S3.2	2	12	5	30	98.45	95	63.6	56.08	56.08			23.39			P	100	–
S3.2	3	12	5	30	98.45	95	63.4	56.94	56.94			23.82			P	100	–
S3.2	4	12	5	30	98.45	95	61.9	53.78	53.78			23.05			P/P_M	85/15	–
S3.2	5	12	5	30	98.45	95	64.2	55.52	55.52			22.94			P	100	–
S3.3	1	12	5	60	98.45	95	65.4	60.73	59.65	56.05	3.48	24.20	23.05	1.67	C/P	25/75	6x6
S3.3	2	12	5	60	98.45	95	62.9	61.08	60.00			25.30			C/P	30/70	6x6
S3.3	3	12	5	60	98.45	95	63.3	55.11	54.14			22.69			C/P	25/75	6x6
S3.3	4	12	5	60	98.45	95	66.5	54.68	53.71			21.42			C/P	25/75	6x6
S3.3	5	12	5	60	98.45	95	64.7	53.70	52.75			21.63			C/P	20/80	6x6
S3.4	1	12	5	90	98.45	95	64.0	44.03	43.25	46.31	4.32	17.92	19.68	2.55	C/P_M	30/70	9x8.5
S3.4	2	12	5	90	98.45	95	64.9	42.91	42.15			17.23			C/P	35/65	8.5x9
S3.4	3	12	5	90	98.45	95	61.7	49.48	48.60			20.90			C/P	35/65	10x10
S3.4	5	12	5	90	98.45	95	59.9	52.14	51.22			22.68			C/P	35/65	9x6
S3.5	1	12	5	120	98.45	95	60.6	48.68	47.82	46.12	3.91	20.93	19.44	2.05	C/P	30/70	10x8.5
S3.5	2	12	5	120	98.45	95	60.9	50.15	49.26			21.46			C/P	55/45	14x12
S3.5	3	12	5	120	98.45	95	63.2	49.24	48.37			20.30			C/P	65/35	21.5x19
S3.5	4	12	5	120	98.45	95	61.7	40.27	39.55			17.01			C/P	35/65	8.5x10
S3.5	5	12	5	120	98.45	95	69.2	46.42	45.60			17.48			C/P	35/65	9x9.9

TABLE C.4: Test results for test program with $M12$ and variation of the bond length (Table 7.4)

Series	No.	Anchor diam.	h_{ef}/d	Config.	Setup diam.	f'_{cc}	Nom. f'_{cc}	Bond length	h_{ef}	N_u	Nom. N_u	$N_{u,m}$	σ	Nom. τ_u	$\tau_{u,m}$	σ	Failure mode	Ratio	Cone dim.
[-]	[-]	[mm]	[-]	[-]	[mm]	[MPa]	[MPa]	[mm]	[mm]	[kN]	[kN]	[kN]	[kN]	[MPa]	[MPa]	[MPa]	[-]	[%]	[cm]
$S4.0-A-C$	1	12	4	a	24	98.45	95	28.40	47.60	39.68	39.68	38.50	2.43	37.06	37.12	1.67	P	100	—
$S4.0-A-C$	2	12	4	a	24	98.45	95	26.40	46.00	39.16	39.16			39.35			P	100	—
$S4.0-A-C$	3	12	4	a	24	98.45	95	29.40	45.90	39.84	39.84			35.94			P	100	—
$S4.0-A-C$	4	12	4	a	24	98.45	95	27.60	48.40	39.65	39.65			38.11			P	100	—
$S4.0-A-C$	5	12	4	a	24	98.45	95	25.80	44.50	34.18	34.18			35.15			P	100	—
$S4.0-A-U$	1	12	4	a	300	98.45	95	23.05	46.10	28.56	26.15	28.14	1.29	30.10	29.70	2.28	C	100	33x31.7
$S4.0-A-U$	2	12	4	a	300	98.45	95	28.90	57.80	30.84	28.24			25.92			C/P	50/50	10.2x10
$S4.0-A-U$	3	12	4	a	300	98.45	95	25.65	51.30	32.42	29.69			30.70			C/P	50/50	11x11.8
$S4.0-A-U$	4	12	4	a	300	98.45	95	23.25	46.50	27.94	27.94			31.87			C/P	50/50	9.5x11
$S4.0-A-U$	5	12	4	a	300	98.45	95	25.45	50.90	31.32	28.68			29.89			C/P	50/50	13.7x9x5
$S4.0-B-C$	1	12	4	b	24	98.45	95	23.80	48.10	35.73	35.73	32.81	3.35	39.83	34.13	3.82	P	100	—
$S4.0-B-C$	2	12	4	b	24	98.45	95	26.00	47.10	30.12	30.12			30.73			P	100	—
$S4.0-B-C$	3	12	4	b	24	98.45	95	24.80	49.40	29.86	29.86			31.94			P	100	—
$S4.0-B-C$	4	12	4	b	24	98.45	95	27.12	47.70	37.06	37.06			36.25			P/P_M	80/20	—
$S4.0-B-C$	5	12	4	b	24	98.45	95	26.00	49.10	31.27	31.27			31.90			P/P_M	80/20	—
$S4.0-B-U$	1	12	4	b	300	98.45	95	24.75	49.50	31.39	28.74	28.56	0.33	30.81	31.85	0.93	C	100	35x24.5
$S4.0-B-U$	2	12	4	b	300	98.45	95	23.25	46.50	30.65	28.07			32.02			C	100	36x33.2
$S4.0-B-U$	4	12	4	b	300	98.45	95	24.15	48.30	31.36	28.71			31.54			C	100	27.9x30
$S4.0-B-U$	5	12	4	b	300	98.45	95	23.05	46.10	31.34	28.70			33.03			C	100	25.5x28.2
$S4-4d-3/4-C$	1	12	4	c	24	98.45	95	10.50	49.80	17.72	17.72	17.75	1.15	44.77	46.10	1.53	P	100	—
$S4-4d-3/4-C$	2	12	4	c	24	98.45	95	10.50	49.30	18.91	18.91			47.77			P	100	—
$S4-4d-3/4-C$	3	12	4	c	24	98.45	95	9.63	46.90	16.61	16.61			45.75			P	100	—
$S4-4d-3/4-U$	1	12	4	c	300	98.45	95	12.25	51.41	20.26	20.26	15.39	5.09	43.87	35.38	9.26	P	—	—
$S4-4d-3/4-U$	2	12	4	c	300	98.45	95	10.50	50.10	10.10	10.10			25.52			P	—	—
$S4-4d-3/4-U$	3	12	4	c	300	98.45	95	11.40	47.70	15.80	15.80			36.76			P	—	—
$S4-4d-4/4-C$	1	12	4	d	24	98.45	95	0.00	50.00	0.49	0.49	0.79	0.39	—	—	—	—	100	—
$S4-4d-4/4-C$	2	12	4	d	24	98.45	95	0.00	49.30	0.64	0.64			—			—	100	—
$S4-4d-4/4-C$	3	12	4	d	24	98.45	95	0.00	48.10	1.23	1.23			—			—	100	—
$S4-4d-4/4-U$	1	12	4	d	300	98.45	95	0.00	47.00	1.01	1.01	0.71	0.26	—	—	—	—	—	—
$S4-4d-4/4-U$	2	12	4	d	300	98.45	95	0.00	46.90	0.57	0.57			—			—	—	—
$S4-4d-4/4-U$	3	12	4	d	300	98.45	95	0.00	51.90	0.56	0.56			—			—	—	—
$S4.1-C$	1	12	5	a	24	98.45	95	31.49	61.20	47.29	47.29	44.04	3.29	39.84	35.01	4.18	P	100	—
$S4.1-C$	2	12	5	a	24	98.45	95	33.91	62.60	45.73	45.73			35.77			P	100	—
$S4.1-C$	3	12	5	a	24	98.45	95	32.18	62.90	46.07	46.07			37.97			P/P_M	90/10	—
$S4.1-C$	4	12	5	a	24	98.45	95	35.12	63.60	41.34	41.34			41.22			P/P_M	50/50	—
$S4.1-C$	5	12	5	a	24	98.45	95	34.88	60.70	39.75	39.75			30.23			P/P_M	40/60	—

TABLE C.4: (continued)

Series	No.	Anchor diam.	h_{ef}/d	Config.	Setup diam.	f'_{cc}	Nom. f'_{cc}	Bond length	h_{ef}	N_u	Nom. N_u	$N_{u,m}$	σ	Nom. τ_u	$\tau_{u,m}$	σ	Failure mode	Ratio	Cone dim.
[–]	[–]	[mm]	[–]	[–]	[mm]	[MPa]	[MPa]	[mm]	[mm]	[kN]	[kN]	[kN]	[kN]	[MPa]	[MPa]	[MPa]	[–]	[%]	[cm]
S4.1 – U	1	12	5	a	300	98.45	95	27.95	55.90	28.76	26.34	32.74	3.78	24.99	29.39	2.66	C/P	50/50	18x20
S4.1 – U	2	12	5	a	300	98.45	95	30.40	60.80	38.31	35.08			30.61			C/P	50/50	16.2x19.2
S4.1 – U	3	12	5	a	300	98.45	95	29.70	59.40	38.24	35.01			31.27			C/P	50/50	22x19.8
S4.1 – U	4	12	5	a	300	98.45	95	29.75	59.50	38.26	35.04			31.24			C/P	50/50	18.2x18.1
S4.1 – U	5	12	5	a	300	98.45	95	29.80	59.60	35.19	32.23			28.69			C/P	50/50	17.3x20.1
S4.2 – C	1	12	5	b	24	98.45	95	30.69	58.10	48.68	48.68	43.78	4.95	42.08	38.66	3.72	P/P_M	60/40	–
S4.2 – C	3	12	5	b	24	98.45	95	29.43	60.40	37.30	37.30			33.62			P/P_M	20/80	–
S4.2 – C	4	12	5	b	24	98.45	95	30.17	59.50	46.34	46.34			40.74			P/P_M	60/40	–
S4.2 – C	5	12	5	b	24	98.45	95	29.72	59.00	42.80	42.80			38.20			P	100	–
S4.2 – U	1	12	5	b	300	98.45	95	29.85	59.70	42.09	42.09	40.67	4.15	37.41	36.86	3.84	P	100	–
S4.2 – U	2	12	5	b	300	98.45	95	28.85	57.70	42.92	42.92			39.46			P	100	–
S4.2 – U	3	12	5	b	300	98.45	95	29.25	58.50	38.40	38.40			34.83			P	100	–
S4.2 – U	4	12	5	b	300	98.45	95	29.15	58.30	45.24	45.24			41.17			P	100	–
S4.2 – U	5	12	5	b	300	98.45	95	29.25	58.50	34.69	34.69			31.46			P/P_M	80/20	–
S4.3 – C	1	12	6	a	24	98.45	95	38.26	71.40	49.79	49.79	48.74	5.33	34.52	33.59	2.80	P	100	–
S4.3 – C	2	12	6	a	24	98.45	95	38.39	73.40	51.48	51.48			35.57			P/P_M	80/20	–
S4.3 – C	3	12	6	a	24	98.45	95	39.90	72.40	53.60	53.60			35.63			P	100	–
S4.3 – C	4	12	6	a	24	98.45	95	39.07	70.30	49.13	49.13			33.36			P/P_M	90/10	–
S4.3 – C	5	12	6	a	24	98.45	95	36.51	72.30	39.72	39.72			28.86			P/P_M	80/20	–
S4.3 – U	1	12	6	a	300	98.45	95	34.65	69.30	39.24	35.93	37.27	2.31	27.51	26.95	1.95	C/P	50/50	30.1x28
S4.3 – U	2	12	6	a	300	98.45	95	39.30	78.60	39.53	36.20			24.43			C/P	50/50	20.1x19.5
S4.3 – U	3	12	6	a	300	98.45	95	36.00	72.00	34.78	34.78			25.63			P/P_M	50/50	–
S4.3 – U	4	12	6	a	300	98.45	95	35.60	71.20	43.14	39.50			29.43			C/P	50/50	29.5x30
S4.3 – U	5	12	6	a	300	98.45	95	38.20	76.40	43.63	39.95			27.74			C/P	50/50	24.2x24.4
S4.4 – C	2	12	6	b	24	98.45	95	36.99	75.30	57.28	57.28	54.20	2.30	41.08	39.94	1.09	P/P_M	70/30	–
S4.4 – C	3	12	6	b	24	98.45	95	35.56	73.90	54.49	54.49			40.64			P	100	–
S4.4 – C	4	12	6	b	24	98.45	95	35.86	71.10	53.05	53.05			39.24			P	100	–
S4.4 – C	5	12	6	b	24	98.45	95	35.53	69.40	51.98	51.98			38.80			P/P_M	95/5	–
S4.4 – U	1	12	6	b	300	98.45	95	34.65	69.30	47.10	47.10	46.54	7.10	36.06	34.76	5.33	P/P_M	70/30	–
S4.4 – U	2	12	6	b	300	98.45	95	35.55	71.10	34.86	34.86			26.01			P	100	–
S4.4 – U	3	12	6	b	300	98.45	95	35.70	71.40	50.01	50.01			37.15			P/P_M	80/20	–
S4.4 – U	4	12	6	b	300	98.45	95	36.20	72.40	46.94	46.94			34.40			P	100	–
S4.4 – U	5	12	6	b	300	98.45	95	35.50	71.00	53.81	53.81			40.21			P	100	–
S4 – 6d – 3/4 – C	1	12	6	c	24	98.45	95	16.60	73.20	26.74	26.74	26.11	1.40	42.73	40.31	2.86	P	100	–
S4 – 6d – 3/4 – C	2	12	6	c	24	98.45	95	17.50	70.50	27.09	27.09			41.06			P	100	–
S4 – 6d – 3/4 – C	3	12	6	c	24	98.45	95	17.50	73.40	24.51	24.51			37.15			P	100	–

TABLE C.4: (continued)

Series	No.	Anchor diam. [mm]	h_{ef}/d [-]	Config. [-]	Setup diam. [mm]	f'_{cc} [MPa]	Nom. f'_{cc} [MPa]	Bond length [mm]	h_{ef} [mm]	N_u [kN]	Nom. N_u [kN]	$N_{u,m}$ [kN]	σ [kN]	Nom. τ_u [MPa]	$\tau_{u,m}$ [MPa]	σ [MPa]	Failure mode [-]	Ratio [%]	Cone dim. [cm]
$S4-6d-3/4-U$	1	12	6	c	300	98.45	95	17.50	71.20	27.33	27.33	27.01	0.40	41.43	43.15	1.66	P	–	–
$S4-6d-3/4-U$	2	12	6	c	300	98.45	95	16.63	68.90	27.15	27.15			43.31			P	–	–
$S4-6d-3/4-U$	3	12	6	c	300	98.45	95	15.75	69.50	26.56	26.56			44.73			P	–	–
$S4-6d-4/4-C$	1	12	6	d	24	98.45	95	0.00	72.30	0.85	0.85	0.90	0.07	–	–	–	–	100	–
$S4-6d-4/4-C$	2	12	6	d	24	98.45	95	0.00	71.70	0.86	0.86			–			–	100	–
$S4-6d-4/4-C$	3	12	6	d	24	98.45	95	0.00	72.30	0.98	0.98			–			–	100	–
$S4-6d-4/4-U$	1	12	6	d	300	98.45	95	0.00	71.50	0.85	0.85	0.91	0.10	–	–	–	–	–	–
$S4-6d-4/4-U$	2	12	6	d	300	98.45	95	0.00	72.50	1.04	1.04			–			–	–	–
$S4-6d-4/4-U$	3	12	6	d	300	98.45	95	0.00	69.20	0.84	0.84			–			–	–	–
$S4.5-C$	1	12	7	a	24	98.45	95	44.18	80.60	65.84	65.84	61.97	3.75	39.53	38.64	2.68	P/P_M	55/45	–
$S4.5-C$	2	12	7	a	24	98.45	95	43.15	82.80	65.52	65.52			40.28			P/P_M	80/20	–
$S4.5-C$	3	12	7	a	24	98.45	95	47.02	79.10	60.37	60.37			34.06			P/P_M	90/10	–
$S4.5-C$	4	12	7	a	24	98.45	95	39.10	76.60	56.93	56.93			38.62			P/P_M	90/10	–
$S4.5-C$	5	12	7	a	24	98.45	95	39.88	80.60	61.19	61.19			40.70			P/P_M	95/5	–
$S4.5-U$	1	12	7	a	440	98.45	95	42.35	84.70	57.13	57.13	48.90	4.68	35.78	30.99	2.71	P	100	–
$S4.5-U$	2	12	7	a	440	98.45	95	41.20	82.40	50.79	46.51			29.94			C/P	50/50	25.1x28x9
$S4.5-U$	3	12	7	a	440	98.45	95	41.50	83.00	45.64	45.64			29.17			P/P_M	55/45	–
$S4.5-U$	4	12	7	a	440	98.45	95	41.90	83.80	51.52	47.17			29.86			C/P	50/50	32.7x36.8
$S4.5-U$	5	12	7	a	440	98.45	95	42.25	84.50	52.50	48.07			30.18			C/P	50/50	26.5x27.8
$S4.6-C$	1	12	7	b	24	98.45	95	40.33	82.80	57.61	57.61	59.18	2.19	37.89	38.37	1.16	P/P_M	95/5	–
$S4.6-C$	2	12	7	b	24	98.45	95	40.71	82.60	60.52	60.52			39.43			P/P_M	95/5	–
$S4.6-C$	3	12	7	b	24	98.45	95	40.84	82.80	56.29	56.29			36.56			P	100	–
$S4.6-C$	4	12	7	b	24	98.45	95	41.94	82.00	61.64	61.64			38.99			P/P_M	70/30	–
$S4.6-C$	5	12	7	b	24	98.45	95	40.76	81.80	59.86	59.86			38.96			P	100	–
$S4.6-U$	1	12	7	b	440	98.45	95	42.25	84.50	65.18	65.18	58.27	4.12	40.92	37.51	2.51	P	100	–
$S4.6-U$	2	12	7	b	440	98.45	95	41.80	83.60	54.08	54.08			34.32			P/P_M	80/20	–
$S4.6-U$	3	12	7	b	440	98.45	95	41.95	83.90	57.05	57.05			36.07			P	100	–
$S4.6-U$	4	12	7	b	440	98.45	95	39.55	79.10	62.95	57.64			38.66			C/P	80/20	52.5x39x5
$S4.6-U$	5	12	7	b	440	98.45	95	40.55	81.10	57.42	57.42			37.56			P/P_M	80/20	–
$S4.7-C$	1	12	8	a	24	98.45	95	50.88	95.00	64.63	64.63	64.84	5.09	33.69	34.73	1.46	P/P_M	55/45	–
$S4.7-C$	2	12	8	a	24	98.45	95	49.76	95.00	66.93	66.93			35.68			P/P_M	60/40	–
$S4.7-C$	3	12	8	a	24	98.45	95	49.61	95.30	64.08	64.08			34.26			P/P_M	90/10	–
$S4.7-C$	4	12	8	a	24	98.45	95	45.69	92.00	57.27	57.27			33.25			P/P_M	50/50	–
$S4.7-C$	5	12	8	a	24	98.45	95	51.41	95.40	71.27	71.27			36.77			P/P_M	80/20	–
$S4.7-U$	1	12	8	a	400	98.45	95	48.10	96.20	50.31	50.31	58.35	4.67	27.74	32.72	2.88	P	100	–
$S4.7-U$	2	12	8	a	400	98.45	95	47.70	95.40	65.08	59.59			33.14			C/P	50/50	38.9x34.6
$S4.7-U$	3	12	8	a	400	98.45	95	46.80	93.60	64.58	59.13			33.51			C/P	50/50	28.1x32
$S4.7-U$	4	12	8	a	400	98.45	95	46.80	93.60	65.81	60.26			34.16			C/P	50/50	36x26.2
$S4.7-U$	5	12	8	a	400	98.45	95	47.25	94.50	68.21	62.46			35.06			C/P	50/50	32.5x27x8

TABLE C.4: (continued)

Series [-]	No. [-]	Anchor diam. [mm]	h_{ef}/d [-]	Config. [-]	Setup diam. [mm]	f'_{cc} [MPa]	Nom. f'_{cc} [MPa]	Bond length [mm]	h_{ef} [mm]	N_u [kN]	Nom. N_u [kN]	$N_{u,m}$ [kN]	σ [kN]	Nom. τ_u [MPa]	$\tau_{u,m}$ [MPa]	σ [MPa]	Failure mode [-]	Ratio [%]	Cone dim. [cm]
S4.8 – C	1	12	8	b	24	98.45	95	46.93	93.00	55.59	55.59	62.19	7.78	31.42	31.67	4.17	P	100	–
S4.8 – C	2	12	8	b	24	98.45	95	47.49	91.00	47.10	47.10			26.31			P/P_M	5/95	–
S4.8 – C	3	12	8	b	24	98.45	95	48.08	95.90	58.95	58.95			32.52			P/P_M	90/10	–
S4.8 – C	5	12	8	b	24	98.45	95	46.13	91.90	63.36	63.36			36.43			P/P_M	70/30	–
S4.8 – U	2	12	8	b	400	98.45	95	47.85	95.70	63.24	63.24	66.64	6.19	35.06	37.34	2.96	P	100	–
S4.8 – U	4	12	8	b	400	98.45	95	46.00	92.00	62.89	62.89			36.27			P	100	–
S4.8 – U	5	12	8	b	400	98.45	95	48.10	96.20	73.77	73.77			40.68			P/P_M	70/30	–
S4 – 8d – 3/4 – C	1	12	8	c	24	98.45	95	21.00	98.10	34.94	34.94	29.97	6.35	44.13	37.29	1.53	P	100	–
S4 – 8d – 3/4 – C	2	12	8	c	24	98.45	95	20.00	96.20	22.82	22.82			30.27			P	100	–
S4 – 8d – 3/4 – C	3	12	8	c	24	98.45	95	22.75	96.00	32.14	32.14			37.47			P	100	–
S4 – 8d – 3/4 – U	1	12	8	c	440	98.45	95	22.75	95.40	32.31	32.31	34.05	1.65	37.67	42.58	9.26	P	–	–
S4 – 8d – 3/4 – U	2	12	8	c	440	98.45	95	20.13	97.10	34.23	34.23			45.11			P	–	–
S4 – 8d – 3/4 – U	3	12	8	c	440	98.45	95	21.00	95.30	35.60	35.60			44.97			P	–	–
S4 – 8d – 4/4 – C	1	12	8	d	24	98.45	95	0.00	96.00	2.47	2.47	1.89	0.51	–	–	–	–	100	–
S4 – 8d – 4/4 – C	2	12	8	d	24	98.45	95	0.00	97.50	1.56	1.56			–			–	100	–
S4 – 8d – 4/4 – C	3	12	8	d	24	98.45	95	0.00	97.20	1.63	1.63			–			–	100	–
S4 – 8d – 4/4 – U	1	12	8	d	440	98.45	95	0.00	98.10	1.27	1.27	0.23	0.04	–	–	–	–	–	–
S4 – 8d – 4/4 – U	2	12	8	d	440	98.45	95	0.00	96.20	1.19	1.19			–			–	–	–
S4 – 8d – 4/4 – U	3	12	8	d	440	98.45	95	0.00	95.90	1.24	1.24			–			–	–	–

TABLE C.5: Test results for axial compression test with $M\,12$ (Table 7.5)

Series [−]	No. [−]	Anchor diam. [mm]	h_{ef}/d [−]	Setup diam. [mm]	f'_{cc} [MPa]	Compression load [kN]	h_{ef} [mm]	N_u [kN]	$N_{u,m}$ [kN]	σ [kN]	Nom. τ_u [MPa]	$\tau_{u,m}$ [MPa]	σ [MPa]	Failure mode [−]	Ratio [%]
S7.R	1	12	6	24	70.22	0	72.8	97.54	78.07	35.71	35.54	34.01	4.53	P	100
S7.R	2	12	6	24	70.22	0	72.2	67.67			24.86			P/P_M	20/80
S7.R	3	12	6	24	70.22	0	71.3	98.80			36.76			P	100
S7.R	4	12	6	24	70.22	0	73.0	99.53			36.17			P	100
S7.R	5	12	6	24	70.22	0	72.5	95.33			34.88			P	100
S7.R	6	12	6	24	70.22	0	73.6	99.57			35.89			P	100
S7.1	1	12	6	24	70.22	112	71.9	72.34	90.53	14.63	26.69	33.09	5.23	P_M	100
S7.1	2	12	6	24	70.22	112	74.8	102.94			36.50			P	100
S7.1	3	12	6	24	70.22	112	90.1	103.75			37.65			P_M	100
S7.1	4	12	6	24	70.22	112	72.4	96.97			35.53			P	100
S7.1	5	12	6	24	70.22	112	73.3	65.06			23.54			P_M	100
S7.1	6	12	6	24	70.22	112	71.2	88.61			33.01			P_M	100
S7.1	7	12	6	24	70.22	112	71.2	92.12			34.32			P	100
S7.1	9	12	6	24	70.22	112	72.5	102.42			37.47			P	100
S7.2	1	12	6	24	70.22	225	72.8	79.59	80.37	11.03	29.00	29.32	4.14	P	100
S7.2	2	12	6	24	70.22	225	71.5	94.19			34.94			P	100
S7.2	3	12	6	24	70.22	225	71.5	82.96			30.78			P	100
S7.2	4	12	6	24	70.22	225	73.2	65.82			23.85			P_M	100
S7.2	5	12	6	24	70.22	225	71.6	78.91			29.23			P/P_M	50/50
S7.2	6	12	6	24	70.22	225	74.4	71.10			25.35			P/P_M	50/50
S7.2	8	12	6	24	70.22	225	74.0	97.59			34.98			P/P_M	60/40
S7.2	9	12	6	24	70.22	225	73.1	72.82			26.42			P/P_M	30/70
S7.3	1	12	6	24	70.22	448	72.9	95.23	84.80	6.92	34.65	31.14	2.28	P/P_M	70/30
S7.3	2	12	6	24	70.22	448	70.5	79.00			29.72			P_M	100
S7.3	3	12	6	24	70.22	448	70.9	87.17			32.61			P/P_M	50/50
S7.3	4	12	6	24	70.22	448	72.6	82.81			30.26			P/P_M	80/20
S7.3	5	12	6	24	70.22	448	72.5	81.04			29.65			P_M	100
S7.3	6	12	6	24	70.22	448	73.5	87.25			31.49			P/P_M	80/20
S7.3	7	12	6	24	70.22	448	73.5	91.79			33.13			P	100
S7.3	8	12	6	24	70.22	448	71.3	74.12			27.57			P	100
S7.4	1	12	6	24	70.22	512	71.9	92.42	86.56	5.26	34.10	34.52	5.38	P/P_M	95/5
S7.4	2	12	6	24	70.22	512	72.1	89.41			32.89			P/P_M	70/30
S7.4	3	12	6	24	70.22	512	52.7	83.33			41.94			P_M	100
S7.4	7	12	6	24	70.22	512	73.8	81.07			29.14			P/P_M	50/50

TABLE C.6: Test results for long-term test with $M\,12$ (Table 7.6)

Series	No.	Anchor diam.	h_{ef}/d	Config.	Setup diam.	f'_{cc}	Sustained load	Bond length	h_{ef}	N_u	$N_{u,m}$	σ	Nom. τ_u	$\tau_{u,m}$	σ	Failure mode	Ratio
[−]	[−]	[mm]	[−]	[−]	[mm]	[MPa]	[kN]	[mm]	[mm]	[kN]	[kN]	[kN]	[MPa]	[MPa]	[MPa]	[−]	[%]
$S8.1-R-A$	1	12	6	a	24	30.13	−	42.7	72.0	53.54	48.39	7.49	33.26	31.30	4.3	P	100
$S8.1-R-A$	2	12	6	a	24	30.13	−	38.5	72.1	35.20			24.25			P/P_M	85/15
$S8.1-R-A$	3	12	6	a	24	30.13	−	44.5	70.1	50.60			30.16			P	100
$S8.1-R-A$	4	12	6	a	24	30.13	−	39.6	72.1	50.34			33.70			P/P_M	50/50
$S8.1-R-A$	5	12	6	a	24	30.13	−	39.5	70.0	52.27			35.13			P/P_M	90/10
$S8.2-R-B$	1	12	6	b	24	30.13	−	34.2	68.5	49.18	47.55	6.35	38.20	35.23	5.10	P	100
$S8.2-R-B$	2	12	6	b	24	30.13	−	37.0	73.5	36.47			26.18			P/P_M	30/70
$S8.2-R-B$	3	12	6	b	24	30.13	−	36.4	71.1	51.41			37.48			P	100
$S8.2-R-B$	4	12	6	b	24	30.13	−	35.5	73.4	48.75			36.45			P	100
$S8.2-R-B$	5	12	6	b	24	30.13	−	36.4	72.1	51.96			37.83			P	100
$S8.3-A$	1	12	6	a	24	30.13	33	39.9	71.7	58.86	57.33	5.62	39.18	38.10	2.70	P	100
$S8.3-A$	2	12	6	a	24	30.13	33	41.1	71.2	62.03			40.08			P	100
$S8.3-A$	3	12	6	a	24	30.13	33	38.7	70.9	51.10			35.03			P	100
$S8.4-R$	1	12	6	−	24	30.13	−	70.7	70.7	100.67	100.72	3.05	37.77	37.06	0.90	P/P_M	50/50
$S8.4-R$	2	12	6	−	24	30.13	−	71.9	71.9	97.70			36.04			P/P_M	70/30
$S8.4-R$	3	12	6	b	24	30.13	−	73.7	73.7	103.81			37.36			P/P_M	80/20
$S8.5-B$	1	12	6	b	24	30.13	33	36.7	72.8	61.08	57.07	5.66	44.20	41.15	4.32	P	100
$S8.5-B$	2	12	6	b	24	30.13	33	37.0	78.7	53.06			38.09			P	100
$S8.7-A$	1	12	6	a	24	98.45	34	42.7	71.4	54.32	60.39	8.37	33.78	38.57	4.90	P	100
$S8.7-A$	2	12	6	a	24	98.45	34	42.8	71.2	72.54			45.01			P	100
$S8.7-A$	3	12	6	a	24	98.45	34	39.8	72.4	59.26			39.50			P	100
$S8.7-A$	4	12	6	a	24	98.45	34	40.9	70.0	55.45			36.00			P/P_M	50/50
$S8.8-B$	1	12	6	b	24	98.45	37	36.8	71.8	60.40	59.95	4.25	43.51	43.83	3.12	P	100
$S8.8-B$	2	12	6	b	24	98.45	37	36.0	70.2	63.94			47.09			P	100
$S8.8-B$	3	12	6	b	24	98.45	37	36.0	71.9	55.49			40.88			P	100

C.1 Diagrams for Table 7.1
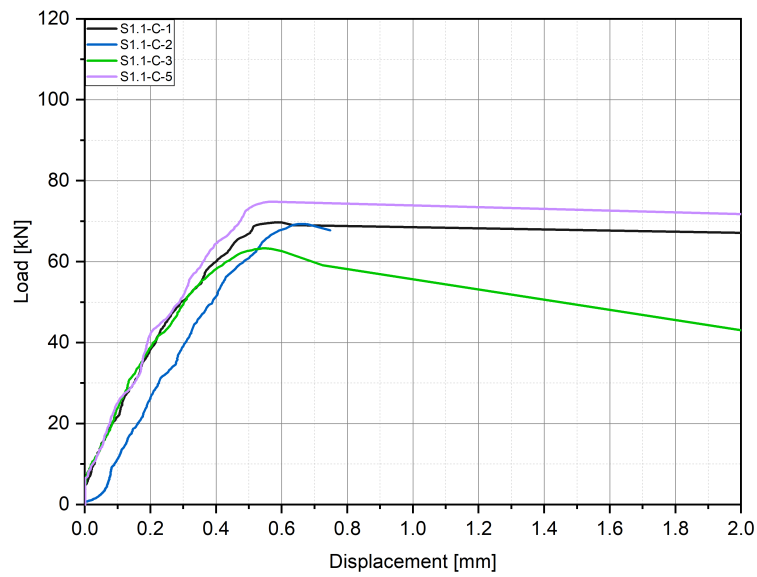
FIGURE C.1: S1.1-C - load versus displacement curves
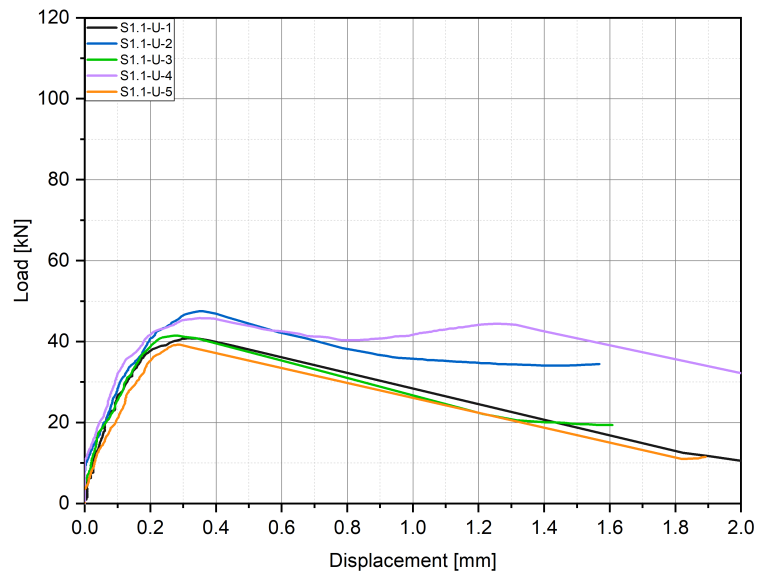
FIGURE C.2: S1.1-U - load versus displacement curves
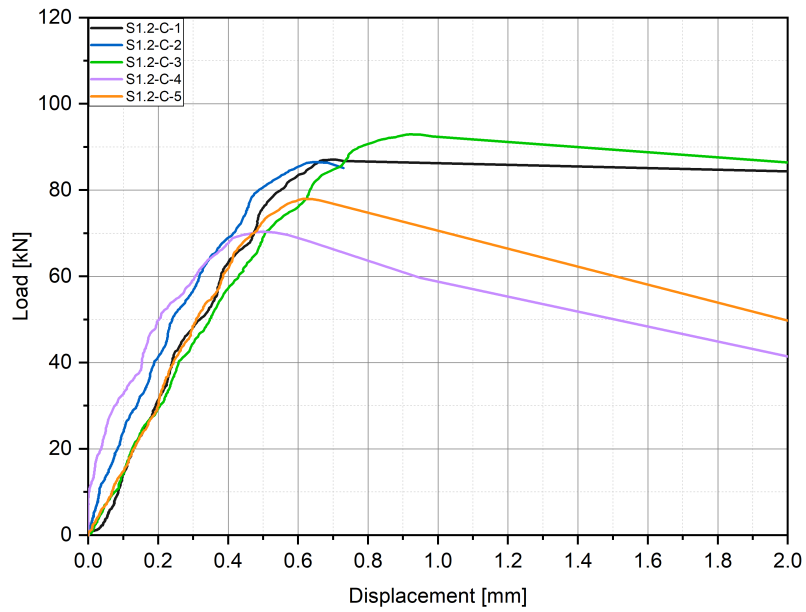
FIGURE C.3: S1.2-C - load versus displacement curves
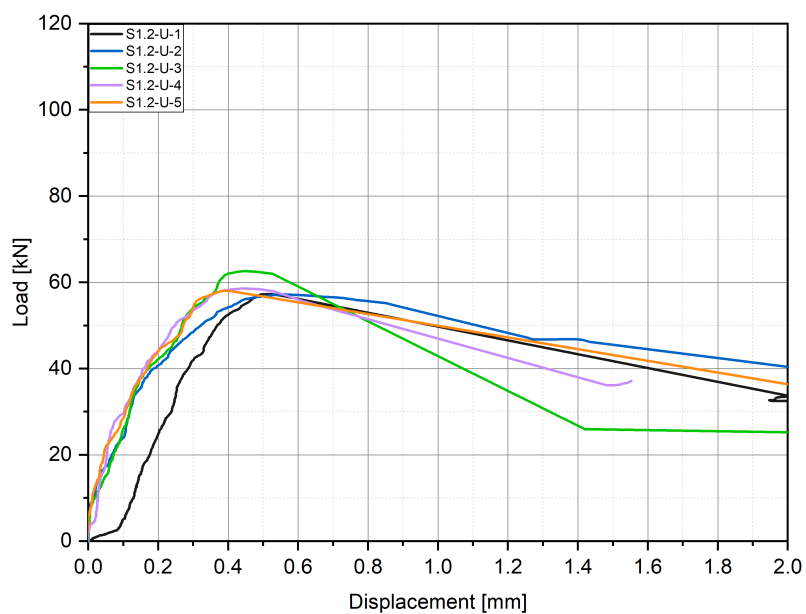
FIGURE C.4: S1.2-U - load versus displacement curves
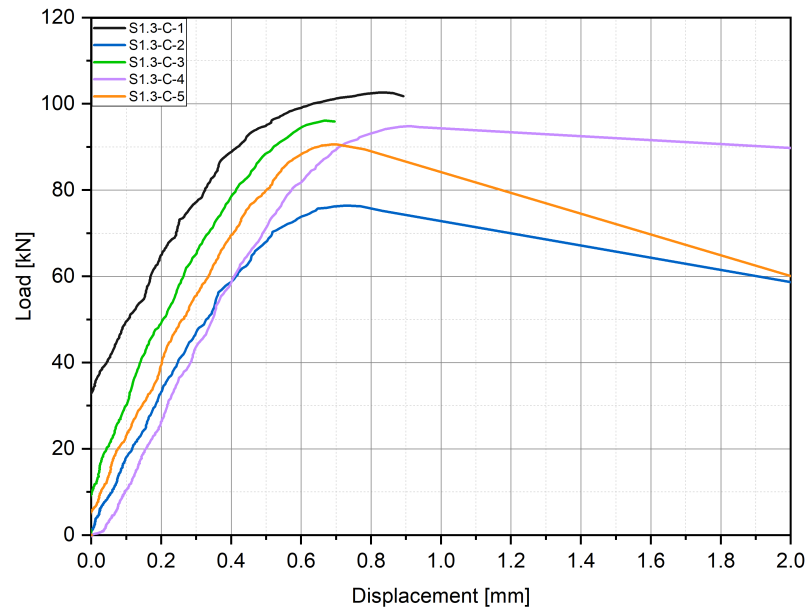
FIGURE C.5: S1.3-C - load versus displacement curves
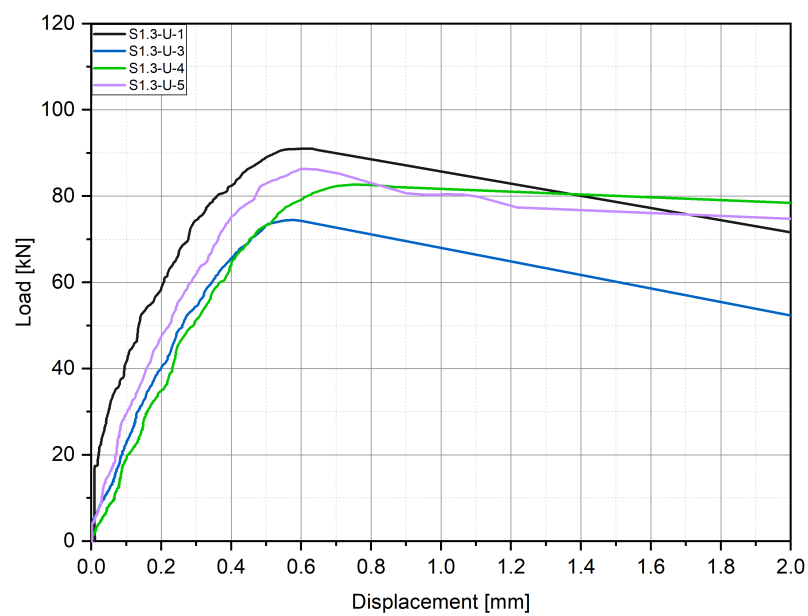
FIGURE C.6: S1.3-U - load versus displacement curves
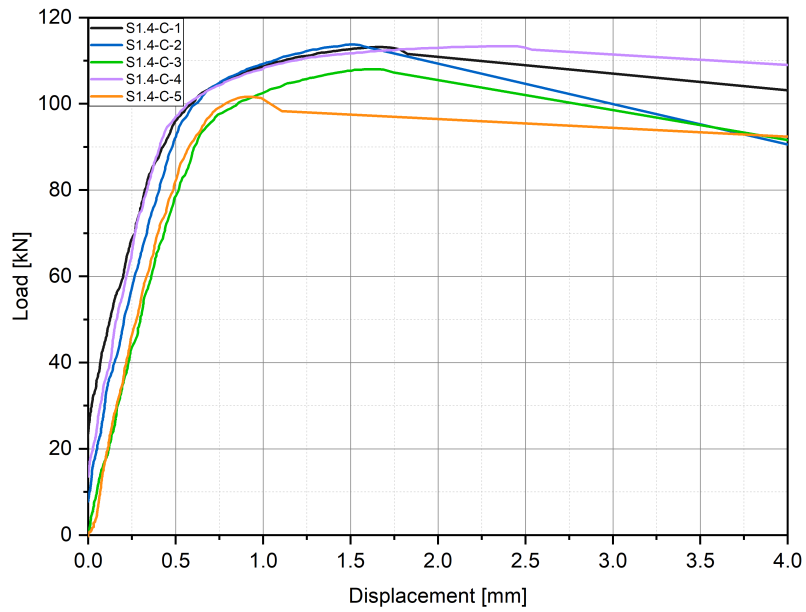
FIGURE C.7: S1.4-C - load versus displacement curves
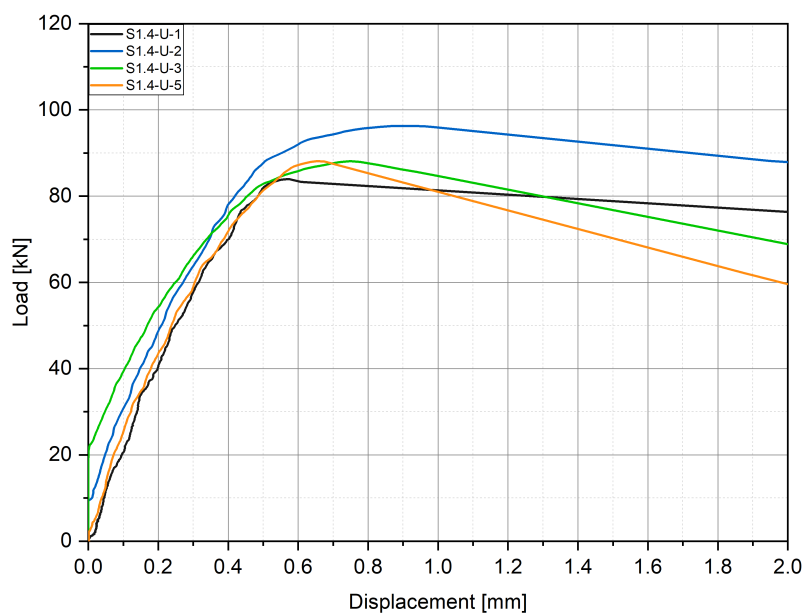
FIGURE C.8: S1.4-U - load versus displacement curves
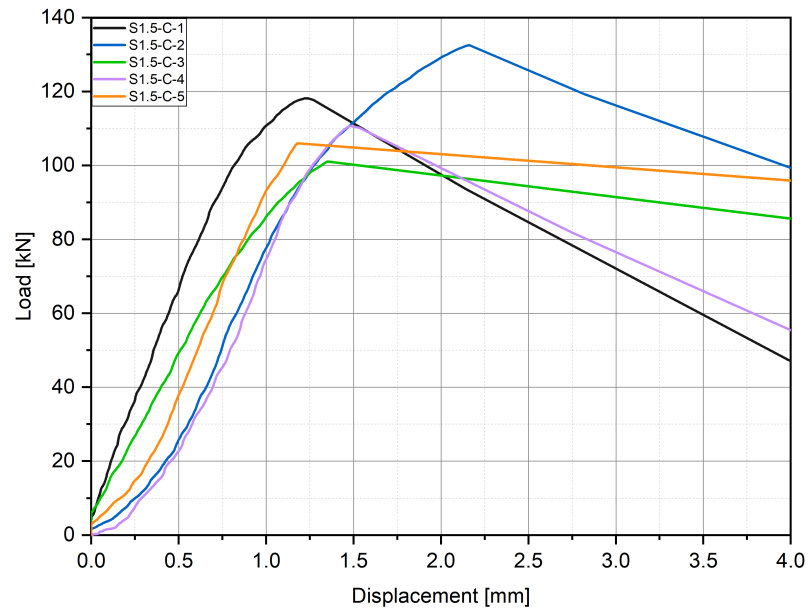
FIGURE C.9: S1.5-C - load versus displacement curves
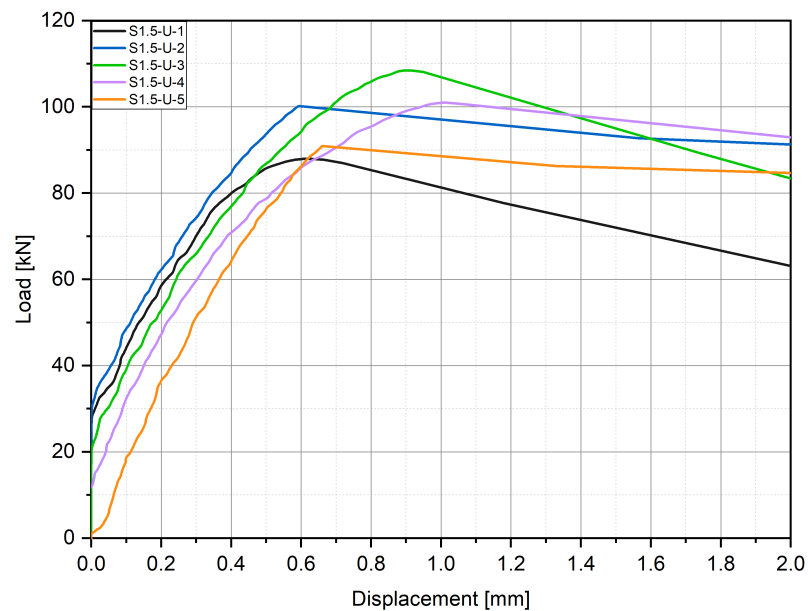
FIGURE C.10: S1.5-U - load versus displacement curves

C.2 Diagrams for Table 7.2
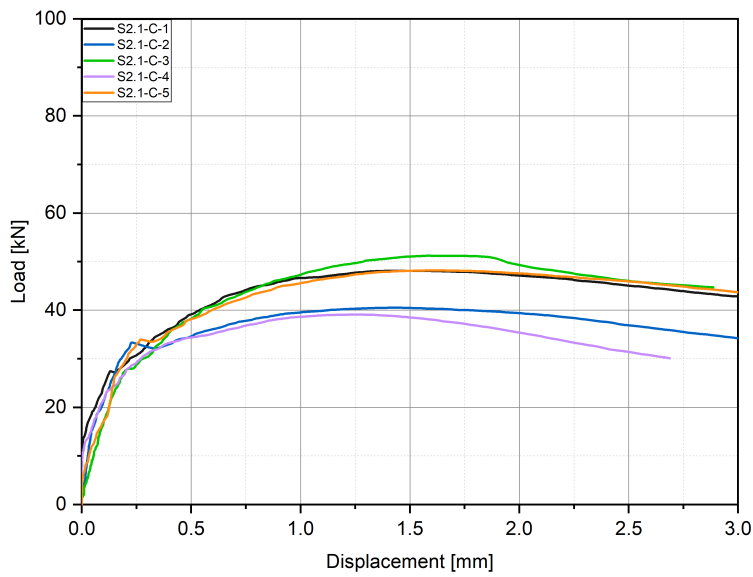
FIGURE C.11: S2.1-C - load versus displacement curves
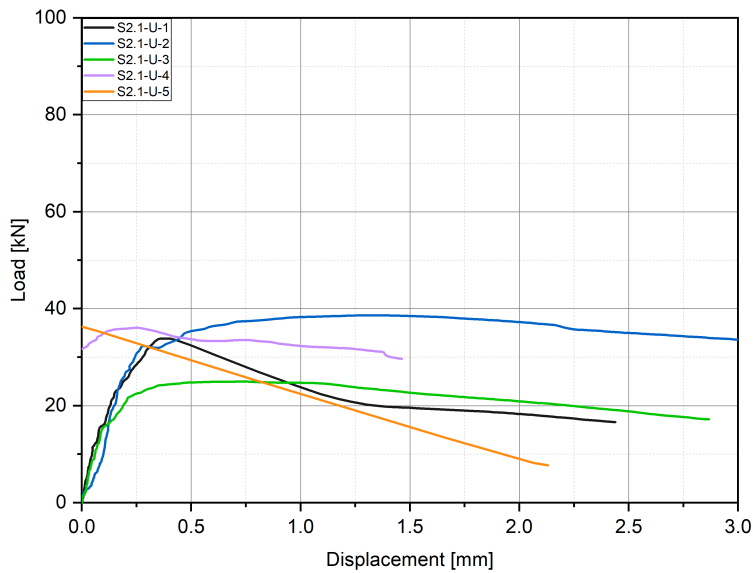
FIGURE C.12: S2.1-U - load versus displacement curves
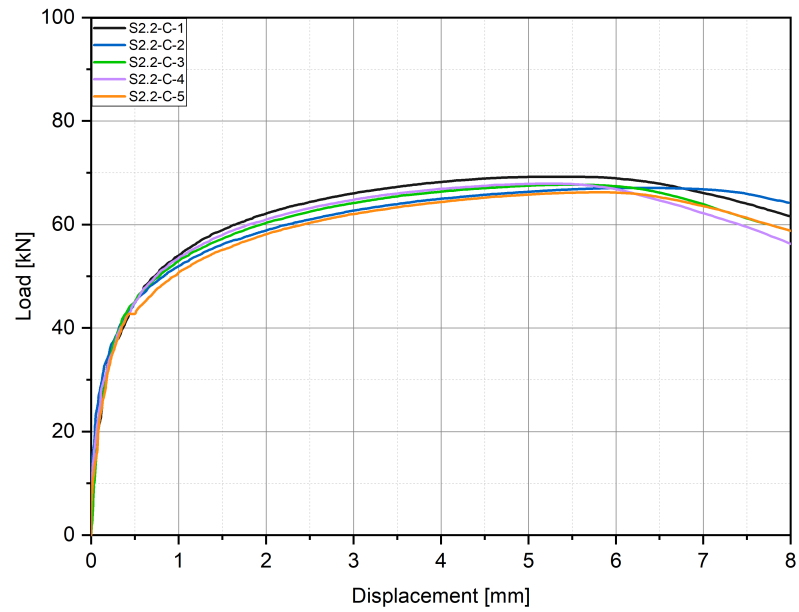
FIGURE C.13: S2.2-C - load versus displacement curves
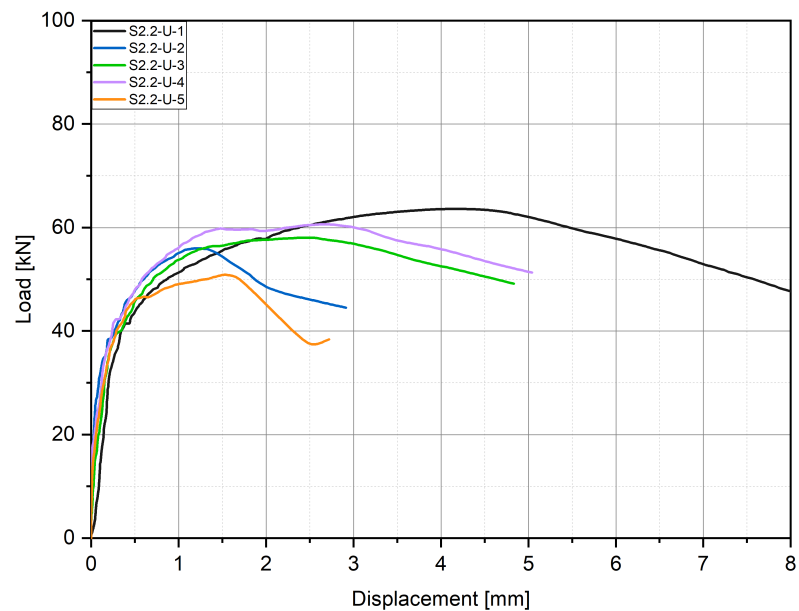
FIGURE C.14: S2.2-U - load versus displacement curves
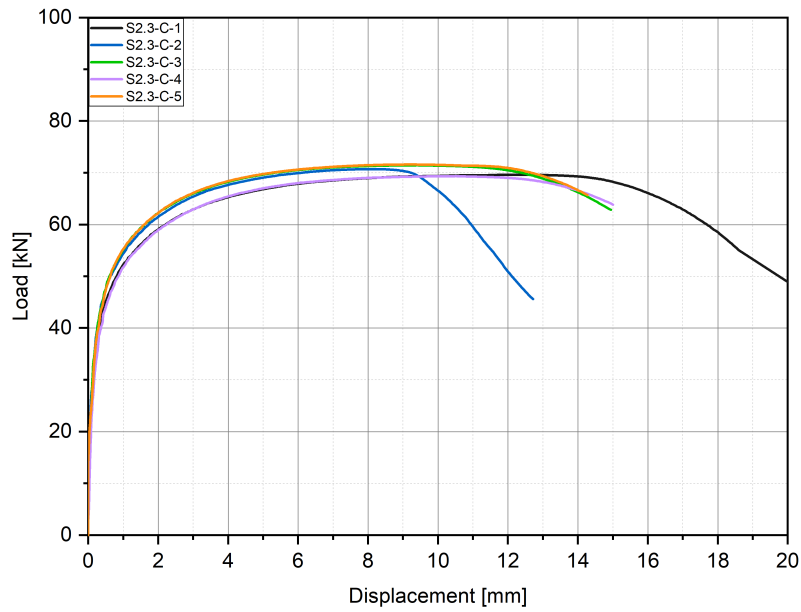
FIGURE C.15: S2.3-C - load versus displacement curves
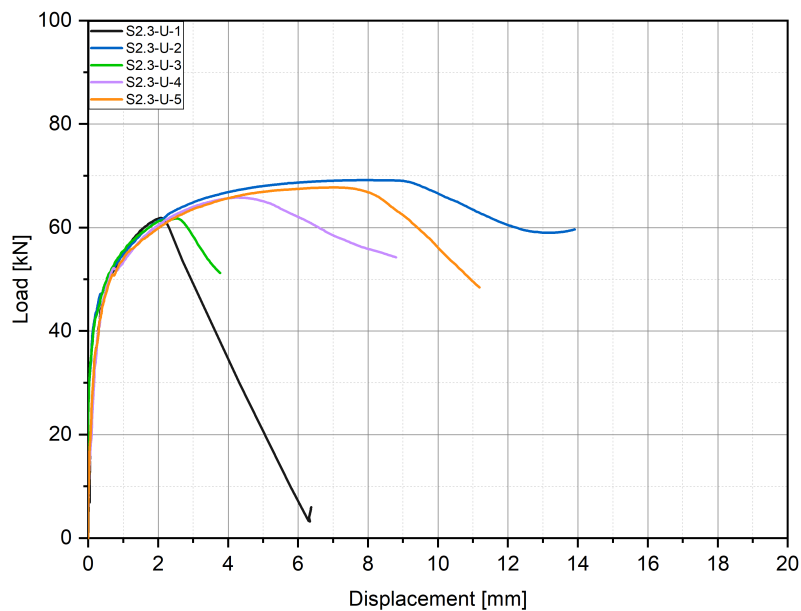
FIGURE C.16: S2.3-U - load versus displacement curves

C.3   Diagrams for Table 7.3
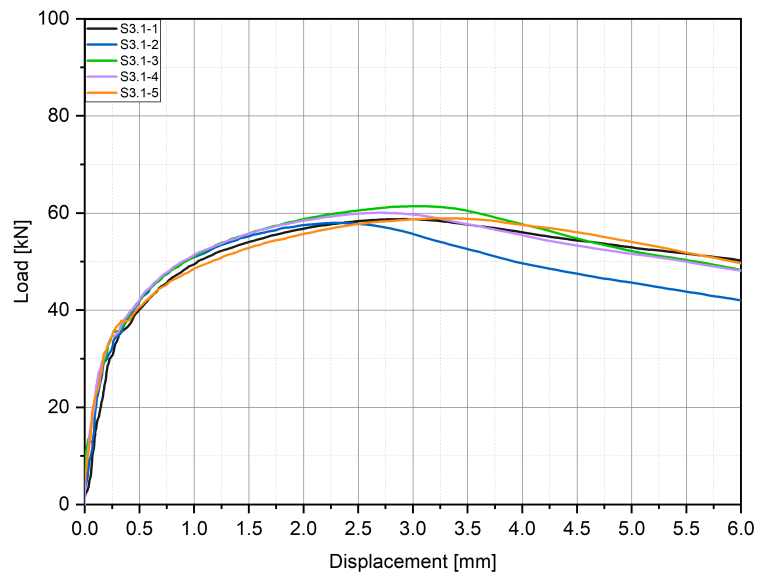
FIGURE C.17: S3.1 - load versus displacement curves
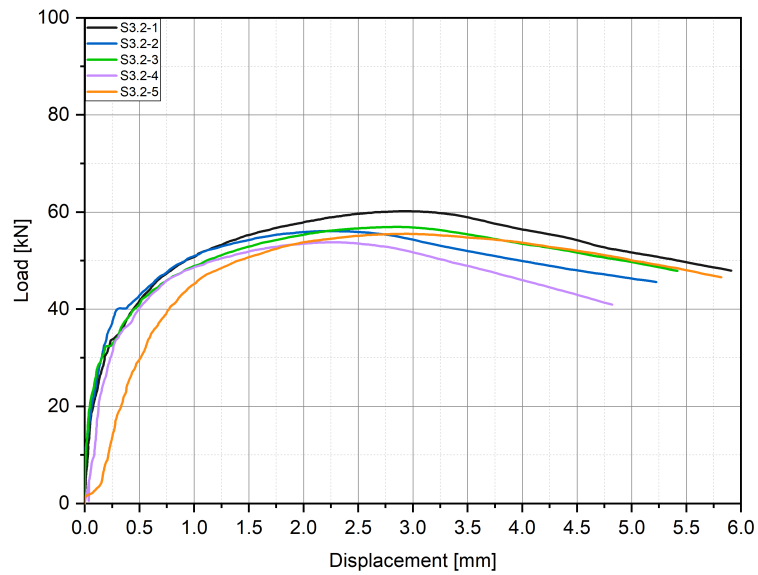
FIGURE C.18: S3.2 - load versus displacement curves
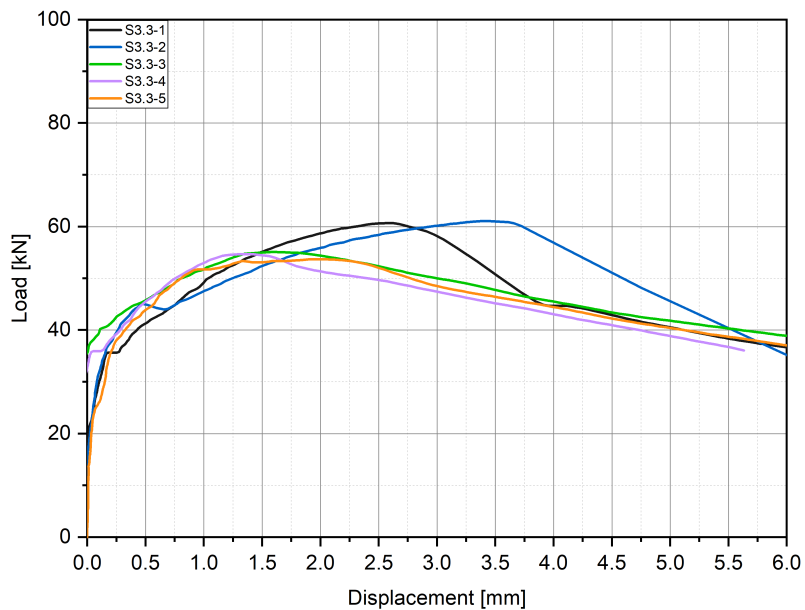
FIGURE C.19: S3.3 - load versus displacement curves
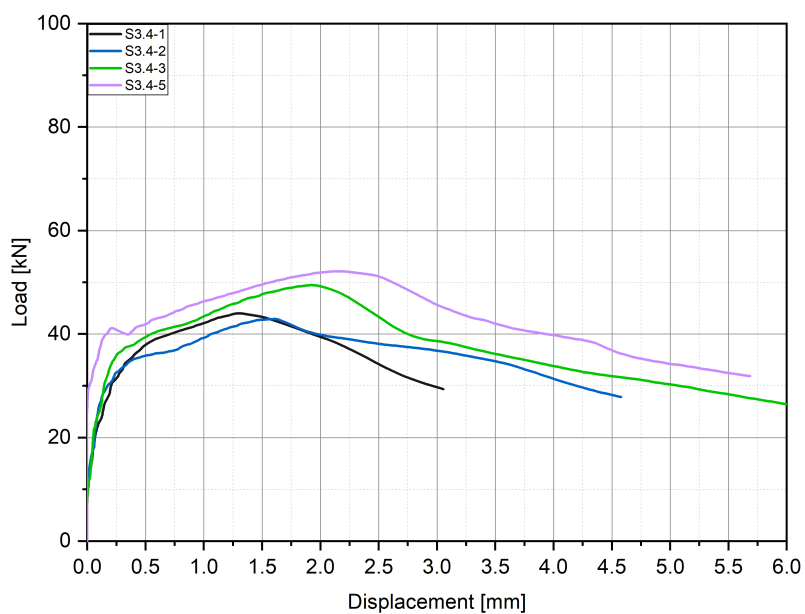
FIGURE C.20: S3.4 - load versus displacement curves
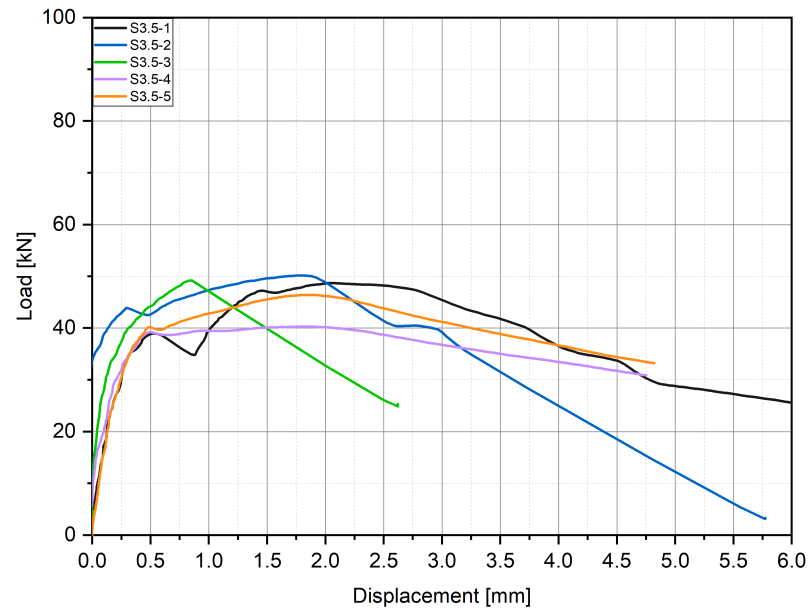
FIGURE C.21: S3.5 - load versus displacement curves

C.4 Diagrams for Table 7.4
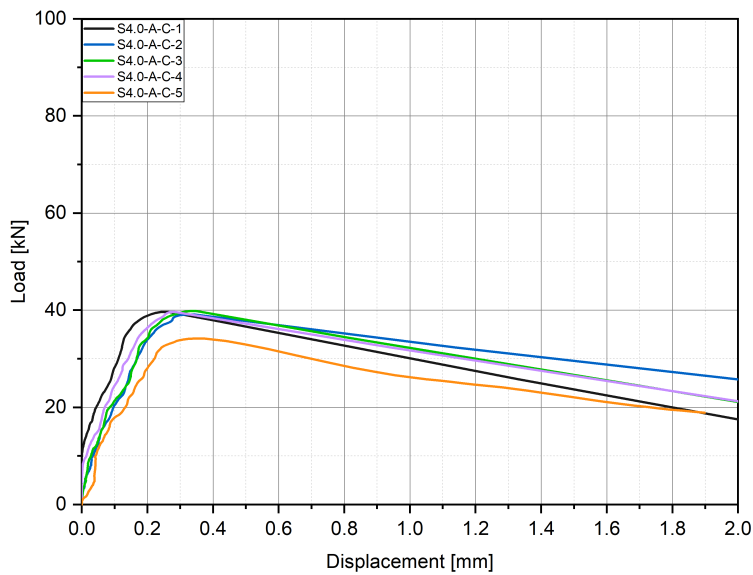
FIGURE C.22: S4.0-A-C - load versus displacement
curves
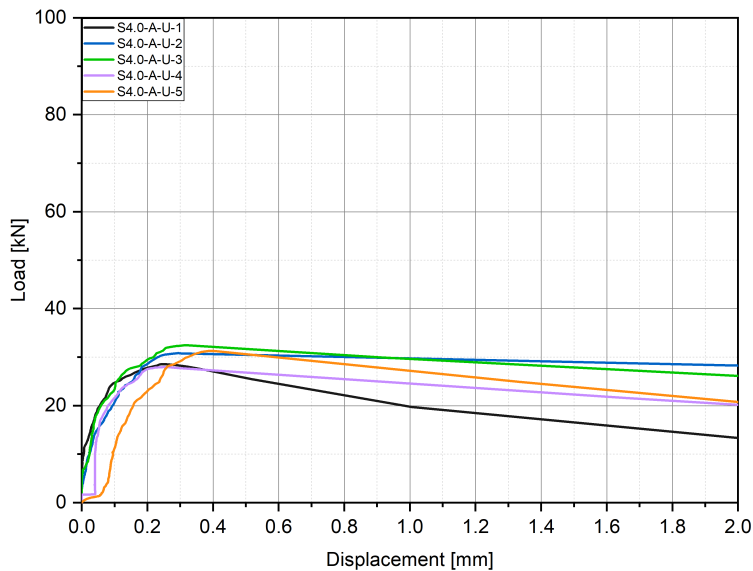
FIGURE C.23: S4.0-A-U - load versus displacement
curves
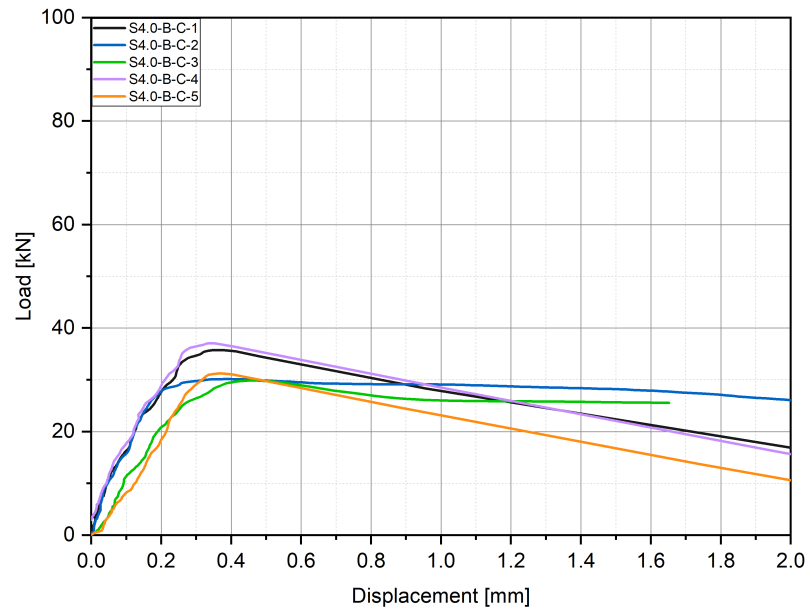
FIGURE C.24: S4.0-B-C - load versus displacement curves
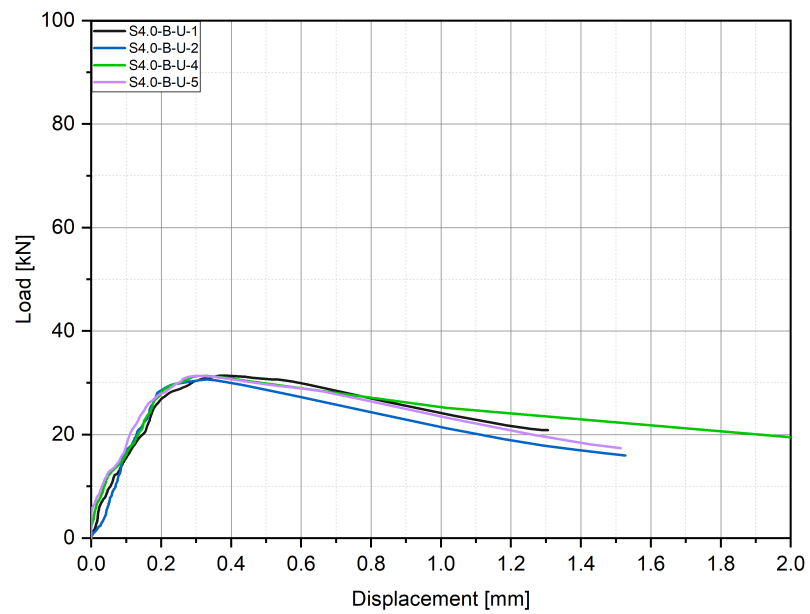
FIGURE C.25: S4.0-B-U - load versus displacement curves
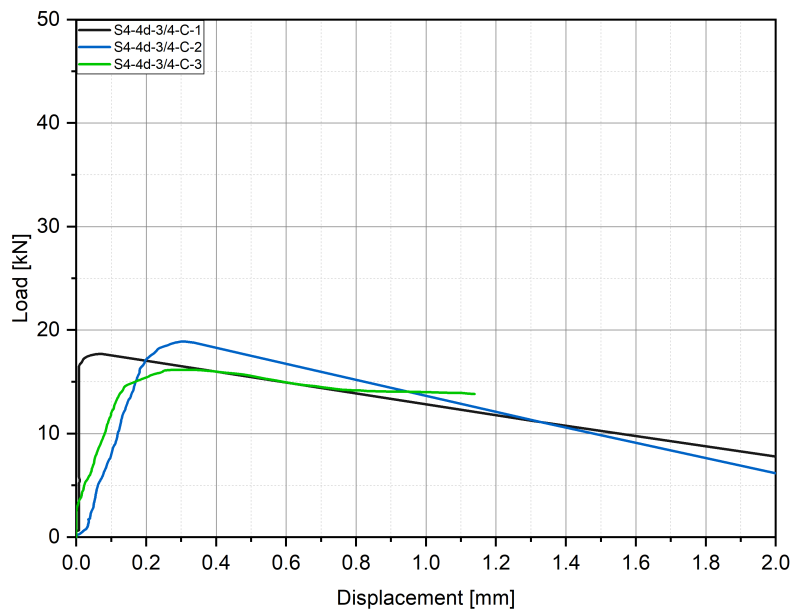
FIGURE C.26: S4-4d-3/4-C - load versus displacement curves
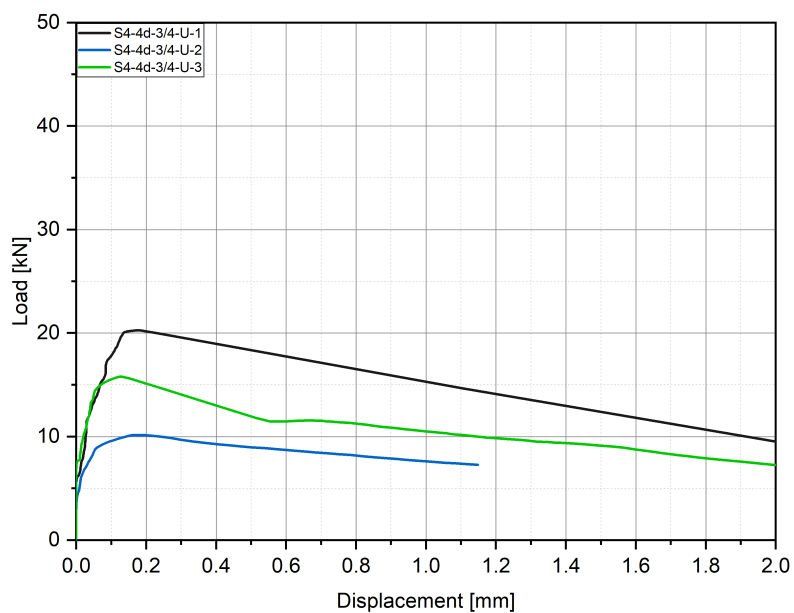
FIGURE C.27: S4-4d-3/4-U - load versus displacement curves
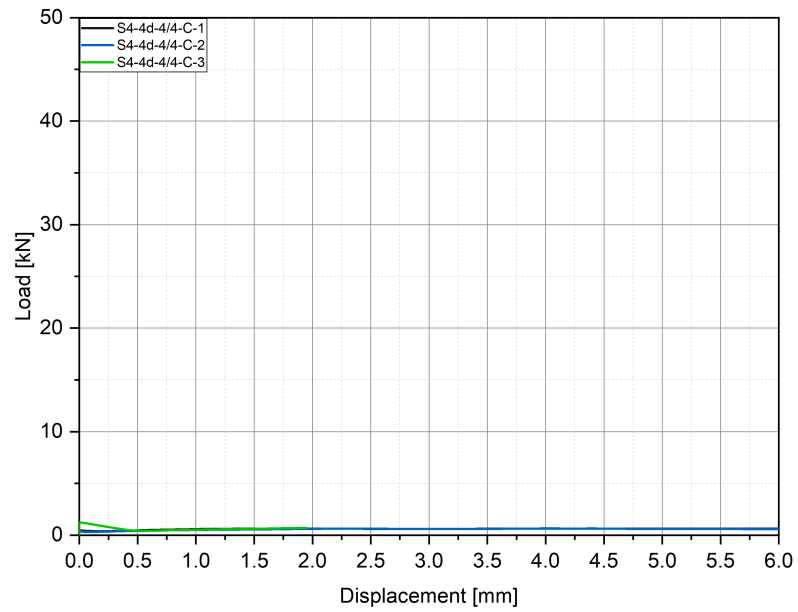
FIGURE C.28: S4-4d-4/4-C - load versus displacement
curves
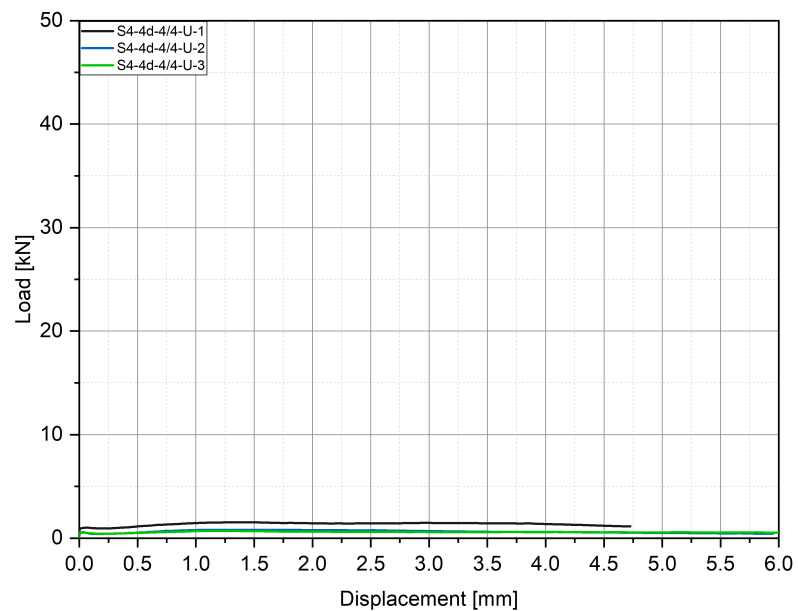
FIGURE C.29: S4-4d-4/4-U - load versus displacement
curves
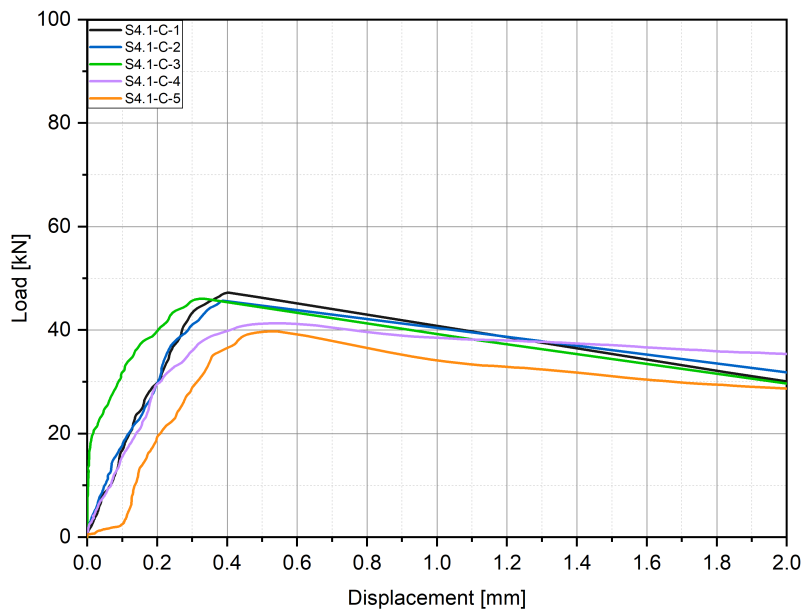
FIGURE C.30: S4.1-C - load versus displacement curves
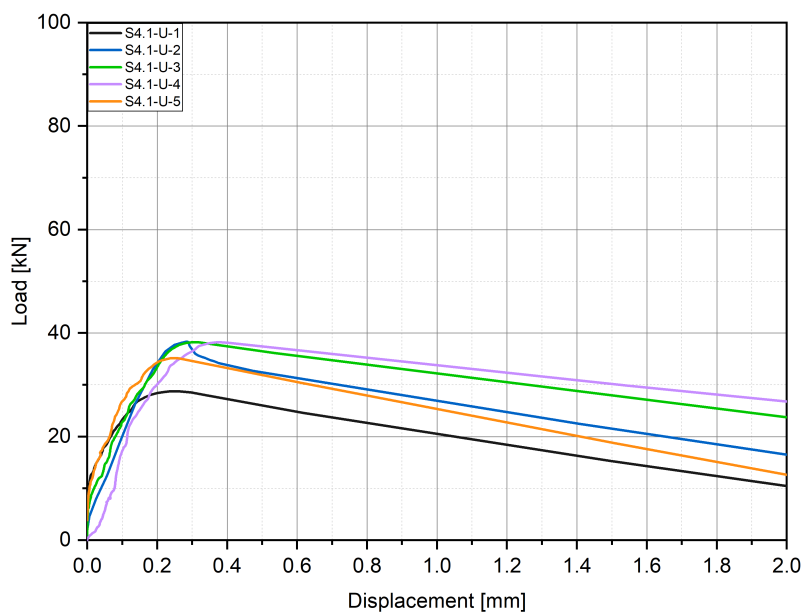
FIGURE C.31: S4.1-U - load versus displacement curves
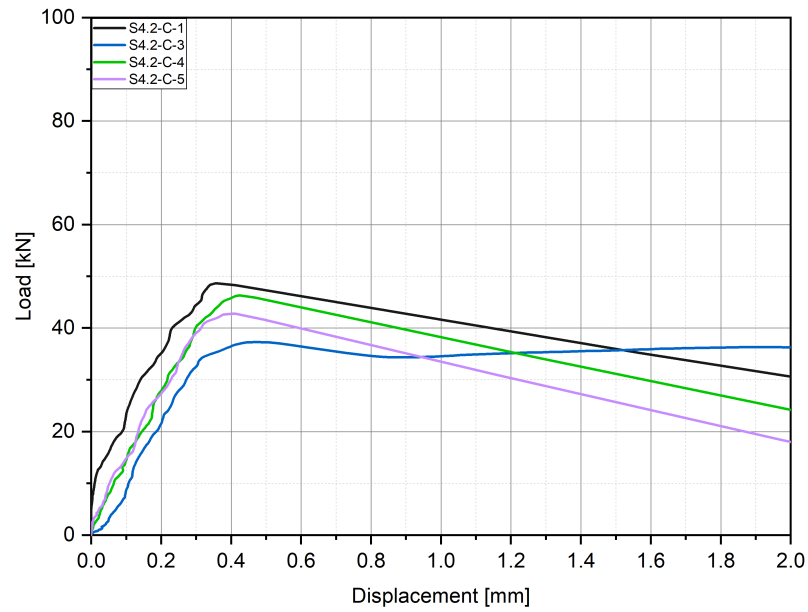
FIGURE C.32: S4.2-C - load versus displacement curves
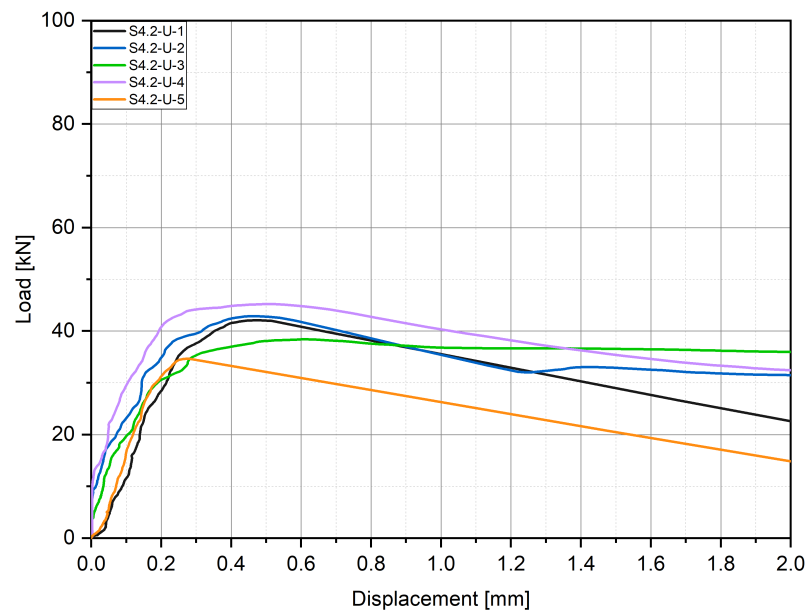
FIGURE C.33: S4.2-U - load versus displacement curves
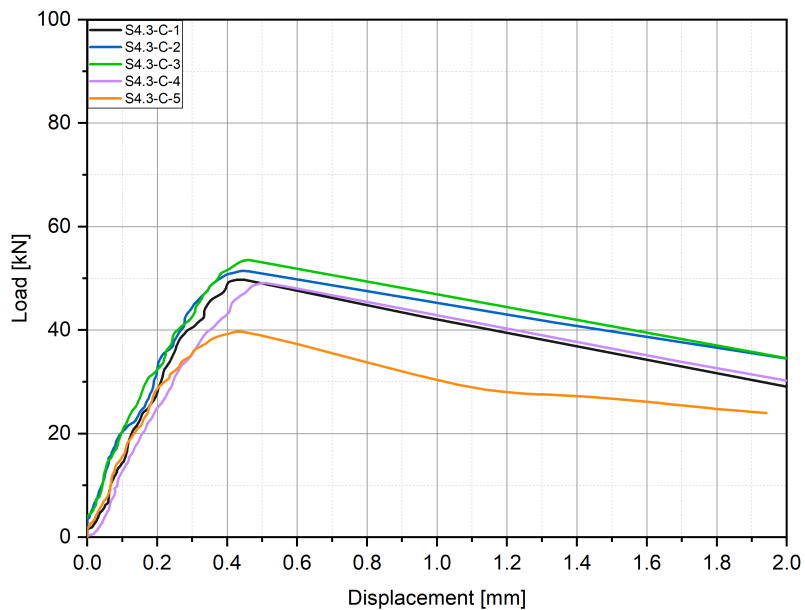
FIGURE C.34: S4.3-C - load versus displacement curves
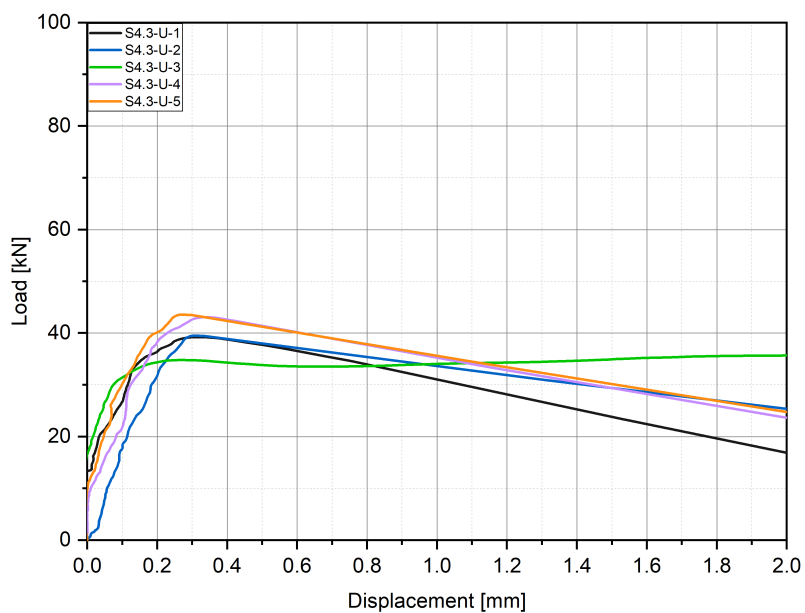
FIGURE C.35: S4.3-U - load versus displacement curves
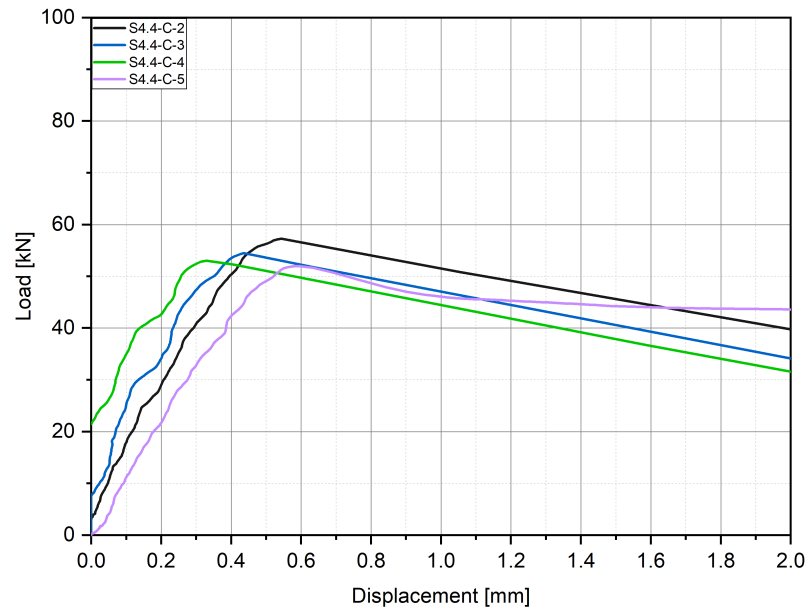
FIGURE C.36: S4.4-C - load versus displacement
curves
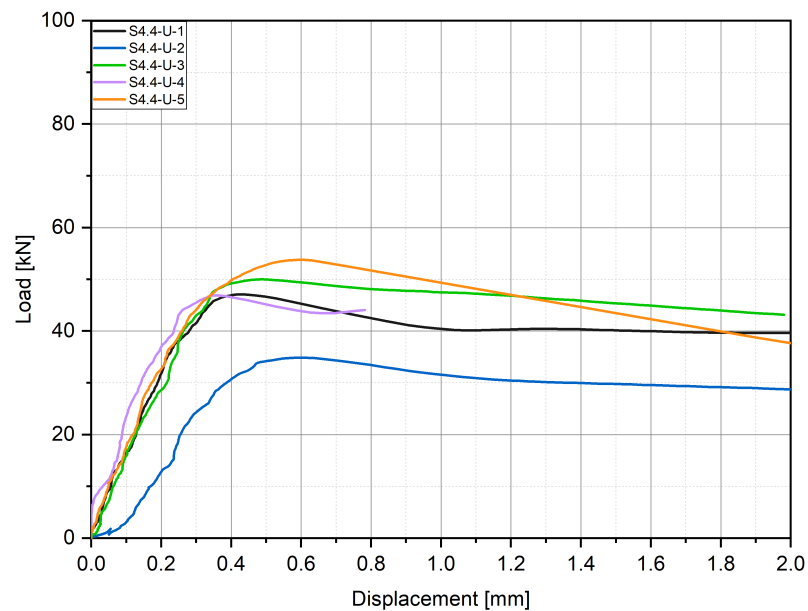
FIGURE C.37: S4.4-U - load versus displacement
curves
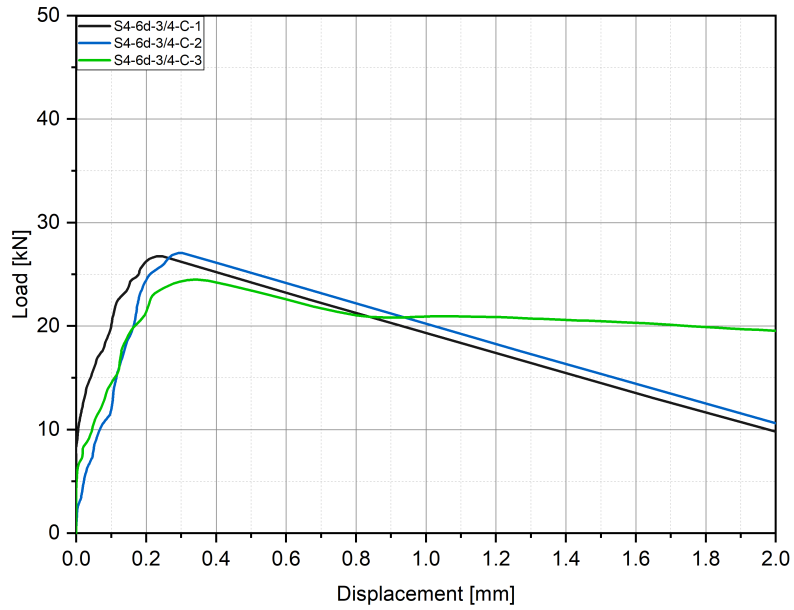
FIGURE C.38: S4-6d-3/4-C - load versus displacement curves
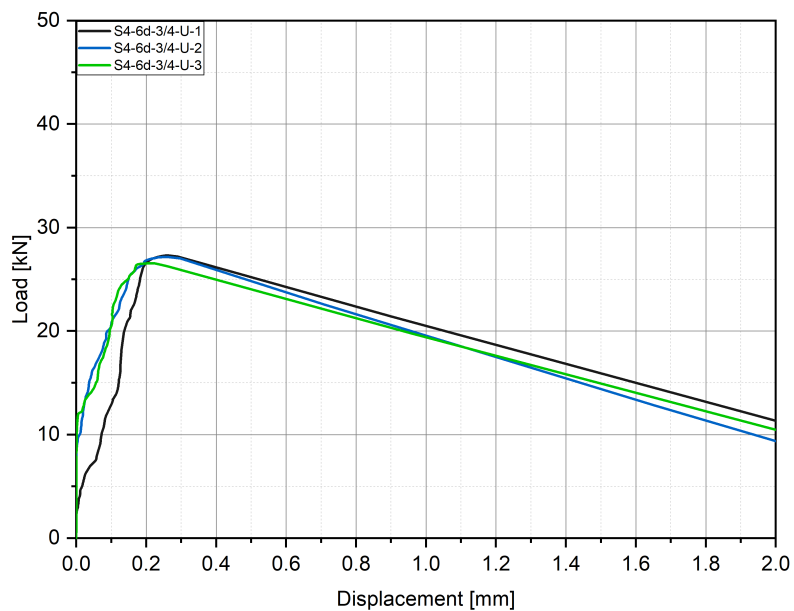
FIGURE C.39: S4-6d-3/4-U - load versus displacement curves
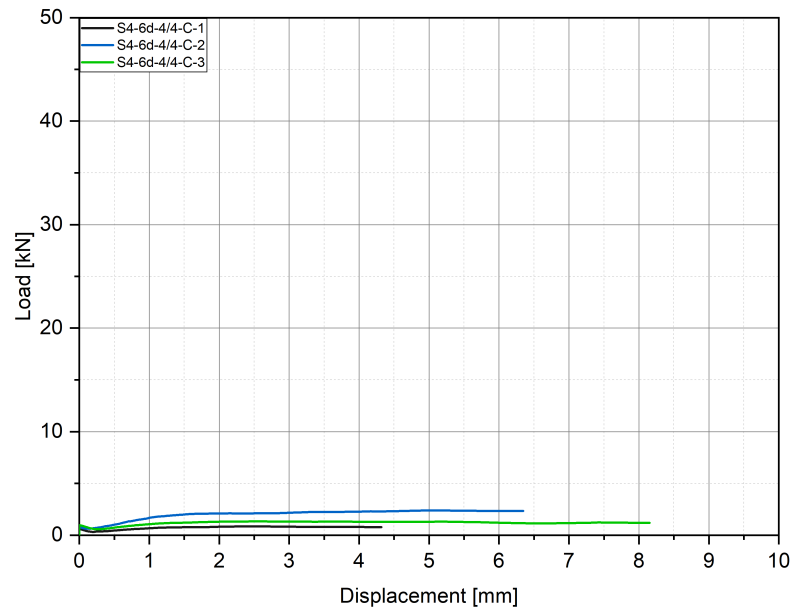
FIGURE C.40: S4-6d-4/4-C - load versus displacement
curves
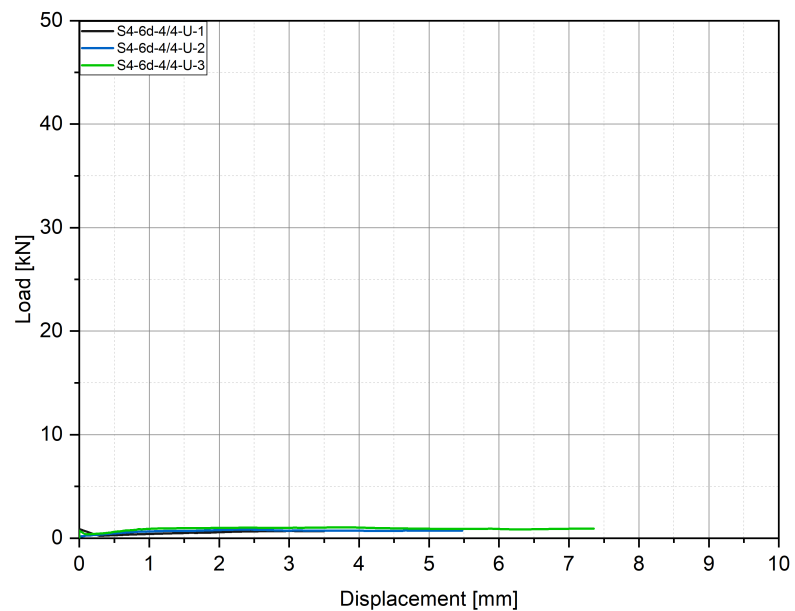
FIGURE C.41: S4-6d-4/4-U - load versus displacement
curves
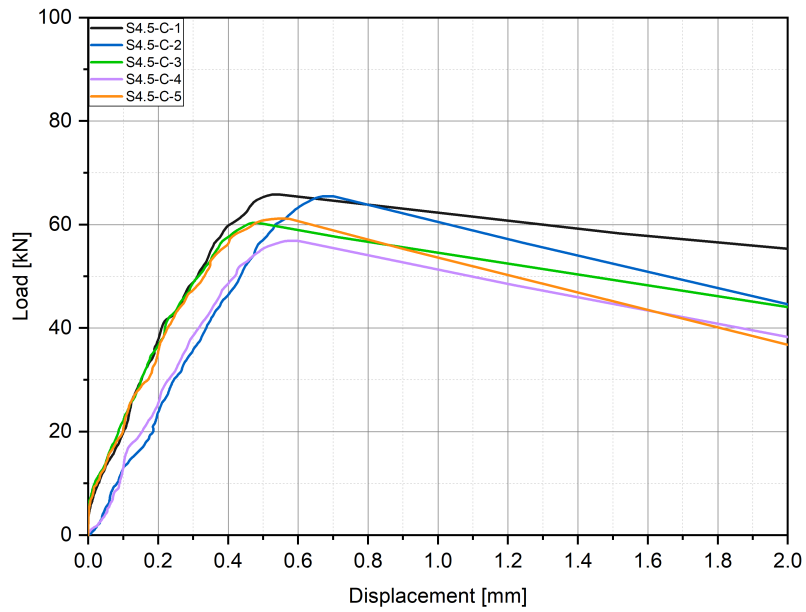
FIGURE C.42: S4.5-C - load versus displacement curves
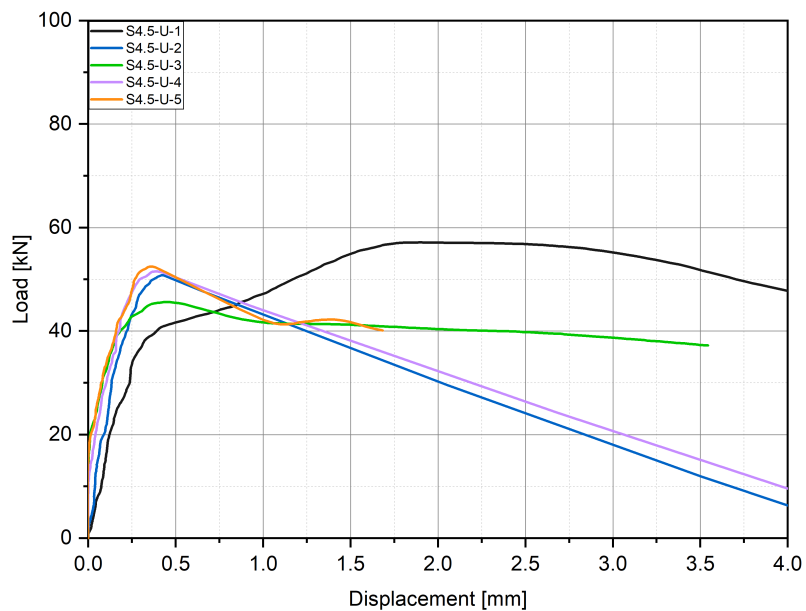
FIGURE C.43: S4.5-U - load versus displacement curves
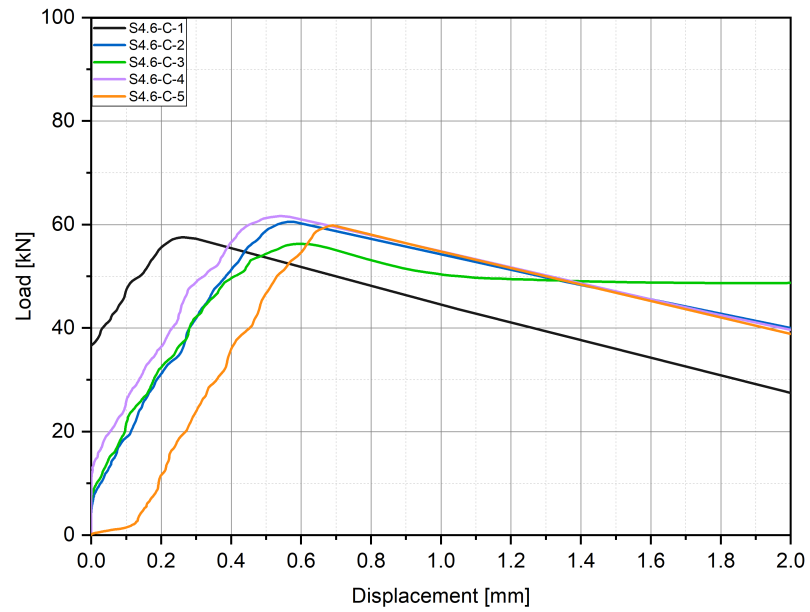
FIGURE C.44: S4.6-C - load versus displacement curves
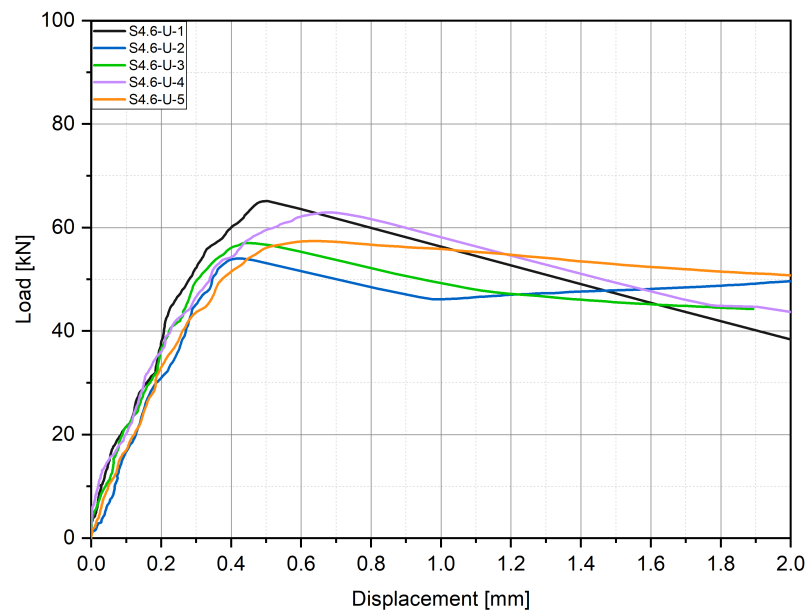
FIGURE C.45: S4.6-U - load versus displacement curves
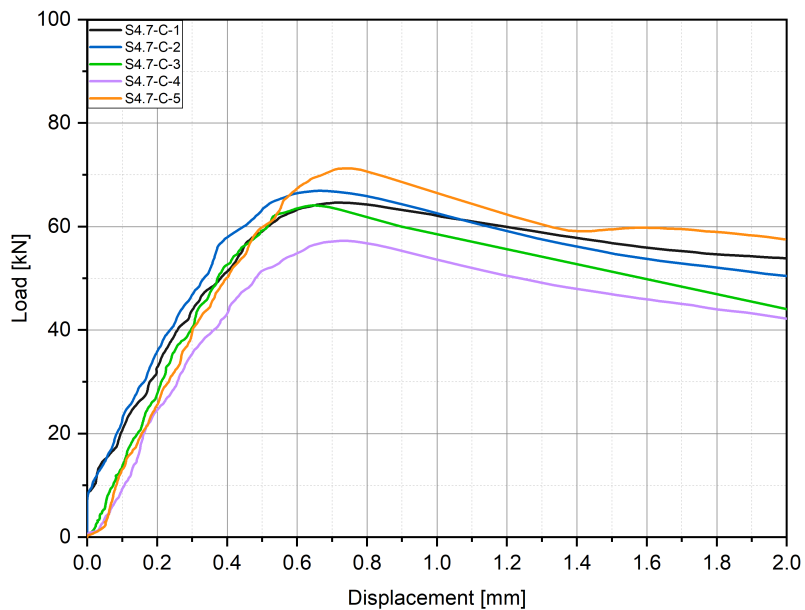
FIGURE C.46: S4.7-C - load versus displacement curves
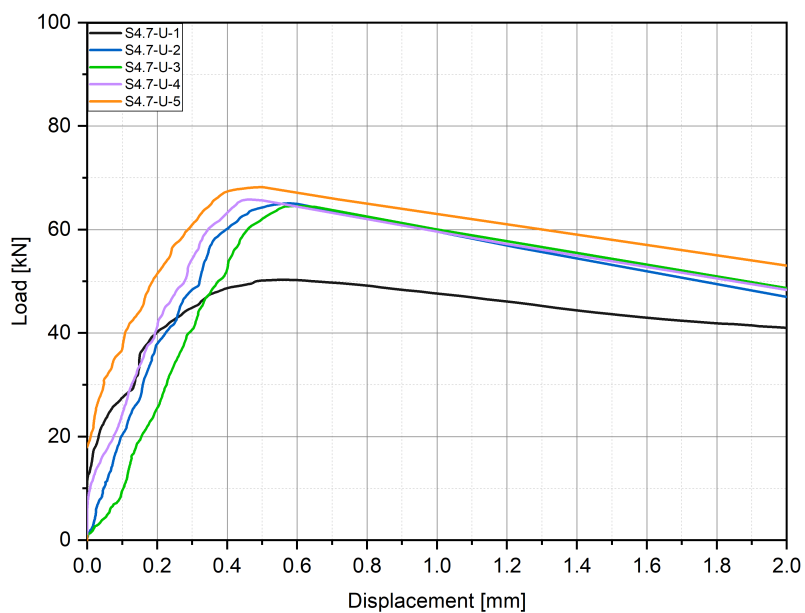
FIGURE C.47: S4.7-U - load versus displacement curves
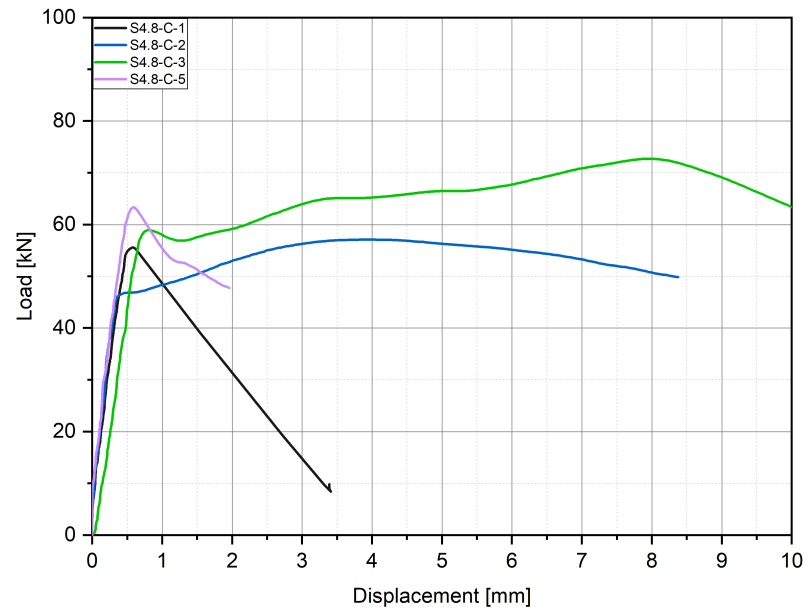
FIGURE C.48: S4.8-C - load versus displacement curves
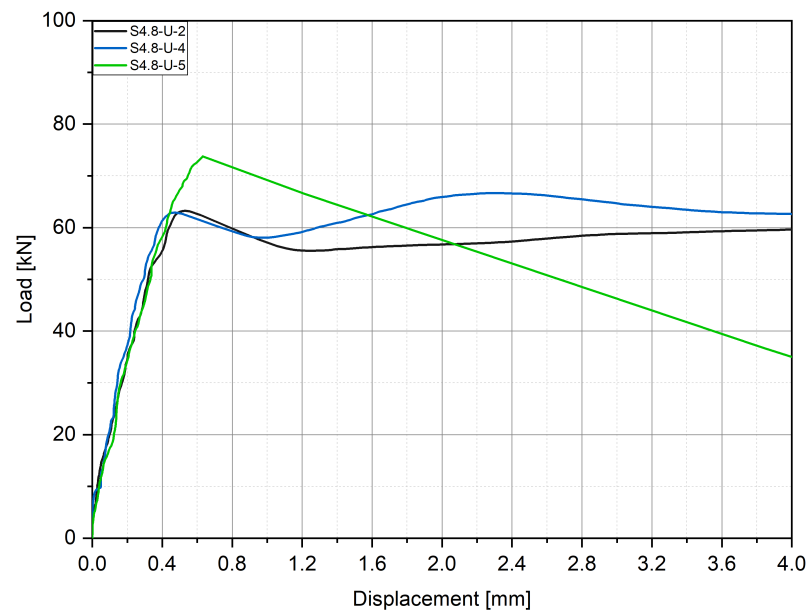
FIGURE C.49: S4.8-U - load versus displacement curves
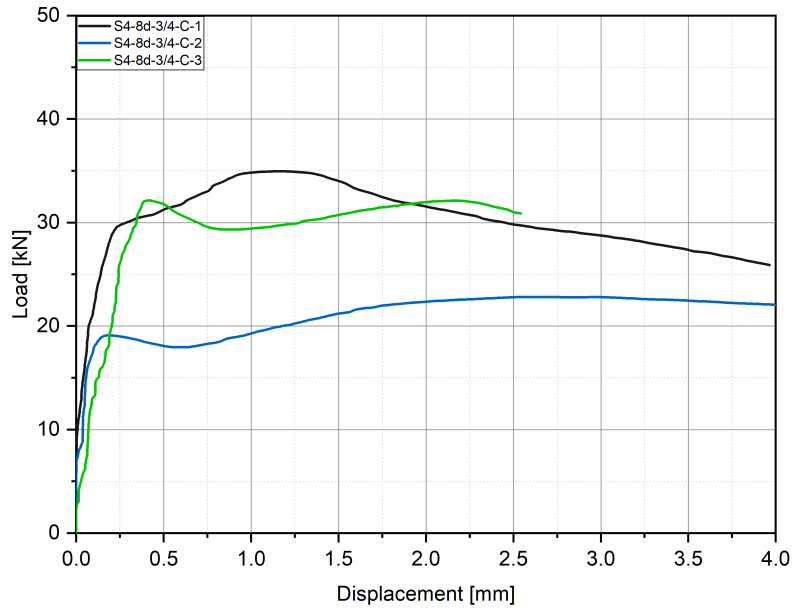
FIGURE C.50: S4-8d-3/4-C - load versus displacement curves
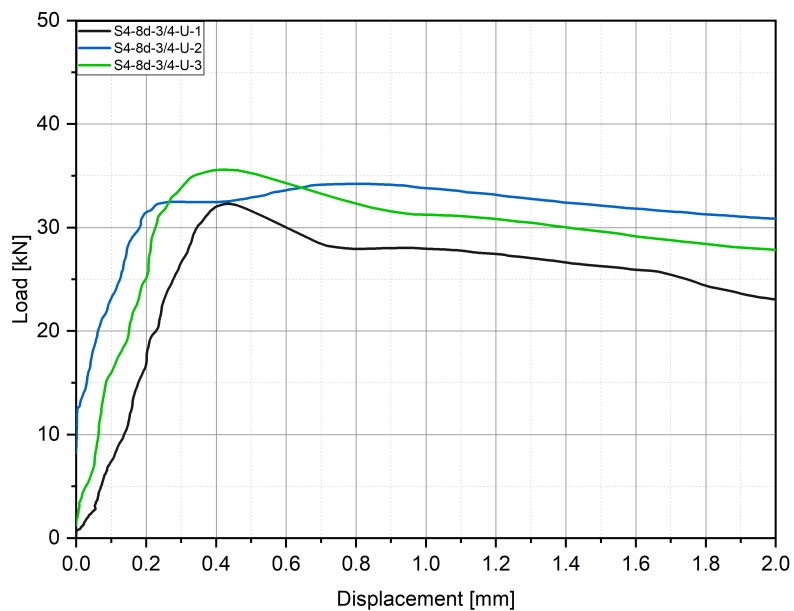
FIGURE C.51: S4-8d-3/4-U - load versus displacement curves
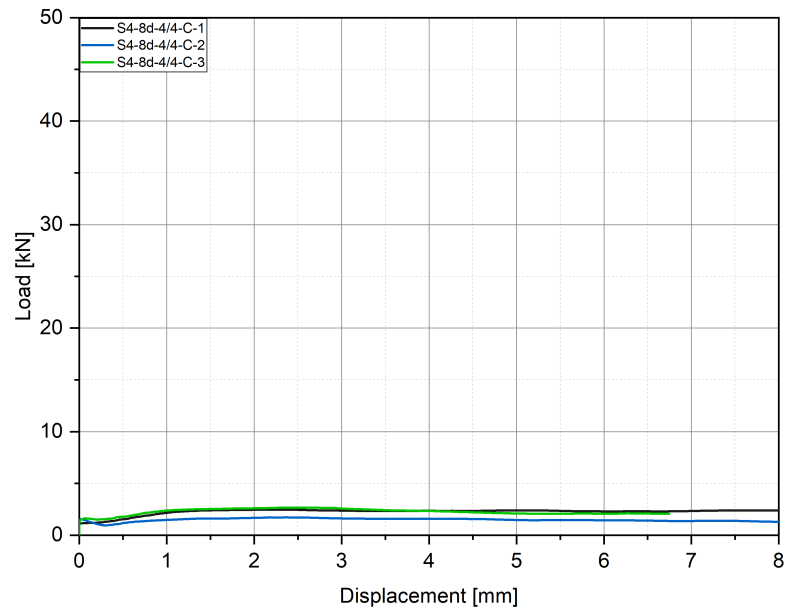
FIGURE C.52: S4-8d-4/4-C - load versus displacement curves
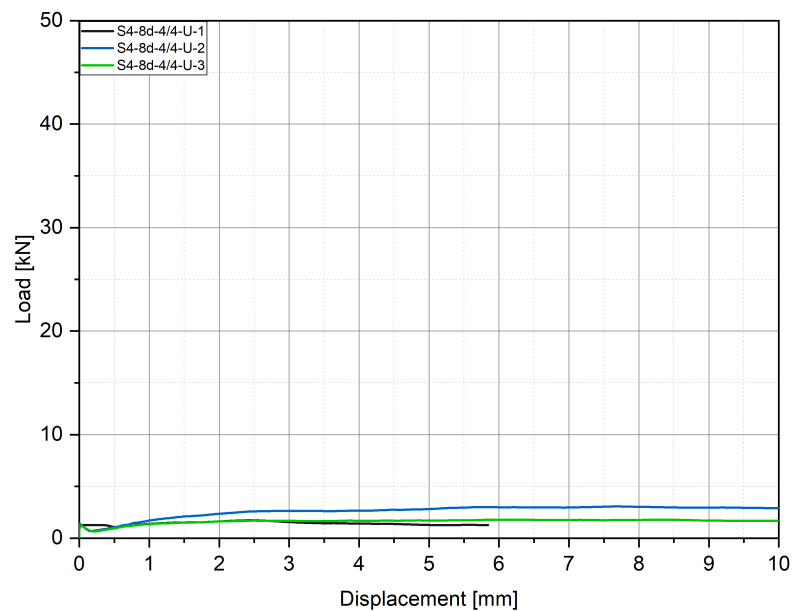
FIGURE C.53: S4-8d-4/4-U - load versus displacement curves

C.5 Diagrams for Table 7.5
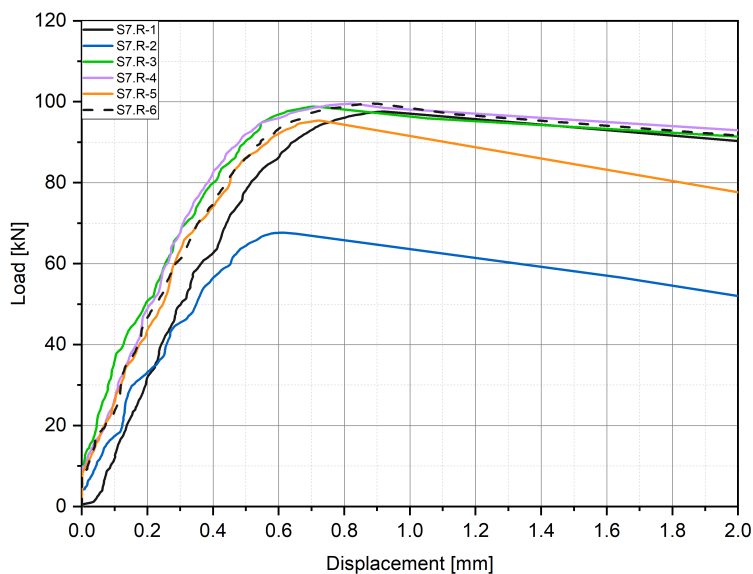
FIGURE C.54: S7.R - load versus displacement curves
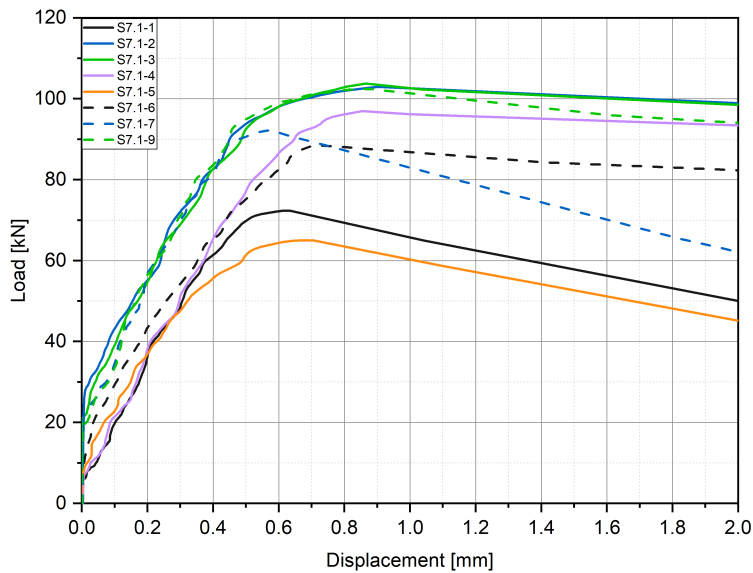
FIGURE C.55: S7.1 - load versus displacement curves
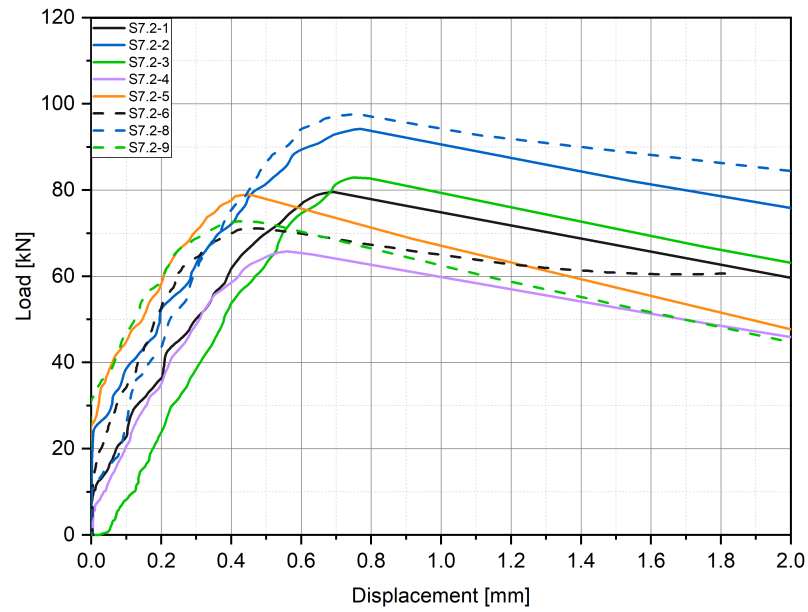
FIGURE C.56: S7.2 - load versus displacement curves
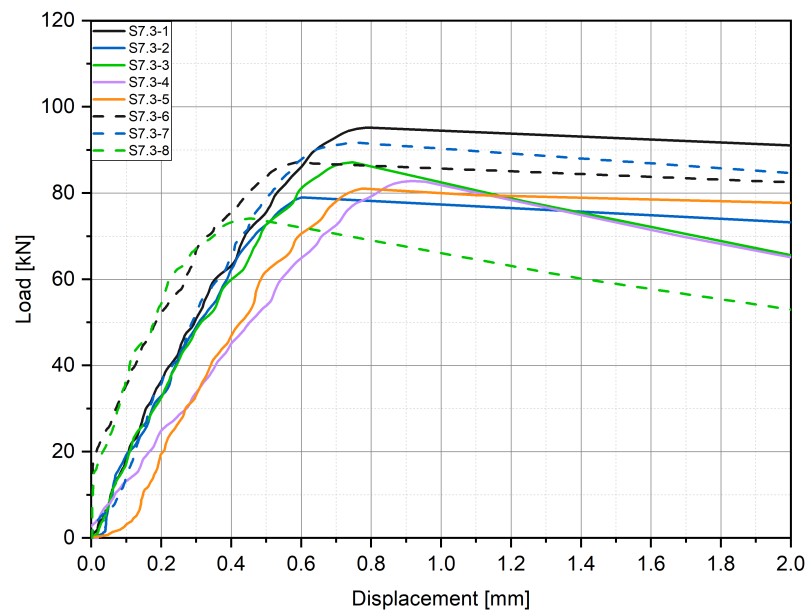
FIGURE C.57: S7.3 - load versus displacement curves
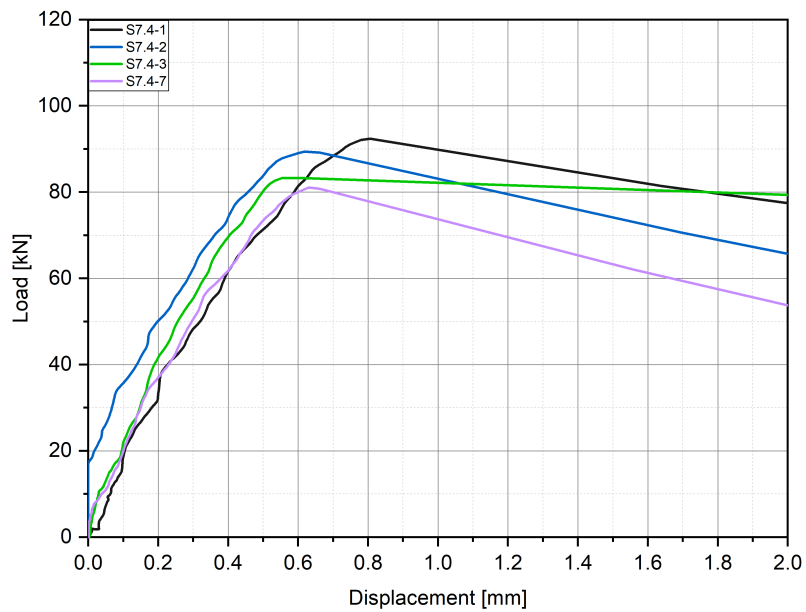
FIGURE C.58: S7.4 - load versus displacement curves

C.6 Diagrams for Table 7.6
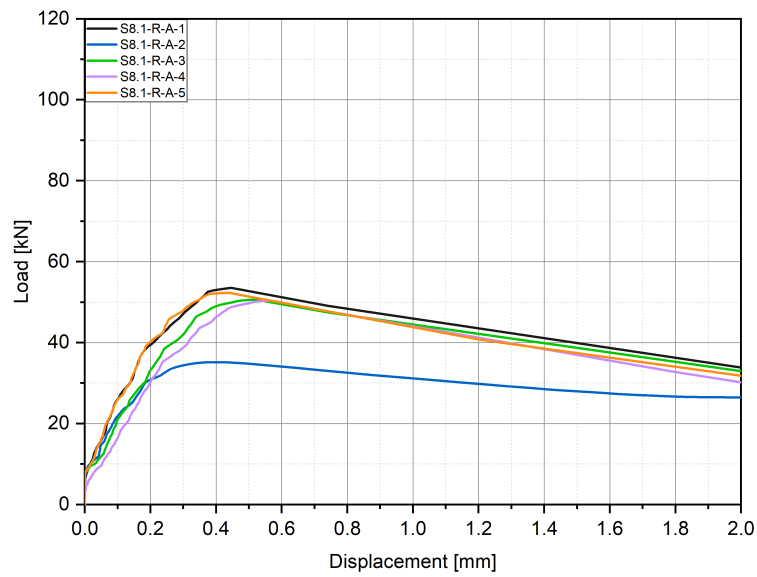
FIGURE C.59: S8.1-R-A - load versus displacement curves
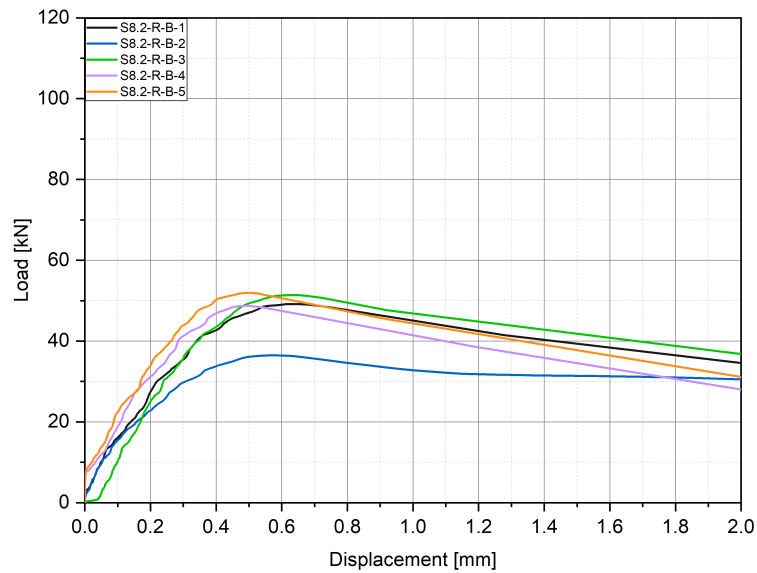
FIGURE C.60: S8.2-R-B - load versus displacement curves
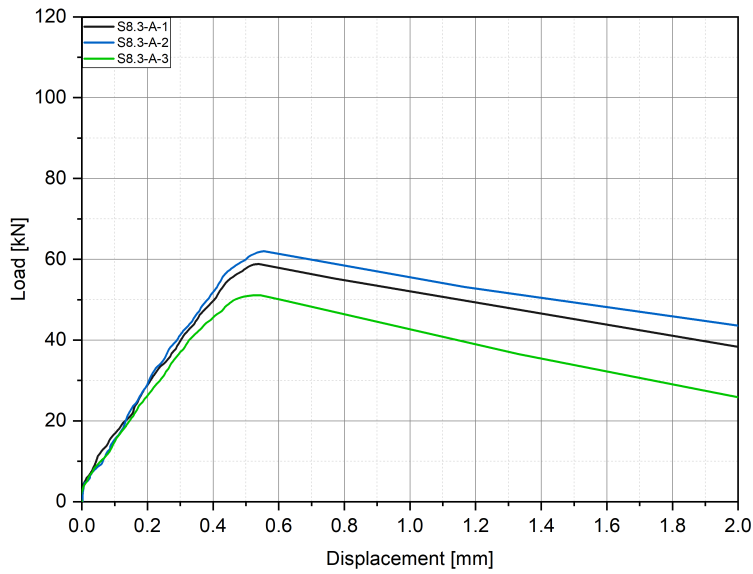
FIGURE C.61:   S8.3-A - load versus displacement
curves
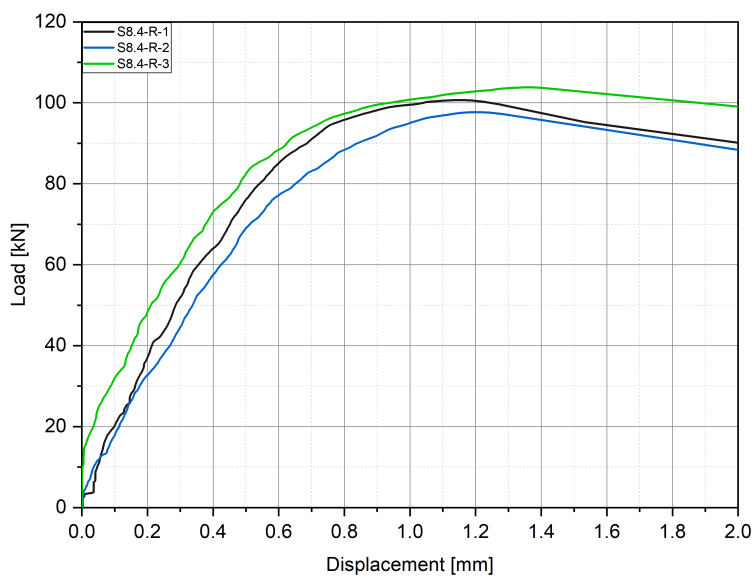
FIGURE C.62:   S8.4-R - load versus displacement
curves
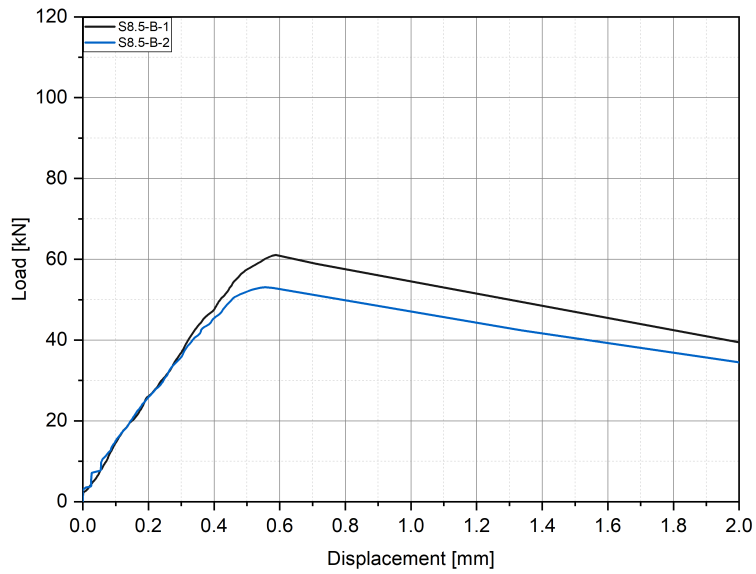
FIGURE C.63: S8.5-B - load versus displacement curves
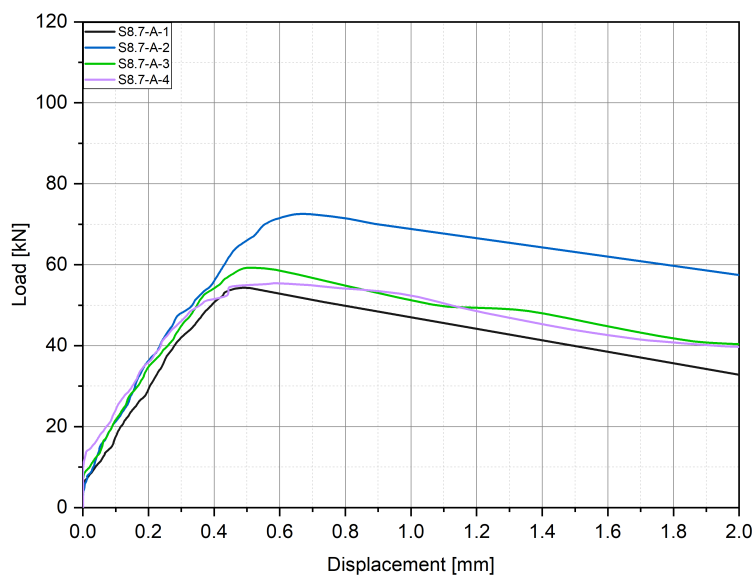
FIGURE C.64: S8.7-A - load versus displacement curves
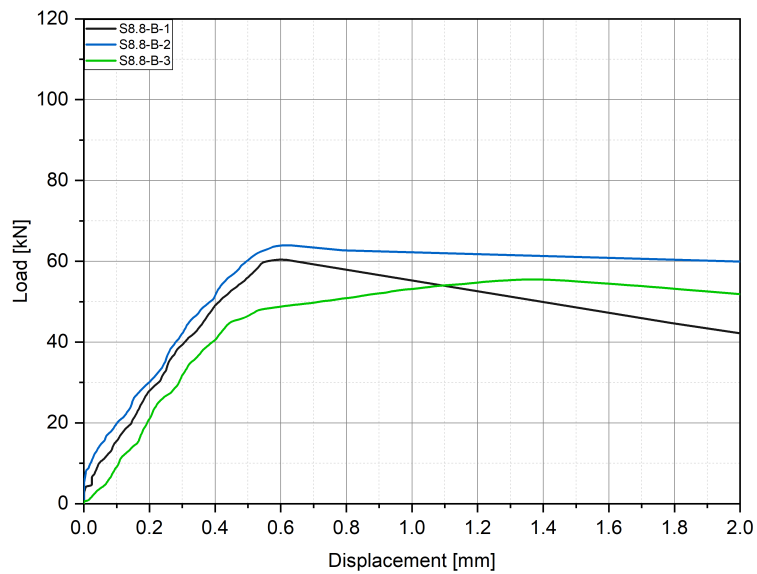
F<small>IGURE</small> C.65:   S8.8-B - load versus displacement
curves

C.7 Failure figures for Table 7.1

FIGURE C.66: S1.1-C - Failure of the anchors
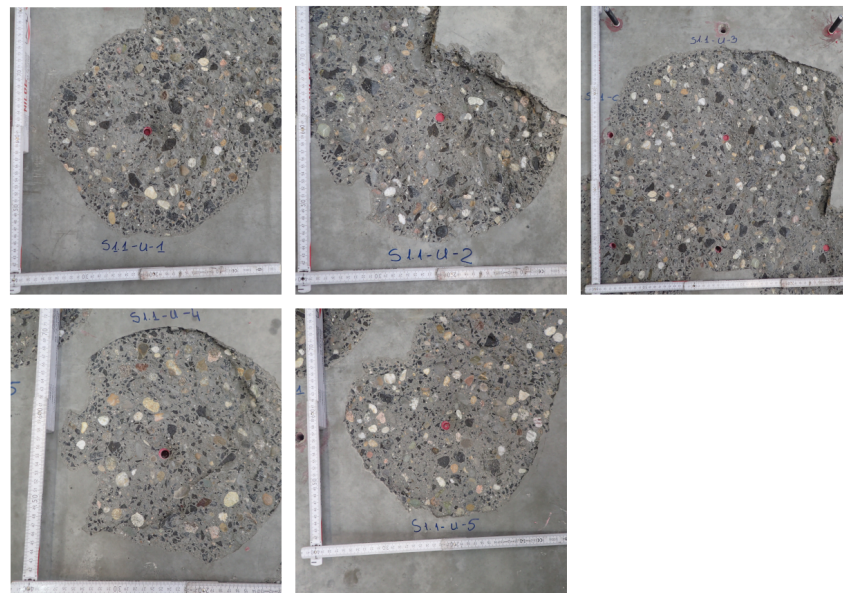
FIGURE C.67: S1.1-U - Failure of the anchors
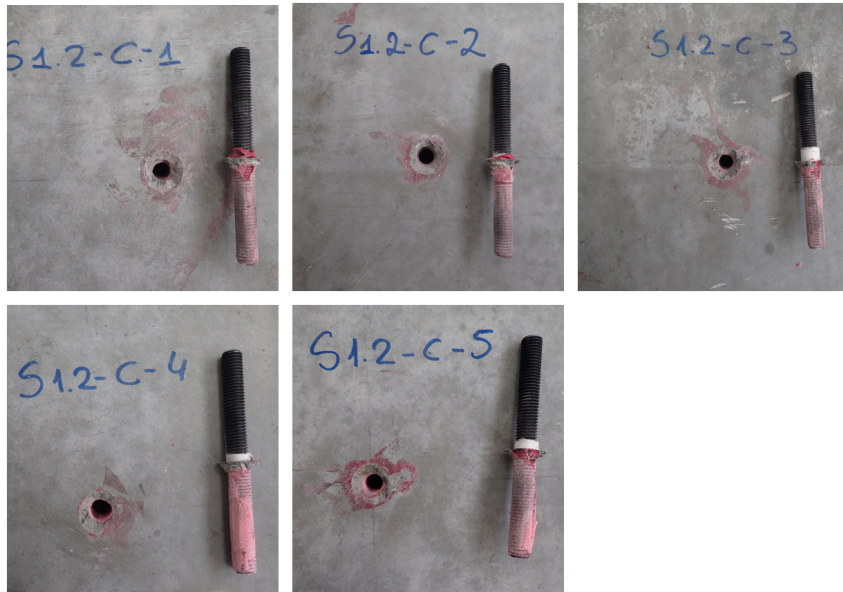
FIGURE C.68: S1.2-C - Failure of the anchors
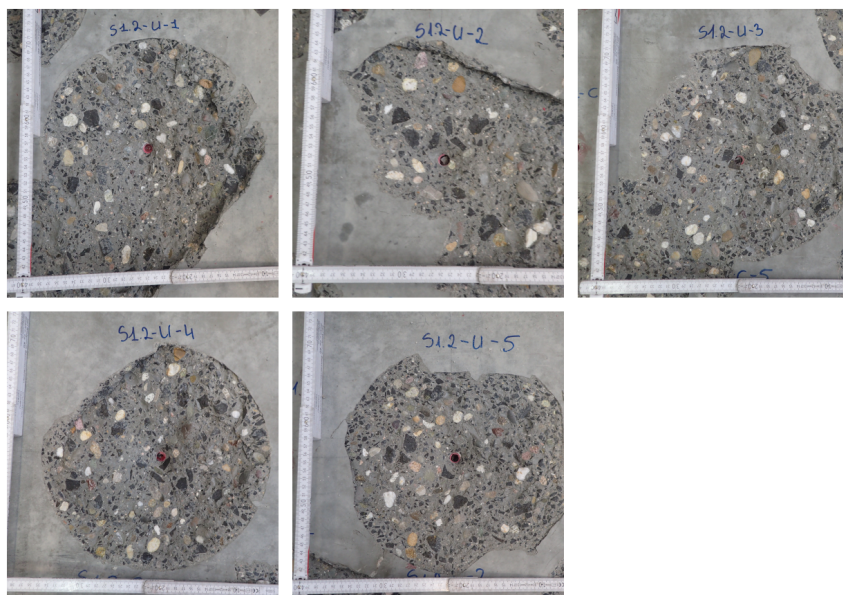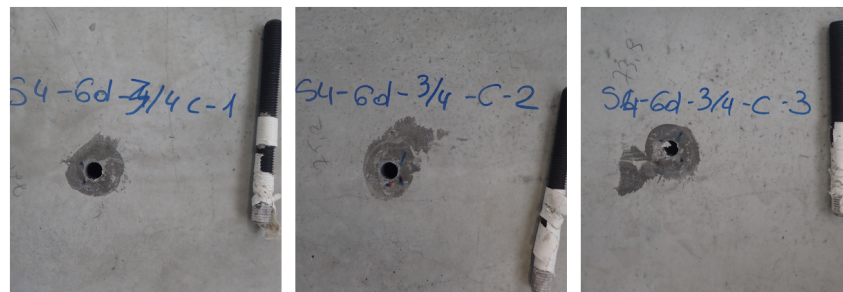

FIGURE C.69: S1.2-U - Failure of the anchors
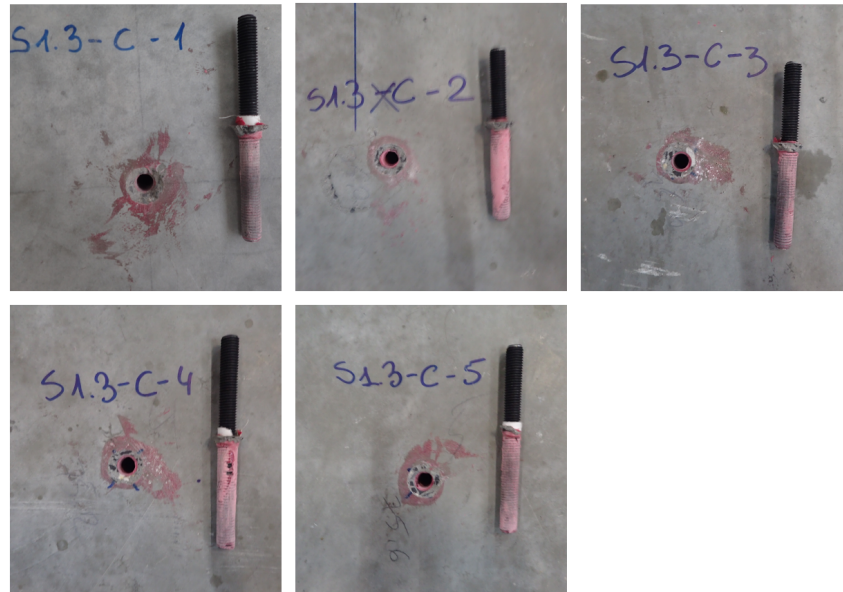
FIGURE C.70: S1.3-C - Failure of the anchors
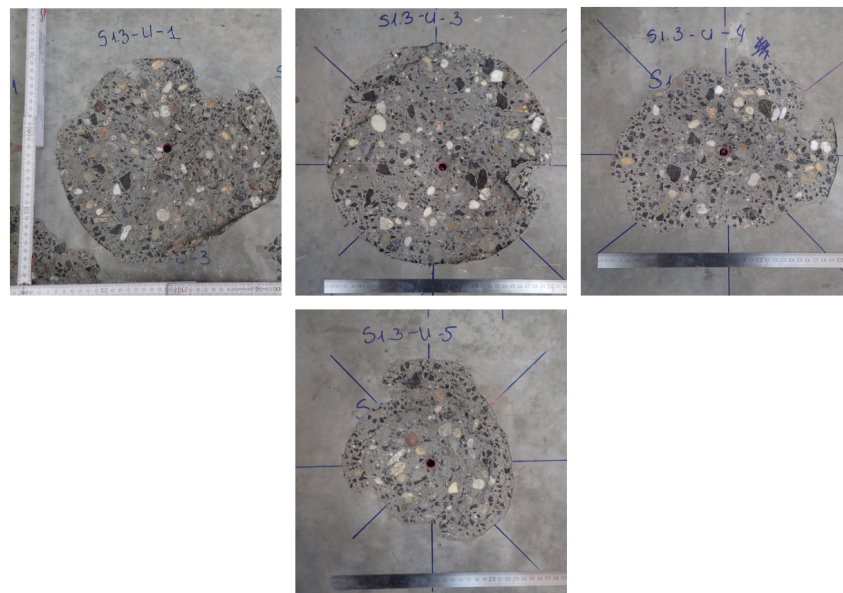
FIGURE C.71: S1.3-U - Failure of the anchors
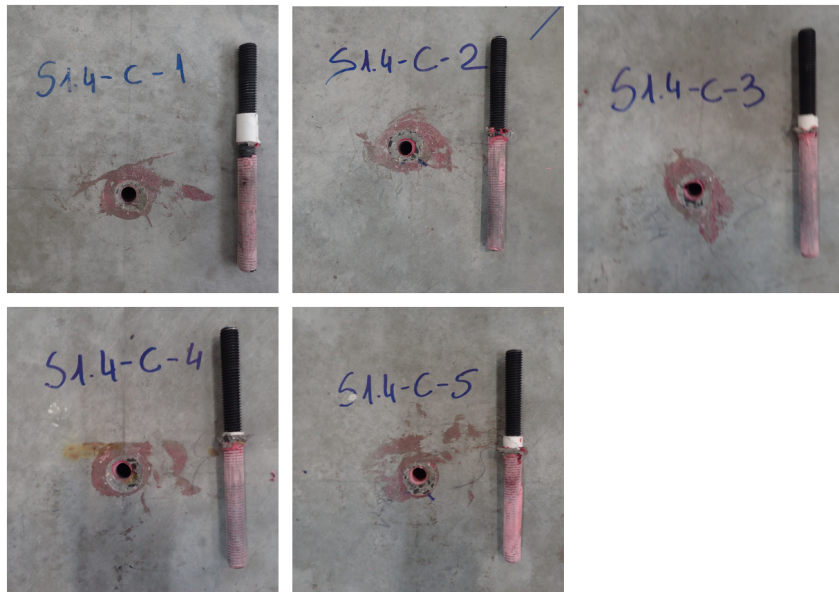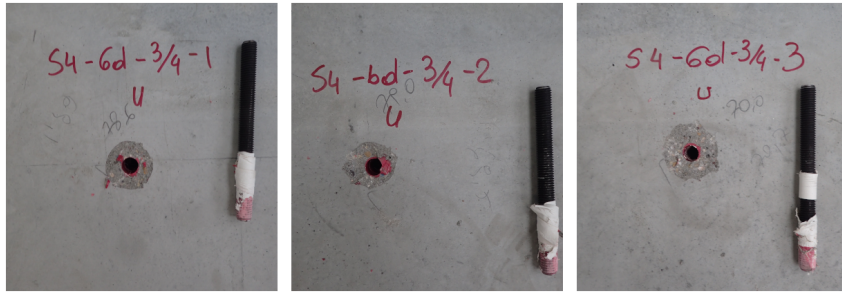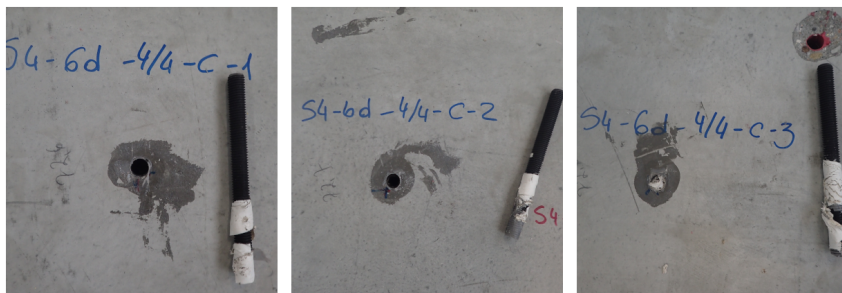
FIGURE C.72: S1.4-C - Failure of the anchors
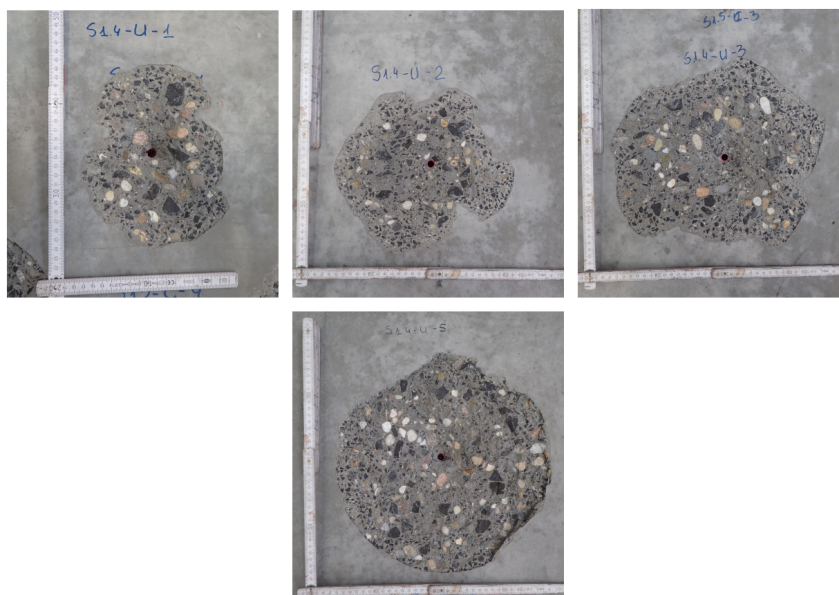
FIGURE C.73: S1.4-U - Failure of the anchors
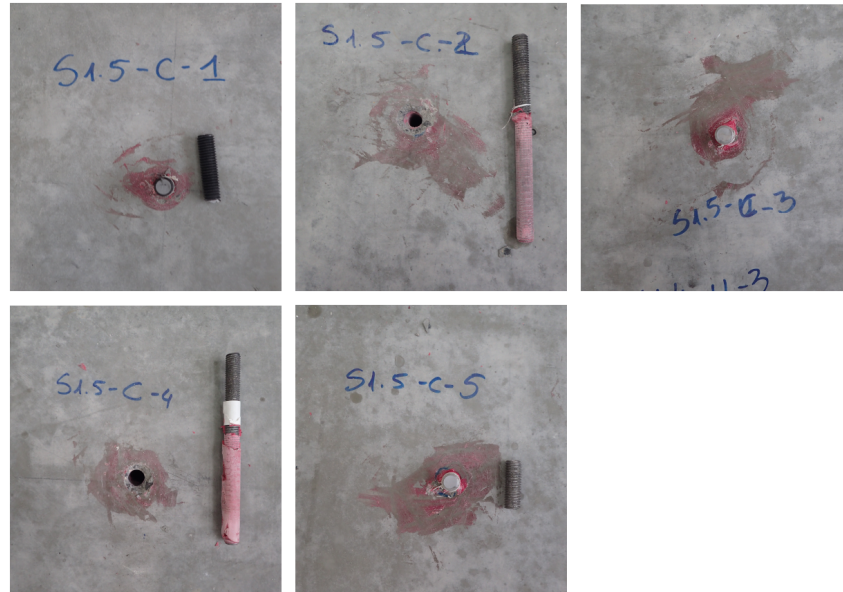
FIGURE C.74: S1.5-C - Failure of the anchors
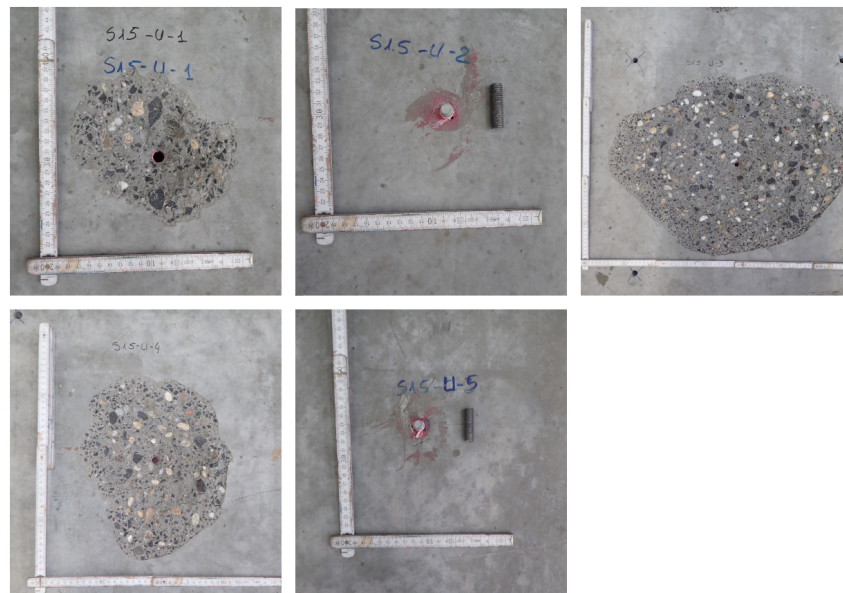
FIGURE C.75: S1.5-U - Failure of the anchors

C.8   Failure figures for Table 7.2
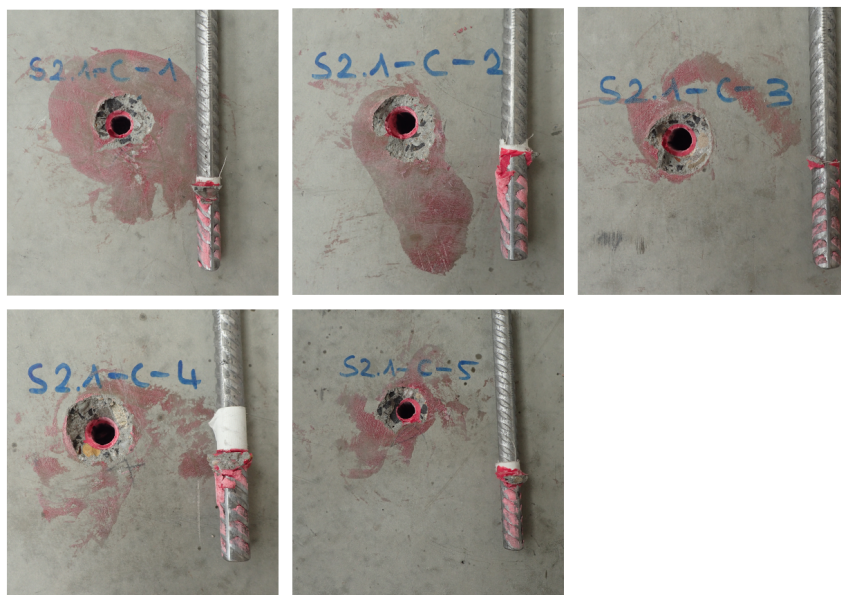
FIGURE C.76: S2.1-C - Failure of the anchors
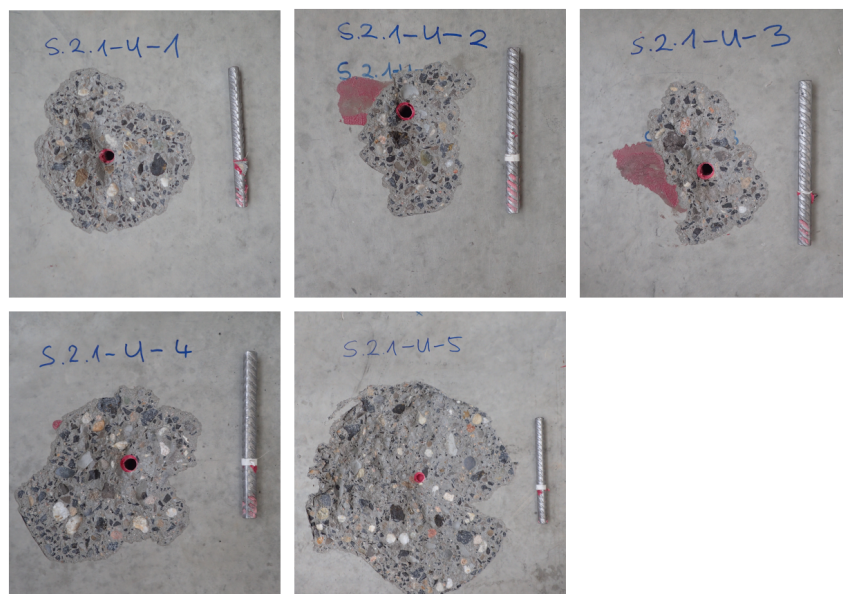
FIGURE C.77: S2.1-U - Failure of the anchors
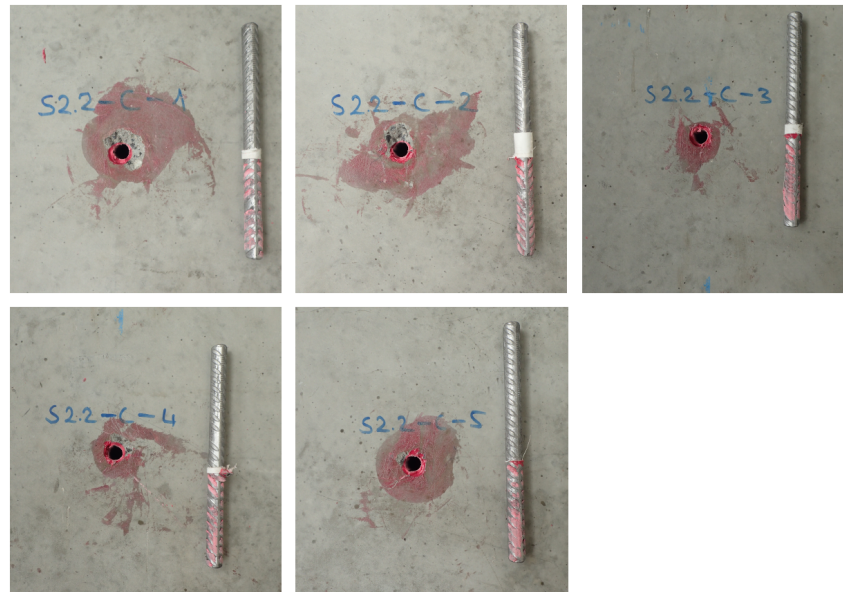
FIGURE C.78: S2.2-C - Failure of the anchors
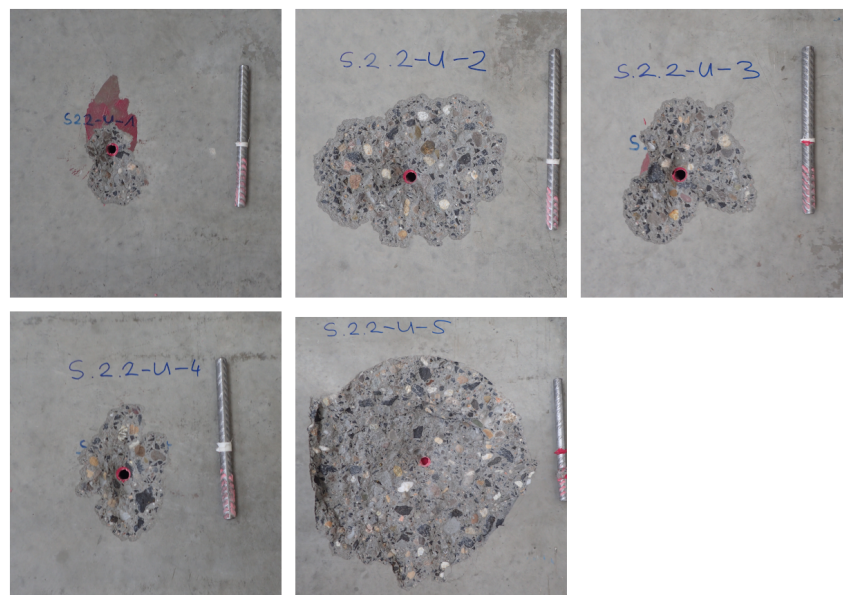
FIGURE C.79: S2.2-U - Failure of the anchors
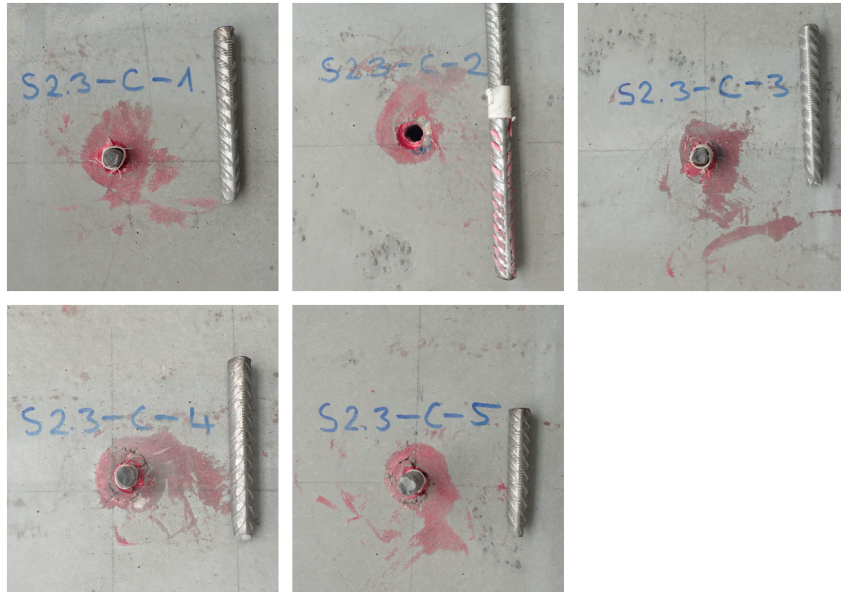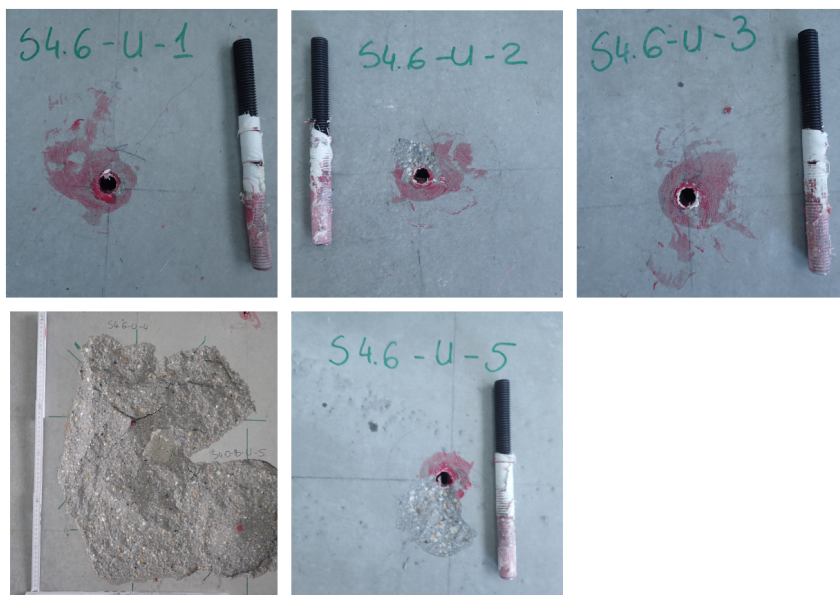
FIGURE C.80: S2.3-C - Failure of the anchors
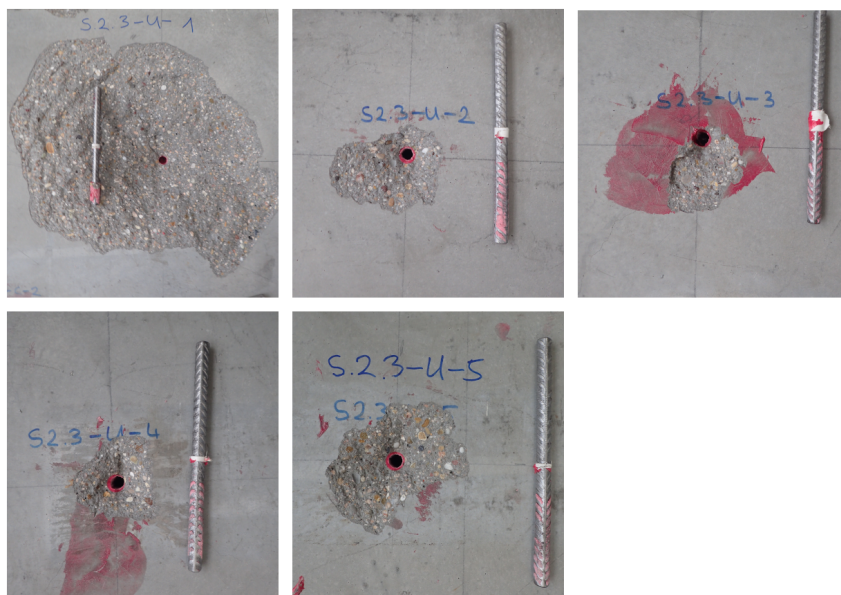
FIGURE C.81: S2.3-U - Failure of the anchors

C.9 Failure figures for Table 7.3
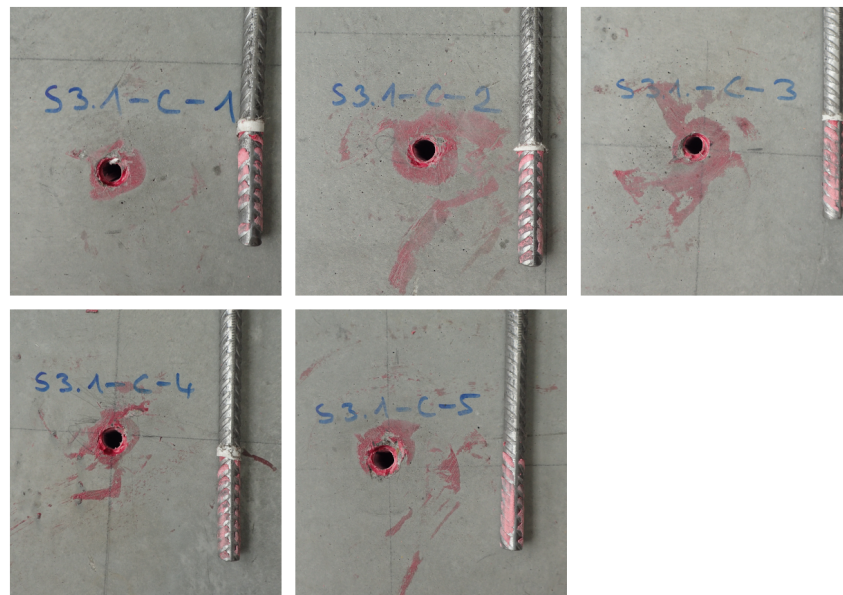
FIGURE C.82: S3.1 - Failure of the anchors
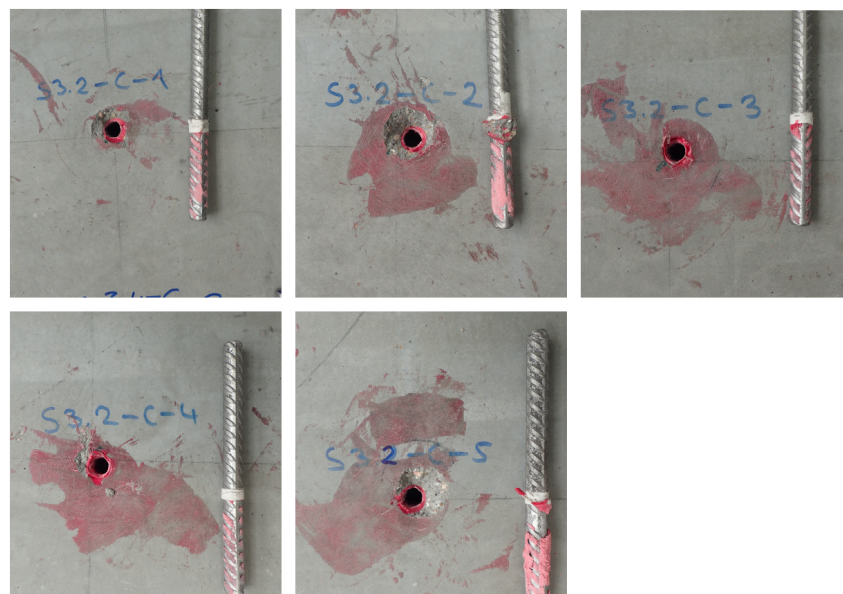
FIGURE C.83: S3.2 - Failure of the anchors
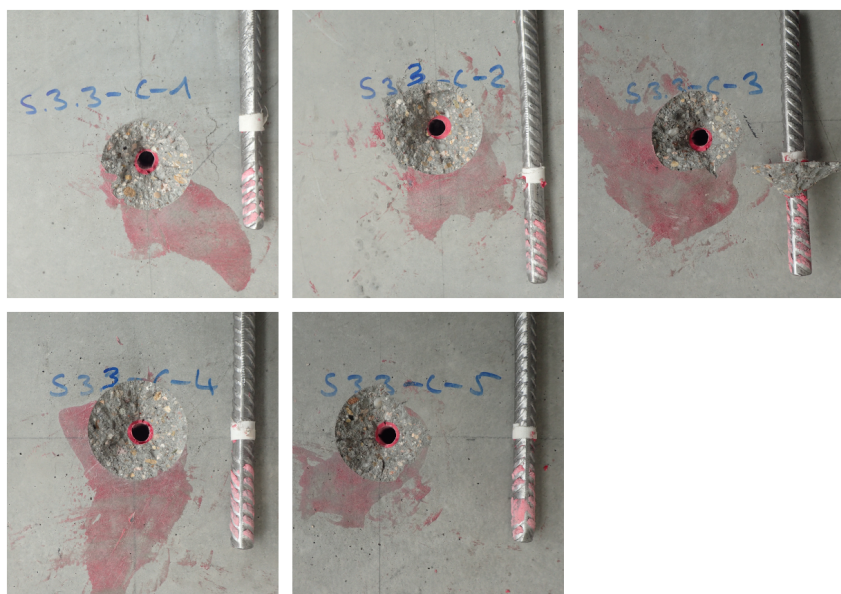
FIGURE C.84: S3.3 - Failure of the anchors
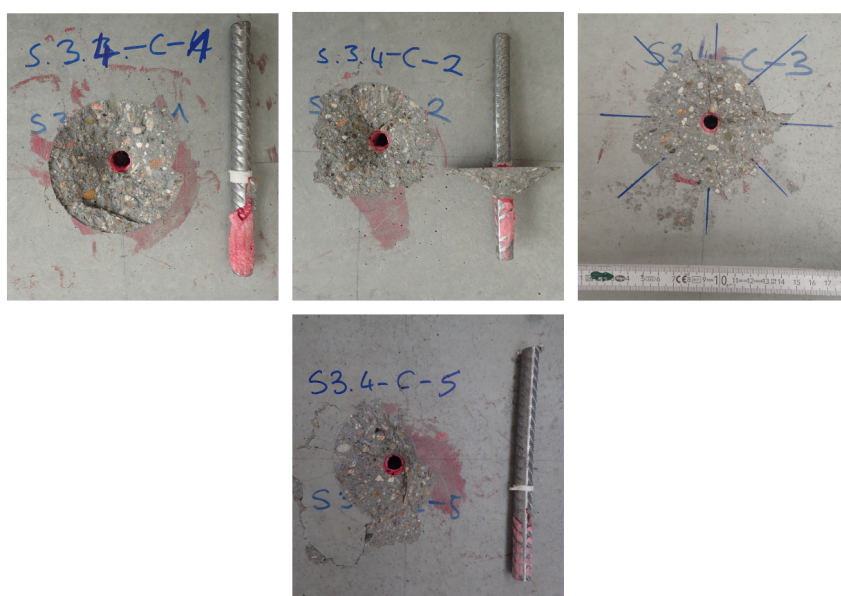
FIGURE C.85: S3.4 - Failure of the anchors
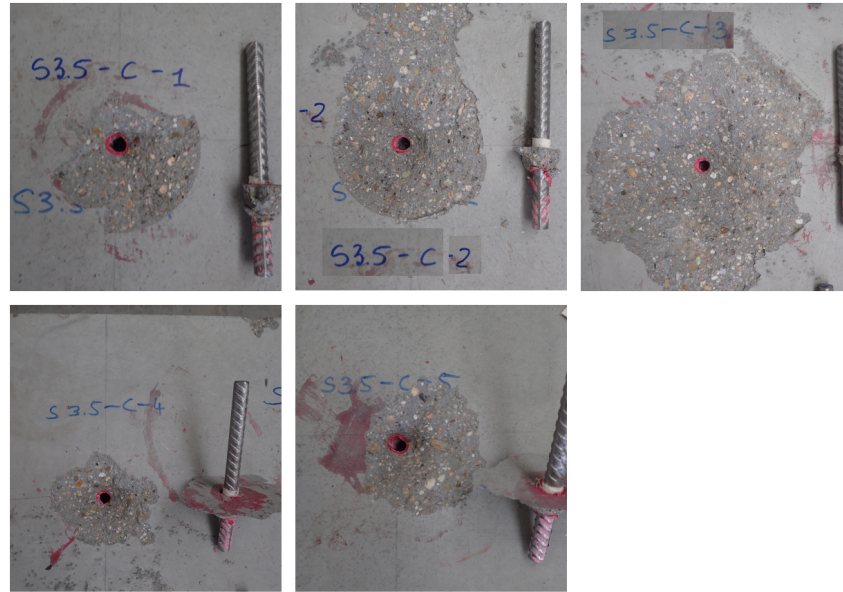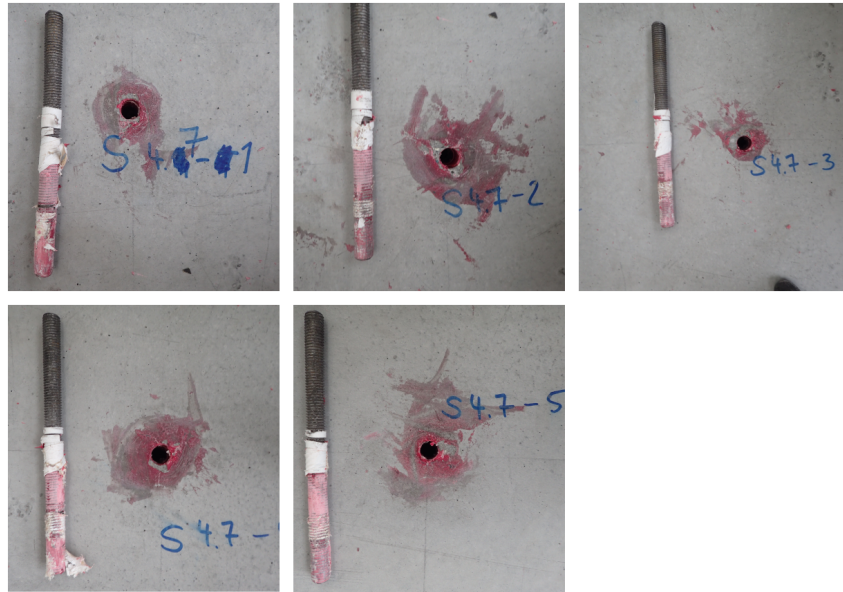
FIGURE C.86: S3.5 - Failure of the anchors

C.10 Failure figures for Table 7.4
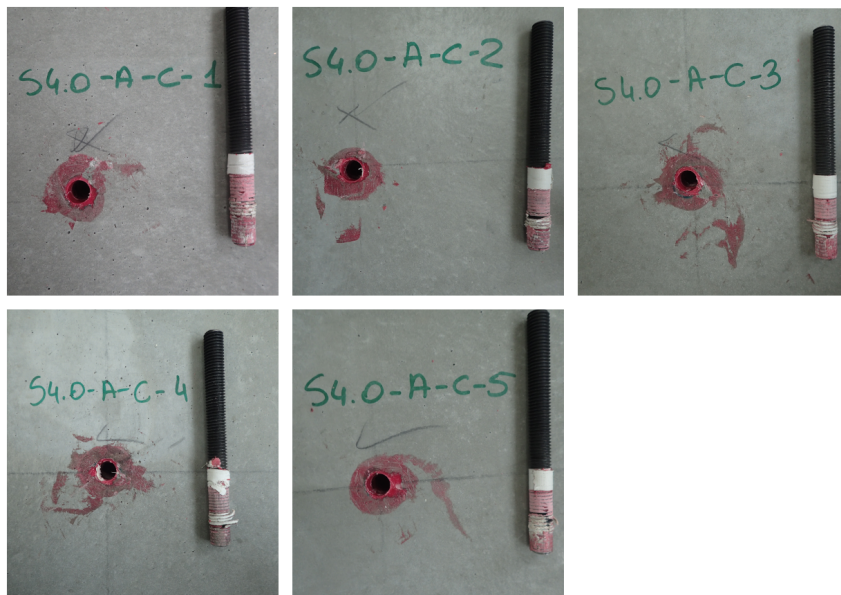
FIGURE C.87: S4.0-A-C - Failure of the anchors
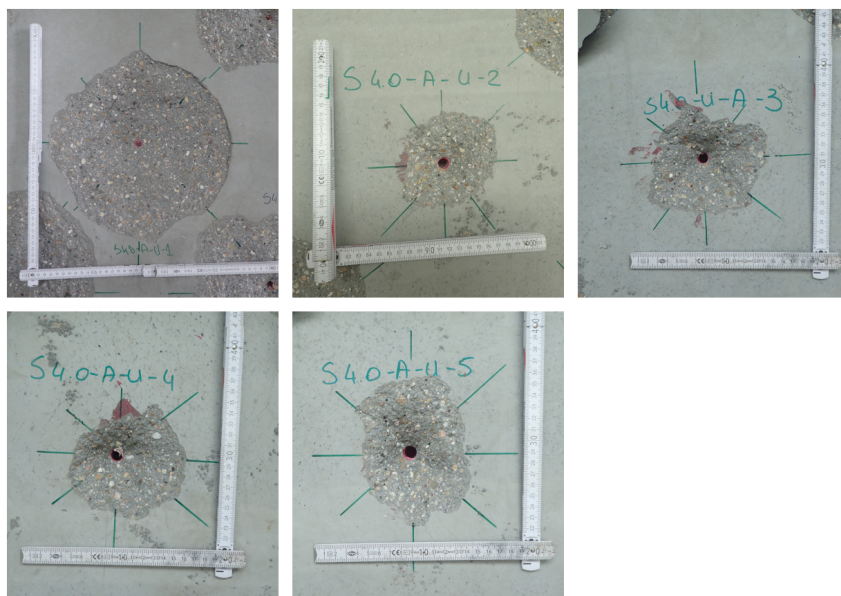
FIGURE C.88: S4.0-A-U - Failure of the anchors
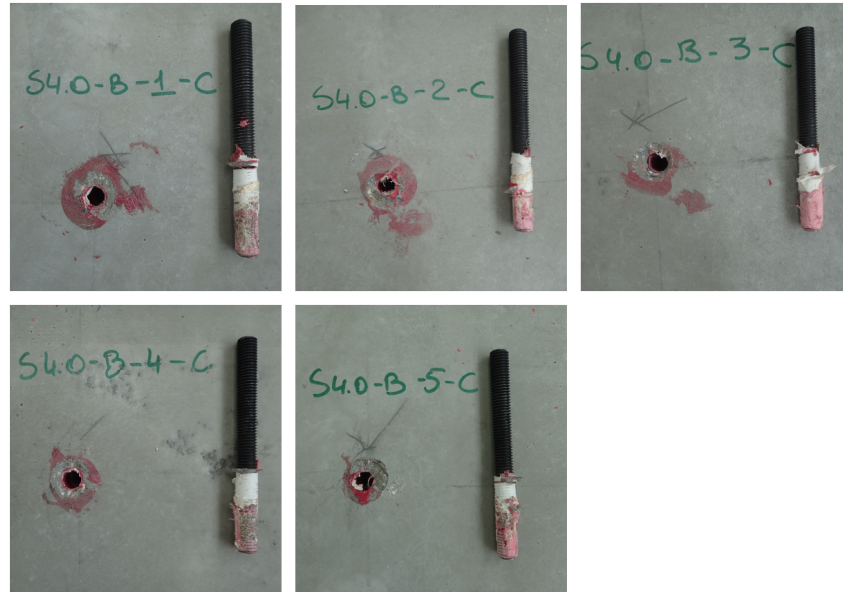
FIGURE C.89: S4.0-B-C - Failure of the anchors
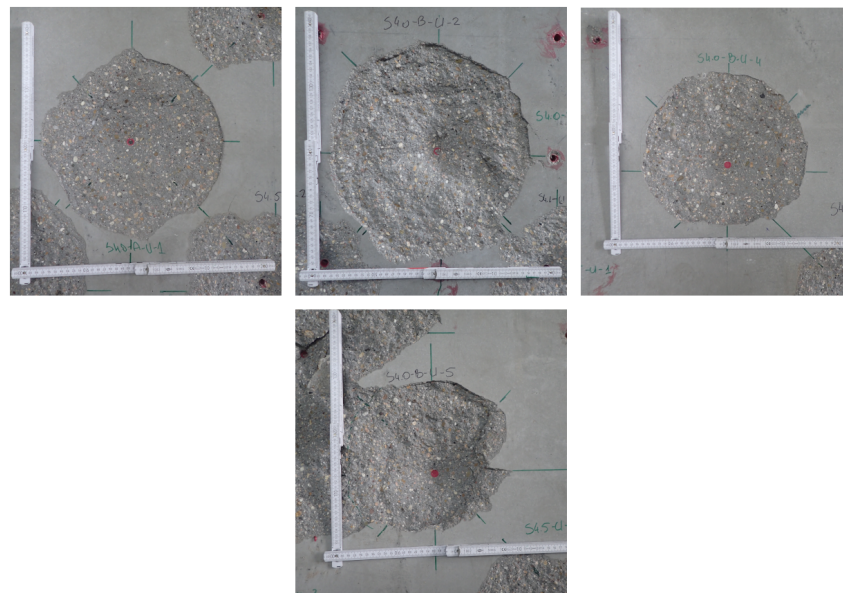
FIGURE C.90: S4.0-B-U - Failure of the anchors
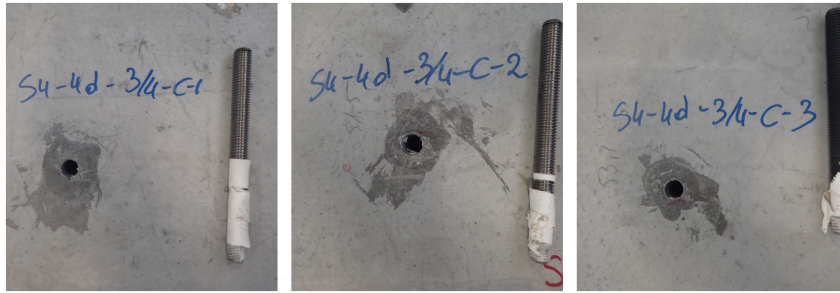
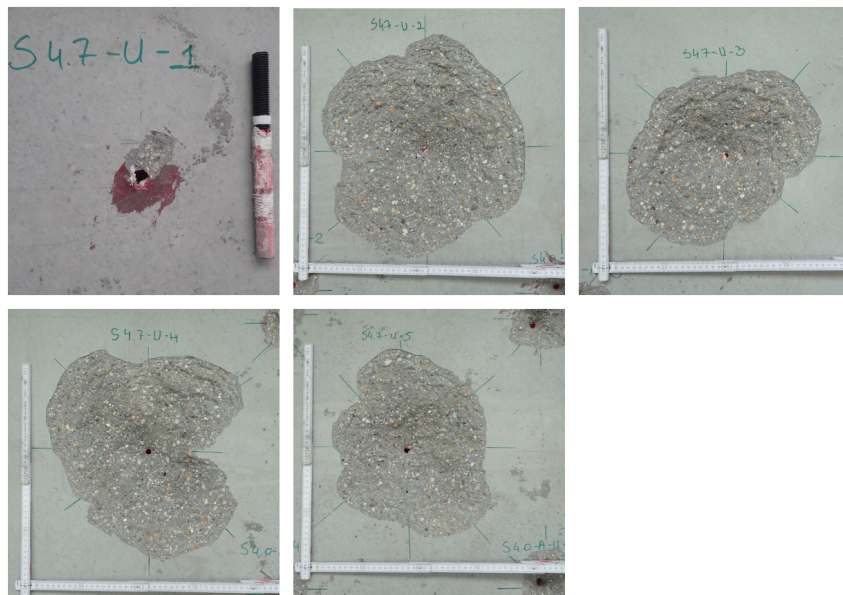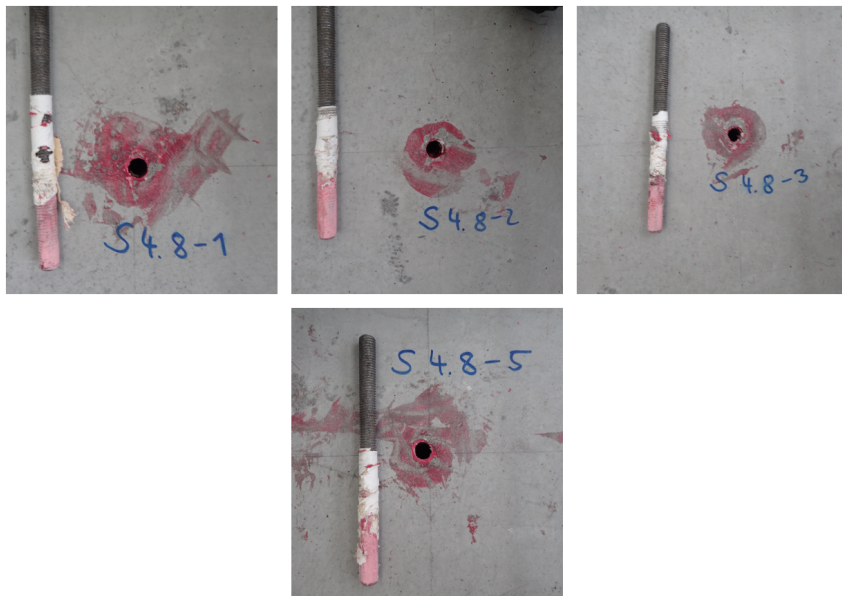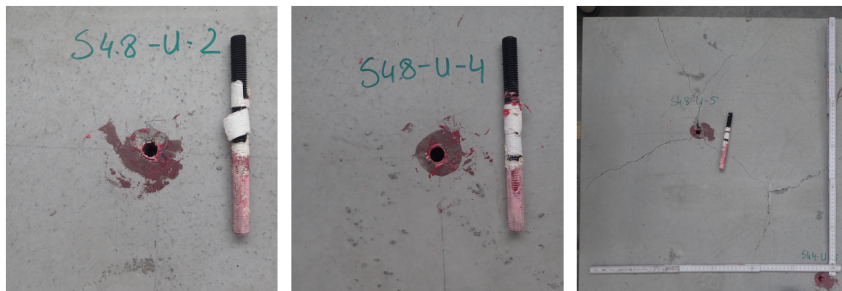FIGURE C.91: S4-4d-3/4-C - Failure of the anchors
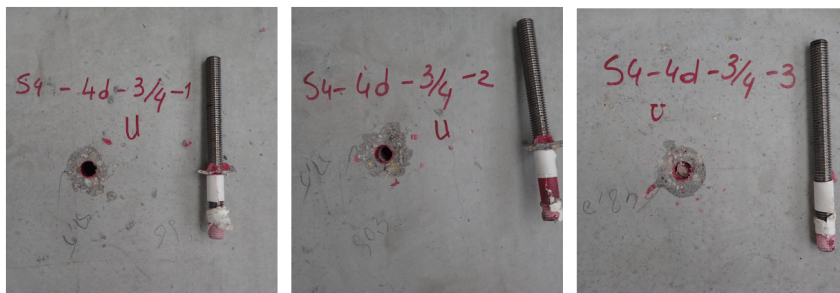
FIGURE C.92: S4-4d-3/4-U - Failure of the anchors
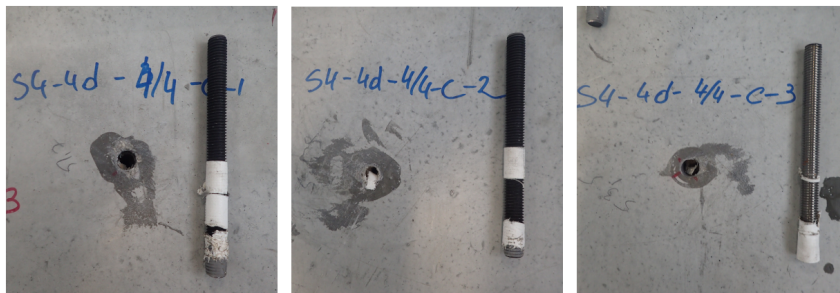
FIGURE C.93: S4-4d-4/4-C - Failure of the anchors
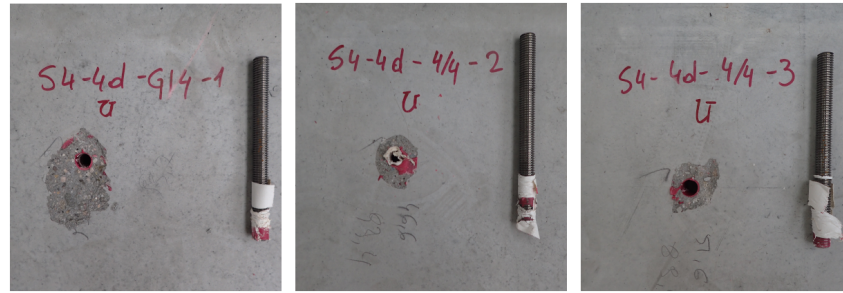
FIGURE C.94: S4-4d-4/4-U - Failure of the anchors

FIGURE C.95: S4.1-C - Failure of the anchors
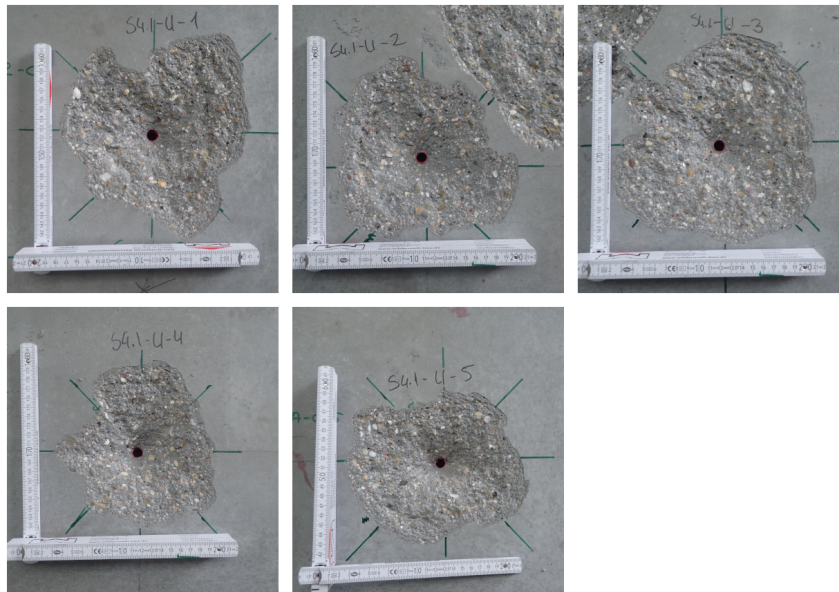
FIGURE C.96: S4.1-U - Failure of the anchors
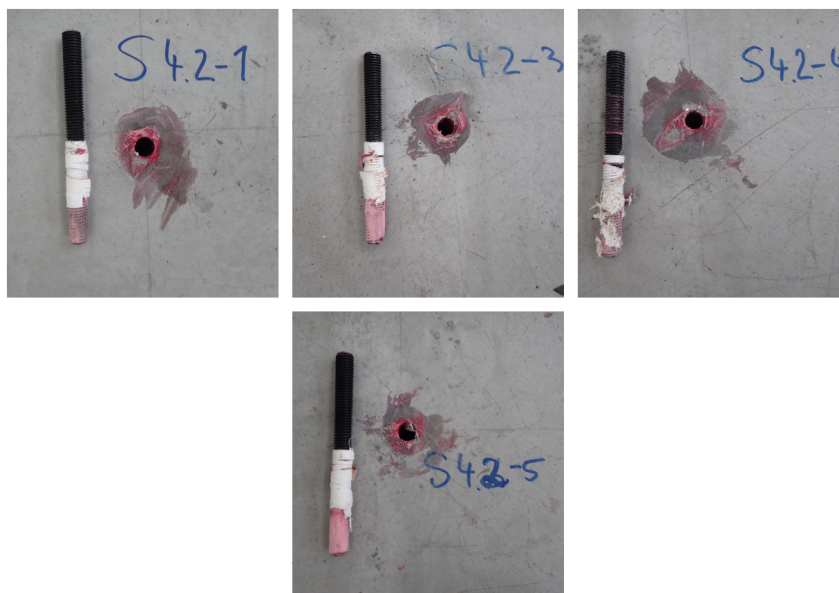
FIGURE C.97: S4.2-C - Failure of the anchors
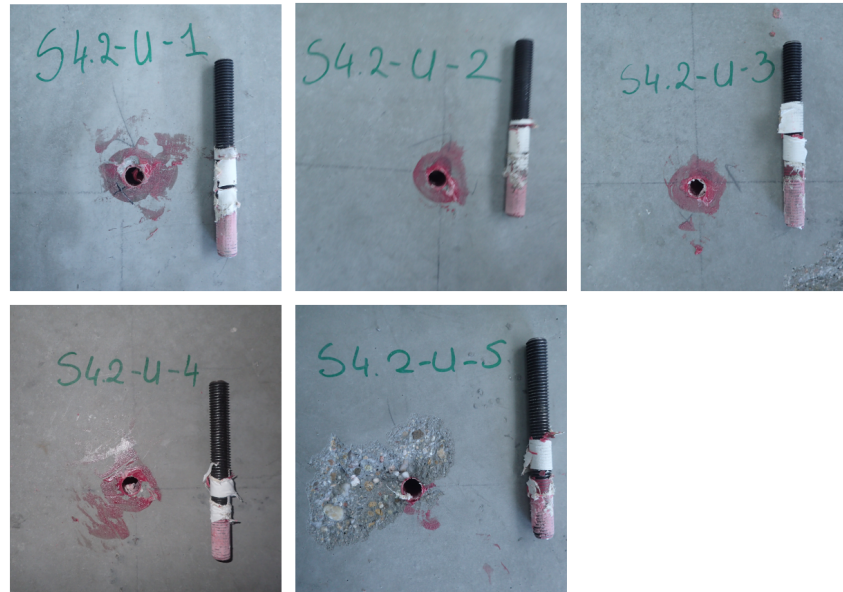
FIGURE C.98: S4.2-U - Failure of the anchors

FIGURE C.99: S4.3-C - Failure of the anchors
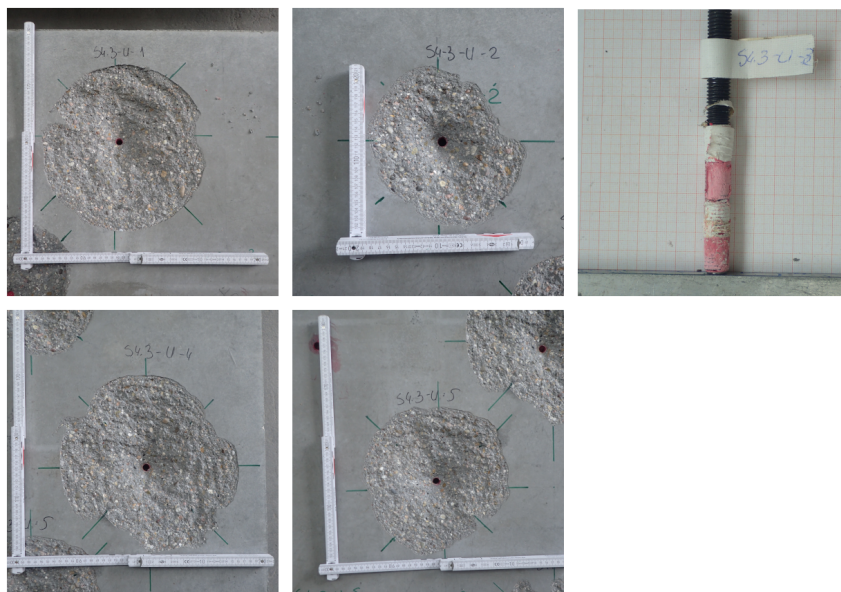
FIGURE C.100: S4.3-U - Failure of the anchors
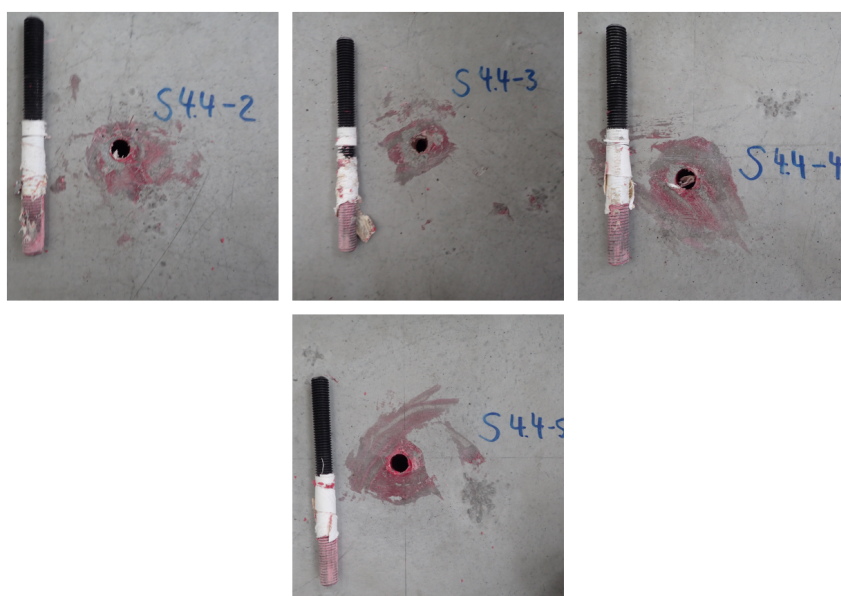
FIGURE C.101: S4.4-C - Failure of the anchors
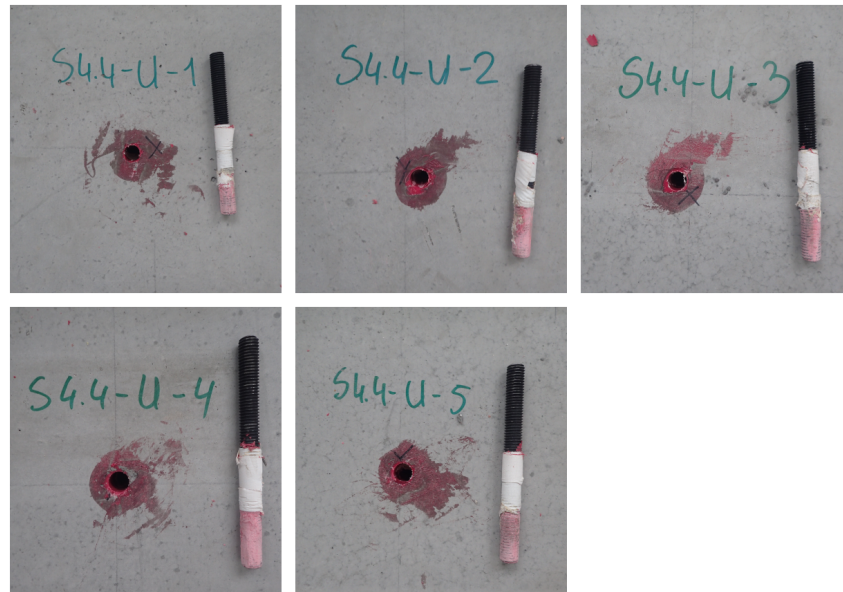
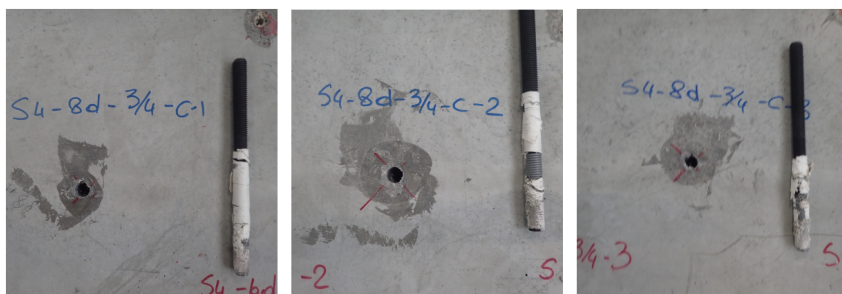FIGURE C.102: S4.4-U - Failure of the anchors

FIGURE C.103: S4-6d-3/4-C - Failure of the anchors
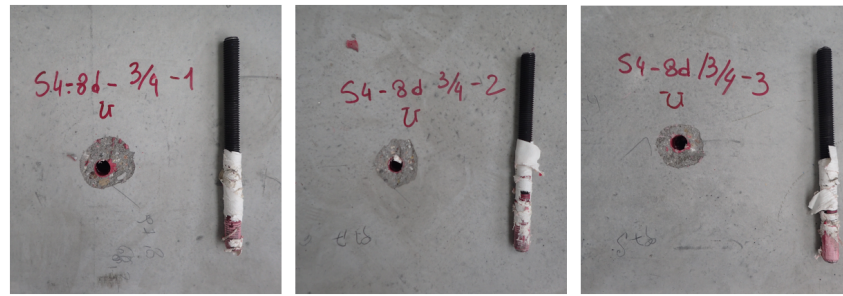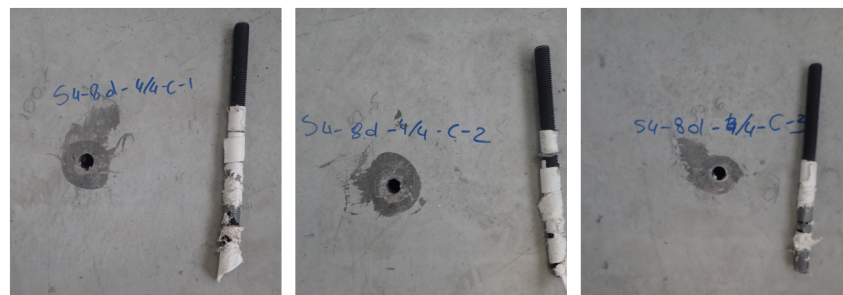
FIGURE C.104: S4-6d-3/4-U - Failure of the anchors

FIGURE C.105: S4-6d-4/4-C - Failure of the anchors
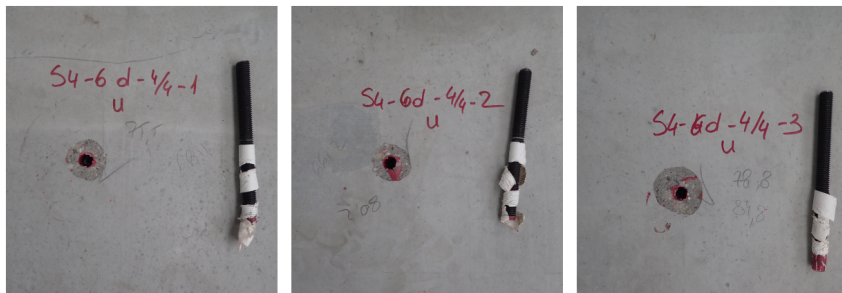
FIGURE C.106: S4-6d-4/4-U - Failure of the anchors

FIGURE C.107: S4.5-C - Failure of the anchors

FIGURE C.108: S4.5-U - Failure of the anchors

FIGURE C.109: S4.6-C - Failure of the anchors

FIGURE C.110: S4.6-U - Failure of the anchors

FIGURE C.111: S4.7-C - Failure of the anchors

FIGURE C.112: S4.7-U - Failure of the anchors

FIGURE C.113: S4.8-C - Failure of the anchors

FIGURE C.114: S4.8-U - Failure of the anchors

FIGURE C.115: S4-8d-3/4-C - Failure of the anchors

FIGURE C.116: S4-8d-3/4-U - Failure of the anchors

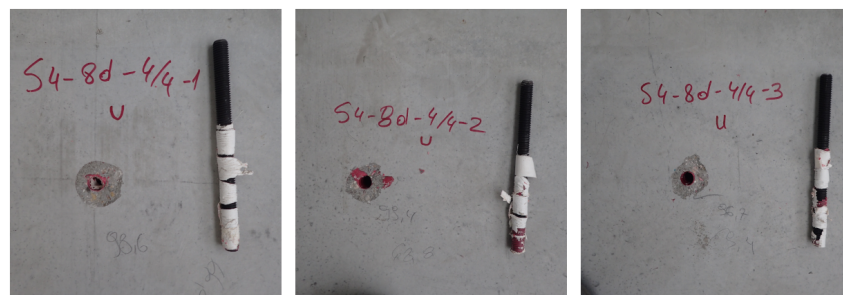FIGURE C.117: S4-8d-4/4-C - Failure of the anchors

FIGURE C.118: S4-8d-4/4-U - Failure of the anchors

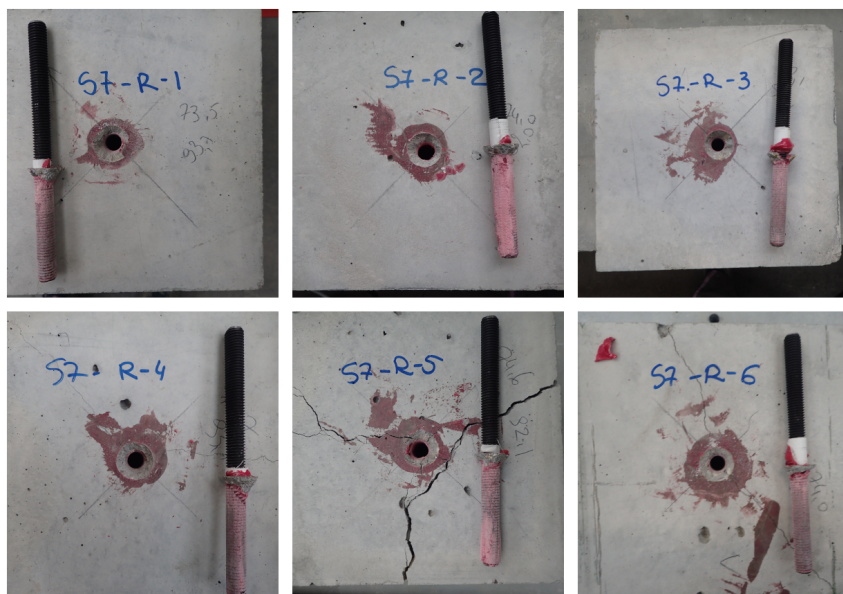## C.11   Failure figures for Table 7.5

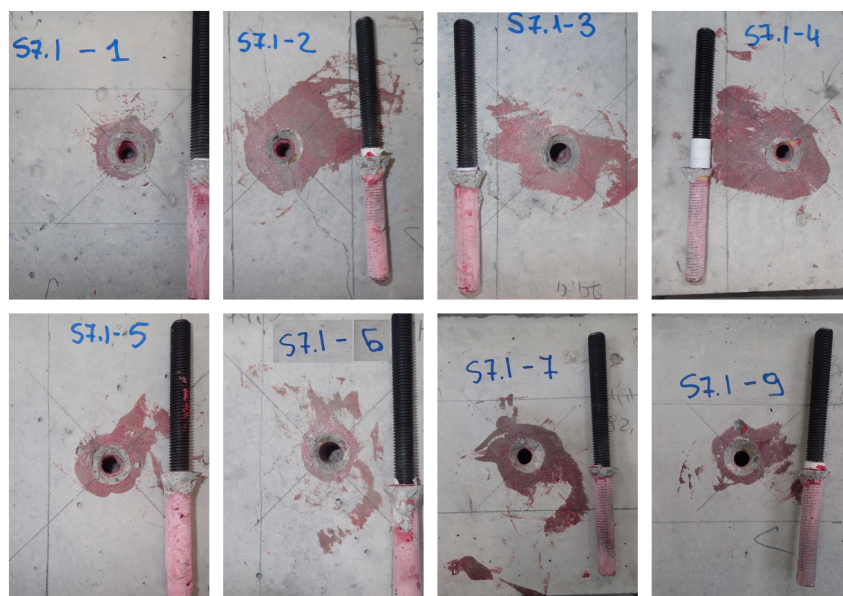

FIGURE C.119: S7.R - Failure of the anchors
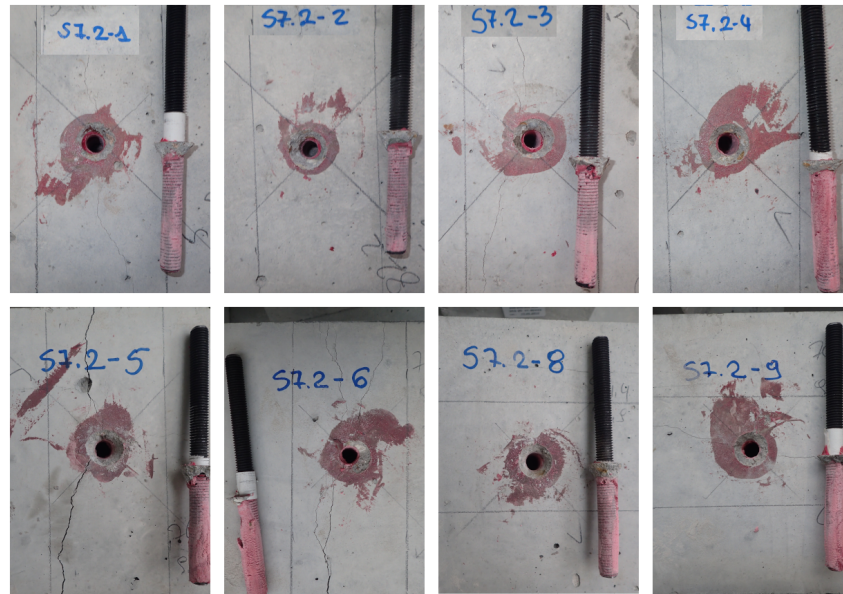

FIGURE C.120: S7.1 - Failure of the anchors

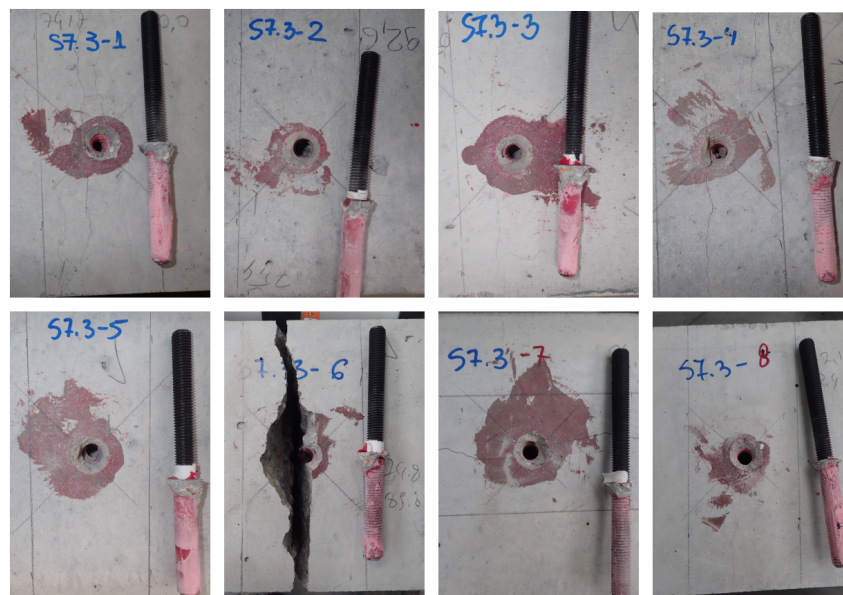FIGURE C.121: S7.2 - Failure of the anchors

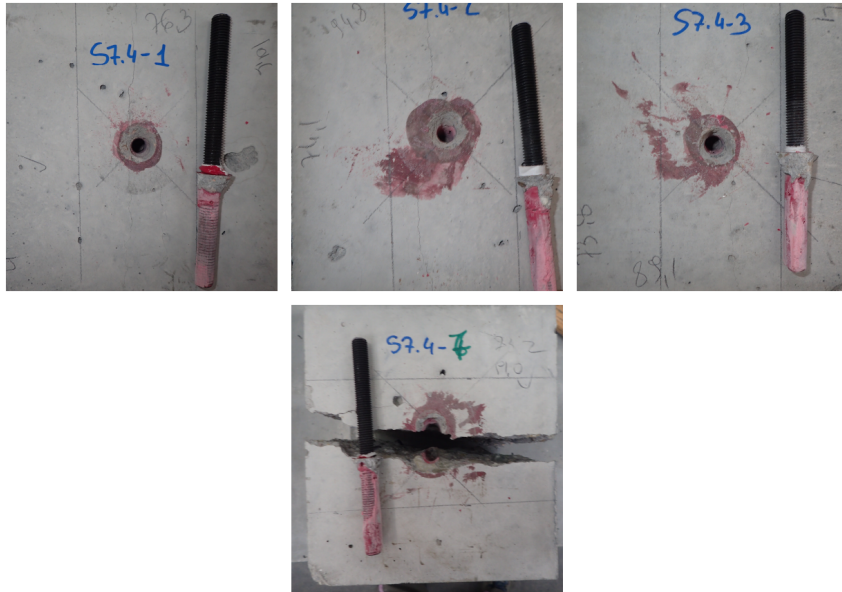FIGURE C.122: S7.3 - Failure of the anchors

FIGURE C.123: S7.4 - Failure of the anchors

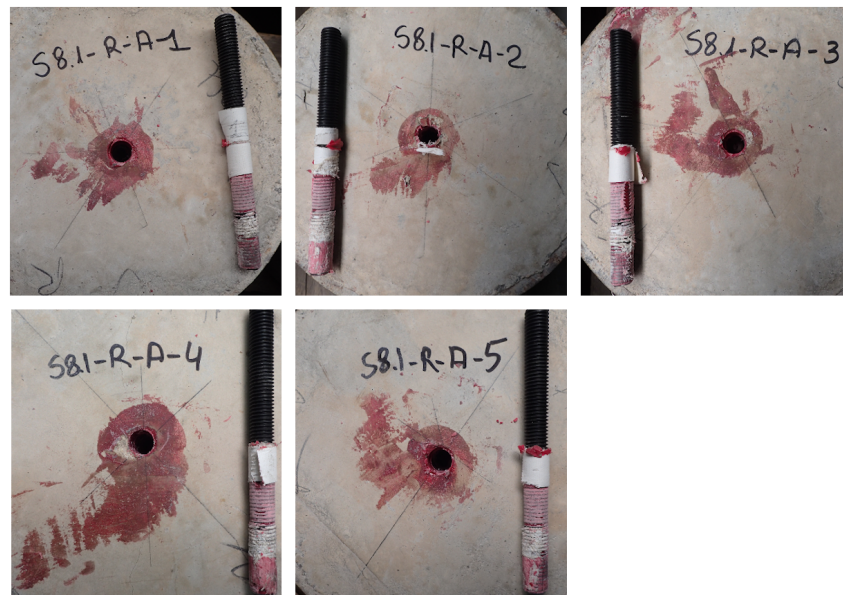## C.12 Failure figures for Table 7.6

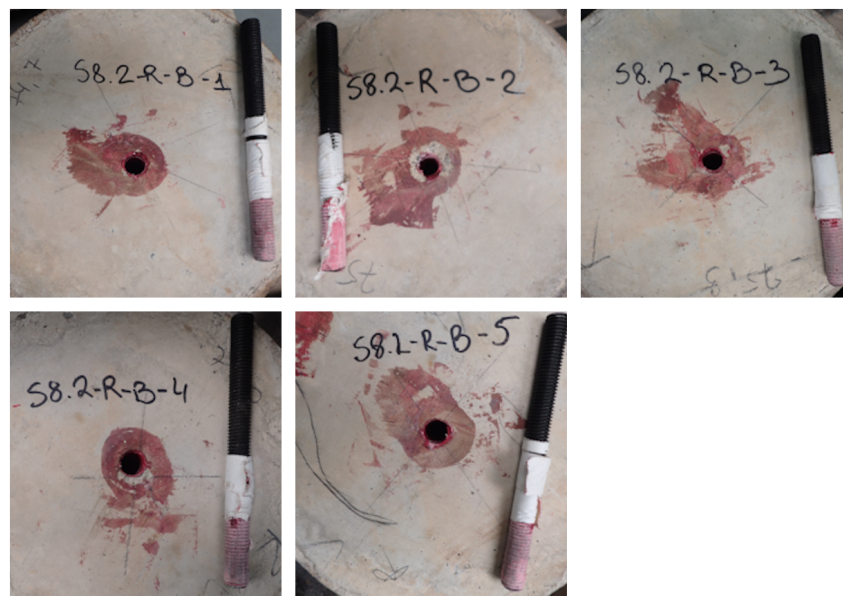FIGURE C.124: S8.1-R-A - Failure of the anchors

FIGURE C.125: S8.2-R-B - Failure of the anchors

FIGURE C.126: S8.3-A - Failure of the anchors

FIGURE C.127: S8.4-R - Failure of the anchors

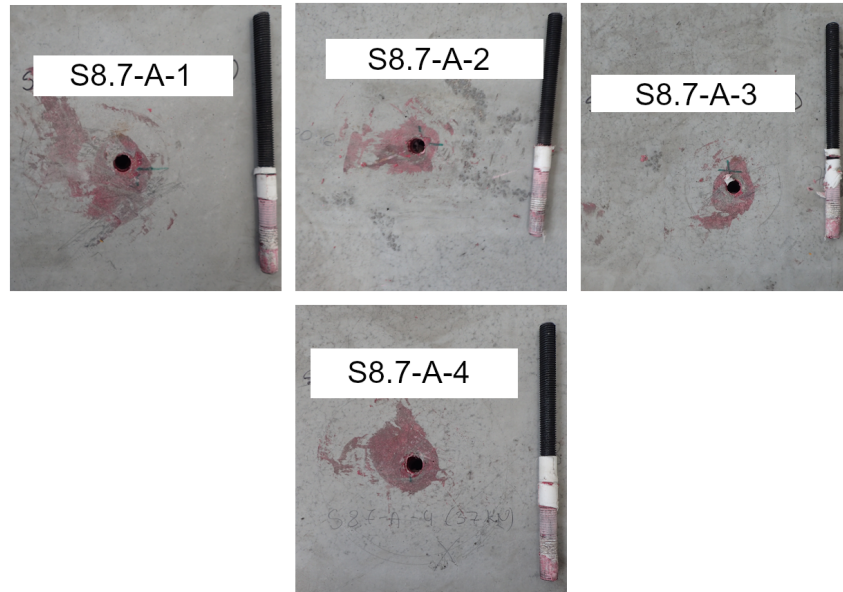FIGURE C.128: S8.5-B - Failure of the anchors
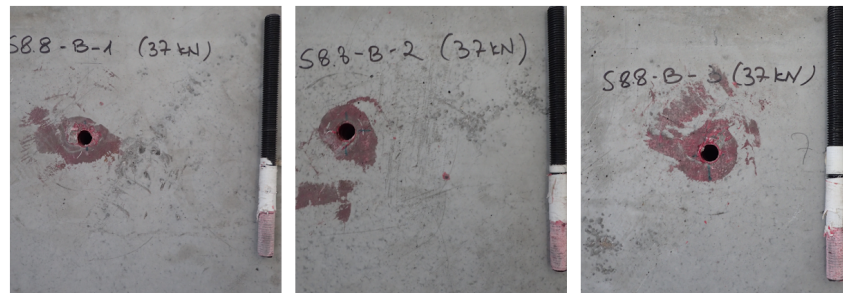
FIGURE C.129: S8.7-A - Failure of the anchors

FIGURE C.130: S8.8-B - Failure of the anchors

Bibliography

AC 308 (2017). *Acceptance criterial for post-installed adhesive anchors in concrete elements.*

ACI 318 (2019). *Building code requirements for structural concrete: commentary on building code requirements for structural concrete (ACI 318R-19).*

Appl, Jörg-Jochen (2009). "Tragverhalten von Verbunddübeln unter Zugbelastung". PhD thesis.

ASTM D2990 (2017). *Test Methods for Tensile, Compressive, and Flexural Creep and Creep-Rupture of Plastics.* West Conshohocken, PA.

Blochwitz, Ronald (2019). "Verbunddübelsysteme unter dauerhafter Lasteinwirkung". PhD thesis.

Cattaneo, Sara, Andrea Locatelli, and Davide Rago (2019). "Reliability of bonded anchors with different installation techniques: experimental assessment". In: *Asian Journal of Civil Engineering* 20.5, pp. 681–692.

Cognard, Philippe (2005). *Handbook of adhesives and sealants.* Amsterdam and London: Elsevier. ISBN: 0-08-044554-3.

Çolak, Adnan (2001). "Parametric study of factors affecting the pull-out strength of steel rods bonded into precast concrete panels". In: *International Journal of Adhesion and Adhesives* 21.6, pp. 487–493.

— (2007). "Estimation of ultimate tension load of methylmethacrylate bonded steel rods into concrete". In: *International Journal of Adhesion and Adhesives* 27.8, pp. 653–660.

Comité Euro-International du Béton (1994). *Fastenings to concrete and masonry structures: State of the art report.* London and New York: T. Telford and American Society of Civil Engineers, Publications Sales Dept. [distributor]. ISBN: 0-7277-3959-X.

Cook, Ronald A. (1993). "Behavior of Chemically Bonded Anchors". In: *Journal of Structural Engineering* 119.9, pp. 2744–2762.

Cook, Ronald A., Mark C. Bishop, et al. (1994). *Adhesive-bonded anchors: Bond properties and effects of in-service and installation conditions. Final project report.* Florida.

Cook, Ronald A., G. T. Doerr, and R. E. Klingner (1993). "Bond Stress Model for Design of Adhesive Anchors". In: *ACI Structural Journal* 90.5, pp. 514–524.

Cook, Ronald A., Elliot P. Douglas, and Todd M. Davis (2009). *Adhesive Anchors in Concrete Under Sustained Loading Conditions.* Washington, D.C.: Transportation Research Board.

Cook, Ronald A. and Robert C. Konz (2001). "Factors Influencing Bond Strength of Adhesive Anchors". In: *ACI Structural Journal* 98.1, pp. 76–86.

Cook, Ronald A., Jakob Kunz, et al. (1998). "Behavior and Design of Single Adhesive Anchors under Tensile Load in Uncracked Concrete". In: *ACI Structural Journal* 95.1, pp. 9–26.

Davis, Todd M. (2012). "Sustained Load Performance of Adhesive Anchor Systems in Concrete". PhD thesis. Florida: University of Florida.

DIN EN 12390-3 (2019). *Prüfung von Festbeton - Teil 3: Druckfestigkeit von Probekörpern; Deutsche Fassung EN_12390-3:2019.* Berlin.

DIN EN 1992-4 (2019). *Eurocode 2 - Bemessung und Konstruktion von Stahlbeton - und Spannbetontragwerken - Teil 4: Bemessung der Verankerung von Befestigungen in Beton; Deutsche Fassung EN 1992-4:2018.* Berlin.

DIN EN 206-01 (2017). *Beton- Festlegung, Eigenschaften, Herstellung und Konformität; Deutsche Fassung EN_206:2013+A1:2016.* Berlin.

DIN EN ISO 899-1 (2018). *Kunststoffe - Bestimmung des Kriechverhaltens - Teil 1: Zeitstand-Zugversuch (ISO_899-1:2017); Deutsche Fassung EN_ISO_899-1:2017.* Berlin.

Doerr, G. T. and R. E. Klinger (1989). "Adhesive anchors: behavior and spacing requirements". In: *1126-2UR - https://trid.trb.org/view/1180418.*

EAD 330499 (2018). *Bonded fasteners for use in concrete.*

Eligehausen, Rolf, Rainer Mallée, and Gallus Rehm (1984). "Befestigungen mit Verbundankern. [Teil 1]". In: URL: `https://elib.uni-stuttgart.de/handle/11682/442`.

Eligehausen, Rolf, Rainer Mallée, and John F. Silva (2006). *Anchorage in concrete construction.* Weinheim: Ernst & Sohn. ISBN: 978-3-433-01143-0.

Findley, William N., James S. Lai, and Kasif Onaran (1976). *Creep and relaxation of nonlinear viscoelastic materials: With an introduction to linear viscoelasticity / by William N. Findley, James S. Lai, and Kasif Onaran.* New York, N.Y.: Dover. ISBN: 978-0-486-66016-5.

Fuchs, Werner, Rolf Eligehausen, and John E. Breen (1995). "Concrete Capacity Design (CCD) Approach for Fastening to Concrete". In: *ACI Structural Journal* 92.1.

González, Francisco et al. (2018). "Influence of construction conditions on strength of post installed bonded anchors". In: *Construction and Building Materials* 165, pp. 272–283.

Grzesik, Peter (2012). "Effect of Fly Ash as Cement Replacement on the Short Term Bond Strength of Adhesive Anchors Systems". In: *ACI Symposium Publication* 283.

Hülder, Gerrit (2008). *Zur Aushärtung kalthärtender Reaktionsharzsysteme für tragende Anwendungen im Bauwesen.* 1. Aufl. Vol. 50. Technisch-wissenschaftlicher Bericht / Lehrstuhl für Kunststofftechnik, Universität Erlangen-Nürnberg. Erlangen: Univ. Erlangen-Nürnberg, Lehrstuhl für Kunststofftechnik. ISBN: 978-3-931864-37-8.

IWB (2019). *Time-to-failure- and Reference-tests with injection mortar.* Stuttgart.

Kränkel, Thomas S. (2017). *Ein rheologischer Modellansatz zur Prognose des Langzeittragverhaltens von Verbunddübeln.* München: Universitätsbibliothek der TU München.

Kunz, Jakob et al. (1998). "Tragverhalten und Bemessung von chemischen Befestigungen". In: *Beton– und Stahlbetonbau* 93.1, pp. 15–19. URL: `https://onlinelibrary.wiley.com/doi/pdf/10.1002/best.199800030`.

Lahouar, Mohamed Amine et al. (2017). "Mechanical behavior of adhesive anchors under high temperature exposure: Experimental investigation". In: *International Journal of Adhesion and Adhesives* 78, pp. 200–211.

Lehr, Bernhard (2003). "Tragverhalten von Verbunddübeln unter zentrischer Belastung im ungerissenen Beton - Gruppenbefestigungen und Befestigungen am Bauteilrand". PhD thesis. Stuttgart: University of Stuttgart.

Lehr, Bernhard and Rolf Eligehausen (1998). *Zusammenfassender Bericht über zentrische Ausziehversuche mit Verbunddübeln M8, M12, M16 mit weiter und enger Abstützung.* Not published.

Marti, P. (1993). *Anchoring of concrete reinforcement using HIT-HY 150.* Kaufering, Germany.

Mészároš, Juraj (2002). "Tragverhalten von Einzelverbunddübeln unter zentrischer Kurzzeitbelastung". PhD thesis.

National Transportation Safety Board NTSB (2006). *Ceiling Collapse in the Interstate 90 Connector Tunnel Boston, Massachusetts.* Washington D.C.

Sell, R. (1973). "Über Festigkeit und Verformung mit Reaktionsharzmörtelpatronen versetzen Betonanker". In: *Verbindungstechnik* Heft 8, pp. 11–16.

Simons, Isabelle Nadine (2007). "Verbundverhalten von eingemörtelten Bewehrungsstäben unter zyklischer Beanspruchung". PhD thesis. URL: `https://elib.uni-stuttgart.de/handle/11682/278`.

Spieth, Hannes A. (2002). "Tragverhalten und Bemessung von eingemörtelten Bewehrungsstäben". PhD thesis. URL: `http://elib.uni-stuttgart.de/bitstream/11682/177/1/Dis_Spieth.pdf`.

Vogelgsang, Christian (2012). "Experimentelle und numerische Untersuchungen des Einflusses der engen Abstützung auf die Verbundspannungen im Zugversuch von eingemörtelten Gewindestangen in Beton". PhD thesis. Stuttgart: Unisersity of Stuttgart.

Curriculum Vitae

Nilde MAÇI, M.Sc.

1990	born in Tirana, Albania
1997 − 2005	"Avni Rustemi" School in Tirana, Albania
2005 − 2009	"Qemal Stafa" High School in Tirana, Albania
2005 − 2009	Bachelor study in civil engineering at the Polytechnic University of Tirana, Albania
2009	Bachelor of Science
2009 − 2012	Master study in Computational Mechanics of Materials and Structures at the University of Stuttgart
2012	Master of Science
2023	Doctor of Engineering
2013 − 2015	Student assistant at COMMAS study program, University of Stuttgart
2015 − 2021	Research associate at the Institute of Construction Materials, University of Stuttgart
2021 −	Managing Director at FixING Solutions GmbH